(NASA-CR-173784) GENERAL AVIATION AIRCRAFT INTERIOR NOISE PROBLEM: SOME SUGGESTED SOLUTIONS (Kansas Univ.) 488 p
HC A21/MF A01 CSCL 20A G3/71

N84-29685
Unclas
19947

CRINC

THE UNIVERSITY of KANSAS CENTER FOR RESEARCH, INC.
2291 Irving Hill Drive-Campus West
Lawrence, Kansas 66045

Progress Report

for

NASA Contract NCCI-6

GENERAL AVIATION AIRCRAFT INTERIOR NOISE PROBLEM: SOME SUGGESTED SOLUTIONS

KU-FRL-417-23

by

Ramasamy Navaneethan

Principal Investigator:
Jan Roskam

Flight Research Laboratory

University of Kansas

Lawrence, Kansas 66045

July 1984

GENERAL AVIATION INTERIOR NOISE PROBLEM: SOME SUGGESTED SOLUTIONS

by

Ramasamy Navaneethan

Abstract of report submitted to the
University of Kansas in partial fulfillment
of the degree of Doctor of Engineering

June 1984

Studies have shown that interior noise levels in general aviation aircraft are generally high and annoying. The airborne noise transmission through aircraft sidewall is one of the important source-path combinations of the sound transmission into an aircraft cabin. This report describes the work completed for an ongoing general aviation interior noise research project. A broad-based approach--i.e., laboratory investigation of sound transmission through panels, use of modern data analysis techniques and application to actual aircraft--was used to determine methods to reduce general aviation interior noise.

The laboratory investigations were carried out in a low-cost acoustic panel test facility. The experimental noise reduction characteristics of stiffened flat and curved panels with damping treatment are discussed. The experimental results of double-wall panels used in the general aviation industry are given. The effects of skin panel material, fiberglass insulation and trim panel material on the noise reduction characteristics of double-wall panels are investigated. These results are compared with the

theoretical predictions from classical sound transmission theory for multilayered panels. The changes needed in the classical sound transmission theory for a better agreement are discussed. It is also shown that the same theory can successfully be used to design the interior noise control treatment of a new aircraft.

The development of the acoustic intensity system for this test facility is described. The use of cepstral analysis techniques to determine the absorption coefficients of interior trim panels in situ is discussed. Also a computer program, which can be used to analyze the problem of high interior noise of the production aircraft and to study the effectiveness of the noise control treatment, is given. The use of this program on aircraft noise control has shown the validity of the models used. The results indicate that with minor modifications the classical sound transmission theory can be used not only to predict the panel sound transmission loss characteristics but also to analyze actual noise control treatment of an aircraft.

ACKNOWLEDGEMENTS

In a program of this magnitude, many organizations and individuals make contributions to the success of the project. I would like to express my gratitude to all who provided invaluable assistance during the course of this project. Many organizations have directly contributed to this project. These are NASA Langley Research Center (financial and technical support), Cessna Aircraft Company (financial and technical support) and other aircraft manufacturers (test specimens).

In particular, at the University of Kansas, I wish to express my sincere appreciation to Dr. Jan Roskam for his guidance, support and encouragement. In addition I am grateful to my committee members for their valuable suggestions. At Cessna Aircraft Company I wish to express my appreciation to Mr. Joe Gault and Mr. Mike Smith. A special word of thanks goes to Mr. Robert L. Howes, who initiated me into the field of Time Series Analysis and suggested many computer programs developed during this project. My sincerest appreciation goes to Mrs. Nancy Hanson for her patient typing and correction of this manuscript.

In addition, I would like to recognize my parents for their understanding and many sacrifices in providing me with opportunity and encouragement. Finally, thanks must also go to Nirmala and Priya for their understanding and support.

R. Navaneethan

TABLE OF CONTENTS

TABLE OF CONTENTS (continued)

TABLE OF CONTENTS (continued)

TABLE OF CONTENTS (continued)

TABLE OF CONTENTS (continued)

TABLE OF CONTENTS (continued)

TABLE OF CONTENTS (continued)

TABLE OF CONTENTS (continued)

LIST OF FIGURES

Number | Title | Page

INTENTIONALLY LEFT OUT

LIST OF FIGURES (continued)

LIST OF FIGURES (continued)

LIST OF FIGURES (continued)

LIST OF FIGURES (continued)

LIST OF FIGURES (continued)

LIST OF FIGURES (continued)

LIST OF FIGURES (continued)

LIST OF FIGURES (continued)

LIST OF FIGURES (continued)

LIST OF FIGURES (continued)

LIST OF TABLES

LIST OF TABLES (continued)

LIST OF SYMBOLS

Symbol	Definition	Dimension
a	Acceleration	[g units]
a	Speed of sound	[m/s]
a	Panel length	[m]
A	Area	[m^2]
A	Maximum input range of the analyzer	-
b	Panel width	[m]
b	Propagation constant	[Nepers]
c	Damping coefficient	[Newton-sec/m]
c	Power cepstrum	-
c	Speed of sound	[m/s]
C	Speed of sound	[m/s]
d	Depth of airgap or insulation	[m]
d	Distance	[m]
D	Flexural rigidity	[Nm]
D	Damping energy	[Nm]
E	Young's modulus	[N/m^2]
$\dot{E}$	Energy flux	[Nm]
E	Expected value function	-
f	Frequency	[Hz]
$\mathscr{F}$	Fourier transform	-
F	Force	[N]
G	Shear modulus	[N/m^2]
G	One-sided spectrum	-

LIST OF SYMBOLS (continued)

Symbol	Definition	Dimension
h	Skin thickness	[m]
h	Impulse response function	-
H	Transfer function	-
i	Integer	-
I	Area moment of inertia	$[m^4]$
I	Intensity	$[Watt/m^2]$
j	$\sqrt{-1}$	-
J	Torsion constant	$[m^4]$
k	Slope factor	$[m^4]$
k	Integer	-
k	Wave number	$[m^{-1}]$
K	Calibration constant	-
ℓ	Distance	[m]
ℓ	Stringer pitch	[m]
L	Panel length	[m]
m	Mass per unit area	$[kg/m^2]$
M	Mass per unit area	$[kg/m^2]$
M	Mach number	-
n	Integer	-
n	Number of cycles	-
n	Number of layers	-
n	Number of ensemble averages	-

LIST OF SYMBOLS (continued)

Symbol	Definition	Dimension
N	Number of ensemble averages	-
N	Number of layers	-
N	Array size of the analyzer	-
p	Pressure	[Pa]
P	Pressure	[Pa]
P	Loads due to pressurization	[N]
q	Circumferential half wave number	-
Q	Quality index (Equation 4.2)	-
r	Distance	[m]
R	Radius of skin panel	[m]
R	Correlation function	-
S	Spectrum	-
t	Panel thickness	[m]
t	Time	[s]
T	Observation time interval	[s]
T	Reverberation time	[s]
u	Particle velocity	[m/s]
U	Particle velocity	[m/s]
U	Elastic energy	[Nm]
V	Output value from the analyzer	-
V	Volume	$[m^3]$
x	Distance	[m]
x	Amplitude of oscillations	[m]

LIST OF SYMBOLS (continued)

Symbol	Definition	Dimension
$\bar{x}$	Sample mean	-
x	Direct signal	-
X	Fourier transform of x(t)	-
y	Composite signal	-
Y	Fourier transform of y(t)	-
z	Complex variable	-
z	Test statistic	-
z	Impedance	[Rayls]
Z	Statistic	-
Z	Characteristic impedance	[Rayls]
Z	Z-transform	-
Greek		
α	Absorption coefficient	-
δ	Logarithmic decrement	-
δ	Difference between test mean and population mean	-
θ	Angle of incidence	[deg]
ζ	Damping ratio	-
μ	Population mean	-
ν	Poisson's ratio	-
η	Loss factor	-
ε	Relative statistical error	-
λ	Variable	-

(Greek)	Definition	Dimension
ρ	Density	$[kg/m^3]$
ω	Angular frequency	[rad/s]
τ	Transmission coefficient	-
τ	Time delay	[s]
τ	Time increment	[s]
γ	Square root of coherence	-
ϕ	Phase difference	[deg]
ψ	Specific damping capacity (Equation 4.3)	-
ψ	Phase angle	-
σ	Standard deviation	-

Subscript	
a	Ambient
A	At location A
av	Average
ax	Axial
B	At location B
B	Airgap or insulation
c	Calibration
C	Critical
cal	Calibration
cir	Circumferential
cp	Complex cepstrum

LIST OF SYMBOLS (continued)

(Subscript)	Definition	Dimension
d	Test of sample	
e	Base of natural logarithm (= 2.171828)	
f	Frame	
i	Integer	
i	Incident	
I	Incident	
inst	Instantaneous	
k	Integer	
n	Resonance	
n	Integer	
p	Panel	
P	Pressure	
pc	Power cepstrum	
r	Receiver	
r	Reflected	
s	Source	
s	Sample	
s	Sabine	
std	Standard	
t	Terminating	
t	Transmitted	
t.s.	Test sample	
v	Particle velocity	

LIST OF SYMBOLS (continued)

(Subscript)	Definition	Dimension
α	Probability of committing Type I error	
β	Probability of committing Type II error	
θ	Angle	
Superscript		
s	Switched	
*	Conjugate	
-	Average	
^	Logarithm	

LIST OF ABBREVIATIONS

Abbreviation	Definition
CRINC	Center for Research, Inc.
DB (dB)	Decibel
DBA (dBA)	A-weighted sound pressure level in decibels
DBL (dbL)	Linear sound pressure level in decibels
FRL	Flight Research Laboratory
KU	University of Kansas
NR	Noise reduction
NRC	Noise reduction coefficient
OSPL	Overall sound pressure levels
PSIL	Preferred speech interference level
SDOF	Single degree of freedom
SLM	Sound level meter
SIL	Speech interference level
TL	Transmission loss
ΔP	Pressure differential

CHAPTER 1

INTRODUCTION

Studies (References 1-3) show that the levels of noise within general aviation aircraft are high when compared to other modes of transportation and in many cases result in annoyance and discomfort for the pilot as well as the passengers. This is despite the use of heavy acoustical treatments. The noise control treatment in present-day general aviation aircraft is based on an after-the-fact approach. Even though high interior noise level is uncomfortable and annoying, it rarely affects the safety of the aircraft. For this reason it does not receive enough attention from the aircraft designers during the initial phases of the design of an aircraft. Only after a prototype is constructed and found to be noisy are the members of acoustic and vibration groups consulted. However, there is a growing awareness of this problem, both in the industry and in research institutions. The noise sources in general aviation are engine, propeller, auxiliary equipment and airflow over fuselage. The noise paths include both structure-borne and airborne paths. In particular, a significant NASA-sponsored research program is being conducted in the area of structural transmission phenomena and prediction. The research program concerns itself with the transmission of the airborne noise from the engines and propellers, through aircraft sidewalls into the fuselage. In this area, three major topics of experimental and theoretical analysis can be identified:

1. Sound transmission through actual fuselage structure;

2. Sound transmission through a cylindrical model;

3. Sound transmission through panel type structures.

It is the third topic that is being investigated at the University of Kansas Flight Research Laboratory (KU-FRL), under a grant from NASA. This ongoing program, titled "A Research Program to Reduce the Interior Noise in General Aviation Airplanes," is funded by NASA Langley Research Center, through continuing Cooperative Agreement NCCI-6. The work conducted by the KU-FRL, in addition to contributing to NASA Langley's general aviation noise programs, also provides information that is more directly applicable to the design and modification of interior noise control treatment of general aviation aircraft. The latter is the reason for general aviation manufacturers to stimulate the KU-FRL research program with valuable information as well as with test specimen.

This research program started in April 1976 and has guaranteed funding up to April 1985. This report presents the organization and results of this program from June 1982 through June 1984. During this period, the research progrm was concentrated in the following aspects of the interior noise problems of general aviation aircraft.

1. Investigation of sound transmission through panel type structures;

2. Development of new data analysis techniques for the test facility;

3. Application of the results of this research program to actual aircraft noise control.

The next chapter describes the project history, the status of the project at the beginning of this report period, the research objectives, and the impact of this project.

Chapters 3-6 deal with the first aspect of the project. In particular, the sound transmission characteristics of panels treated with damping tapes are presented in Chapter 3. The effects of three different damping tapes are analyzed. Chapter 4 describes the test methods developed to measure the loss factors of panels installed at this test facility. These values are needed for use in theoretical prediction programs. Also discussed in this chapter are effects of various parameters on the loss factors of panels installed in this test facility. Chapters 5 and 6 deal with the sound transmission characteristics of double-wall panels. Chapter 5 presents the results of a systematic experimental investigation of double-wall panels. Chapter 6 describes the computer program developed to calculate the noise reduction values of such panels. Analytical and experimental results are also compared in this report.

Chapter 7 describes the design development and testing of the acoustic intensity techniques at this facility. With the installation of this technique, sound intensity radiation of panel type structures can be studied. A method to measure the absorption coefficients in situ based on the principle of deconvolution of composite signals is presented in Chapter 8.

The application of the results obtained in Chapters 5 and 6 to actual aircraft noise control design is described in Chapter 9. A computer program, based on the conventional sound transmission theory to troubleshoot high interior noise problems of individual aircraft, is presented in Chapter 10.

Conclusions and recommendations based on this research project are given in Chapter 11.

CHAPTER 2

PROJECT HISTORY AND MANAGEMENT

2.1 PROJECT HISTORY

In April 1976, the request by the University of Kansas for a grant to do research in the field of general aviation interior noise was approved by the Noise Effect Branch of the NASA Langley Research Center. The broad objective of this research program is expressed by its title, "A Research Program to Reduce the Interior Noise of General Aviation Airplanes." The first year of this research program was exploratory in nature. It was used to define a long-range, follow-up research program in interior airplane noise. During the latter part of the project year 1976-77 and the first part of the project year 1977-78, the design and construction of the KU-FRL acoustic test facility was undertaken. During the second project year onwards, the program objectives (Reference 3) remained as follows:

1. To determine the sound transmission loss characteristics of various structural panels and panel treatments (experimentally);
2. To compare test results with predictions from pertinent analytical methods;
3. To provide a systematic collection of sound attenuation characteristics of panels based on both experimental and analytical considerations;

4. To use these results to extend or develop prediction methods.

By the end of the second project year the following tasks were accomplished:

1. Design and construction of an acoustic test facility: A description of the test facility is given in Appendix A of this report.
2. Design and construction: special test sections to measure sound transmission loss characteristics at oblique angles of incidence.
3. Determination of transmission loss data for single panels.
4. Empirical and theoretical insertion loss prédiction methods.

During the next two project years (1978-79 and 1979-80), a systematic study was undertaken to determine the parameters that affect noise transmission through single-wall panels. The parameters studied include mass; thickness; stiffness; angles of incidence; radius of curvature; riveted, bonded and clamped edge conditions; and tensile stress. During this period, the effect of the cavity of the termination box of the test facility on the measured sound transmission loss of the panels was also investigated. A systematic study was also undertaken to investigate the sound transmission loss characteristics of single-pane and dual-pane plexiglass windows. During this investigation, use of flat, depressurized, integral, dual-pane windows was also explored. The

results of these two years of study are presented in the Doctor of Engineering Report (Reference 4).

During the years 1980-81 and 1981-82, the sound transmission charcteristics of interior trim panels, multilayer panels and composite panels were studied. Also investigated were the concepts of Helmholtz resonators for dual-pane windows and tuned dampers for structures (References 5 and 6). During this period, tests were also performed on panels with damping tape.

The author, Ramasamy Navaneethan, started working on this project in August 1979. The work performed between June 1980 and June 1981 was used for his Master of Science thesis (Reference 5). He continued to work for his doctoral program on this project. During 1981-82, he familiarized himself with actual aircraft interior noise problems and developed methods to apply the results of this test facility to actual aircraft applications. He became the student project manager for this continuing NASA project from June 1982. This project report covers the period from June 1982 to June 1984 and the relevant work on actual aircraft applications.

During the project years 1982-83 and 1983-84, the following additional objective was added to the primary objectives of the project:

> To develop new analysis techniques at the KU-FRL acoustic test facility.

During this project period, the following tasks were proposed.

1. To investigate the effect of damping material on the sound transmission loss characteristics of skin panels;
2. To investigate the damping characteristics of panels used in general aviation aircraft;
3. To document the sound transmission loss characteristics of double-wall panels;
4. To investigate the parameters which affect sound transmission through double-wall panels;
5. To develop a simple, theoretical model which will predict the sound transmission loss characteristics of double-wall panels;
6. To develop a computer program to apply the results obtained in 3 through 5 in the noise control treatment design of an aircraft;
7. To develop a method for troubleshooting high interior noise problems of existing production aircraft;
8. To develop procedures to calculate sound transmission values using acoustic intensity measurements;
9. To develop cepstral analysis techniques for the measurement of absorption coefficients of nonstandard size panels.

PARAGRAPHS 2.2 AND 2.3

INTENTIONALLY LEFT OUT

CHAPTER 3

NOISE REDUCTION CHARACTERISTICS OF SINGLE PANELS WITH DAMPING MATERIALS

3.1 INTRODUCTION

Experimental investigations have already been performed at the KU-FRL acoustic test facility to determine the individual effects of structural stiffening, curvature and damping on the sound transmission loss characteristics of panel-type structures used in general aviation industry (Reference 4). But in practice, all three of these factors occur together; i.e., the aircraft skin is always stiffened by stringers and frames, it is often pressurized to add comfort for the passengers, and invariably some sort of damping treatment is added. In this series of experimental investigations, the sound transmission characteristics of the panels containing damping material were investigated.

Earlier studies (References 3 and 4) indicate that the use of stiffeners on panels increases the stiffness of the panel, which increases the noise reduction in the stiffness-controlled region (or low-frequency region). Curving a panel increases the low-frequency noise reduction if the curvature is low, because of the stiffening effect of the curvature. However, when the curvature is very high, other effects such as oblique incidence become dominant. These effects reduce the noise reduction, offsetting the effect of stiffening. In the high-frequency region, the effect of curvature is to reduce the noise reduction. The effect of increasing damping

of panels by means of additional damping treatment is to increase the noise reduction at the fundamental resonance frequency and also to reduce the severity of the resonance peaks and dips in the high-frequency region. In this series of tests, the above results were kept in mind in choosing the test parameters to be varied. Two panels, representative of the actual aircraft panels, were used. Three different types of damping treatment were investigated.

The KU-FRL acoustic test facility was used for these tests. It consists of three main systems: testing apparatus, signal generating and analyzing equipment, and depressurization system. Figure 3.1 shows the test facility. Figure 3.2 shows the test facility configuration for flat panels. Figure 3.3 shows the adapter required for a curved, stiffened panel. The data acquisition system and noise generation equipment are illustrated in Figure 3.4. Finally, the schematic diagram of the depressurization subsystem is presented in Figure 3.5. The description and characteristics of the test facility are summarized in Appendix A. In the following section the modifications done to the test facility, the test panels, and the parameters tested will be described. The results for each group of tests performed will also be presented in the subsequent sections.

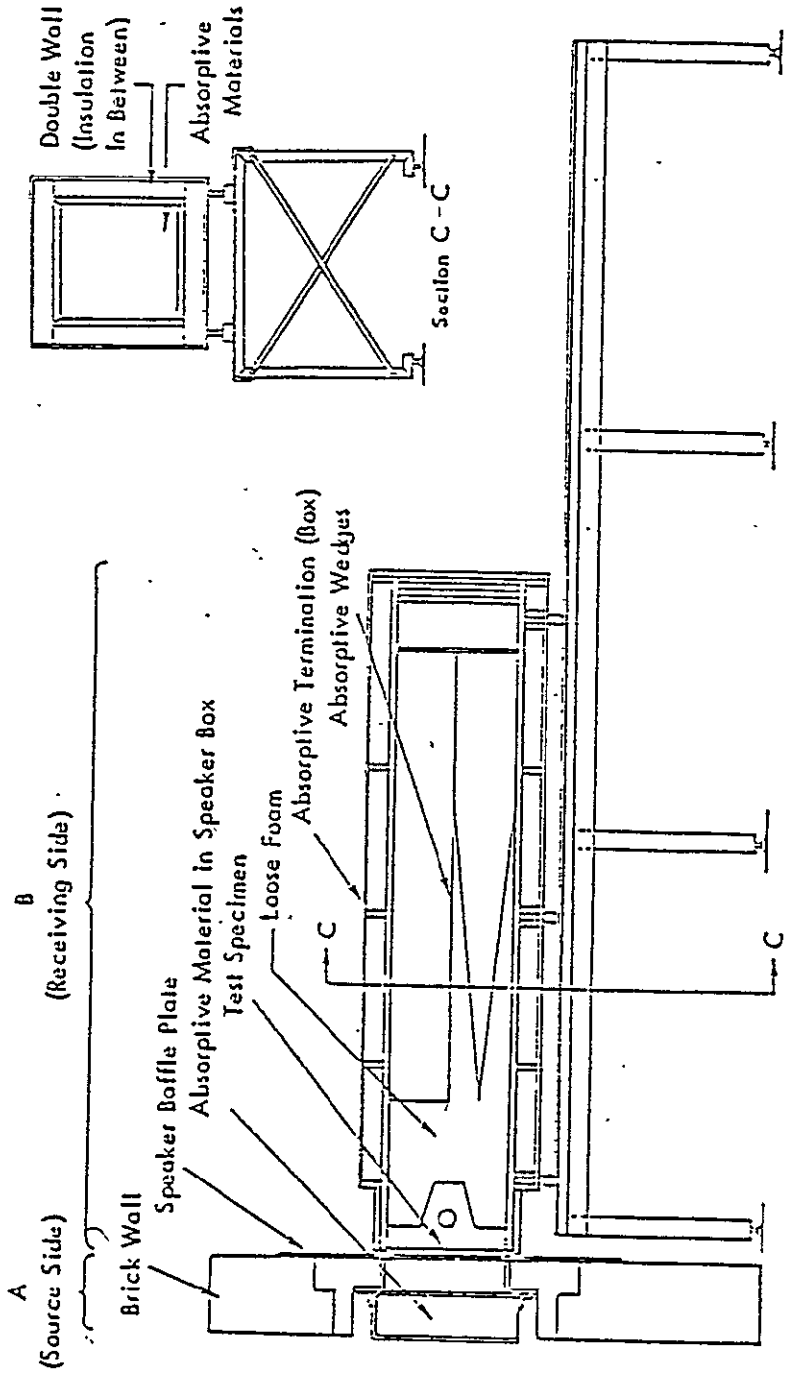

Figure 3.1: Test Set-Up in the KU-FRL Acoustic Test Facility

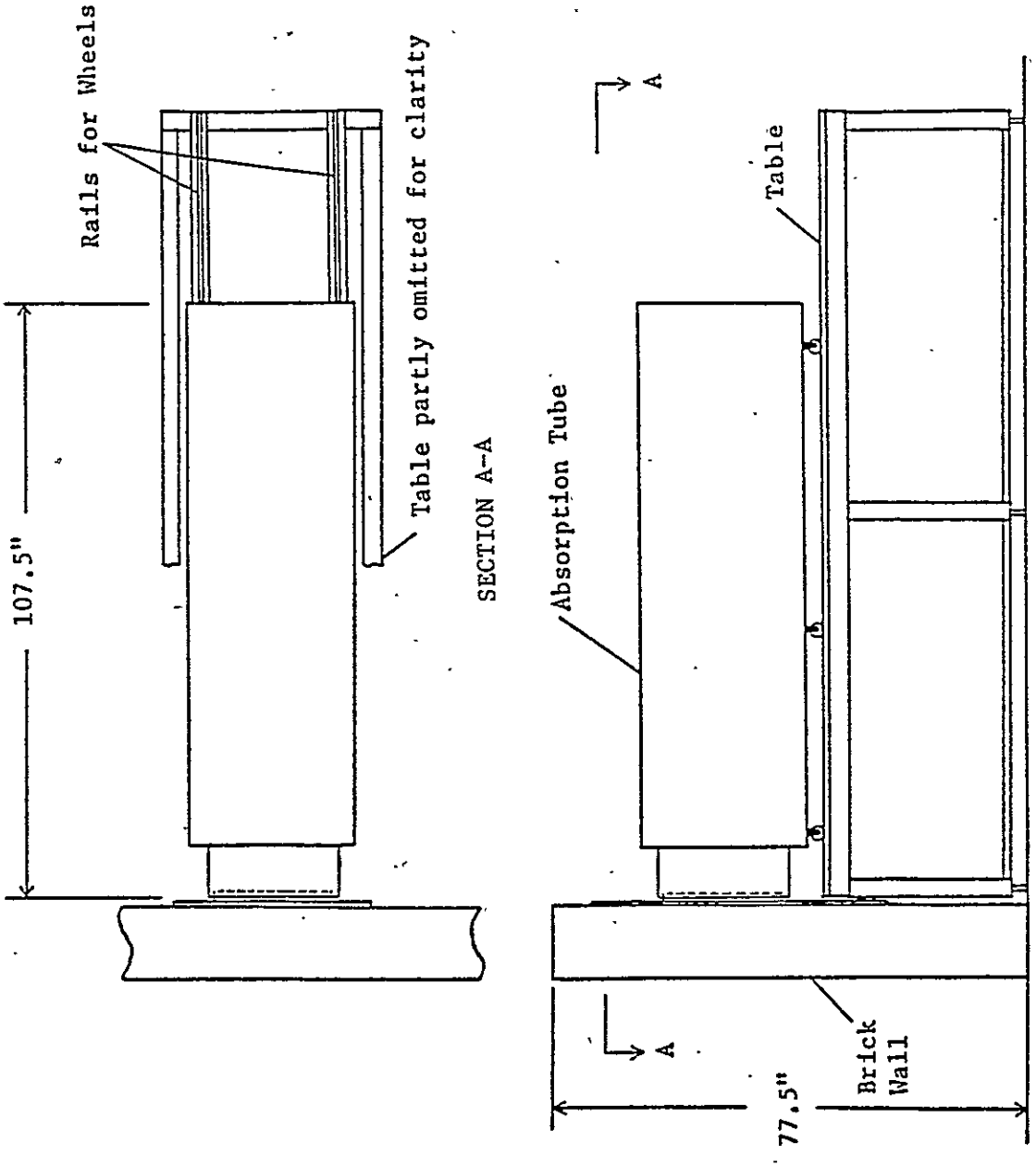

Figure 3.2: Test Facility Set-Up for Flat Panel

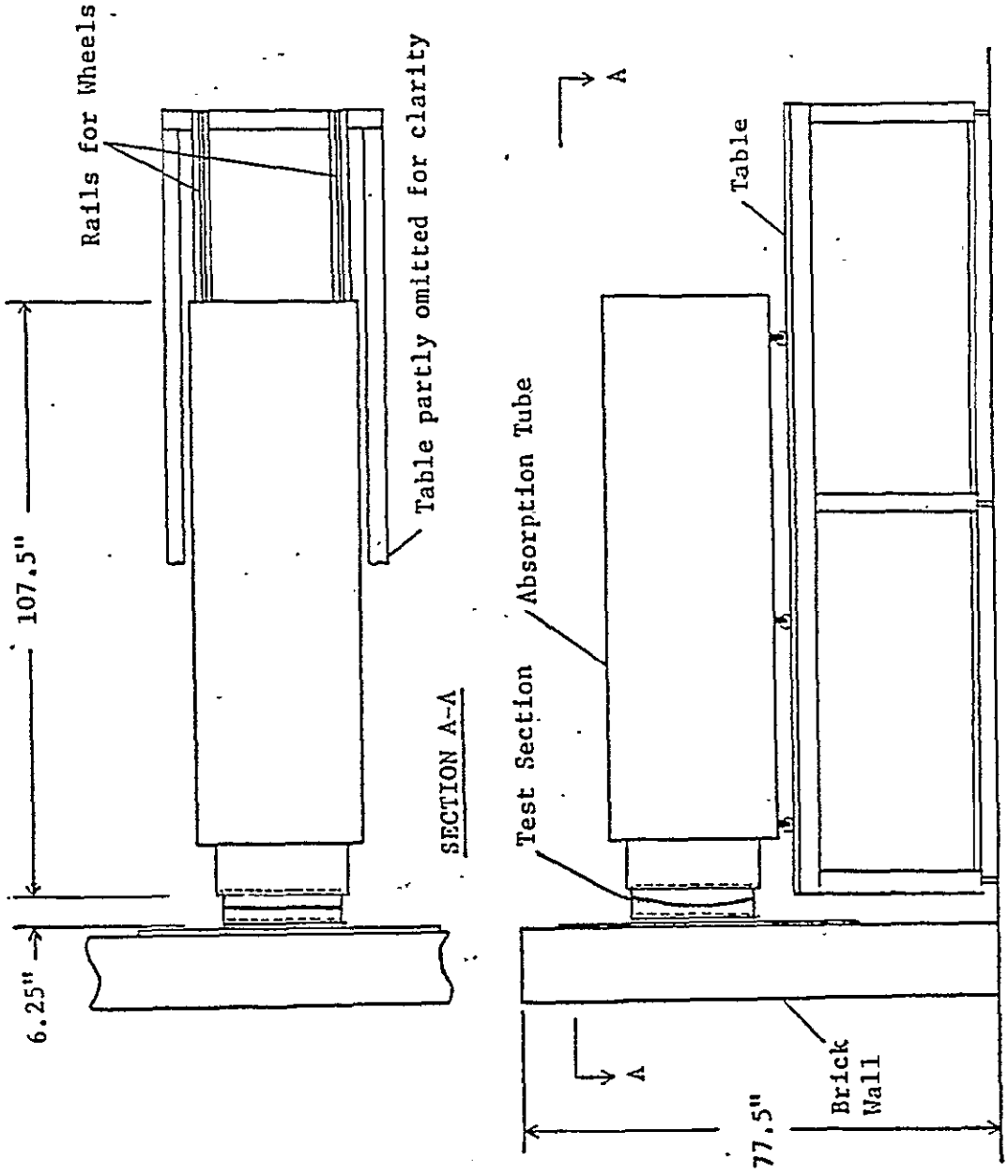

Figure 3.3: Test Facility Set-Up for Curved Panel

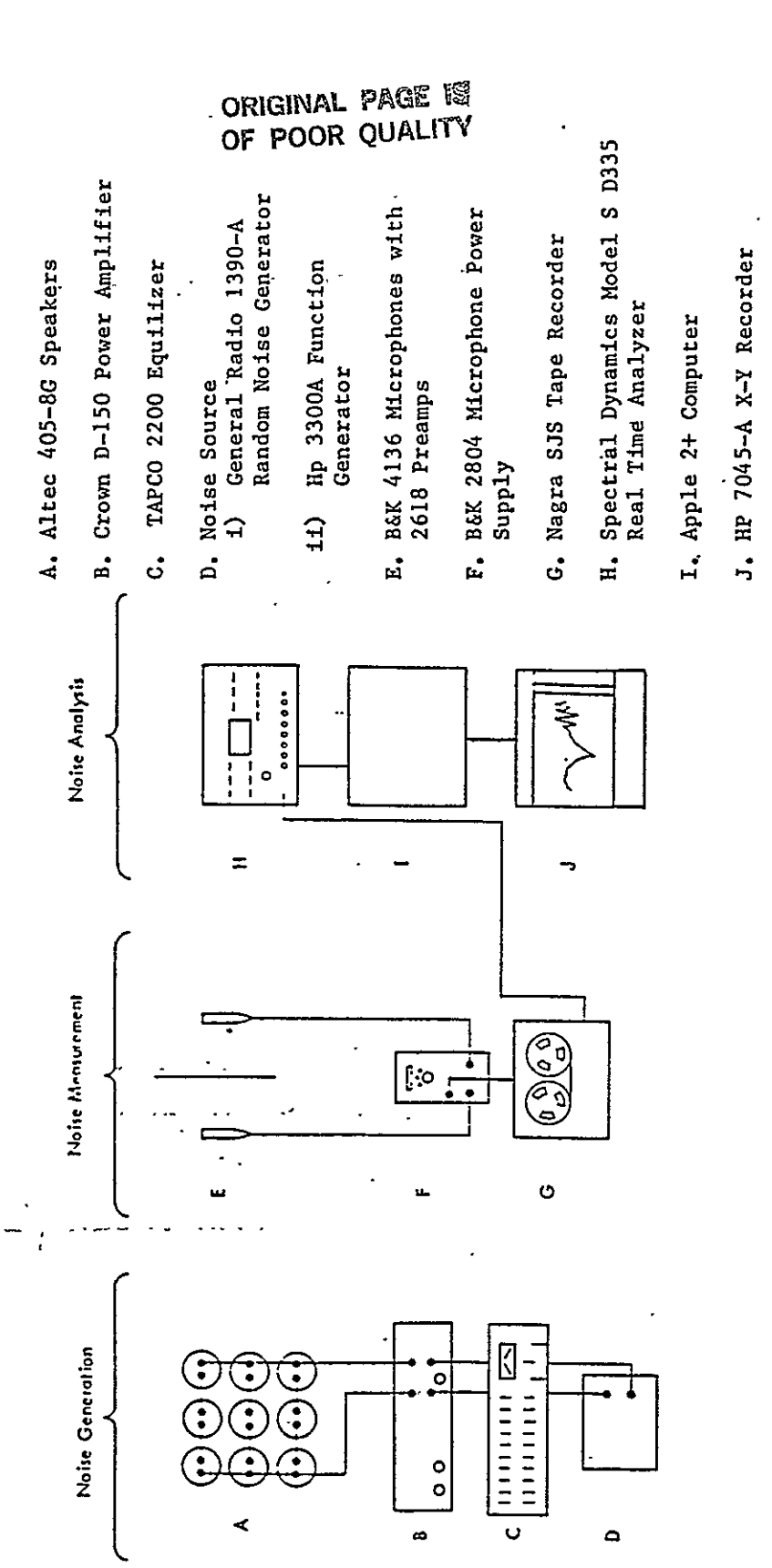

Figure 3.4: Noise Generation and Data Acquisition Equipment

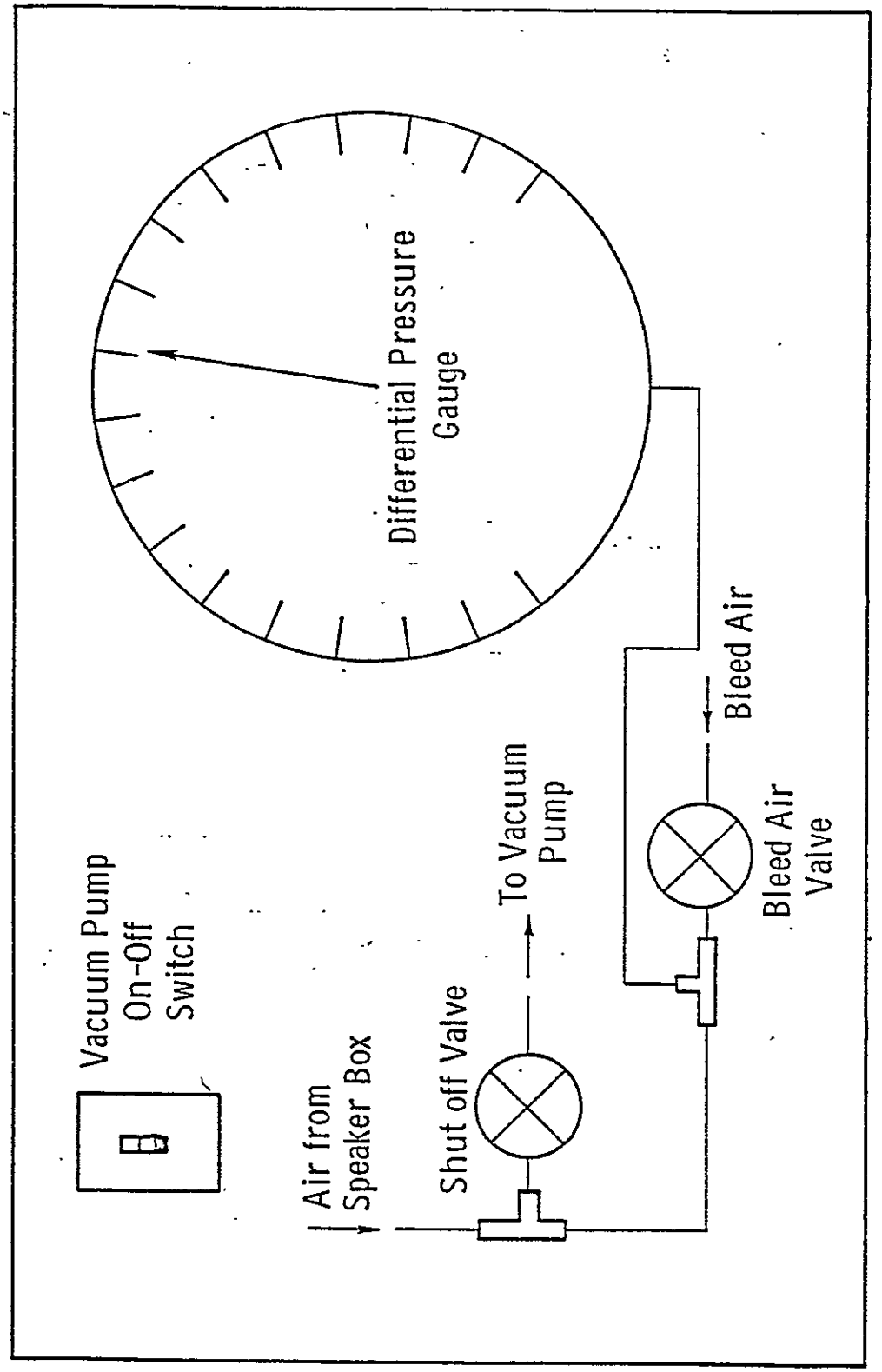

Figure 3.5: Depressurization Subsystem

3.2 MODIFICATIONS TO THE TEST FACILITY

These tests with the flat and curved panels with pressure differential across the test specimen demanded some modifications to the test facility. These are described below.

3.2.1 DEPRESSURIZATION SYSTEM

As previously mentioned, testing was also done with pressure differential across the test panel. A depressurization system had already been used in the KU-FRL acoustic test facility (Reference 3). This system was reactivated for use in this phase. The schematic diagram of the system is shown in Figure 3.5. The system was recalibrated to determine the line losses. The system proved to be reliable and posed little problem during the tests. Pressure differentials up to 3 psi could be generated.

3.2.2 ADAPTER FOR CURVED PANEL

Unlike the flat panel, which can be directly clamped to the test section, the curved panel required an additional curved support on both sides of the panel so that a simply-supported edge condition could be simulated. Figure 3.3 shows the adapter used and its relative location in the test facility. This adapter was constructed from 3/4 inch particle board and had the same outside dimensions as the standard test section. The adapter shifted the centerline of the test specimen back to three inches from the noise

source, as compared to the standard one inch for the flat panel. No corrections were made for the additional cavity produced by this adapter. However, the distance between the microphones was maintained constant at eight inches.

3.3 DESCRIPTION OF THE TEST PANELS AND MATERIALS

3.3.1 FLAT PANEL

The flat panel, made from standard aluminum sheet, was stiffened in one direction by "L" stringers. The sheet was 0.04 inches thick and 20 inches by 20 inches in outside dimensions. The extruded stiffeners were riveted to the skin. Figure 3.6 gives the geometrical details of the panel.

3.3.2 CURVED PANEL

The curved aluminum panel was stiffened in two directions. The sheet thickness was .04 inch. The panel was curved in one direction and stiffened in both directions, thus approximating a typical general aviation type sidewall. The radius of the curvatuve of the panel was 33.5 inches. This radius of curvature is representative of the radius used in the general aviation industry. The stiffeners and the frames were riveted to the skin. The outside dimensions were 20 inches by 20 inches. The geometric details of the panel are given in Figure 3.7.

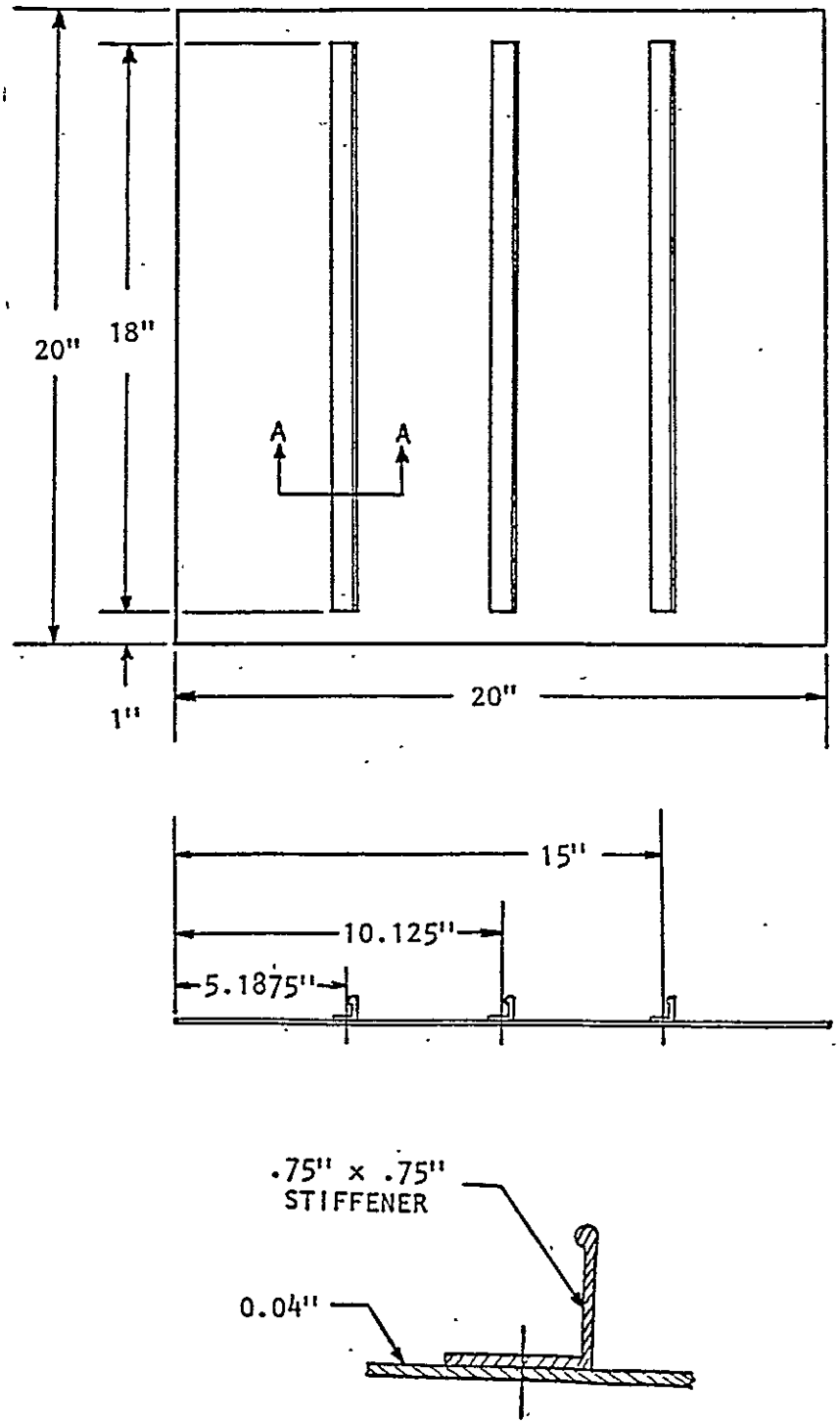

Figure 3.6: Flat Panel Dimensions

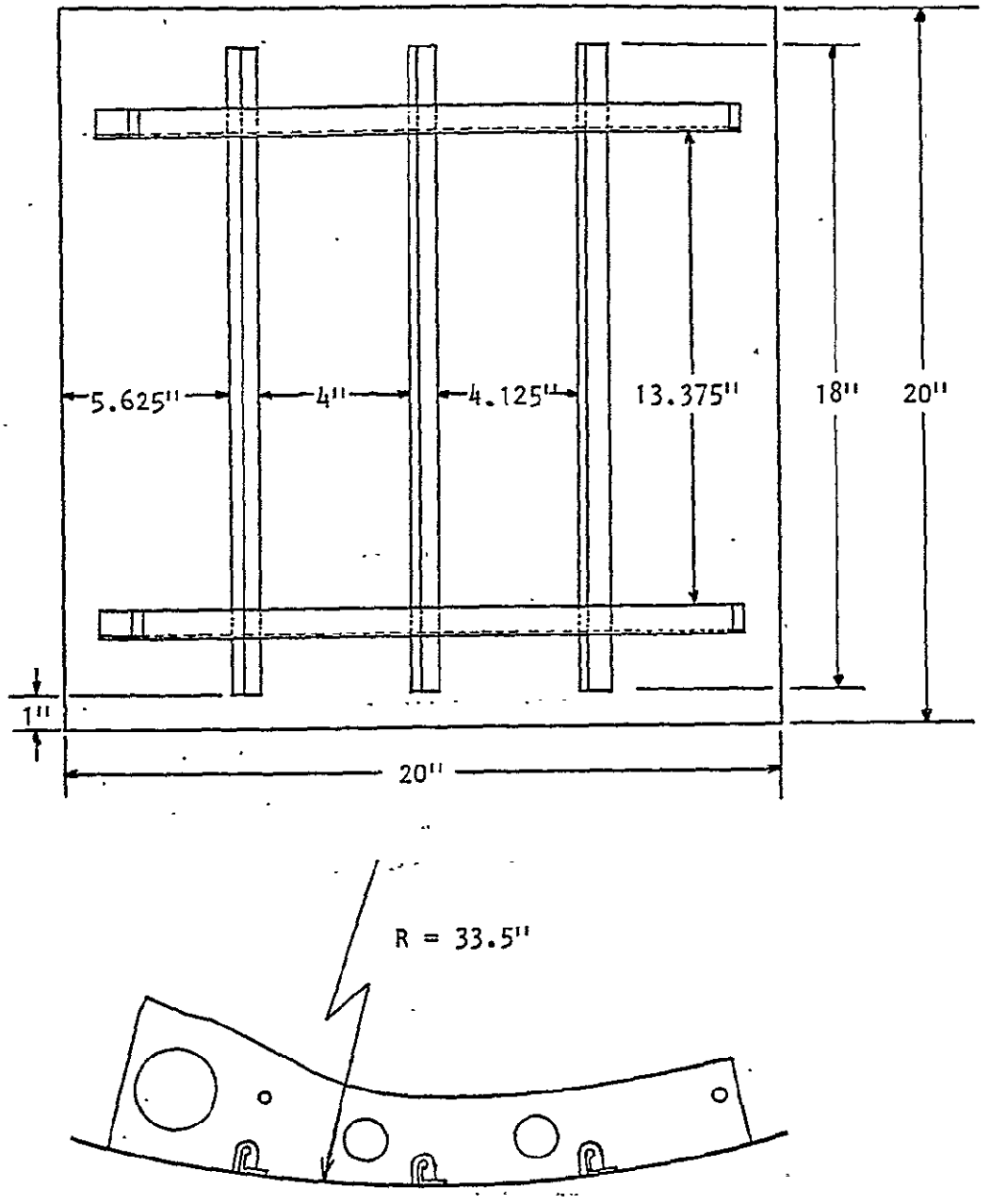

Figure 3.7: Curved Panel Dimensions

3.3.3 DAMPING TAPES

Three damping tapes were used in the investigations. They were Y-370, Y-434, and Y-436, manufactured by the 3M Company. They provided constrained layer damping. Y-434 has a 7.5-mil constraining layer, and Y-436 has 17-mil constraining layer. Y-370 is the commonly used damping tape in the general aviation industry. These tapes were self adhesive; and, as a result, application to the test specimen was easy. The tapes were applied in amounts of 30%, 60%, and 100% of the panel test area (18 inch by 18 inch). During tests with partial coverage, the application was limited to the central part of the test panel. This was in conformity with existing industry practices. The stringers and frames were not treated with damping tape. All tests were done at room temperature, as it was not possible to vary the temperature within the acoustic test facility. The damping properties of these materials will degrade when they are soaked in very low temperatures that can be expected in cruise conditions. The results of the present series should be considered in this context.

3.4 TEST RESULTS

Table 3.1 summarizes the variables considered in this series of tests. At least one noise reduction test was conducted for each combination of variables considered. These variables were chosen after consultation with the industry. As already explained, the tests were conducted only at room temperature. Tests with the sweep

Table 3.1: List of Variables Considered

Panels:

a. Flat, stiffened aluminum, thickness = .040" (.85 kg or 1.88 lb)
b. Curved, stiffened aluminum, thickness = .040" (1.09 kg or 1.240 lb)

Noise Source:

a. Sine wave sweep oscillator
b. Random Noise Generator

Depressurization, ΔP:

a. 0 psi
b. 1 psi
c. 2 psi
d. 2.5 or 3 psi

Damping Material:

a. Y-370
b. Y-434
c. Y-436

Percentage of Coverage:

a. 0% (Bare panel)
b. 30%
c. 60%
d. 100% (18" x 18" area)

oscillator were carried out in two steps to improve the resolution at low frequencies. In the first sweep, the frequency range from 20 to 500 Hz was covered. The effective bandwidth in this frequency range was three Hz. In the second sweep the frequency range from 500 to 5000 Hz was covered, with an effective bandwidth of 15 Hz. In both cases, the linear sweep time was 100 seconds. The analysis of tests with the random noise generator was also carried out with the two frequency ranges (500 and 5000 Hz) for the same reason. The random noise generator, however, produced a flat spectrum up to 20 kHz. From the narrow band analysis, the one-third octave analysis is done by energy-summing the narrow band levels within each one-third octave band. This was achieved through a computer program. The results of the individual tests are published in Reference 7. A typical output is given in Figure 3.8. The result obtained from the test facility is the noise reduction as a function of frequency. It is a continuous curve from 20 Hz to 500 Hz and from 500 Hz to 5000 Hz. In the subsequent sections, however, the effect of various parameters on the result obtained will be discussed only at two frequency values, one from the low-frequency region (stiffness-controlled region) and the other from the high-frequency region (mass-controlled region). These results are representative for these regions. Previous tests at this facility have also confirmed these trends (References 4, 5, and 7).

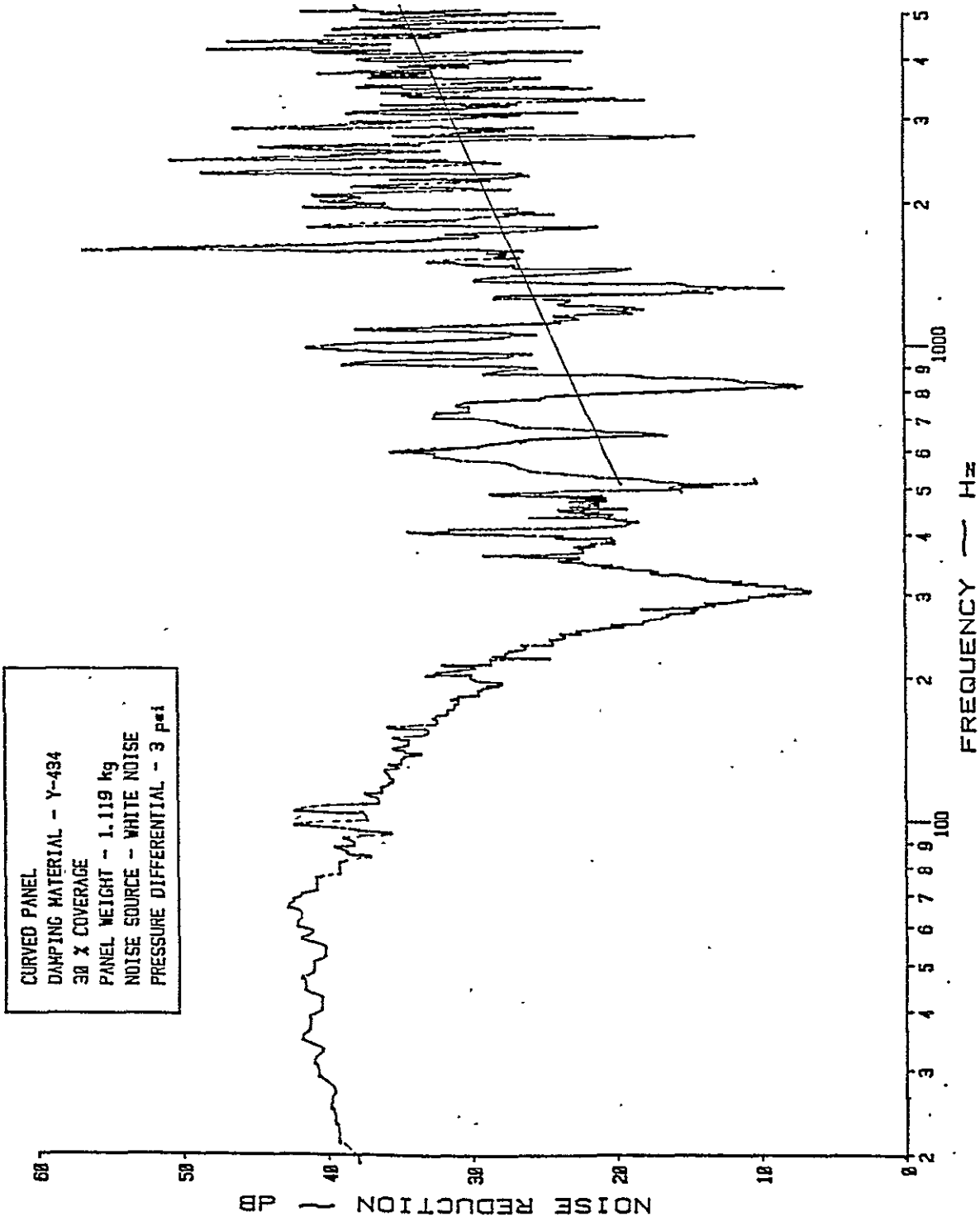

Figure 3.8: A Typical Output

3.4.1 EFFECT OF NOISE SOURCE

The test results of both excitations matched within the experimental scatter (±2 dB) in the low-frequency region. In the high frequency region, due to the resonance peaks and dips, it was not possible to identify the scatter for individual filter location. However, the least-square values of the results were within the ± 2dB. These results are consistent with the earlier test results with the unstiffened panels. For all the cases considered--i.e., stiffened and depressurized panels--no significant differences exist in the results between these two noise excitations.

3.5 NOISE REDUCTION CHARACTERISTICS OF BARE FLAT AND CURVED PANELS

3.5.1 FLAT PANEL

Before the application of damping treatment, the noise reduction characteristics of the bare panels were investigated. Earlier studies had indicated that depressurization increases the low-frequency noise reduction by the stiffening effect (Reference 4). The purpose, in this case, was to study the extent of the gain in noise reduction that can be obtained by a pressure differential in an already stiffened structure. In all cases the pressure on the source side was reduced to simulate the actual aircraft conditions. Depressurization of up to three psi differential was investigated. The effect of depressurization is easily seen by

studying the variation at two selected frequency values, 100 and 3000 Hz. The frequency value of 100 Hz is within the stiffness-controlled region, and 3000 Hz is in the mass-controlled region. The effect of depressurization of the flat panel is similar to that of the unstiffened panel (see Reference 4). The maximum increase in the noise reduction occurs in the first one psi, and after that the effect is minimal (Figure 3.9). At 100 Hz, the noise reduction increased from 17 dB to 28 dB for the first one psi and increased only by three dB for the next two psi pressure differential. Compared to the unstiffened panel (see Reference 4), these results are not impressive. This is because the panel is already stiffened, and hence the increase in stiffness is not proportionally high. This can be seen from the resonance frequency. The depressurization increases the stiffness without varying the mass, and hence the resonance frequency should increase (Figure 3.10). In this case the increase is from 120 Hz to 230 Hz. As can be seen from Figure 3.10, this increase in the resonance frequency directly translates into higher noise reduction in the stiffness-controlled region. At 3000 Hz, there is a slight decrease in noise reduction with increase in pressure differential. This result is in variance with the earlier results for the unstiffened panel (Reference 4), where it was reported that it remained the same. However, the present results confirm the published theoretical results by Koval (Reference 8), which reported a decrease of up to three dB.

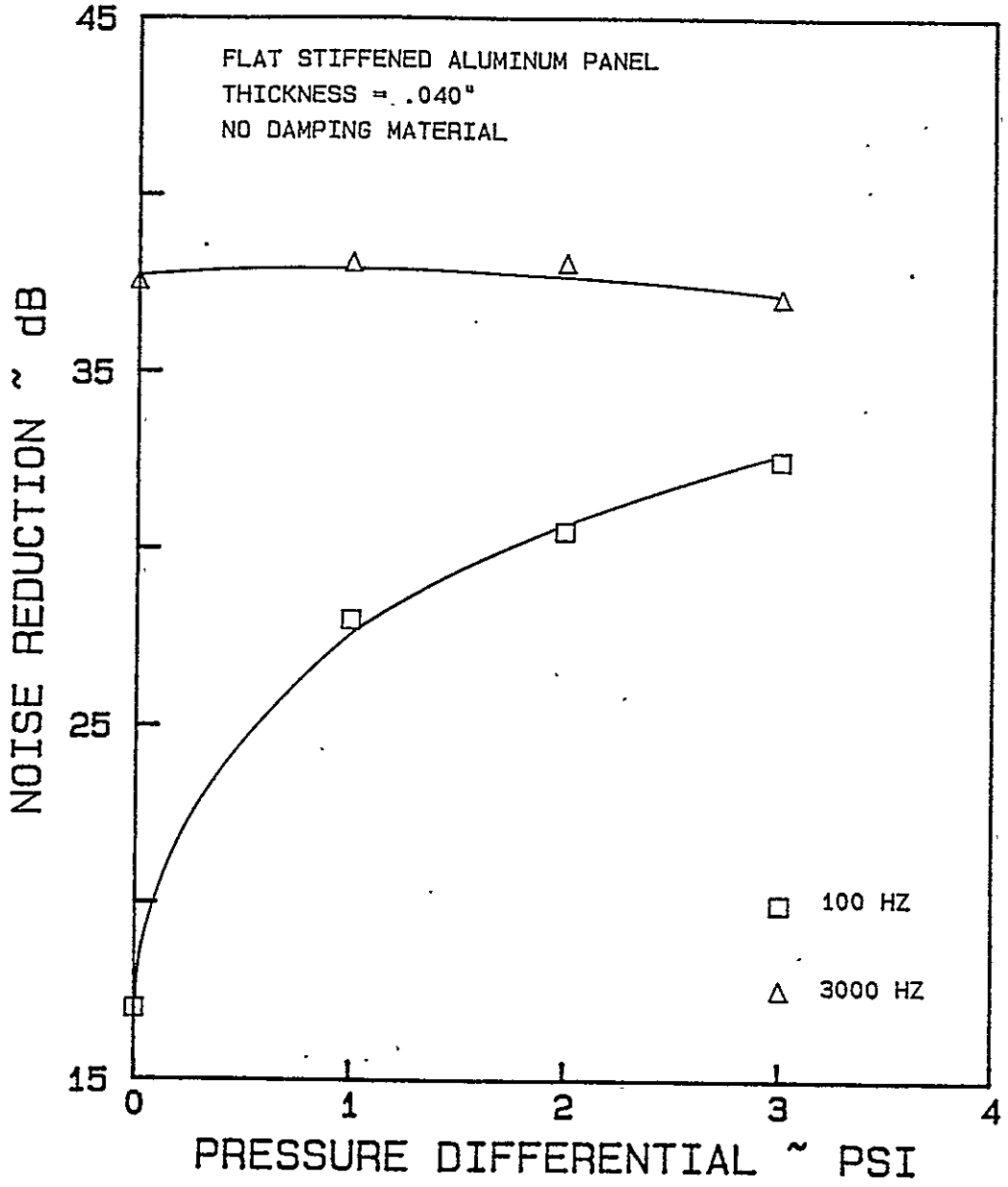

Figure 3.9: Effect of Pressure Differential on Noise Reduction Characteristics of a Bare, Flat Panel

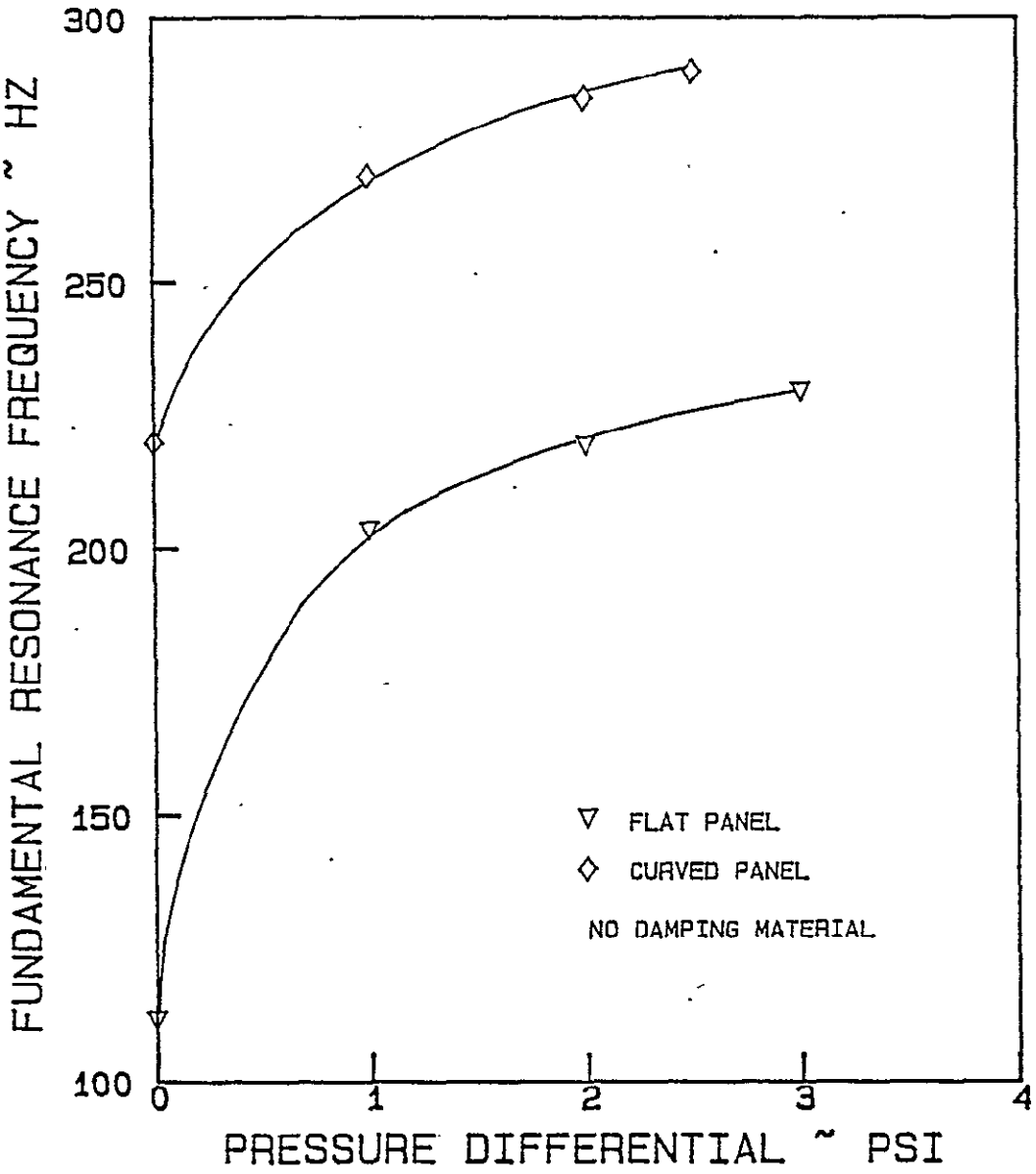

Figure 3.10: Effect of Pressure Differential on the Fundamental Resonance Frequency for Flat and Curved, Stiffened Panels

3.5.2 CURVED PANEL

Earlier experimental investigation on curved, unstiffened panels (Reference 4) indicates that the low-frequency noise reduction of the unstiffened, curved panel increases up to a certain value and then decreases. Curving a panel stiffens the panel and also changes the angle of incidence of the panel. Stiffening of the panel increases low-frequency noise reduction. The low-frequency noise reduction decreases when the angle of incidence is not normal. The combination of these two effects determines the final low-frequency noise reduction. During these tests, the effect of radius of curvature was not investigated. Only one radius (33.5 inches) was used.

The results of the tests with the curved panel confirm the trend observed with the bare, flat panel. A plot of noise reduction at 100 and 3000 Hz is given in Figure 3.11 as a function of pressure differential. As the panel is already stiffened, due to the stiffeners as well as the curvature, the noise reduction at 100 Hz is higher compared to the flat panel tested: 30 dB as opposed to 17 dB for the flat panel. But the additional increase in noise reduction due to pressurization was smaller, as can be seen from Figure 3.11. This can be attributed to the initial high stiffness of the panel. Without any damping treatment it can be concluded that the increase in noise reduction due to pressurization is much smaller in an already stiffened structure than in an unstiffened structure. The same conclusions can be drawn from the measured

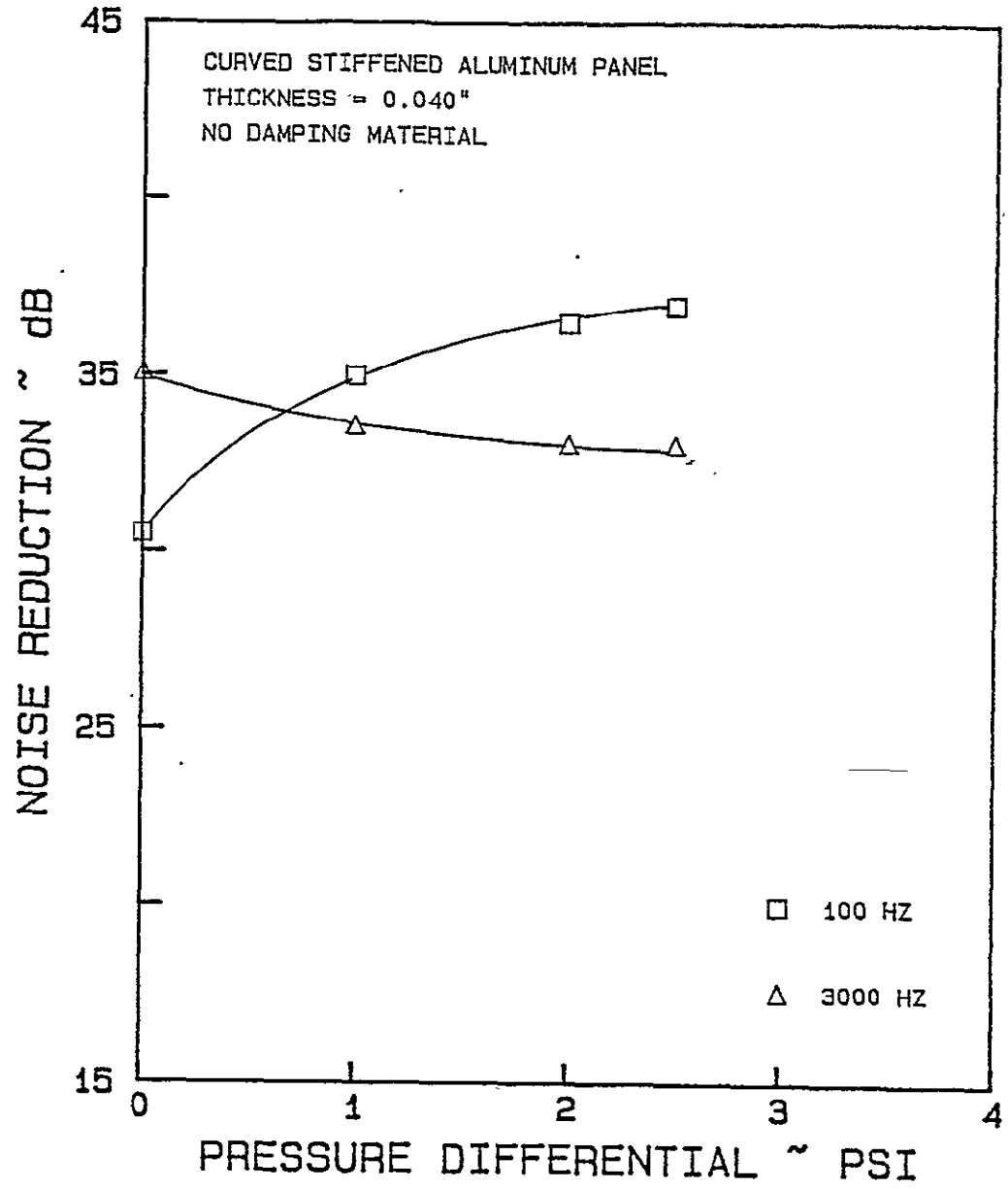

Figure 3.11: Effect of Pressure Differential on Noise Reduction Characteristics of a Bare, Curved Panel

fundamental frequency of the panel, as shown in Figure 3.10. The resonance frequency increases 220 Hz to 295 Hz for 2.5 psi pressure differential. Once again the major increase occurs during the first one psi pressure differential. In the mass-law (or high-frequency) region, the decrease in noise reduction due to depressurization is slightly more pronounced in the curved panel than in the flat panel. This result is also in conformity with the theoretical results published in Reference 8.

3.6 Y-370 DAMPING MATERIAL

3.6.1 FLAT PANEL

The effect of Y-370 damping material on the flat, stiffened panel has been discussed in Reference 5. Y-370 was found to decrease the fundamental resonance frequency and the noise reduction values in the stiffness-controlled region. But the noise reduction at the resonance frequency was higher. Also the effect of the damping tape in the high frequency region was to smooth out the peaks and dips in the noise reduction curve and also to increase the noise reduction due to the increased mass of the damping tape (Reference 5). During the present tests, the effects of depressurization and partial application of the damping tape were investigated, with the purpose of verifying those trends.

The effect of partial treatment of the damping material on the noise reduction characteristics of the flat test panel are given in

Figure 3.12. At low frequencies (~100 Hz), the effect of partial coverage on the noise reduction characteristics of the flat panel is negligible. Except for the initial 30% application, there is no effect in the low frequency noise reduction by the Y-370 damping treatment. Even the increase at 30% is noticed only at 0 psi. Hence, this is considered to be an experimental error. At other pressure differentials, no gain is achieved in the sound transmission loss of airborne noise excitation, with the appliction of the damping tape. In the high frequency region (shown in Figure 3.12 for 3000 Hz), there is an increase in the noise reduction due to the additional damping tape. This increase occurs at all the pressure differentials tested. As observed in Reference 5, the increase is due to the increased mass of damping tape.

The effect of depressurization on the noise reduction characteristics of panels treated with Y-370 damping tape is shown in Figure 3.13 at 100 and 3000 Hz. The noise reduction values are shown for three areas of treatment: 30%, 60%, and 100%. Also shown in the same figure are the noise reduction values for panels without any treatment. At 100 Hz, the effect of depressurization on the noise reduction values of the treated panel is similar to that of the untreated panel. The increase in noise reduction is more pronounced during the first one psi than at any other time. At higher pressure differentials, the effect of treatment is negligible. In the high frequency region (Figure 3.13), the untreated flat panel shows nearly constant noise reduction values at

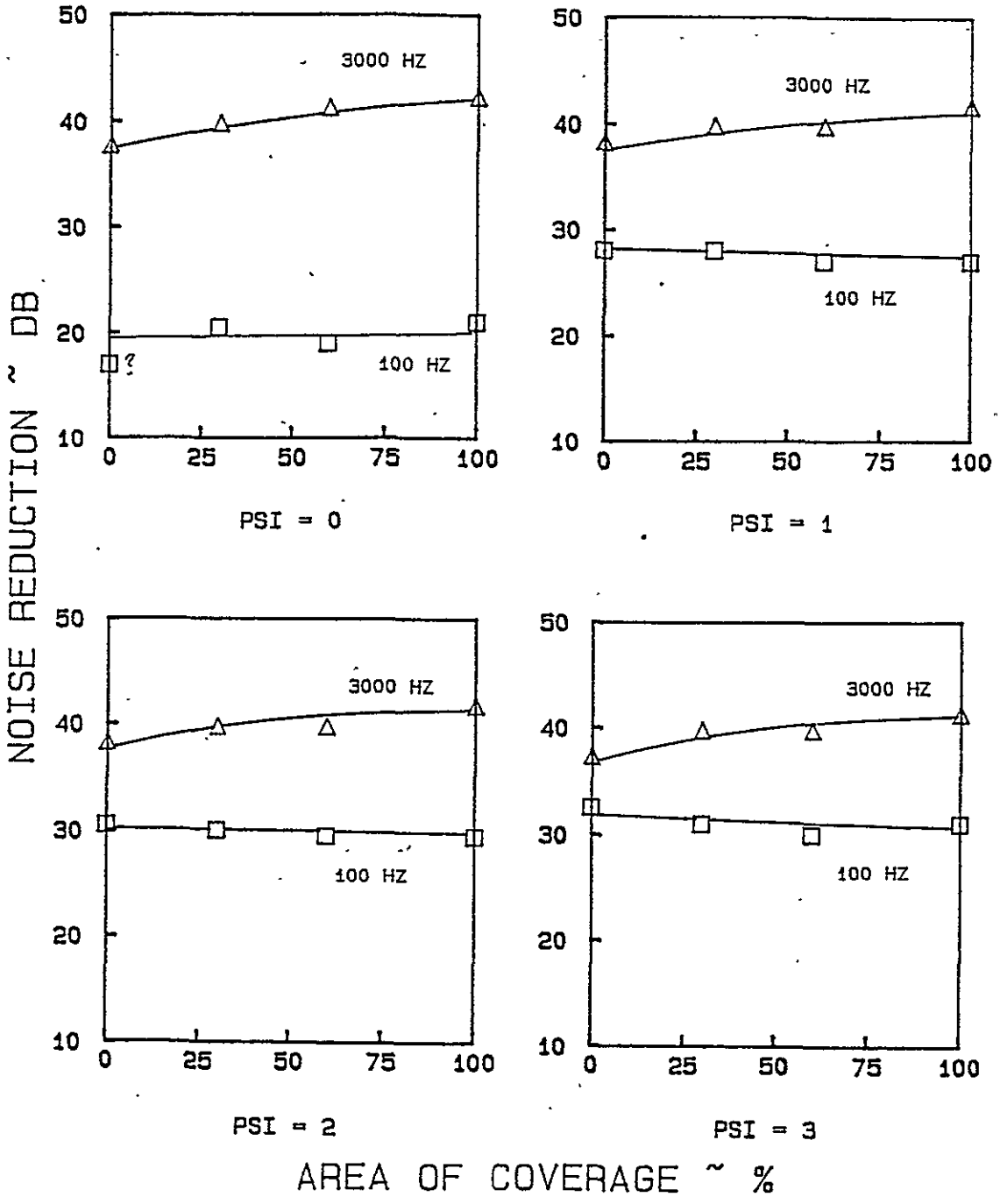

Figure 3.12: Effect of Coverage of Y-370 Damping Tape on Noise Reduction Characteristics of a Flat, Stiffened Panel at Different Pressure Differentials

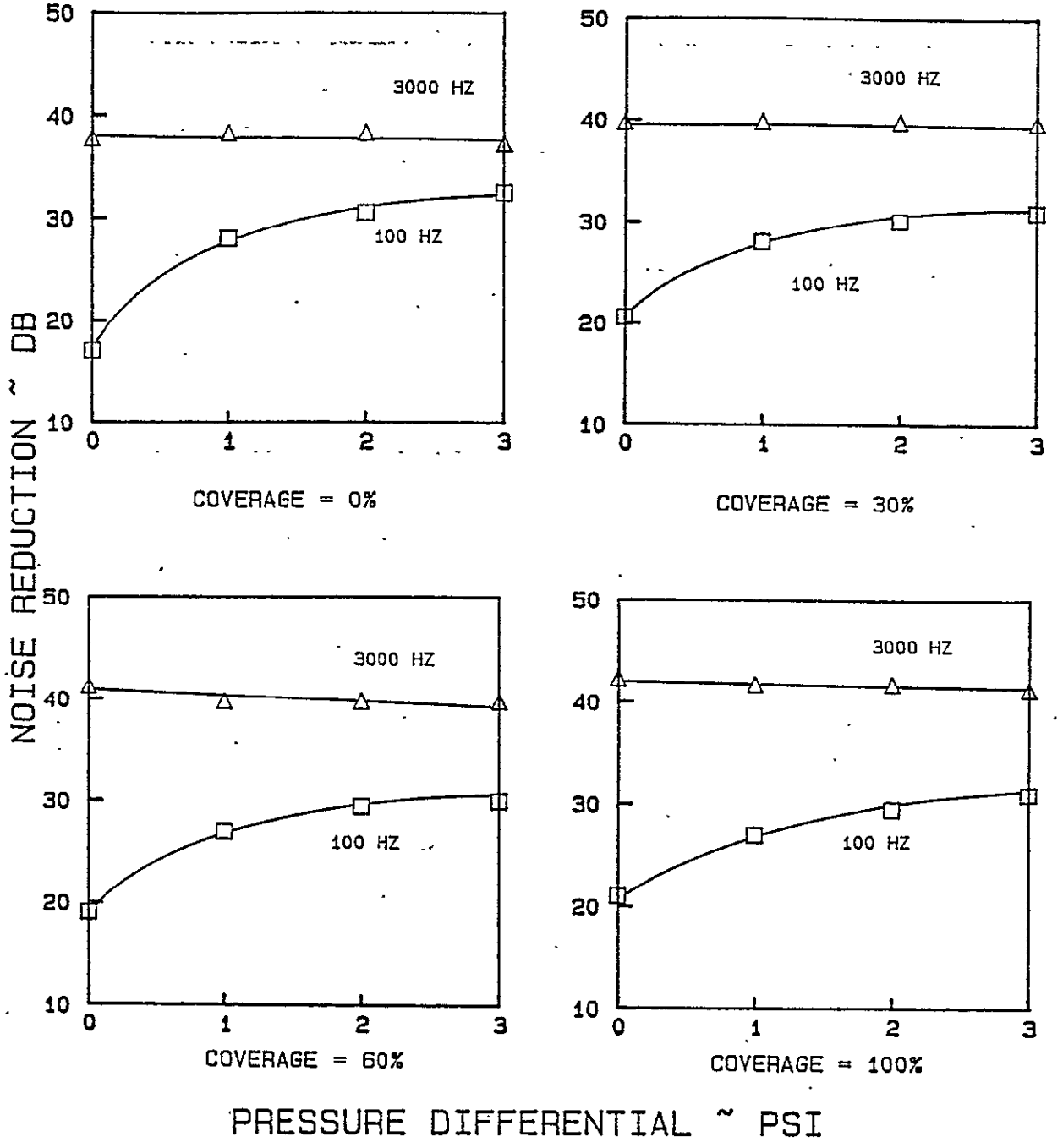

Figure 3.13: Effect of Pressure Differential on Noise Reduction Characteristics of a Flat, Stiffened Panel with Y-370 Damping Tape

all pressure differentials. However, with the application of the treatment, there is a slight decrease (2-3 dB) in the noise reduction as the pressure differential is increased. These decreases are of two to three dB.

The effect of depressurization on the fundamental resonance frequency is given in Figure 3.14. In all areas of treatment tested, the resonance frequency increases with an increase in pressure differential. This increase is more pronounced when the area of application is smaller. This effect can be attributed to the increased mass of damping treatment.

3.6.2 CURVED PANEL

Tests similar to those described in Section 3.6.1 were carried out with the curved panel. The parameters were maintained nearly the same to make one-to-one comparison between the flat and the curved panel. As already explained, all tests were performed with both swept and random noise as excitation sources. The differences between the results obtained from these two excitation sources were still within the experimental accuracy of the test facility.

The trends of results obtained with the curved panel are similar to the results obtained with the flat panel. The noise reduction values as a function of the area of coverage are given in Figure 3.15 for 100 and 3000 Hz. As the stiffness of the curved panel is already high, the low-frequency noise reduction is higher than that of the flat panel. It remains constant up to 60%

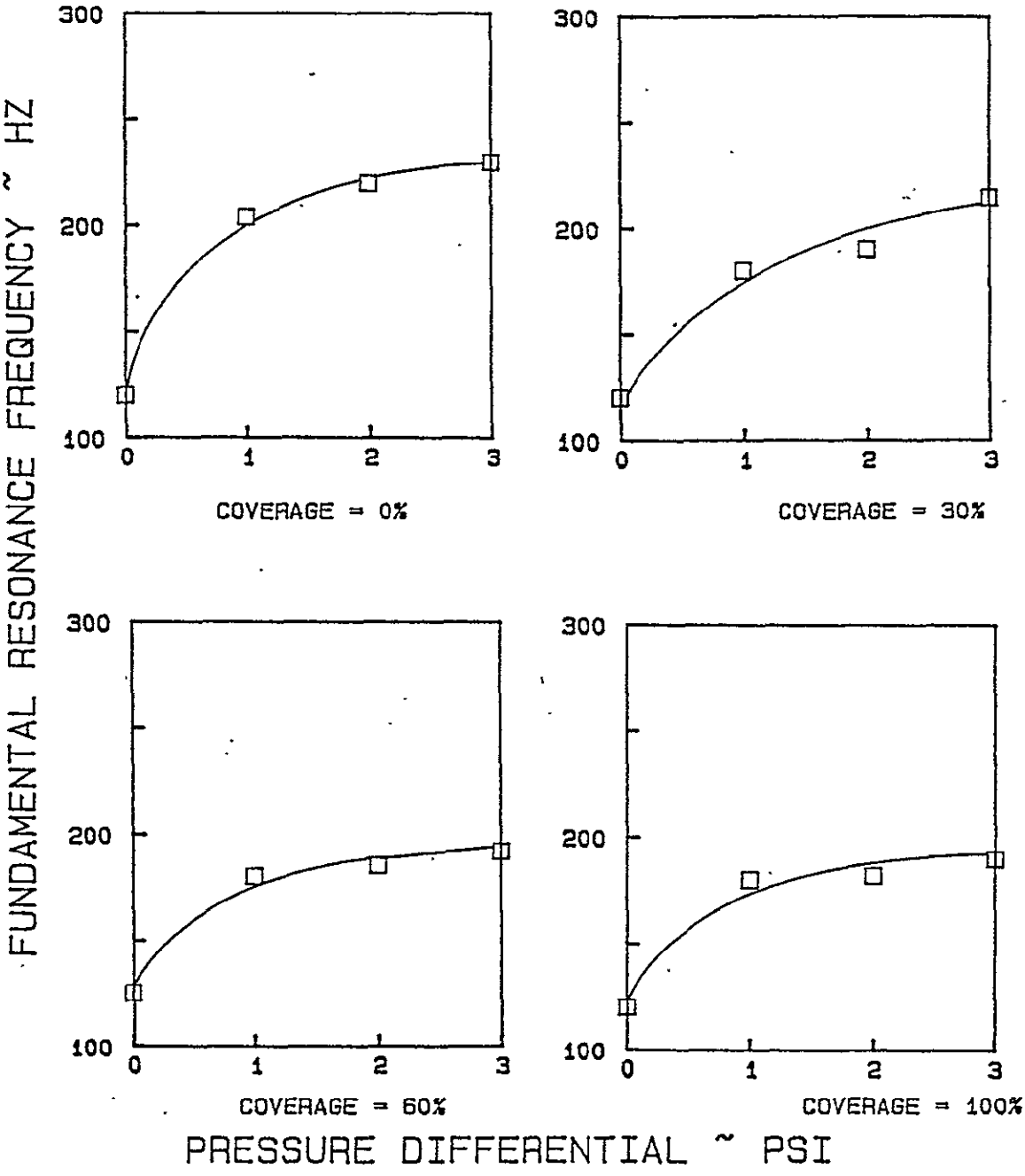

Figure 3.14: Effect of Pressure Differential on the Fundamental Resonance Frequency of a Flat, Stiffened Panel with Y-370 Damping Tape

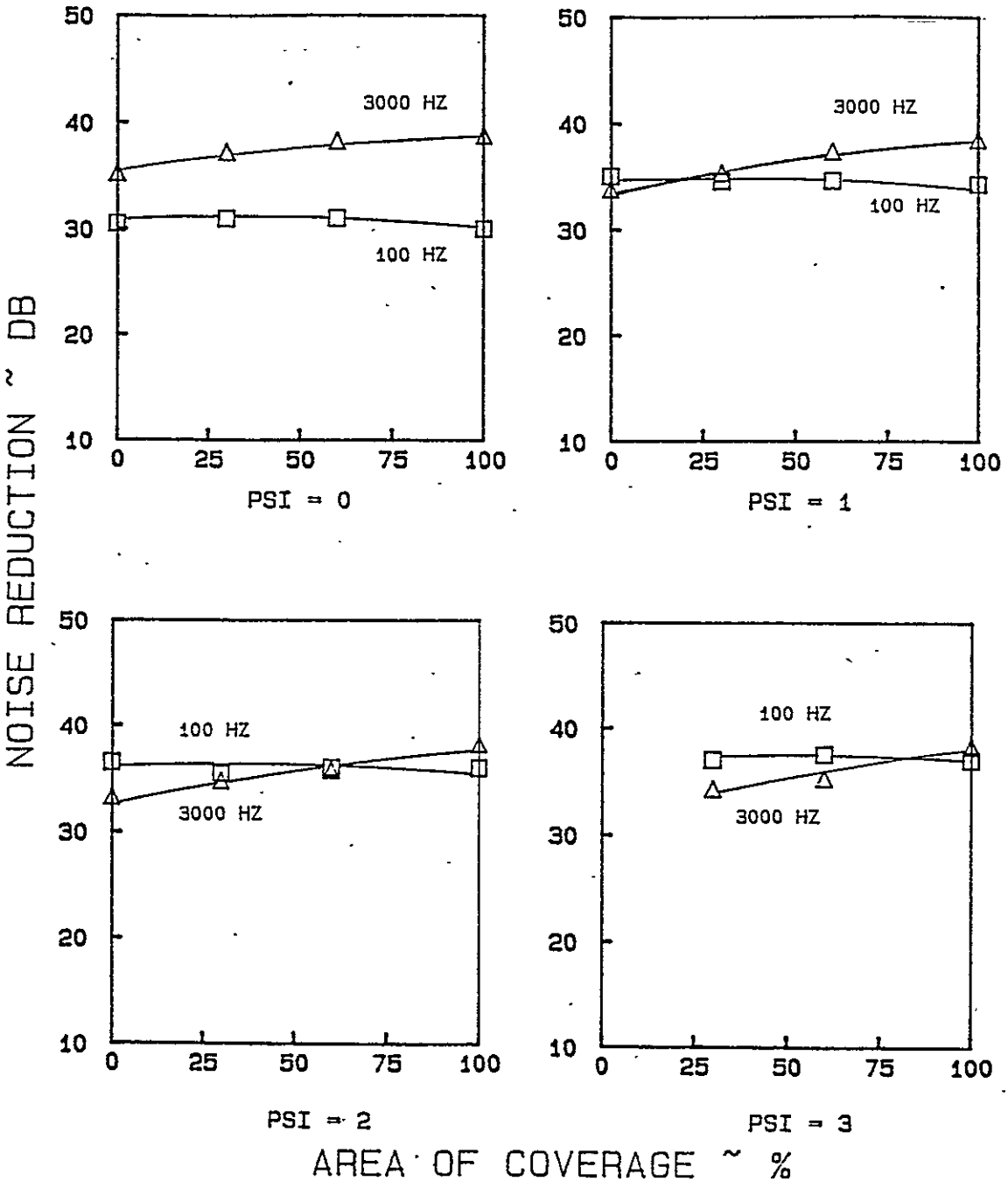

Figure 3.15: Effect of Coverage of Y-370 Damping Tape on Noise Reduction Characteristics of a Curved, Stiffened Panel at Different Pressure Differentials

treatment and thereafter shows one to two dB decrease. In the high-frequency region at 3000 Hz there is a gradual increase in the noise reduction as the area of application is increased. This increase is similar to the one observed with the flat panel.

Figure 3.16 shows the noise reduction values as a function of the pressure differential. The effect of pressurization with the Y-370 damping treatment is similar to that without the treatment. With the curved panel the increase in low-frequency noise reduction is smaller; i.e., 30 dB to 37 dB. In the high-frequency region, the decrease in the noise reduction values observed without the treatment becomes less and less severe as the area of application is increased.

The measured resonance frequency as a function of the pressure differential is shown in Figure 3.17. As with the flat panel, pressurization stiffens the panels and increases the resonance frequency. For example, the resonance increases from 195 Hz to 260 Hz when the pressure differential increases from zero to three psi with 100% treatment. However, at a given pressure differential, increasing the area of application decreases the fundamental resonance frequency. For example, at two psi the resonance frequency decreases by 30 Hz from 285 Hz without the treatment to 255 with the treatment. This also confirms the experimental results of Reference 5 where it was found that the Y-370 material does not increase the stiffness. Addition of mass alone decreases the resonance frequency.

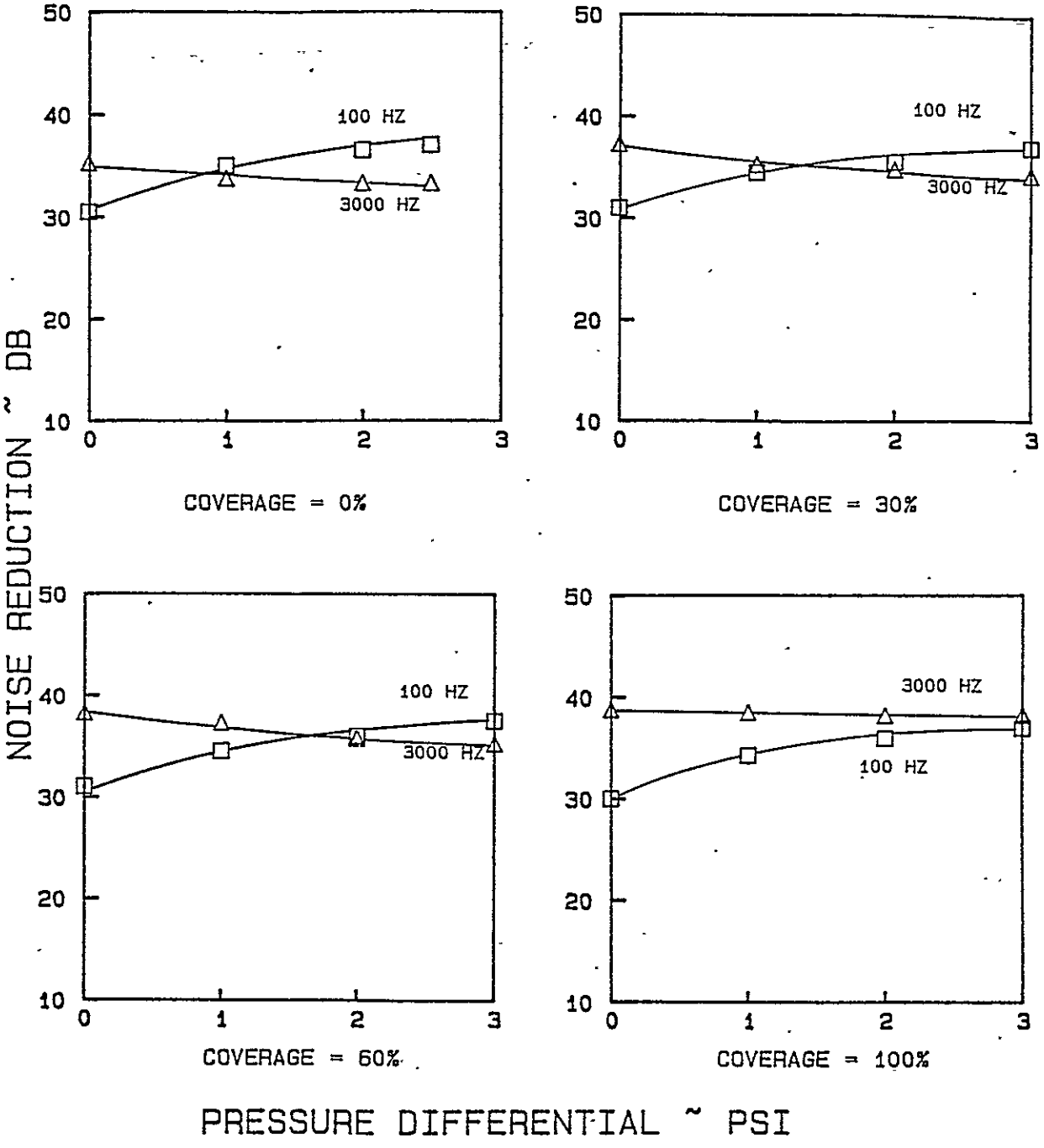

Figure 3.16: Effect of Pressure Differential on Noise Reduction Characteristics of a Curved, Stiffened Panel with Y-370 Damping Tape

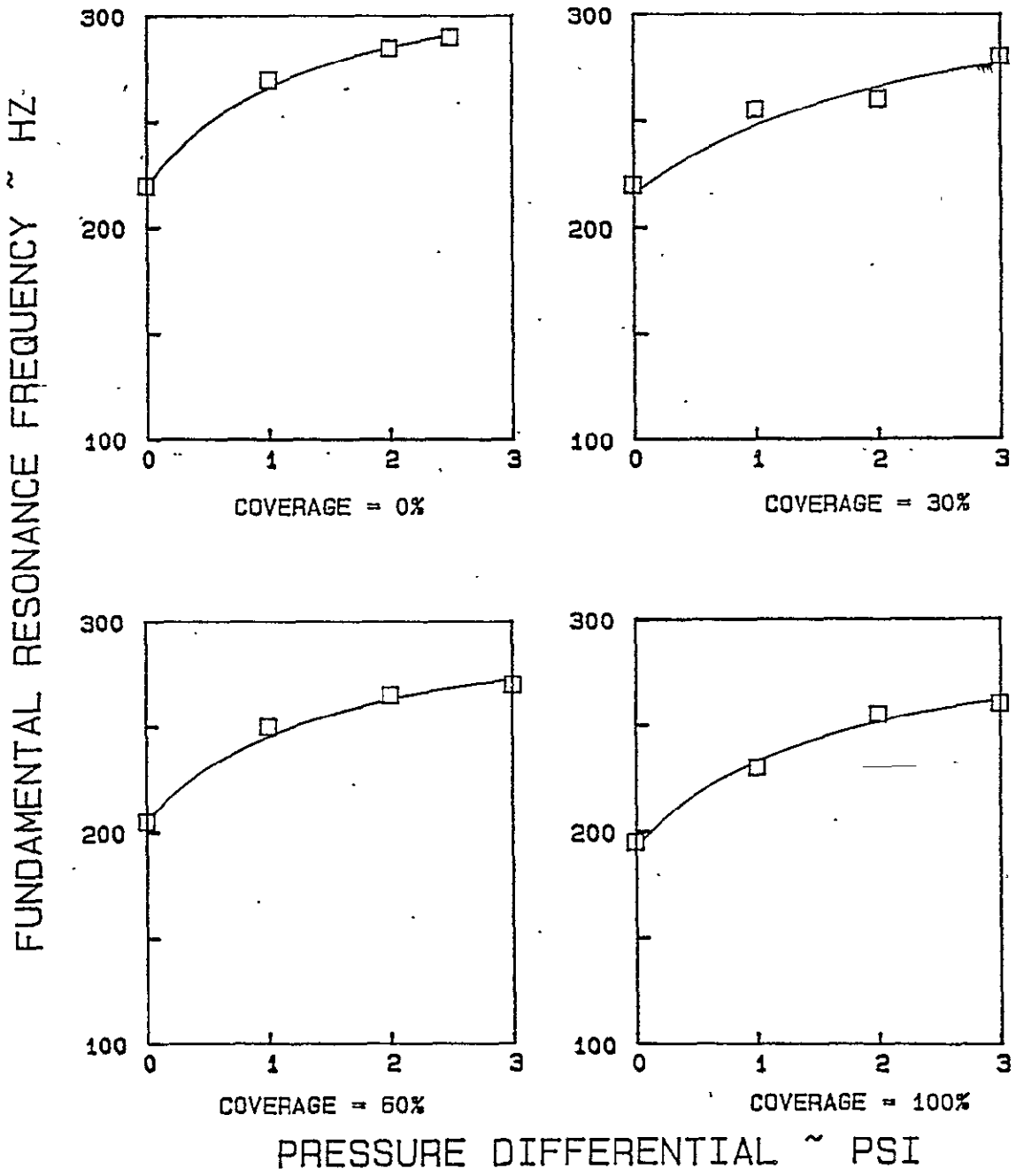

Figure 3.17: Effect of Pressure Differential on the Fundamental Resonance Frequency of a Curved, Stiffened Panel with Y-370 Damping Tape

3.7 Y-434 DAMPING MATERIAL

Y-434 damping tape has a seven-mil constraining aluminum layer. But it does not contain the foam material present in the Y-370 material. The purpose of these tests is to compare the sound transmission loss characteistics of panels with this damping material with those of Y-370. Y-434 material is the lightest of the three damping materials tested. The parameters investigated were the same as for damping tape Y-370: four pressure differentials (0, 1, 2, and 3 psi), two types of noise sources (white noise, and swept sine), and three different areas of coverage (30%, 60%, and 100%). The results of these tests are also given in Reference 9.

3.7.1 FLAT PANEL

The effect of Y-434 material is very similar to that of Y-370 material. Once again, because the difference in the results obtained with sweep oscillators and random noise generator were negligible, the results will be valid for both types of excitations.

The effect of partial treatment of the Y-434 damping material on the noise reduction characteristics of the flat panel are given in Figure 3.18. At low frequencies, the effect of the area of treatment on the noise reduction is small. These results are similar to the results with the Y-370 damping tape. In the high frequency region, the increase due to the treatment is smaller because the Y-434 material is lighter. The weight of Y-434 material

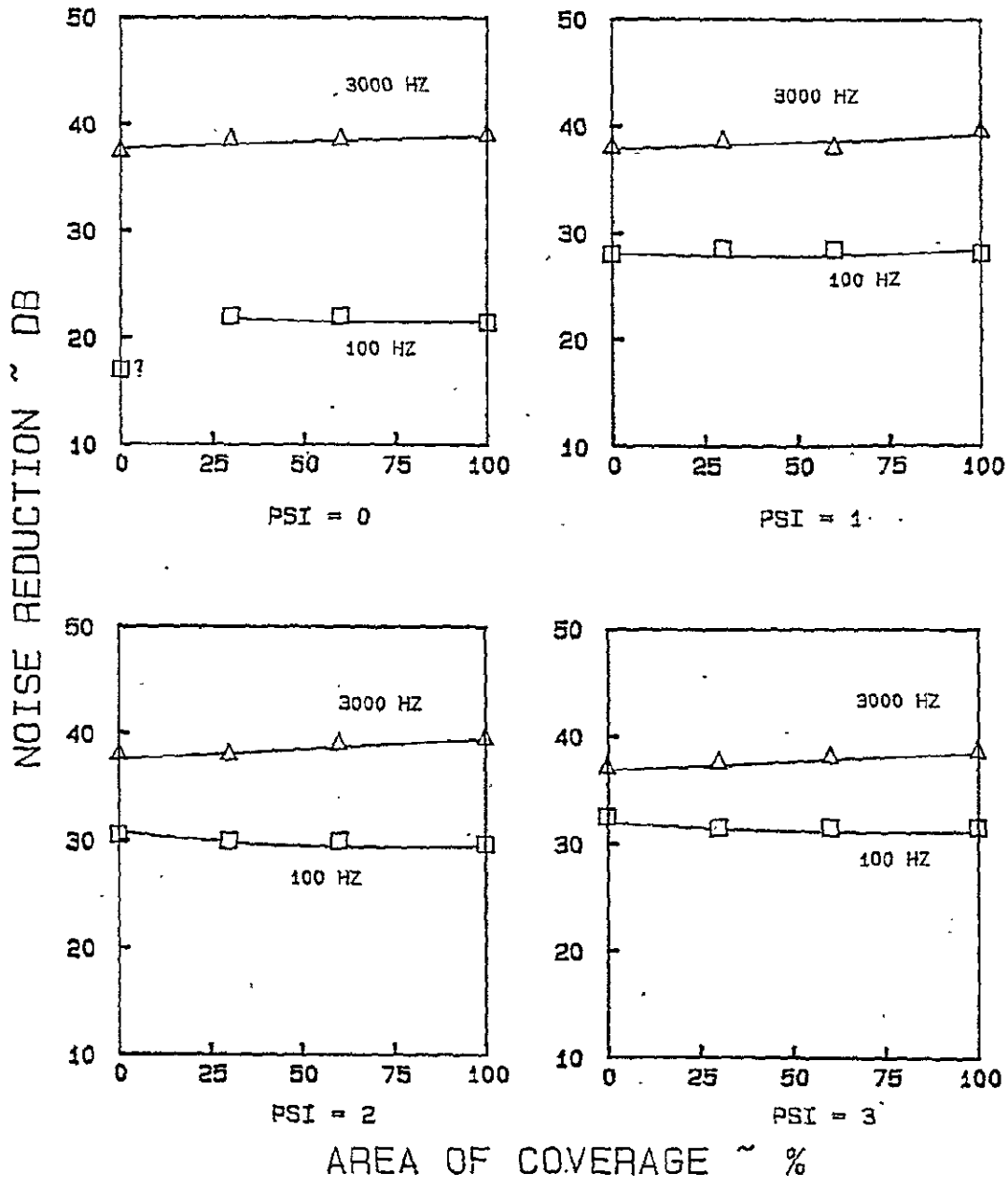

Figure 3.18: Effect of Coverage of Y-434 Damping Tape on the Noise Reduction Charactristics of a Flat, Stiffened Panel at Different Pressure Differentials

for 18" x 18" treatment is 0.2 lbs, while that of Y-370 is 0.62 lbs. In this case the increase in mass is smaller; hence the increase in noise reduction due to this effect is also smaller.

The effect of depressurization is given in Figure 3.19. If a constraining layer is attached atop the damping material, then bending of the composite produces not only bending and extensional strains in all three layers, but also shear, primarily of the middle (damping) layer. The shear-strain energy storage tends to dominate the damping action of constrained damping layers (Reference 9). The action also increases the stiffness of the panel. Because of this increase in stiffnes, the noise reduction in the stiffness-controlled region is higher (1-2 dB) at zero psi. However, with increase in pressure differential, this increase vanishes. At high frequency, the results are very similar to Y-370 material.

The cross plot of the resonance frequency vs pressure—differential is given in Figure 3.20. The resonance frequency in fact slightly increases at zero psi, indicating that the stiffness effects of the tape are more predominant than the mass effects. However, at three psi, the mass effects overshadow the stiffness effects.

3.7.2 CURVED PANEL

Similar cross plots for curved panel with Y-434 are given in Figures 3.21-3.23. The results are very similar to Y-370 treatments. The only noticeable difference is in the resonance

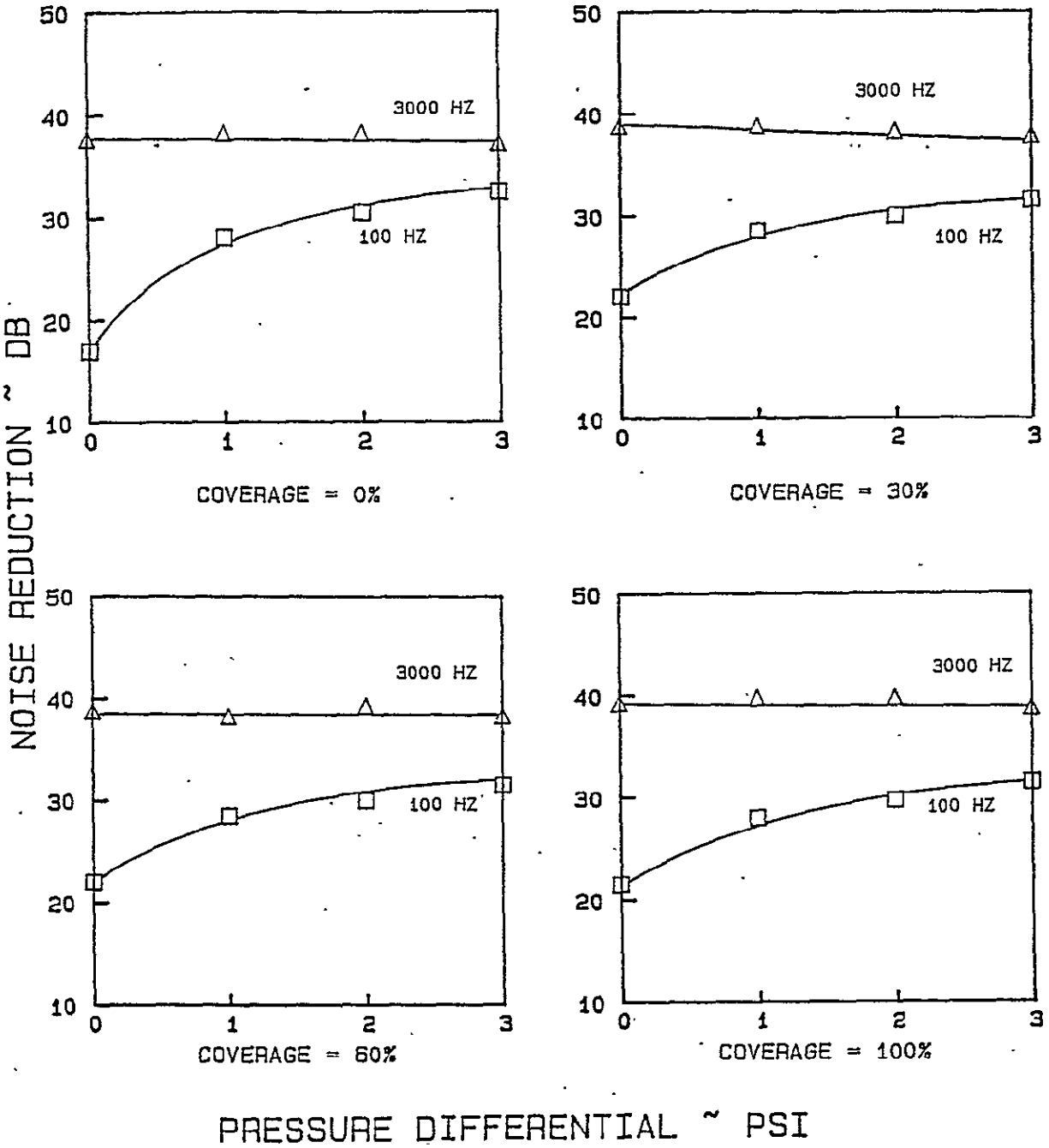

Figure 3.19: Effect of Pressure Differential on Noise Reduction Characteristics of a Flat, Stiffened Panel with Y-434 Damping Tape

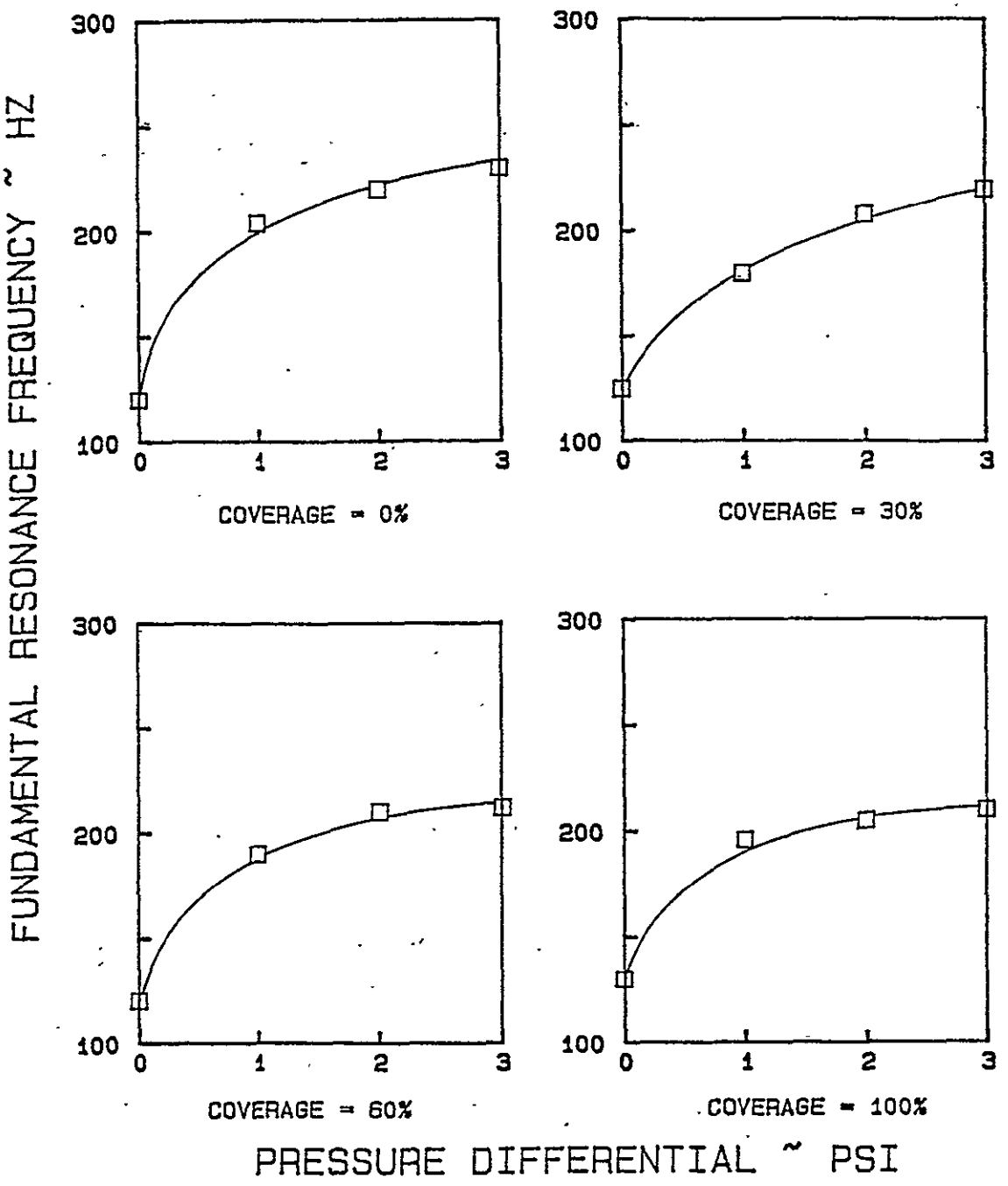

Figure 3.20: Effect of Pressure Differential on the Fundamental Resonance Frequency of a Flat, Stiffened Panel with Y-434 Damping Tape

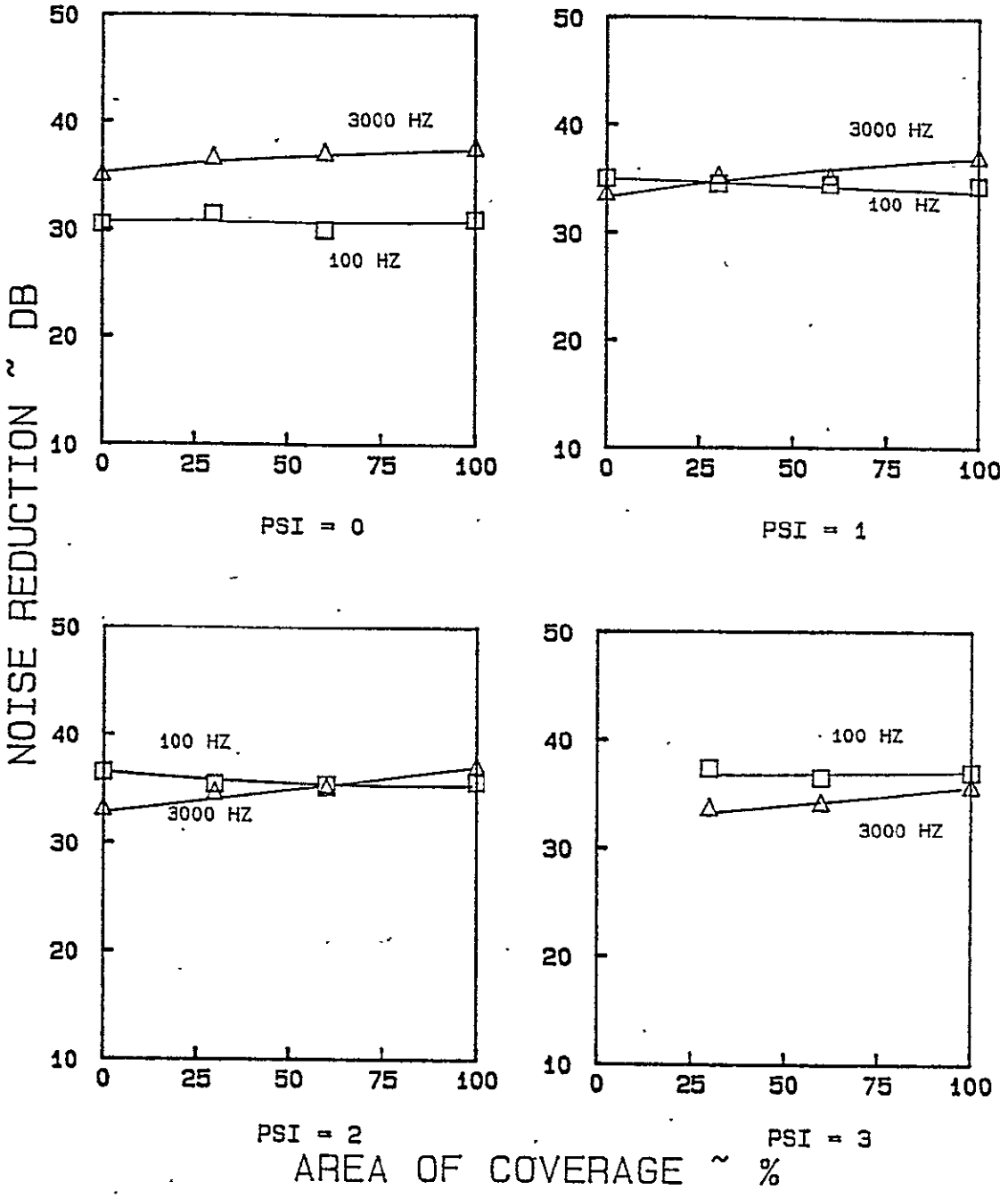

Figure 3.21: Effect of Coverage of Y-434 Damping Tape on the Noise Reduction Characteristics of a Curved, Stiffened Panel at Different Pressure Differentials

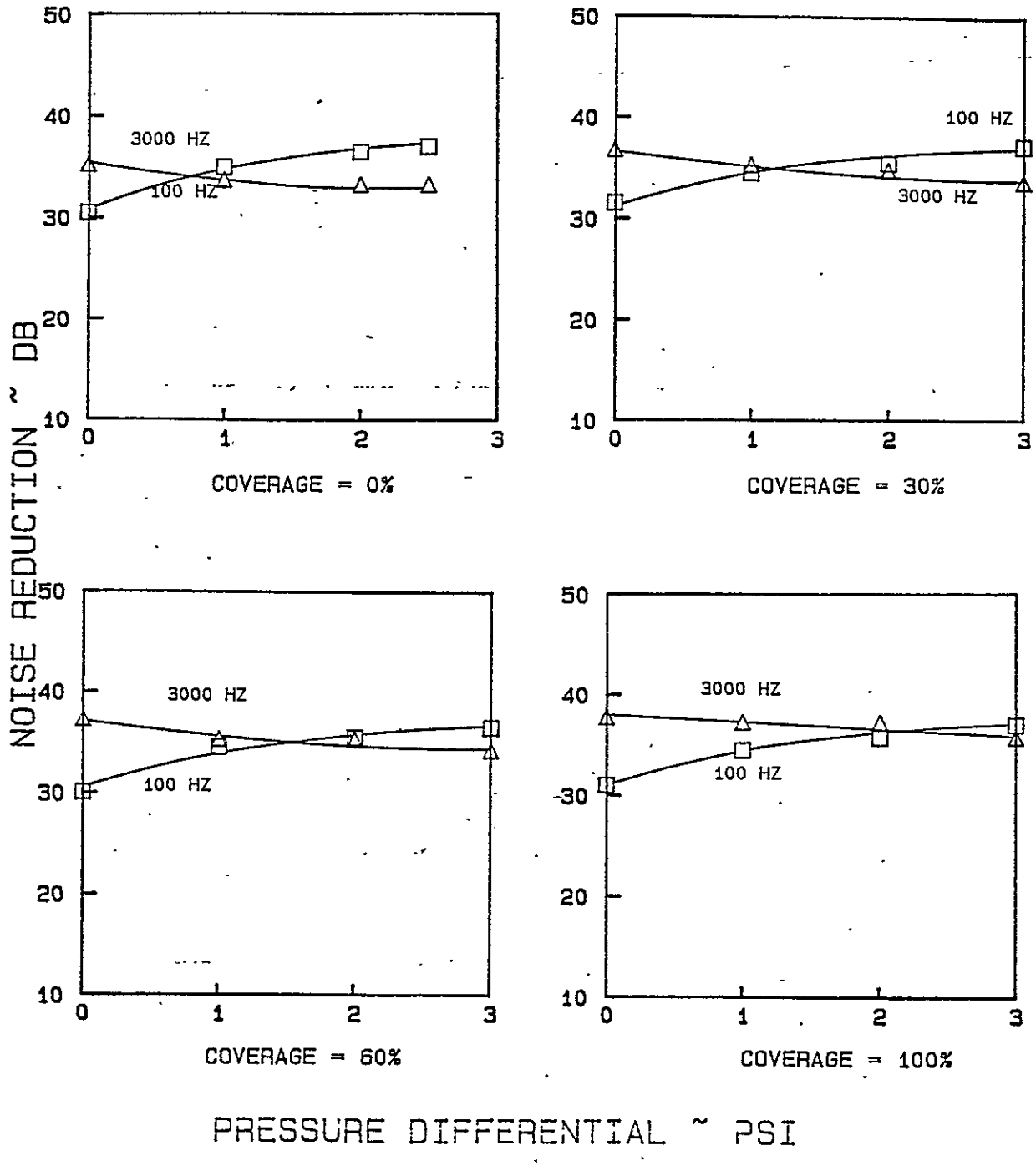

Figure 3.22: Effect of Pressure Differential on Noise Reduction Characteristics of a Curved, Stiffened Panel with Y-434 Damping Tape

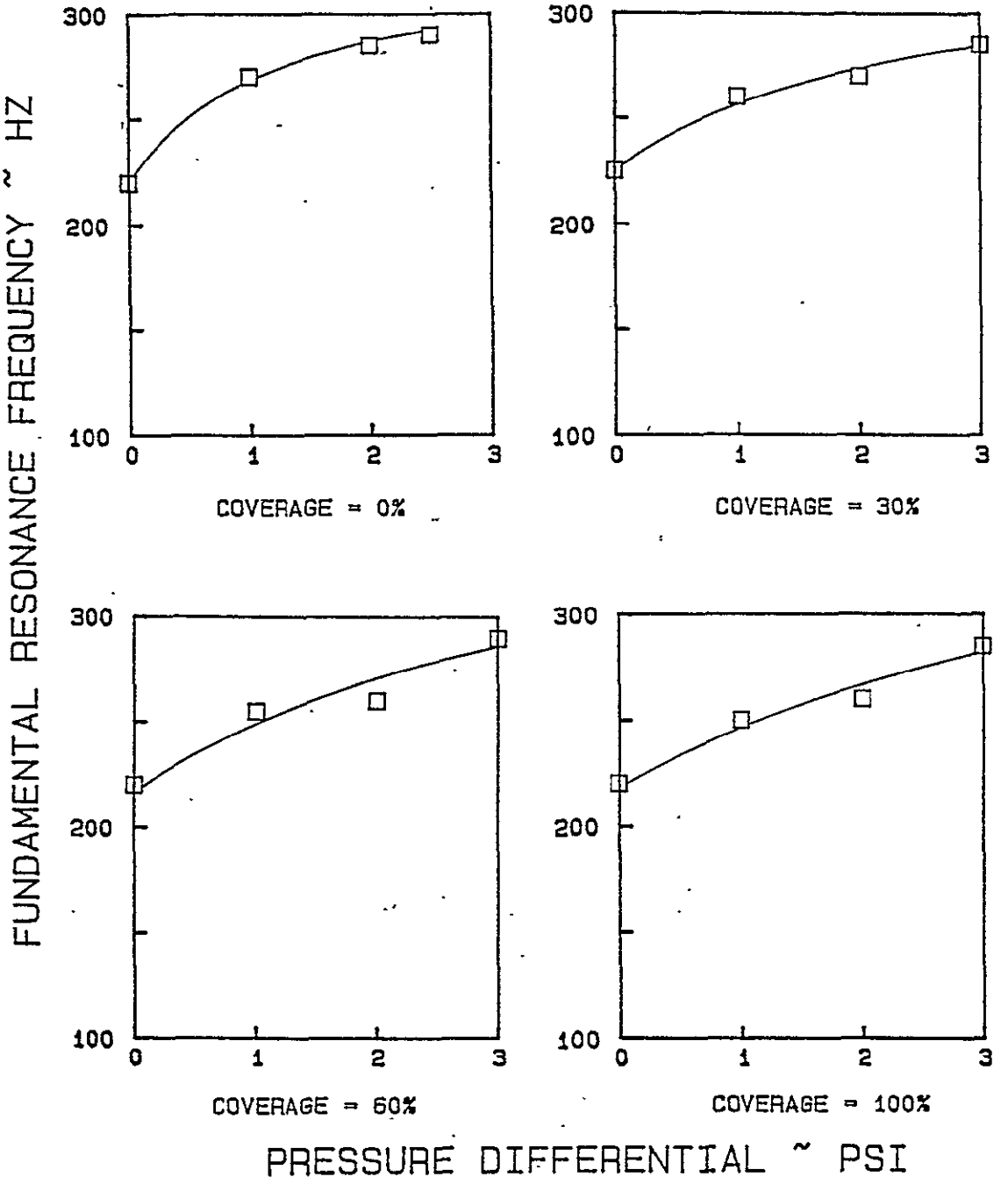

Figure 3.23: Effect of Pressure Differential on the Fundamental Resonance Frequency of a Curved, Stiffened Panel with Y-434 Damping Tape

frequency vs pressure differential (Figure 3.23). With Y-370 damping tape, the resonance frequency tends to flatten at high pressure differential, while with Y-434 material the resonance frequency continues to increase even at three psi differential.

3.8 Y-436 DAMPING MATERIAL

Y-436 damping material has 17 mil constraining layer. Otherwise it is similar to Y-434. The full application of Y-436 material weighed 0.4 lbs, as opposed to 0.62 lb for Y-370 and 0.2 lb for Y-434. The parameters varied during this investigation were essentially the same: four pressure differentials (0, 1, 2, and 3), two types of noise sources, and three different coverages (30%, 60%, and 100%).

3.8.1 FLAT PANEL

The cross plots at 100 and 3000 Hz are shown in Figures 3.24, 3.25, and 3.26. The trends of the curves are very similar to the trends observed with the flat panel with Y-370 damping tape. In the high frequency region, the increase in the noise reduction (Figure 3.24) is higher because of the higher mass of Y-436 compared to Y-434. The effect of pressurization on the high frequency noise reduction on flat panels with Y-370 and Y-434 is to decrease slightly (Figure 3.13 and 3.19). But with the Y-436 material this

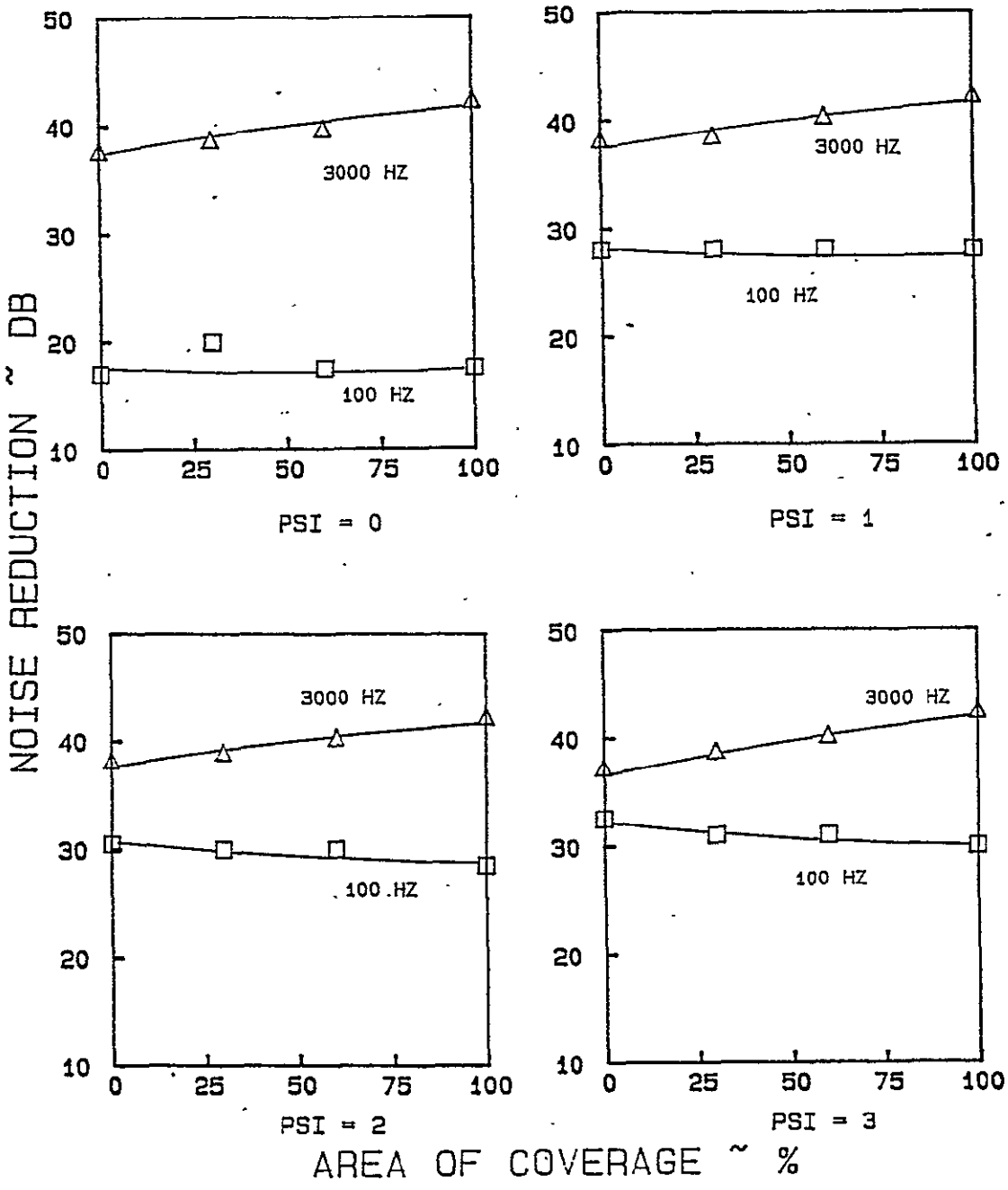

Figure 3.24: Effect of Coverage of Y-436 Damping Tape on the Noise Reduction Characteristics of a Flat, Stiffened Panel at Different Pressure Differentials

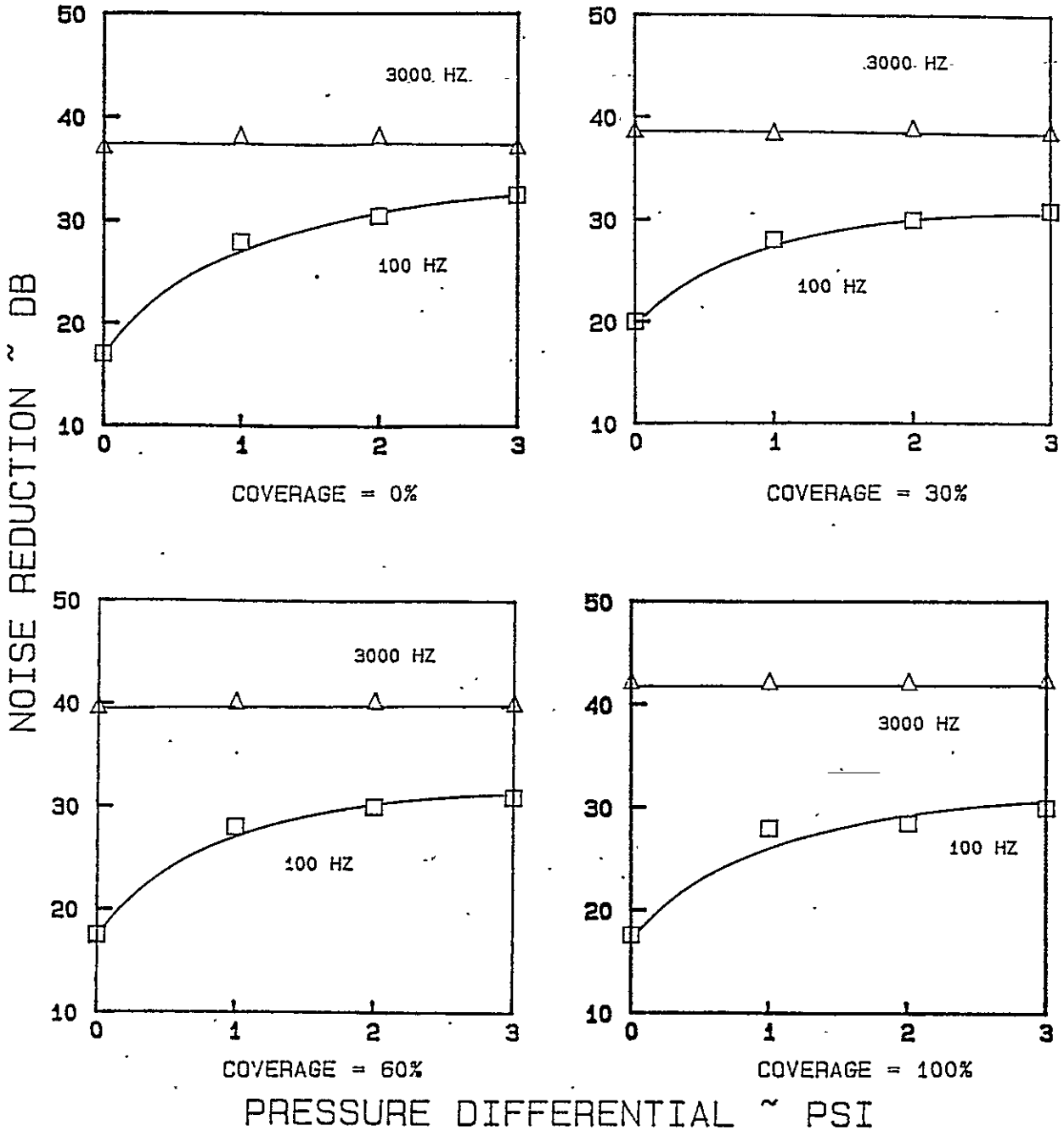

Figure 3.25: Effect of Pressure Differential on Noise Reduction Characteristics of a Flat, Stiffened Panel with Y-436 Damping Tape at Low and High Frequencies

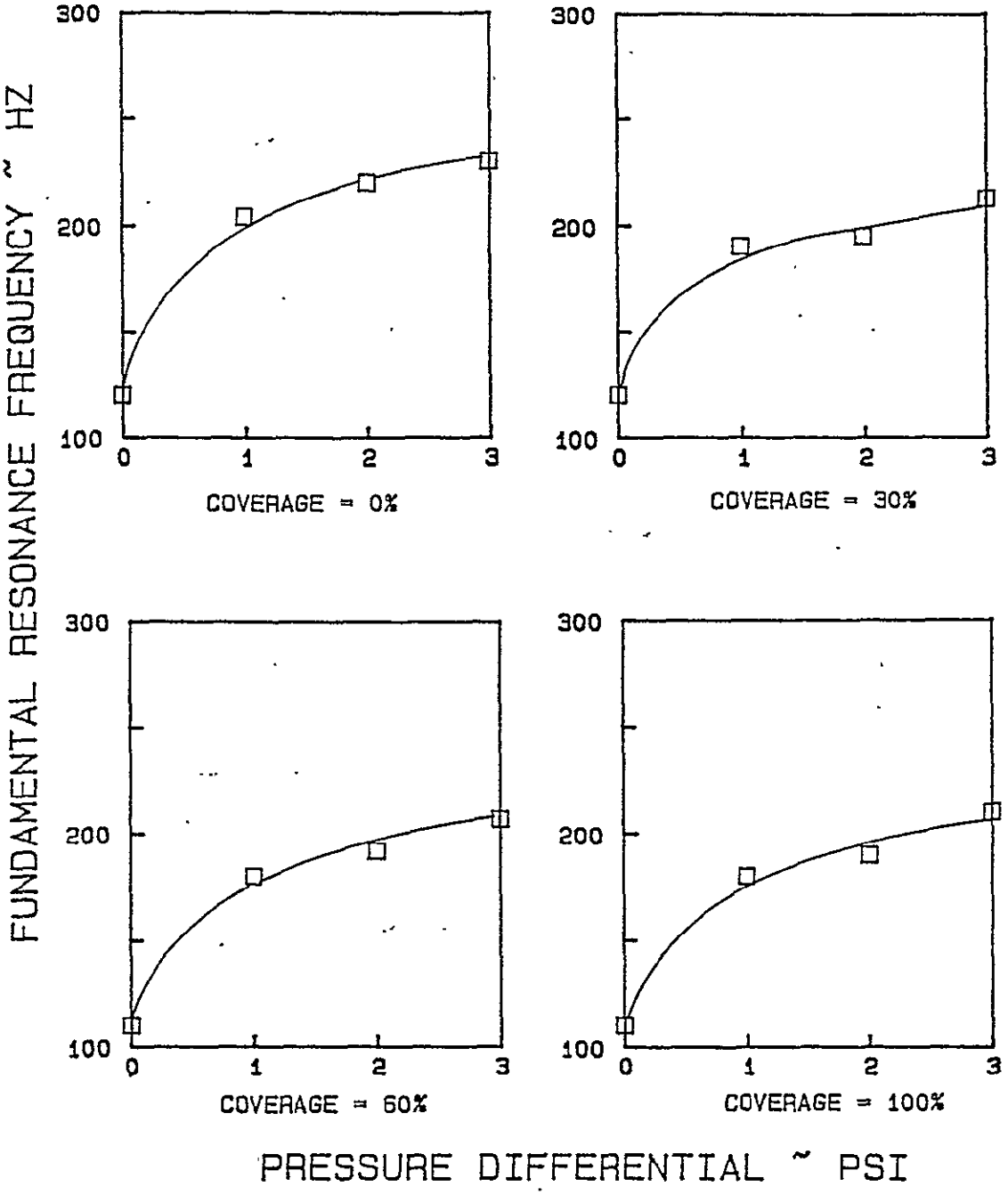

Figure 3.26: Effect of Pressure Differential on the Fundamental Resonance Frequency of a Flat, Stiffened Panel with Y-436 Damping Tape

decrease is not observed (Figure 3.25). The resonance frequency (Figure 3.26) behaves exactly like the resonance frequency with the Y-434 material (Figure 3.20).

3.8.2 CURVED PANEL

Similar cross plots are given for a curved panel with Y-436 material in Figures 3.27-3.29. Once again the results are similar, except that the increased stiffness due to 17 mil constraining layer is more visible. Because of the increased stiffness, the noise reduction does not decrease with the application of the treatment (Figure 3.27). With the curved panel, the decrease with the pressure differential is still high (see Figure 3.28). The resonance frequency vs pressure differential is nearly similar to that with the Y-434 material.

3.9 DISCUSSION AND CONCLUSIONS

Reference 9 discusses the effect of damping material on infinite panels. With the infinite panels the damping tapes do not have any effect below the coincidence frequency. In the KU-FRL acoustic test facility the coincidence frequency of aluminum panels is well above 5000 Hz. This is because of the normal angles of incidences. However, the studies (discussed in Reference 51) indicate that the sound transmission of finite panels is controlled by the resonant transmission; i.e., by the various resonance

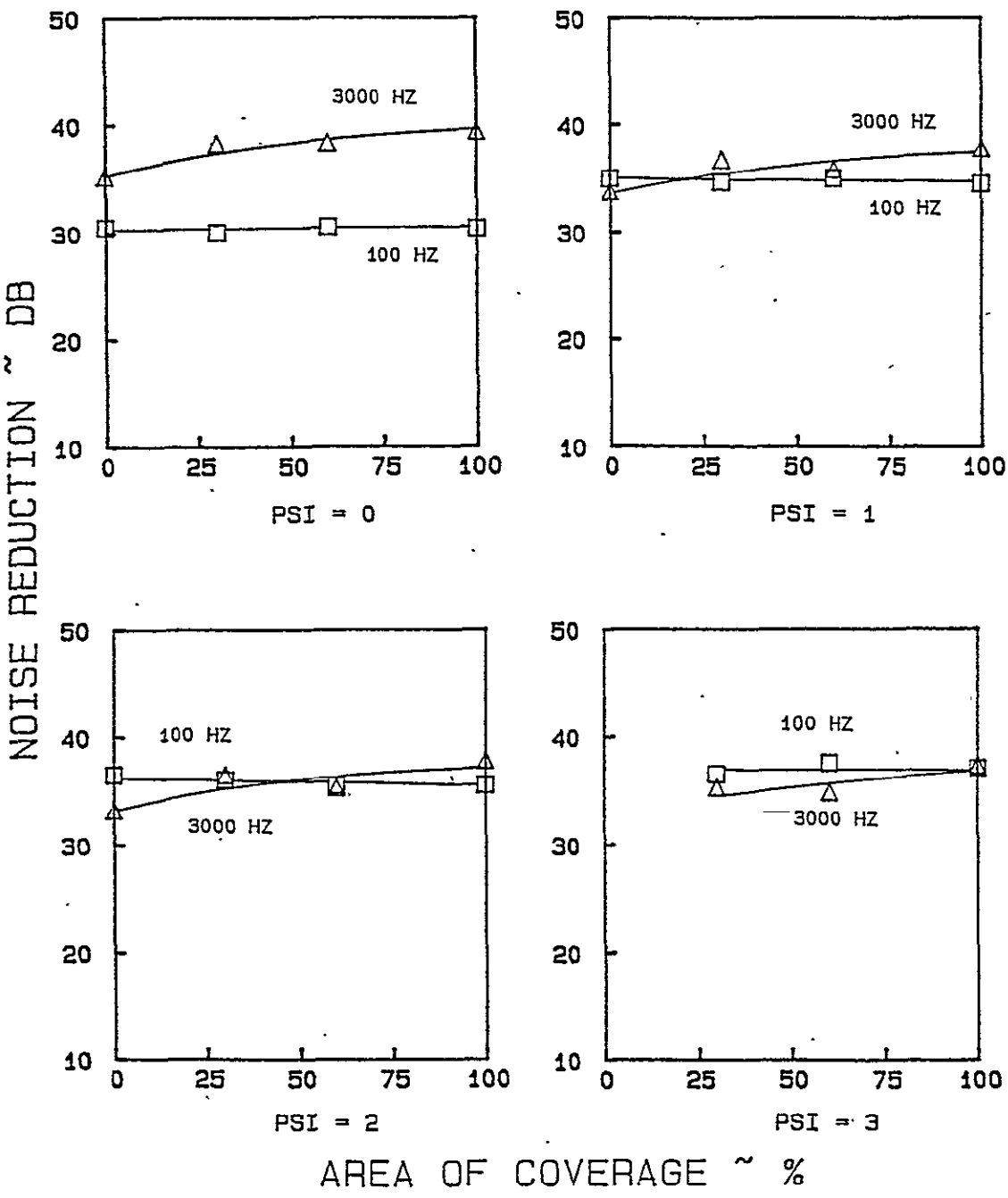

Figure 3.27: Effect of Coverage of Y-436 Damping Tape on the Noise Reduction Characteristics of a Curved, Stiffened Panel at Different Pressure Differentials.

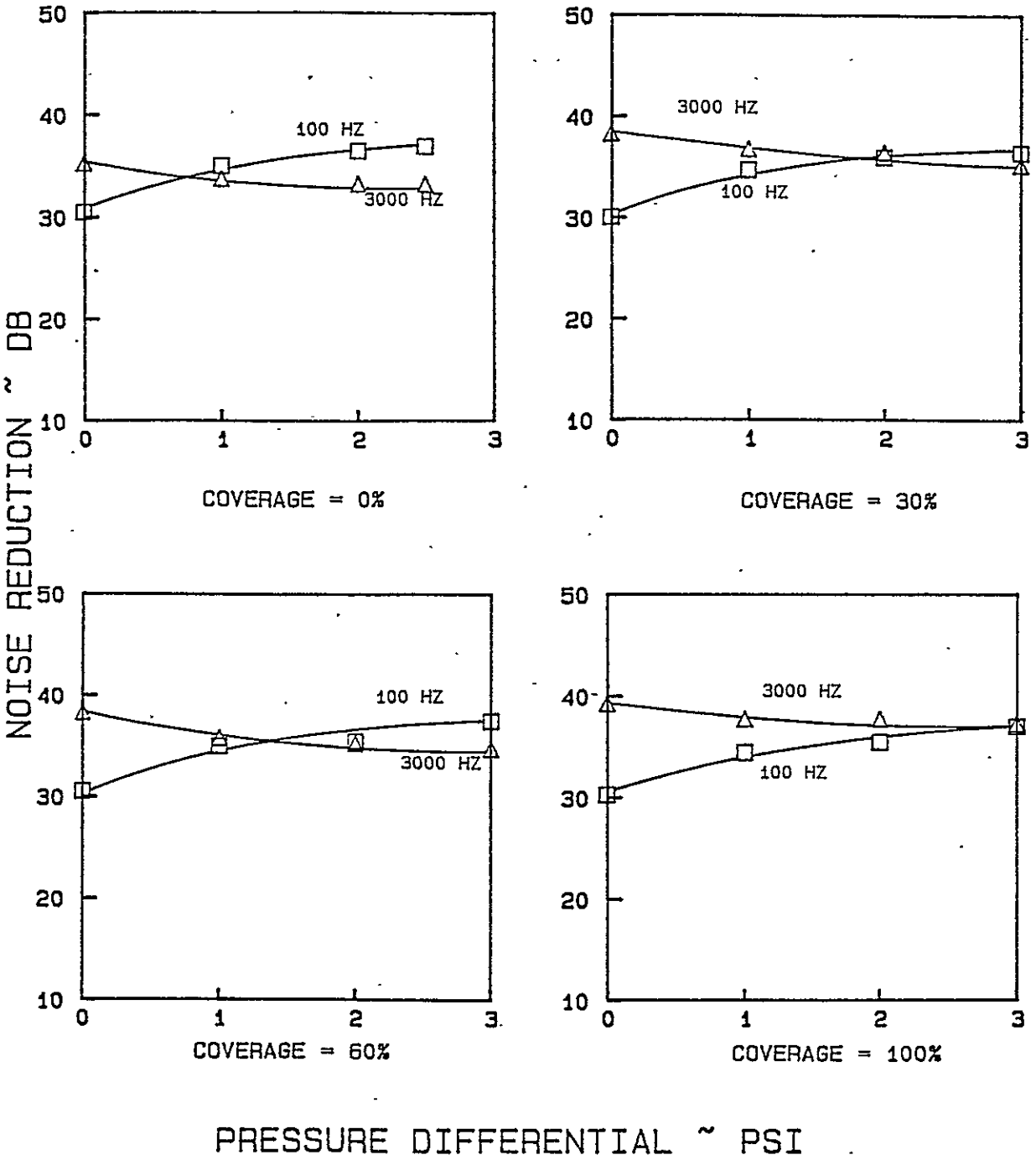

Figure 3.28: Effect of Pressure Differentials on Noise Reduction Characteristics of a Curved, Stiffened Panel with Y-436 Damping Tape

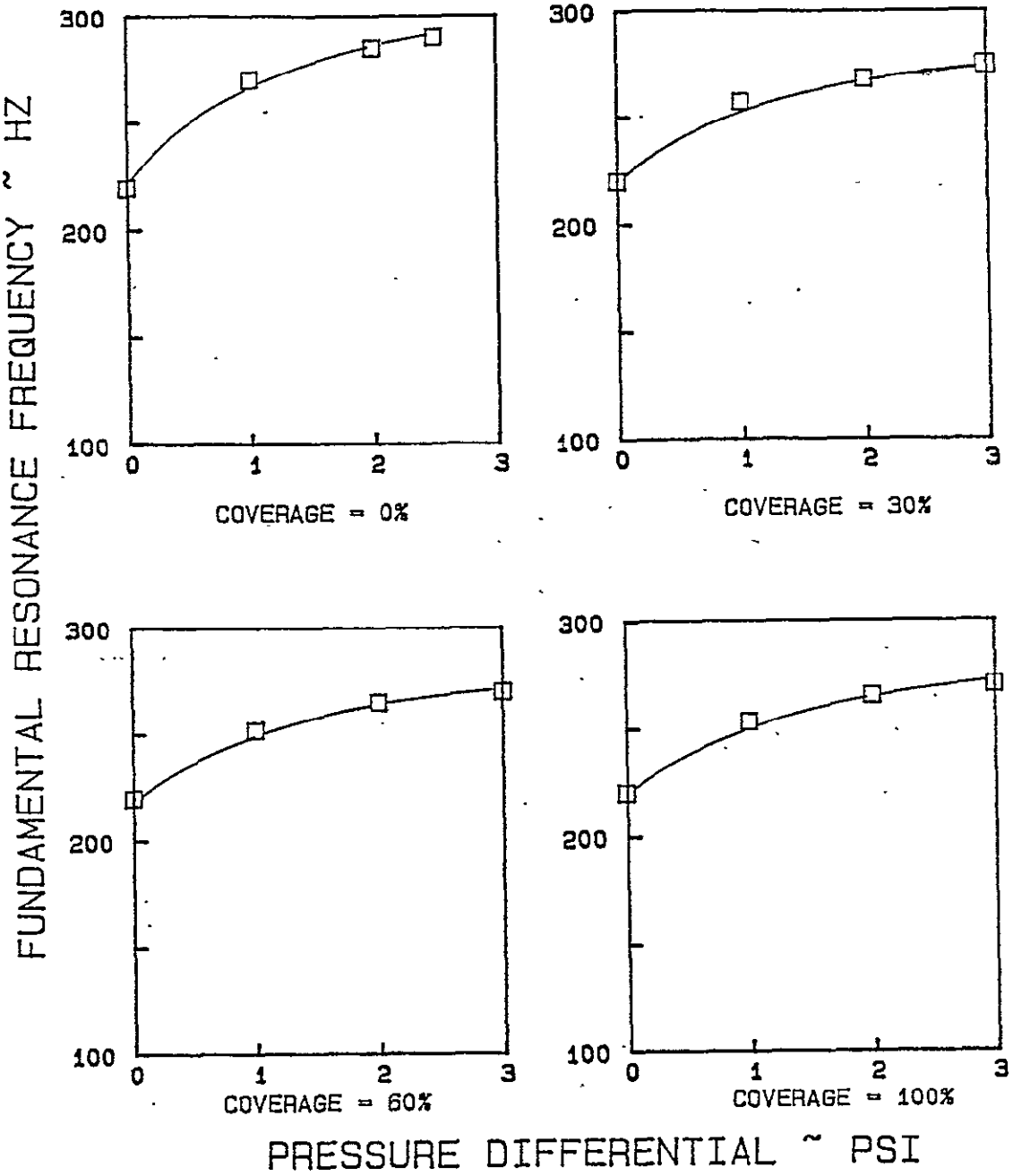

Figure 3.29: Effect of Pressure Differential on the Fundamental Resonance Frequency of a Curved, Stiffened Panel with Y-436 Damping Tape

modes. The sound transmission at each mode is controlled by the damping of the mode. In the KU-FRL acoustic test facility the panel size tested was 18" x 18". Hence, this panel will have both longitudinal and circumferential (or lateral) resonance frequencies. Earlier tests (References 3 and 4) indicated that the severity of the resonance peaks and dips are higher with the pressure differentials. Hence it was initially expected that the effect of damping tape would be more than just the effects of mass and stiffness. However, results of all three damping tapes tend to show that these panels behave more like infinite panels, for airborne noise excitation.

In particular, based on the experimental investigations, it is concluded that the noise source has negligible effect on the noise attenuation characteristics of the specimens under all conditions tested. This is considered to be so, due to the normal incidence of the panel in the Beranek tube and the very high sweep time of the sweep oscillator. The effect of curvature on a bare panel is to stiffen the panel, thereby increasing low frequency noise reduction. The maximum increase in noise reduction occurs in the first one psi pressure differential in all cases. The gain in noise reduction for the curved panel is smaller compared to that of the flat panel, since it is inherently stiffer. In the high-frequency region the noise reduction decreases by one to three dB due to pressurization. This result is consistent with published theoretical results (Reference 4).

Even at room temperature, the effct of damping tapes on the noise reduction is negligible at frequencies other than the resonance frequencies. This is consistent with the classical mass law predictions. When the mass of the damping tapes constitutes a large percentage of the mass of the specimen, as in the case of 100% coverage, the effect is essentially to increase noise reduction in the high frequency region. The test results indicate that with greater application of Y-370 material, the fundamental resonance frequency decreases. This is due to the fact that only mass--not stiffness--is added. With Y-436 and Y-434 materials which have constraining layers, the resonance frequency shift is negligible, indicating that the additional stiffness produced by the constraining layer balances out the effect of added mass on the resonance frequency. The effect of percentage of coverage is to decrease low-frequency noise reduction and to increase noise reduction at high frequencies. Decreases were very slight for all the pressure differentials tested.

Scatter of the noise reduction values at the fundamental resonance frequency precludes any general conclusion about the effect of percentage of coverage of the damping material. In general, the resonance peaks and dips are reduced by the application of damping material.

CHAPTER 4

DETERMINATION OF LOSS FACTORS

4.1 INTRODUCTION

This test program was conducted in the KU-FRL acoustic test facility to determine the damping of panels mounted in the Beranek tube. Damping is defined as energy dissipation of a structure as it deforms and the conversion of ordered mechanical energy into thermal energy. Unlike mass and stiffness, damping does not refer to a unique physical phenomenon; and that is the reason damping is very difficult to predict in general. Damping mechanisms include interface friction, acoustic radiation, magnetic hysteresis, mechanical hysteresis (also called material damping), and any other way of converting mechanical into thermal energy. In practical cases one or two mechanisms generally predominate (Reference 9). For example, the material damping in aluminum alloy structures is known to contribute only a tiny proportion to the total damping (Reference 10). Likewise, magnetic hysteresis has a very small effect.

The panel damping is an important factor for noise reduction at the fundamental frequency and in the mass law region (higher frequencies) depending on the particular mode; as a result, the boundary conditions of the panel play a significant role in the damping of the installed panel (Reference 11). Since the damping varies considerably with different installations, it is not readily

predicted. For this reason, this evaluation of a technique for the determination of the damping in panels in the KU-FRL acoustic test facility was undertaken.

This chapter details the equipment and the method used to obtain the required data and the techniques for reducing the data to usable terms. Also described are the tests used to validate the results obtained for the panels installed in this facility, and the conclusions reached as a result of these tests are presented.

4.2 DEFINITION OF TERMS

There are many units and terms used for designating damping in materials. Of these the loss coefficient, η (or loss factor, as it is commonly called) is often used in structural mechanics and will be used in this paper. Loss coefficient is a relative energy unit defined as the ratio of damping energy to strain energy and is applicable to both liner and nonlinear materials.

$$\eta_s = D_s/2U_s \qquad (4.1),$$

where D_s is the damping energy dissipated in the total specimen

U_s is the total elastic energy stored in the specimen.

The subscript s denotes that these values are specimen properties. These properties are dependent on the specimen configuration, such

as panel size and shape, as well as the material properties. This subscript will be dropped subsequently with the understanding that all values for η are specimen loss factors.

For purposes of comparison of results with those of other investigators, the relations with several other common measures of damping are given below.

1. Quality factor, Q: Physically this is amplification at resonance.

$$Q = 2\pi U/D = 1/\eta \qquad (4.2).$$

2. Specific damping capacity, ψ:

$$\psi = D/U = 2\pi\eta \qquad (4.3).$$

3. Damping ratio, ζ: Fraction of critical damping:

$$\zeta = C/C_c = \eta/2 \qquad (4.4);$$

C is the viscous damping coefficient, lbf-sec/in;

C_c is the critical damping coefficient, lbf-sec/in.

4. Logarithmic decrement, δ:

$$\delta = \ln(x_o/x_1) = \pi\eta \qquad (4.5);$$

x_o = the amplitude of the damped wave at point 0;

x_1 = the amplitude of the following wave after 1 cycle.

For further explanation of measures and nomenclature of damping, see References 9 and 11.

4.3 TECHNIQUES FOR DAMPING EVALUTION

Several methods have been used to determine the damping of a specimen. Those that can be applied to a panel include bandwidth, energy measurements, amplification factor, and decay rate.

For the bandwidth method a frequency sweep is made, and the bandwidth is measured at a specified fraction of maximum amplitude. Problems arise when modes are closely spaced, as is the case with most panels for all but the first one or two modes.

The energy measurement method involves directly measuring the energy input (amplitude and phase) and the specimen output (amplitude and phase) and using these to calculate the energy loss directly. This requires more elaborate and expensive equipment.

Measurement of amplification factor is difficult to use for absolute measurement of damping, since the reference level may be hard to find.

Decay rate or logarithmic decrement tests are easy to do and are widely used (References 9 and 15). Here the excitation force is turned off and the panel is allowed to vibrate freely with the response, as measured by vibration pickup, recorded. The logarithmic decrement, δ, can then be obtained from this record using the relation $\delta = \ell n(x_o/x_1)$. The limitation on this method is the assumption that the decay curve is logarithmic. Physically this means that δ must be independent of amplitude (viscous damping). When this assumption is violated (the curve is not logarithmic), a logarithmic curve can be fitted to the decay curve and an equivalent

value for δ can be found. Because of the simplicity and reliability of this method, the damping values were determined using the decay rate tests.

4.4 EQUIPMENT

The equipment set-up for the decay rate tests is shown in Figure 4.1. The panel displacement can be measured by several devices, including capacitance pickups or accelerometers. An accelerometer was chosen over the capacitance pickup because of the ease of installation and operation. Since the mass of the accelerometer is very small, the loading on the panel is insignificant, as shown in the next section. The integrator on the sound level meter (SLM) has a switch to select output of acceleration, velocity, or displacement. The active filter was used when the third octave filter was out of service. A comparison test run with each filter yielded the same results. For the first tests the Techni-rite hot stylus recorder was used with a capability of recording up to 125 Hz and 100 mm/sec. This was inadequate for the modes above the first; so the Honeywell oscillograph, with a capability of recording up to 1000 Hz and 80 inches per second, was used for all sebsequent tests. The sweep oscillator was chosen over random noise generator because tests with the random noise generator produced nonanalyzable results.

A switch was installed in the wires between the amplifier and the speakers, as shown in Figure 4.1. This single throw switch

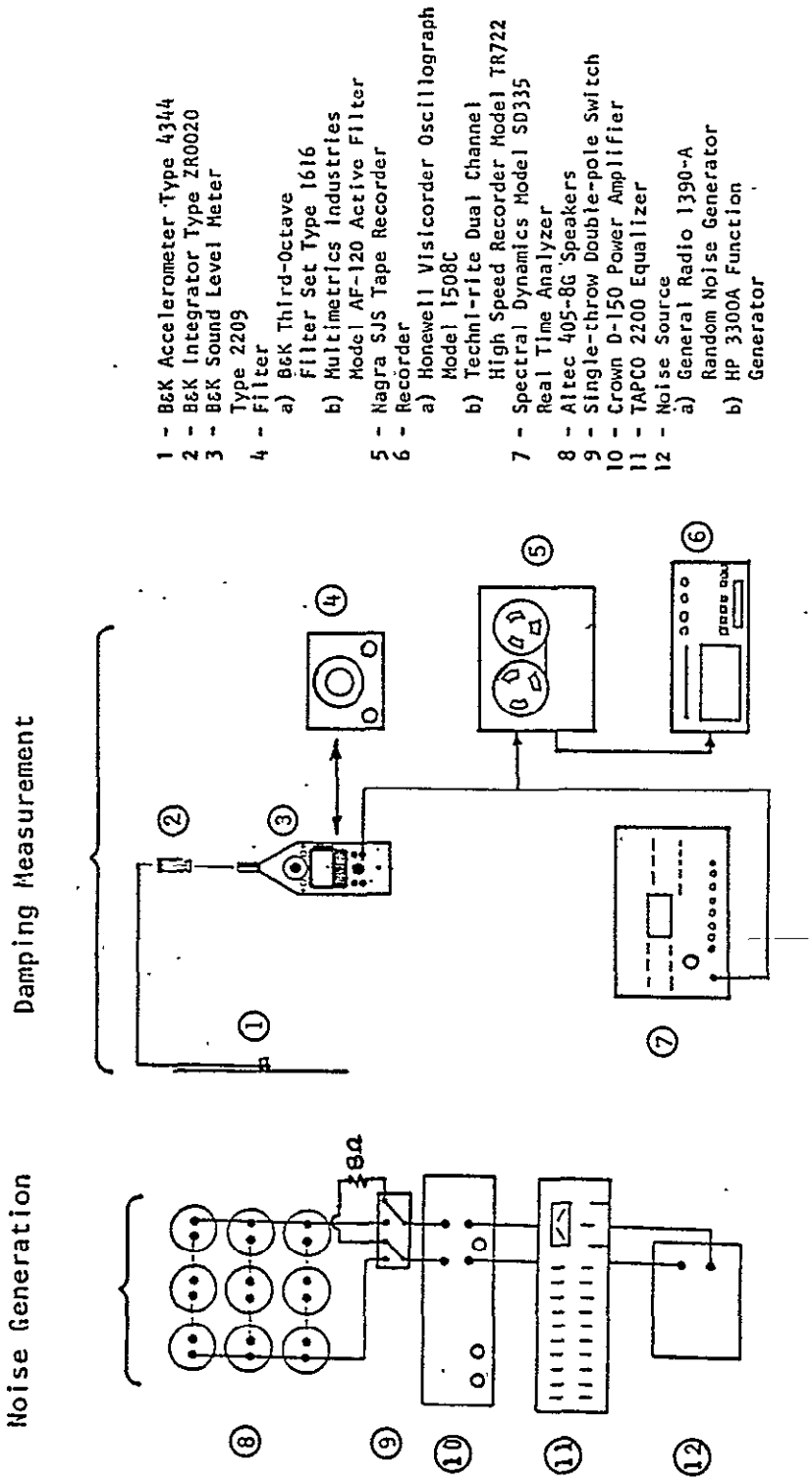

Figure 4.1: Equipment Set-Up for Noise Generation and Damping Measurements

C-2

diverts the current to an 8Ω to prevent damage to the amplifier when the speakers are shut off for the decay tests.

4.5 TEST METHOD

The most important factor to consider in damping testing is to test the specimen in a configuration which bears a close resemblance to the application of the results. For this reason the damping will be evaluated with the panel in the same installation used for the noise reduction tests.

4.5.1 PANEL INSTALLED IN BERANEK TUBE

For the decay rate tests the accelerometer was mounted on the panel as described in Reference 12. For the first few tests the accelerometers were mounted with the cement, but for later tests bee's wax was used because of the ease of installation and removal. The accelerometer cable was routed toward the top of the panel and taped with electrical insulation tape at three points to minimize triboelectric noise caused by vibration of the cable. The panel was then placed in the Beranek tube (Figure 4.2), and the eight clamping bolts were torqed to 25 in-lb. At first, frequency sweep was made from 20 Hz to 1000 Hz to locate the resonant peaks for the panel. This frequency response was then stored on the analyzer and the output of the SLM was connected to the tape recorder for signal amplification. The amplified signal was then sent to the oscillograph.

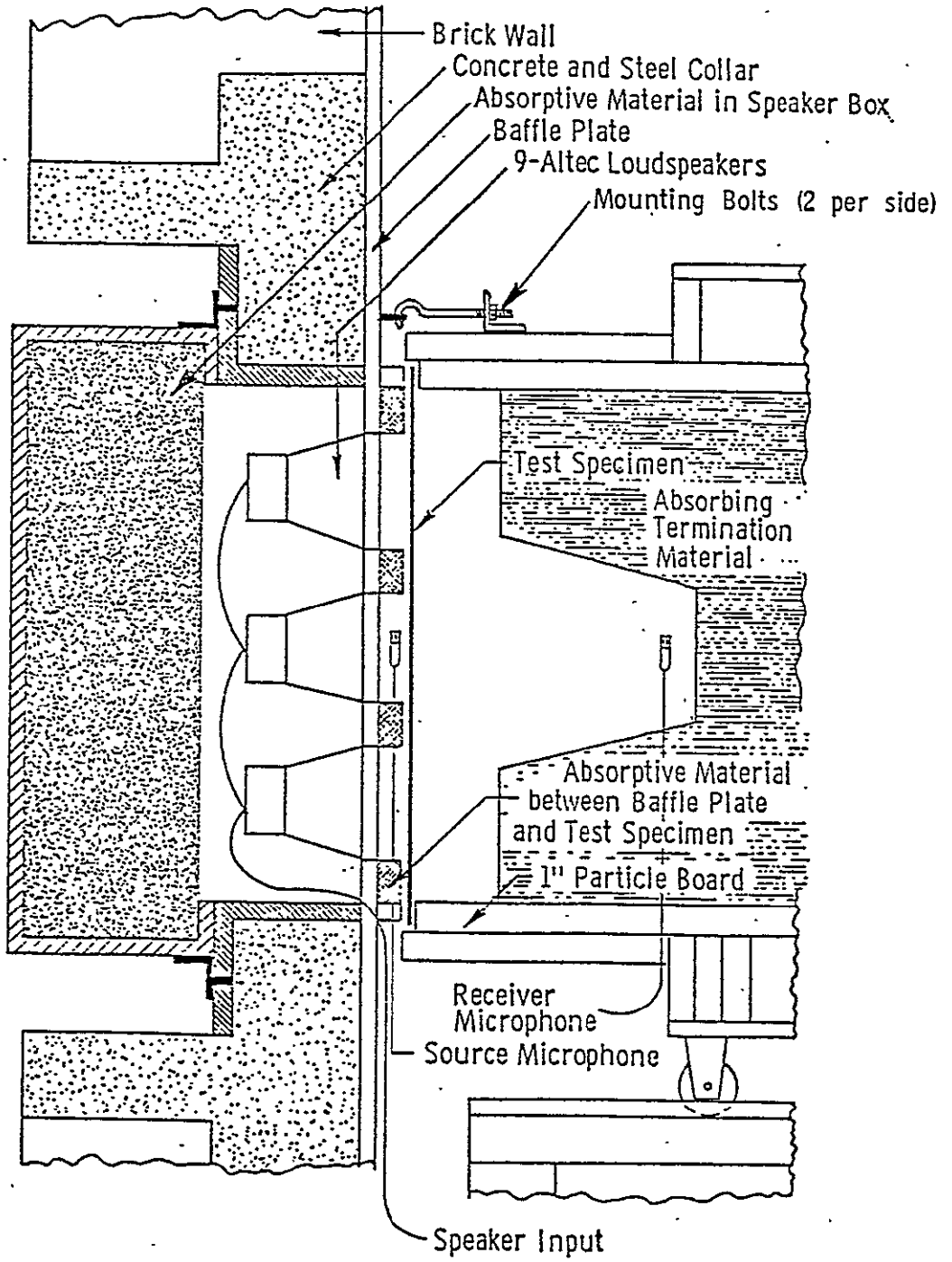

Figure 4.2: Panel Installation in the KU-FRL Acoustic Test Facility

For the actual tests the first resonant peak was located on the scope and the frequency read. This frequency was then tuned on the oscillator and minor adjustments made to yield the maximum acceleration as indicated on the SLM. This peak does not necessarily correspond to the resonant frequency of a specific mode but was very close. Acceleration was used as output, since the displacements were so small that the meter was operating at its lower limits for even the low frequencies and was registering mostly noise at the higher frequencies. The gain on the recorder was then adjusted to yield the widest signal available on the oscillograph (approximately 3 inches, but this varied with frequency). The speaker was then switched off to obtain a record of the signal decay. The paper speed was then adjusted to give a decay of about three inches for more accurate analysis and the test repeated until three good decays were obtained. After the three decays were recorded, the next peak (one which is not closely coupled or overshadowed by another peak) was located; and the preceding steps were repeated for each subsequent peak up to 1000 Hz.

4.5.2 FREE PANEL TESTS

Several tests were performed on panels hung by a wire in front of the speakers, as shown in Figure 4.3, to minimize the effects of support-related damping (see Reference 9). These tests were used to check the validity of this decay test set-up by comparing the results for the free panel with those obtained by other

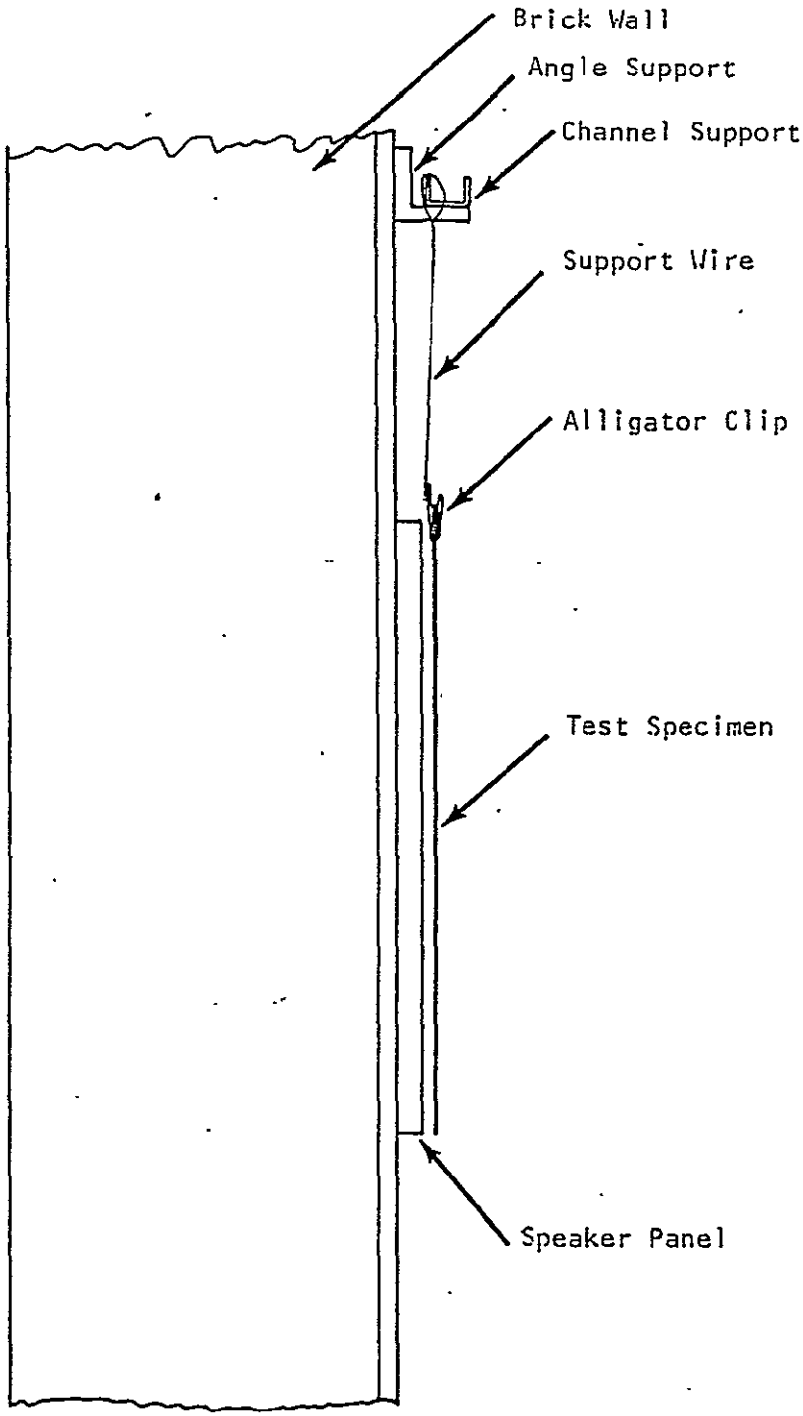

Figure 4.3: Hanging Panel Installation for the Free-Free Modes (Side View)

investigators and for comparison with the panel installed in the tube to determine the support-related damping. The test procedure remained unchanged except that the accelerometer was mounted on a diagonal, as shown in Figure 4.4, since the middle of the panel is the intersection of two nodal lines for the first and several other modes. The cable from the accelerometer was routed to the nearest nodal line and off the panel at the intersection of the nodal line with the edge of the panel. Difficulties arose here at low frequencies because the fundamental resonance frequency for the free panels was generally <10 Hz, which is far below the frequency range of the speaker set-up.

4.5.3 SPECIAL CONSIDERATIONS

1. Mass Effect of Accelerometer: The effect of the accelerometer mass on the natural frequency of the panel was checked using natural frequency relations for a beam with both ends supported and a central mass. These relations of Reference 13 yielded a 0.7% decrease in the natural frequency due to the accelerometer, for an accelerometer mass of 2.7 gm and the mass of the lightest panel at 298 gm. This is certainly a negligible change. The cable and tape will similarly have an even smaller effect due to their mass and also should not affect the stiffness.

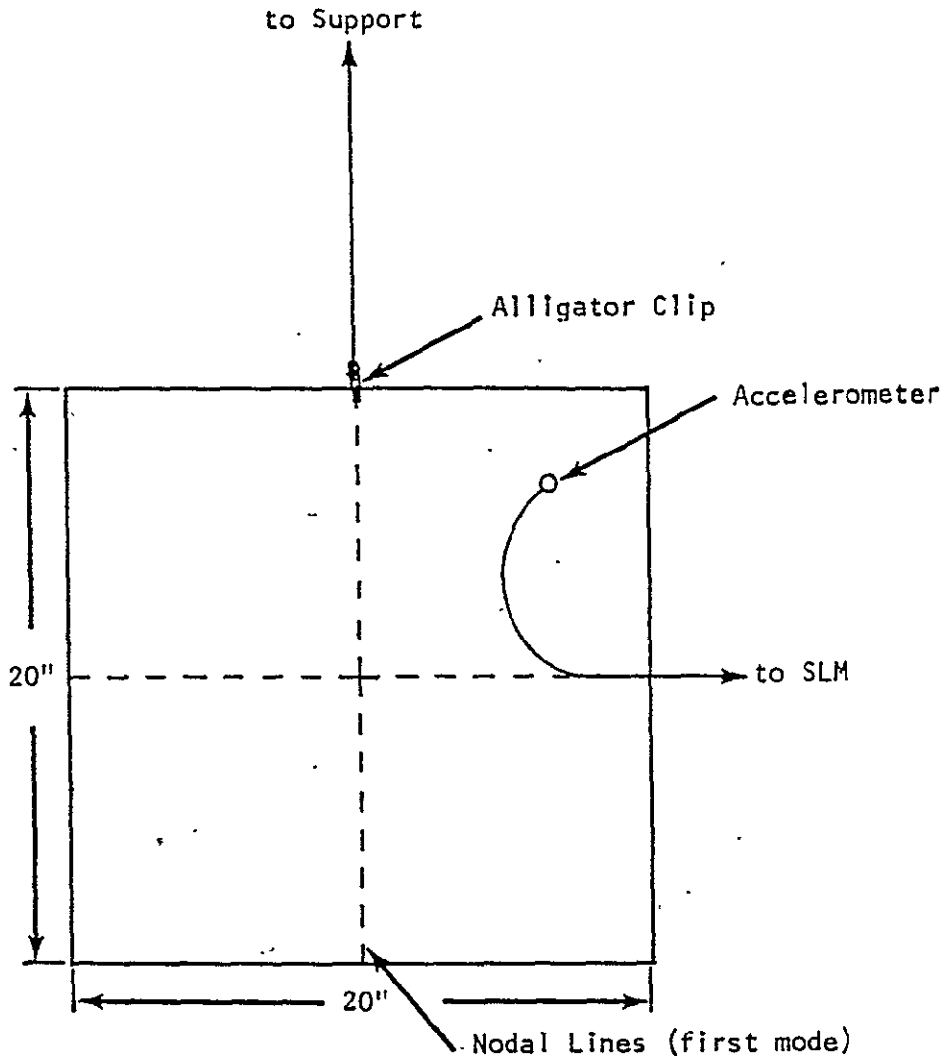

Figure 4.4: Front View of Hanging Panel Installation

2. Effect of a Closed Cavity: By placing the panel in a closed cavity, the effect of the pressure within the cavity could be significant, especially in the small space between the panel and the speakers. This effect was checked by recording the microphone signal simultaneously with the accelerometer signal. The results of these tests showed that for some modes, there was a significant effect. That is, for the worst case the microphone signal decay rate was only two times faster than the panel decay rate. For a viable damping test, the decay of the noise source should be an order of magnitude greater than the decay of the panel. The case presented here certainly violates this rule, but this was the worst case. For most panels, the microphone signal decay rate was significantly greater.

4.6 DATA ANALYSIS

To obtain the loss factor, η, from the decay curves, a workable relation was first obtained as follows:

$$\delta = \frac{1}{n} \ell n(x_0/x_n) \qquad (4.6);$$

δ = the logarithmic decrement

x_0 = the amplitude of the damped wave at point 0

x_n = the amplitude of the damped wave after n cycles

n = the number of cycles.

For consistent results Plunkett (Reference 14) suggested counting the number of cycles, n_e, for the amplitude to decay to x_0/e.

$$\delta = \frac{1}{n_e} \ln(e) \qquad (4.7),$$

or $$\delta = \frac{1}{n_e} \qquad (4.7a);$$

but $$n_e = f*t_e \qquad (4.8),$$

f = the frequency of vibration

t_e = the time to decay to x_0/e

and $$t_e = d_e/s \qquad (4.9),$$

d_e = the distance to decay to x_0/e

s = the recording paper speed

with the result that

$$\delta = s/f*d_e) \qquad (4.10);$$

or in terms of

$$\eta = s/(\pi*f*d_e) \qquad (4.11).$$

4.6.1 CURVE FIT

The following procedure was then used to measure d_e from the decay curve:

1. Using a French curve (logarithmic) draw a curve to fit the overall decay,
2. locate the first good peak and measure its height: This is x.
3. Divide x_0 by the numerical value of e.
4. On the decaying curve find where the value of x is equal to the result of step 3: This is point e.

5. Measure the distance between point 0 and point e: This is d_e.

A problem noted with the above procedure was that variation of the loss coefficient occurred depending on which part of the curve was fitted. This was only a problem with curves which deviated significantly from the logarithmic decay, such as when mode interaction was evident or when Coulomb type damping was present. The variation introduced here was minimized by fitting the curve to the entire decay rather than a minor portion of it.

4.6.2 LINEAR REGRESSION CURVE FIT

This method involves digitizing the peaks of the decay curve and fitting a curve through the points. Both a linear and a logrithmic curve were fitted using linear regression for both. The correlation coefficient for each curve is used as a measure of the quality of the fit to indicate whether the damping is primarily Coulomb (indicated by a good linear fit) or viscous (indicated by a good logarithmic fit).

4.6.3 COMPARISON

A comparison of the two data analysis methods was done to check if there was any difference between the results. Three tests of a 0.032 inch thick aluminum panel were analyzed by both methods. The results for the second method are consistently higher (by 8.7%) than those from the first method, but the overall trends for each method

are nearly identical. The regression curve fit method would be expected to be more accurate than the mechanical curve fit. Either method predicts the overall trends of damping with the frequency; and results from the first method can be corrected to match those of the second method. One consideration is that the second method takes up a lot of analysis time and was not possible at high frequencies due to masking of individual peaks.

4.7 RESULTS

To check the validity of this test set-up and panel installation, several tests were run with panels of various materials and configurations. Panels mounted to vibrate in the free-free modes were used to check the basic test set-up and for comparison with the installed panels to see what effects this installation has on the damping of the panels. Various clamping bolt torques were checked to approximate simply supported and clamped boundaries, and a heavy steel frame was used for a closer approximation of the clamped condition. The trends of damping variation with stress and frequency were measured and compared with results of other investigators. The effects of various stiffened, riveted, and bonded panel configurations were checked for comparison. Finally, the effect of damping materials and composite material panels were measured. A list of the tests is given in Table 4.1.

Table 4.1: Damping Test Log

Test #	Test Description
1	0.020 Al, Free Panel
2	0.020 Al, Free, Stress effect
3	0.020 Al, Free
4	0.032 Al, Free
5	0.025 Al, Free, Active and 1/3 octave filter
6	0 032 Al, Free, 100% Y-370
7	0.025 Al, Stiffened (Channel & Z), Free
8	0.016 Al, 15" x 15", Bonded
9	0.016 Al, 15" x 15", Bolted edge strip
10	0.020 Al, 15" x 15", Bonded
11	0.020 Al, 15" x 15", Riveted
12	0.020 Al, new recorder set-up
13	0.025 Al, Standard
14	0.032 Al, Standard
15	0.032 Al, Effect of foam contact
16	0.032 Al, Test w/o foam over speakers
17	0.032 Al, 2 in. wide clamping frame
18	0.025 Al, Stiffened (Channel & Z) crossed
19	0.032 Al, 100 % Y-370
20	2 x 0.016 Al, Bonded with IC-998
21	0-0-0, Graphite/epoxy
22	45-0-45, Graphite/epoxy
23	0.032 Al, Standard
24	0.032 Al, Standard
25	0.032 Al, Standard
26	45-0^{u}-45, Graphite/epoxy
27	0-45-0, Graphite/epoxy
28	0-0-0, Kevlar/epoxy
29	45-0-45, Kevlar/epoxy
30	0-45-0, Kevlar/epoxy

4.7.1 FREE PANEL

The results from the free hanging panel tests on the bare aluminum panels of thickness 0.020 to 0.032 inch show that the loss factor at the lowest obtainable frequency was 0.002 to 0.004. This compares rather well with the loss factors from Heckl (Reference 15) for a free hanging bare panel of 0.0022. Large variations occurred for some frequencies. These were likely caused by the panel vibrating in a mode which caused the clip to vibrate, thus dissipating more energy and resulting in an increase in the measured damping.

4.7.2 INSTALLED PANEL

To show the effect of the boundary conditions in the tube on the damping, a plot of the damping results for a 0.032 inch panel is shown in Figure 4.5 for both types of mounting. In addition, a plot for a 0.032 inch panel with a 2 inch wide by 0.25 inch thick steel clamping frame is shown. The figure shows that the installation has increased the damping of the panel by more than an order of magnitude. This same effect was also observed with the 0.020 and 0.025 inch thick aluminum panels. Comparison of the loss factors for the installed panel and the clamped panel shows that at the first two modes the frequencies and loss factors are in fair agreement. However, above this the installed panel damping is higher than for the clamped panel; and the frequencies are altered. This indicates that the boundary conditions for the

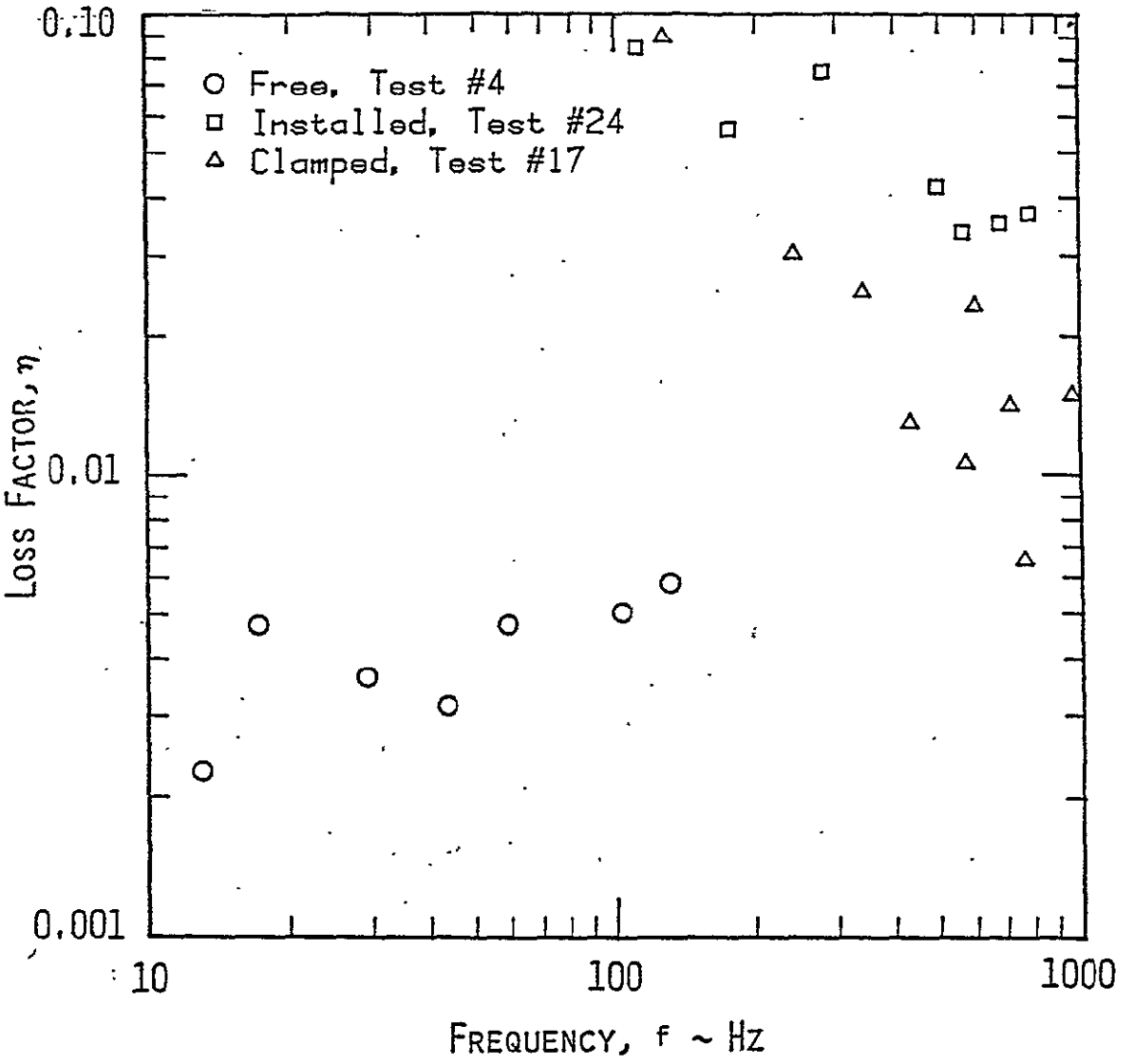

Figure 4.5: Effects of Boundary Conditions for a 0.032 Inch Aluminum Panel

installed panel approximate those for clamped panel for the lower modes. This was not the case at higher frequencies. Further tests should be done to check how well these boundary conditions approximate simply supported conditions. The loss factors for the clamped panel approach those for the free panel, as they should for the ideal case of no dissipation at the boundaries.

1. Repeatability of Runs: The consistency of the test method and the data reduction method can be checked by calculating the standard deviation in the results for several successive runs at each frequency. This was done for tests #23 and #24 with the 0.032 inch panel, with results shown in Table 4.2. The results of 4.9% and 3.7% for the average percentage standard deviation indicate that the loss factor for a given installation is within 4-5% of that measured.

2. Clamping Torque: The effect of the clamping bolt torque on the loss factor was measured for a 0.020 inch panel, with the results shown in Figure 4.6. The clamping torques were varied from 20 in-lb to 50 in-lb. Also shown are the results of tests with the clamping frame. The change in loss factor is negligible, as it should be. The only factor affecting this is the decreased amplitude due to the increased clamping on the panel causing a decrease in air damping, but this is compensated by the increase in stiffness of the "compliant" boundaries.

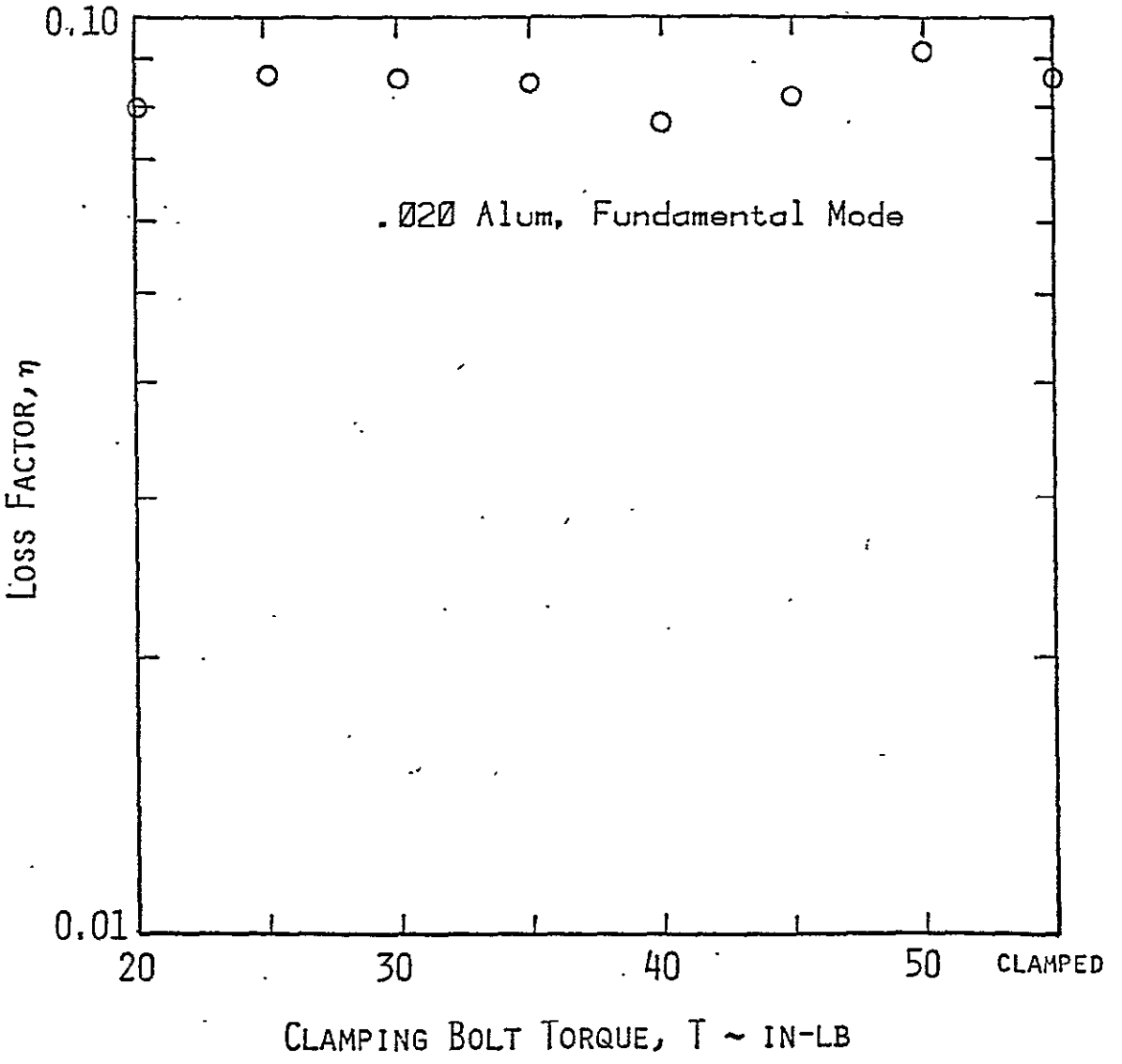

Figure 4.6: Effect of Clamping Bolt Torque on the Loss Factor for the Fundamental Mode of a 0.020 Inch Aluminum Panel

Table 4.2: Percentage Standard Deviation for Tests #23 and #24

Test #23		Test #24	
f	$\sigma/\bar{x}$ (%)	f	$\sigma/\bar{x}$ (%)
116	0.1	112	4.9
178	1.4	177	3.7
289	5.8	281	6.0
502	15.1	498	5.1
572	5.8	564	1.5
689	4.6	680	2.2
792	1.6	785	2.1
Average	4.9%		3.7%

3. Successive Installations: Three tests were run on a standard 0.032 inch panel on different days to check the variations introduced due to the panel mounting technique. The results are shown in Figure 4.7. For the frequencies of 100 to 500 Hz, the variations are very small; but for the first mode and at the higher frequencies (<500 Hz), the variations were fairly large. For the fundamental mode this variation can be attributed to the fact that the logarithmic curves did not fit the decay curves very well. The liner correlation factor was 0.99, while the logarithmic correlation factor was 0.95, indicating that the damping present was primarily Coulomb. At the higher frequencies this variation is possibly due to the alteration of the closely spaced higher modes upon each successive installation. Test #24

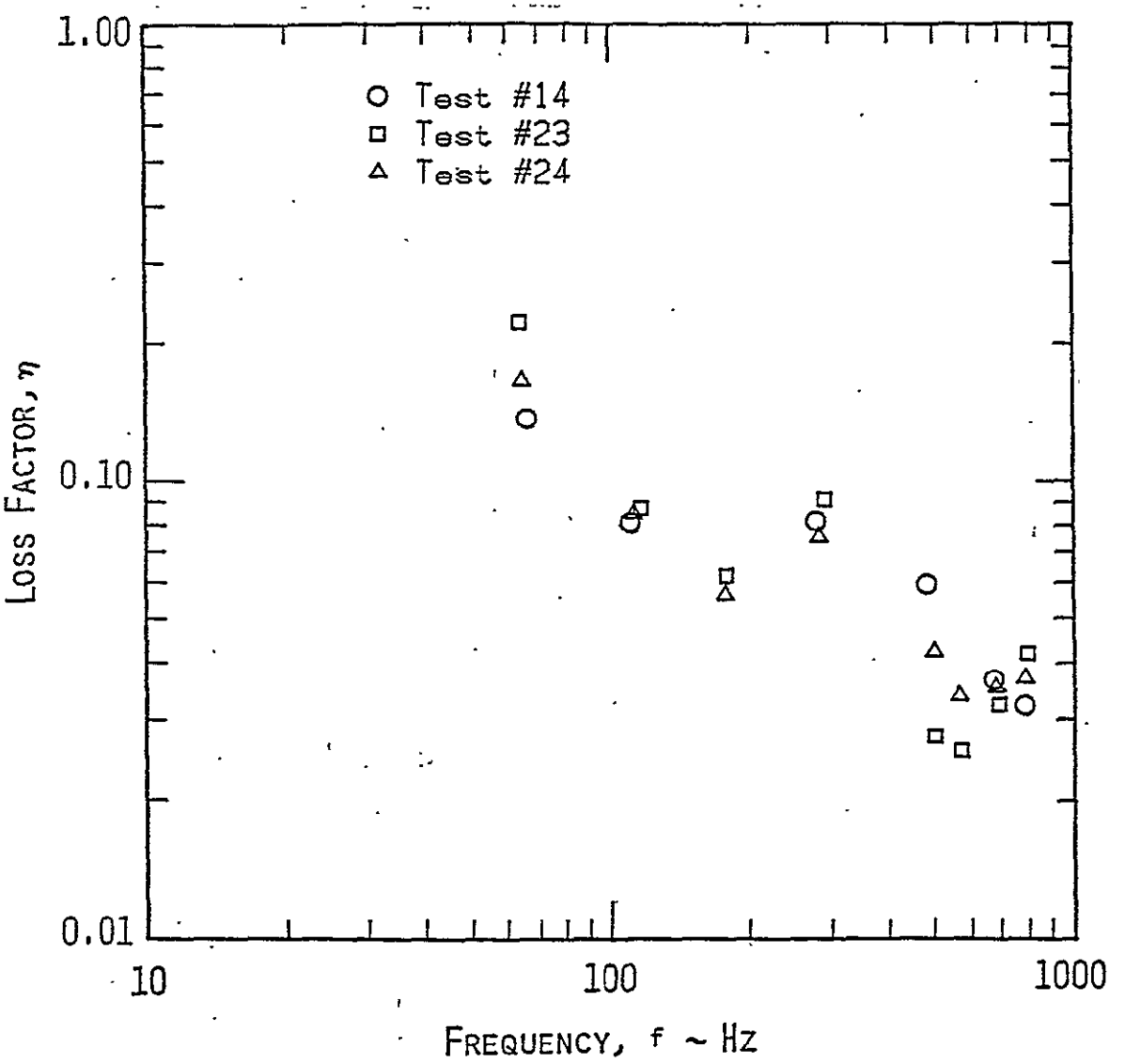

Figure 4.7: Comparison of Loss Factors for Successive Installations of a 0.032 Inch Aluminum Panel

represents an average of the three, so this test will be used for comparison purposes in the following section.

4.7.3 EFFECT OF STIFFENERS

To test the effect of stiffeners, a 0.025 inch aluminum panel with a channel stiffener and a "Z" stiffener crossed in the middle was tested, both free and mounted in the tube.

1. Free: A comparison of the loss factors for a stiffened plate with those of a bare plate as plotted in Figure 4.8 shows that at low frequencies there is no effect. At higher frequencies there is a noticeable increase in the damping. This increasing loss factor contribution with frequency agrees with the investigations by Ungar and Carbonell (Reference 16) and by Heckl (Reference 15), who show that this effect is caused by air pumping at the joints.
2. Installed: For the panels mounted in the tube, the results are shown in Figure 4.9. Here the effect of the stiffeners is masked by the effect of the boundary conditions.

4.7.4 EFFECT OF DAMPING MATERIAL

For the evaluation of the testing of damping materials, two damped panels were tested. The effect of damping material on the noise reduction characteristics were discussed in Chapter 3. The

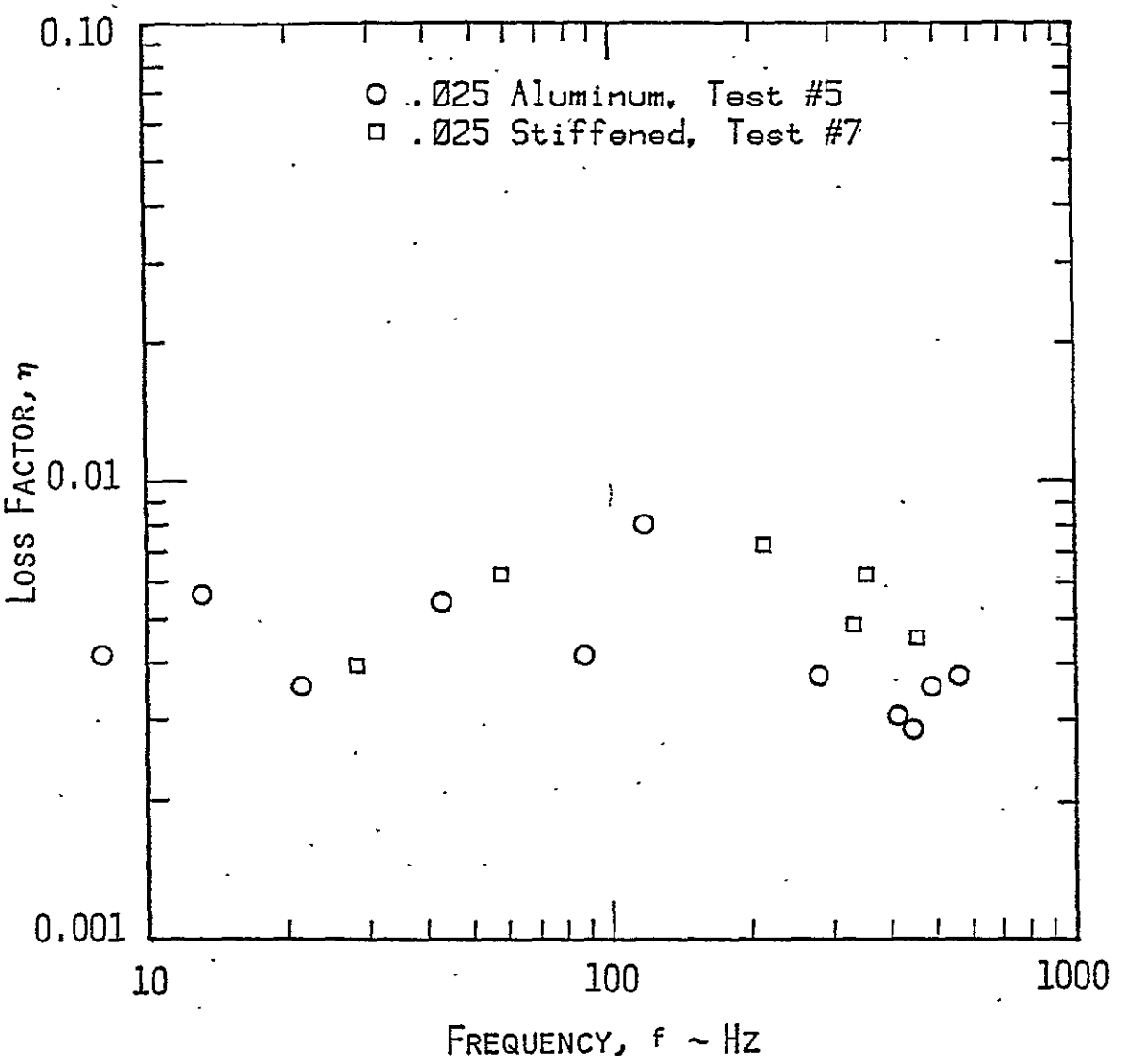

Figure 4.8: Effect of Stiffeners on Damping of a 0.025 Inch Aluminum Panel with Free Boundaries

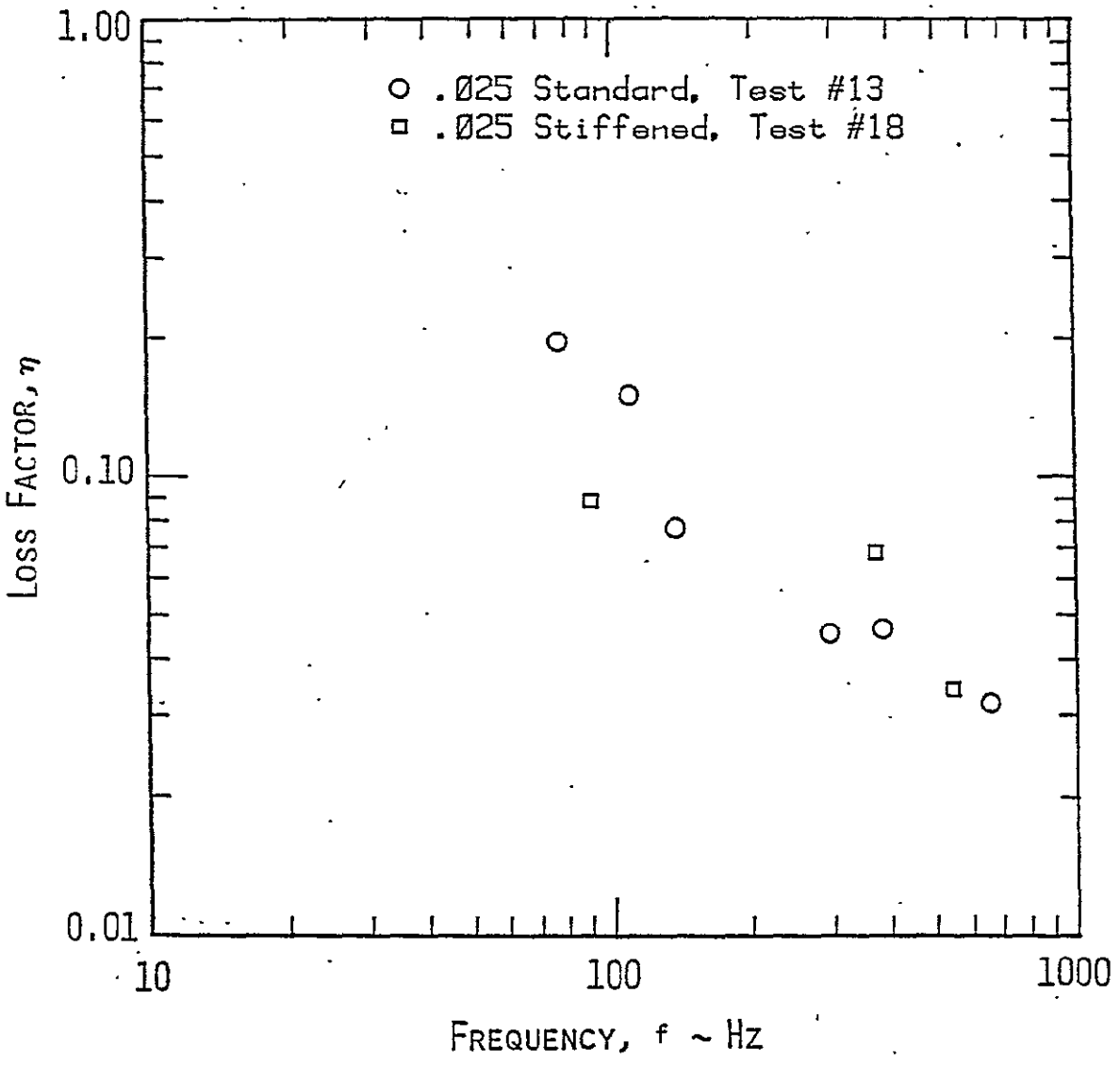

Figure 4.9: Effect of Stiffeners on Damping of a 0.025 Inch Aluminim Panels, Installed

first panel was a 20 x 20 x 0.032 inch aluminum panel with Y-370 damping material over an 18 x 18 inch area of the panel. The second panel consisted of a 20 x 20 x 0.016 inch aluminum panel with a 17.6 x 17.6 x 0.016 inch aluminum panel bonded to this with IC-998 viscoelastic adhesive. The first panel was tested for both free and installed mounting, while the second was tested only for the installed condition.

1. Free: As shown in Figure 4.10, the damping material had a definite effect on the loss factor with a $\Delta\eta$ of about 0.075. This increase by more than order of magnitude corresponds well with the results of Crandall (Reference 17) for a free-free beam.
2. Installed: Figure 4.11 shows the results for the two damped panels mounted in the tube, comparing them with the results for the bare panel. The overall effect is seen to be an increase in damping at the higher frequencies and not much effect at the lowest frequency. The two materials seem to behave the same over the entire range. The $\Delta\eta$ is about the same for the frequency range 500-1000 Hz as it was for the free panels.

4.7.5 COMPOSITE PANELS

Graphite/epoxy and Kevlar panels of various ply orientations were tested in the installed conditions with loss factor results as shown in Figure 4.12 and 4.13. There are no particular ply

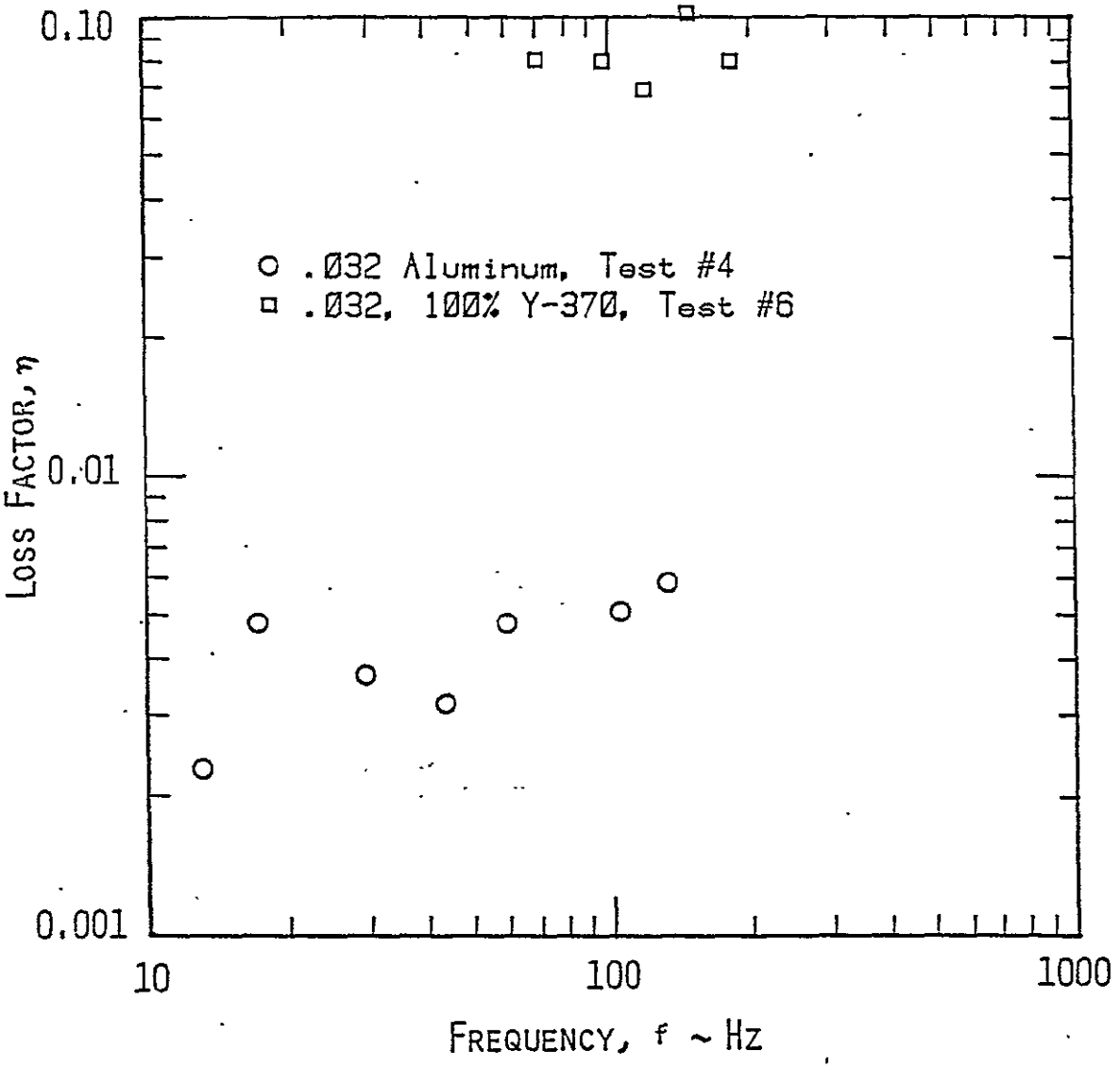

Figure 4.10: Effect of 100% Y-370 Damping Material on Dampin of a 0.032 Inch Aluminum Panel with Free Boundaries

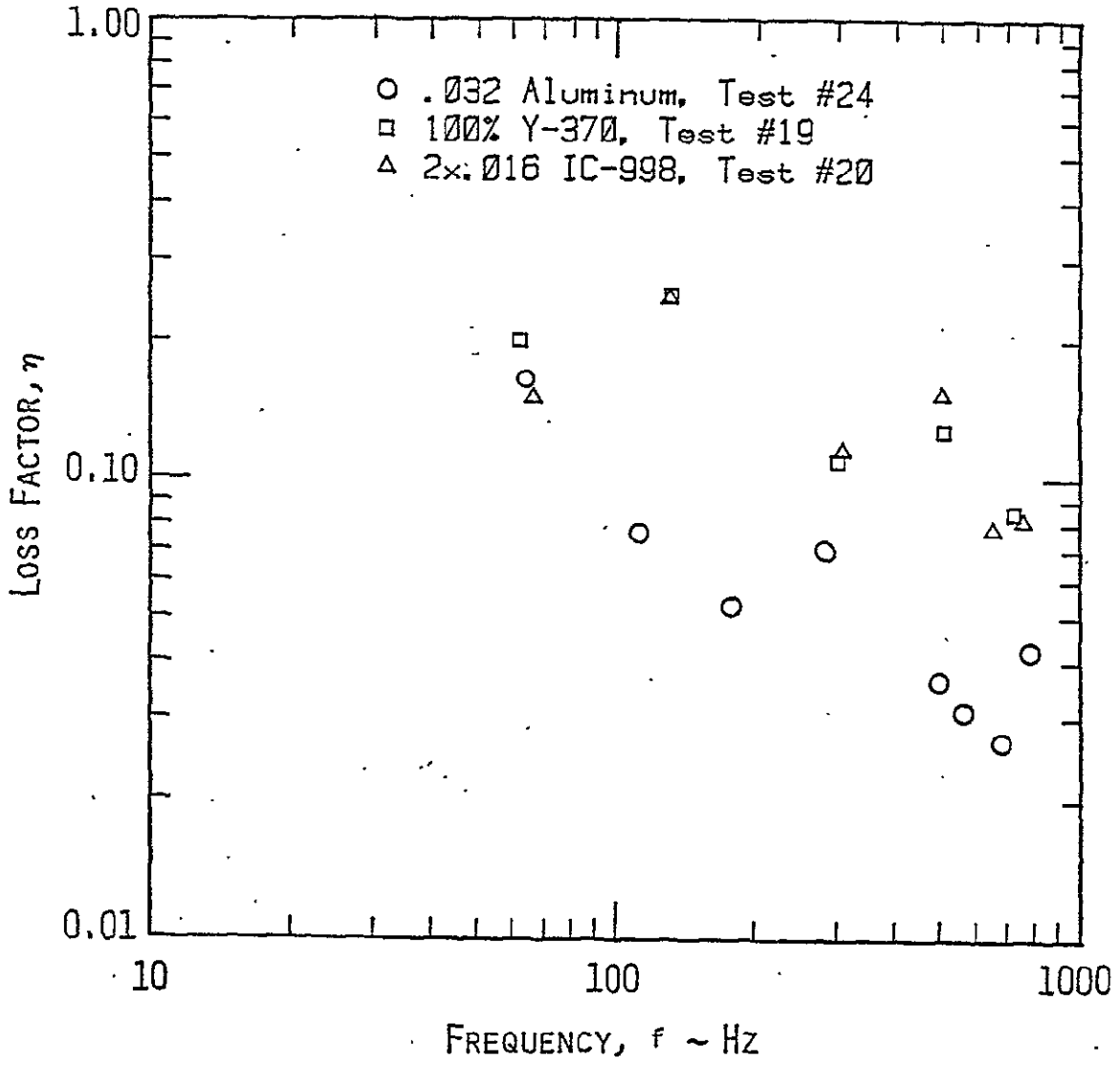

Figure 4.11: Effect of 100% Y-370 and IC-998 Adhesive on Damping of Aluminum Panel, Installed

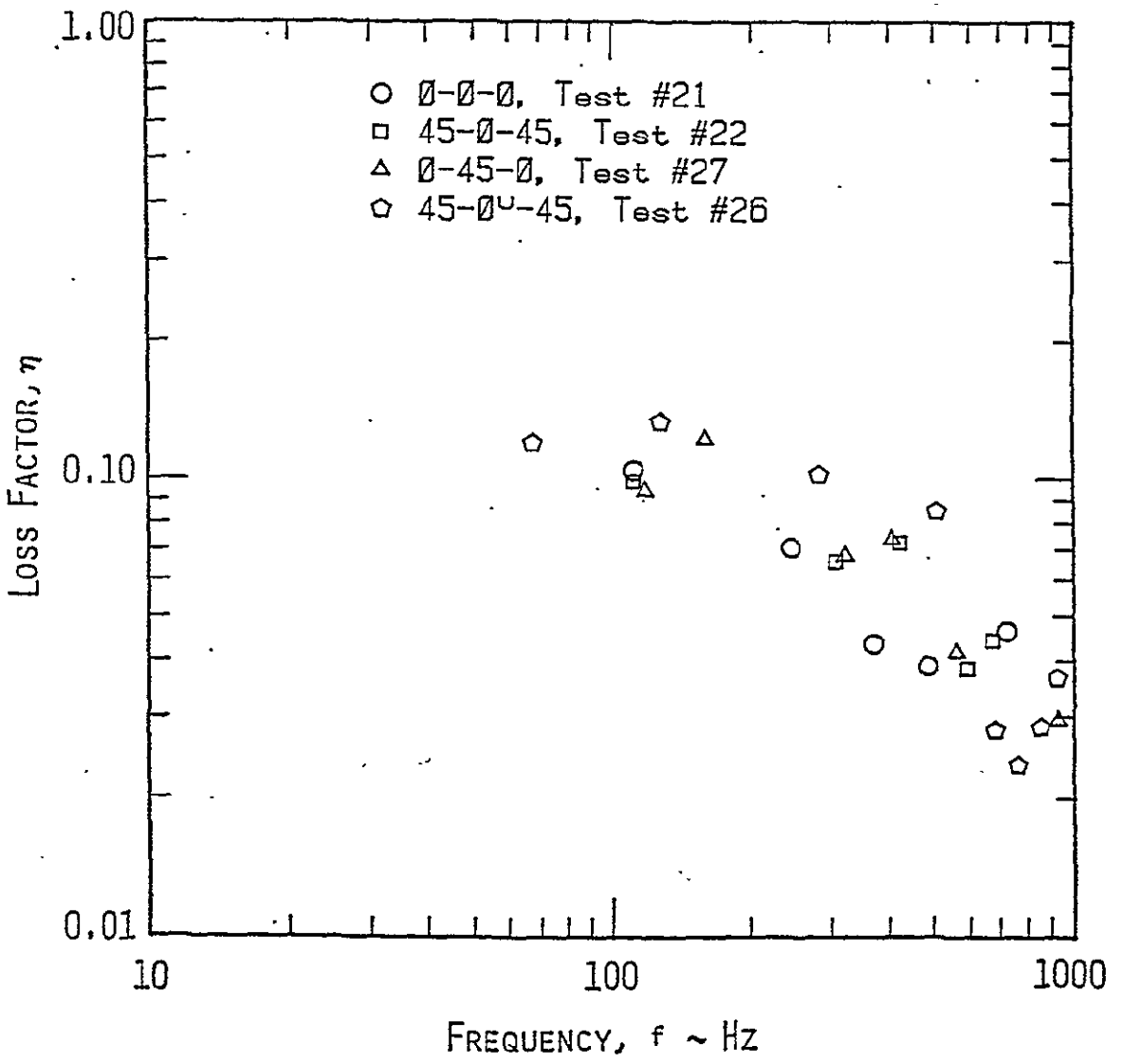

Figure 4.12: Damping in Graphite/Epoxy Panels of Various Ply Orientations, Installed

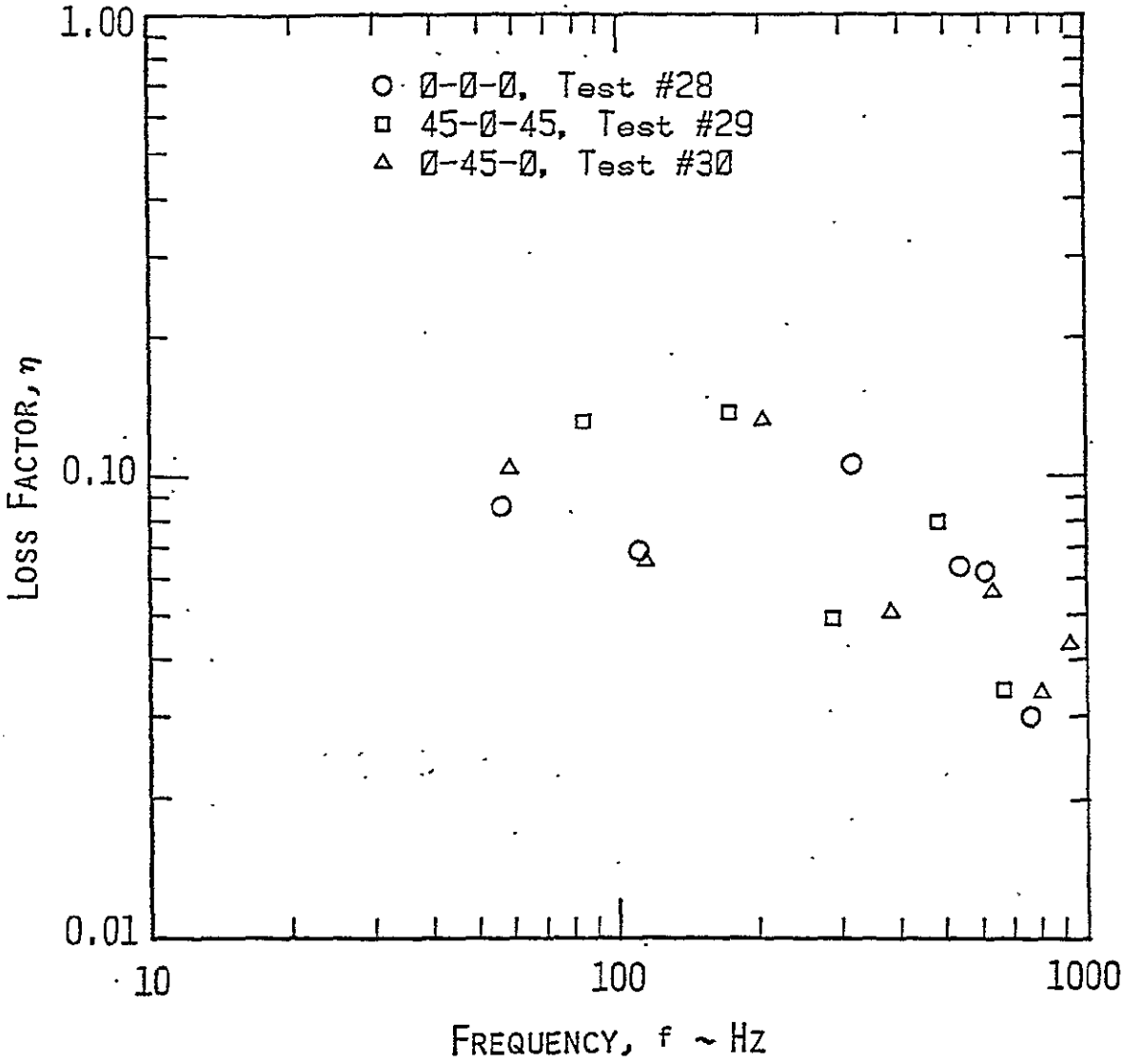

Figure 4.13: Damping in Kevlar/Epoxy Panels of Various Ply Orientations, Installed

orientations that stand out as having much better damping than the others for either the graphite or the Kevlar panels. The scatter for the Kevlar panels is larger than for the graphite composites, possibly due to manufacturing tolerances; but the average damping and the decrease with frequency are very close. These panels show approximately a 30% increase in damping ($\Delta\eta$ = .03) over the aluminum panel of comparable thickness (0.032) at the lowest frequency and none at the higher frequencies. The effects of ply orientations here are partially masked by the boundary losses. The scatter in the data here is mainly due to the many factors which affect the damping of composite panels in addition to the previously mentioned effects of this installation on aluminum panels. One of these factors is the fiber volume fraction of the composite (References 18 and 19) which is unknown for these panels.

4.8 CONCLUSIONS AND RECOMMENDATIONS

The decay rate tests worked very well with the existing equipment at the KU-FRL acoustic test facility. The testing method used here produced results which were consistent within 5% for each installation, which is very good for this type of installation. Both methods of data analysis produced comparably consistent results over a wide frequency range, with a difference of less than 10% between the two.

Tests conducted on panels suspended by wire at the nodal point verified the basic equipment set-up and test procedure and provided

a comparison with the results for the installed panels, showing the contribution of the boundary conditions to the overall damping of the panel. The torque on the clamping bolts showed no effect on the damping. Variations in the experimental damping for successive installations were within 10% for lower frequencies but varied considerably for the higher frequencies. There was a 50% decrease in the effect of stress as a result of the panel installation. The effects of the panel installation tended to mask the increased damping due to stiffeners, damping material, and composite materials; but their effects were still generally noticeable.

As a result of this series of checks, the damping test procedure as described here can be used to obtain loss factors accurate to within 10% for frequencies up to about 500 Hz as panels installed in the acoustic test facility. For the fundamental frequency and for higher frequencies, care must be taken in using these results. For general use, these loss factors can be obtained by averaging the results for several successive installations. When more specific results are required, it is suggested that the decay tests and the noise reduction tests be done successively without removing the panel. It is recommended that the effects of acoustic radiation on the panel damping be analyzed theoretically and/or experimentally. Also panels should be tested in a device which approximates a simply supported boundary conditions to check how closely the regular panel installation approximates the simply supported boundary conditions.

CHAPTER 5

NOISE REDUCTION CHARACTERISTICS OF DOUBLE-WALL PANELS

5.1 INTRODUCTION

The double-wall panels are made up of two panels (one representative of the skin and the other of the trim) separated either by an airgap or by a fiberglass thermal insulation material. In industry this configuration is widely used. The skin panel normally is designed for the structural integrity of the airplane. The interior trim panel is used for decorative purposes. Typically, inexpensive, light-weight trim materials are used in commercially oriented, general aviation airplanes; but more luxurious materials such as carpet, leather, etc., are used in business and executive type aircraft. In pressurized aircraft and in aircraft flying at high altitudes, fiberglass insulation is used to provide thermal insulation. The objective of this investigation is to study the sound attenuation characteristics of such panels and to use them as a part of the treatment to reduce externally generated noise. In this investigation both aluminum and fiber-reinforced materials were used as the skin materials. The trim panels investigated are the ones used in the industry. Beech Aircraft Corporation and Cessna Aircraft Company (Wallace Division) provided the test specimens. The details of the panel and the configurations tested are described in Section 5.2. The results of the experimental investigation are presented in Chapter 5.3.

5.2 DESCRIPTION OF THE TEST FACILITY AND TEST PANELS

5.2.1 DESCRIPTION OF THE ACOUSTIC TEST FACILITY

The KU-FRL acoustic test facility was used in this investigation. A detailed description of this test facility and its characteristics is given in References 20 and 21. Salient features are excerpted from these reports and presented in Appendix A. In the same appendix the limitations of the facility are also described. All the panels tested were 20 inches by 20 inches with 18-inch-by-18-inch exposed area. The tests were conducted under normal incidence at room temperature. Three adapter tubes were added to accommodate the three panel depths tested. This was the only modification to the test facility. A diagram of the facility with the adapters is shown in Figure 5.1. The output from the test facility is in the form of noise reduction curves plotted as a function of frequency. The noise reduction across a structure is defined as

$$NR = 10 \text{ Log}|p_s/p_r|^2 \qquad (5.1)$$

where NR = Noise reduction (dB)

p_s = Measured pressure on the source side (Pa)

p_r = Pressure on the receiver side (Pa).

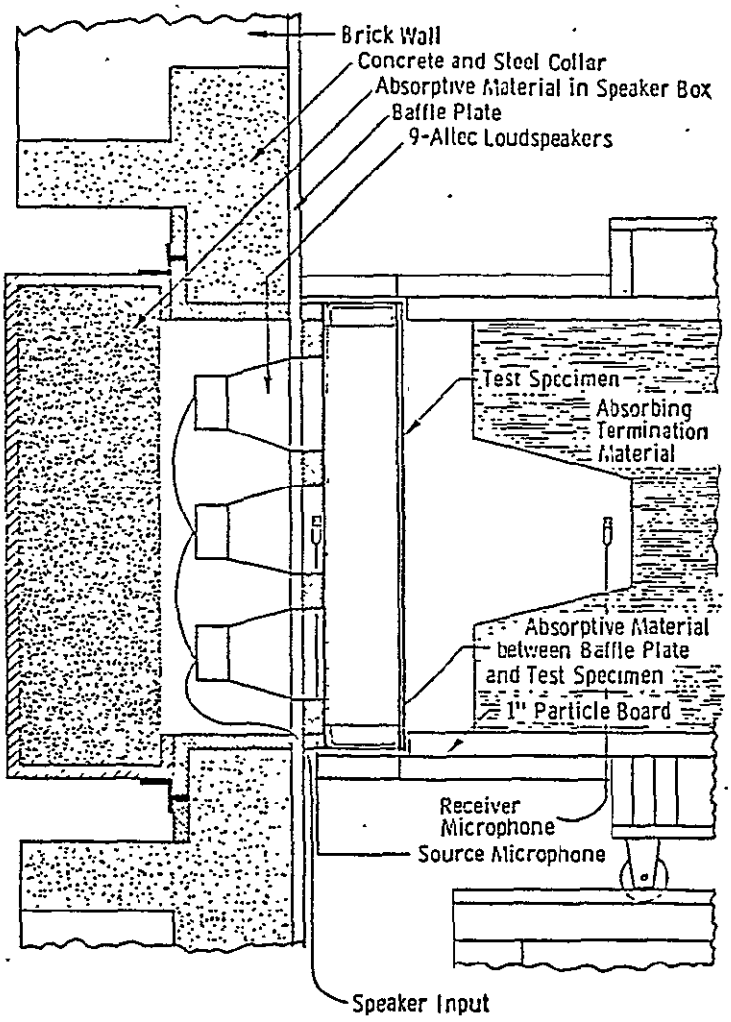

Figure 5.1: Schematic Diagram of the Test Facility with the Adapter to Test Double-Wall Panel

5.2.2 DESCRIPTION OF THE TEST PANELS

The double-wall test specimens were made of skin, airgap or fiberglass insulation, and a trim panel. Figure 5.2 shows a typical double-wall configuration tested. Three types of skin panels were used in the investigation. The first type was .032" aluminum panel. This panel was stiffened with a single extruded "T" section stiffener, riveted down the center. This stiffener divided the panel into two equal-area bays (see Figure 5.2a). Three test panels of this type were used. These three panels vary only in the depth of the edge members riveted to the edge of the skin panel. This permits the installation of the panel depth of one, two, and three inches. The second type of skin panel was made of .029" thick graphite-epoxy. Each of the three layers of the panel was made of a woven cloth material with the two main directions of the fibers perpendicular to each other. The ply orientation for the three layers is 45°-0°-45°. Only one panel of this type was used in the present investigation. This particular panel had two "hat" stiffeners (see Figure 5.2c). The mechanical properties of this panel are given in Reference 6. The third type of skin panel used was made of .029" thick Kevlar* material. Once again it had three layers of equal thickness with ply orientation 45°-0°-45°. Two panels of this type were used: one with one "hat" stiffener, and the other with two "hat" stiffeners. Refer to Table 5.1 for further

*Made by DuPont Corporation

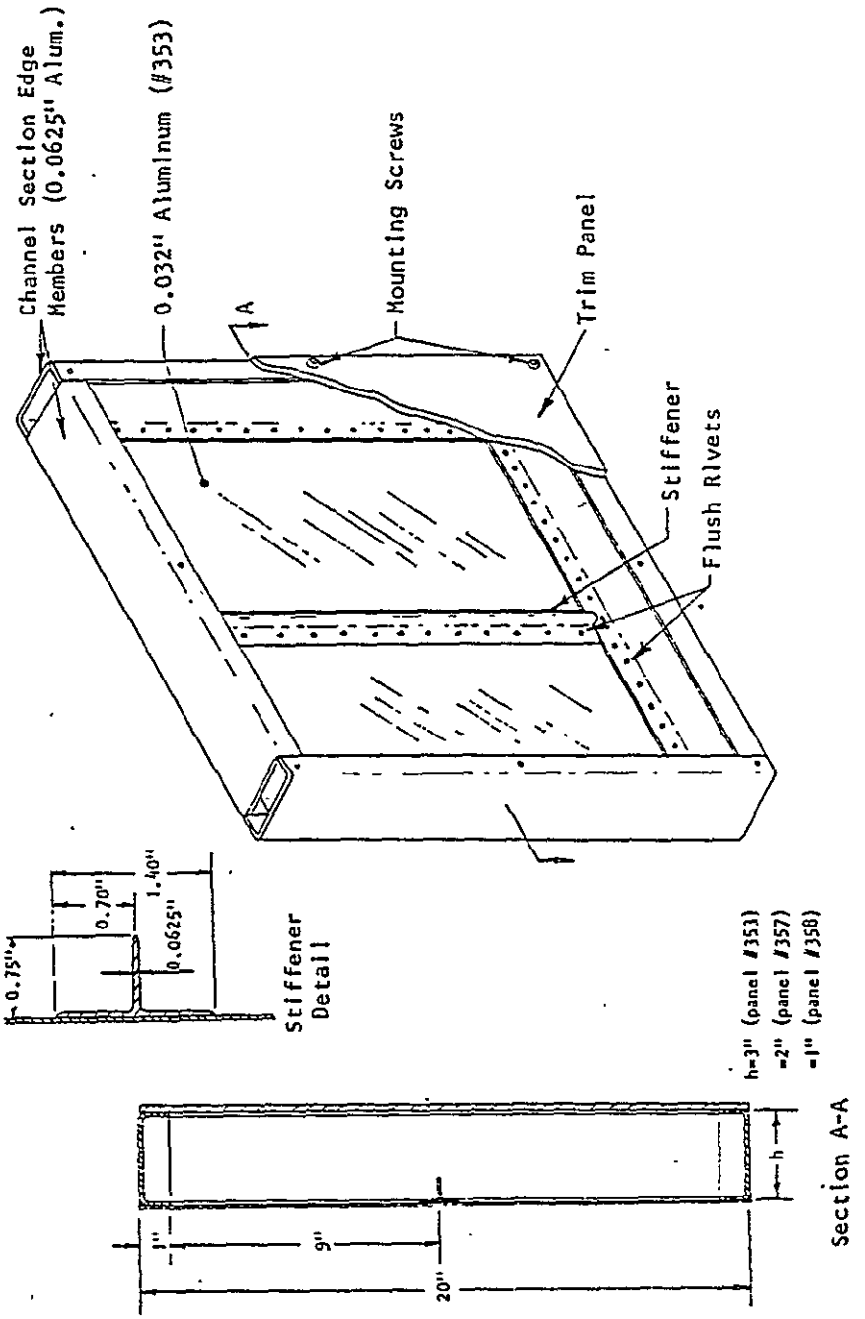

Figure 5.2a: Details of Typical Skin Panels Tested: Group 1, Aluminum with 1 Stiffener

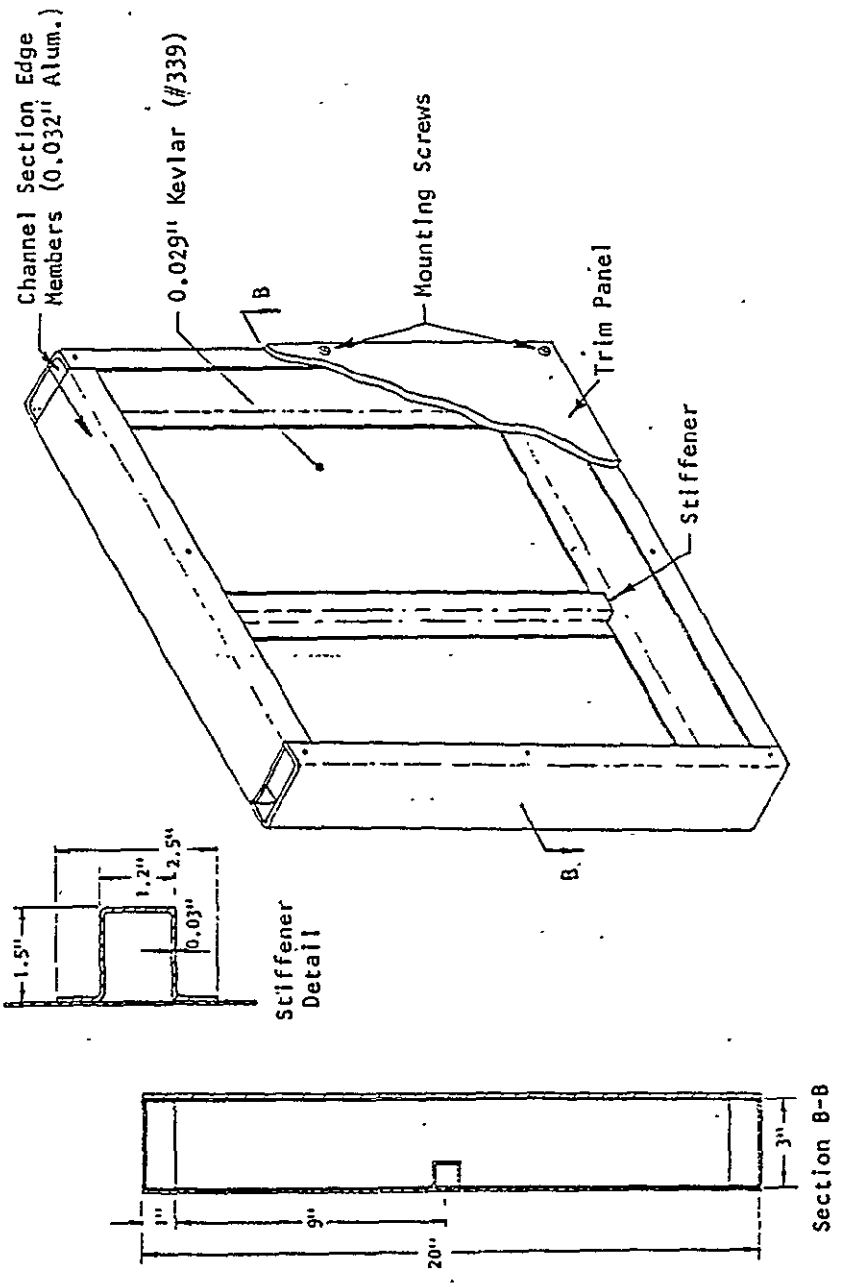

Figure 5.2b: Details of Typical Skin Panels Tested: Group 2, Kevlar with 1 Stiffener

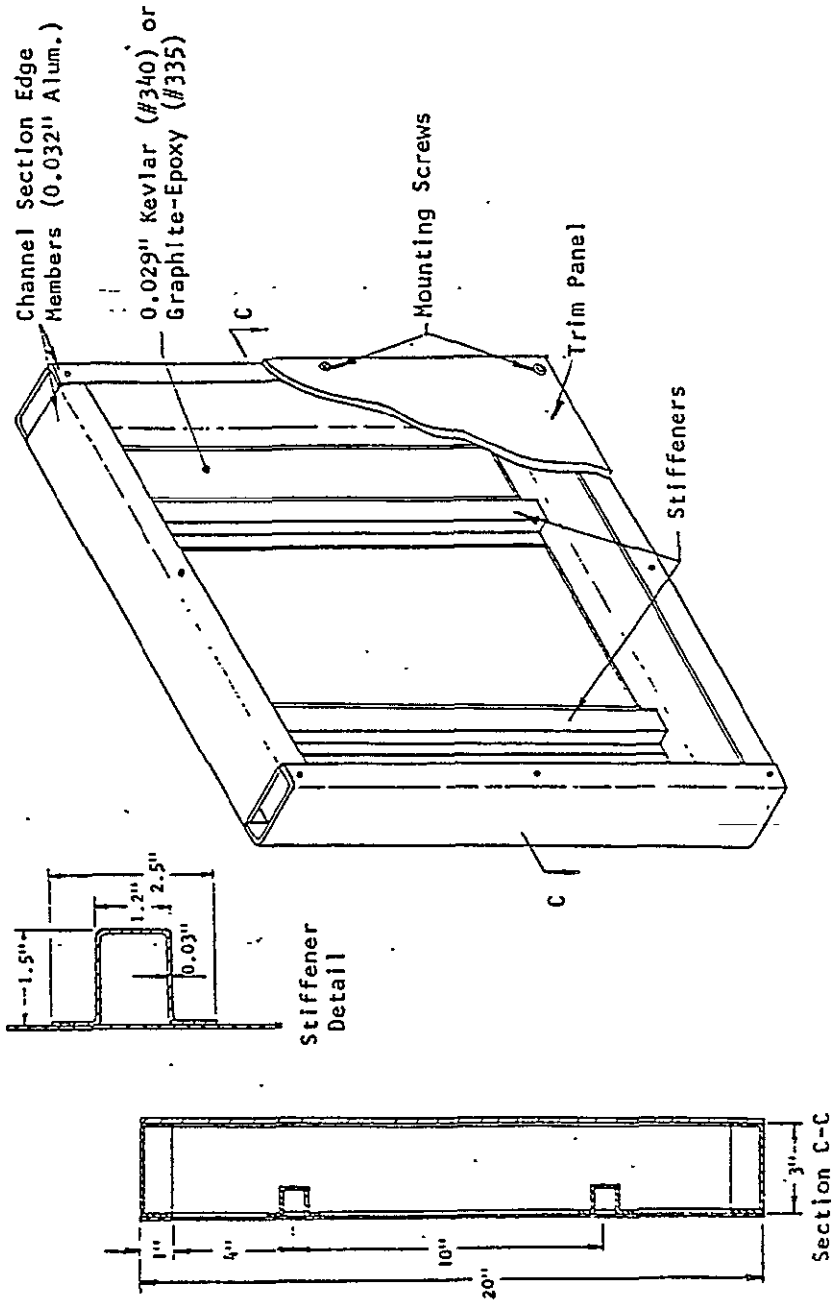

Figure 5.2c: Details of Typical Skin Panels Tested: Group 3, Kevlar or Graphite-Epoxy with 2 Stiffeners

information. The effects of the material and stiffeners were studied using these panels.

Table 5.1: Skin Panels Tested at the KU-FRL Acoustic Test Facilty

Panel	Material	Number of Stiffeners Depth		Thick-ness	Weight*
		(in.)		(in.)	(lb.)
		Group 1			
353	2024-T3 Aluminum	3	1	0.032	1.53
357	2024-T3 Aluminum	2	1	0.032	1.53
358	2024-T3 Aluminum	1	1	0.032	1.53
		Group 2**			
339	Kevlar	3	1	0.029	0.70
340	Kevlar	3	2	0.029	0.85
335	Graphite-Epoxy	3	2	0.029	0.90

*Skin and stiffener weight only

**All composite panels have three layers of the same thickness. Ply orientation is 45°-0°-45°.

The insulation used was loose fiberglass material with a density of 0.7 lb/cubic ft, or 11 kg/m^3. This material came enclosed in very thin vinyl bags and thicknesses of 3, 2, and 1 inch.

The trim panels tested were the typical trim panels being used or being proposed to be used in the general aviation aircraft. The trim panels were constructed of lightweight base materials such as closed-cell polyvinyl chloride foam, aluminum, and fiberglass. The foam panels were usually coated with a protective sheathing to give the foam damage tolerance. Over the base material some type of decorative material (called hereafter "trim panel treatment"), such as leather, simulated leather, upholstery fabric, carpet, etc., is usually applied. The trim panels tested have been divided into three groups, depending on their base material. Group 1 have a Klegecell base, while Group 2 have a Rohacell base. The panels in these groups vary in the thickness of their base material and in their trim panel treatment. Group 3 panels have miscellaneous base material such as compressed fiberglass, 45% open-pore aluminum, and Lexan. These panels and their relevant characteristics are described in Table 5.2.

The skin panel and the trim panel were attached by means of the channel section members (see Figure 5.2). The channel section was riveted along the edges to the aluminum skin. In the case of composite skin panels, they were epoxied. Two types of attachment of the trim panel to this channel section were investigated. In the

Table 5.2: Trim Panels Tested at the KU-FRL Acoustic Test Facility

Panel	Trim Panel Material and Treatment	Area Density (lb/ft^2)
	Group 1	
317	0.125" Klegé-Cell type 75 with 1 layer type A fiberglass both sides	0.128
315	0.25" Klege-Cell type 75 with 1 layer type A fiberglass both sides	0.168
318	Same as #317 but with 0.020" Royalite covering	0.258
	Group 2	
341	0.125" Rohacell grade 51 with 1 layer 120 phenolic pre-preg skin both sides	0.134
323	0.25" Rohacell grade 51 with 1 layer 120 phenolic pre-preg skin both sides	0.180
347	Same as #323 but with 2 layers 120 phenolic pre-preg skin both sides	0.301
342	Same as #341 but with 0.020" Royalite covering	0.279
343	Same as #341 but with 0.5" carpet	0.674
344	Same as #341 but with 0.25" neoprene + leather covering	0.432
325	Same as #323 but with 0.125" neoprene + wool covering	0.428
	Group 3	
312	45% open 0.025" Aluminum with 0.5" foam + leather covering	0.472
314	0.090" Lexan 0.596	
352	0.187" compressed fiberglass with 0.2" carpet	0.450

first case, the trim panel was screwed to the flange by means of eight screws. Most of the tests were carried out in this configuration. The effect of "floating" the trim panel was investigated by using a pressure-sensitive, double-sided adhesive tape. The flange of the channel section was 1" all around; hence, it was not exposed to the direct sound pressure field.

5.3 EXPERIMENTAL INVESTIGATION

5.3.1 INTRODUCTION

The noise reduction tests of the double-wall structures were conducted at the KU-FRL acoustic test facility. Various trim and skin panel combinations were investigated. For each skin and trim panel configuration, the effect of the fiberglass insulation was also tested. The noise reduction curve as a function of frequency was obtained by slowly sweeping the frequency, measuring the source and the receiver microphone levels, and subtracting the receiver microphone level from the source microphone level at each frequency. This was done in two stages: first from 20 Hz to 500 Hz, and then from 500 Hz to 5000 Hz. In the first case the analysis bandwidth was 2 Hz (effective bandwidth 3 Hz), and in the second case it was 10 Hz (effective bandwidth 15 Hz). This was done to get narrow bandwidth at low frequencies as well as to cover a broader frequency range. The gains of output signals could also be changed between these two frequency ranges. All tests were performed at normal angle of incidence and at room temperature and pressure. There was no pressure differential between the source and the receiver side.

Most of the tests were done at least twice to ensure repeatability. The repeatability of the tests was generally good, the results agreeing within 1-2 dB in the low-frequency region. In the high-frequency region the least square lines agreed within 2-4

dB. The noise reduction curves for all the tests are presented in Reference 22.

A typical noise reduction curve of a double-wall structure is shown in Figure 5.3, taken from Reference 22. It can be divided into three parts. In the very low frequency the noise reduction is a function of the stiffness of the skin and the trim panel. This region can be called the stiffness-controlled region. In the second frequency region, varying anywhere from 50 to 600 Hz, two resonance dips dominate the noise reduction. The first one normally corresponds to either the skin or the trim panel fundamental resonance frequency. For the panels tested, resonance frequencies of trim and skin panels are so close that it is not possible to separate them. The second major resonance corresponds to the panel-air-panel described in Reference 9. In the high frequency region (above 600 Hz) the narrow-band analysis (analysis bandwidth 10 Hz) indicates a multitude of resonances, resulting in dips and peaks in the noise reduction curve. These resonances are due to the higher order skin and trim panel modes, double-wall modes, and the cavity modes of the test facility itself. In order to study the trends in this frequency region, a least-square line approximation is used. Previous studies at this facility have indicated that the slope of the least-square lines of simple panels corresponds to the calculated mass law slope (i.e., 6 dB/octave). In general, for the double-wall structure, the slope of the least mean-square line lies anywhere between 6 dB/octave (predicted by mass law for single

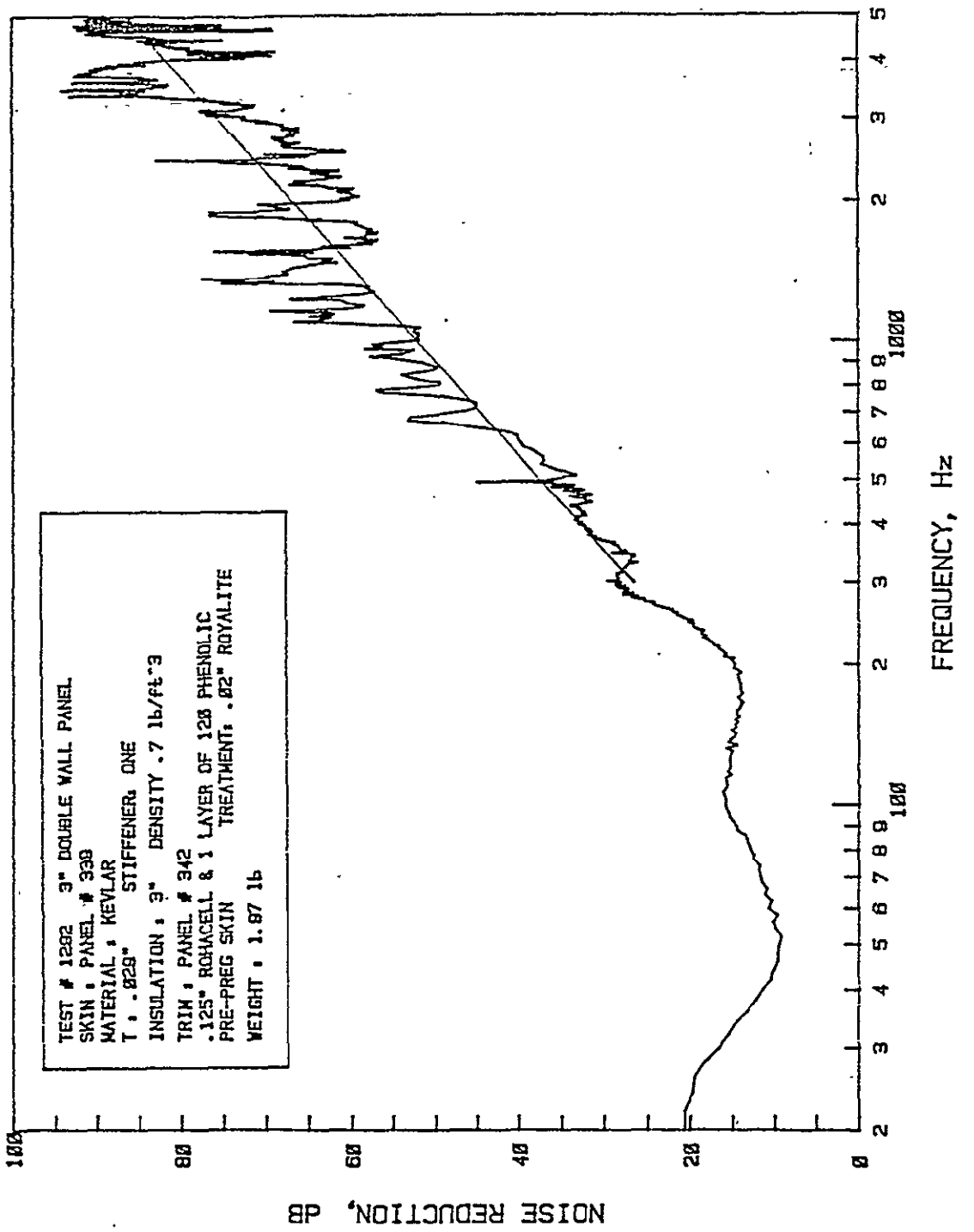

Figure 5.3: Typical Noise Reduction Characteristics of a Double-Wall Panel

panels) and 12 dB/octave (predicted by classical transmission theory for double-wall structures; see Reference 9). The effects of various parameters on the noise reduction values will now be studied at selected frequencies. These frequencies cover the three frequency regions described above. In the high-frequency region only the least-square line will be used. The choice of these frequencies is rather arbitrary and at times can be misleading because of the wide variations in the characteristics of the panels tested. For a complete review, the original noise reduction curves in Reference 22 should be consulted.

Some of these double-wall panels tested showed very high noise reduction values in the high frequency region. This posed some problems in the measurement of the receiver microphone sound pressure levels. At the KU-FRL acoustic test facility the panels could be excited either by a random noise signal or by a slowly-swept sine wave signal. Previous measurements at this facility had shown that the differences in the noise reduction characteristics due to either type of excitation were small, when analyzed through a narrow band analyzer. Because of this, the latter type of excitation was chosen for this series of tests to improve the accuracy in the measurement of receiver microphone signals. With slowly swept sine waves it is possible to concentrate the sound energy over a very small frequency range. This produced a source sound pressure level of 110-120 dB at these frequencies. Hence the receiver microphone signal was correspondingly higher. Even with

this type of excitation the problem was not completely solved. The signal to (ambient) noise ratio was still low in many cases. In addition, during many tests the change in the signal strength within a frequency sweep exceeded the dynamic range of the instrumentation used. As described above, the noise reduction characteristics were investigated by dividing the analysis in two frequency ranges: a) 20-500 Hz with 2 Hz nominal bandwidth, and b) 500-5000 Hz with 10 Hz nominal bandwidth. The dynamic range of the spectrum analyzer used (Spectral Dynamnics Model 335) was 60 dB. Hence the maximum change in the receiver microphone level that could be measured in either of the two passes was only 60 dB. This did not pose any problem either during the low-frequency sweep or with panels exhibiting lower high-frequency noise reduction. However, this was not enough for panels with noise reduction higher than 80 dB in the high-frequency region. In such cases the receiver microphone level was near the maximum level of the analyzer at 500 Hz and was below the minimum level above 3000 Hz. Hence true signal level could not be found at some frequencies above 3000 Hz. The only way this problem could have been overcome was to further subdivide the frequency range. But as mentioned above, the signal levels were so low that further amplification did not improve the results very much, due to deteriorating signal-to-noise ratio. This dynamic range limitation produced scatter in the data when the noise reduction values were higher than 80 dB. Even though this appears to be a serious limitation, it is not so. This phenomenon also occurs in aircraft

interior noise measurements. At very high transmission loss values of the fuselage sidewall, the ambient noise level inside the aircraft may be higher than the level transmitted from the sidewall. Under these conditions it may not be worthwhile to have higher noise reduction for the fuselage sidewall. Also, more importantly, the noise level inside the aircraft is normally dominated by the low frequency noise. Hence, the overall inside aircraft is determined by the low-frequency noise level. The contribution of the sound pressure level at these high frequencies (>3000 Hz) to the overall noise level will be negligible. In practice, if the sound pressure level at any frequency range is below 20 dB of the highest band level, then it may safely be neglected without affecting the overall sound pressure level. Hence a dynamic range of 60 dB is more than adequate to predict the interior levels accurately. Hence, no further attempt was made to increase the dynamic range of the instrumentation used in the test facility.

5.3.2 EFFECT OF SKIN PANEL

The effect of skin panels was investigated using four different types of panels. They were the following:

a. .032" aluminum panel with one "T" stiffener (panel 353)

b. .029" thick, 3-ply (45°-0°-45°) graphite-epoxy laminate with two hat stiffeners (panel 335)

c. .029" thick, 3-ply (45°-0°-45°) Kevlar panel with one hat stiffener (panel 339)

d. .029" thick, 3-ply (45°-0°-45°) Kevlar panel with two hat stiffeners (panel 340).

The parameters investigated with these panels are the effects of the panel material and stiffeners. The noise reduction values of these four panels are compared under similar configurations in Figures 5.4 through 5.11. These figures show the noise reduction values at four selected frequencies: two in the low-frequency region (40 and 100 Hz) and two in the high-frequency region (1000 and 3000 Hz). The noise reduction values at 300 and 500 Hz are not plotted, as they fall in the resonance frequency region. Because the panels are so different in their characteristics, the X-axes in these figures are panel numbers and do not represent any continuously varying parameters. Hence these figures are essentially bar charts with values at four frequencies. The influence of the skin panels is plotted for trim panels 312, 314, 315, 318, 425, 342, 344, and 352. For each trim panel two figures are given: one with the fiberglass insulation between the skin and the trim panel, and the other without (i.e., air gap). In all cases the depth of the double wall was maintained at three inches.

The effect of the skin panel material can be studied by comparing the noise reduction values of panels 335 (graphite-epoxy), 340 (Kevlar), and 353 (aluminum). There is a slight difference in their thickness: both Kevlar and graphite-epoxy panels are .029"

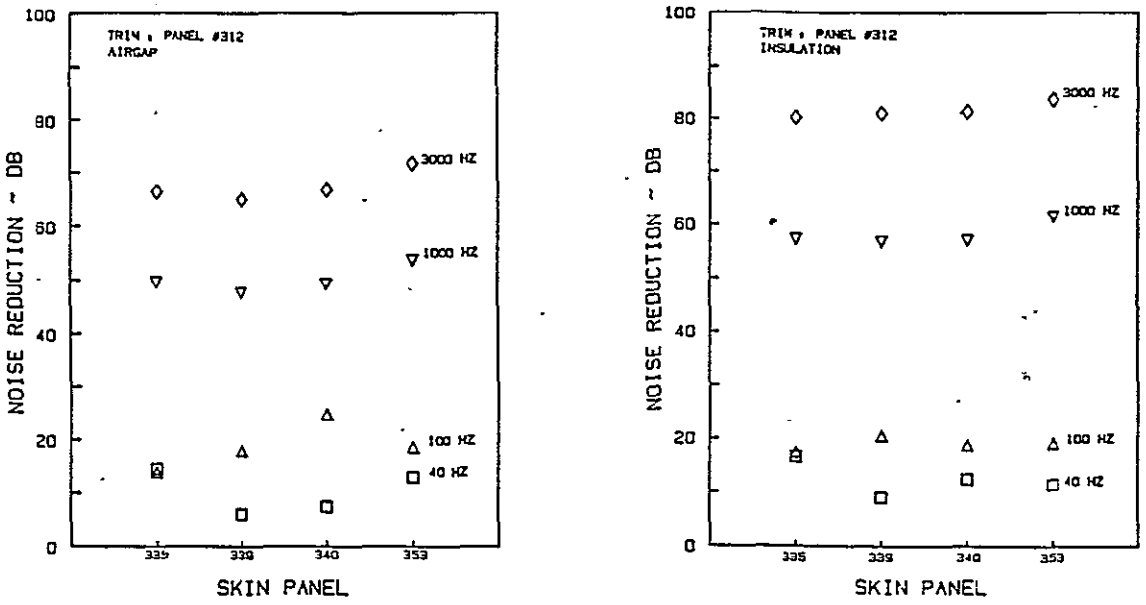

a. Airgap

b. Fiberglass Insulation

Figure 5.4: Effect of Skin Panel on the Noise Reduction Characteristics of a Double-Wall Panel with Trim Panel 312

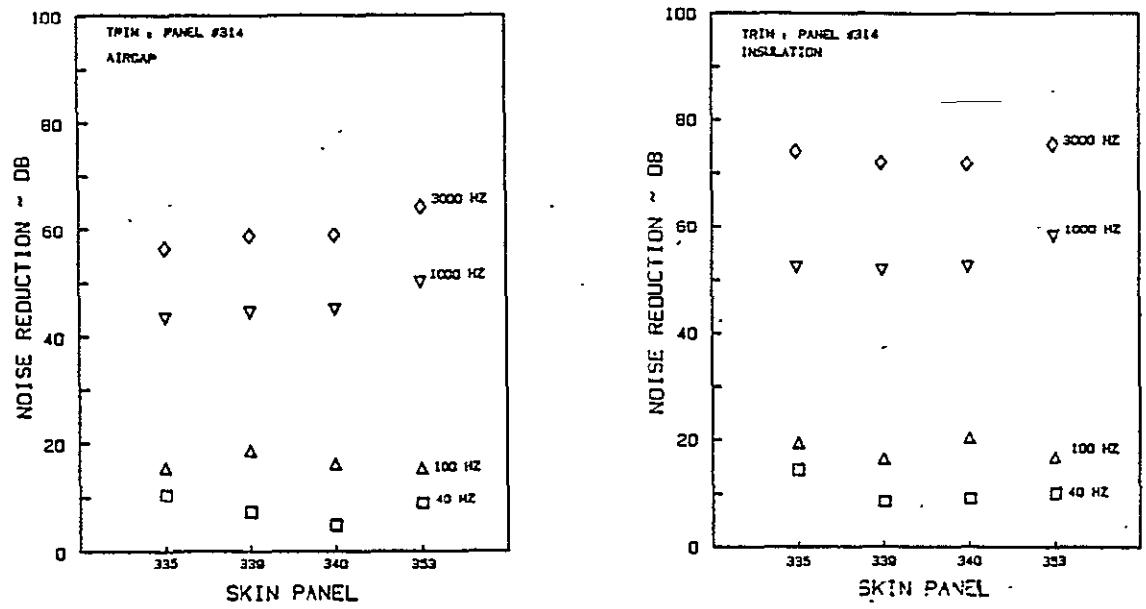

a. Airgap

b. Fiberglass Insulation

Figure 5.5: Effect of Skin Panel on the Noise Reduction Characteristics of a Double-Wall Panel with Trim Panel 314

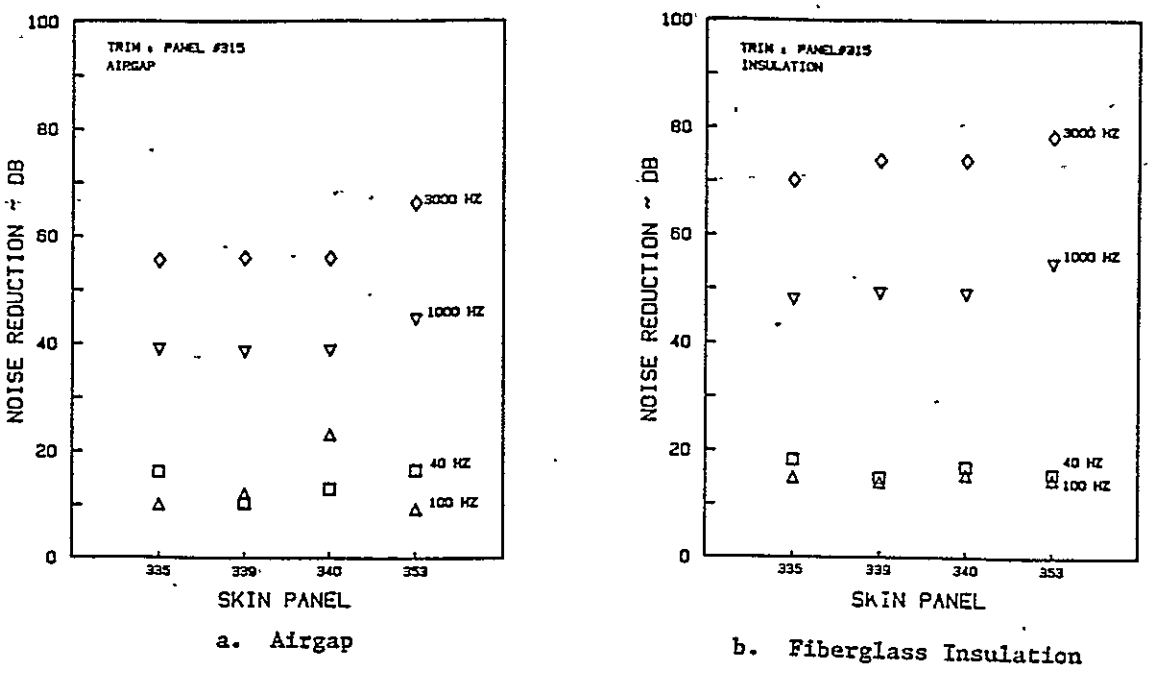

a. Airgap

b. Fiberglass Insulation

Figure 5.6: Effect of Skin Panel on the Noise Reduction Characteristics of a Double-Wall Panel with Trim Panel 315

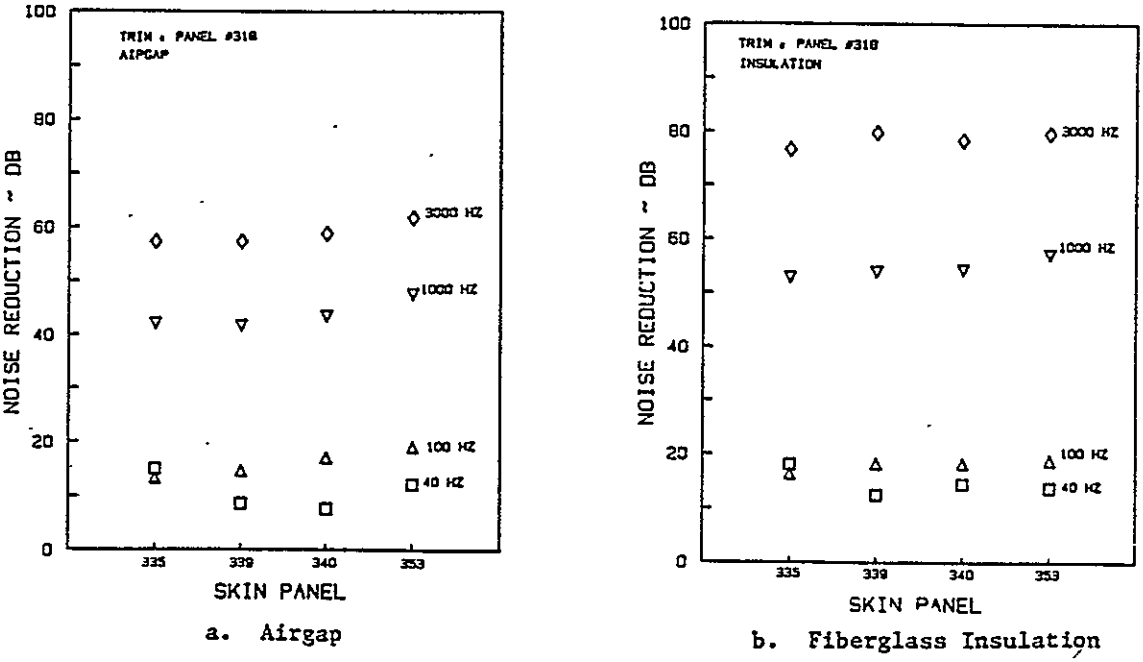

a. Airgap

b. Fiberglass Insulation

Figure 5.7: Effect of Skin Panel on the Noise Reduction Characteristics of a Double-Wall Panel with Trim Panel 318

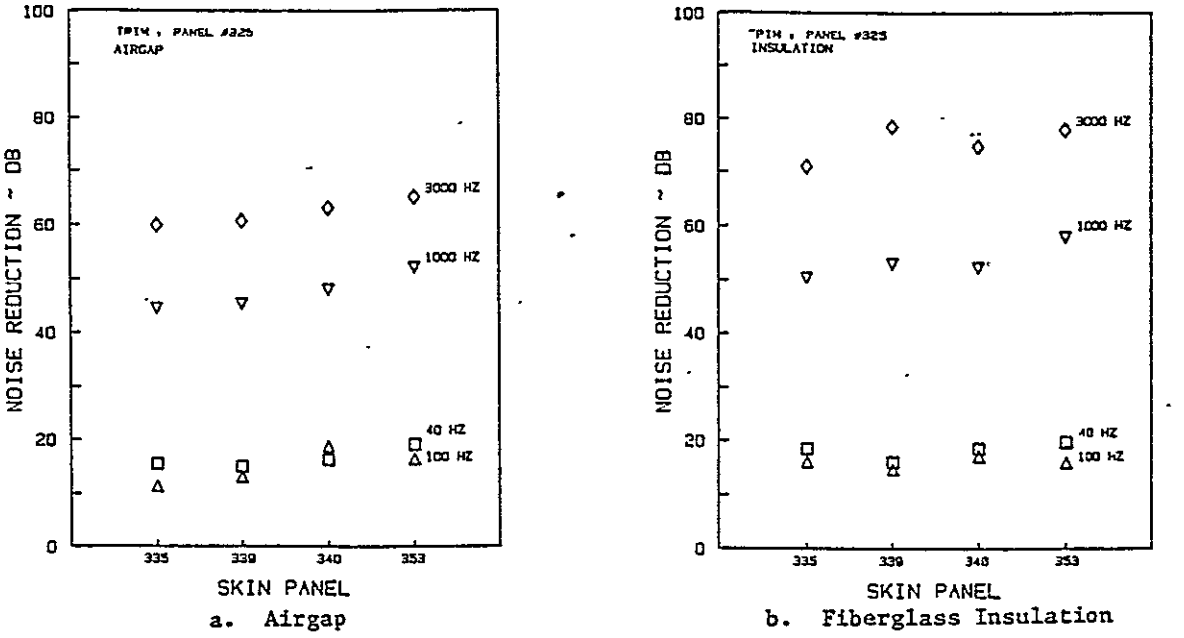

Figure 5.8: Effect of Skin Panel on the Noise Reduction Characteristics of a Double-Wall Panel with Trim Panel 325

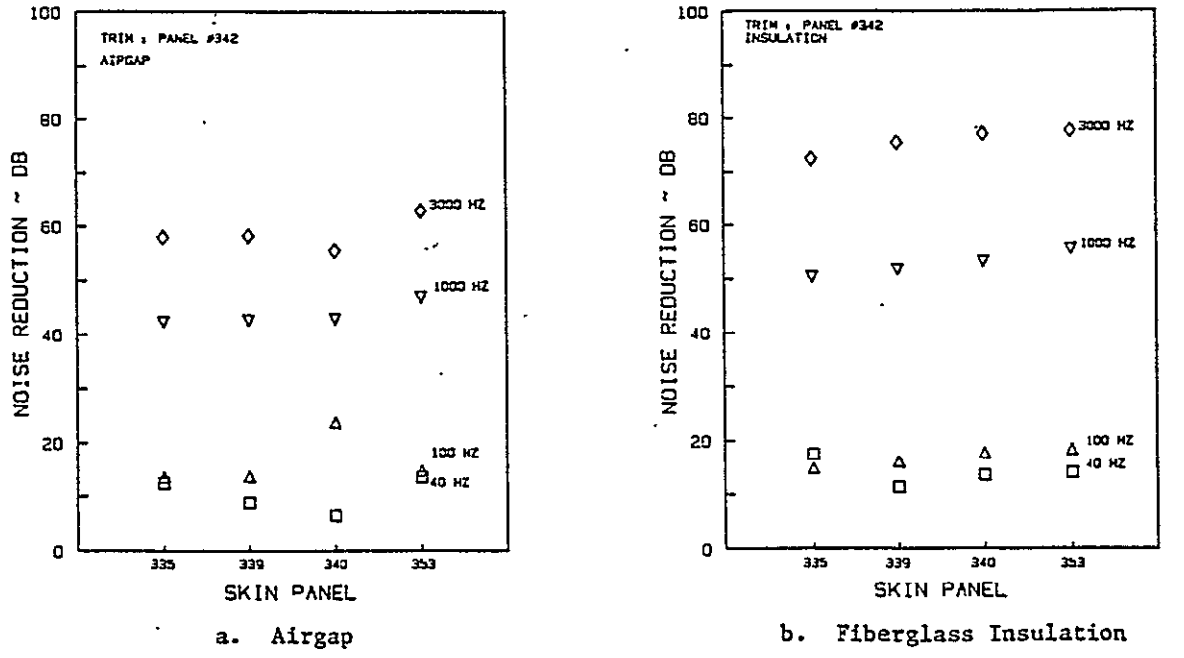

Figure 5.9: Effect of Skin Panel on the Noise Reduction Characteristics of a Double-Wall Panel with Trim Panel 342

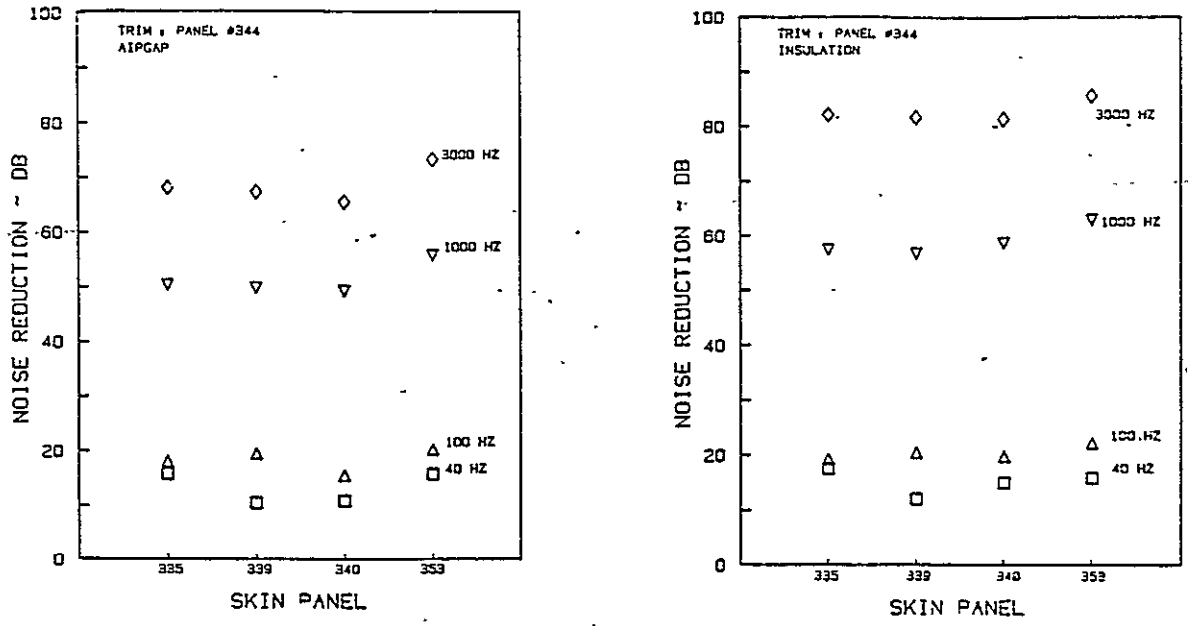

a. Airgap

b. Fiberglass Insulation

Figure 5.10: Effect of Skin Panel on the Noise Reduction Characteristics of a Double-Wall Panel with Trim Panel 344

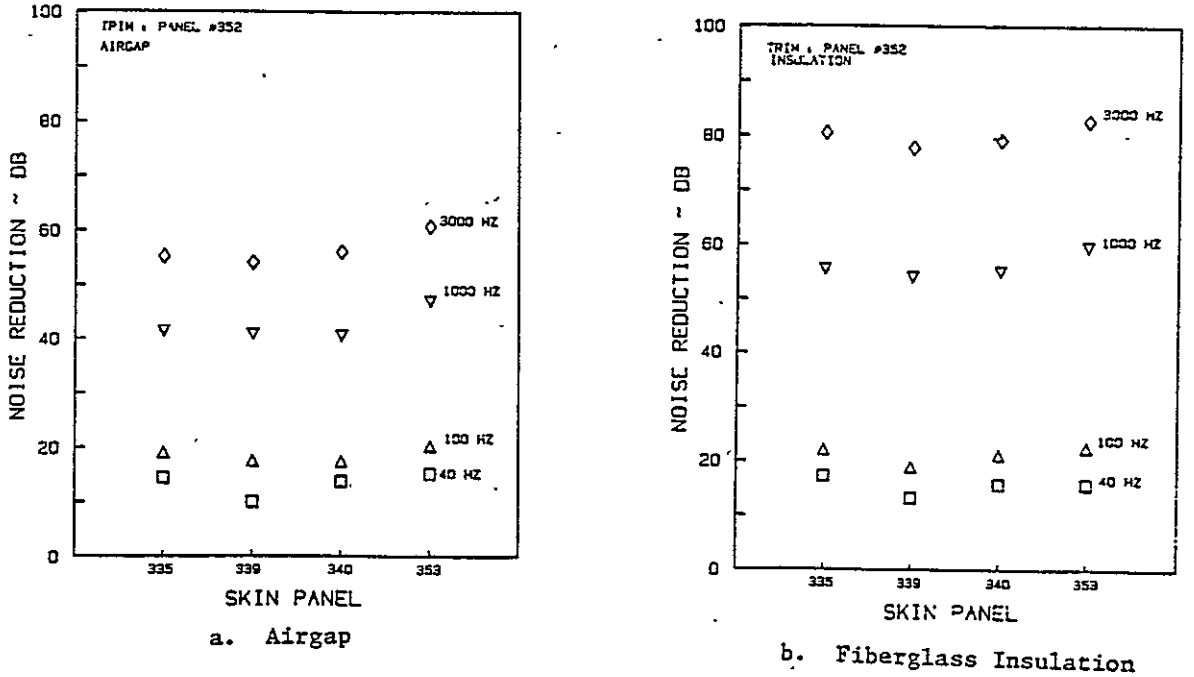

a. Airgap

b. Fiberglass Insulation

Figure 5.11: Effect of Skin Panel on the Noise Reduction Characteristics of a Double-Wall Panel with Trim Panel 352

thick, and the aluminum panel is .032" thick. The mass and the stiffness are the major variables. The weights of these individual panels are .9 lb (graphite-epoxy panel 335), .85 lb (Kevlar panel 340), and 1.35 lb (aluminum panel 353). Kevlar panel 339, which has one stiffener, weighs .7 lb. At low frequencies the noise reduction of double-wall panels is a function of the stiffness of the skin and the trim panel. In these figures, the trim panel has been kept the same for each plot. Hence the noise reduction at 40 Hz in each plot is a function only of the stiffness of the skin panel being studied. However, the stiffness of the skin panel is a function not only of the material properties but also of the number and the type of the stiffeners used. The aluminum and the composite panels had different types of stiffeners. In the case of aluminum it was an extruded "T" section. For composite panels it was a hat section. This precludes any conclusions about the relative stiffness effects of the various skin materials. In general, for the skin panels tested, the graphite-epoxy skin panel and the aluminum skin panel have the same noise reduction at 40 Hz, while the Kevlar skin panel has up to 7 dB less noise reduction. This is consistent with the single panel tests reported in Reference 6. The noise reduction values at 100Hz vary very widely because they are very close to either the skin or the trim panel fundamental resonance frequency.

At frequencies of 1000 Hz and 3000 Hz, the noise reduction is mainly a function of the surface density of the double-wall panel. All other parameters being constant, it is a function of the skin

panel surface density. Since the surface densities of the graphite-epoxy panel (panel 335) and the Kevlar panel (panel 340) are nearly equal, they have nearly the same noise reduction. The aluminuim skin panel (panel 353) is considrably heavier and hence has higher noise reduction. For double-wall panels with an air gap, the increase in noise reduction values closely match the theoretically predicted 3-4 dB at 1000 Hz. At 3000 Hz two phenomena occur. First, the first harmonic of the double-wall resonance falls in this frequency region. The dips in the noise reduction introduced by this resonance are strong enough to mask the increased noise reduction due to higher surface density of the aluminum skin panel. Second, this is the frequency region with very high noise reduction. Hence, as explained in Section 5.3.1, the variations in the noise reduction values are not truly reflected in the results, due to dynamic range limitations. Hence the effect of the increased mass of the aluminum skin panel is not seen in the experimental results. This is especially true with fiberglass insulation. Panels with insulation show very high noise reduction (>80 dB) above 3000 Hz.

The effect of the stiffener can be studied by comparing the results of the Kevlar panel with one stiffener (panel 339) and with two stiffeners (panel 340). In this case other parameters of the double-wall panels are the same. At very low frequency of 40 Hz, the effect of the stiffener is to increase the noise reduction by the increase in the stiffness of the skin panel. This trend is

confirmed in all but three cases tested (see Figure 5.4 through 5.11). The exception occurred in two cases with air gap. These exceptions are considered to be due to experimental scatter. The increase in noise reduction at 40 Hz due to increased stiffness is less than three dB. Once again at 100 Hz, near the fundamental resonance frequency of the skin/trim panel, there is a wide fluctuation in the test results. The results show a very small increase in noise reduction at 1000 and 3000 Hz due to the two stiffeners. However, this increase is so small that it is within the scatter of the experimental results.

5.3.3 EFFECT OF PANEL DEPTH

In general aviation aircraft the space available for the installation of double-wall type structures for interior noise cotrol is very limited, due to already small interior dimensions. A quick survey among the manufacturers indicated that two-three inches is about the maximum depth that can be allowed. Hence the effect of the double-wall depth was investigated for only three cases: one inch, two inches, and three inches. For this investigation, aluminum skin panel and four trim panels were used. The trim panels tested were one from each group of the base materials described in Section 5.2. These panels were 312, 318, 325, and 352. The tests were performed both with and without the fiberglass insulation in the space between skin and trim panels. The results from the tests

have been cross plotted in Figures 5.12 through 5.15 for the cases investigated. For each test condition six frequencies are shown.

At 40 Hz, which is below the fundamental resonance frequency of the skin or trim panels, the experimental results show a very small decrease with increase in panel depth. The decrease was less than three dB in all cases. This trend was not predicted by the simple theory described in Chapter 6.. It is believed to be due to the trim panel attachment procedure used in the investigation. The trim panel was attached to the edge channel members by means of screws. The depth of these channel sections determines the panel thickness (see Figure 5.2). It is possible that with higher panel depth, the stiffness of this member decreases, decreasing the double-wall panel stiffness. This decrease in stiffness may cause the reduction experienced in the test results. This effect is present even with the insulation. An opposite phenomenon occurs at 100 Hz. This frequency is on the other side of the fundamental resonance frequency for most of the panels, and hence a slight increase is expected with increase in panel depth. The increase was 3-5 dB. The decrease in stiffness as described above can cause such a trend.

The noise reduction values at 300 and 500 Hz are also plotted in Figures 5.12 through 5.15. This frequency region is the most important region for the interior noise control of the general aviation aircraft. The noise reduction values at 300 Hz show an increase, with the increase in panel depth. The shape of the curves, however, is different for different trim panels. This is

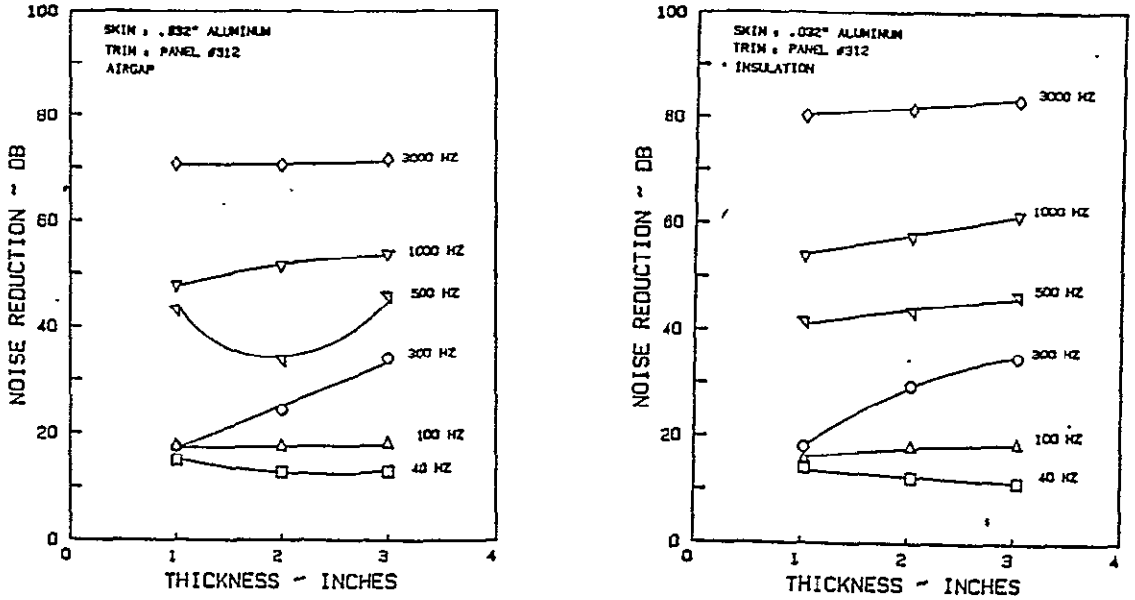

a. Airgap

b. Fiberglass Insulation

Figure 5.12: Effect of Panel Depth on the Noise Reduction Characteristics of a Double-Wall Panel with Aluminum Skin and Trim Panel 312

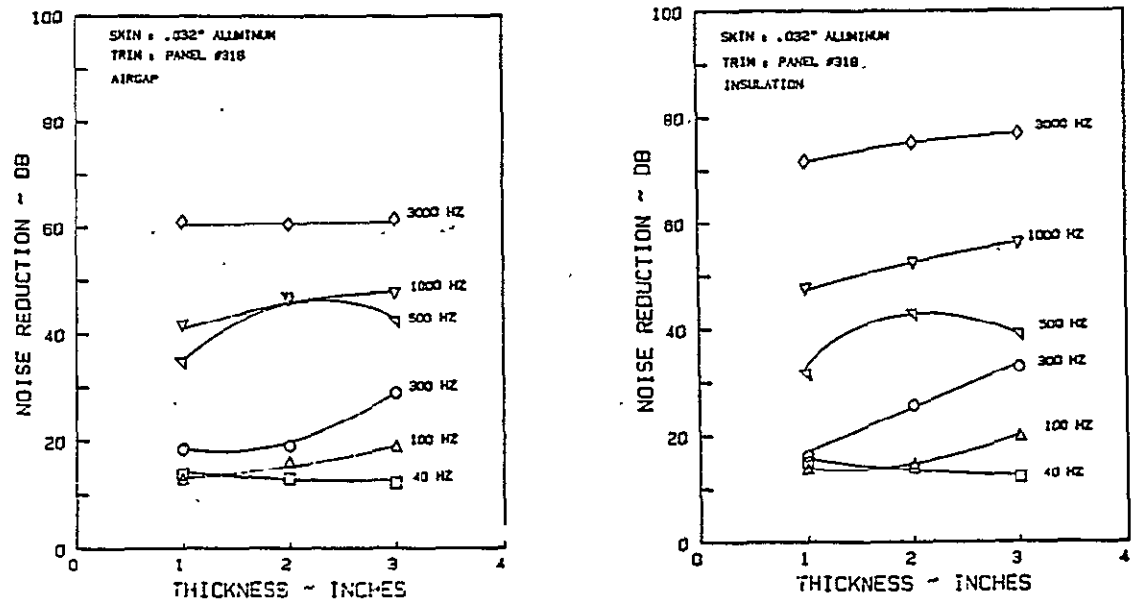

a. Airgap

b. Fiberglass Insulation

Figure 5.13: Effect of Panel Depth on the Noise Reduction Characteristics of a Double-Wall Panel with Aluminum Skin and Trim Panel 318

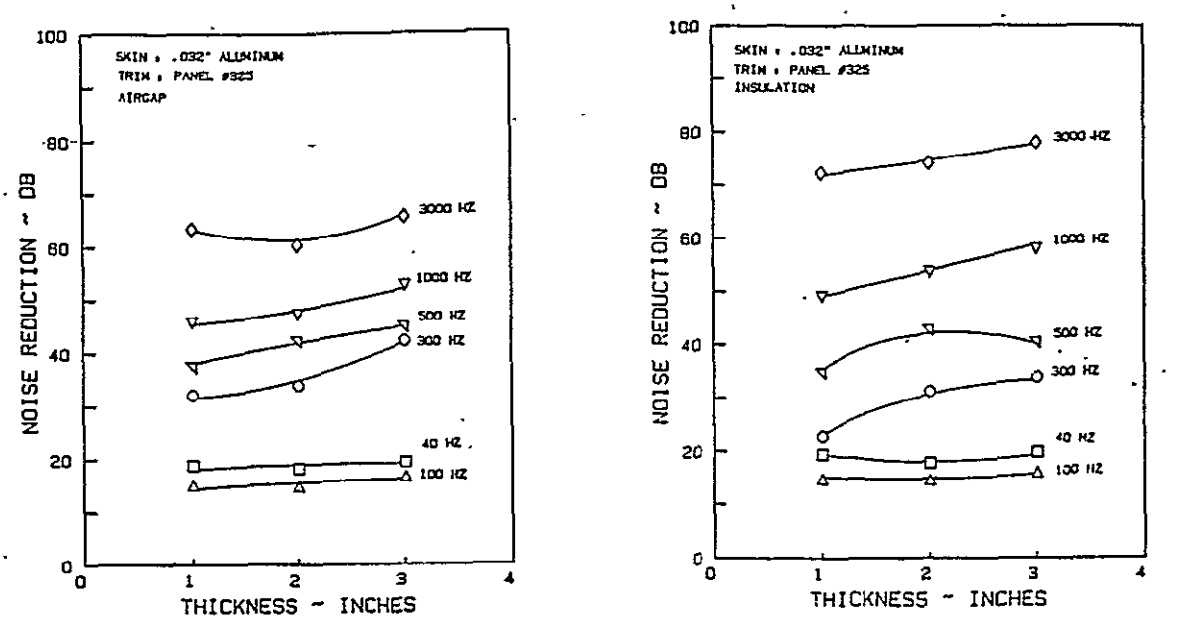

a. Airgap

b. Fiberglass Insulation

Figure 5.14: Effect of Panel Depth on the Noise Reduction Charactistics of a Double-Wall Panel with Aluminum Skin and Trim Panel 325

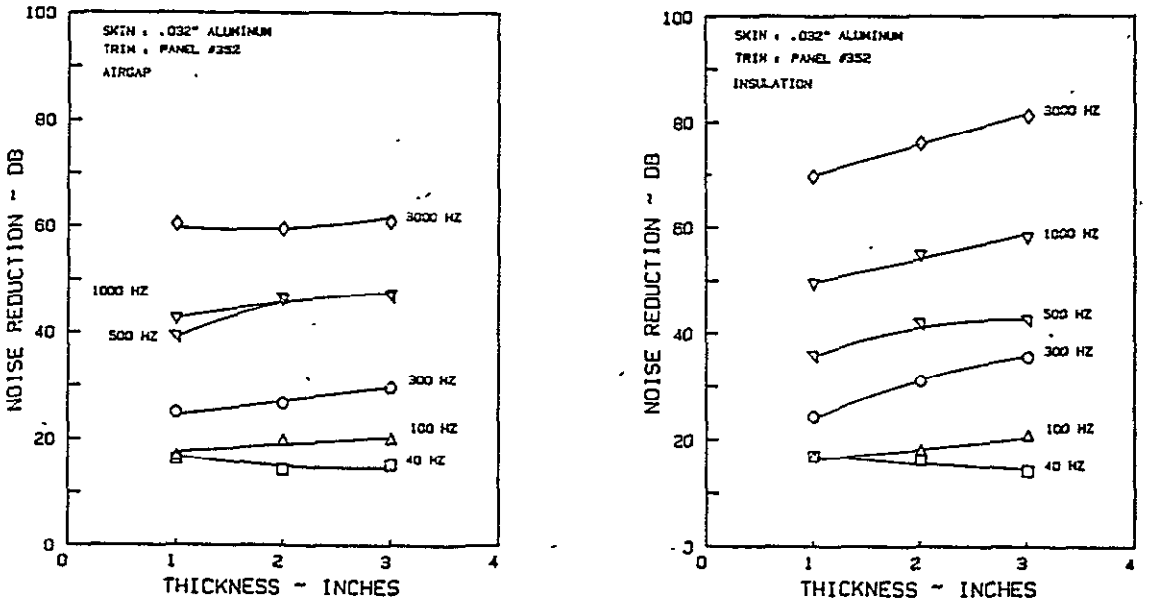

a. Airgap

b. Fiberglass Insulation

Figure 5.15: Effect of Panel Depth on the Noise Reduction Characteristics of a Double-Wall Panel with Aluminum Skin and Trim Panel 352

because the experimental double-wall resonance frequency occurs in this region. The noise reduction values depend very much on the value of the double-wall resonance frequency. The simple theory used in the theoretical analysis overpredicts the double-wall resonance frequency (see Chapter 6). Hence comparisons of the trend of the noise reduction values at 300 Hz could not be made. The trend of the frequency values themselves is the same--only shifted by 75-100 Hz depending on the panel configuration. Similarly, at 500 Hz the variations in noise reduction could not be explained in terms of the simple theory. Except for trim panel 312 with air gap, the experimental results show either a steady increase or a slight peaking at two-inch depth. The double-wall panel with trim panel 312 has a definite dip at 500 Hz at 2" panel depth. It is believed that the porous aluminum base material may contribute to this phenomenon.

At 1000 Hz, for all cases tested the noise reduction shows a steady increase with increase in panel depth. As the panel depth is increased, the first harmonic of the double-wall resonance frequency decreases. On either side of this frequency, the slope of the noise reduction curve will be high. At 1000 Hz we are in this region for all three depths tested. This slope is higher if the resonance frequency is closer to 1000 Hz. Because of this the noise reduction of the three-inch depth panel is higher than that of the two-inch panel. The increase is smaller for the air gap (6 dB max.) than for the insulation (11 dB max.). Some of the increase in noise reduction of the panels with insulation is due to the viscous shear

in the insulation. This shear loss manifests itself as the real part of the complex propagation constant (see Reference 9). The effect of the harmonic of the double-wall resonance frequency is more apparent at 3000 Hz with air gap. The resonance in this case is so strong that it lowers the overall noise reduction of the double-wall panels with two-inch depth at this frequency. Hence the cross plot of noise reduction vs thickness shows a dip at two inches at this frequency. These results are consistent with the theoretical predictions and also with the results of the dual pane window tests (Reference 9) carried out at this test facility. The addition of the insulation damps out this dip. In addition, viscous shear losses in the insulation increase the noise reduction beyond 80 dB for three (panels 312, 318, and 325) out of the four trim panels tested. As described in Section 5.3.1, any increase in the noise reduction over this value does not get truly reflected in the test results. In the case of trim panel 352, which has a lower noise reduction at one-inch panel depth (>70 dB), the effect of increase in depth is more prominent.

5.3.4 EFFECT OF FIBERGLASS INSULATION

Even though all double-wall tests have been done with and without air gaps, aluminum skin panel and four trim panels (312, 318, 325, and 352) were chosen for comparative study. The cross plots at 40, 100, 1000, and 3000 Hz are given in Figures 5.16 through 5.19. The Y-axis of these figures is the change in noise

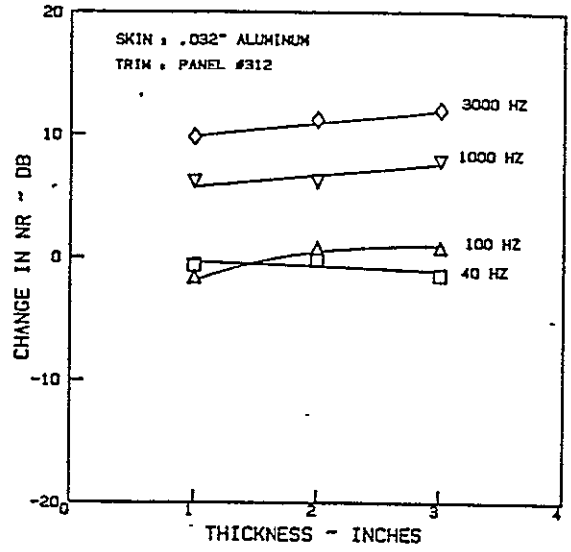

Figure 5.16: Effect of Fiberglass Insulation on the Noise Reduction Characteristics of a Double-Wall Panel with Aluminum Skin and Trim Panel 312

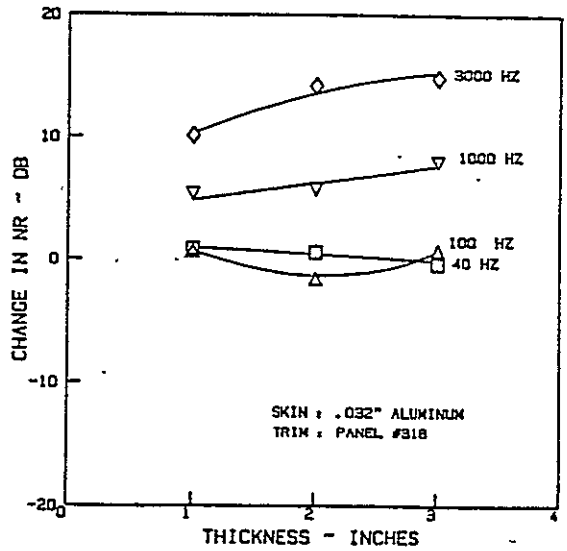

Figure 5.17: Effect of Fiberglass Insulation on the Noise Reduction Characteristics of a Double-Wall Panel with Aluminum Skin and Trim Panel 318

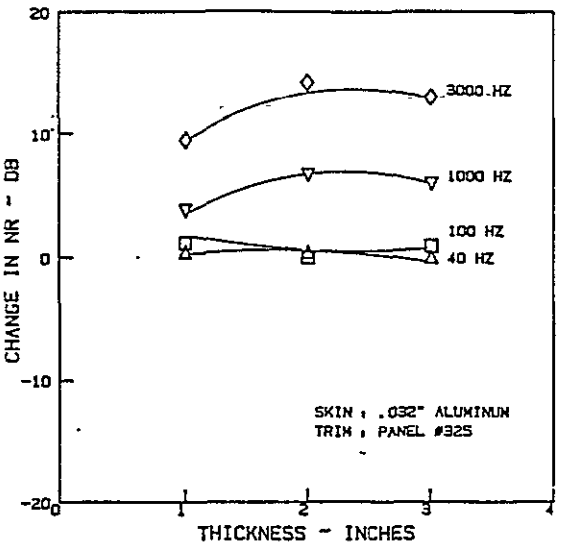

Figure 5.18: Effect of Fiberglass Insulation on the Noise Reduction Characteristics of a Double-Wall Panel with Aluminum Skin and Trim Panel 325

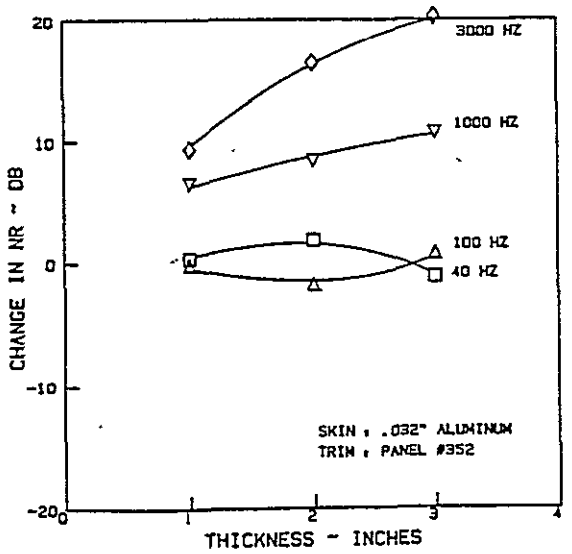

Figure 5.19: Effect of Fiberglass Insulation on the Noise Reduction Characteristics of a Double-Wall Panel with Aluminum Skin and Trim Panel 352

reduction due to the fiberglass insulation of density , .7 lb/cu.ft or 11 kg/m^3. These values were obtained by subtracting the noise reduction values of the panels with insulation, from those without the insulation (shown in Figures 5.12 through 5.15). At 40 and 100 Hz the effect of the fiberglass is negligible. In fact, in some cases it is even negative. At high frequencies the fiberglass has two effects, as described in the previous section. First, it eliminates the dip in the noise reduction curve observed due to the harmonics of the double-wall resonance frequencies. Secondly, the sound level is also attenuated by the viscous shear losses when it travels through the porous media (Reference 9). At any given frequency the attenuation due to this effect is linearly proportional to the thickness of the insulation. The experimental results tend to confirm this trend in those cases, where the noise reduction measurements are not affected by the limitation of the dynamic range of the instruments. At 3000 Hz the increase due to the insulation varies from 3 dB (for trim panel 312) to 11 dB (for trim panel 352) for two inch variation in the panel depth.

5.3.5 EFFECT OF TRIM PANELS

The interior trim panels are used in the general aviation industry for decorative purposes. They also form a part of the interior noise control treatment. But it is the decorative purpose which determines the type of material and treatment that will be used. Normally a trim panel has a base material, which provides the

stiffness and also makes it easier to install. The treatment such as leather, simulated leather, upholstery, etc., is applied solely for decorative purposes. Theoretically, these panels are treated as limp panels having mass-law impedance. Tests at this facility of various materials have shown that such an assumption may not be valid (References 6). During the present series of tests, the effect of these panels was investigated when used as a part of a double-wall struture. As described in Section 5.3, the trim panels were divided into three groups, based on their base material. Tables 5.3 and 5.4 give the noise reduction values at 40 and 3000 Hz for four skin panels. As expected, there is considerable scatter in the data. Figures 5.20 through 5.27 show this effect as a function of the total panel surface density. For each skin panel the noise reduction obtained is plotted as a function of the surface density of the panel. Since the other panel parameters have been held constant for each plot, the variation of the surface density in each figure is due to the variation of the panel surface (area) density of the trim panels.

Table 5.3: Effect of Trim Panels on Noise Reduction Characteristics of Double-Wall Panel; 40 Hz

	Airgap				Insulation			
	Skin Panel				Skin Panel			
Trim Panel	353	335	339	340	353	335	339	340
312	13	15	6	7	12	17	9	13
314	9	11	7	7	10	15	9	9
315	17	16	11	13	16	18	15	15
317	13	12	7	8	13	16	12	15
318	12	15	9	8	13	17	11	13
323	19	17	16	15	19	21	15	17
325	18	15	15	15	20	19	16	18
341	14	14	7	8	15	16	13	15
342	14	12	9	8	14	18	12	14
343	9	12	7	6	13	13	11	11
344	14	15	9	9	14	16	10	13
* 347	24	25	19	20	23	24	19	22
352	15	16	10	13	14	16	12	13

*Has the highest noise reduction at 40 Hz.

Table 5.4: Effect of Trim Panels on Noise Reduction Characteristics of Double-Wall Panel; 3000 Hz

		Airgap				Insulation			
		Skin Panel				Skin Panel			
	Trim Panel	353	335	339	340	353	335	339	340
*	312	72	66	65	67	84	80	80	80
	314	64	58	59	59	76	75	73	73
	315	66	56	56	56	78	70	73	74
	317	61	57	57	55	71	69	71	70
	318	62	57	57	59	78	75	77	78
	323	58	54	52	58	74	69	76	74
	325	65	60	61	63	78	71	78	77
	341	59	56	57	55	75	69	75	73
	342	63	58	55	58	78	73	76	77
	343	68	65	67	66	77	74	75	74
*	344	72	67	66	64	84	80	80	80
	347	60	54	54	54	73	69	74	72
	352	61	55	54	56	80	78	76	77

*Have the highest noise reduction at 3000 Hz

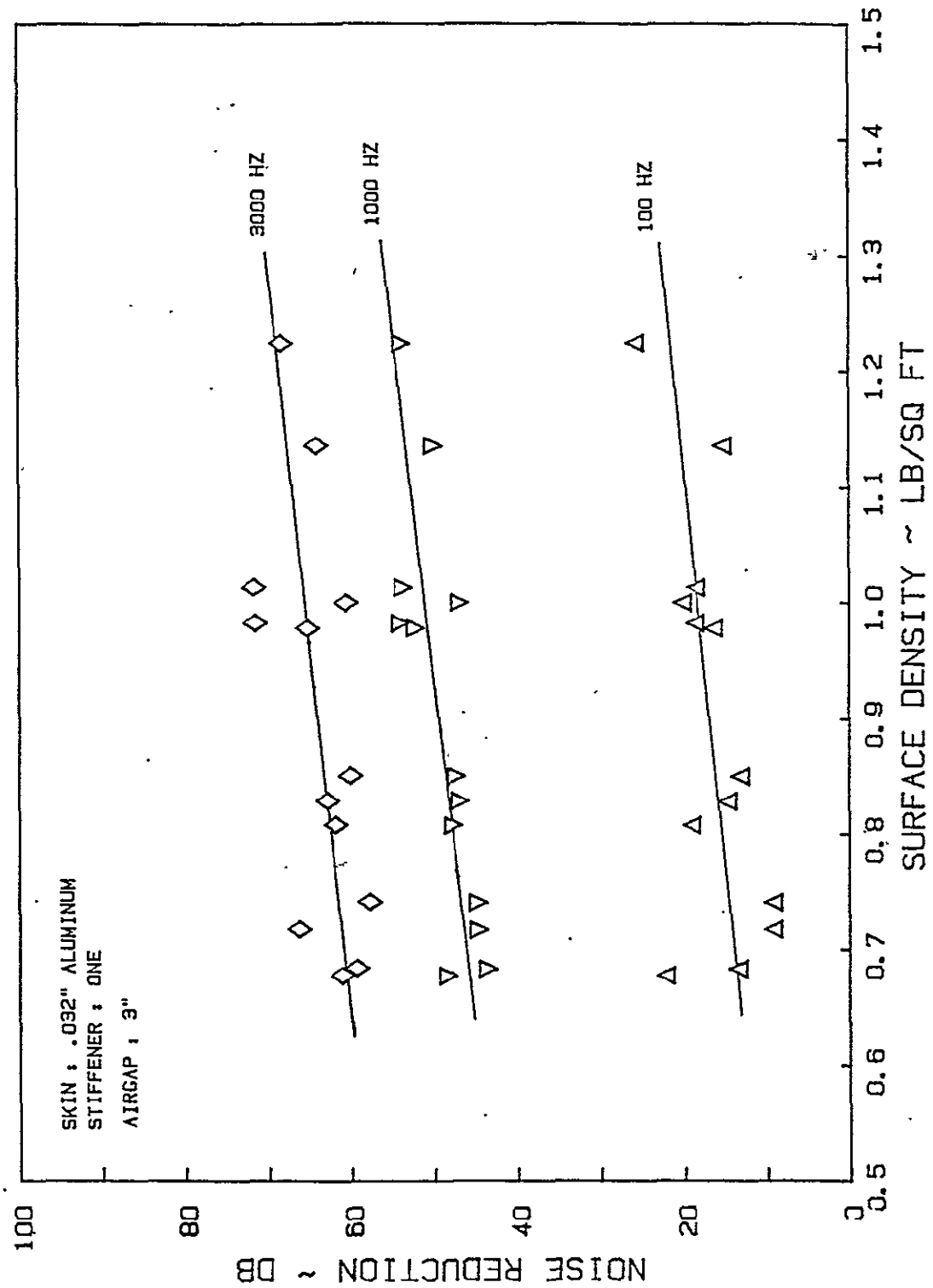

Figure 5.20: Effect of Total Panel Area Density on the Noise Reduction Characteristics of a Double-Wall Panel with Aluminum Skin (Panel 353)and Airgap

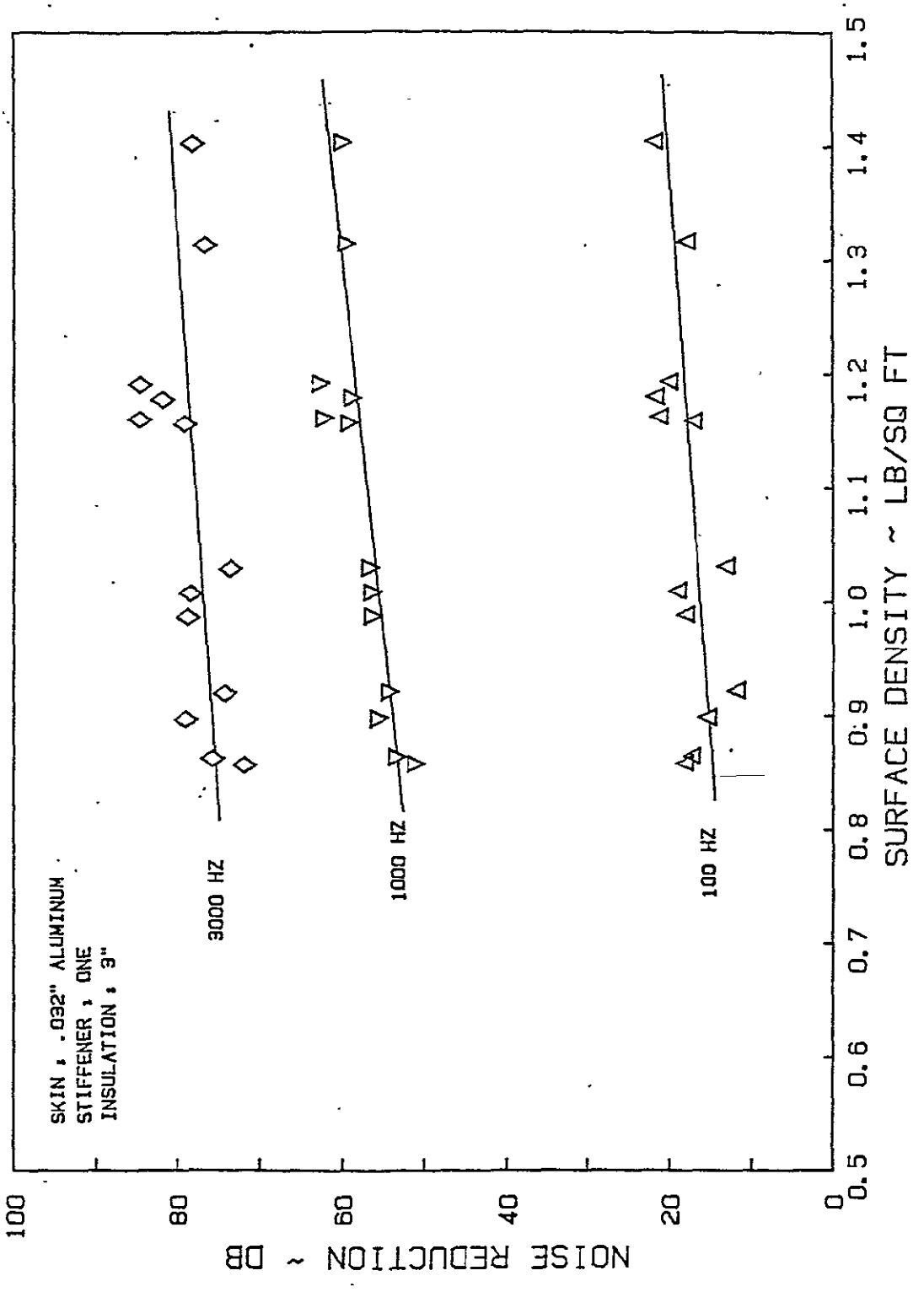

Figure 5.21: Effect of Total Panel Area Density on the Noise Reduction Characteristics of a Double-Wall Panel with Aluminum Skin (Panel 353) and Insulation

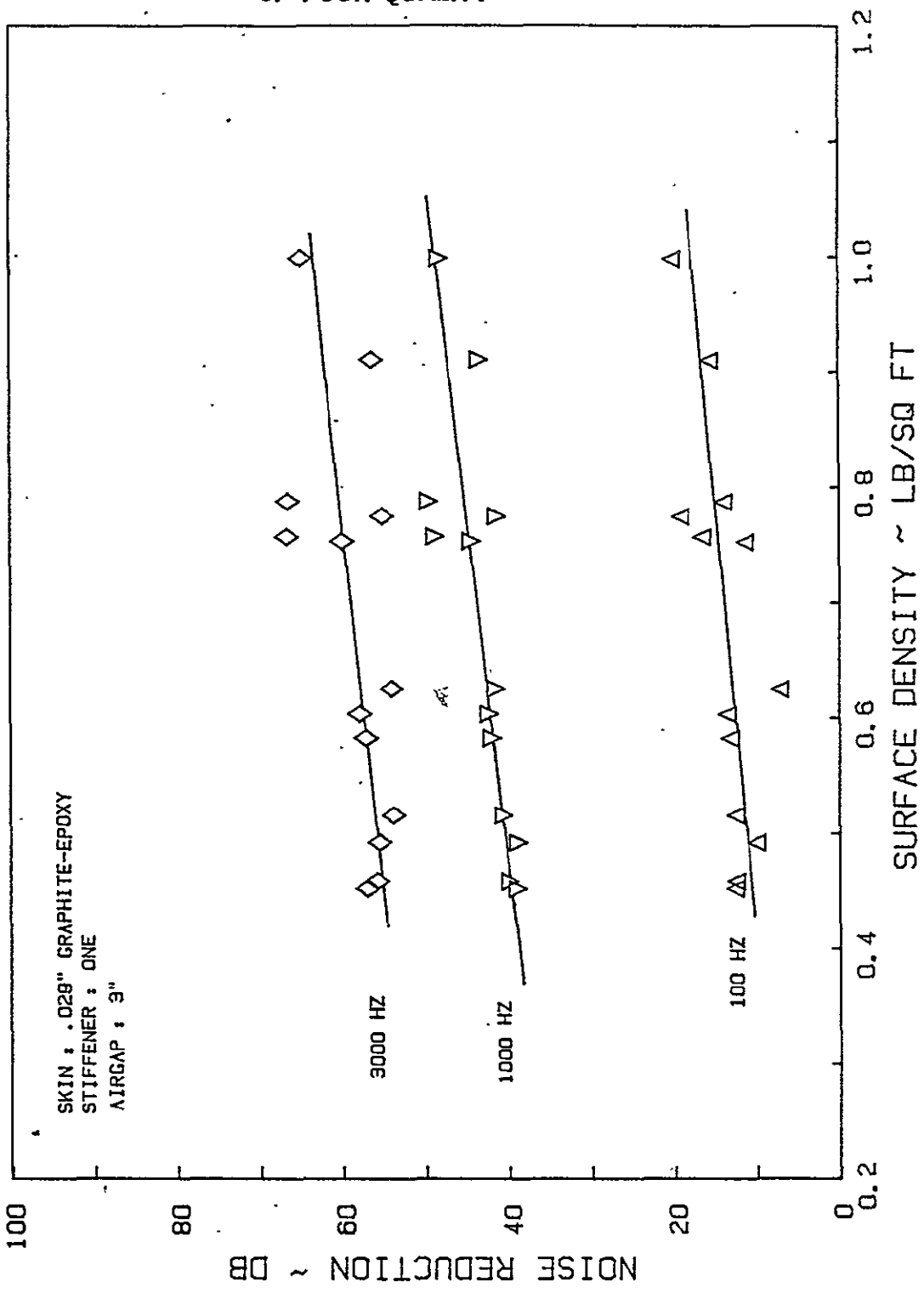

Figure 5.22: Effect of Total Panel Area Density on the Noise Reduction Characteristics of a Double-Wall Panel with Graphite-Epoxy Skin (Panel 335) and Airgap

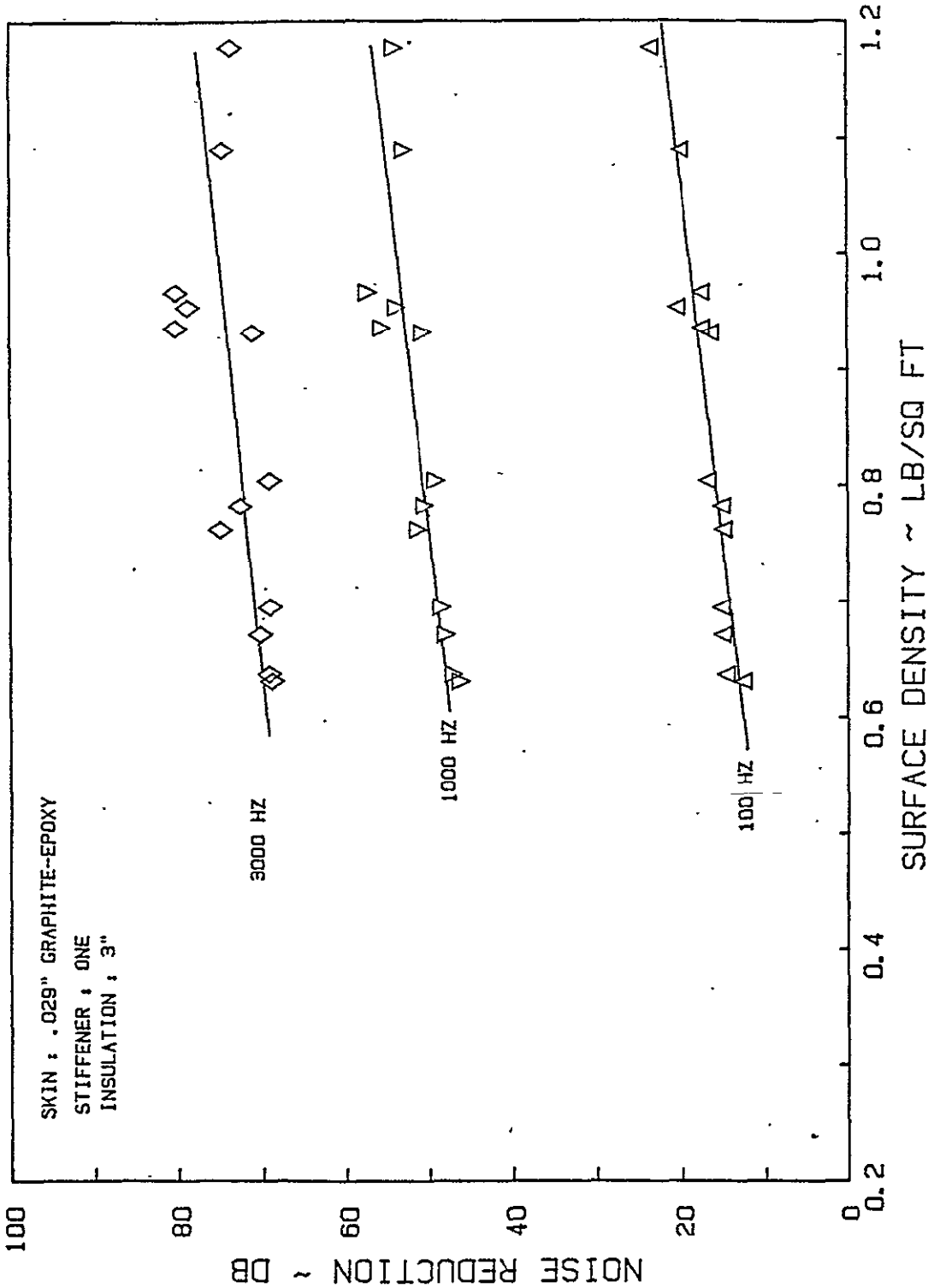

Figure 5.23: Effect of Total Panel Density on the Noise Reduction Characteristics of a Double-Wall Panel with Graphite-Epoxy Skin (Panel 335) and Insulation

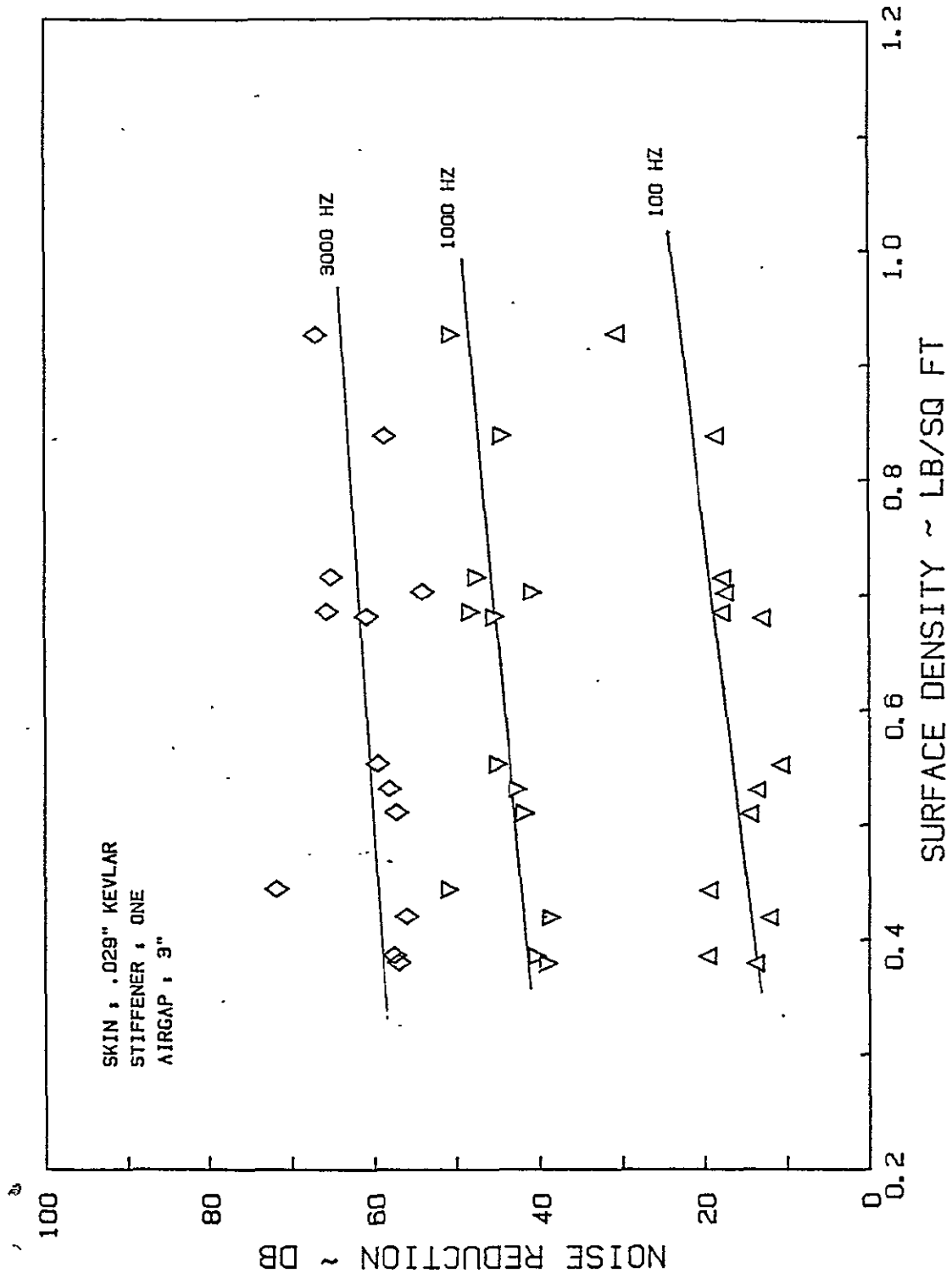

Figure 5.24: Effect of Total Panel Area Density on the Noise Reduction Characteristics of a Double-Wall Panel with Kevlar Skin (Panel 339) and Airgap

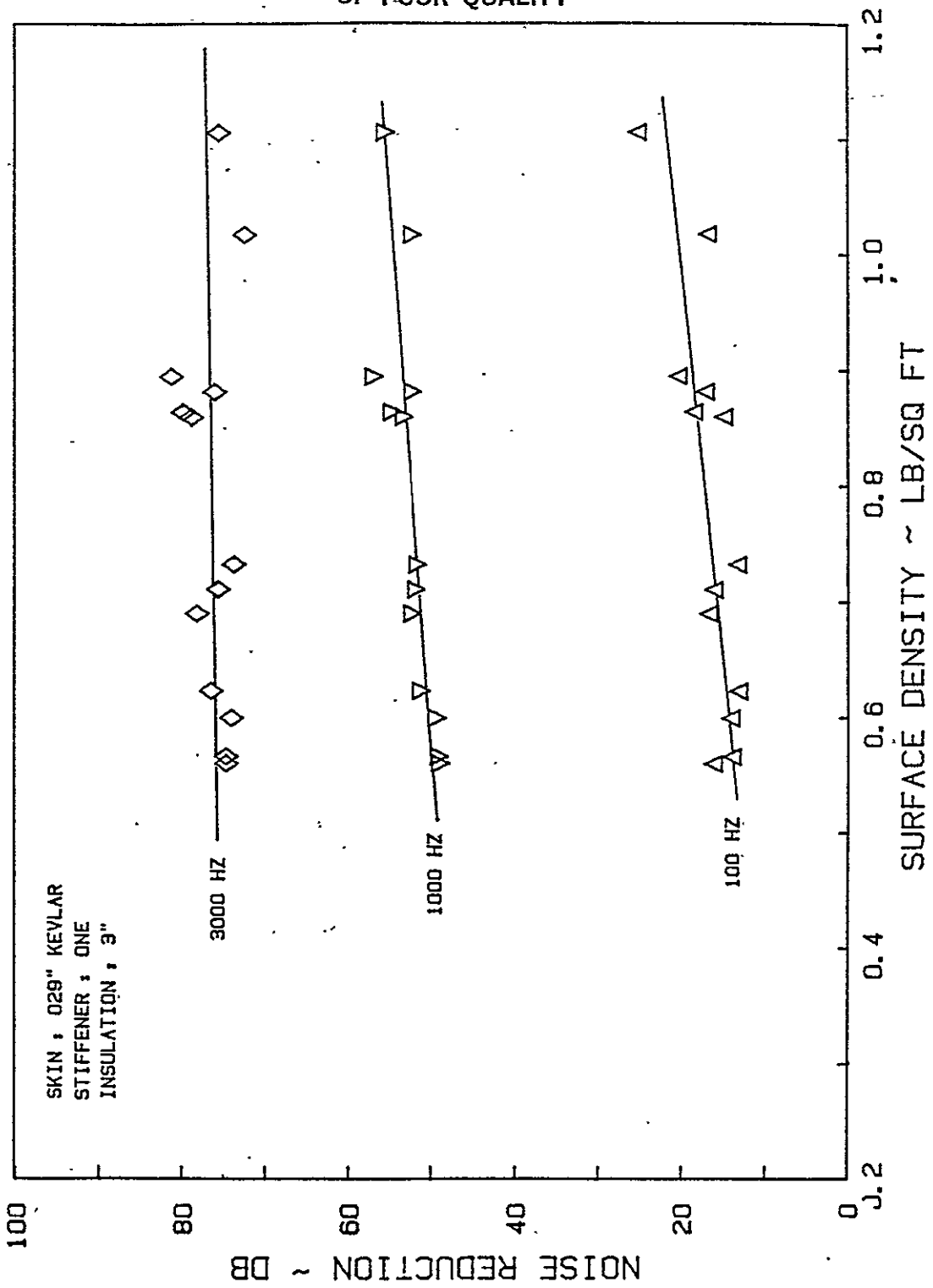

Figure 5.25: Effect of Total Panel Area Density on the Noise Reduction Characteristics of a Double-Wall Panel with Kevlar Skin (Panel 339) and Insulation

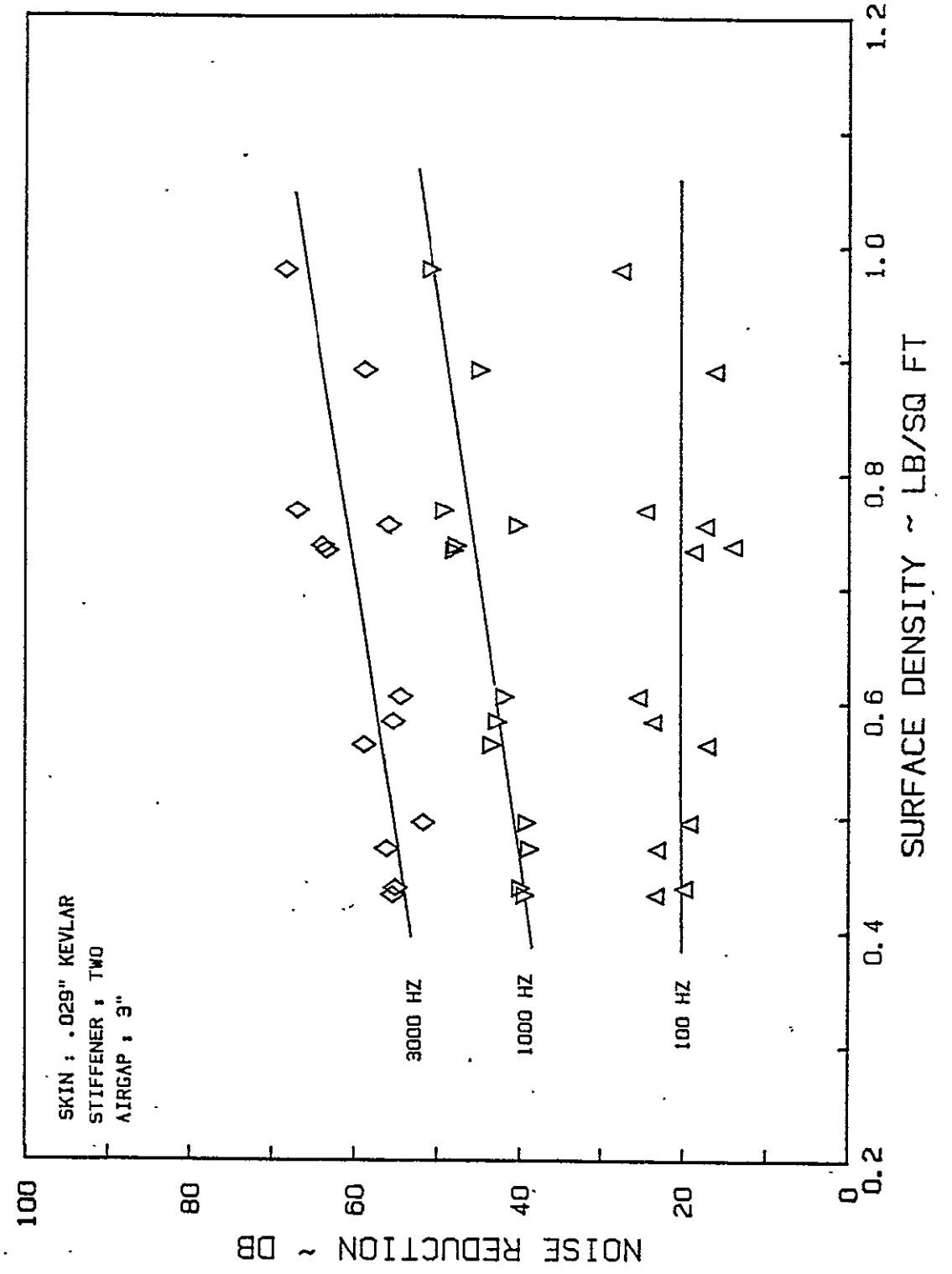

Figure 5.26: Effect of Total Panel Area Density on the Noise Reduction Characteristics of a Double-Wall Panel with Kevlar Skin (Panel 340) and Airgap

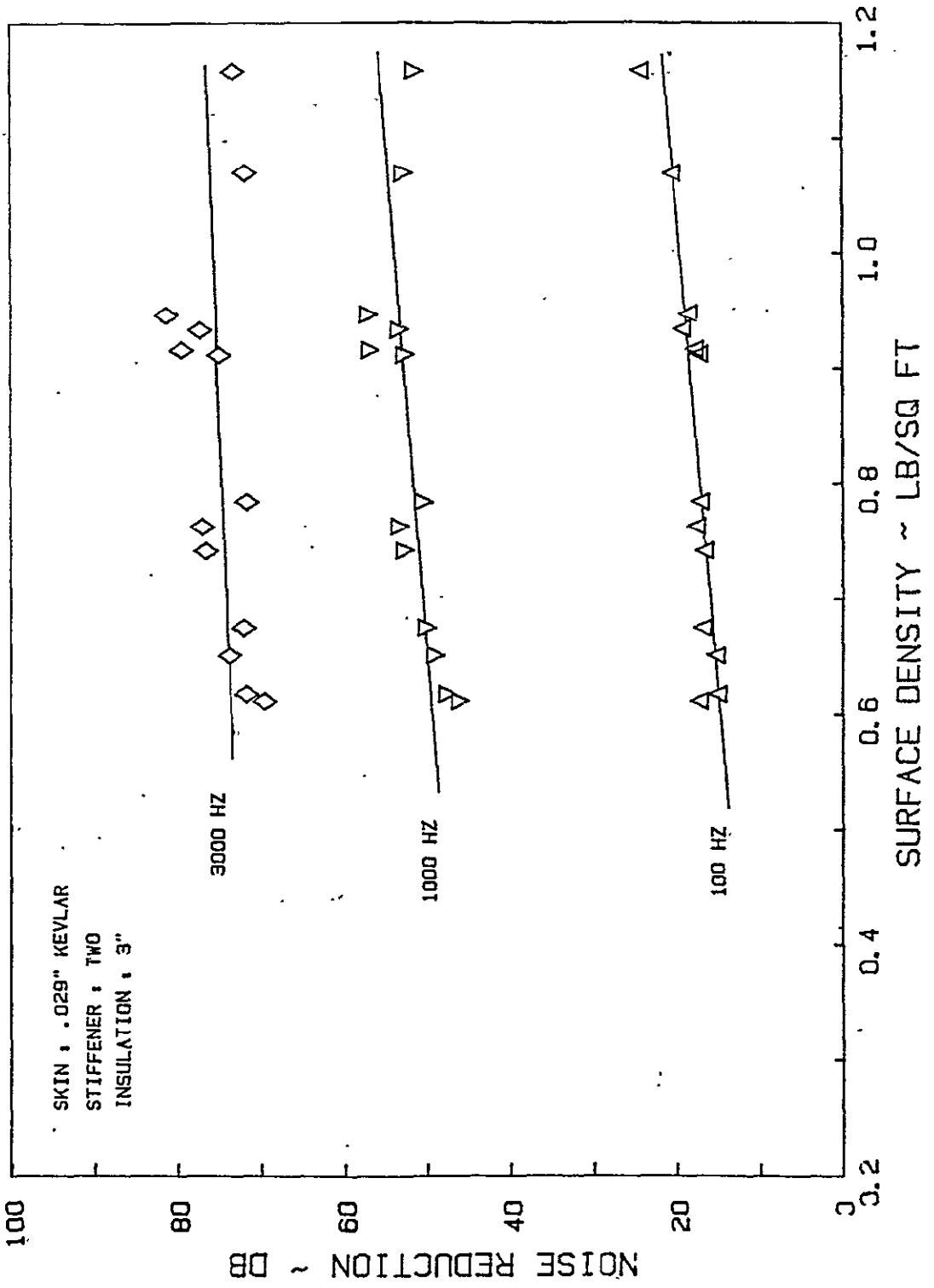

Figure 5.27: Effect of Total Panel Area Density on the Noise Reduction Characteristics of a Double-Wall Panel with Kevlar Skin (Panel 340) and Insulation

These cross plots must be interpreted with care. The noise reduction due to the trim panel at any frequency is not a function solely of the mass of the panel, which explains the considerable scatter seen in these plots. However, the mass of the trim panel is still (at least in the high frequency region) a major factor and represents the trade-off parameter that most often decides what material will be selected for use. Because of the scatter, mean square lines are shown, which indicate, as expected, increasing noise reduction with increase in mass. From Tables 5.3 and 5.4 it can be seen that trim panels 312 and 344 perform consistently better than the other panels, even after consideration of their higher area density. Both these panels are treated with flexible 1/2" foam material, over which a leather covering is applied. The thickness of the foam may be one of the reasons for the better performance of these panels.

Four trim panels--312, 318, 325, and 352 (one each from groups 1 and 2, and two from group 3)--were selected for further investigation. Each of these panels has a different base material: 312 has 45% open pore aluminum, 318 has Rohacell core, 325 has Klege-cell base, and 352 has compressed fiberglass core. These trim panels are representative of the trim panels being used in the general aviation industry. Single panel noise reduction tests were performed, and the results are given in Figures 5.28 through 5.31. These results confirm that the limp panel assumption may not be valid for these panels. At this test facility, the noise

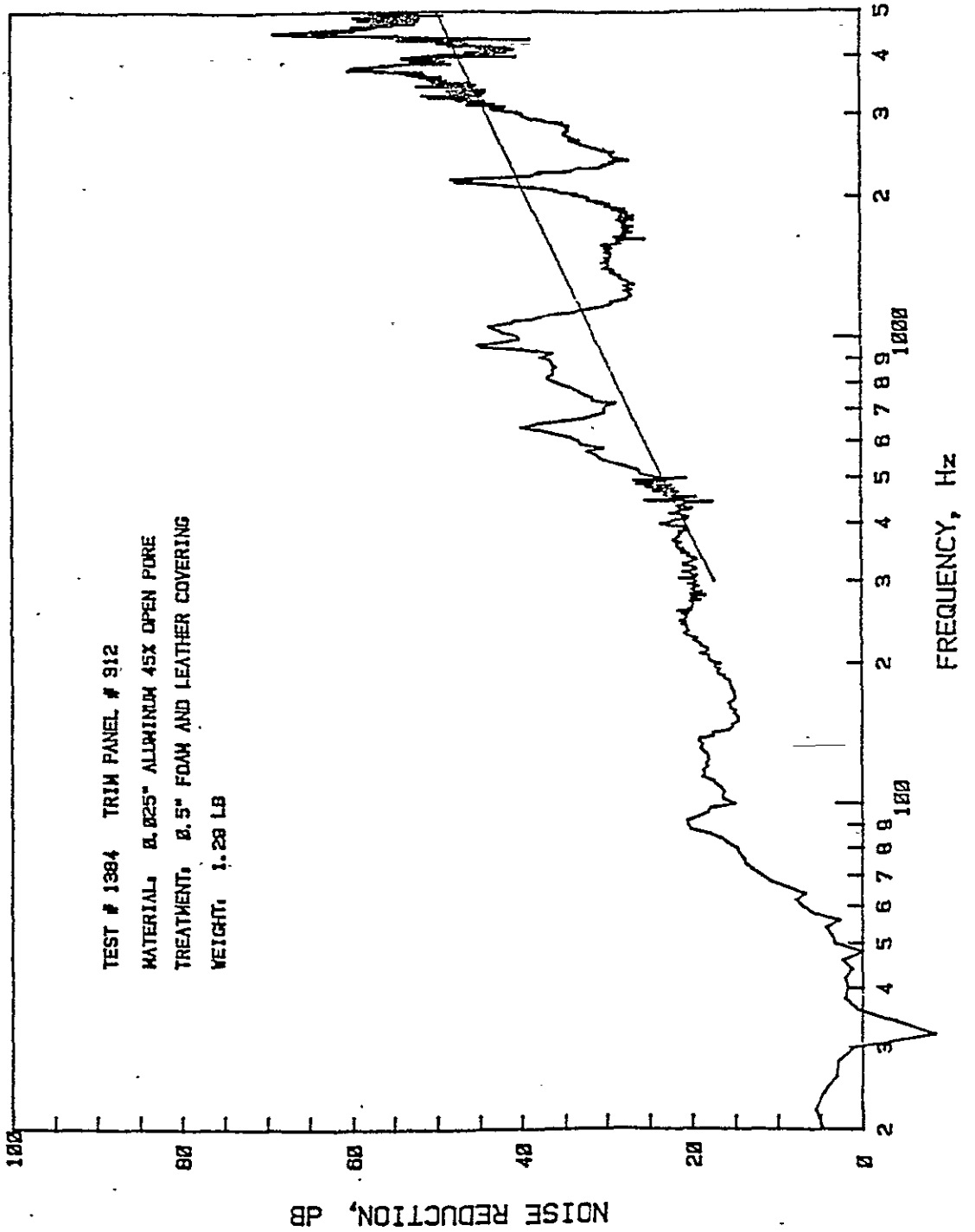

Figure 5.28: Noise Reduction Characteristics of Trim Panel 312

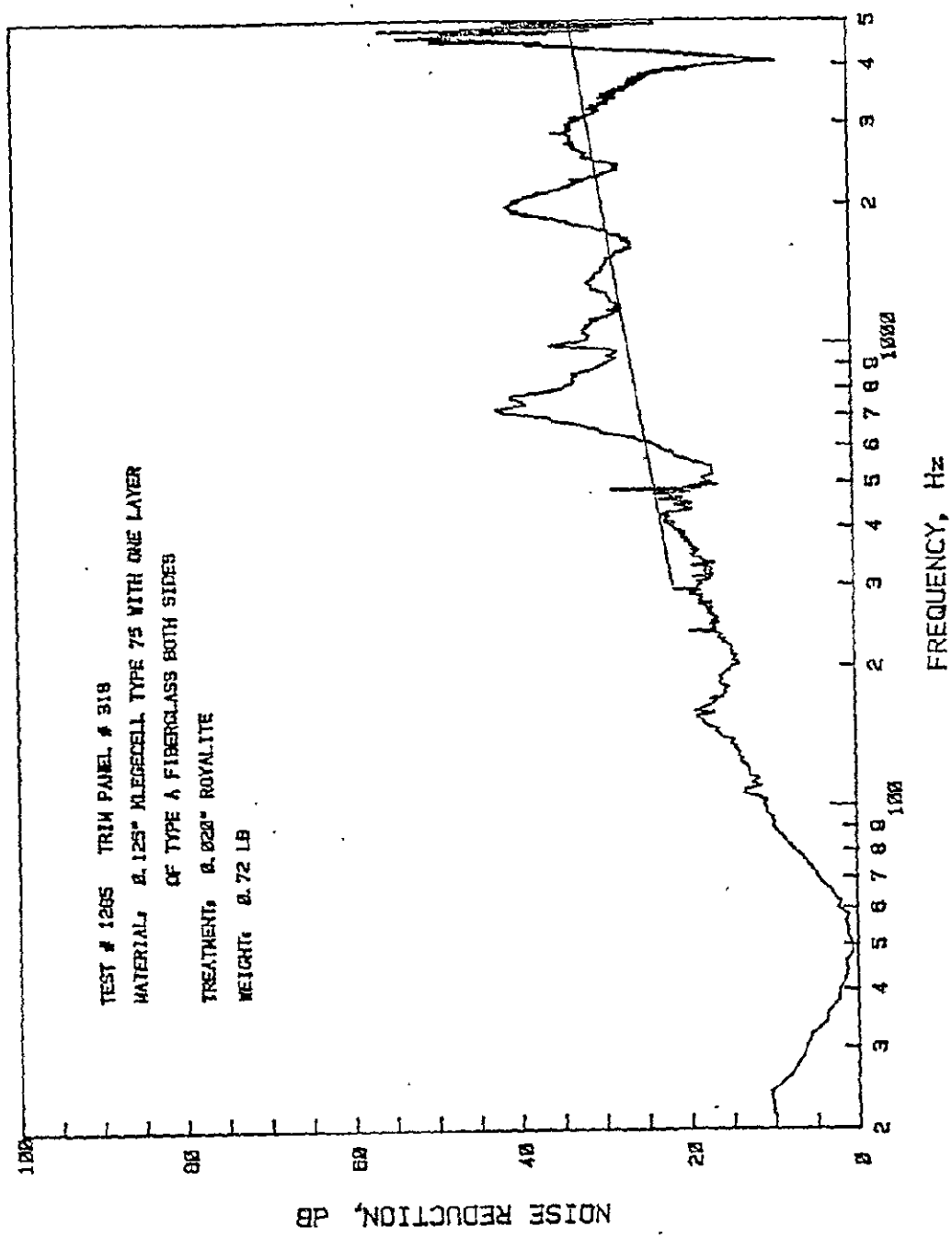

Figure 5.29: Noise Reduction Characteristics of Trim Panel 318

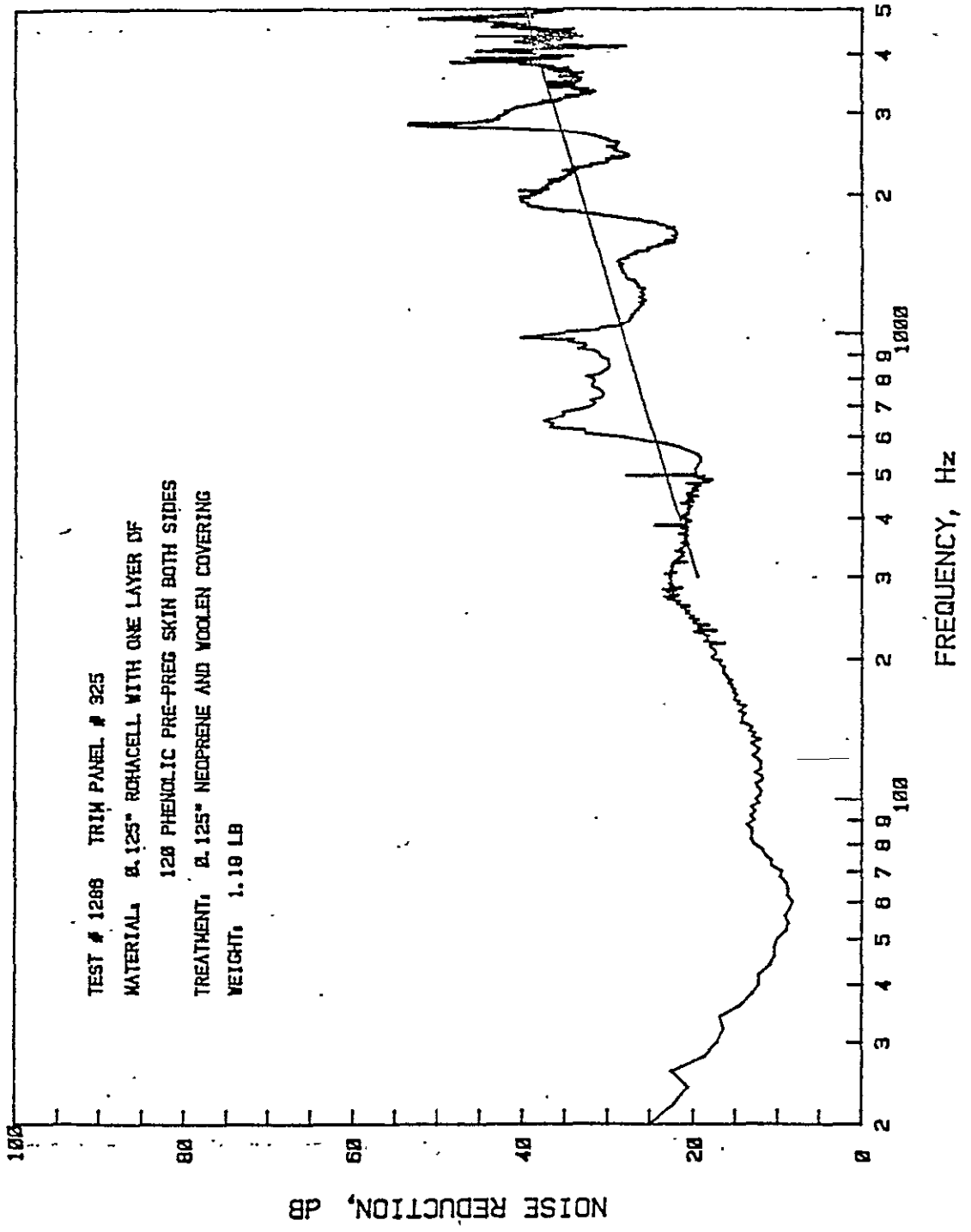

Figure 5.30: Noise Reduction Characteristics of Trim Panel 325

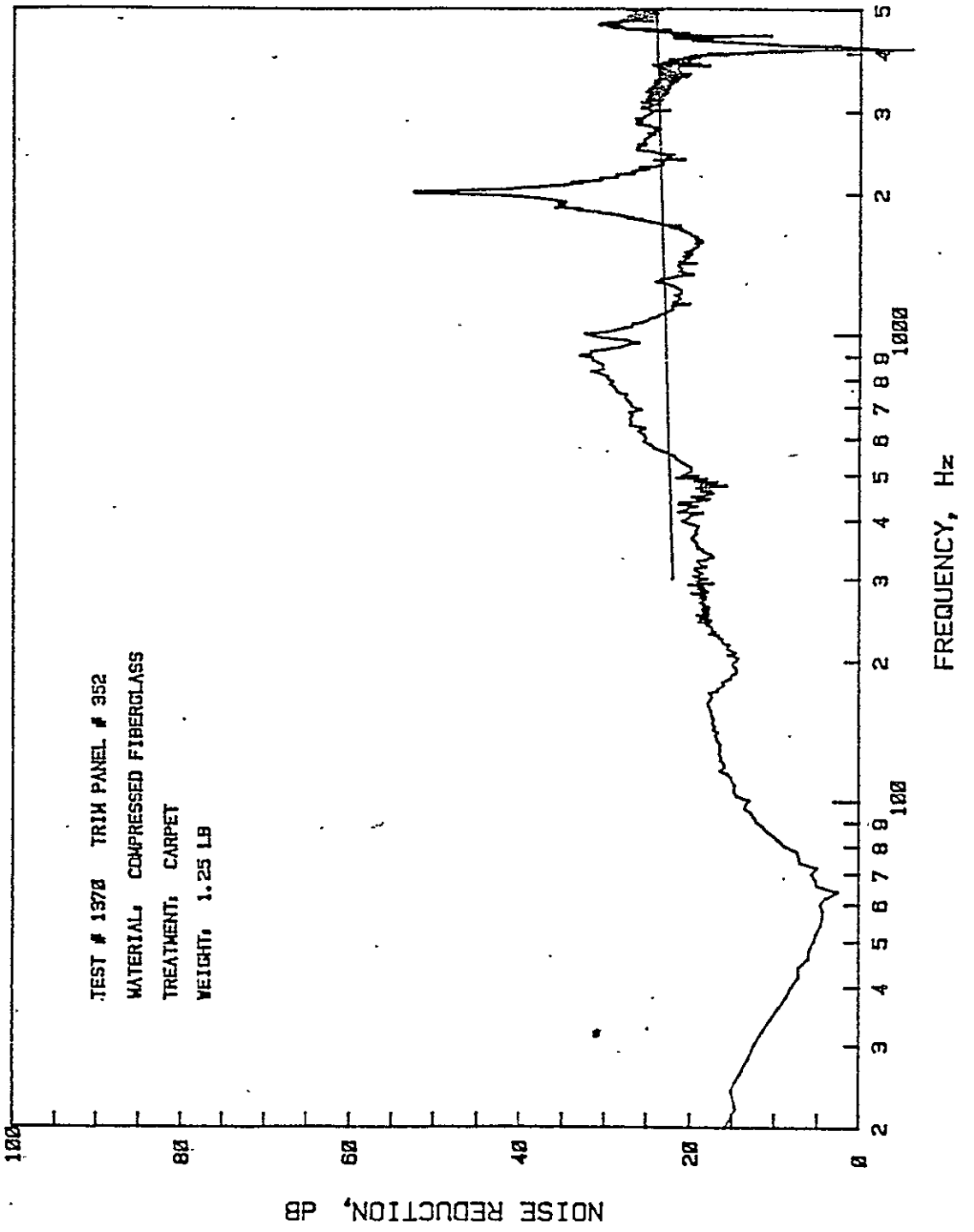

Figure 5.31: Noise Reduction Characteristics of Trim Panel 352

reduction curve of a standard .032" aluminum panel shows a slope of 6 dB/octave, which corresponds to mass-law value. However, three of the four trim panels tested had less than 6 dB/octave slope. These values are tabulated in the next chapter. Only panel 312 had a slope of 8 dB/octave, far higher than mass-law slope. Panel 352 had a near zero slope, as can be seen from Figure 5.31. Both these panels have nearly the same area density. While double-wall tests confirmed these trends, they also indicated that the effectiveness of panel 312 decreased and that of panel 352 increased, thus evening out the difference. This aspect is further discussed in the next chapter.

In the low-frequency region of 40-1000 Hz, panel 347 was superior to all other panels tested. Panel 347 was the thickest panel in group 2 and has two layers of 120 phenolic skin applied to both sides to stiffen the base material. Also it is made of light Rohacell material. This property of high stiffness and low mass increases its fundamental resonance frequency. This makes panel 347 superior to other panels in the low-frequency, stiffness-controlled region.

The effect of attachment of the trim panel to the channel section was also investigated. Two types of attachment procedures were tried. In one case the trim panel was screwed to the channel section by means of eight screws as shown in Figure 5.2. The second attachment was to simulate free-free edge conditions for the trim panel. This was done by using 1/8" thick pressure-sensitive

adhesive tape. The results are compared in Tables 5.5 through 5.7. The results indicate that the effect of the attachment is felt only in the very low-frequency region. An increase of 0-2 dB is observed with the free-free edge condition. This might be due to the better isolation of the trim panel at very low frequencies. At 100 Hz the results were inconclusive. It is possible that the vibration isolation of this tape is not effective at and above 100 Hz. At very high frequencies the panels with tape attachment indicate a gain of 0-3 dB. The results are within the experimental scatter observed in this frequency region. Increased mass of the 1/8" tape all around might have caused some of the increase.

5.4 CONCLUSIONS

The results of the tests described in this chapter have demonstrated the following characteristics of the sound transmission through double-wall structures.

At very low frequencies (below 100 Hz) the noise reduction is a function only of the stiffness of either skin or trim panel. Hence use of a double-wall panel presents no additional gain over use of the single-wall structure. At frequencies of 100 to 500 Hz, the overall noise reduction of the double-wall panel is normally lower than the noise reduction of the single panel with the same panel weight. However, the noise reduction at these frequencies is so much a function of the double-wall, panel-air-panel, resonance

Table 5.5: Effect of Trim Panel Attachment on the Noise Reduction Characteristics of Double-Wall Panels with Aluminum Skin; Depth 3"

a. Trim Panel 318

Frequency (Hz)	Airgap		Insulation	
	Screw	Tape	Screw	Tape
40	12	14	13	16
100	18	18	17	17
300	29	32	30	31
500	42	41	39	46
1000	48	50	56	59
3000	62	63	78	80

b. Trim Panel 325

Frequency (Hz)	Airgap		Insulation	
	Screw	Tape	Screw	Tape
40	18	18	20	20
100	16	16	16	16
300	42	43	34	35
500	45	46	41	46
1000	53	53	59	59
3000	65	65	78	78

Table 5.6: Effect of Trim Panel Attachment on the Noise Reduction Characteristics of Double-Wall Panels with Aluminum Skin; Depth 2"

a. Trim Panel 318

Frequency (Hz)	Airgap		Insulation	
	Screw	Tape	Screw	Tape
40	13	14	14	16
100	16	15	14	15
300	19	26	26	26
500	45	42	43	42
1000	47	50	53	57
3000	61	63	78	80

b. Trim Panel 325

Frequency (Hz)	Airgap		Insulation	
	Screw	Tape	Screw	Tape
40	16	16	18	20
100	14	14	15	14
300	34	35	32	35
500	42	45	43	41
1000	47	49	54	56
3000	61	63	74	76

Table 5.7: Effect of Trim Panel Attachment on the Noise Reduction Characteristics of Double-Wall Panels with Aluminun Skin; Panel Depth 1"

a. Trim Panel 318

Frequency (Hz)	Airgap		Insulation	
	Screw	Tape	Screw	Tape
40	14	15	15	16
100	13	13	13	14
300	19	21	16	17
500	35	32	32	36
1000	42	43	48	51
3000	61	62	72	75

b. Trim Panel 325

Frequency (Hz)	Airgap		Insulation	
	Screw	Tape	Screw	Tape
40	17	18	20	20
100	15	12	15	15
300	32	30	23	24
500	37	41	35	35
1000	46	46	50	51
3000	63	64	73	73

frequencies that any conclusion on the efficiency of the double wall without knowledge of the excitation frequency and the double-wall characteristics will not be valid. By proper designing of the double-wall panel treatment, the coincidence of the panel-air-panel resonance frequency and the excitation frequency may be avoided. The double wall may also be designed to give a higher noise reduction at the excitation frequencies. In the high-frequency region, even though the slope of the noise reduction curve of the double-wall panel exceeds that of the single-wall panel, the experimental values are lower than the theoretically predicted 12 dB/octave. One of the causes for the discrepancy is the assumption that the trim panel behaves like a limp panel following mass-law impedance.

In particular for the double-wall panels investigated, the effect of the airgap depth in the high frequency region is negligible outside the range of the harmonics of the panel-air-panel resonance frequencies. Of the skin panels tested, the aluminum skin panel offers higher high-frequency noise reduction by virtue of its greater mass. At low frequencies, graphite-epoxy panels have up to seven dB higher noise reduction than the Kevlar panels. One-to-one compariosn between these panels is not possible, due to the varied nature of the thickness and the stiffener characteristics. The effect of an additional stiffener in the skin panel is to increase the low-frequency noise reduction by about 4 dB. The additional stiffener has a negligible effect on the noise reduction at high frequencies.

The effect of the fiberglass insulation in the low-frequency region is small and at times slightly negative. In the high frequency region the installation of the fiberglass insulation damps out the resonance effects and also increases the noise reduction due to the viscous losses. This increse is directly proportional to the insulation thickness.

The effect of the trim panel is not significant in the low-frequency region. Increase in the trim panel mass results in a slightly lower noise reduction. At high frequencies the base material and the treatment of the trim panel play a major role in the noise reduction characteristics of both double-wall and single-wall panels. Of the trim panels tested, panels with .5" foam as part of the treatment had the best noise reduction in the high-frequency region, even after consideration of their increased mass.

Due to the instrument limitation, the effect of very high trim panel density on the high-frequency noise reduction could not be accurately determined. However, as the noise reduction is well above 80 dB, it is considered that this may not be worthwhile.

CHAPTER 6

THEORETICAL ANALYSIS OF SOUND TRANSMISSION THROUGH DOUBLE-WALL PANELS

6.1 INTRODUCTION

The main purpuse of the theoretical analysis of double-wall panels was to compare the results obtained from experimental investigations of Chapter 5 with the computer-calculated theoretical results. The secondary purpose is to use this theoretical model for the future design of double-wall noise control treatment. The double-wall panels tested include skin, airspace, fiberglass insulation and trim. Hence, one of the requirements for the selection of the theoretical model is that it should be able to handle these variables.

A literature survey was conducted to determine the methods available (Reference 51). Recent studies to determine the interior noise of propeller aircraft (References 23 and 24) still use the classical sound transmission loss model originally proposed in Reference 25. It was decided to use the same model, with some modifications to accommodate the type of panels tested in Chapter 5.

6.2 THEORETICAL FORMULATION

For a plane wave with partial absorption on the receiver side, the noise reduction across a panel is expressed as (References 23-25):

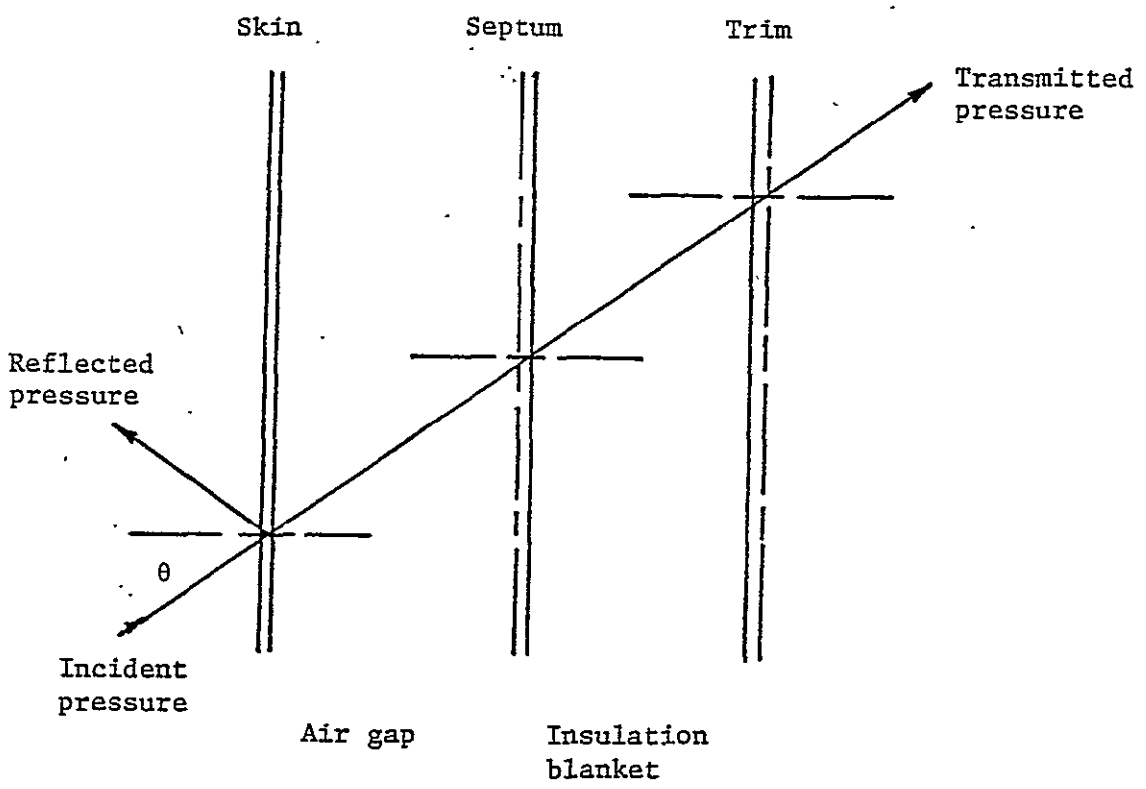

Figure 6.1: Schematic Diagram of a Multilayer Panel

$$NR = 10 \log \left|1 + \frac{\alpha}{\tau}\right| \qquad (6.1),$$

where NR = Noise reduction across a panel (dB)

τ = Panel transmission loss coefficient

α = Absorption coefficient of the receiver cavity.

The transmission loss across a panel is calculated from

$$TL = 10 \log\left(\frac{1}{\tau}\right) \qquad (6.2),$$

where TL = Transmission loss.

In case the receiver cavity is fully absorptive, as in the case of the KU-FRL acoustic test facility, the noise reduction and transmission loss will be the same. A typical multilayered panel is shown in Figure 6.1. The transmission loss across this panel can be written as

$$TL = 10 \log\left(\frac{1}{\tau}\right) = 10 \log \left|\frac{p_s}{p_t}\right|^2 \qquad (6.3),$$

where TL = Transmission loss across a panel (dB)

p_s = Measured sound pressure at the source side (Pa)

p_t = Measured sound pressure at the receiver side.

The sound pressure measured by a microphone on the source side will measure not only the incident sound wave but also the reflected sound wave. The measured sound pressure is also called "blocked sound pressure." Following the classic derivation from Reference 26, this pressure ratio can be written in terms of the pressure ratios across the successive interfaces as

$$\left|\frac{p_s}{p_t}\right|^2 = \left|\frac{p_s}{p_2} \cdot \frac{p_2}{p_3} \cdots\cdots \frac{p_k}{p_{k+1}} \cdots\cdots \frac{p_N}{p_t}\right|^2 \qquad (6.4),$$

where N = Number of layers

$\frac{p_k}{p_{k+1}}$ = Pressure ratio across layer k.

For the purpose of calculating the pressure ratios across successive interfaces, both airspace and fiberglass insulation (porous medium) will be considered as similar media. The pressure in a porous insulation or airspace is calculated from the solution of the one-dimensional wave equation (Reference 26):

$$p = A \cosh(bx + \Psi_b) \qquad (6.5),$$

where A = Pressure amplitude

p = Pressure at any point along axis of sound propagation x

x = Distance from a terminal impedance Z_t

b = Propagation constant for the medium (neper)

Ψ_b = Phase angle dependent on the characteristic impedance of the medium and is given by

$$\psi_b = \coth^{-1}\left(\frac{Z_t}{Z_o}\right) \qquad (6.6),$$

where Z_o = Characteristic impedance of the medium.

Equation 6.6 is derived from the equation of impedance (Reference 26):

$$Z = Z_o \coth (bx + \Psi_b) \qquad (6.7).$$

In this case at $x = 0$, $Z = Z_t$. Therefore,

$$\psi_b = \coth^{-1}\left(\frac{Z_t}{Z_o}\right) \qquad (6.8).$$

For an airspace between two solid boundaries, the propagation constant

$$b = j\omega c = \text{ and } Z_o = \rho c. \qquad (6.9).$$

For the porous insulation, both b and Z_o are complex. Reference 9 gives a method to calculate these values for any porous insulation material given its porosity, resistivity, and density. Hence, knowing b and Ψ_b, the pressure ratio across a porous fiberglass insulation or airspace can be calculated.

The pressure ratio across septum or skin or trim panel can be found by the impedance ratio across these layers because the particle velocity across these layers should be continuous. The impedance is defined as the ratio of pressure to particle velocity. Therefore, across any septum,

$$Z_1 = \frac{p_1}{u_1} \text{ and } Z_2 = \frac{p_2}{u_2} \qquad (6.10).$$

Since u_1 and u_2 are equal,

$$\frac{p_1}{p_2} = \frac{Z_1}{Z_2} \qquad (6.11).$$

Therefore, if the impedances at the interfaces of successive layers are known, then the pressure ratios can be calculated. The impedance of airspace and porous media are calculated using Equation 6.8. The impedance in front of a septum (or skin or trim) is found by adding the impedance of the septum to the terminating impedance for that layer. For example, in Figure 6.1, if the impedance at

z_{k+1} is known, then the impedance at k is calculated by adding the impedance of septum k to the impedance at k+1. In classical sound transmission theory, the impedance of the septum is given by the mass-law impedance (= $j\omega m_k$). Therefore,

$$Z_k = Z_{k+1} + j\omega m_k \qquad (6.12),$$

where Z_k = Impedance at location k

Z_{k+1} = Impedance at location k+1

ω = Circular frequency

m_k = Surface mass density of septum at k.

The above model has been corrected for the oblique incidence and airflow in Reference 24. In the following subsections, the pressure ratios and the impedance values across the individual layers are given. These equations are taken from References 23 to 25, and 21.

6.2.1 SKIN PANEL

For a skin panel subjected to an obliquely incident sound wave with an airflow, the pressure ratio is obtained from (Reference 24):

$$\frac{p_I}{p_2} = \left[1 + \frac{Z_p \cos\theta_2}{Z_2} + \frac{\rho_1 c_1 \cos\theta_1}{\cos\theta_1 (1 + M \sin\theta_1) Z_2}\right] \qquad (6.13),$$

where p_I = Blocked incident pressure

p_2 = Transmitted pressure

Z_p = Characteristic impedance of skin panel

Z_2 = Terminating impedance for the skin panel

θ_2 = Angle of incidence in Region 2

θ_1 = Angle of incidence

$\rho_1 c_1$ = Impedance of air on the source side

M = Mach number.

Equation (6.13) can be simplified when the external flow is not considered.

$$\frac{p_I}{p_2} = \left[1 + \frac{Z_p \cos\theta_2}{Z_2} + \frac{\rho_1 c_1 \cos\theta_2}{Z_2 \cos\theta_1}\right] \qquad (6.14).$$

The impedance of a panel is modeled in the KU-FRL program in four ways:

a. The first model used for skin impedance is derived from simple mass law and is given by

$$Z_p = j\omega m \qquad (6.15).$$

b. The second impedance model is for a stiffened and pressurized cylindrical panel. It is given by (Reference 24):

$$Z_p = \frac{\omega_n^2}{\omega} m\eta + \frac{\omega^3 D\eta}{c_1^4} \frac{\sin^4\theta}{(1 + M \sin\theta)^4} + j\left[\omega m - \frac{\omega_n^2 m}{\omega} - \frac{\omega_n^3 D}{c_1^4} \frac{\sin^4\theta}{(1 + M \sin\theta)^4}\right] \qquad (6.16),$$

where η = Loss factor

D = Flexural rigidity $[Eh^3/12(1 - \upsilon^2)]$

c_1 = Speed of sound on the source side

θ = Angle of incidence

M = Mach number

m = Mass per unit area

E = Young's modulus

υ = Poisson's ratio

h = Skin thickness

ω_n = Fundamental resonance frequency.

For a cylindrical stiffened panel, neglecting the membrane stiffness, it is given by (Reference 23):

$$\omega_n^2 = \frac{\pi^4 D}{mL_x^4}\left\{p^4(1+\delta^2)^2 + p^4\left[\frac{E_s I_s}{D\ell_y} + \delta^2\left(\frac{G_s J_s}{D\ell_y} + \frac{G_f J_f}{D\ell_x}\right) + \delta^4 \frac{E_f I_f}{D\ell_x}\right] + \right.$$

$$\left. + \Delta p \frac{R}{2} \frac{p^2 L_x^2}{\pi^2 D}(1+2\delta^2)\right\} \qquad (6.17),$$

where D = Flexural rigidity as defined above

L_x = Length of the panel

ℓ_x = Frame pitch

ℓ_y = Stringer pitch

E = Young's modulus

m = Mass per unit area

I = Moment of inertia

G = Shear modulus

J = Torsion constant

p = Axial wave number (= 1 for fundamental mode)

R = Radius of curvature

$$\delta = \frac{qL_x}{p\pi R} \qquad (6.18)$$

q = Circumferential full wave number (= .5 for fundamental mode; see Reference 23).

c. The third impedance model is for a flat panel with in-plane stresses to simulate pressurization and is given by (Reference 24):

$$Z_p = \frac{\omega_n^2}{\omega} m\eta + \frac{\omega^3 D\eta}{c_1^4} \frac{\sin^4\theta}{(1 + M \sin\theta)^4} + j[\omega m - \frac{\omega_n^2 m}{\omega} - \frac{\omega_n^3 D}{c_1^4} \frac{\sin^4\theta}{(1 + M \sin\theta)^4}] \quad (6.19),$$

where ω_n = Fundamental angular resonance frequency for a panel bounded by sides a and b and pressurization loads P_x and P_y. It is given by

$$\omega_n = \frac{\pi}{(m)^{1/2}} [(\frac{P_x}{a^2} + \frac{P_y}{b^2}) + D\pi^2(\frac{1}{a^2} + \frac{1}{b^2})^2]^{1/2} \quad (6.20);$$

η = Loss factor

D = Flexural rigidity $[Eh^3/12(1 - \upsilon^2)]$

c_1 = Speed of sound on the source side

θ = Angle of incidence

M = Mach number

P_x = Load in x direction due to pressurization

P_y = Load in y direction due to pressurization

m = Mass per unit area

E = Young's modulus

υ = Poisson's ratio

h = Skin thickness

a, b = Panel length and width

d. The fourth model is for cases where the fundamental resonance frequency and damping ratio (= loss factor/2) are known. In this case the panel impedance is calculated as (Reference 27):

$$Z_p = 2\zeta\omega_n m + \omega m(1 - [\frac{\omega_n}{\omega}]^2) \qquad (6.21),$$

where ζ = Damping ratio

ω_n = Natural frequency

m = Mass per unit area

ω = Circular frequency.

6.2.2 SEPTUM

When a thin, impervious layer (leaded vinyl or vinyl) is present, the following equation is used to determine the pressure ratio across that layer:

$$\frac{p_i}{p_{i+1}} = \frac{Z_i \cos\theta_i + 1}{Z_{i+1}} \qquad (6.22),$$

where $Z_i = Z_p + Z_{i+1}$ (6.23),

$Z_p = j\omega m_i$ (6.24),

$\omega = 2\pi f$

m_i = mass per unit area of layer i

f = frequency

Z_{i+1} = Terminating impedance for layer i, calculated from impedance downstream of layer i + 1.

The input impedance Z_i is simply the sum of the layer impedance and the terminating impedance.

6.2.3 AIR GAP OR FIBERGLASS INSULATION

The pressure ratio across an airspace or a soft porous fiberglass insulation subjected to an obliquely incident ray is given by (References 23-25):

$$\frac{p_i}{p_{i+1}} = \frac{\cosh\left[bd\cos\theta + \coth^{-1}\left(\frac{Z_{i+1}\cos\theta}{Z_B}\right)\right]}{\cosh\left[\coth^{-1}\left(\frac{Z_{i+1}\cos\theta}{Z_B}\right)\right]} \qquad (6.25),$$

where b = Complex propagation constant (calculated from equations and data in Reference 9 for fiberglass insulation

$$b = j\omega c \text{ for air gap} \qquad (6.26)$$

Z_{i+1} = Termination impedance

Z_B = Characteristic impedance of the layer (calculated from Reference 9 for fiberglass insulation)

$Z_B = \rho c$ for air gap.

The input impedance of the airgap blanket is given by (Reference 23):

$$Z_i = \frac{Z_B}{\cos\theta}\coth\left[bd\cos\theta + \coth^{-1}\left(\frac{Z_{i+1}\cos\theta}{Z_B}\right)\right] \qquad (6.27).$$

6.2.4 TRIM PANEL CHARACTERISTICS

The pressure ratio across the trim panel is calculated using Equation 6.22. Two models exist for the panel impedance. The first is the same as Equation 6.24. The second model uses the experimental values obtained at the KU-FRL acoustic test facility. In general, a single mode impedance model is given by (Equation 6.21)

$$Z_p = 2\zeta\omega_n m + j\omega m(1 - [\frac{\omega_n}{\omega}]^2) \qquad (6.28),$$

where ζ = Experimental damping ratio

ω_n = Experimental resonance frequency

m = Mass per unit area.

Equation (6.28) has been modified to change the slope of the noise reduction curve in the high frequency region by a factor called "slope factor" (see Section 5.3.5) to correspond to the experimental value of the slope obtained. The model for panel impedance uses Equation (6.28) in the low-frequency region and experimental slope in the high frequency region.

6.3 COMPUTER PROGRAM

The equations described in Section 6.2 are used in a computer program, which calculates the transmission loss of multilayer panels. The program is written in PDP-11 Fortran, which is an enhanced version of Fortran-66. It is intended for use on the DEC

MINC-11, 16 bit, 64 k byte minicomputer. Five difference types of layers can be studied. These are skin, airspace, porous fiberglass insulation, septum and trim. The program is written in such a way as to permit the user to vary both the type and the order of the layers. The flow diagram and the listing of the computer program are given in Appendix B. The input data required, input data format and output formats are given in the user's manual, Reference 28.

When this computer program is used for the calculation of transmission loss of panels tested, several aspects should be kept in mind. These are given below. It should also be noted that even though the program can allow up to 10 layers, in the tests only three layers were used; i.e., skin, airgap or fiberglass, and trim panel.

a. Actual transmission loss should measure only the incident pressure on the source side. But at the KU-FRL acoustic test facility the source microphone measures the blocked sound pressure, which consists of both incident and reflected pressures. This effect has been taken into account in the program.

b. The receiver microphone measures both the transmitted sound pressure and the reflected pressure from the receiver cavity. As explained in Appendix A, the receiver cavity absorbs most of the transmitted energy. Hence the contribution of the reflected pressure is assumed to be negligible. In other words, the absorption coefficient of the cavity has been assumed to be equal to 1.

c. At low frequency the receiving cavity stiffens the panel due to Helmholtz effect. This effect increases the measured fundamental resonance frequency of the single panel. Hence the measured resonance frequency is greater than the calculated resonance frequency. This effect can also be expected for the double-wall panels. No modifications have been done to account for this effect. This effect can be taken into account by inputting the measured single panel resonance frequency of the trim and the skin panel, instead of calculating their resonance frequencies within the program.

d. In practice the trim panel is modelled as a limp panel. In classical sound transmission loss theory, limp panel impedance is directly proportional to the surface density and the frequency. The transmission loss resulting from this impedance is known as mass-law transmission loss. Under these assumptions the transmission loss increases by 6 dB for doubling of either the mass or the frequency. In a transmission loss vs frequency plot, this produces 6 dB/octave slope. However, as can be seen from the test results (Figures 5.28 through 5.31), the slope of the least mean-square line of the trim panels varies considerably. Hence a simple mass-law assumption seems to be invalid for such trim panels. Three out of the four panels tested had slopes less than the theoretical

C-3

values. Hence the use of mass-law approximation produces a higher transmission loss for a double panel. In order to overcome this problem, an additional option for the trim panel was introduced for the trim panel impedance. In this option the measured slope is used. The model uses mass law impedance for low frequency and impedance corresponding to the measured slope at high frequency. The experimental slope is input as a ratio of the measured slope to theoretical slope (6 dB/octave), and this ratio is called the slope factor. Values of these factors for various trim panels are given in Reference 28. For this study these values were measured from Figures 5.28 through 5.33.

e. The absorption coefficient is normally less than one. But when the cavity is nearly absorptive, ($\alpha \approx 1$), as in the case of the KU-FRL acoustic test facility, the noise reduction and transmission loss will nearly be the same. In case the cavity is not fully absorptive, noise reduction values in general will be less than transmission loss. At cavity resonance frequencies such simplifications will not be valid. At the KU-FRL experimental test facility the receiver microphone measures both the transmitted pressure and the very weak reflections from the cavity walls. Hence the sound attenuation characteristics measured from this facility

are called "noise reduction." The theoretical values calculated from the program do not contain any corrections and hence are transmission loss values. This should be borne in mind when making the comparison between the theoretical and experimental values.

6.4 DETAILS OF THE INPUT DATA

For the theoretical investigation the parameters chosen to vary were

a. Panel depth

b. Effect of sound insulation

c. Effect of skin structure

d. Effect of trim panel material and treatment.

Four skin panels and four trim panels were used for the comparison of the theoretical and the calculated values. The skin panels tested are given in Table 6.1. Trim panels used were 312, 318, 325, and 352. The details of these panels are presented in Table 6.2. The impedance model used for the skin and trim panels was the single mode approximation. This approximation, described in detail in Reference 28, required single panel resonance frequencies of the skin panel and its damping ratio around that frequency region. The single panel test results from 6 were used for the resonance frequencies. The damping values of these panels had been

measured and were reported in Reference 28. These values were used in the calculation of the impedance. These values are tabulated in Table 6.1.

The mechanical properties of the fiberglass insulation were unknown. This insulation material was very similar to the PF 105 fiberglass insulation discussed in Reference 9. Also the sensitivity analysis indicated that the minor variations in porosity and resistivity of the insulation did not significantly change the transmission loss values. Hence the porosity and the resistivity of PF 105 material were used. However, actual fiberglass density was input.

The input data required for the trim panels were fundamental resonance frequency, damping ratio, and the experimental slope of the noise reduction and damping tests of the trim panels alone. These values are tabulated in Table 6.2.

6.5 RESULTS

The outputs from the computer runs are plotted in Figures 6.2 through 6.25 for the 48 combinations considered. These calculated values are plotted as dotted lines over the experimental values. Each figure contains two plots: one with the fiberglass insulation between the skin and the trim panel and the other without the insulation.

Table 6.1: Input Data for Skin Panels

Skin Panel	Resonance Frequency (Hz)	Damping Ratio	Surface Density (kg/sq m)
353, 357, 358	50	.015	2.24
335	70	.03	1.58
339	40	.02	1.23
340	55	.02	1.48

Table 6.2: Input Data for Trim Panels

Trim Panel	Resonance Frequency (Hz)	Damping Ratio	Surface Density (kg/sq m)	Slope Factor
312	0	.042	2.26	1.33
318	50	.060	1.26	0.58
325	60	.074	2.04	0.83
352	62	.063	2.20	0.05

$$\text{Slope Factor} = \frac{\text{Measured Slope}}{6}$$

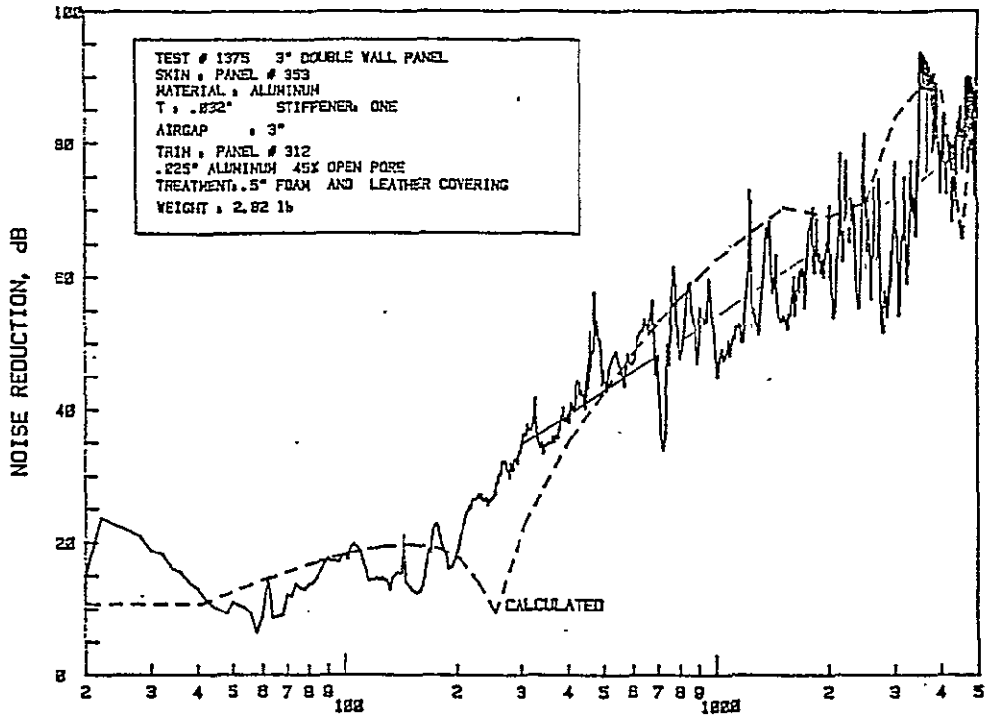

a. Airgap

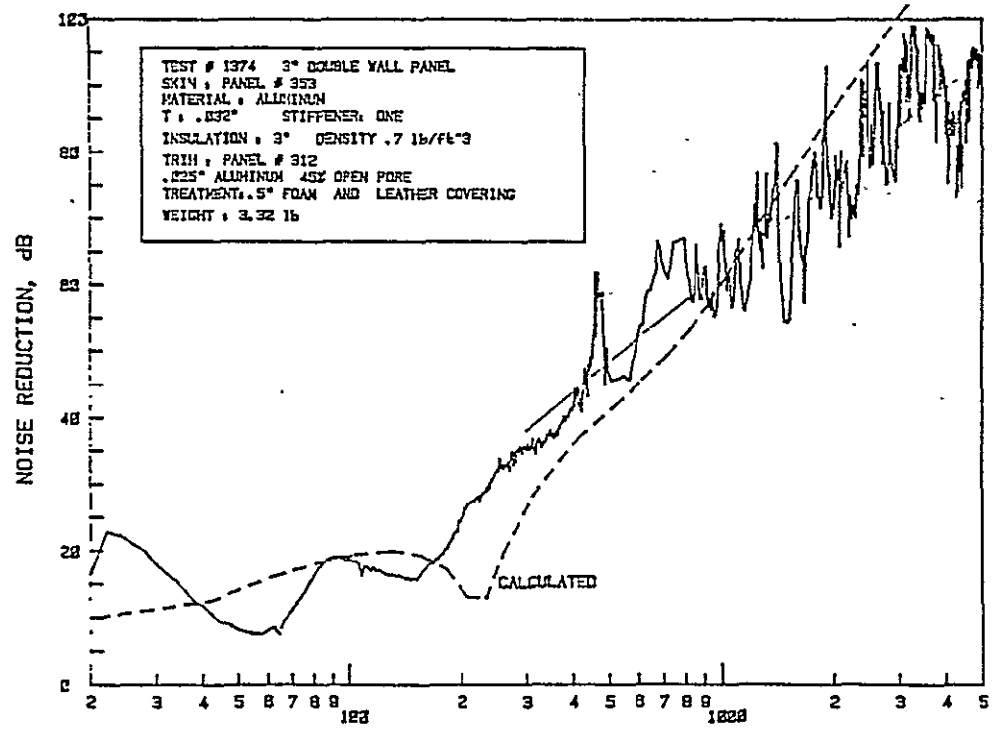

b. Fiberglass Insulation

Figure 6.2: Comparison of Experimental and Theoretical Noise Reduction Characteristics of a Double-Wall Panel Made of Aluminum Skin (Panel 353) and Trim Panel 312; Panel Depth 3"

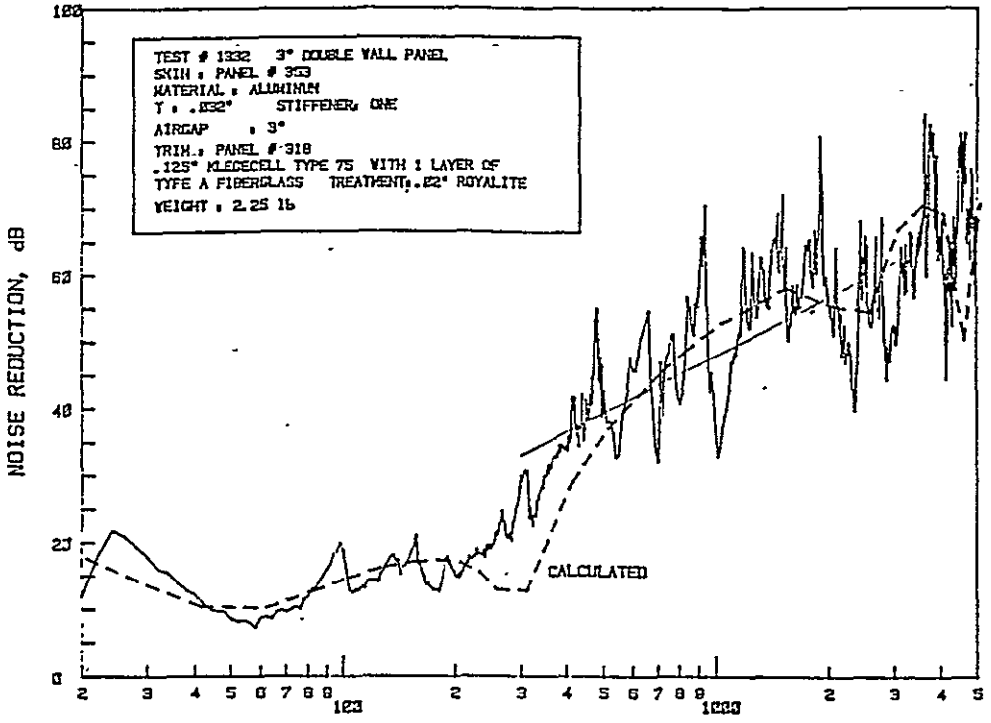

a. Airgap

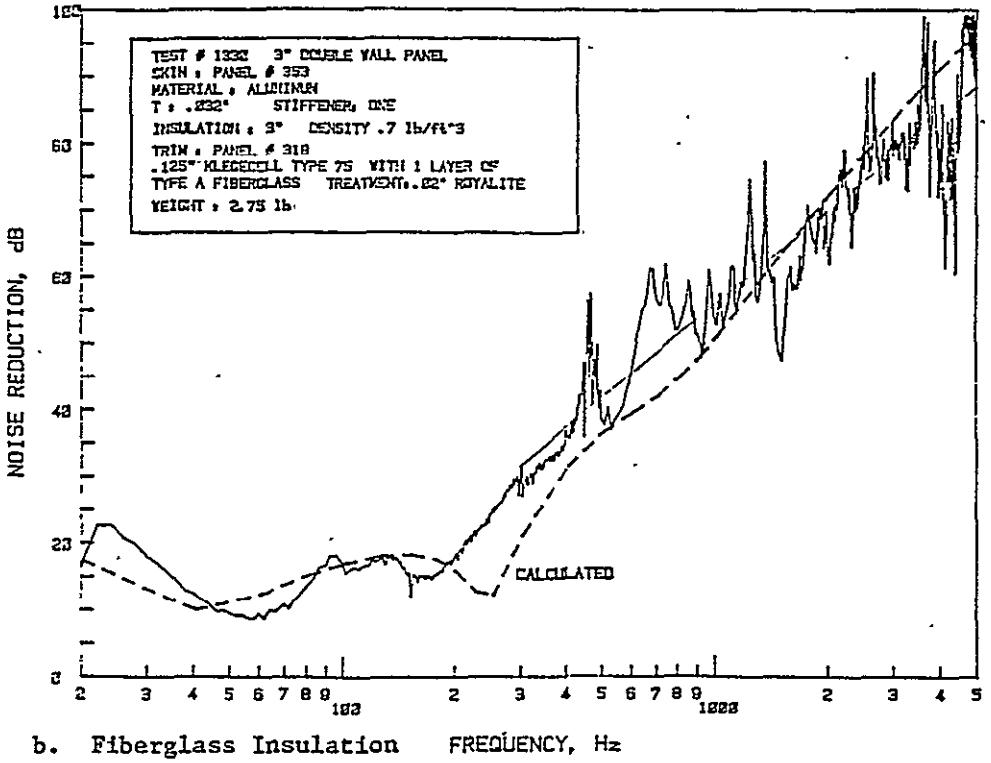

b. Fiberglass Insulation

Figure 6.3: Comparison of Experimental and Theoretical Noise Reduction Characteristics of a Double-Wall Panel Made of Aluminum Skin (Panel 353) and Trim Panel 318; Panel Depth 3"

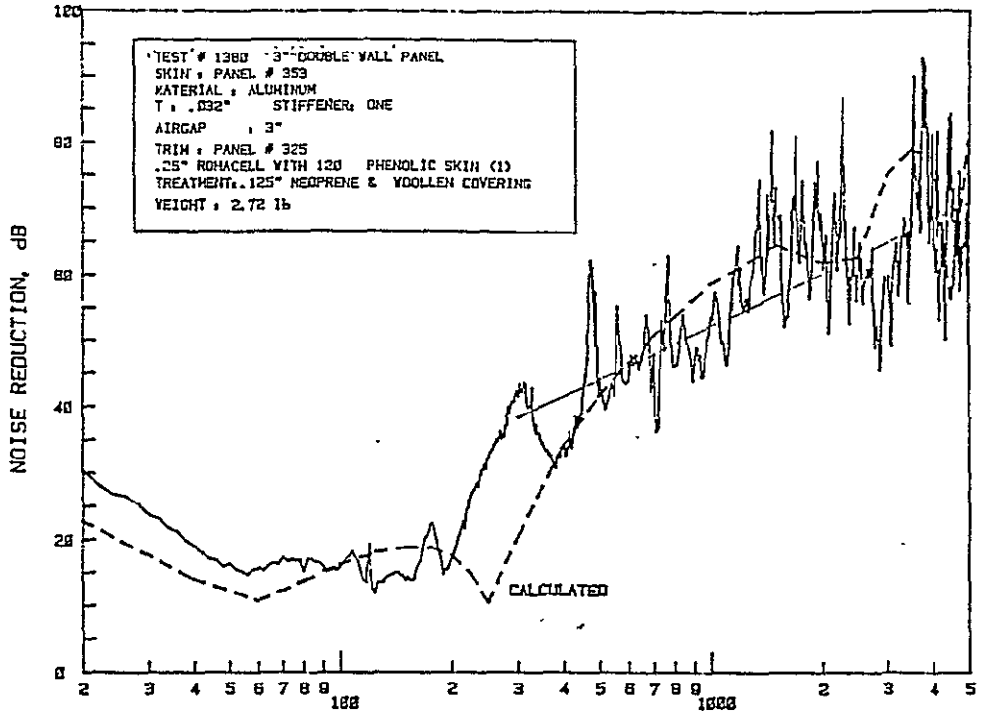

a. Airgap

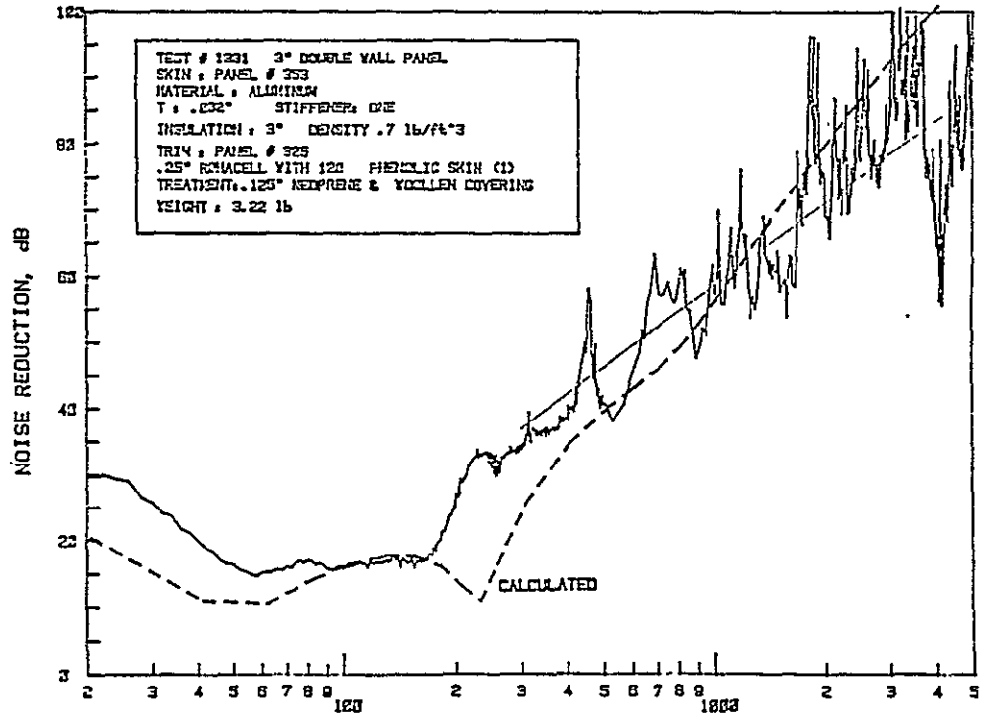

b. Fiberglass Insulation

Figure 6.4: Comparison of Experimental and Theoretical Noise Reduction Characteristics of a Double-Wall Panel Made of Aluminum Skin (Panel 353) and Trim Panel 325; Panel Depth 3"

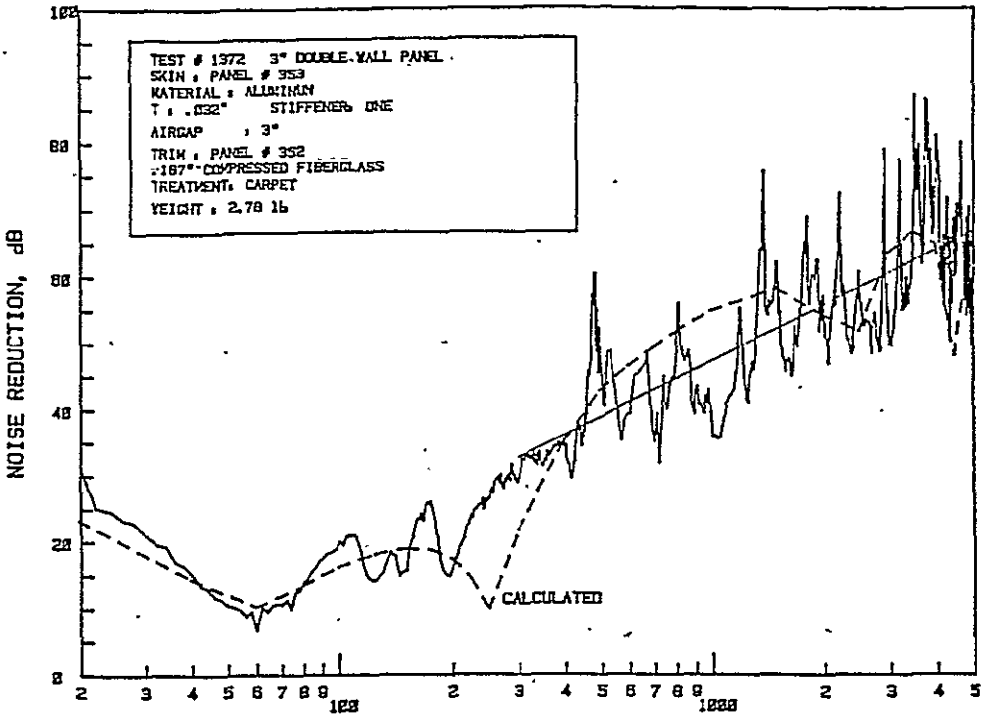

a. Airgap

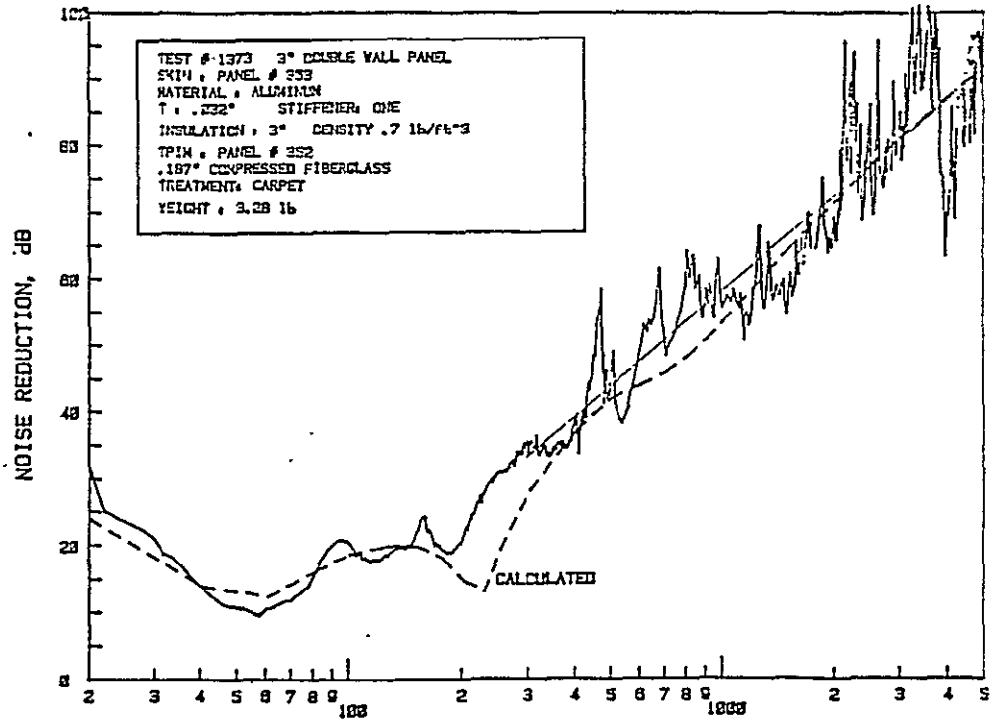

b. Fiberglass Insulation

Figure 6.5: Comparison of Experimental and Theoretical Noise Reduction Characteristics of a Double-Wall Panel Made of Aluminum Skin (Panel 353) and Trim Panel 352; Panel Depth 3"

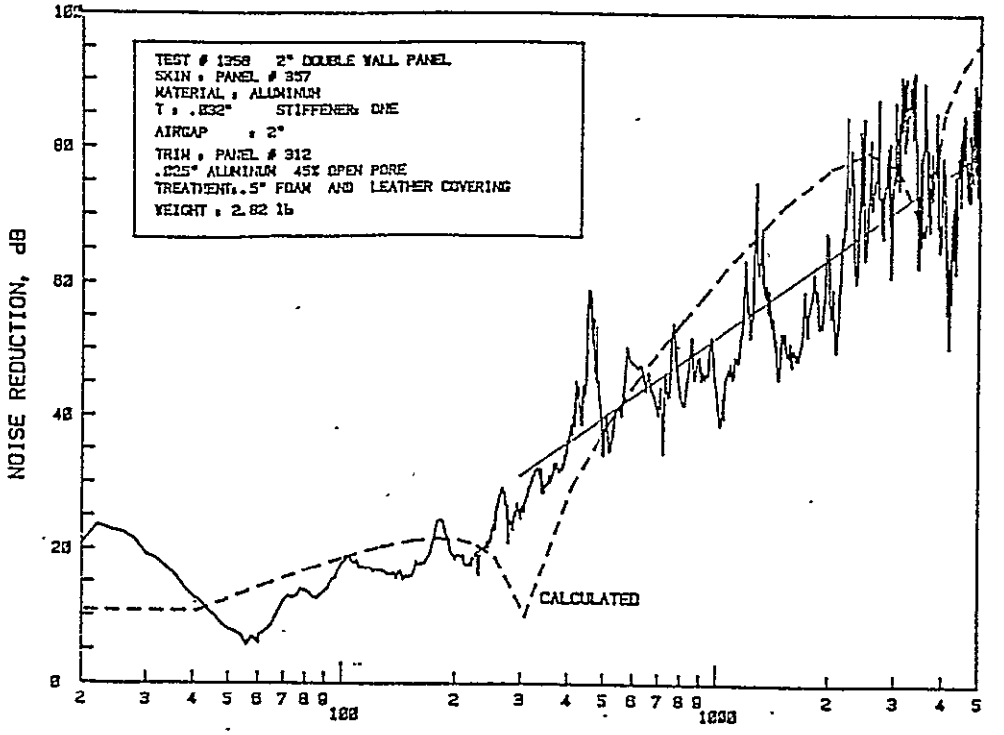

a. Airgap

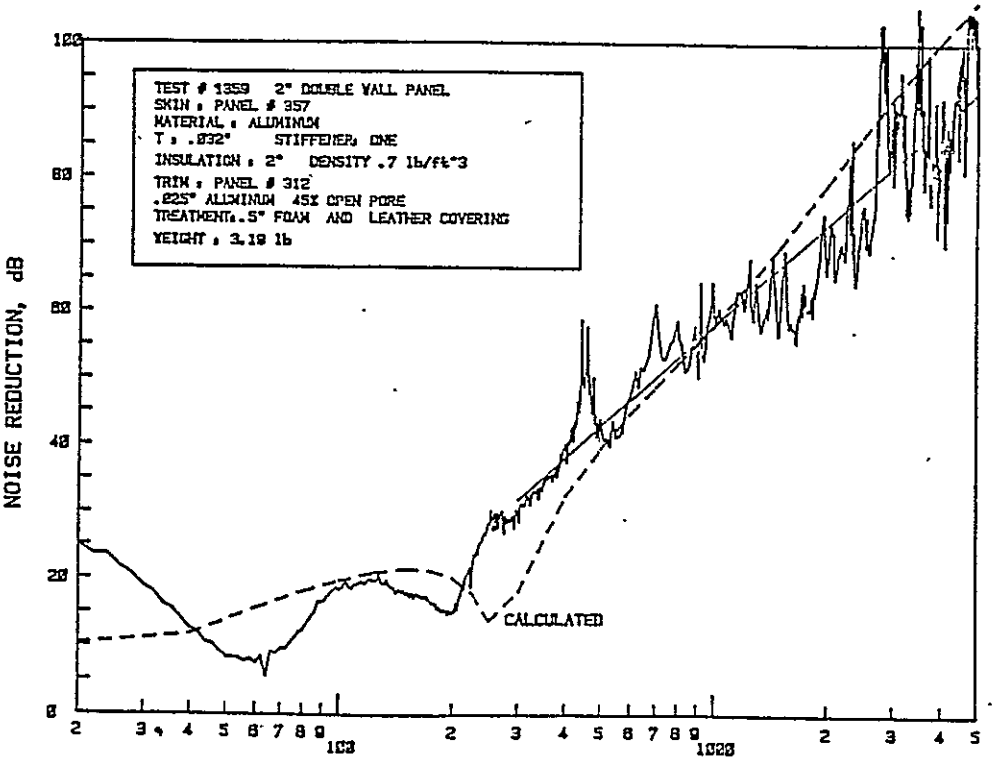

b. Fiberglass Insulation

Figure 6.6: Comparison of Experimental and Theoretical Noise Reduction Characteristics of a Double-Wall Panel Made of Aluminum Skin (Panel 357) and Trim Panel 312; Panel Depth 2"

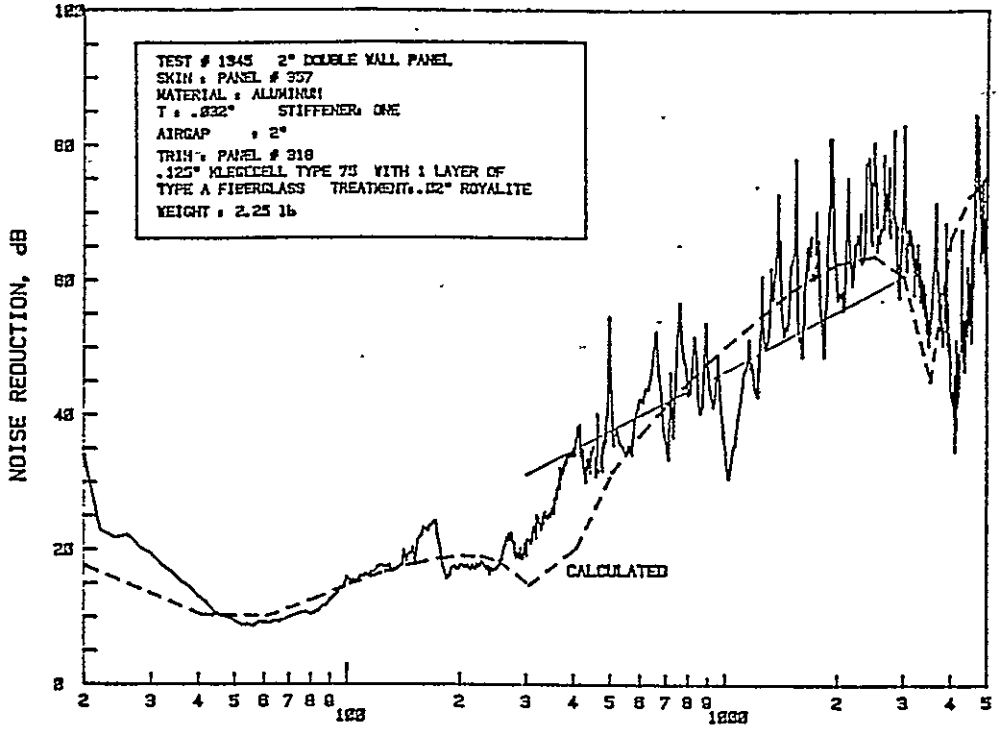

a. Airgap

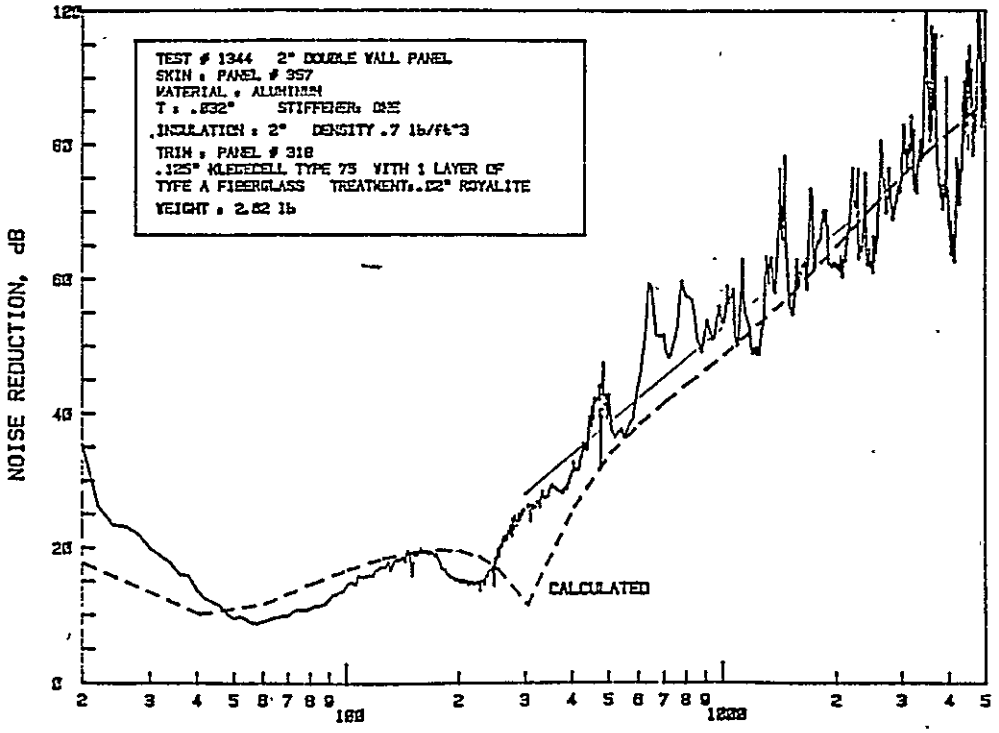

b. Fiberglass Insulation

Figure 6.7: Comparison of Experimental and Theoretical Noise Reduction Characteristics of a Double-Wall Panel Made of Aluminum Skin (Panel 357) and Trim Panel 318; Panel Depth 2"

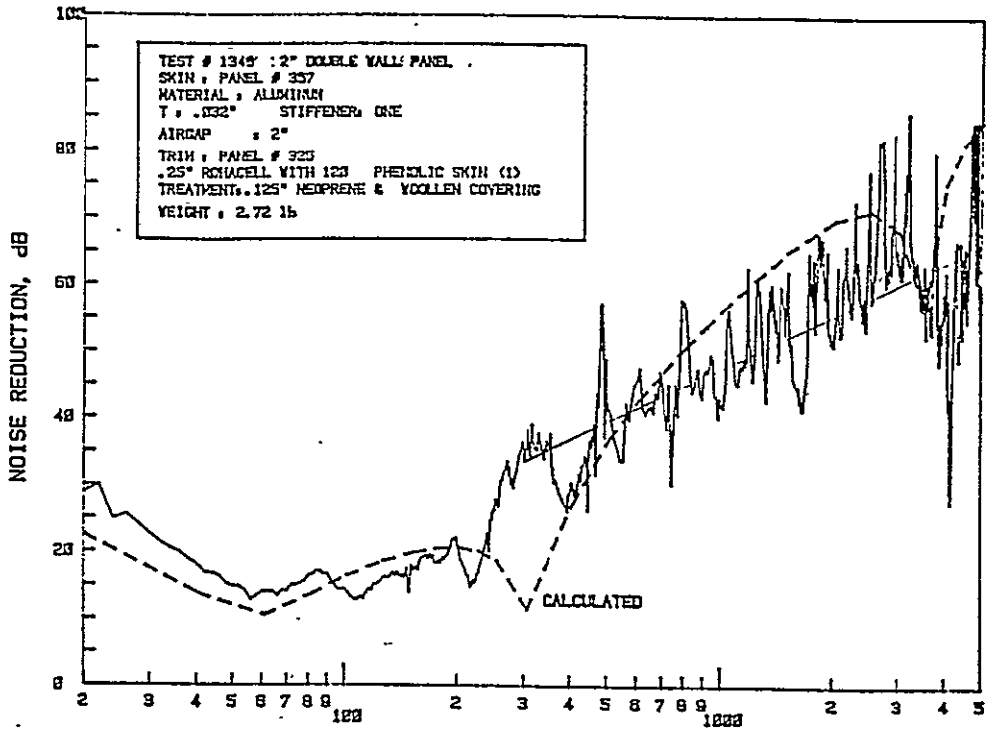

a. Airgap

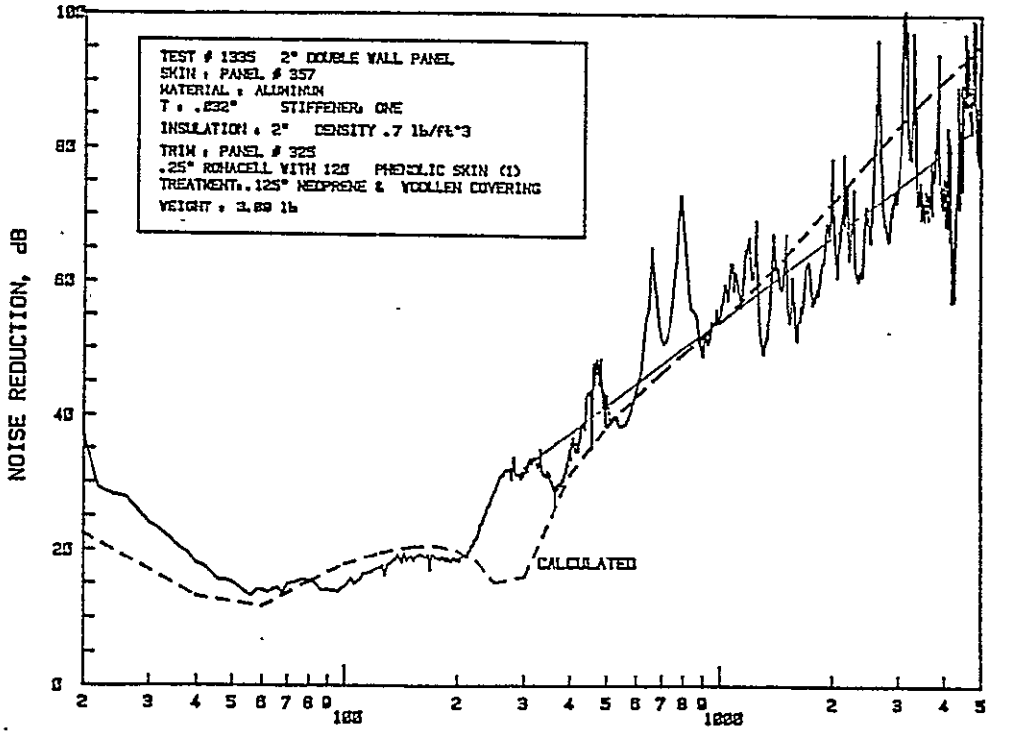

b. Fiberglass Insulation

Figure 6.8: Comparison of Experimental and Theoretical Noise Reduction Characteristics of a Double-Wall Panel Made of Aluminum Skin (Panel 357) and Trim Panel 325; Panel Depth 2"

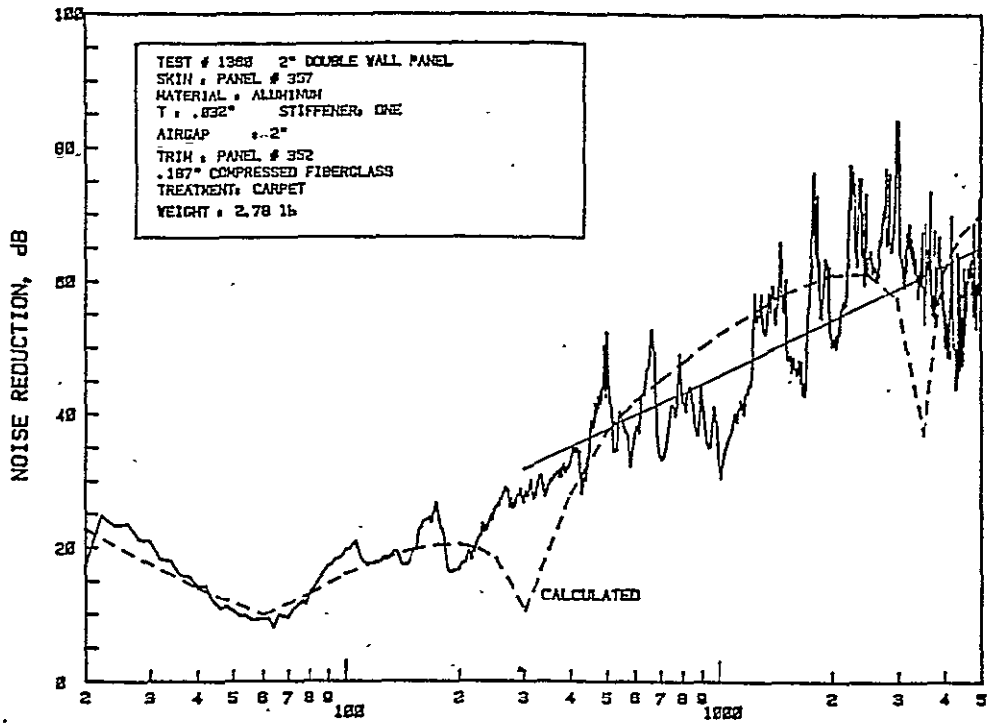

a. Airgap

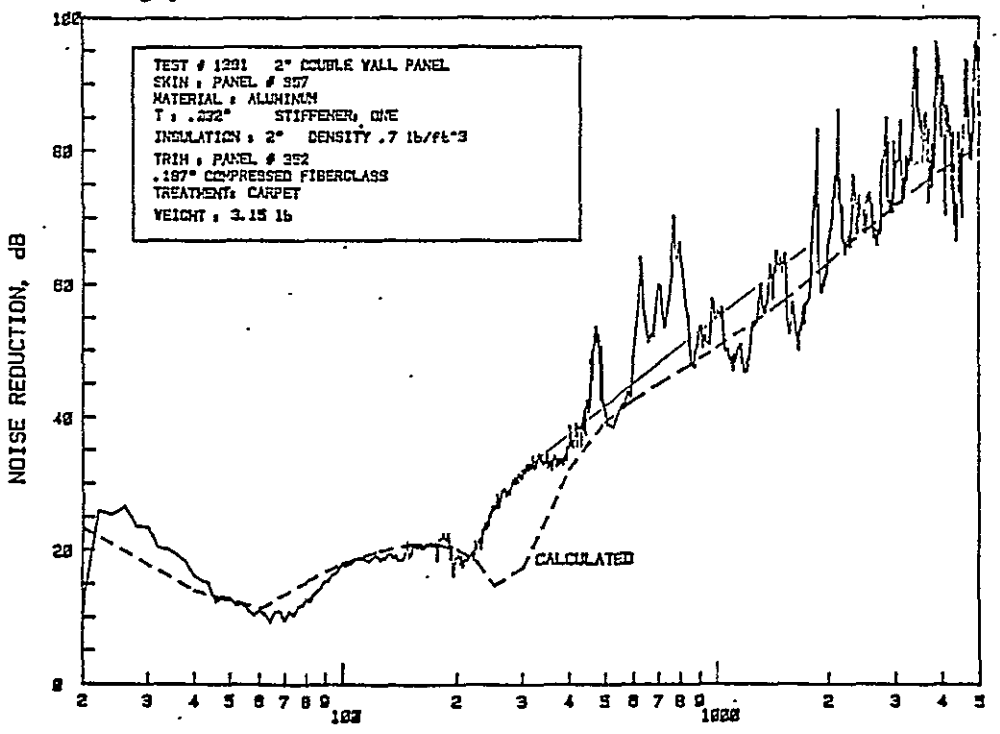

b. Fiberglass Insulation

Figure 6.9: Comparison of Experimental and Theoretical Noise Reduction Characteristics of a Double-Wall Panel Made of Aluminum Skin (Panel 357) and Trim Panel 352; Panel Depth 2"

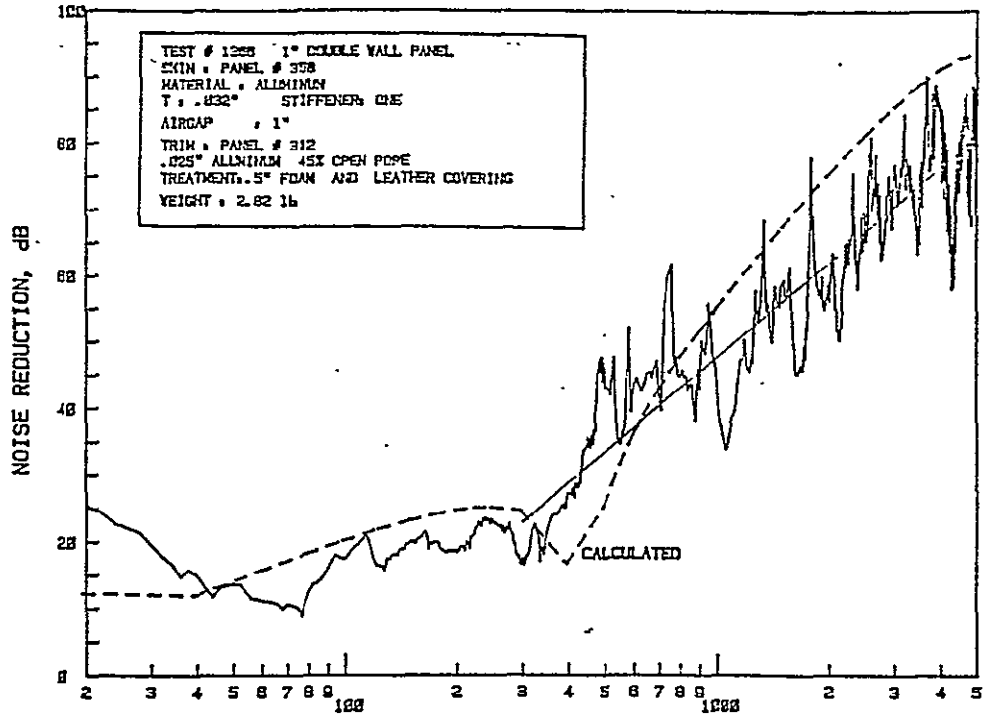

a. Airgap

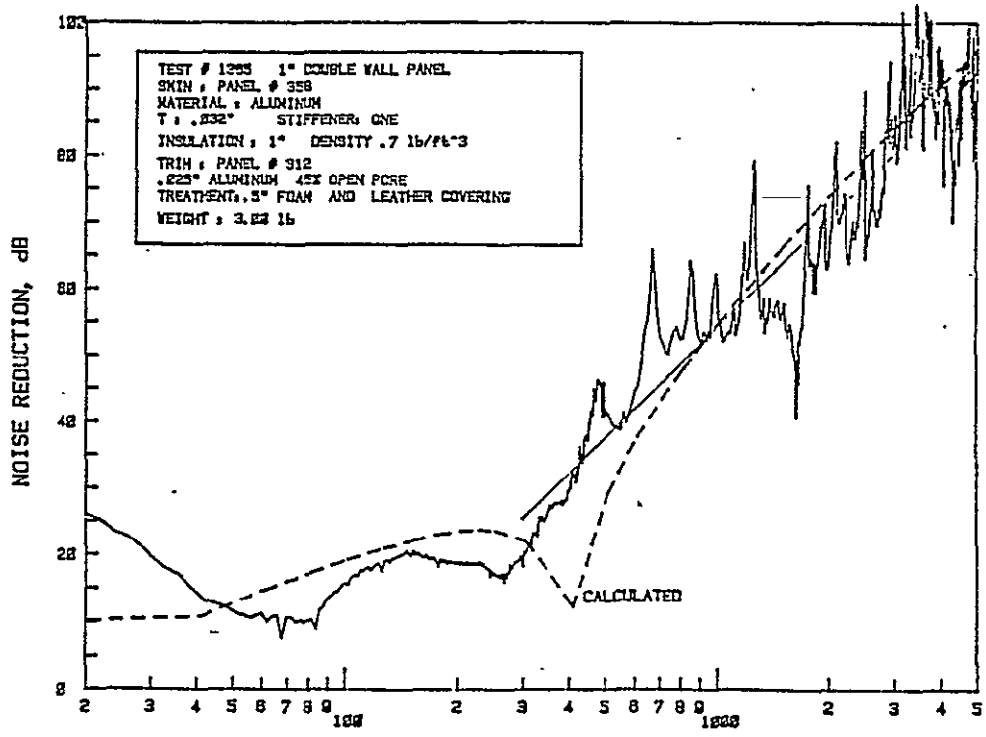

b. Fiberglass Insulation

Figure 6.10: Comparison of Experimental and Theoretical Noise Reduction Characteristics of a Double-Wall Panel Made of Aluminum Skin (Panel 358) and Trim Panel 312; Panel Depth 1"

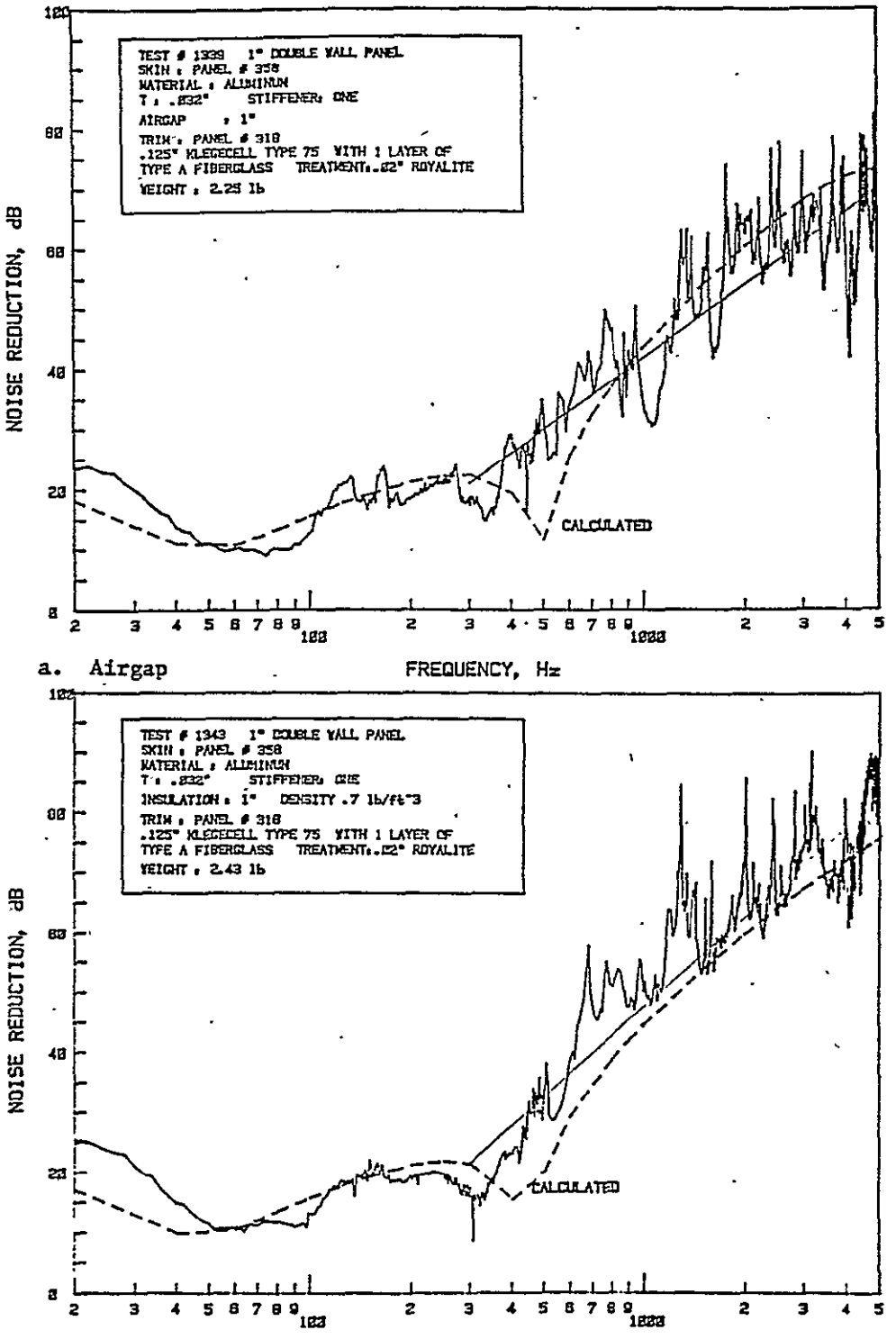

Figure 6.11: Comparison of Experimental and Theoretical Noise Reduction Characteristics of a Double-Wall Panel Made of Aluminum Skin (Panel 358) and Trim Panel 318; Panel Depth 1"

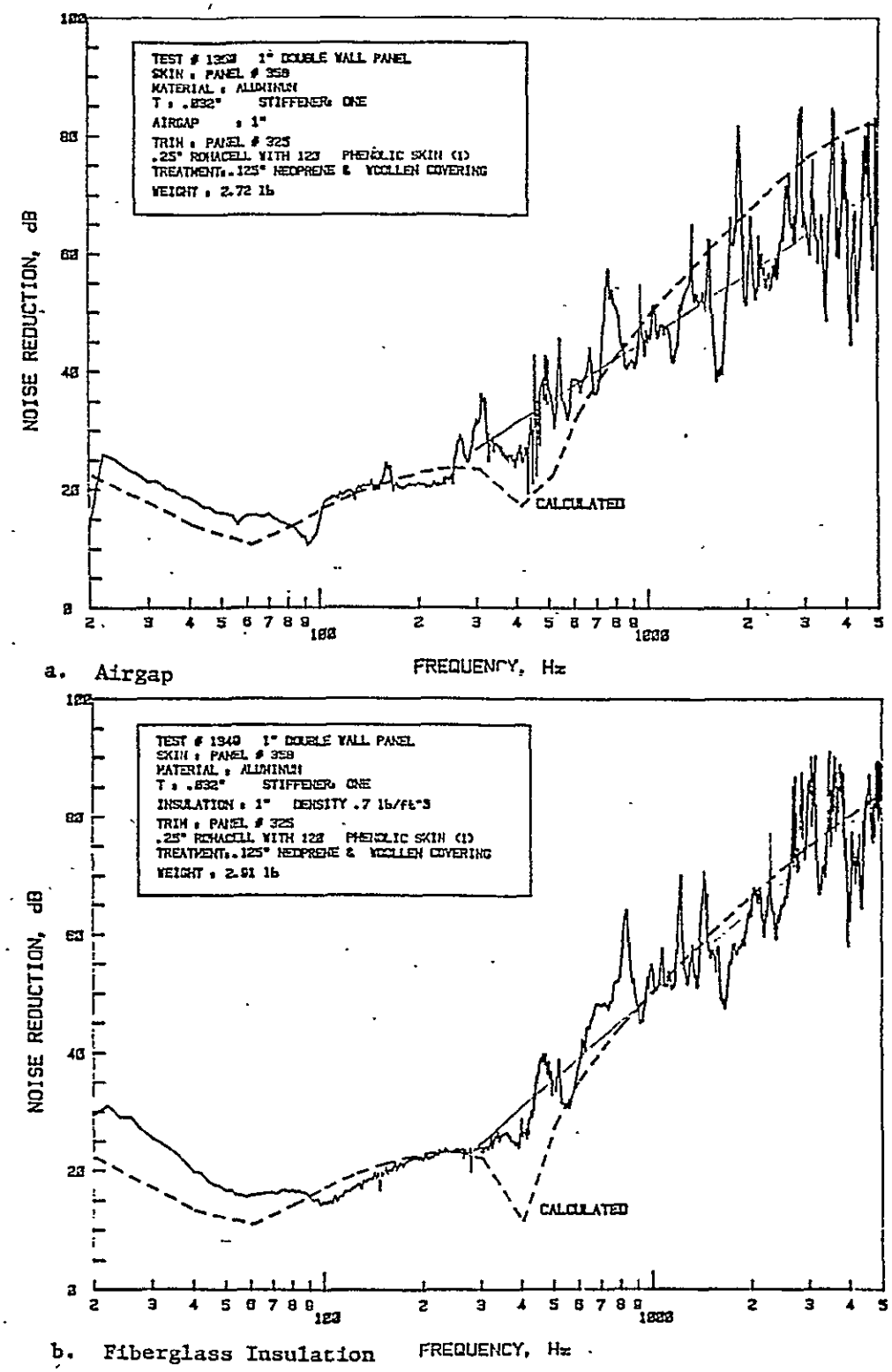

Figure 6.12: Comparison of Experimental and Theoretical Noise Reduction Characteristics of a Double-Wall Panel Made of Aluminum Skin (Panel 358) and Trim Panel 325; Panel Depth 1".

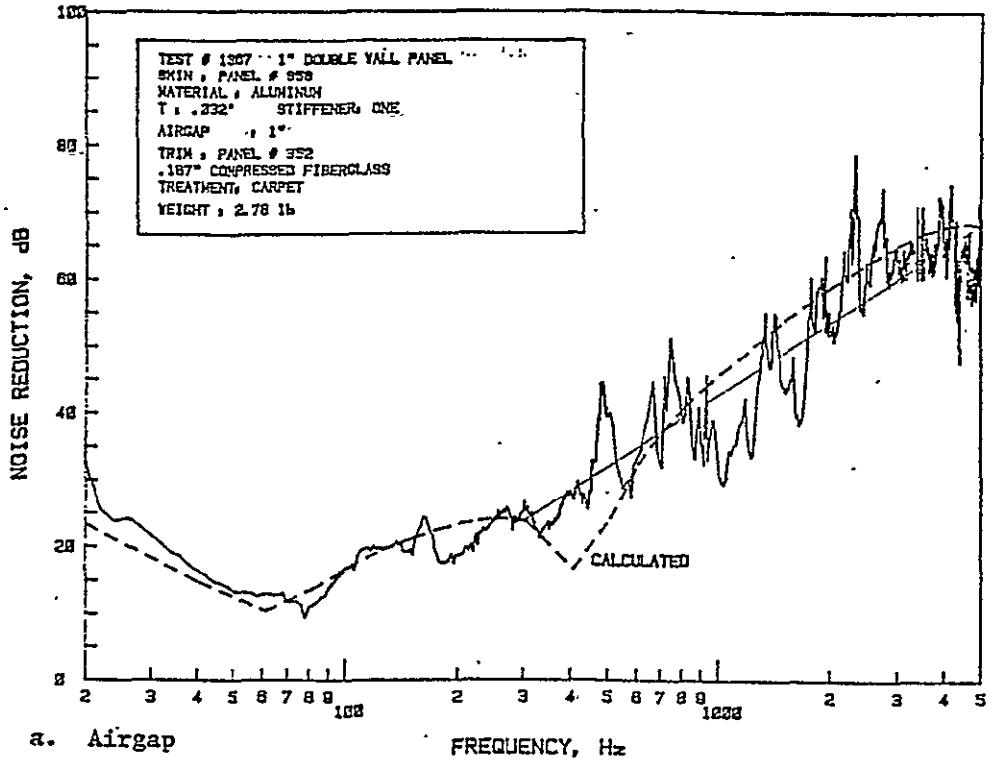

a. Airgap

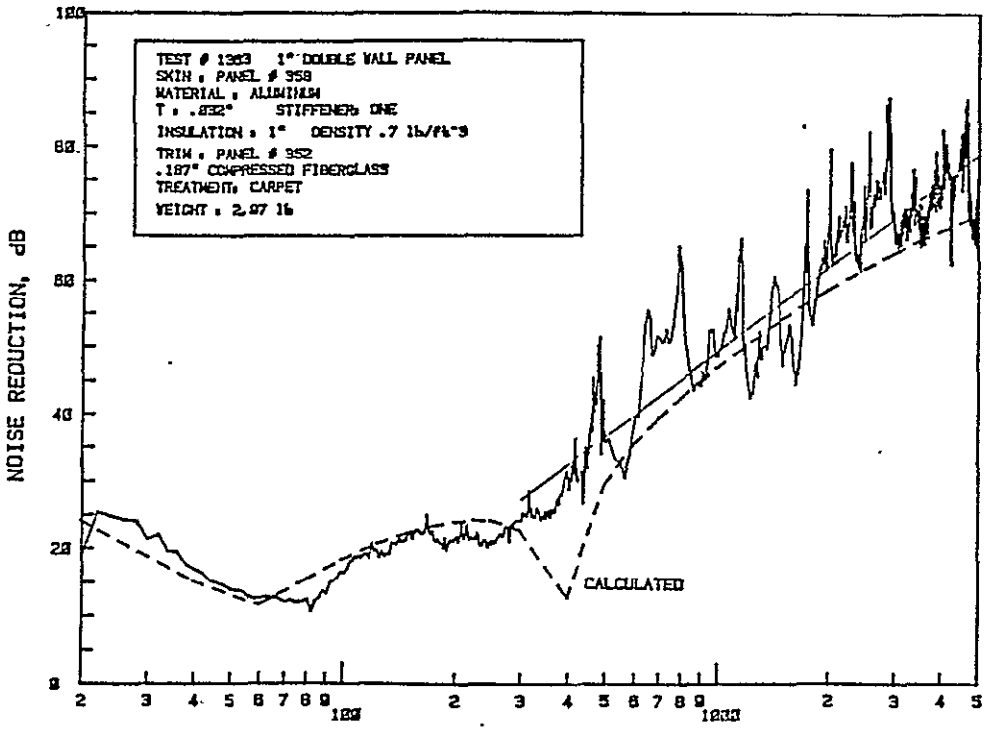

b. Fiberglass Insulation

Figure 6.13: Comparison of Experimental and Theoretical Noise Reduction Characteristics of a Double-Wall Panel Made of Aluminum Skin (Panel 358) and Trim Panel 352; Panel Depth 1"

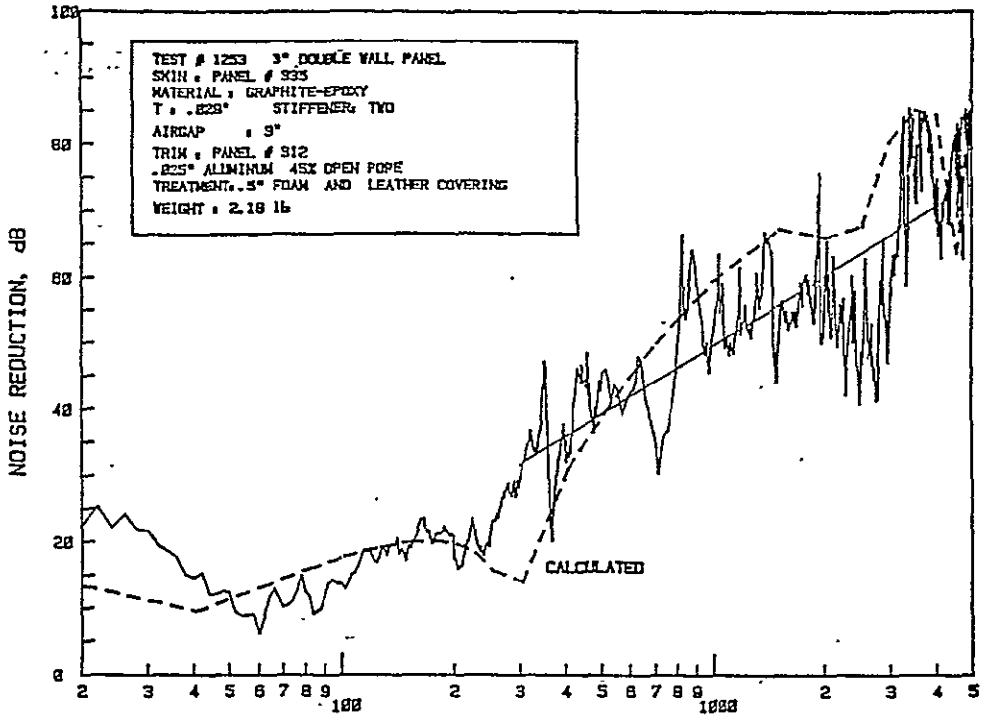

a. Airgap

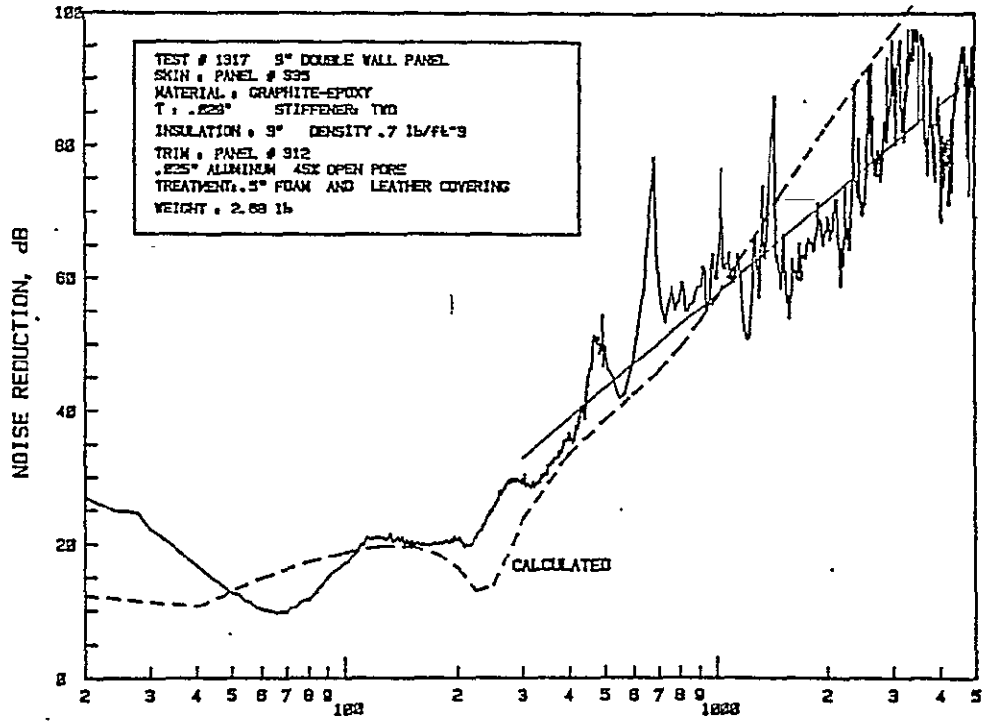

b. Fiberglass Insulation

Figure 6.14: Comparison of Experimental and Theoretical Noise Reduction Characteristics of a Double-Wall Panel Made of Graphite-Epoxy Skin (Panel 335) and Trim Panel 312; Panel Depth 3"

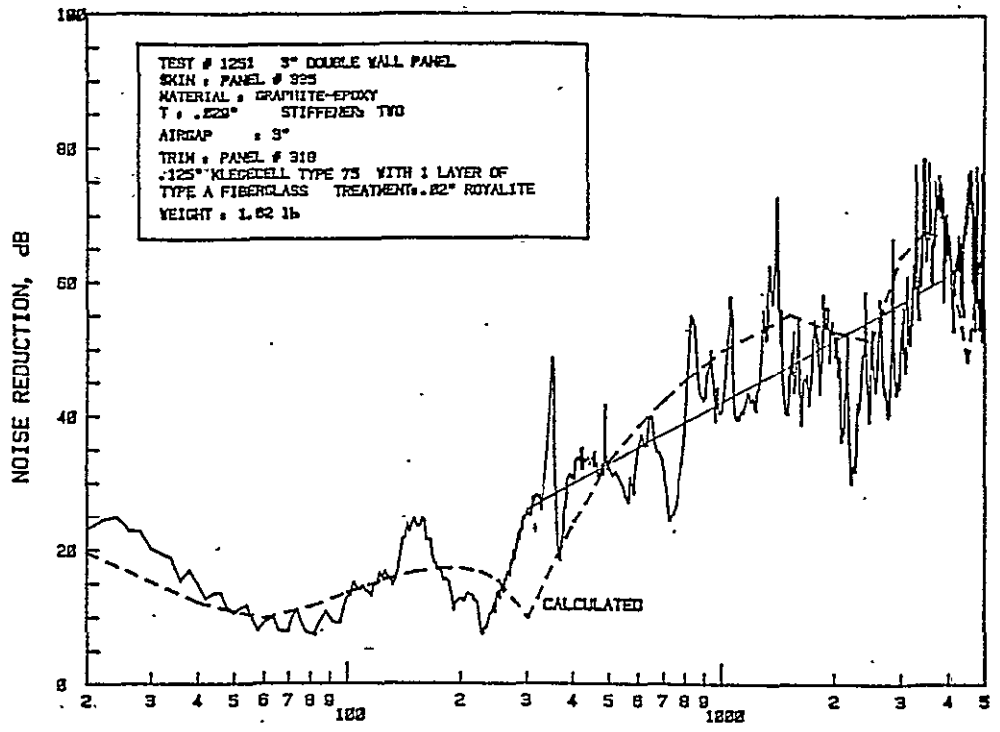

a. Airgap

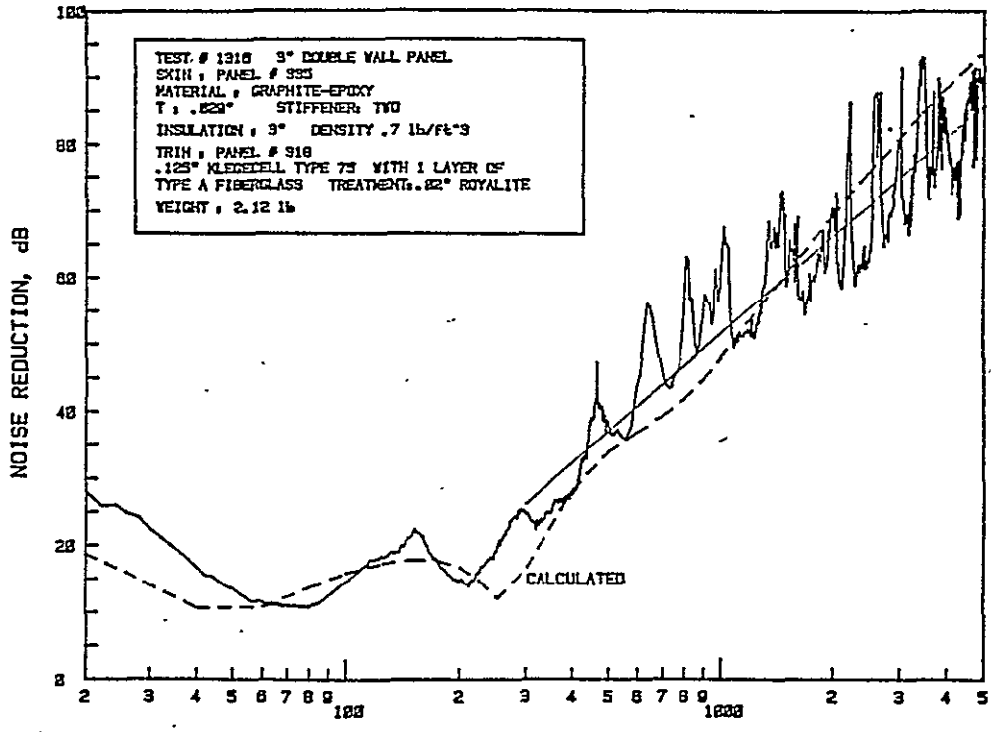

b. Fiberglass Insulation

Figure 6.15: Comparison of Experimental and Theoretical Noise Reduction Characteristics of a Double-Wall Panel Made of Graphite-Epoxy Skin (Panel 335) and Trim Panel 318; Panel Depth 3"

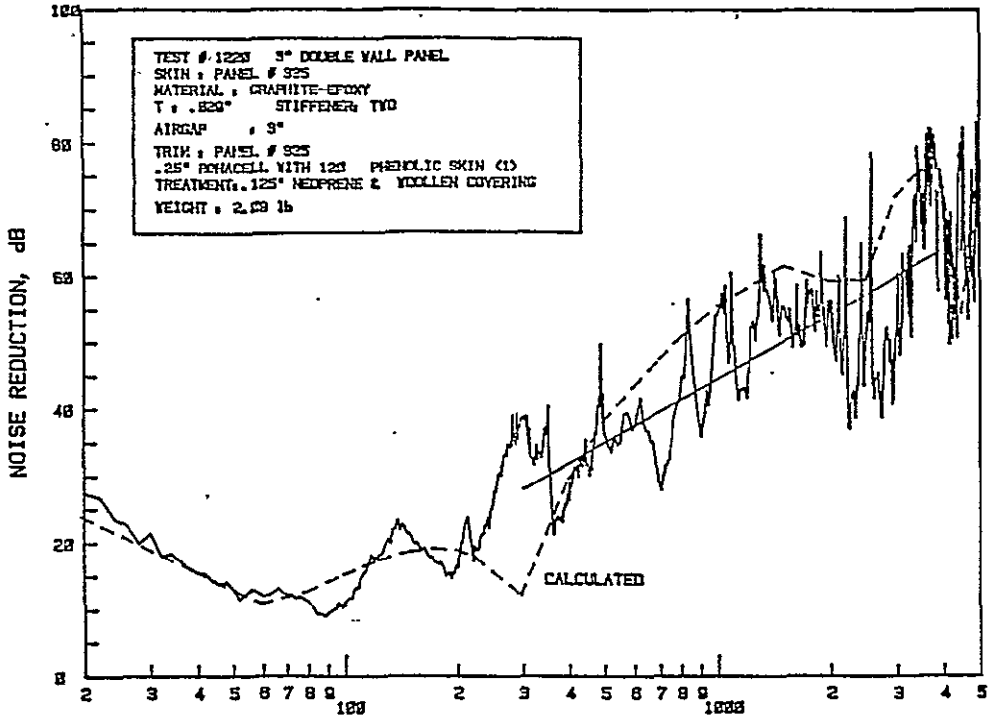

a. Airgap

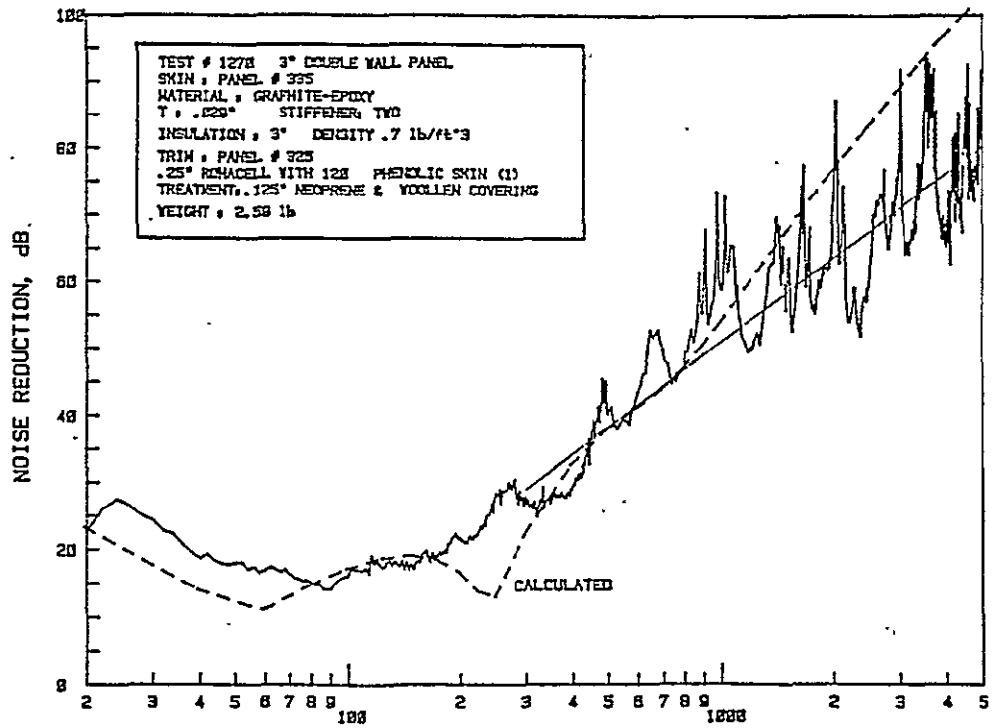

b. Fiberglass Insulation

Figure 6.16: Comparison of Experimental and Theoretical Noise Reduction Characteristics of a Double-Wall Panel Made of Graphite-Epoxy Skin (Panel 335) and Trim Panel 325; Panel Depth 3"

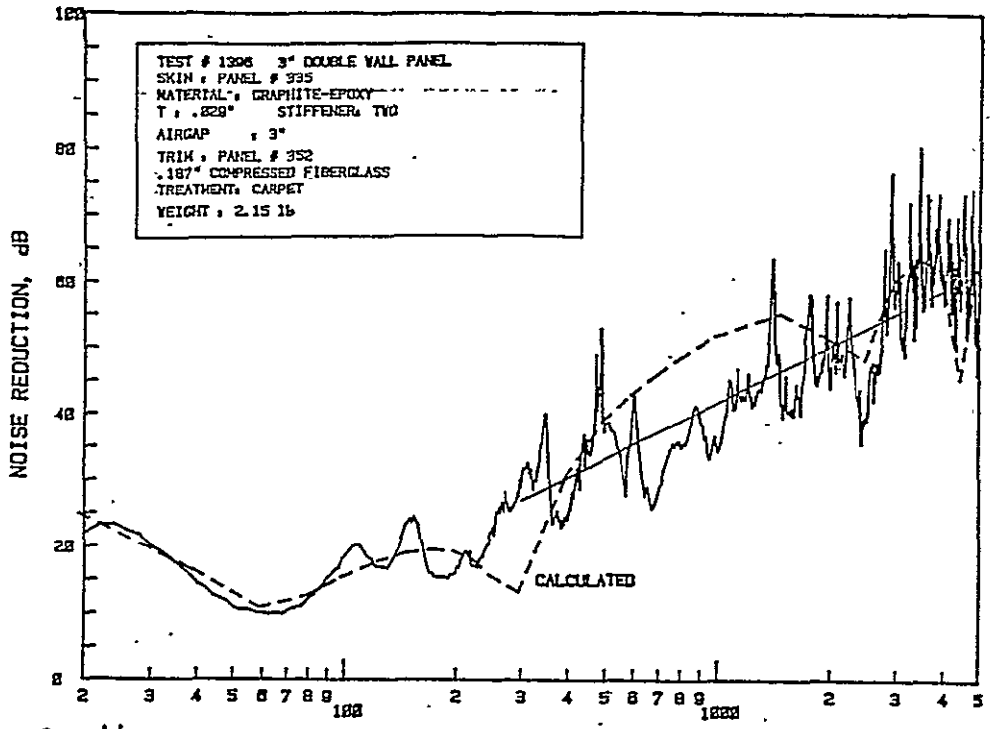

a. Airgap

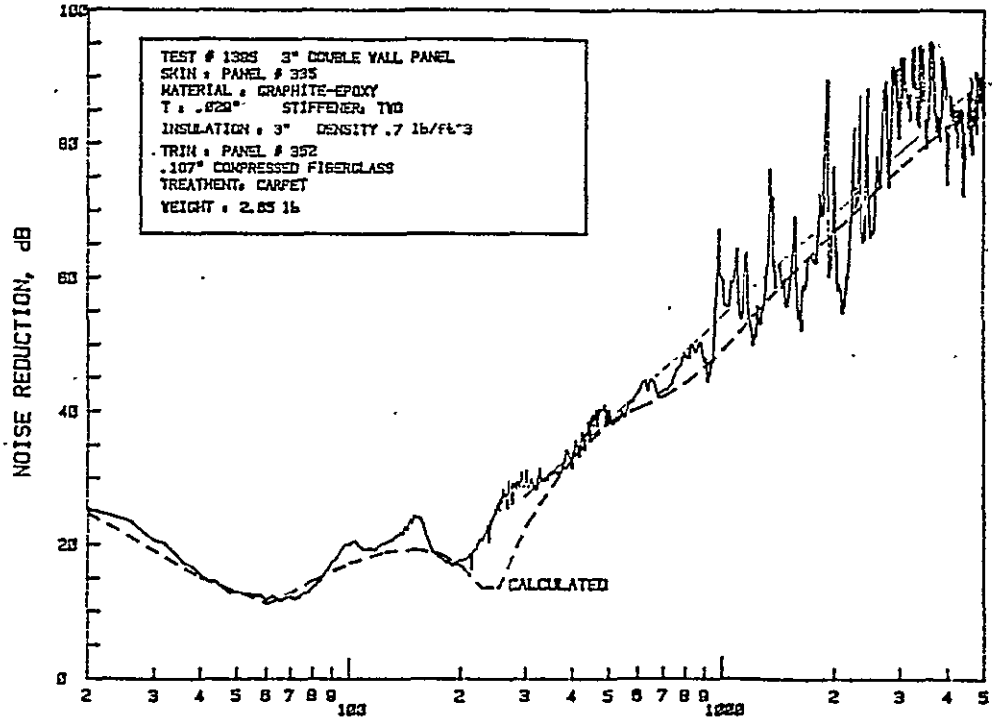

b. Fiberglass Insulation

Figure 6.17: Comparison of Experimental and Theoretical Noise Reduction Characteristics of a Double-Wall Panel Made of Graphite-Epoxy Skin (Panel 335) and Trim Panel 352; Panel Depth 3".

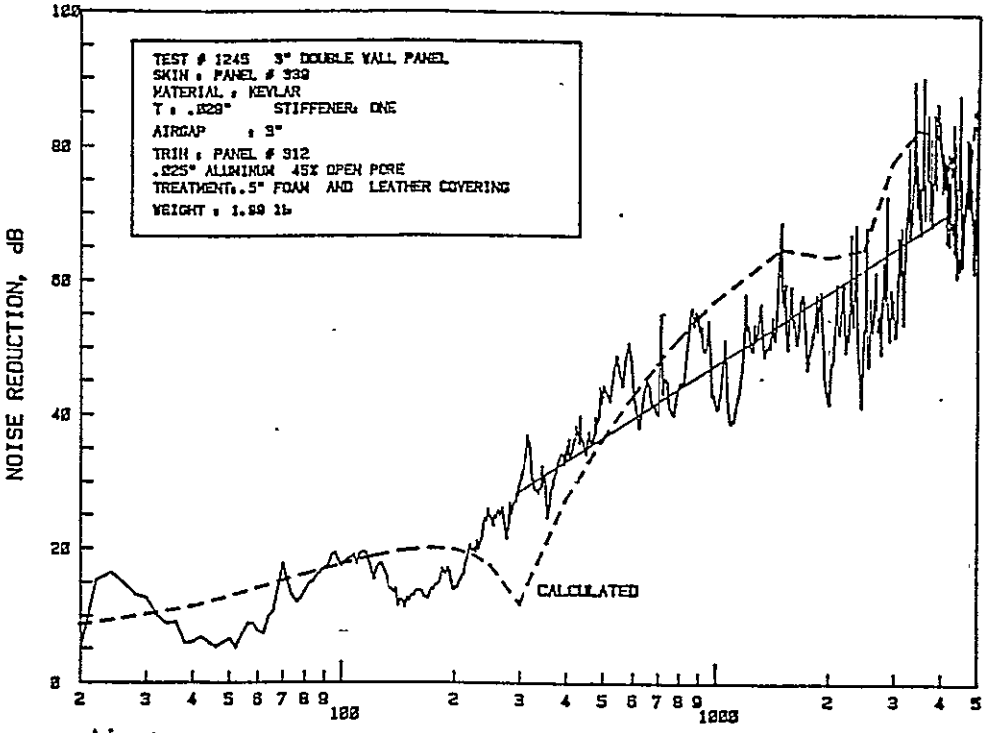

a. Airgap

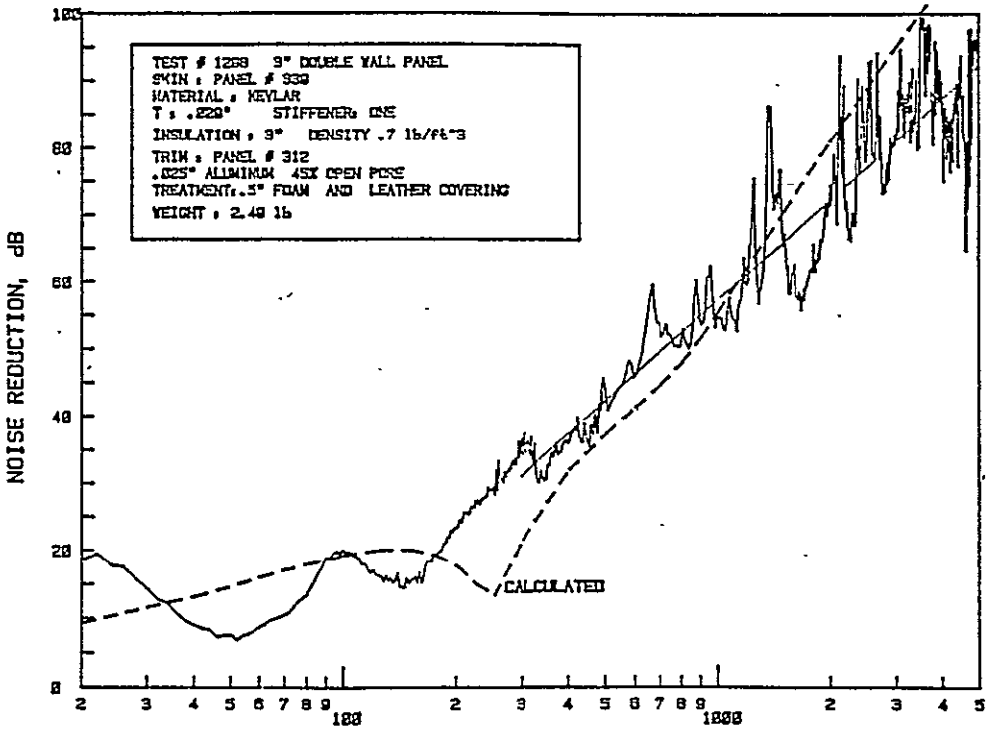

b. Fiberglass Insulation

Figure 6.18: Comparison of Experimental and Theoretical Noise Reduction Characteristics of a Double-Wall Panel Made of Kevlar Skin (Panel 339) and Trim Panel 312; Panel Depth 3"

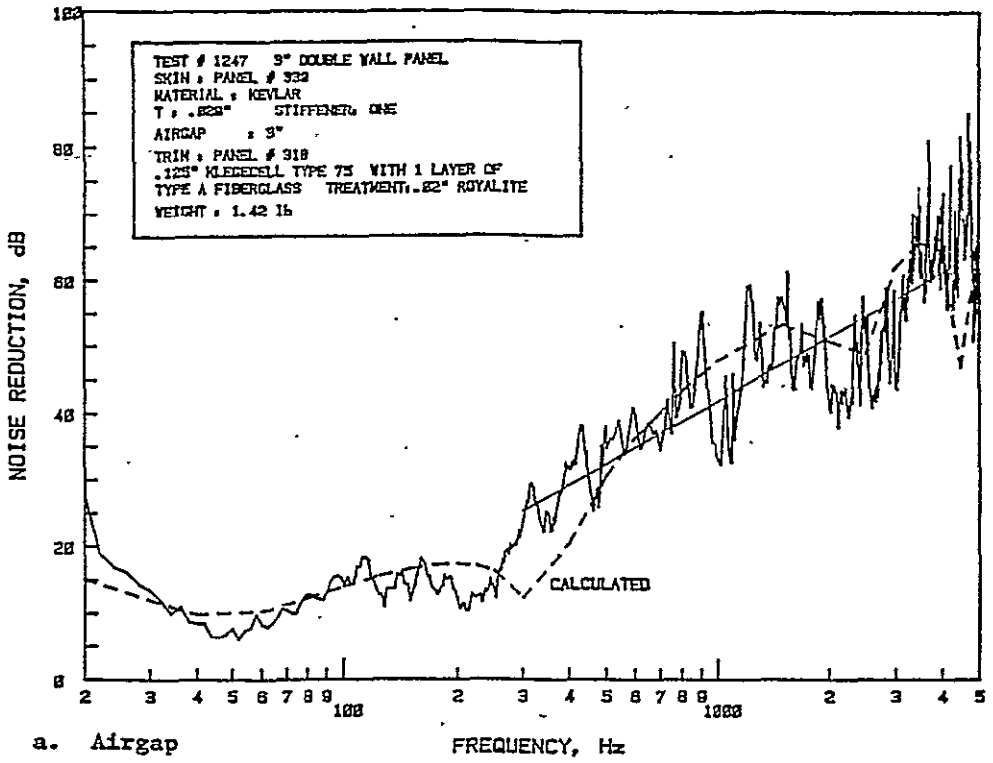

a. Airgap

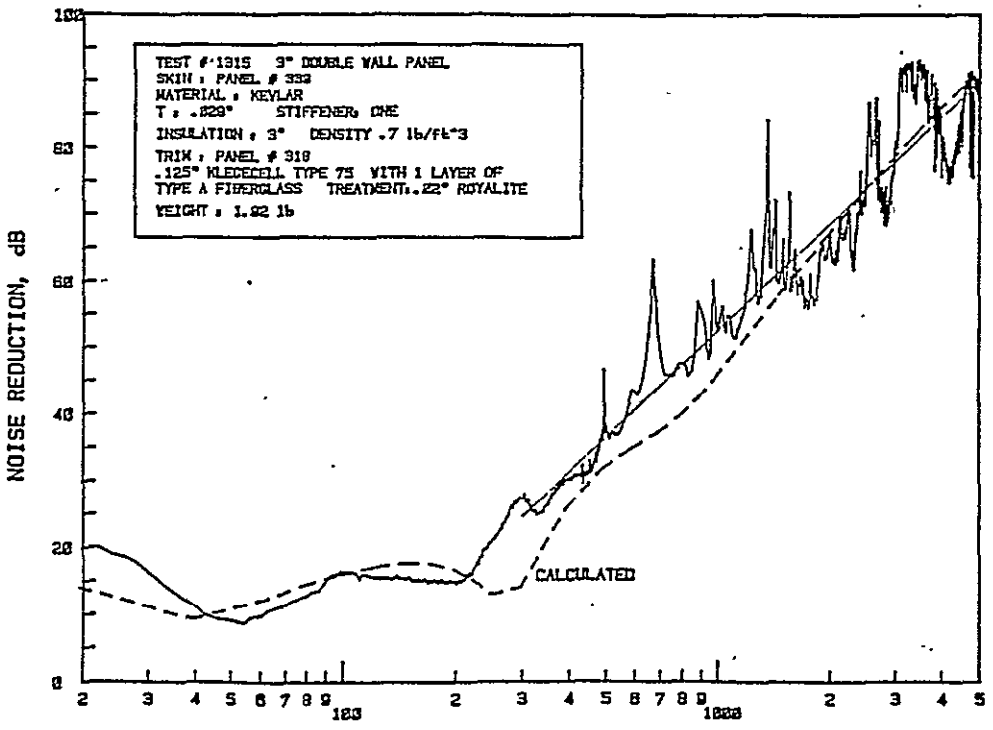

b. Fiberglass Insulation

Figure 6.19: Comparison of Experimental and Theoretical Noise Reduction Characteristics of a Double-Wall Panel Made of Kevlar Skin (Panel 339) and Trim Panel 318; Panel Depth 3"

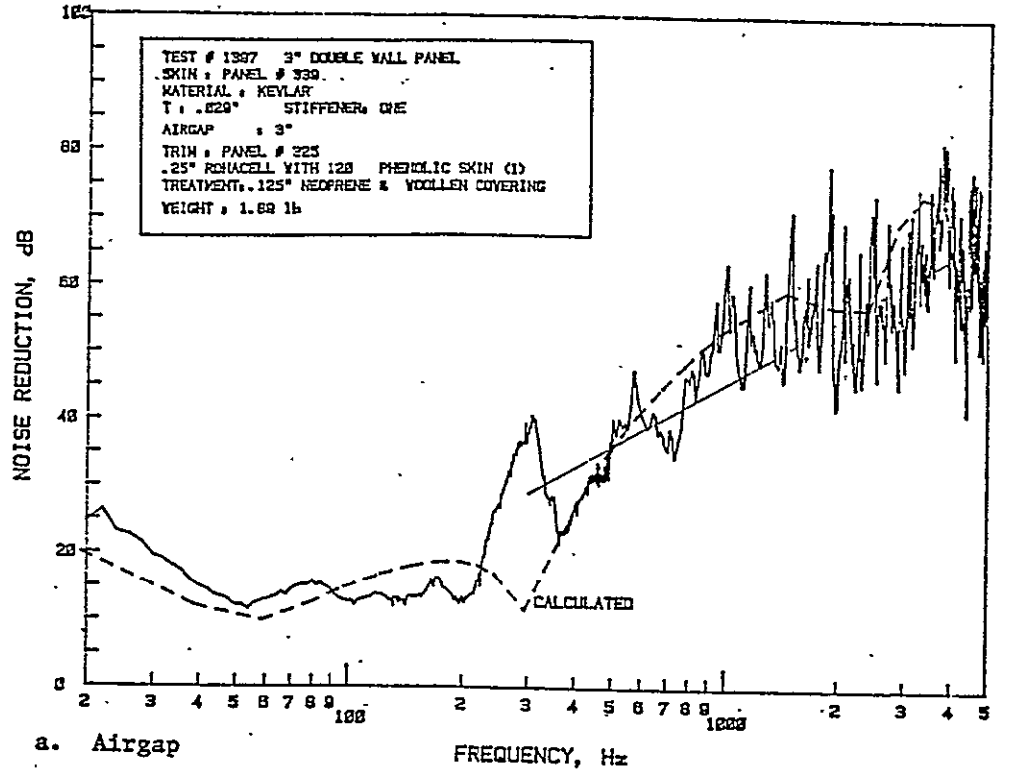

a. Airgap

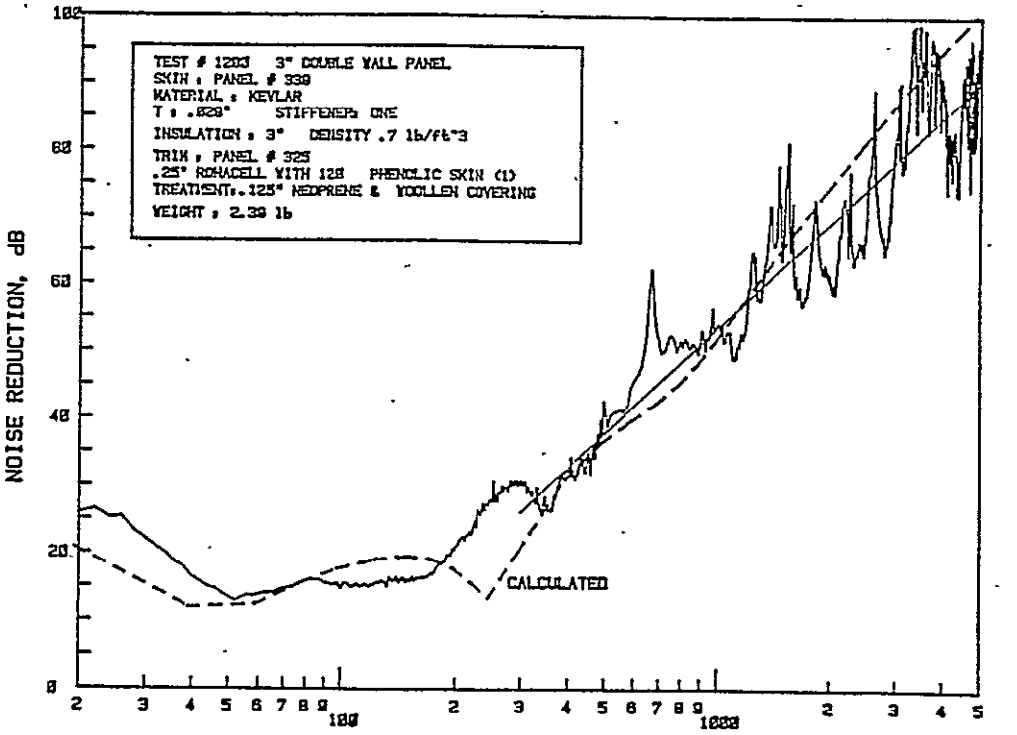

b. Fiberglass Insulation

Figure 6.20: Comparison of Experimental and Theoretical Noise Reduction Characteristics of a Double-Wall Panel Made of Kevlar Skin (Panel 339) and Trim Panel 325; Panel Depth 3"

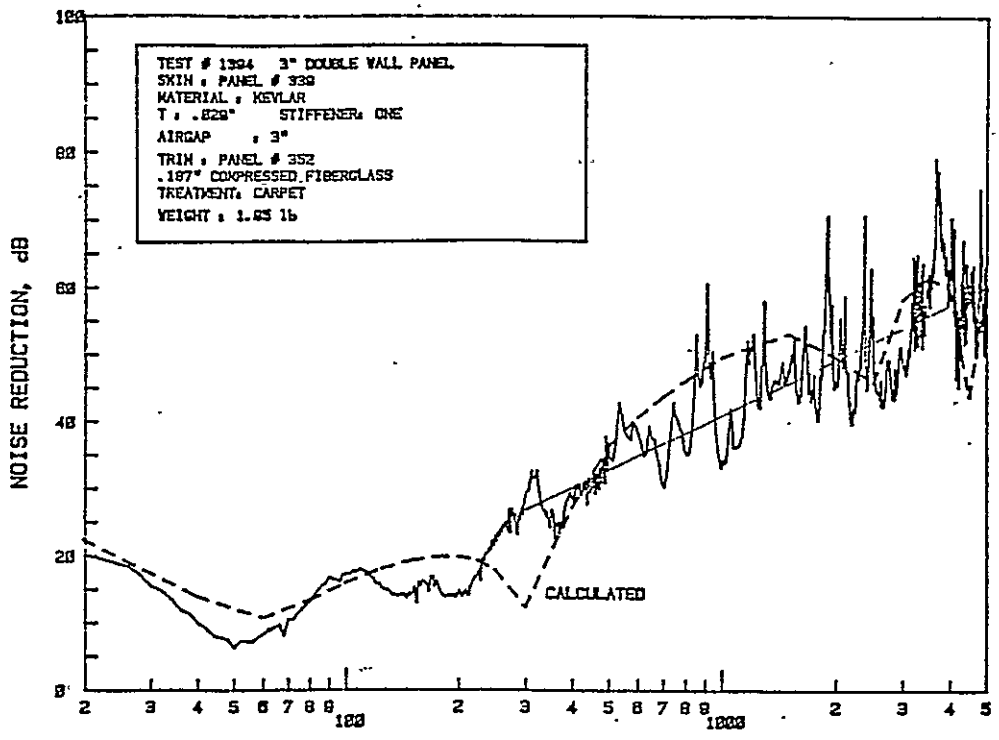

a. Airgap

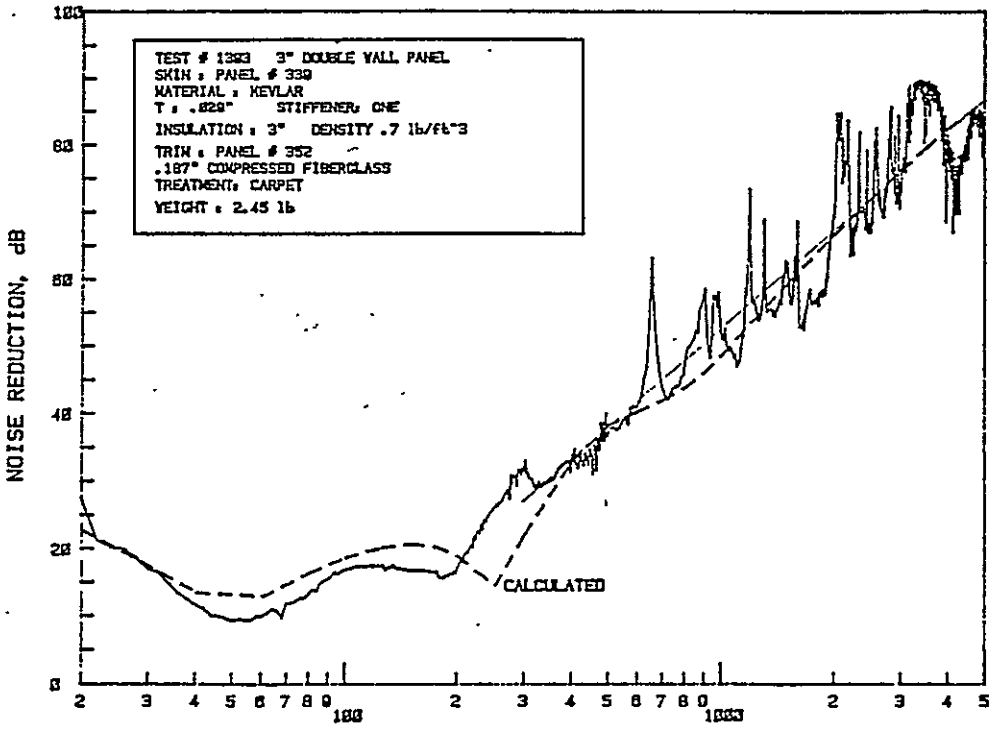

b. Fiberglass Insulation

Figure 6.21: Comparison of Experimental and Theoretical Noise Reduction Characteristics of a Double-Wall Panel Made of Kevlar Skin (Panel 339) and Trim Panel 352; Panel Depth 3"

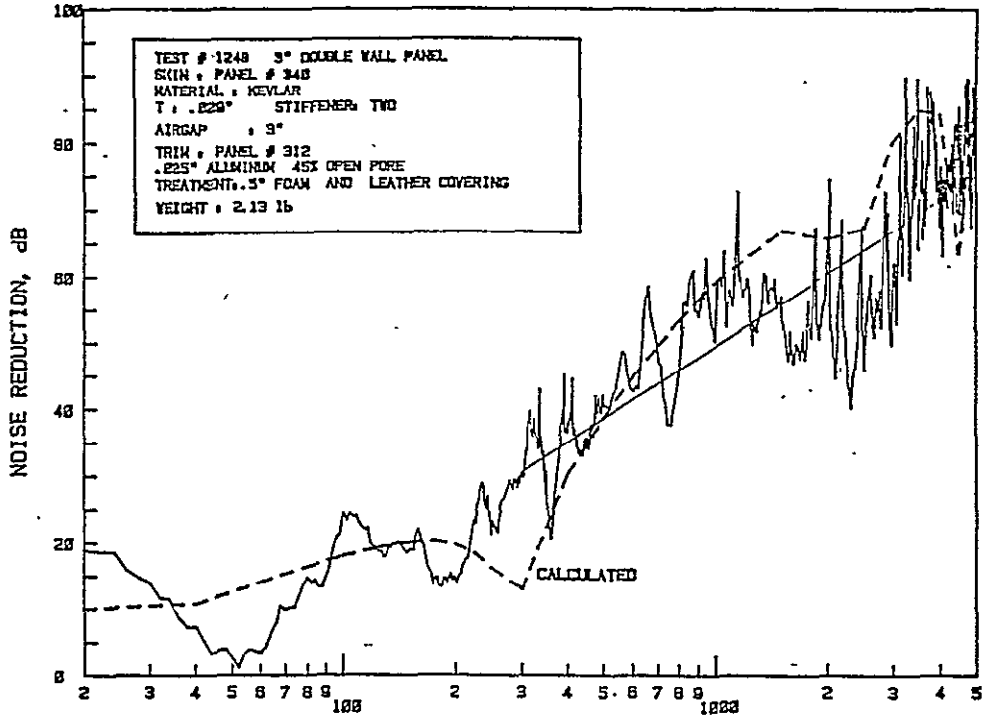

a. Airgap

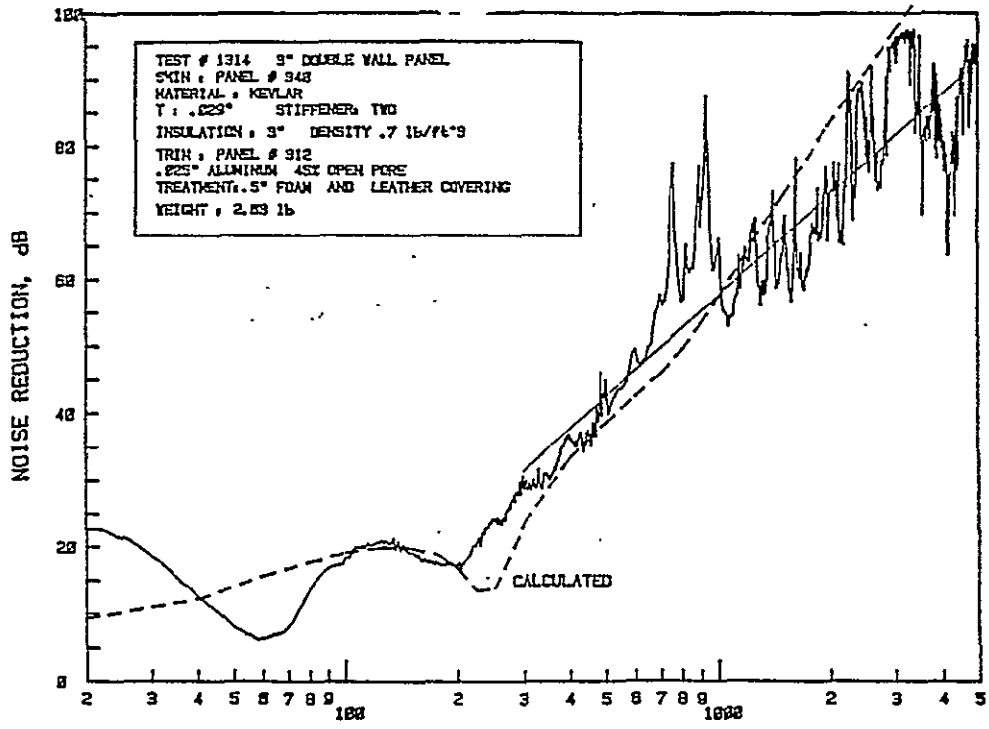

b. Fiberglass Insulation

Figure 6.22: Comparison of Experimental and Theoretical Noise Reduction Characteristics of a Double-Wall Panel Made of Kevlar Skin (Panel 340) and Trim Panel 312; Panel Depth 3"

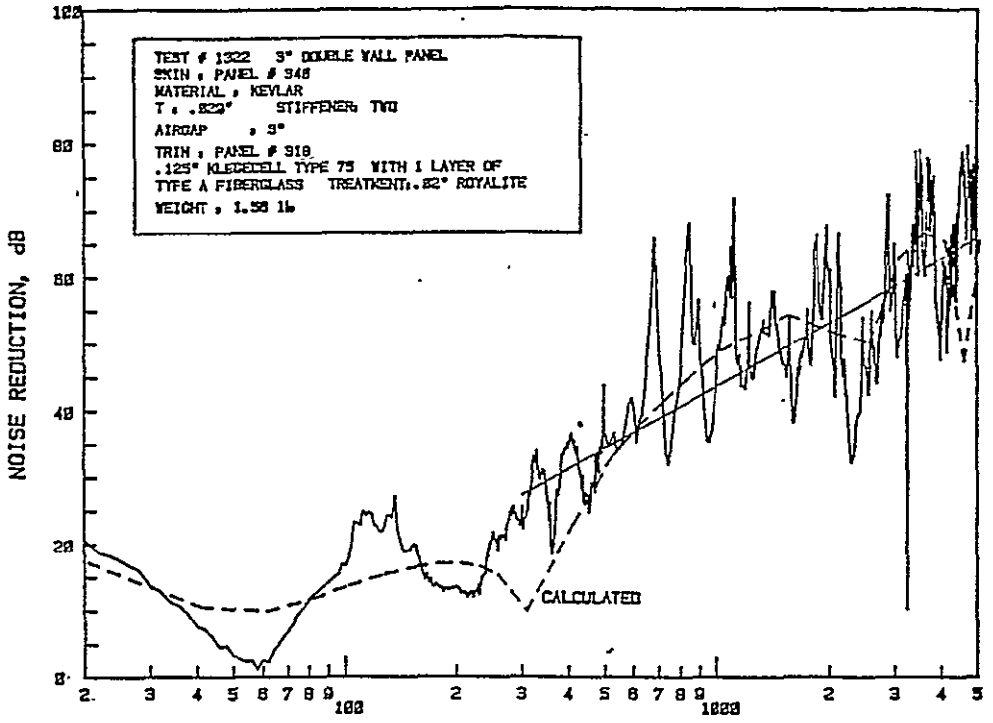

a. Airgap

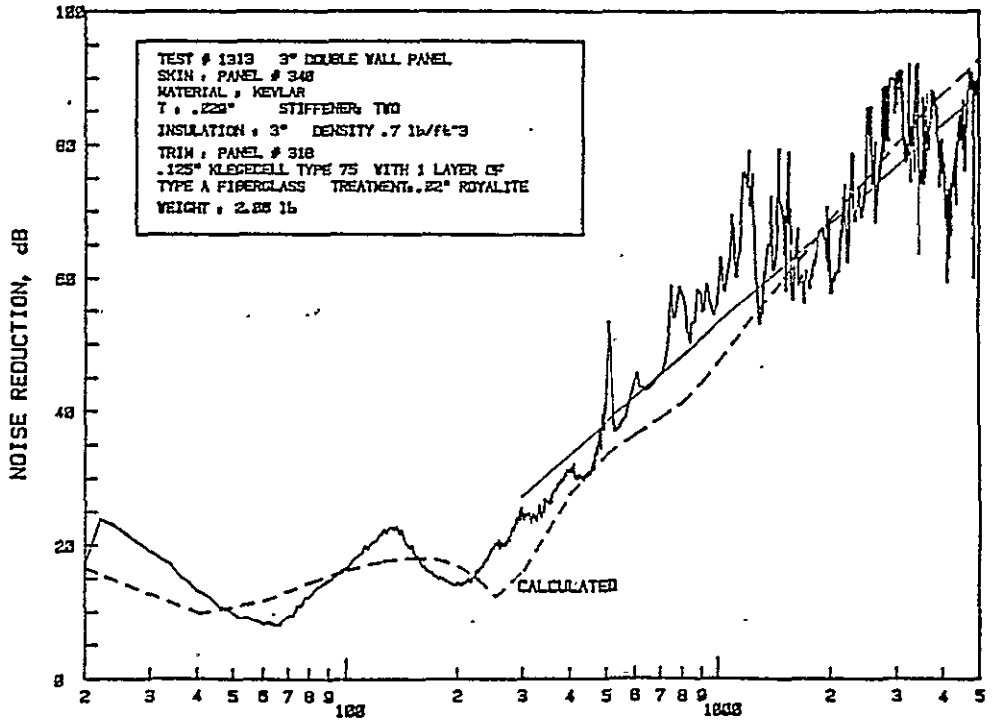

b. Fiberglass Insulation

Figure 6.23: Comparison of Experimental and Theoretical Noise Reduction Characteristics of a Double-Wall Panel Made of Kevlar Skin (Panel 340) and Trim Panel 318; Panel Depth 3"

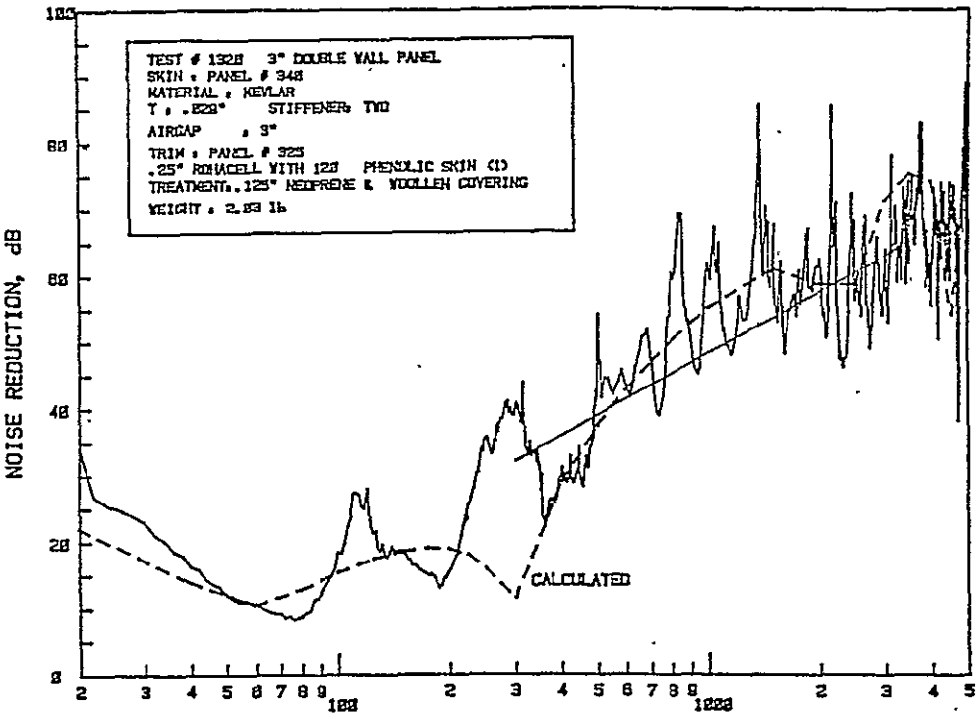

a. Airgap

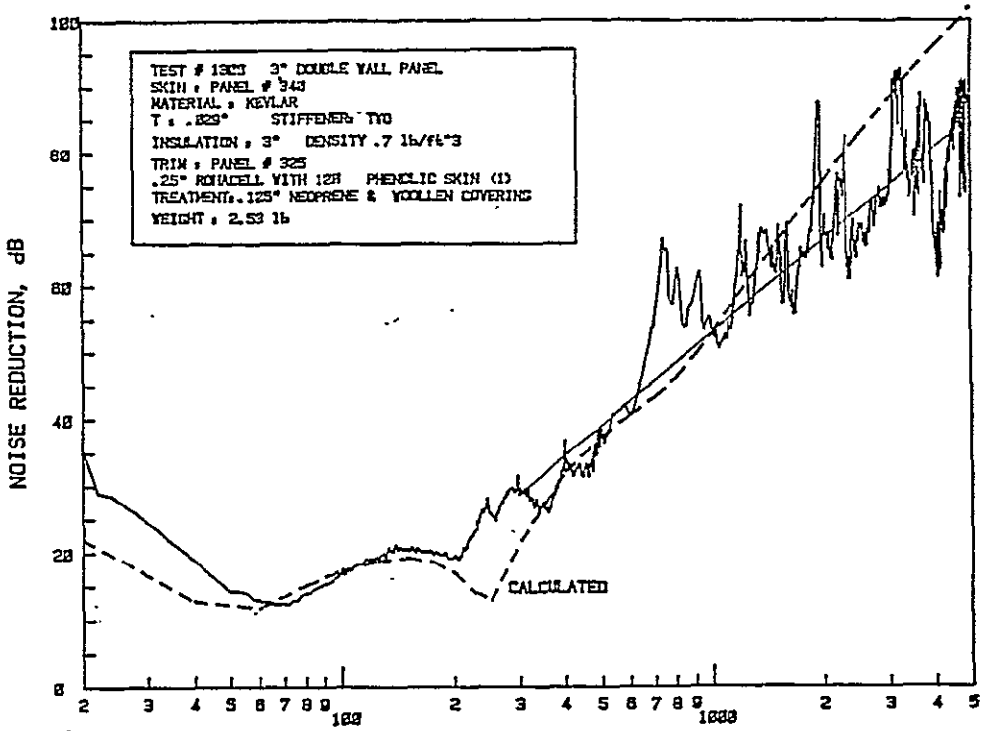

b. Fiberglass Insulation

Figure 6.24: Comparison of Experimental and Theoretical Noise Reduction Characteristics of a Double-Wall Panel Made of Kevlar Skin (Panel 340) and Trim Panel 325; Panel Depth 3"

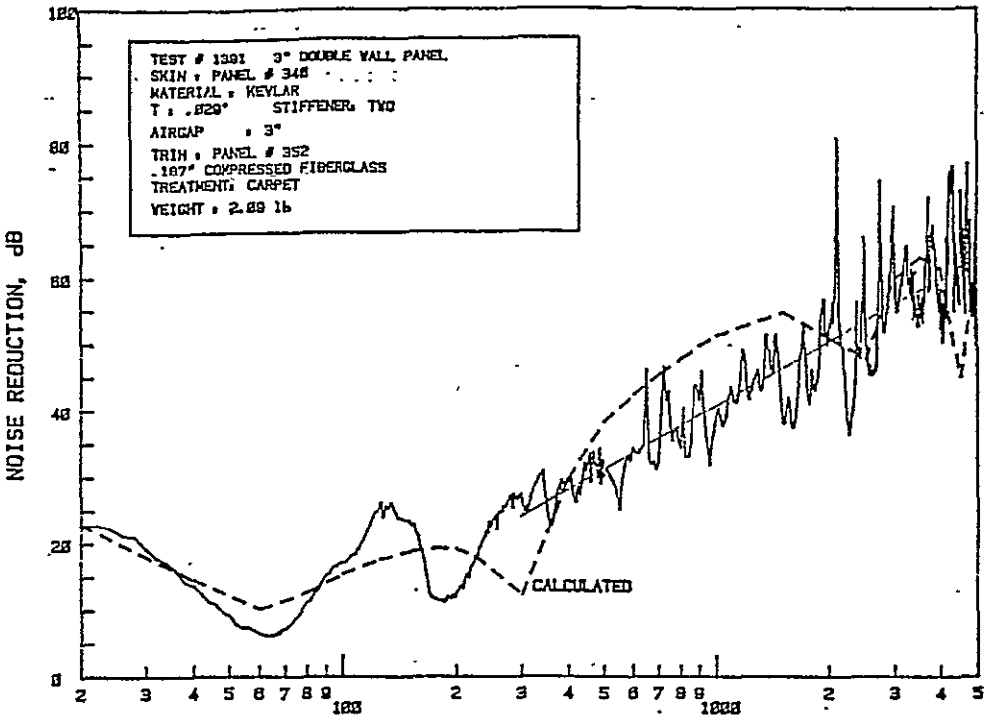

a. Airgap

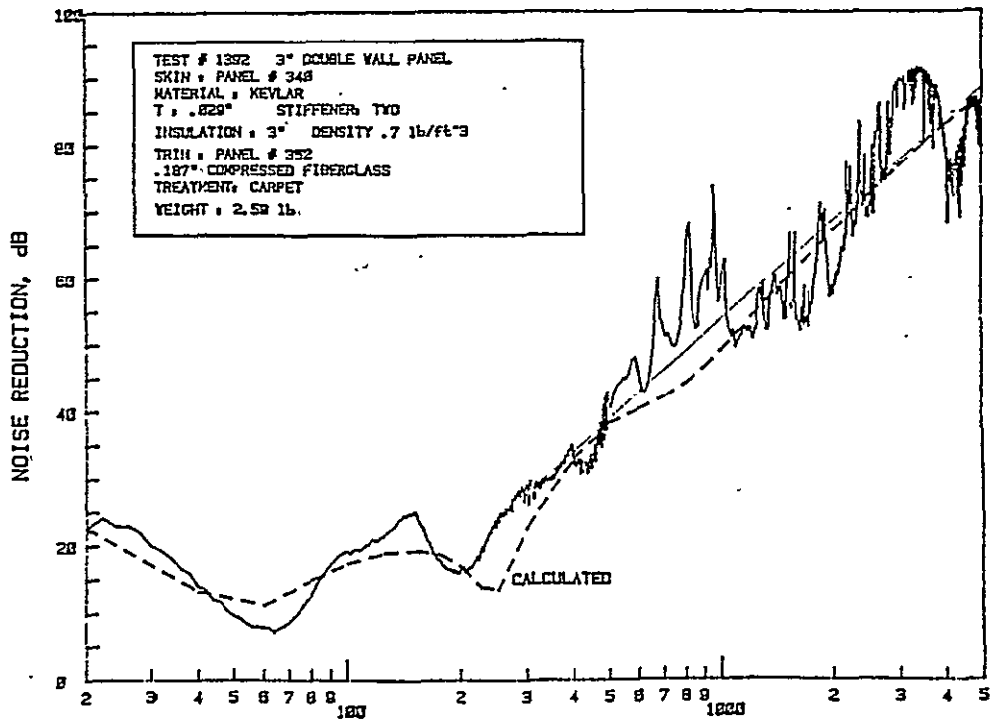

b. Fiberglass Insulation

Figure 6.25: Comparison of Experimental and Theoretical Noise Reduction Characteristics of a Double-Wall Panel Made of Kevlar Skin (Panel 340) and Trim Panel 352; Panel Depth 3"

In general, it can be seen that the agreement is reasonable for most of the cases tested. Due to the single mode approximation used in the program, the higher order modes of the skin and the trim panel are not present. Also not present are the higher order cavity modes of the receiver cavity. As the theory does not ignore the higher harmonic of the double-wall panel-air-panel resonance frequencies, they are present and can be seen at higher panel depths without any insulation between the walls.

At low frequency region the calculated values agree well with the experimental double-wall results. These results are expected, since the input values are experimental, single-panel, fundamental resonance frequencies of skin and trim panels. This indicates that at low frequencies the transmission loss is a function of single-panel stiffness. This is true when the frequency is well below the fundamental resonance frequency of either the skin or the trim panel.

In the frequency region between 100 and 500 Hz, which is the region of greatest importance for general aviation interior aircraft noise, the fundamental skin or trim resonance frequency and the fundamental double-wall, panel-air-panel frequency occur. As can be seen, the theoretical values overpredict the measured values by a large value (75 Hz). The reason for this is not understood. Figure 6.26 shows the measured and the calculated double-wall resonance frequency as a function of the thickness of the double-wall panel. The effect of the panel depth on the measured and the calculated

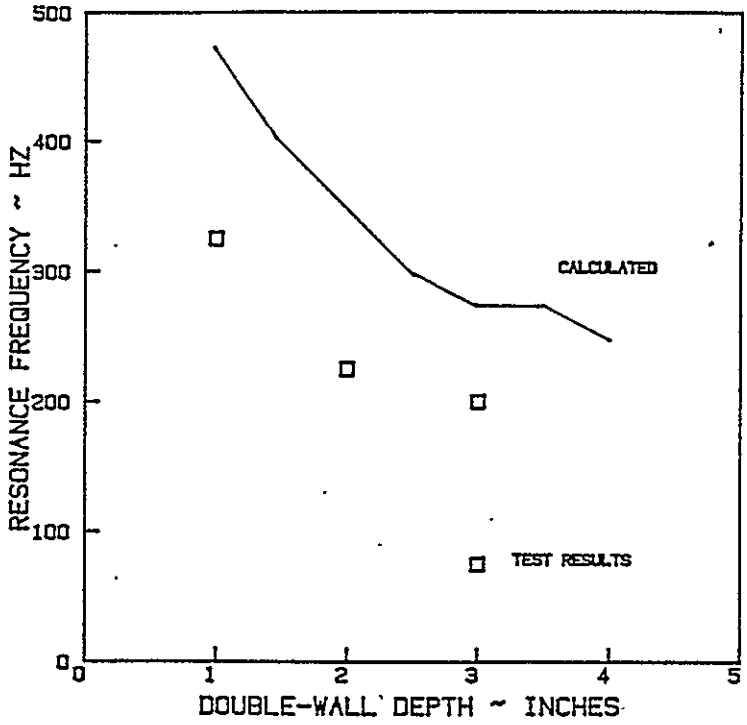

Figure 6.26: Comparison of Experimental and Theoretical Fundamental Panel-Air-Panel Resonance Frequency of the Double-Wall Panel

resonance frequencies is the same; the experimental values are always lower by 75 to 100 Hz, depending upon the trim panel. Around this frequency region, measured values of noise reduction do not agree with the calculated transmission loss values. However, the trends are still maintained.

In the high-frequency region (above 500 Hz) the higher order panel modes and the cavity modes are not predicted. With airgaps the harmonics of panel-air-panel resonances are visible. The agreement with the test results depends on the trim panel and the depth of panel. Increase in panel depth decreases the fundamental panel-air-panel resonance by the same amount as the experimental results, as can be seen from Figure 6.26. At 3000 Hz frequency the calculated transmission loss dips at 2" depth because of this resonance frequency. This has also been observed in the experimental results. With the insulation no decrease in noise reduction is observed near the harmonic of the panel-air-panel resonance frequency. Whenever the theoretical results are above 90 dB, the difference between the experimental values and the theoretical values is large. This is due to the limitation of the dynamic range of the instrumentation.

The theoretical results overpredict the high frequency noise reduction of the double-wall panel with trim panel 312, and they underpredict the noise reduction of the double-wall panel with trim panel 352. This is because of the variation in the actual slope of the trim panels. The slope of panel 312 is 8 dB/octave, and that of

panel 352 is nearly zero. These results indicate that the double-wall evens out these differences. Reasonably good fit is obtained when the slope is less than the theoretical 6 dB/octave slope. Hence it can be concluded that the double wall acts as though the trim panel slope is somewhere between .5 and .8 times the theoretical slope.

6.6 CONCLUSIONS

In this chapter a computer program developed using classical sound transmission theory is described. The computer program can accept up to 10 layers. The layers can consist of skin, airgap, fiberglass insulation, septum, and trim. Different options are available to model various impedance characteristics of the skin and trim panels.

The results obtained from the computer program were compared with the experimental results from double-wall panels with three layers. The agreement is considered reasonable, considering the simplifying assumptions of the model. The theoretically determined panel-air-panel resonance frequencies do not match with the experimental values. However, both follow the same trend. The use of slope factor improves the agreement. The agreement is good if the slope factor is between 0.5 and 0.8.

CHAPTER 7

MEASUREMENT OF TRANSMISSION LOSS OF PANELS USING ACOUSTIC INTENSITY TECHNIQUE

7.1 INTRODUCTION

The characteristics and the limitations of the measurement techniques currently used are described in Reference 21. Most of the limitations mentioned in Reference 21 are due to the small size of source and receiver sections of this test facility and the use of acoustic pressure levels instead of acoustic sound power levels as a measure of sound power. Also, in the present method, the sound pressure levels are measured at only one location. Even though this location had been chosen after a careful experimental study, it is possible that this location may not be ideal for some cases. Measurement of the sound power by the integration of the acoustic intensity levels over the entire panel will eliminate a few of these limitations. The direct measurement of the acoustic intensity has now been made possible by the development of the two-microphone, cross-spectral method. This chapter describes the adoption of this measurement technique at this test facility to measure transmission loss values of the panel.

Theoretical developments for the calculation of the acoustic intensity from the pressure measurements by two microphones separated by a known distance is given in Section 7.2. In Sections 7.3 and 7.4 some of the limitations of this method and ways to reduce some of the errors encountered are also described. The

present test set-up had to be changed to introduce the intensity method at this test facility. The modified test set-up is presented in Section 7.5 Also presented in this section is the description of the computer programs and the modified test procedures. A typical test result from this test facility obtained using the acoustic intensity technique is given in Section 7.6. The chapter is concluded with a discussion of results obtained.

7.2 THEORETICAL ANALYSIS

7.2.1 ACOUSTIC INTENSITY

The acoustic intensity at any point is defined as the rate of acoustic energy flow across a surface of unit area (Reference 29). By definition:

$$I_{r,inst} = \frac{\delta E_r}{\delta t \delta A} \qquad (7.1).$$

This energy flux, δE_r , is equal to the amount of work done upon the area A in the direction r due to the total force, F_r; i.e.,

$$\delta E_r = F_r \cdot \delta r = p_t \delta A \cdot \delta r \qquad (7.2),$$

where p_t is the total pressure comprising the ambient pressure p_a and the sound (perturbed) pressure p. This gives

$$I_{r,inst} = p_a u + pu \qquad (7.3),$$

where $u = \partial r/\partial t$ is the particle velocity in the direction r. Both the sound pressure and the particle velocity are functions of spatial coordinates and time. For sinusoidal processes, the time-averaged value of the first term is zero if the averaging time is an integral number of half periods. For other processes, it will be zero if the averaging time is sufficiently long. If the processes are stationary random, the same result can be obtained by

$$E\{I_r\} = E\{p_a u_r\} + E\{pu_r\}$$

$$= p_a E\{u_r\} + E\{pu_r\}$$

$$= p_a u_{r_{mean}} + E\{pu_r\} \qquad (7.4).$$

If the mean flow is zero, then

$$E\{I_r\} = E\{pu_r\} \qquad (7.5).$$

Direct measurement of intensity using pressure-velocity product has proved very difficult in field conditions (Reference 30). An indirect measurement, wherein two microphones are used to measure the acoustic intensity, has gained wide attention in recent years (Reference 30). In the next section, equations required for the

measurement of acoustic intensity using this method will be derived. This derivation closely follows References 30 and 31.

7.2.2 ESTIMATION OF ACOUSTIC INTENSITY USING TWO-MICROPHONE METHOD

With zero mean flow of the medium, the time-averaged intensity is given by Equation (7.5). For ease of calculation, let us consider both $p(r,t)$ and $u(r,t)$ to be stationary random processes. Fourier transforms of stationary random processes exist if their autocorrelations and cross correlation are aperiodic (Reference 32). In such cases the Fourier transforms of $p(r,t)$ and $u(r,t)$ are defined as

$$P(r,\omega) = - \int_{-\infty}^{\infty} p(r,t) e^{-j\omega t} dt \qquad (7.6),$$

$$U(r,\omega) = - \int_{-\infty}^{\infty} u(r,t) e^{j\omega t} dt \qquad (7.7).$$

From Euler's equation (Reference 29), the relationship between the particle acceleration and the pressure is obtained as

$$\rho \frac{\partial u}{\partial t} = - \text{grad } p \qquad (7.8).$$

In one direction, namely r,

$$\rho \frac{\partial u_r}{\partial t} = - \frac{\partial p}{\partial r} \qquad (7.9).$$

In subsequent discussions, it is assumed that the particle velocity is in the direction r, and hence the subscript r will be dropped. The particle velocity is obtained by integrating Equation (7.9):

$$u = -\frac{1}{\rho} \int_{o}^{t} \frac{\partial p}{\partial r} dt \qquad (7.10).$$

To measure intensity using two microphones, an intensity measurement apparatus as shown in Figure 7.1 is used. In practice, the pressure at the center of closely spaced points A and B can be approximated by taking the mean of p_A and p_B. The pressure gradient, to a first order, can be calculated by dividing the difference in pressures at p_A and p_B by the separation distance, δr. These approximations give the following estimates for p(r,t) and u(r,t):

$$p(r,t) = \frac{1}{2} \{p_A(r,t) + p_B(r,t)\}$$

$$u(r,t) = -\frac{1}{\rho \delta r} \int_{o}^{t} (p_B - p_A) dt \qquad (7.11).$$

These approximations can be considerd valid as long as the separation is small compared to the wavelength, λ (Reference 31). Following Laplace transform procedures, the time integral of the transform can be replaced by

$$\mathcal{F}[\int u dt] = \frac{U(\omega)}{j\omega} \qquad (7.12).$$

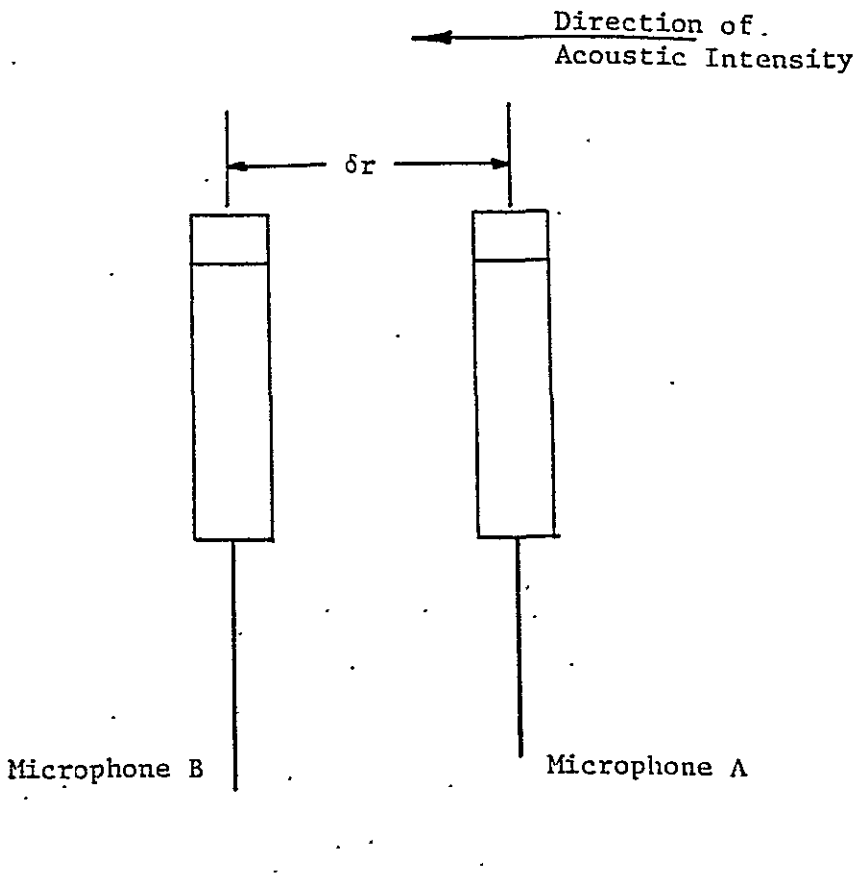

Figure 7.1: Acoustic Intensity Measurement Apparatus

Reference 31 states that even though this procedure is mathematically incorrect, it gives valid results in practice. Hence Fourier transforms of p(r,t) and u(r,t) can be written as

$$P(r,\omega) = \frac{1}{2}\{P_A(r,\omega) + P_B(r,\omega)\} \tag{7.13},$$

$$U(r,\omega) = -\frac{1}{j\omega\delta r\rho}\{P_B(r,\omega) - P_A(r,\omega)\} \tag{7.14}.$$

From Equation (7.5):

$$i_{r,av} = E\{p(r,t)u(r,t)\} \tag{7.15}.$$

Both p and u are functions of the spatial coordinates of r. The cross correlation function of p and u is defined by (Reference 32):

$$R_{pu}(t_1 t_2) = E\{p(t_1)u(t_2)\} \tag{7.16}.$$

Because of the stationarity, this equation can be written as

$$R_{pu}(\tau) = E\{p(t)u(t + \tau)\} \tag{7.17}.$$

At $\tau = 0$,

$$R_{pu}(0) = E\{p(t)u(t)\} \tag{7.18}.$$

The right hand side of the equation is equal to the averaged intensity. Therefore,

$$I_{r,av} = R_{pu}(0) \qquad (7.19).$$

By definition, the cross spectrum of these two processes is given by (Reference 32)

$$S_{pu}(r,\omega) = \int_{-\infty}^{\infty} R_{pu}(\tau)e^{-j\omega\tau}d\tau \qquad (7.20),$$

and its inverse Fourier transform is

$$R_{pu}(\tau) = \frac{1}{2\pi}\int_{-\infty}^{\infty} S_{pu}(\omega)e^{j\omega\tau}d\omega \qquad (7.21).$$

With $\tau = 0$,

$$R_{pu}(0) = \frac{1}{2\pi}\int_{-\infty}^{\infty} S_{pu}(\omega)d\omega = \int_{-\infty}^{\infty} S_{pu}(f)df \qquad (7.22),$$

and

$$R_{pu}(0) = R_{up}(0).$$

If the Fourier transform of p(t) and u(t) exist, the cross spectrum can be written as (Reference 32)

$$S_{pu} = E\{P(f)U^*(f)\} \qquad (7.23).$$

Substituting the values for P(f) and U(f) from Equations (7.13) and (7.14),

$$E\{PU^*\} = E\{\frac{1}{2}(P_A + P_B)[-\frac{1}{j\omega\delta r\rho}(P_B - P_A)]^*\} \qquad (7.24).$$

Simplifying this equation,

$$E\{PU^*\} = -\frac{j}{2\omega\delta r\rho}[E\{P_BP_B^*\} - E\{P_AP_A^*\} + E\{P_AP_B^*\} - E\{P_BP_A^*\}] \qquad (7.25).$$

By definition,

$E\{P_BP_B^*\}$ = Power spectrum of pressure at B = S_{BB}.

$E\{P_AP_A^*\}$ = Power spectrum of pressure at A = S_{AA}.

$E\{P_AP_B^*\}$ = Cross power spectrum between pressure at B and A = S_{AB}.

$E\{P_BP_A^*\}$ = Cross power spectrum between pressure at B and A = S_{BA}.

Because $S_{BA} = S_{AB}^*$,

$$j(S_{AB} - S_{BA}) = +2Im(S_{BA}) .$$

Substituting these relations in the equation,

$$E\{PU^*\} = \frac{1}{2\omega\delta r\rho}\{j(S_B - S_{AA}) + 2Im(S_{BA})\} \qquad (7.26).$$

If the cross correlation is real, which normally is the case, the real part of the cross spectrum will be even and the imaginary part of the cross spectrum will be odd. Hence, when integrated from $-\infty$ to ∞, the odd part integrates to zero. Using only the real part,

$$I_{r,av} = -\int_{-\infty}^{\infty} \frac{1}{\omega\delta r\rho} Im(S_{BA})d\omega \qquad (7.27).$$

$$I_{r,av} = -\int_{-\infty}^{\infty} \frac{1}{\omega\delta r\rho} \cdot Im(S_{BA})d\omega \qquad (7.27).$$

Fourier analyzers use only one-sided spectrum. The values on the positive frequency side are doubled to keep the energy the same. One-sided cross spectrum is normally denoted by G_{BA}.

$$I_{r,av} = -\int_{o}^{\infty} \frac{1}{\omega\delta r\rho} Im(G_{BA})d\omega \qquad (7.28).$$

The negative sign in the equation can be avoided if the microphone closest to the source is connected to channel B of the analyzer (see Equation 7.11). For this case, the intensity can be written as

$$I_{r,av} = \int_{o}^{\infty} \frac{1}{\omega\delta r\rho} Im(G_{AB})d\omega \qquad (7.29).$$

In practice, the digital form of the estimate will be used:

$$I_{r,av} = \frac{1}{\rho\delta r} \sum_{n=1}^{N/2} \frac{ImG_{AB}(n\Delta f)}{n\Delta f} \qquad (7.30),$$

where Δf is the calculation bandwidth and N is the block size of the analyzer. Intensity as a function of frequency is

$$I_r(n\Delta f) = \frac{1}{\rho\delta r} \frac{ImG_{AB}(n\Delta f)}{n\Delta f} \qquad (7.31).$$

7.3 LIMITATIONS

References 29-31 discuss the inherent limtations of the two-microphone cross-spectral method to estimate the acoustic

intensity. The limitations arise due to two types of error that occur: a) a systematic error and b) a statistical error. The systematic error is due to the finite difference approximation used in the formulation of acoustic intensity. The statistical errors are due to the random source excitation and other random variations in measurement. In addition there are some more limitations that are specific to the KU-FRL acoustic test facility. All these limitations are discussed below.

7.3.1 HIGH FREQUENCY LIMITATION

At the KU-FRL acoustic test facility there are two possible sources of error in the high frequency region. The first limitation is due to the finite difference approximation for pressure and pressure gradient. This produces a systematic error in the estimation of these two quantities. The approximations used are (Equation 7.11)

$$p = \frac{p_A + p_B}{2} \qquad (7.32),$$

$$\frac{\partial p}{\partial r} = \frac{p_B - p_A}{\delta r} \qquad (7.33).$$

By the mean value theorem, these approxmations tend to the actual values only when the separation distance tends to zero. Otherwise, they produce a systematic error in the entire frequency range. However, the error is most severe in the high frequency range. For

a plane sinusoidal wave, the estimate of the intensity, using this approximate method, is related to the actual intensity by (Reference 31.)

$$\frac{I}{I_r} = \frac{\sin(k\delta r)}{k\delta r}$$

where I = actual intensity,

I_r = calculated intensity,

k = wave number (ω/c),

$\omega = 2\pi f$

f = frequency.

(Sin x/x) tends to 1 when x tends to zero. Otherwise, it is less than 1. Hence at high frequency (high k) and large separation distance, the acoustic intensity will be underestimated. At the KU-FRL acoustic test facility, this is minimized by limiting the separation distance to 25 mm (1") at frequencies above 500 Hz.

The second limitation is due to the band pass characteristics of microphones. Because low frequency noise reduction is the major concern in aircraft noise reduction, microphones with higher sensitivity are preferred in this region. Only the low frequency region is important in aircraft noise control applications. Hence, 1/2" B&K microphones were chosen for the measurement of transmission loss of panels. These microphones are accurate only up to 3500 Hz. With 1" separation and up to 400 Hz, the error due to the approximation will be less than 3 dB for a plane wave with sinusoidal wave. However, because this is a systematic error,

similar error occurs both with and without the panel. Hence, when the transmission loss is calculated, these errors tend to cancel out each other.

7.3.2 LOW FREQUENCY LIMITATION

According to Reference 30, there is no evidence of any low frequency limit due to the approximation errors. Reference 31 shows that the estimation of the particle velocity results in the estimation of the phase angle difference between the two microphones. The term "$k\delta r$" in Equation (7.34) is the phase difference between the microphones. This term is very small at low frequencies because k is small. Hence, at low frequencies, the measurement error of the phase angle becomes significant. The measurement error is due to the channel mismatch between the two microphone channels. This error can be eliminated (or reduced) either by using phase-matched microphones or by correcting for the difference in the phase angles when both the microphone channels are exposed to the same sound field. While the use of phase-matched microphones will make measurement easier, it cannot account for the phase mismatch in the rest of the measurement channels (like signal amplifier, etc.). Because of this, a phase calibration procedure is being adopted at the KU-FRL acoustic test facility. These procedures are discussed in Section 7.4.

7.3.3 NEAR FIELD LIMITATION

The third limitation occurs when this method is used in cases where the intensity changes rapidly along the probe. When this occurs, the intensity is very different at the two microphone locations. Such a situation arises when the measurements are made in near field. Several expressions have been derived to estimate the effect of near field for simple sources such as monopole, dipole, and quadropole. The following table, taken from Reference 31, gives the following criteria for limiting this error.

Source Type	Proximity error less than 1 dB if source is away by
Monopole	1.1 δr
Dipole	1.6 δr
Quadropole	2.3 δr.

While these results will not be valid for a complex source such as a thin panel, they do provide some guidance in using the acoustic intensity techniques near the sound sources.

7.3.4 LIMITATIONS DUE TO STATISTICAL ERRORS

Because of the random excitation, an estimate of $G_{AB}(f)$ is made. This estimation gives an additional error due to the variance of the quantity being measured. Reference 33 gives the normalized random error, $\varepsilon(I) = (Var(I)^{1/2}/I)$, in this type of measurement as

$$\varepsilon(I) = (n)^{-1/2}[1/\gamma^2 + \cot^2\phi_{AB}(1 - \gamma^2)/2\gamma^2]^{1/2} \quad (2.35),$$

where n is the number of ensemble averages for cross spectrum, and γ^2 is the coherence between the acoustic pressure at the two measurement points.

As can be seen, the statistical error can be minimized by selecting a large number of ensemble averages and by making sure that the coherence level is high. Since the tests are conducted inside a closed cavity where no other sources exist, the measured coherence values are normally very high. In the KU-FRL aoustic test facility an ensemble average of 256 and coherence values of above .8 are used. The tests are repeated if the coherence in general is below 0.8. However, at some discrete values the coherence can be lower than 0.8. For an assumed phase difference of .18 rad, with these values for ensemble averages and coherence, the statistical error ($\varepsilon(I)$) will be less than .194. For a plane wave, a phase angle difference of .18 rad corresponds to 100 Hz at 4" microphone separation.

7.4 CORRECTIONS FOR PHASE MISMATCH

As discussed in Section 7.3, phase mismatch between the two microphones can be minimized either by using phase-matched microphones or by correcting for the error. One of the disadvantages of using the phase-matched microphone is that the error due to phase mismatch of the rest of the measurement channel cannot be corrected. At times these errors may become significant. Hence at the KU-FRL acoustic test facility, phase

correction by prior calibration of microphones is used. A literature search was conducted. Based on the results, the following four methods were chosen (References 30, 31, and 34): 1) phase angle correction, 2) transfer function method, 3) microphone switching method, and 4) modified microphone switching technique.

7.4.1 PHASE ANGLE CORRECTION

In this method the phase difference between the two measurement channels (including microphones) is measured when the microphones are subjected to the same sound field. The phase angles of the cross spectrum measured during the intensity tests are corrected for this difference. The magnitude correction is done separately. If the same sound field is applied to both the microphones, shown in Figure 7.2, the measured cross spectrum is given by

$$S_{AB} = S_{p_1 p_2} \cdot H_A^* \cdot H_B \qquad (7.36),$$

where $S_{p_1 p_2}$ is the cross spectrum of the sound field at the position of the two microphones, S_{AB} is the measured cross spectrum, and H_A and H_B are the transfer functions of the two measuring channels. The phase angle of the measurement channels is the phase angle of the transfer function.

This is one of the methods chosen at the KU-FRL to correct for the phase angle difference. This method is useful at low frequencies. The exact realization is discussed in the next

chapter. The magnitude calibration is done separately using B&K Pistonphone 4220.

7.4.2 TRANSFER FUNCTION METHOD

Reference 31 shows that when two microphones are exposed to the sound field, both magnitude and phase correction for channel mismatch can be done using the relation:

$$S_{p_1 p_2} = \frac{S_{AB}}{(H_A)^2 \cdot H_{AB}} \qquad (7.37),$$

where H_{AB} is the transfer function between the measurement channels. Since this method is very similar to the previous method, this was not tried.

7.4.3 MICROPHONE SWITCHING METHOD

Chung, et al. (Reference 30), originally proposed this method for correcting phase mismatch. In this method, tests are done twice. Tests are first performed with the microphones in normal locations; tests are then repeated with the microphones interchanged. Under these conditions Reference 30 gives the actual cross spectrum as

$$Im = \{[G_{AB}{}^{S} \cdot G_{AB}]^{1/2}\}/\rho\delta r\omega \cdot |H_A| \cdot |H_B| \qquad (7.38),$$

where G_{AB} = cross spectrum between microphones,

G_{AB}^{S} = cross spectrum with microphones switched,

$|H_A|$, $|H_B|$ = gain factors, microphones A and B.

In this method every test has to be done twice; also, the test section has to be opened for every mesurement. For these reasons this method is not being used at the KU-FRL acoustic test facility.

7.4.4 MODIFIED MICROPHONE SWITCHING TECHNIQUE

This method is a combination of the transfer function method and the microphone switching method. In this method, before the start of the tests, the microphones are exposed to a sound field and the cross spectrum (G_{AB}) is measured. Now the microphones are switched, the measuring system is exposed to the same field, and once again the cross spectrum is measured (G_B^S). From Reference 34, we get

$$e^{i\phi} = \frac{G_{AB}^{*}(\omega)}{G_{AB}(\omega)} \qquad (7.39),$$

where ϕ is the phase angle between the measurement channel. By assuming that the magnitudes are the same, the complex root computation is avoided. The phase angle is calculated by dividing the phase angle of the cross spectral division by 2.

This method is used to correct the measured intensity values during the actual tests. The implementation of this method at the KU-FRL acoustic test facility is discussed in the next chapter. The

advantages of this method are 1) the microphones need not be exposed to the same sound field, 2) tests need not be peformed twice, 3) the method is valid even at high frequencies. The only requirement is that the sound field should be stationary.

7.5 EXPERIMENTAL SET-UP

7.5.1 HARDWARE DESCRIPTION

7.5.1.1 General Test Set-Up Description

The general arrangement of the acoustic intensity test set-up is shown schematically in Figure 7.2. The system shown was designed to take and process data as quickly and efficiently as possible. Since each transmission loss test requires 324 intensity spectra at 402 frequency values each (324 spectra = 81 points for high and low frequency tests for both the source and receiver side), the need for speed in data processing and efficiency in data storage becomes obvious. The operation of the system is described below.

The heart of the system is the Nicolet 660B dual channel FFT analyzer. The analyzer provides temporary data storage and performs all required FFT calculations. It is controlled by a Zenith Z-100 microcomputer which provides data reduction and permanent data storage capability. The 660B and Z-100 are linked through their respective RS-232C ports at a 9,600 baud rate. The communication software used to transfer data from the 660B to the Z-100 is written in a compiled Basic language.

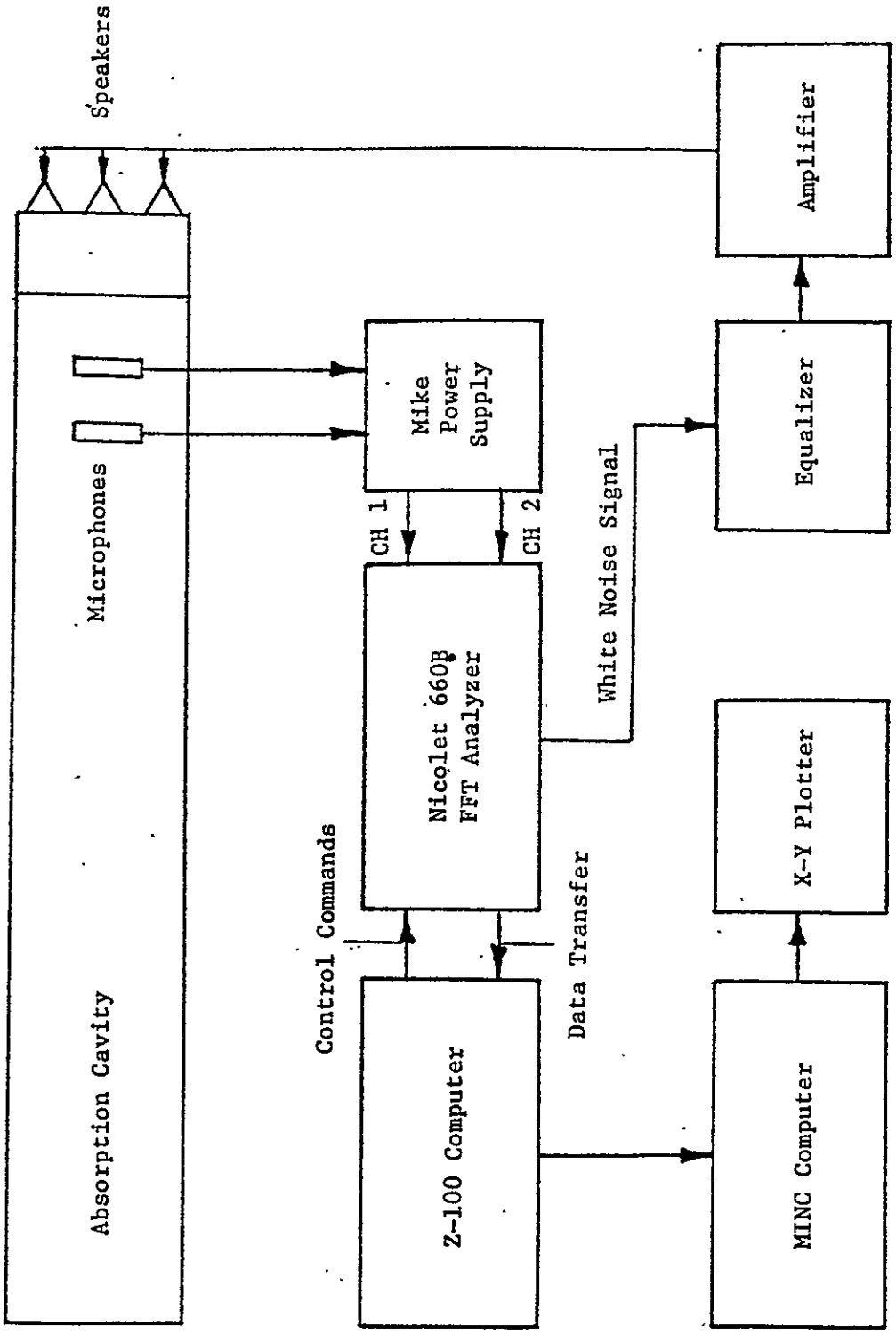

Figure 7.2: General Arrangement of the Acoustic Intensity Test Set-Up

In addition to its data acquisition role, the Nicolet 660B also provides the excitation signal that drives the speakers in the Beranek tube. This excitation signal is a band-limited binary white noise output from the analyzer's rear panel. It is passed through a TAPCO 2200 equalizer for the purpose of modifying the speaker inputs to achieve a flat speaker output. The equalizer output is gained up through a Crown D-150 power amplifier to drive the nine Altec 405-8H loudspeakers. It is necessary to insert a high-pass filter between the analyzer and the equalizer when testing panels with large transmission losses. This is required to avoid overloading the analyzer inputs in the low frequency range when attempting to gain up the microphone outputs in the high frequency range.

Two B&K 4165 microphones with B&K 2619 preamps are positioned in the Beranek tube by the microphone positioning device (MPD). The microphone preamplifier outputs are fed into the two channels of the 660B FFT analyzer (although tests involving panels with very high transmission losses may require additional amplification of microphone signals--such as the Nagra SJS tape recorder--between the microphone power supply and the analyzer). From the analyzer, the cross spectrum of the two microphones is transferred to the Z-100 microcomputer where it is stored on 5 1/4 inch disks. Data transferred to the Z-100 are cataloged in files by microphone location, analysis (frequency) range, and source or receiver spectra so that batch processing of data is simplified. Data reduction routines are run on the Z-100 to generate point intensity values and

overall panel transmission loss. The values are plotted on a Hewlett Packard 7475A digital plotter.

7.5.1.2 Description of Microphone Positioning Device (MPD)

The microphone positioning device was designed and built at the KU-FRL for the purpose of accurately positioning the microphones within the Beranek tube. The design requirements specified that the MPD be able to position two microphones anywhere in a 16-inch-by-16-inch plane parallel to and directly behind the test panel without opening the tube. Movement of the microphones had to be done easily and accurately from the outside. In addition, provisions for varying the spacing between the microphones had to be made, and "blockage" due to the device (interference with the sound paths within the tube) had to be kept to a minimum.

The MPD is shown in Figure 7.3. It is an extension tube constructed of particle board into which the positioning mechanism is built. Vertical and horizontal motion is provided by a system of cross beams. A Lucite block is attached to the vertical and horizontal beams at their inersection and is allowed to slide freely on both. The block is therefore constrained by the cross beams (guide rods) such that when the rods are moved, the Lucite block maintains its position at their intersection. The microphones are attached to the Lucite block through an aluminum beam protruding

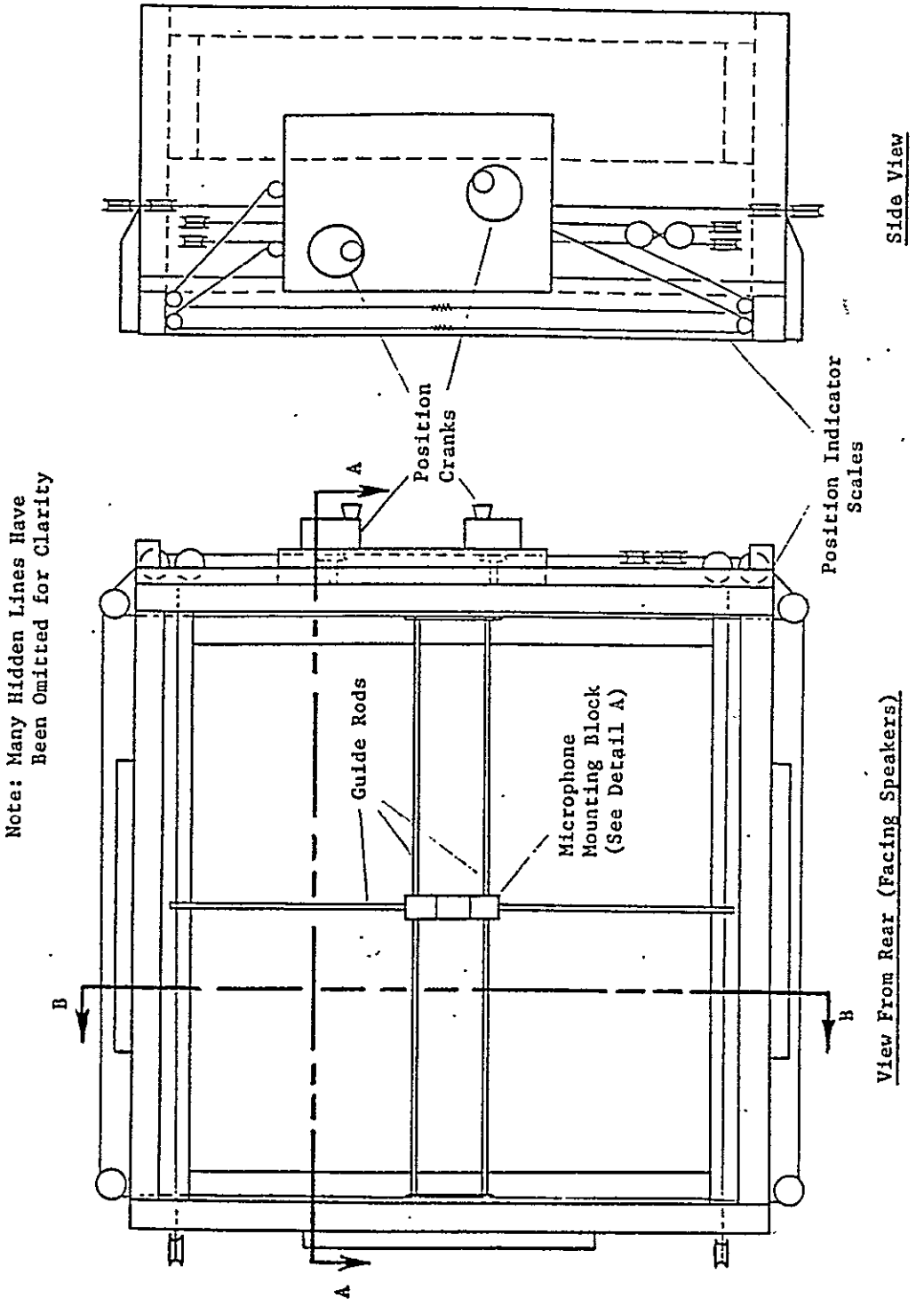

Figure 7.3: Description of Microphone Positioning Device

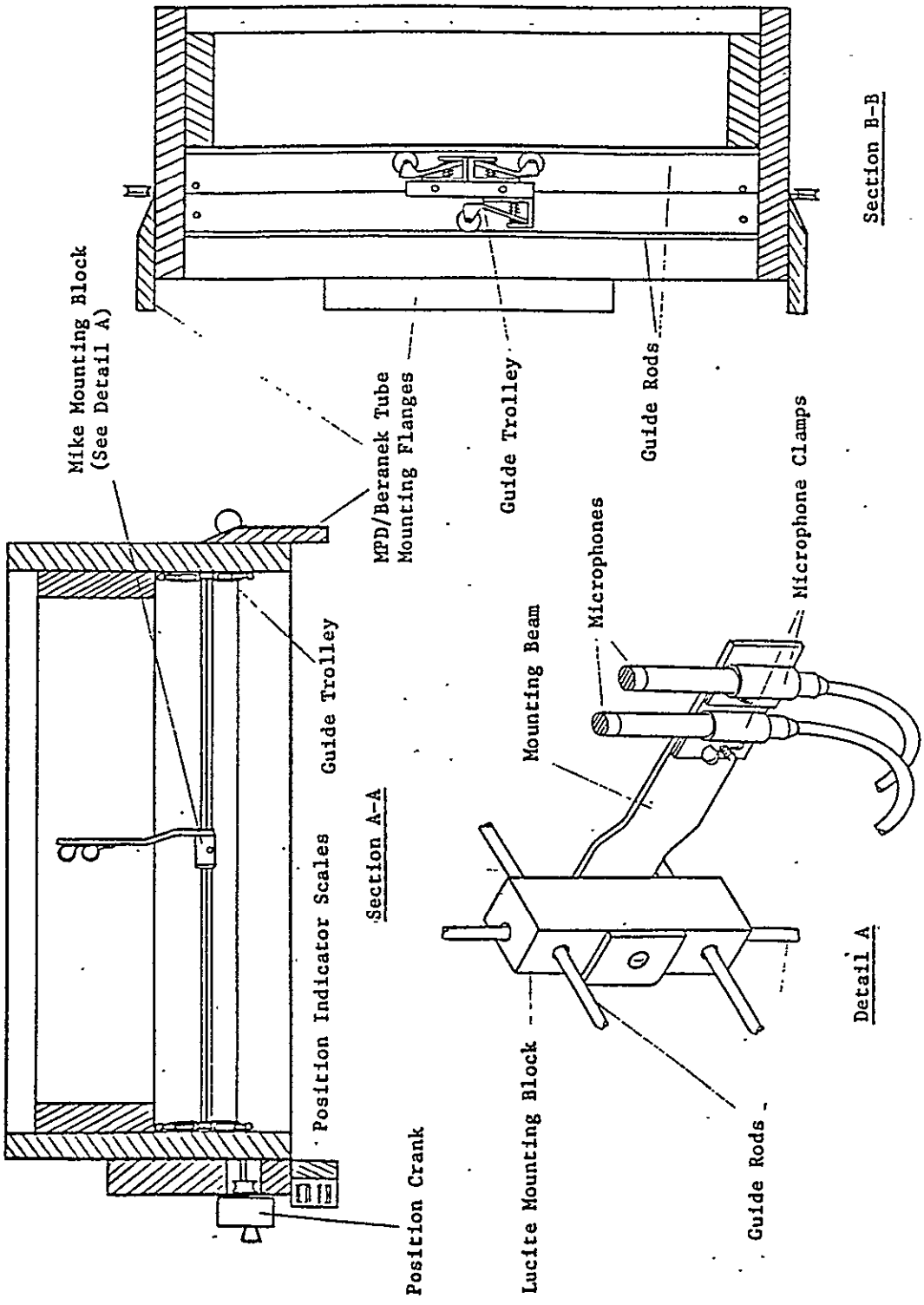

Figure 7.3: (continued)

from it (see Detail A of Figure 7.3). The microphones can be positioned at different locations along the beam to provide for different microphone spacings.

The guide rods in the MPD are controlled externally by a cable and manual crank system. Position information is displayed on scales by a secondary cable system driven off the cranks.

The MPD operates smoothly and positions the microphones with reasonable accuracy. However, due to interference of the microphone cables with the bottom of the MPD at low positions, it is not possible to cover the entire 16-inch-by-16-inch sweep area. The solution to this problem is to turn the microphones face down when they are positioned near the bottom of the MPD. However, this, requires that the Beranek tube be opened midway through a test. While this is not a significant problem, it increases testing time.

7.5.2 SOFTWARE DEVELOPMENT

Because of the large amount of data that will have to be processed using this method, the computer program had to be split into many subparts before it could be handled by the Z-100 computer. Depending upon the ease of programming and the amount of calculations involved, either Fortran or Basic language was chosen to write these programs. The flow diagram shown in Figure 7.4 describes the steps involved. The individual steps and the relevant equations are described in subsequent sections.

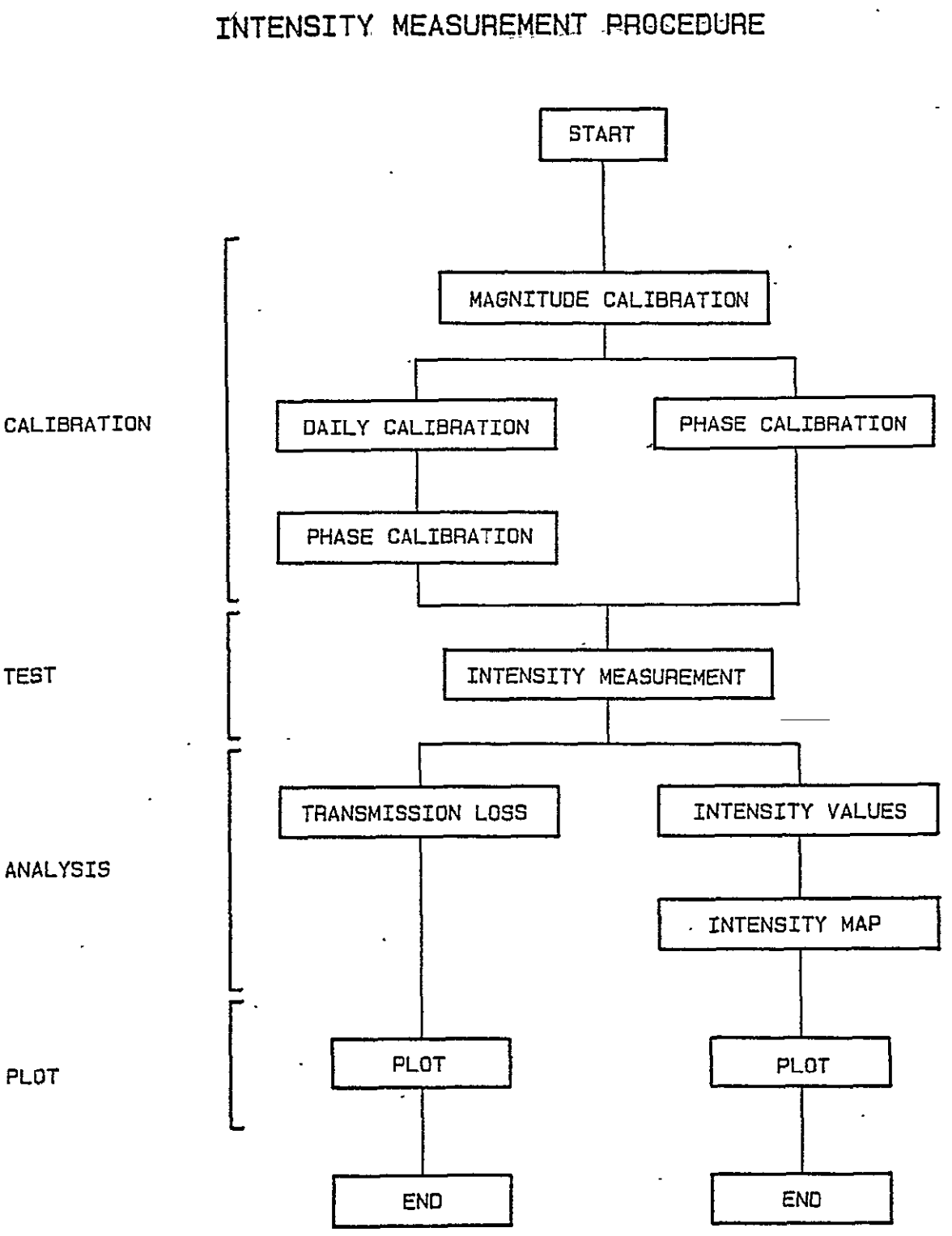

Figure 7.4: Test and Analysis Flow Diagram

7.5.2.1 Magnitude Calibration

A B&K "Pistonphone" is used to calibrate the microphones. Because the 660B outputs unscaled values, the actual output from calibration tests is a function not only of the pressure but also of the input max amplitude setting and number of ensemble averages. In converting the output of the 660B to the actual BNC input volt level and then to pressure, these two additional variables will have to be considered. The B&K 4220 Pistonphone outputs calibrated sound pressure level 124 dB (reference 20 micro pascals) at 250 Hz. Hence,

$$20 \log\left(\frac{p_{cal}}{p_{ref}}\right) = 124 \text{ dB}$$

$$p_{cal} = 10^{\left(\frac{124}{20}\right)} p_{ref} \qquad (7.40),$$

where p_{cal} = pressure corresponding to pressure level of 124 dB

p_{ref} = reference pressure (20 micro pascals).

At a given input channel maximum amplitude setting for a given number of ensemble averages, the pressure (p_i) at any location i will be proportional to the value output by the 660B (v_i).

$$p_i \propto v_i$$

or $$p_i = Kv_i \qquad (7.41),$$

where K is the calibration constant. The Pistonphone outputs 125 dB sound level at 250 Hz. There is a small tolerance about 250 Hz.

Also, spectral leakage always exists in digital signal processing. Whenever the energy is concentrated at a discrete frequency which is in between two adjacent cell (filter) locations, the energy is smeared across the neighboring cells. See Reference 35 for discussion on spectral leakage. In order to minimize the effect of spectral leakage during calibration, the power-spectral values of three adjacent cells on either side are summed to obtain the total energy. The calibrated pressure can be equated to

$$\sum_{i=i_0-3}^{i_0+3} p_i^2 = K \sum_{i=i_0-3}^{i_0+3} v_i^2 \qquad (7.42),$$

$$p_{cal}^2 = K \cdot \sum_{i=i_0-3}^{i_0+3} v_i^2 \qquad (7.43),$$

where i_0 is the filter location corresponding to 250 Hz, v_i is the value output by the 660B at a given maximum amplitude setting and for a given number of ensemble averages, and p_{cal} is the pressure corresponding to 124 dB. The calibration constant K can then be calculated from Equation (7.43). This needs to be done for both channels. The functional relationship between the output and the ensemble averages and the maximum amplitude setting is given in Reference 36. The relationship between the true value and the value output from the analyzer 660B during any one test was derived as follows.

RMS spectrum of channel A:

$$TV = K_A V_t \frac{A_t}{A_c} \frac{N_c}{N_t} \qquad (7.44);$$

Power spectrum of channel A:

$$TV = K_A^2 V_t \left(\frac{A_t}{A_c}\right)^2 \frac{N_c}{N_t} \qquad (7.45);$$

Cross spectrum:

$$TV = K_A K_B V_t \frac{(A_{A,t} A_{B,t})}{(A_{A,c} A_{B,c})} \frac{N_c}{N_t} \qquad (7.46);$$

where TV = true value,

V = value output,

A = maximum input amplitude setting,

N = number of ensemble averages,

K = calibration constants obtained from Equation (7.43),

and the subscripts t, c, A and B correspond to test, calibration, channel A and channel B, respectively. These relationships were confirmed by experimentation. They are used in obtaining calibration constants. The actual test and analysis procedure developed, based on the above equations, is described in Reference 37. The listings of programs PSP660 and MAGCAL, used for the determination of magnitude calibration constants, are given in Appendix C. The output from these programs are stored in a file named CALDAT.DAT. It stores calibration factor, number of averages, and maximum amplitude setting for both channels. This file is accessed by other routines to convert the test values into true values.

7.5.2.2 Phase Calibration

As described in Section 7.4, two different calibration techniques are used at the KU-FRL acoustic test facility. Method 1 calculates the phase angle difference between the two microphone channels when both the microphones are exposed to the same field. Method 2 uses the modified transfer function method described in Section 7.4.

7.5.2.2.1 Method 1

In this method both the microphones are exposed to the same field, and any difference in the phase angle measured is due to the difference in the channels. Subsequent tests can then be corrected for this difference in phase angle. Figure 7.5 shows the schematic diagram for the microphone phase calibration system. In this method, the two microphones are inserted into a long tube with faces of the microphones parallel. A random noise is generated at the other end. Hence both the microphones are exposed to the same sound field. Only the cavity resonance effects affect the actual sound field incident at the microphone. By selecting the tube diameter of two inches, the fundamental circumferential resonance frequency is made to occur at a frequency greater than 5000 Hz, which is the maximum frequency of interest. Thus the effect of circumferential resonance frequency is avoided. The effect of longitudinal resonance frequency could not be eliminated fully, but it is

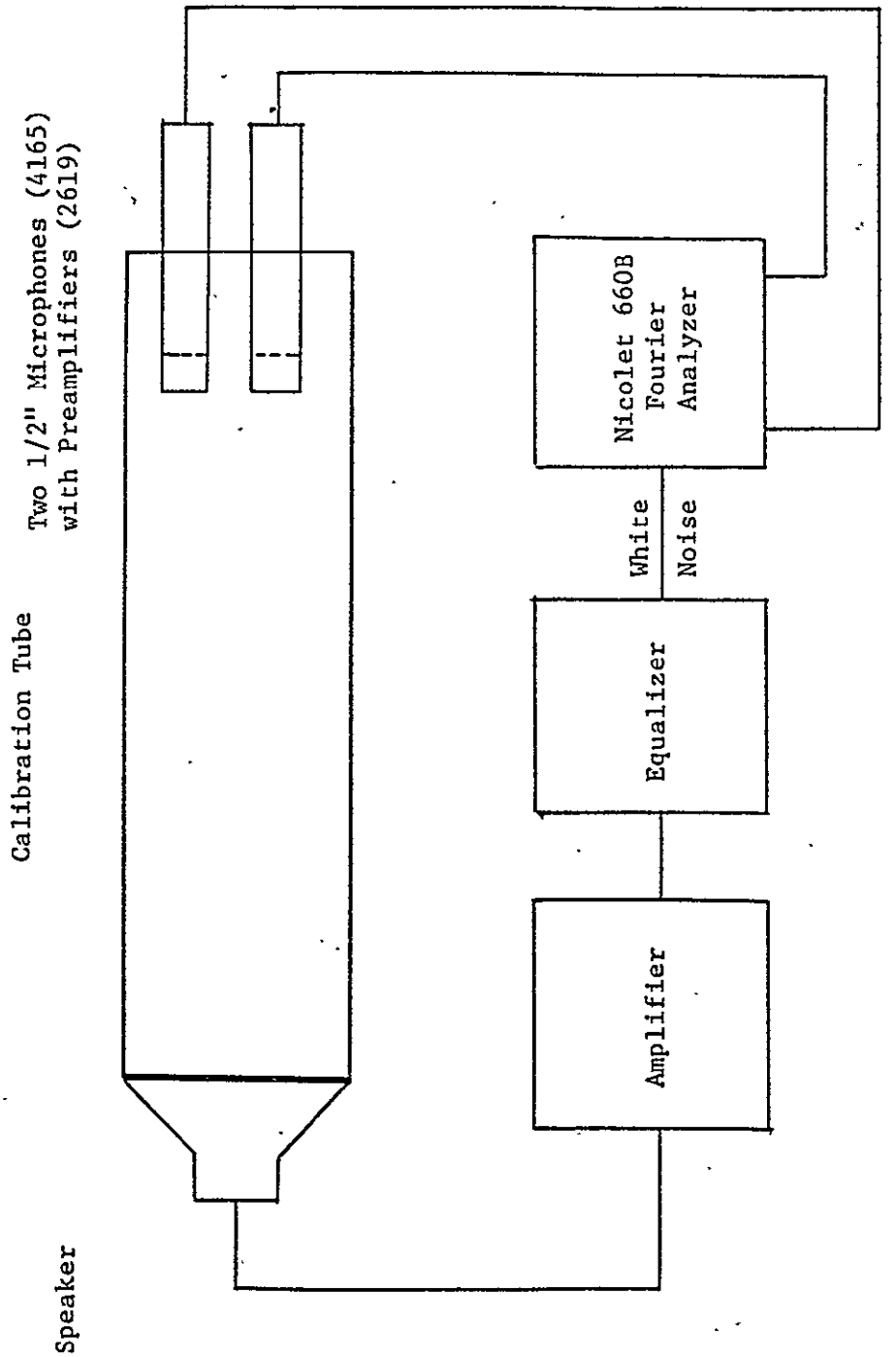

Figure 7.5: General Arrangement of the Microphone Calibration

minimized by having absorptive fiberglass materials on the ends of the calibration tube.

During the initial determination of the phase angles, it was noticed that a certain amount of scatter was unavoidable in the phase angle differences measured. Since this scatter may affect the results during daily calibration, a statistical approach was taken to minimize the effects of this scatter. It was decided to perform tests many times to cover the entire range of parameters that cannot be controlled exactly during any test. These parameters involve the humidity, temperature, amount of time the calibration speaker has been on, etc.

Thirty tests were conducted to cover the range of variables. A mean of the results of these thirty tests can be considered to be a good estimate of the mean of the population of all possible phase angle measurements (see Reference 38). However, thirty calibration tests every day to cover all possible random combinations is not practicable. Hence it was decided to use significance testing to obtain acceptable calibration values. In this procedure, the population mean and standard deviation are first determined only once. Thereafter, only a small number of tests need to be done every day. The mean values of these tests are compared with the population mean values, and the significance tests are used to accept or reject the new values.

An estimate of population mean can be obtained by taking a mean of a large number of tests. If the number of samples is greater

than thirty, it can be assumed that the mean and the standard deviation of the sample are equal to the mean and the standard deviation of the population (Reference 38). Hence, thirty tests that are conducted in the beginning of a test series can be assumed to be a very good estimate of the population mean and the standard deviation. Daily calibration values are then compared with these values for acceptability. In this case, while committing type I error can be tolerated, committing type II error should be avoided. The probability of committing type II is denoted by "β." The probability of committing type I error is denoted by "α." This is also known as the level of significance. When the alternate hypothesis is nonspecific (i.e., the mean of the test is not equal to the population mean) as in this case, it is not possible to compute the probability of type II error (Reference 38). However, with a higher sample size, both α and β can be reduced. Reference 38 also gives the following equation for the two-tailed test to obtain the power $(1 - \beta)$ for a specified alternative as

$$n_2 \simeq \frac{(z_{\alpha/2} + z_{\beta})^2 \sigma^2}{\delta^2} \qquad (7.47),$$

where n_2 is the number of observations required, σ is the standard deviation, and δ is the difference between the sample mean and the population mean. For .05 level of significance (α), $z_{\alpha/2}$ is 1.96 for normal distribution, and for .05 probability of computing type II error (β), $z_{\beta} = 1.645$. Using Equation (7.50) as a guide and by

trial and error, n = 5 was observed to be adequate for our calculations.

These equations have been modeled into the computer program. At the beginning of a series of tests, the calibration is performed 30 times, varying the uncontrollable parameters (such as temperature, humidity, etc.) as much as possible. These tests are performed once for low-frequency range and again for high-frequency range. The results are analyzed using STAT.BAS. The outputs (the population mean and the confidence interval at 95% confidence level) are stored into two files.

During the day of the tests, calibration is done only five times. The analysis program, CALII.EXE, is run to perform the significance tests. This has to be done for both frequency ranges. The output file from this program is called CALII.DLO, or CALII.DHI. These files contain the phase angle correction at each filter location. These files are accessed by other routines to correct measured phase angles.

7.5.2.2.2 Method 2

The second method for phase correction uses the modified microphone switching technique described in Section 7.4.4. Equation (7.39) is used to obtain the correction. In this method, the tests are done only once every day. First, the microphones are clamped in normal location in the MPD and the cross spectrum is measured. Then the microphones are switched and the switched cross spectrum is

measured. From these two cross spectra, the phase angle correction as a function of freuency is obtained using Equation (7.39). The listing of the programs involved is given in Appendix C.

7.5.2.3 Intensity Tests

The test procedure for measuring acoustic intensity values at the KU-FRL acoustic test facility is given in Reference 37. The intensity is calculated from the measured cross-spectral values by Equation (7.31). The program INTSTY performs this calculation. It also performs relevant magnitude and phase corrections. At present, the intensity values are calculated at 81 grid points on an 18-inch-by-18-inch cross sectional area. These intensity values are used either to plot an intensity map or to calculate transmission loss. The relevant programs are identified in Figure 7.4. The listing of programs is given in Appendix C.

7.5.2.4 Plotting

The analyzed programs are plotted using the HP7475 digital plotter with serial interface. The Basic plot programs TL7475 and PIN7475 are used to plot transmission loss and intensity map, respectively. The listings of these plot programs are given in Appendix C.

7.6 TEST RESULTS

This chapter describes the tests conducted to check out the acoustic intensity procedures developed at the KU-FRL acoustic test facility. The tests decribed in this chapter are in addition to the tests conducted to verify the accuracy of the programs. In all cases, phase corrections were performed.

7.6.1 SOURCE INTENSITY MAP

One of the important aspects of the plane wave tube is the behavior of the speaker array. It is desirable for all speakers to produce identical outputs with the same phase angle. Also the spectrum produced by the speakers should be flat for a random white noise excitation. During the initial calibration tests of the test facility, it was concluded (Reference 21) that the incident wave can be considered plane only up to 800 Hz. With the acoustic intensity technique, this aspect can be easily verified. To determine the sound field characteristics of the test facility, an acoustic intensity survey was carried out along the cross section of the plane wave tube. The test facility has a cross section of 18 inches by 18 inches. Tests were conducted to measure intensity every two inches, using the procedures outlined in Reference 37. This gave intensity values of 81 grid points. During these tests, the gain values at the frequency ranges of the equalizer were set to zero.

The results of the tests are plotted in Figures 7.6 and 7.7,

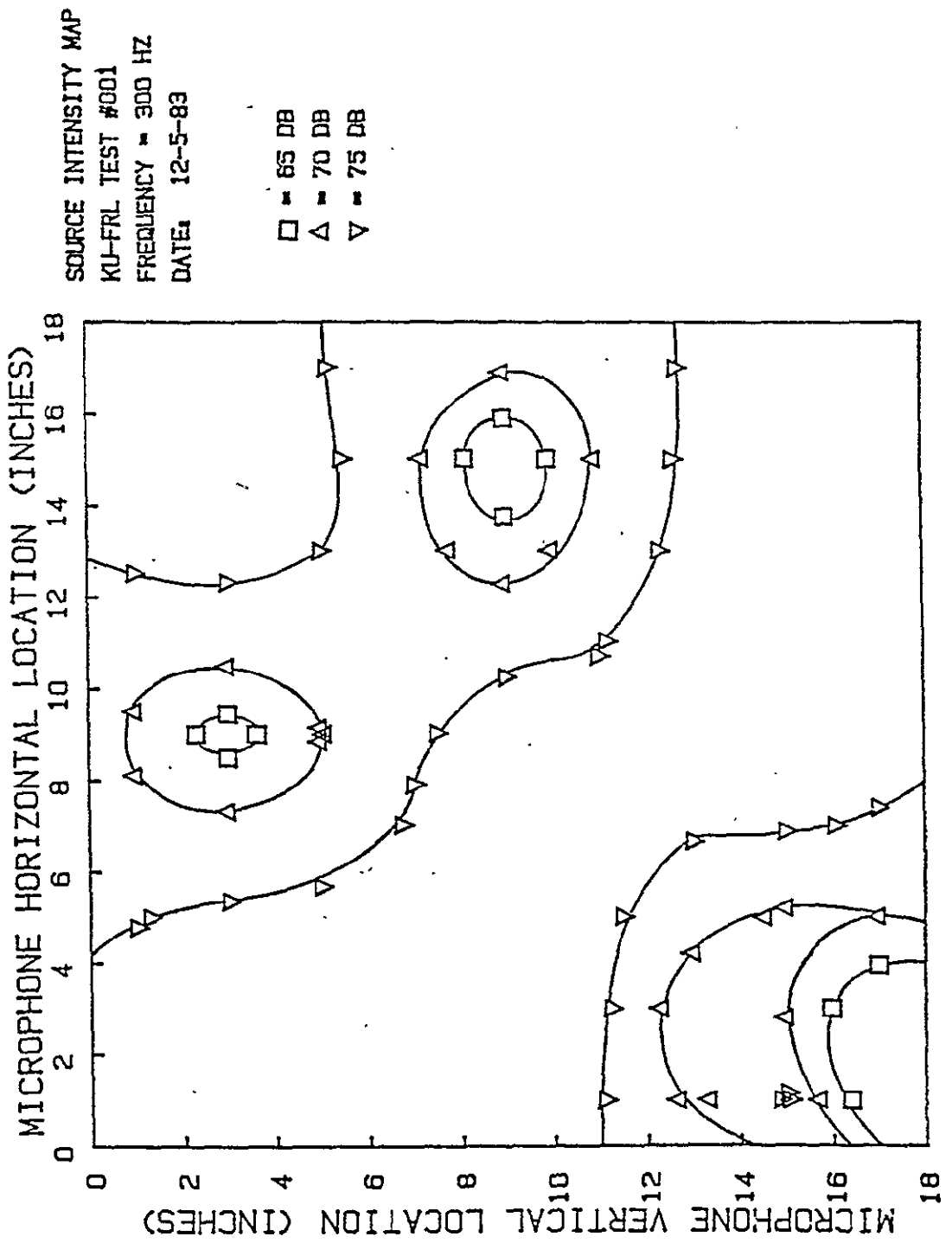

Figure 7.6: Source Intensity Map at 300 Hz

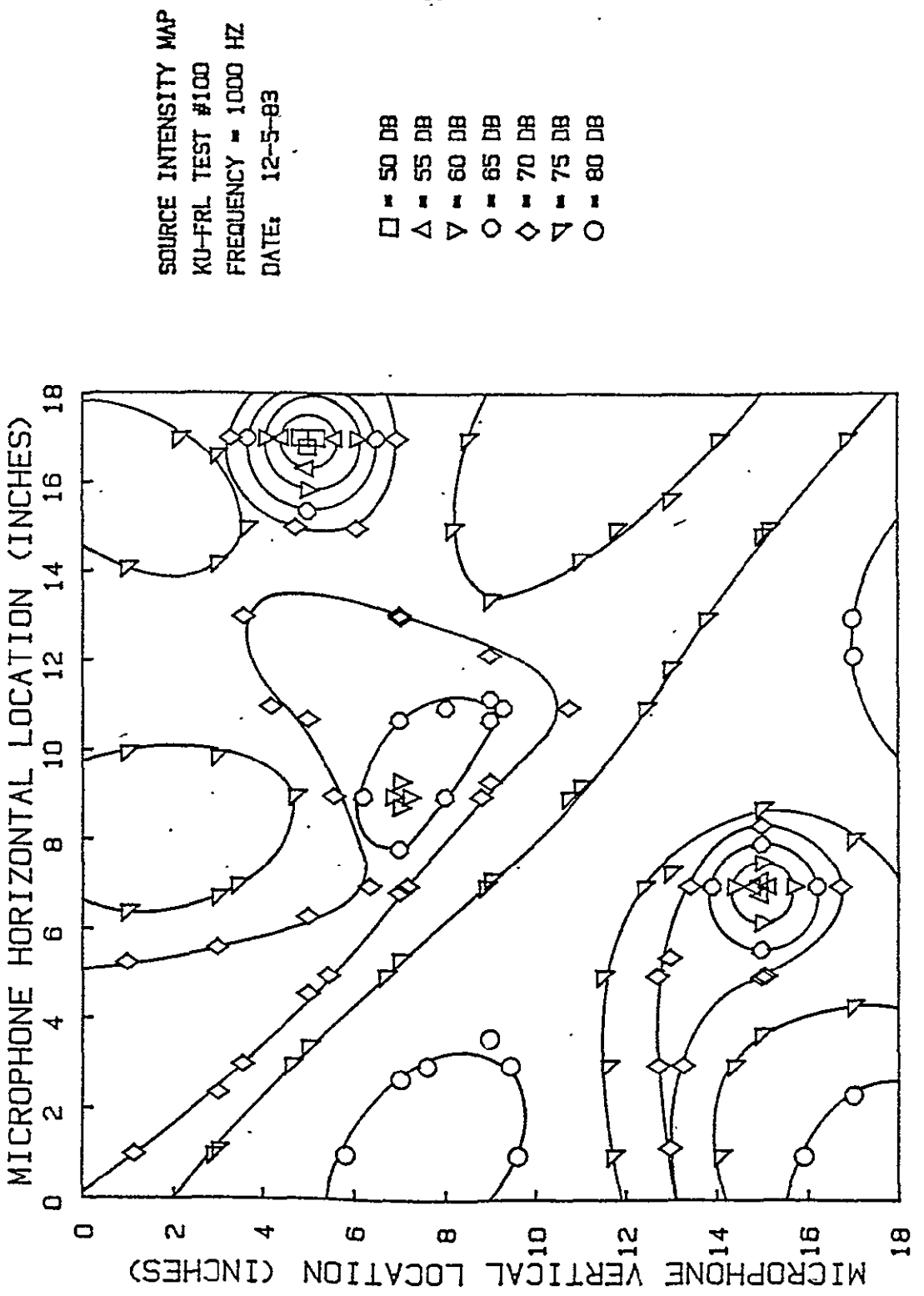

Figure 7.7: Source Intensity Map at 1000 Hz

for 300 Hz and 1000 Hz, respectively. The results are also available for every 1.25 Hz up to 500 Hz, and for every 12.5 Hz from 500 Hz up to 5000 Hz. The software programs developed seem to work well for the type of analysis being done. From the tests, it was found that the number of grid points needs to be increased at high frquencies to obtain a good quality intensity map.

From Figure 7.6, it can be seen that two speakers (#2 and #6) are producing less power (10 dB lower than the other speakers). This phenomenon was seen at frequencies from 250 to 400 Hz. Thereafter, these speakers behaved normally. But for these two areas, the output was reasonably flat. At 1000 Hz, the variations were much more severe. This could be due to the cavity resonances present in the test facility. In general, the intensity was higher around the edges than at the center. The reason for this is not fully understood. However, based on this test, it is concluded that the KU-FRL acoustic test facility cannot be considered a plane wave facility above 1000 Hz.

7.6.2 INTENSITY MAP WITH ALUMINUM PANEL

At the KU-FRL test facility, a 0.032" aluminum panel is used as the standard panel. The transmission loss (or noise reduction) values obtained with this panel are used for calibration. To determine the acoustic intensity characteristics of this panel, an intensity survey was carried out at the same 81 grid points as before, this time with the 0.032" aluminum panel installed between

the source and the microphones. Figures 7.8 and 7.9 show the results at 300 Hz and 1000 Hz, respectively. At 300 Hz, the intensity variation was within 10 dB at all points. At 1000 Hz, while the maximum variation was only 20 dB, the actual intensity value was 40 dB. It is anticipated that this low value of transmitted intensity may pose problems in accurate estimation of the intensity, especially if the panel exhibits higher transmission loss characteristics. This aspect was expected. At higher frequencies, the transmission loss will be higher because of the mass law. Several methods could be used to overcome this problem. They are 1) installation of amplifier in the measurement channel, 2) increasing the input signal strength, and 3) filtering away the low frequency in the excitation signal using high-pass filters and then amplifying the signal. The third method will involve performing each test twice: once at low frequency, say up to 500 Hz; and the second time, from 500 Hz to 5000 Hz.

7.6.3 TRANSMISSION LOSS OF PANELS

To compare the measured transmission loss values with theoretical values, two panels were tested: a 0.032" aluminum panel and 40 oz/sq yd leaded vinyl. These specimens were tested at the KU-FRL acoustic test facility using the test procedures outlined in Reference 37. The resulting transmission loss characteristics are compared with the mass law. The behavior of the test panels is illustrated in Figures 7.10 and 7.11.

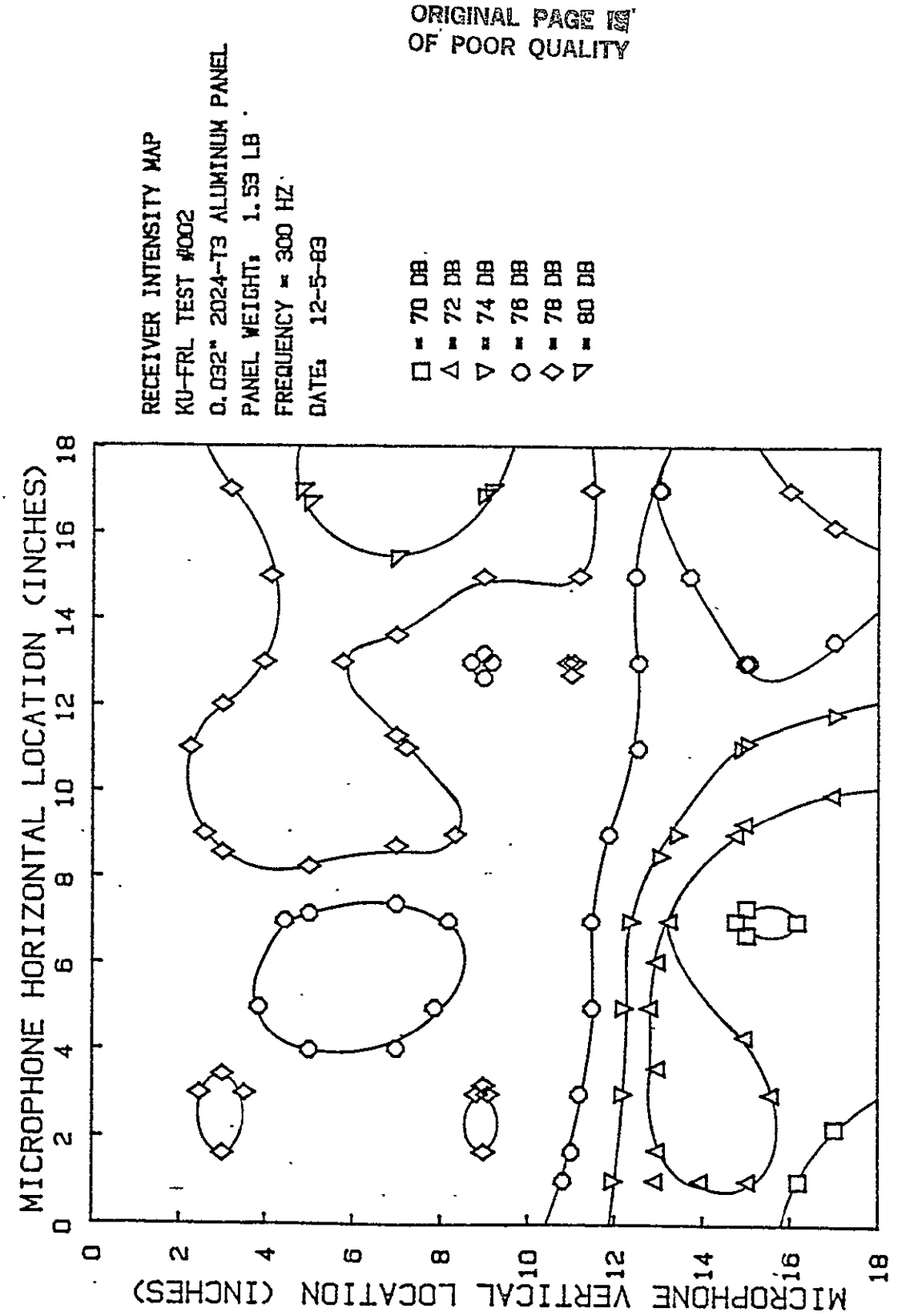

Figure 7.8: Intensity Map with 0.032" Aluminum Panel at 300 Hz

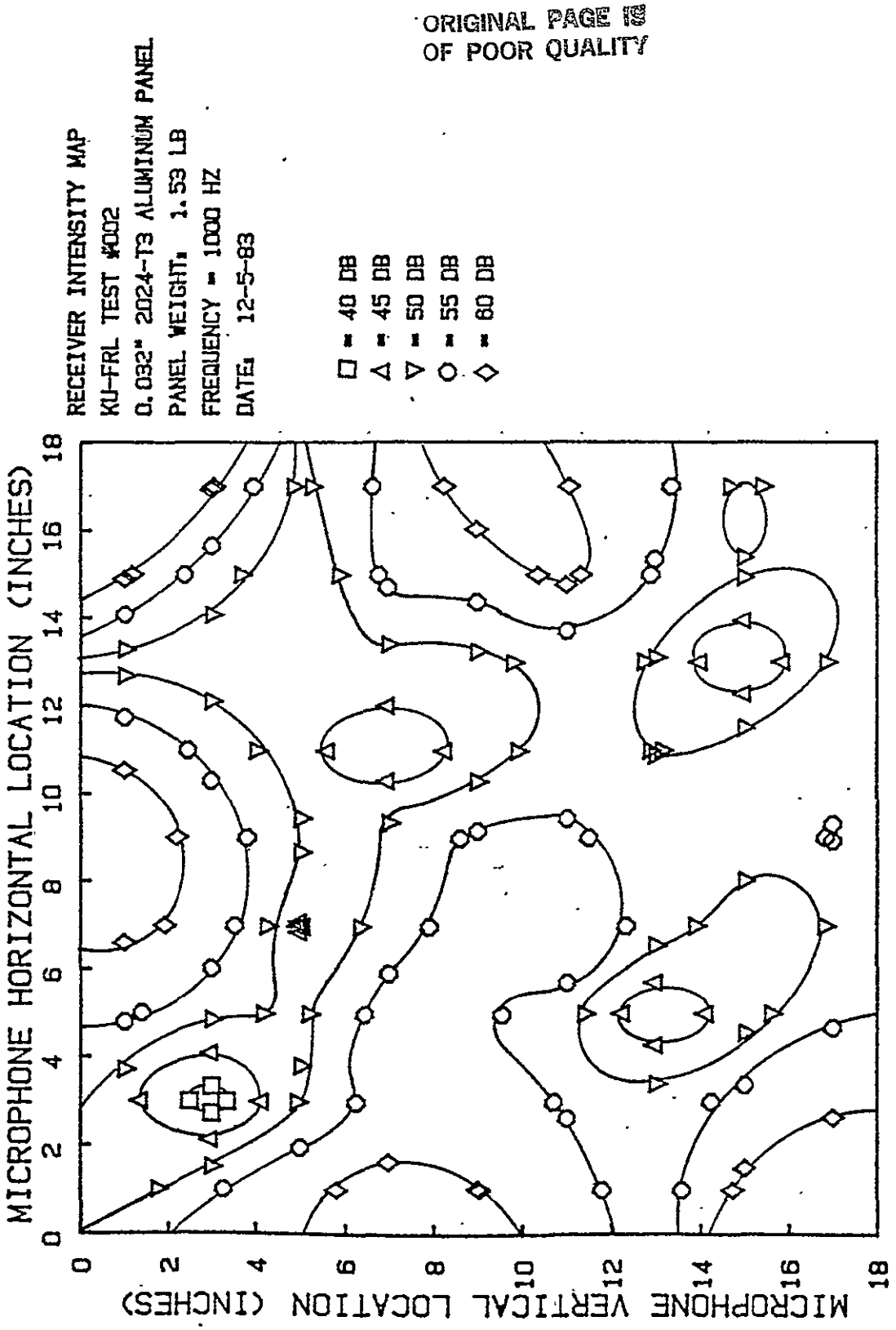

Figure 7.9: Intensity Map with 0.032" Aluminum Panel at 1000 Hz

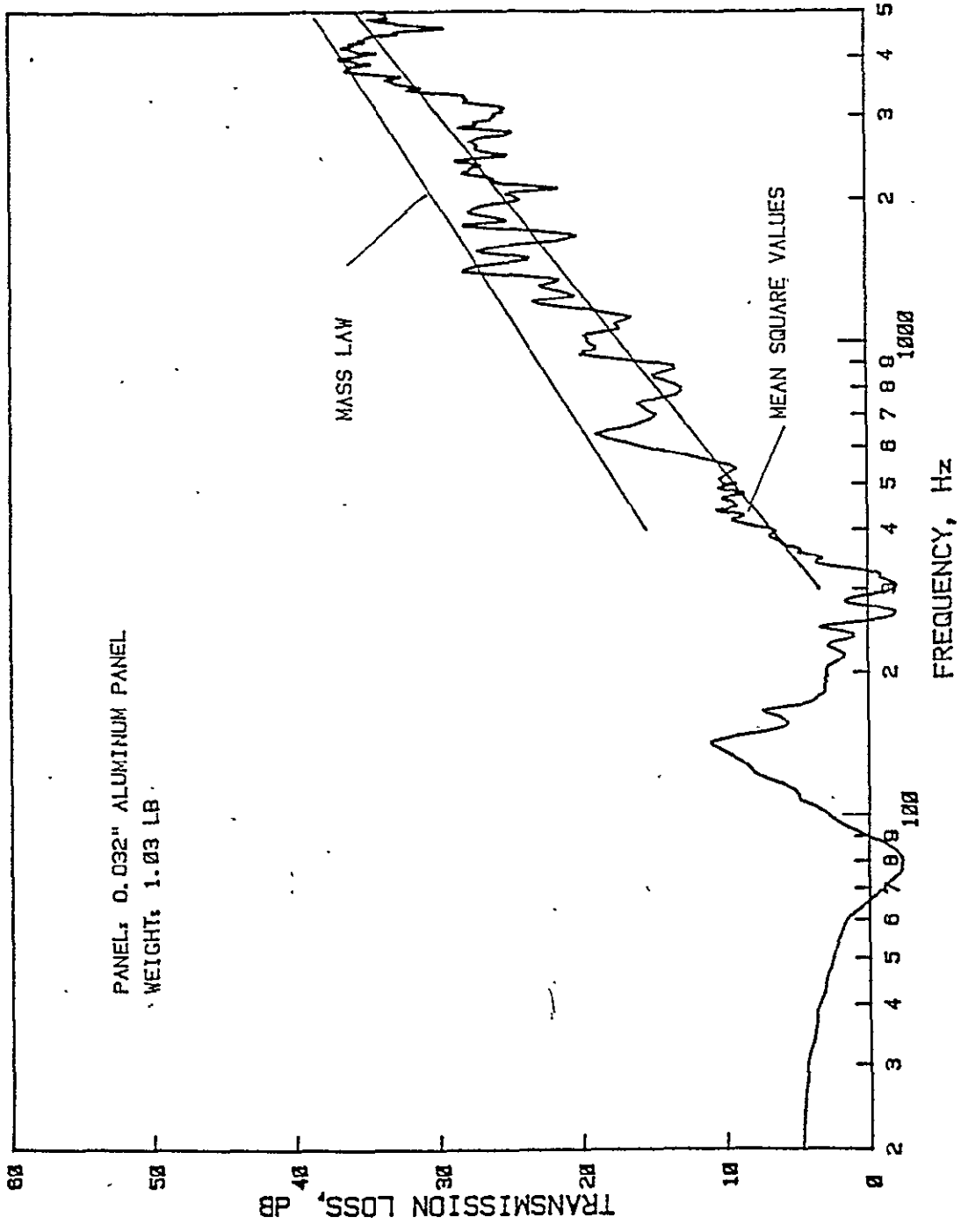

Figure 7.10: Transmission Loss Characteristics of 0.032" Aluminum Panel

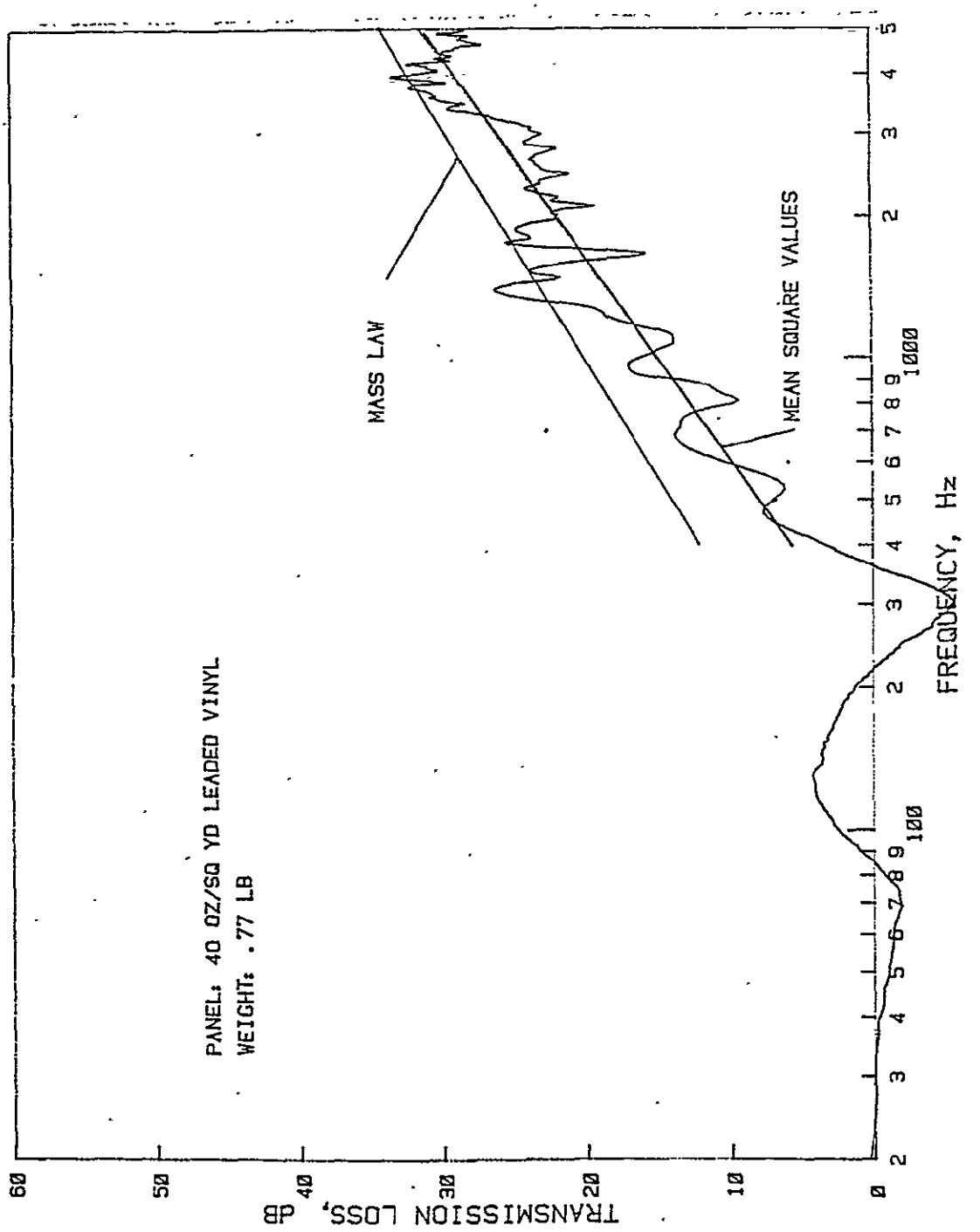

Figure 7.11: Transmission Loss Characteristics of 40 oz/sq yd Leaded Vinyl

The transmission loss (TL) curve for a particular panel is obtained in the following manner. An intensity level survey is conducted without any panel. The intensity level is integrated over the entire panel area, and the incident sound power level is estimated. Then the tests are repeated with the panel installed between the source and the microphones, and the transmitted sound power level is estimated. The differece in sound power level between these two measurements will give the transmission loss. This test procedure is similar to the measurement of insertion loss. However, because the intensity is measured close to the source and the panel is thin, the difference between this procedure and the two-room transmission loss measurement method is expected to be small. This procedure had to be adopted because the measurement of only the incident intensity of the source side is not possible with this technique. The reflected intensity from the test specimen will affect the intensity being measured. This problem existed even in the old procedure. That is the reason the term "noise reduction" was used instead of "transmission loss."

Mass law values are also plotted in Figures 7.10 and 7.11. The mean square transmission loss measured in each case is approximately 2 to 5 dB lower at 5000 Hz. The integration of the several intensity values for both with and without panels, used in this procedure, is expected to yield an average transmission loss value. This is in comparison to the use of just one microphone situated close to both source and receiving side, which will result

in position-dependent transmission loss values. Hence, a difference between the two measurements was anticipated. The results with the old test procedure gave up to 6 dB higher noise reduction than the calculated noise reduction values. Hence, one-to-one comparison between the present procedure and the single-microphone procedure is not considered valid.

7.7 CONCLUSIONS

Based on the tests conducted, the following conclusions have been reached with regard to use of acoustic intensity techniques at the KU-FRL acoustic test facility.

The acoustic intensity technique can be adapted to measure the transmission loss characteristics of panels. Use of this method will give average transmission loss values as opposed to the position-dependent values obtained from single-microphone measurements.The same technique and installation can also be used to plot the intensity maps of vibrating panels. Use of the microphone-positioning device greatly simplifies correct grid positioning.The acoustic intensity programs can easily be written on a microcomputer. (Total cost of the microcomputer is less than $2500.) The initial results indicate that transmission loss values measured using this method are lower than theoretically predicted values. This facility cannot be considered a plane wave facility at high frequencies above 800 Hz.

CHAPTER 8

MEASUREMENT OF ABSORPTION COEFFICIENTS

8.1 INTRODUCTION

When a noise source is situated inside a room and operates continuously, the acoustic intensity at any point in the room will be higher than the value that will exist if the same source is operated in the open air. This is because of the partial reflection of the sound energy by the walls. The sound absorbing efficiency of a wall is expressed in terms of an absorption coefficient. It is also true for the ambient levels inside an aircraft. The acoustic transmission through sidewalls, cockpit, rear bulkhead and floor is the most significant to be considered in determining the interior noise levels. However, a high internal absorption will tend to minimize the ambient noise level produced by those sounds that do penetrate into the fuselage. Also, there are sound sources inside the fuselage such as the air-conditioning ducts.

The effect of internal absorption on ambient sound levels can approximately be found from the following equation. Neglecting the effect of internal sources, the noise reduction of a sidewall can be written as (Reference 23)

$$NR = 10 \left(\log \left(\alpha/\tau\right)\right) \qquad (8.1),$$

where NR = Noise reduction of sidewall

τ = Transmission coefficient

α = Total absorption coefficient.

Separating the effects of transmission loss and the internal absorption, Equation (8.1) can be written as

$$N = -10 \log\tau + 10 \log\alpha \qquad (8.2).$$

The following table, calculated based on Equation 8.2, shows the effect of the internal absorption on the noise reduction:

Average Absorption Coefficient	Change in Noise Reduction (dB)
.01	-20.0
.1	-10.00
.2	-7.0
.5	-3.0
.9	-0.45
.99	-0.04

For example, the internal sound levels will increase by 3 dB if the absorption coefficient is only 0.5. For a bare aluminum panel, the value of absorption coefficient is -1 (Reference 23), while that of the carpet is 0.9. Hence, a knowledge of the absorption inside an aircraft is useful for the noise control engineer.

8.2 DEFINITION OF ABSORPTION COEFFICIENT

The absorption of a material is quantified by means of a coefficient. In the literature, this coefficient is defined in several ways (References 9 and 39).

8.2.1 SOUND ABSORPTION COEFFICIENT AT A GIVEN ANGLE OF INCIDENCE

The sound absorption coefficient (α_θ) is defined as a ratio of the sound energy absorption by a surface to the sound energy incident upon that surface at a given angle of incidence (θ). Accordingly, this coefficient is always less than one. However, because the absorption will vary as a function of the angle of incidence, the practical value of this coefficient will be limited.

8.2.2 STATISTICAL SOUND ABSORPTION COEFFICIENT

The statistical absorption coefficient ($\bar{\alpha}$) is defined (for an absorbing surface of infinite extent) as the ratio of the sound energy absorbed by the surface to the sound energy incident upon the surface, when the incident sound field is perfectly diffuse (Reference 9). This coefficient provides a single-number index for general use.

8.2.3 SABINE ABSORPTION COEFFICIENT

Most of the sound absorption coefficients published are obtained by measuring the time rate of decay of the sound energy density in an approved reverberation room with and without a patch of the sound absorbing material under test laid on the floor (References 9 and 39). The sound absorption coefficient (α_s)

measured using this procedure varies at times considerably from the statistical absorption coefficient (α). This absorption coefficient is called the Sabine Absorption Coefficient.

8.2.4 NOISE REDUCTION COEFFICIENT

This coefficient is different from the noise reduction defined by Equation (8.1). Noise reduction coefficient (NRC) is obtained by averaging (to the nearest multiple of 0.05), the Sabine Absorption Coefficients (or Sabine Absorptivities) at 250, 500, 1000, and 2000 Hz (References 9 and 39).

8.2.5 REVERBERATION TIME AND SABINE ABSORPTION COEFFICIENT

The time rate of decay, used in the measurement or the Sabine Absorption Coefficient, is normally expressed in terms of the reverberation time. The reverberation time is defined as time in seconds required for the sound intensity level to decrease by 60 dB (Reference 9). The average Sabine Absorption Coefficient of a room is defined by the following equation (Reference 9):

$$\alpha_s = \sum \alpha_i S_i / S \qquad (8.3),$$

where $\bar{\alpha}_s$ = Average Sabine Absorption Coefficient

S = Total surface area of the reverberation room

α_i = Sabine Absorption Coefficient of the surface, i

S_i = Area of surface, i

The reverberation time and the average Sabine Absorption Coefficient are related (neglecting air absorption) by the equation (Reference 9),

$$T = 0.161V/(S\bar{\alpha}_s) \quad \text{in MKS units}$$

$$= 0.049V/(S\bar{\alpha}_s) \quad \text{in English units} \qquad (8.4),$$

where T = Reverberation time

V = Volume of the chamber

S = Total surface area of the chamber

$\bar{\alpha}_s$ = Average Sabine Absorption Coefficient.

The Sabine Absorption Coefficient of a test sample can be determined from Equations (8.3) and (8.4) knowing the absorption coefficient of a standard sample of the same size. One of the primary difficulties in measuring the Sabine Absorption Coefficient is that this procedure is valid only in rooms with diffused distribution of acoustic energy. This assumption is not valid for rooms i) which are well defined and have sound focusing characteristics, 2) which have odd-shaped cavities with deep recesses, and 3) which are small and can produce local anomalies resulting from standing wave patterns. To avoid these difficulties, the ASTM method (References 9 and 39) requires that the test chamber be of volume 200 m^3 with sample size eight feet by eight feet. Such a chamber may not be available to general aviation manufacturers who want to test many interior trim panels. Also the sample sizes of these materials available to the noise control engineers will most often be smaller than the required eight feet by eight feet. Under

these circumstances the measurement of Sabine Absorption Coefficient may not be possible. A new method to measure absorption coefficient is necessary, even if it gives only a reasonable estimate of the absorption coefficient. It is noted that no other method will give the same results as the standard Sabine Absorption Coefficient method. But a new method can be used for comparison of the absorption coefficients of various trim materials. The method proposed uses the deconvolution technique. If a transient signal is made to hit an absorption material, a part of the sound energy will be absorbed. The absorption will not, in general, be uniform across the frequency range. Hence, the reflected signal will be not only reduced in amplitude but also distorted. Comparing the direct and the distorted signals, the characteristics of the reflecting surface can be determined. The central part of the analysis when this method is used will be the separation (or deconvolution) of the direct and indirect signals.

8.3 DECONVOLUTION AND CEPSTRUM

A schematic diagram of a system which illustrates the deconvolution is shown in Figure 8.1. The receiver, a microphone, receives both direct signal from source along the path ℓ_1, and the reflected signal along the path ℓ_2. A simple way to deconvolve would be to increase ℓ_2 over ℓ_1 such that the total duration of the signal is less than the time it takes for the signal to travel the extra distance $(\ell_2 - \ell_1)$. A typical case using a mathematical

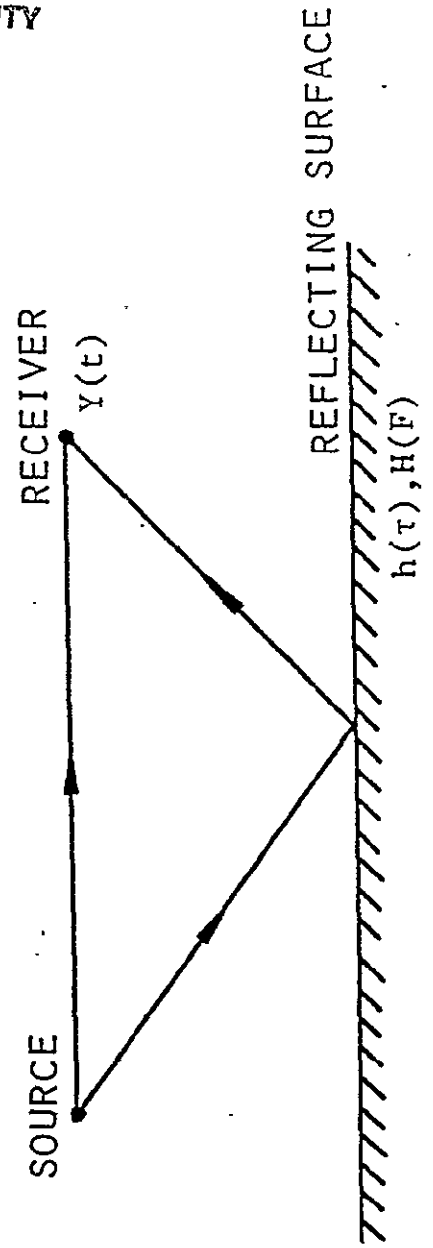

Figure 8.1: Schematic Diagram of Geometry for Absorption Measurement

example taken from Reference 40 is shown in Figure 8.2(a). The time series in this example are generated by

$$y(t) = 50e^{(t-1)} + 30e^{(t-2)} \qquad (8.5).$$

The direct signal is sensed approximately one second after record is started. The reflected signal, which is reduced in amplitude but not distorted, is received one second thereafter. Because the duration of the signal is smaller than the delay time, it can easily be deconvolved. However, achieving deconvolution in time domain is normally not practicable, due to extraneous noise.

Using the autocorrelation method, it is possible to detect the presence of the echoes in the composite signal. However, reconstruction of the characteristics (or impulse response) of the reflecting surface is not possible (Reference 40). The third technique is the use of cepstral technique, which is described in References 40-43.

8.4 BASIC THEORY

8.4.1 DEFINITION OF CEPSTRUM

There are two types of cepstra defined in the literature. Both can be used for deconvolving the composite signal with the distorted echo, power cepstrum and complex cepstrum.

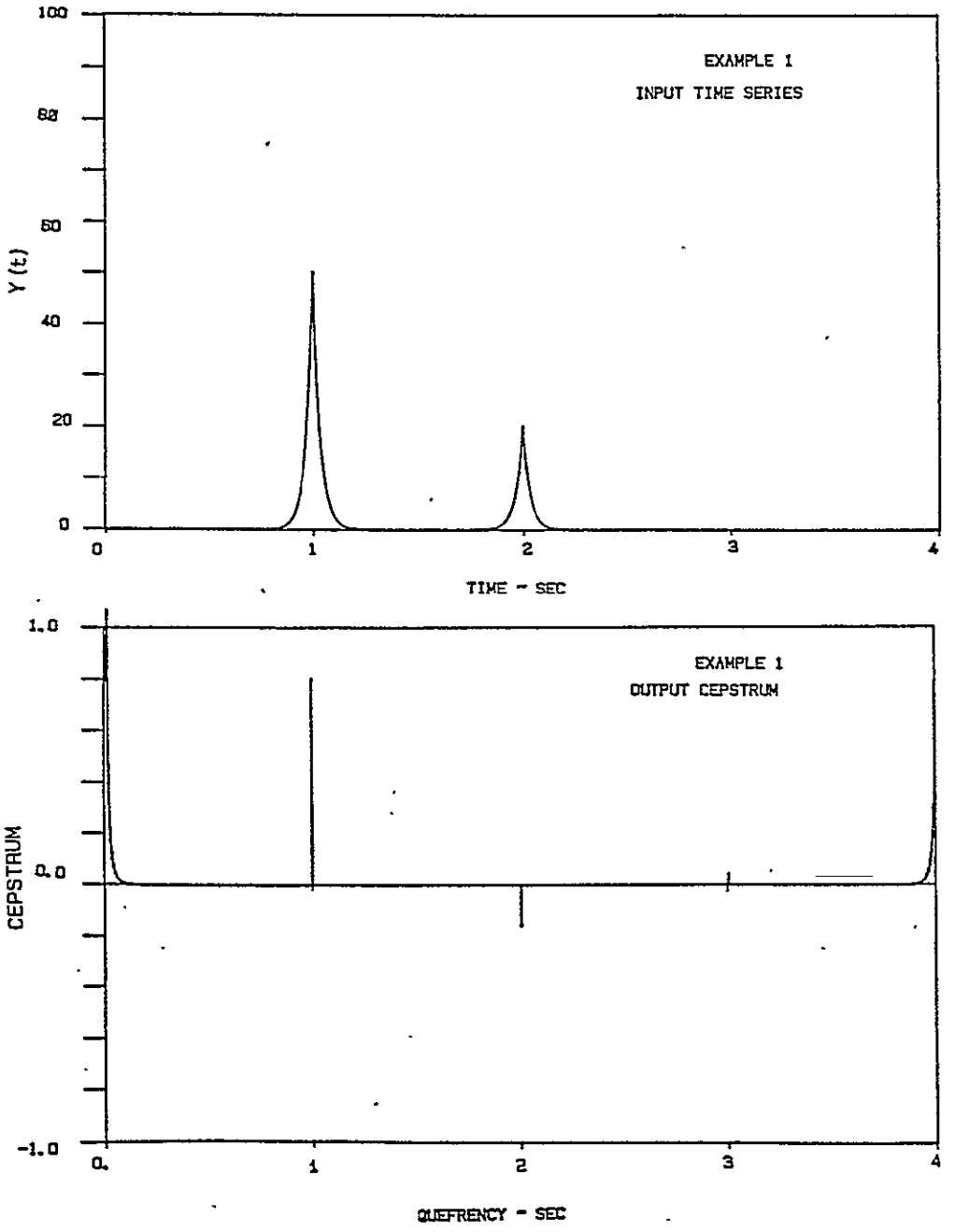

Figure 8.2: A Data Sequence with Reflection and Its Cepstrum

The present-day definition of the power cepstrum is as follows (Reference 44): The power cepstrum of a data sequence is the square of the inverse Z-transform of the logarithm of the magnitude square of the Z transform of the data sequence. Mathematically,

$$x_{pc}(nt) = (Z^{-1}[\ell n|X(z)|^2])^2 \qquad (8.6);$$

x_{pc} = Power cepstrum at nt

n = An integer

t = Sampling interval

Z = Z-Transform

X(z) = Fourier transform of x(z)

x(z) = Data sequence.

Normally the final squaring is not performed. Computationally, the Z-transform is performed using the discrete Fourier transform. The computational procedure for obtaining power cepstrum is shown in Figure 8.3 (taken from Reference 40). The power cepstrum is then the inverse discrete Fourier transform of the logarithm of the power spectrum.

The complex cepstrum of signal x(t) is written as x_{pc} and is defined as the inverse Z-transform of the complex logarithm of Z-transform (Reference 44).

$$x_{cp}(nt) = \frac{1}{2\pi j} \oint \ell n(X(z))\ z^{n-1} dz \qquad (8.7);$$

where $x_{cp}(0)$ is logarithm of x(0), X(z) is the Z-transform of the data sequence x(nt). Computationally this definition of complex cepstrum is equivalent to finding the inverse Fourier transform of

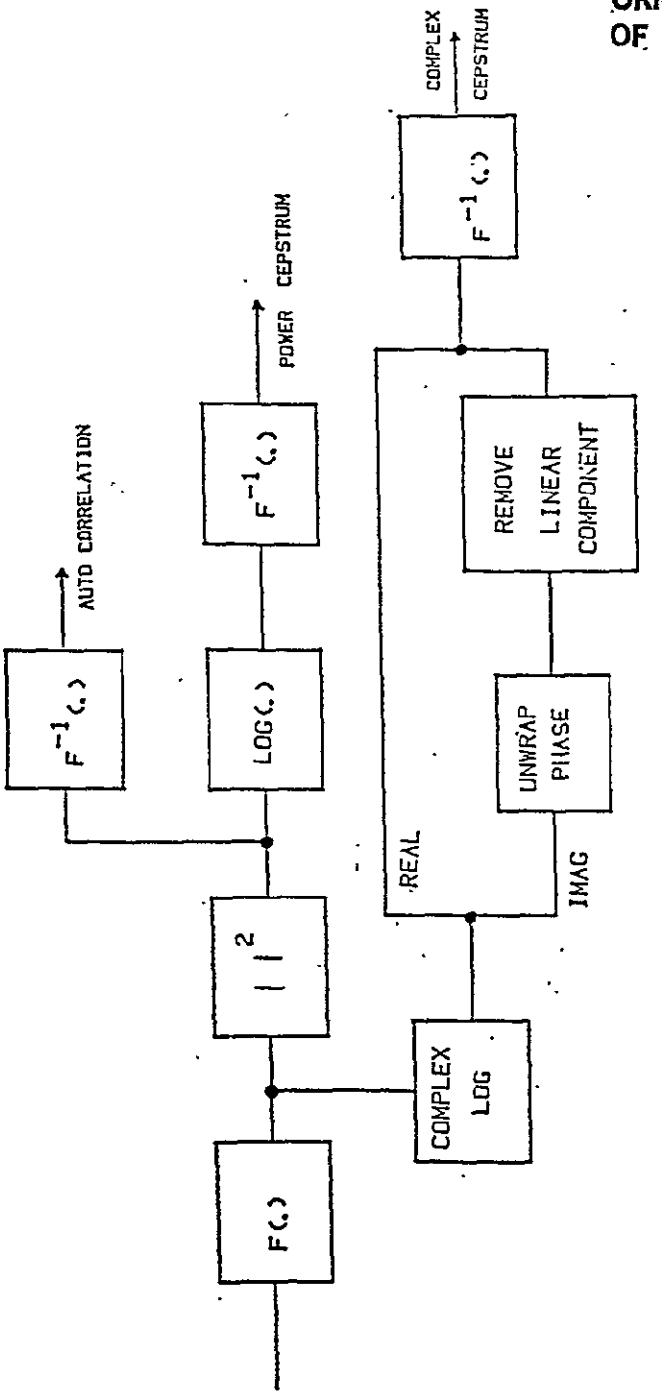

Figure 8.3: Block Diagram for the Calculation of Cepstrum

the complex logarithm of the Fourier transform of a data sequence. The calculation sequence of complex cepstrum is also shown in Figure 8.3.

8.4.2 Theory

The basic theory of calculating absorption coefficient using cepstral technique is reported in References 42 and 43. The following derivation of deconvolution of signals using this technique closely follows References 40-42. Consider the signal measured by a system shown in Figure 8.1. The signal y(t) received at the microphone (output) is a sum of the direct signal x(t) and the reflected signal, distorted and attenuated by the reflecting surface. Let the impulse response of the reflecting surface be $h(\tau)$. The Fourier transform of the $h(\tau)$ yields the reflection frequency response H(f) of the surface. The magnitude of H(f) represents the ratio of the energy reflected to the incident energy. Hence, in terms of H(f), the energy absorption coefficient for a given angle of incidence is given by (see Reference 46)

$$\alpha(f) = 1 - |H(f)|^2 \qquad (8.8).$$

Referring to Figure 8.1, the signal received at the microphone y(t) can be represented by the equation,

$$y(t) = x(t) + \frac{\ell_1}{\ell_2} \int_0^T h(t - \tau - \lambda)x(\lambda)d\lambda \qquad (8.9),$$

or in the operator form,

$$y(t) = x(t) + \frac{\ell_1}{\ell_2} h(t - \tau) * x(t) \qquad (8.10),$$

where $x(t)$ is the direct signal, ℓ_1/ℓ_2 represents the effect of spherical spreading of the source. The reflected wave is assumed to be plane waves (see Reference 42); and ℓ_1/ℓ_2 is always less than 1, τ is the time delay between the arrival of the direct and reflected surfaces, (or echo delay time), and T is the observation interval. The total observation time is assumed to be much larger than the delay time, correlation time of direct signal, and the impulse response $H(\tau)$. As can be seen, the signal arriving along the reflected path is not just an attenuated, delayed replica of $x(t)$ but is also distorted. This distortion is due to the form of the impulse response $h(\tau)$ and occurs as a convolution at an echo delay of τ. This time delay is given by

$$\tau = \frac{\ell_1 - \ell_2}{c}$$

where a is the speed of sound, ℓ_1 is the distance travelled by the direct signal, and ℓ_2 is the distance travelled by the reflected signal.

The Fourier transform of 8.10 yields

$$Y(f) = X(f)[1 + \ell_1/\ell_2 H(f)e^{-i2\pi f\tau}] \qquad (8.12),$$

where f is the frequency; and X, Y and H are the Fourier transforms of x, y and h respectively. The power spectrum is obtained as the modulus squared:

$$|Y(f)|^2 = |X(f)|^2\{[1 + \frac{\ell_1}{\ell_2} H(f)e^{-i(2\pi f)\tau}][1 + \frac{\ell_1}{\ell_2} H(f)e^{-i2\pi f\tau}]^*\} \quad (8.13).$$

Taking logarithm,

$$\ell n|Y(f)|^2 = \ell n|X(f)|^2 + \ell n[1 + \frac{\ell_1}{\ell_2} H(f)e^{-i(2\pi f)\tau}] + \ell n[1 + \frac{\ell_1}{\ell_2} H^*(f)e^{+i(2\pi f)\tau}] \quad (8.14).$$

The series expansions of the second and third term are convergent if the ratio ℓ_1/ℓ_2 and the magnitude of the transfer function are less than one. From the geometry of the problem, the ratio ℓ_1/ℓ_2 is always less than one. For sound absorption materials, the magnitude of the transfer function is normally less than one. The series expansion of logarithmic function $\ell n(1 + p)$ is given by

$$\ell n(1 + p) = p - p^2/2 + p^3/3 \cdot \cdot \cdot \cdot \cdot \cdot \quad (8.15).$$

Using this expansion for the second and third terms in Equation (8.14), it follows that

$$\ell n|Y|^2 = \ell n|X|^2 + \frac{\ell_1}{\ell_2} He^{-i2\pi f\tau} - (\frac{\ell_1}{\ell_2})^2 \frac{1}{2} H^2 e^{-2i(2\pi f)\tau} + (\frac{\ell_1}{\ell_2})^3 \frac{1}{3} H^3 e^{-3i(2\pi f)\tau} - \cdot \cdot \cdot \cdot + \frac{\ell_1}{\ell_2} H^* e^{+i2\pi f\tau} - (\frac{\ell_1}{\ell_2})^2 \frac{1}{2} H^{*2} e^{+2i2\pi f\tau} + (\frac{\ell_1}{\ell_2})^3 \frac{1}{3} H^{*3} e^{+3i2\pi f\tau} - \cdot \cdot \cdot \cdot \cdot] \quad (8.16).$$

Inverse Fourier transforming:

$$y_{pc}(t) = x_{pc}(t) + \frac{\ell_1}{\ell_2} h(t - \tau) - (\frac{\ell_1}{\ell_2})^2 \frac{1}{2} h(t - \tau) * h(t - \tau) + \cdots$$
$$+ \frac{\ell_1}{\ell_2} h(-t - \tau) - (\frac{\ell_1}{\ell_2})^2 \frac{1}{2} h(-t - \tau) * h(-t - \tau) + \cdots$$

(8.17),

where $y_{pc}(t)$ and $x_{pc}(t)$ are the power ceptra of composite and direct signals, respectively. This equation indicates that the power cepstrum is a sum of the power cepstrum of the direct signal and a series of delta functions at delay time τ (both negative and positive) apart. The mirror image at negative delay times occurs because the power spectrum is an even function from 0 to Nyquist frequency. The delay time equivalent in cepstral analysis is known as "quefrency" (References 40, 41, and 44). Because of the logarithmic operation, the effect of convolution type of system in Equation (8.1) is now transformed into a simple additive type. Also, the existence and the delay times of the echoes from the reflecting surface are easier to establish, when the data is transformed to cepstral domain.

The procedure of estimation of the characteristics of the reflecting surface from the cepstrum is called channel estimation (Reference 40). A typical cepstrum is shown in Figure 8.4. To obtain the impulse response of the reflecting surface and hence the transfer function from a cepstrum, such as the one shown in Figure 8.4, the cepstrum should be so arranged that the effect of the

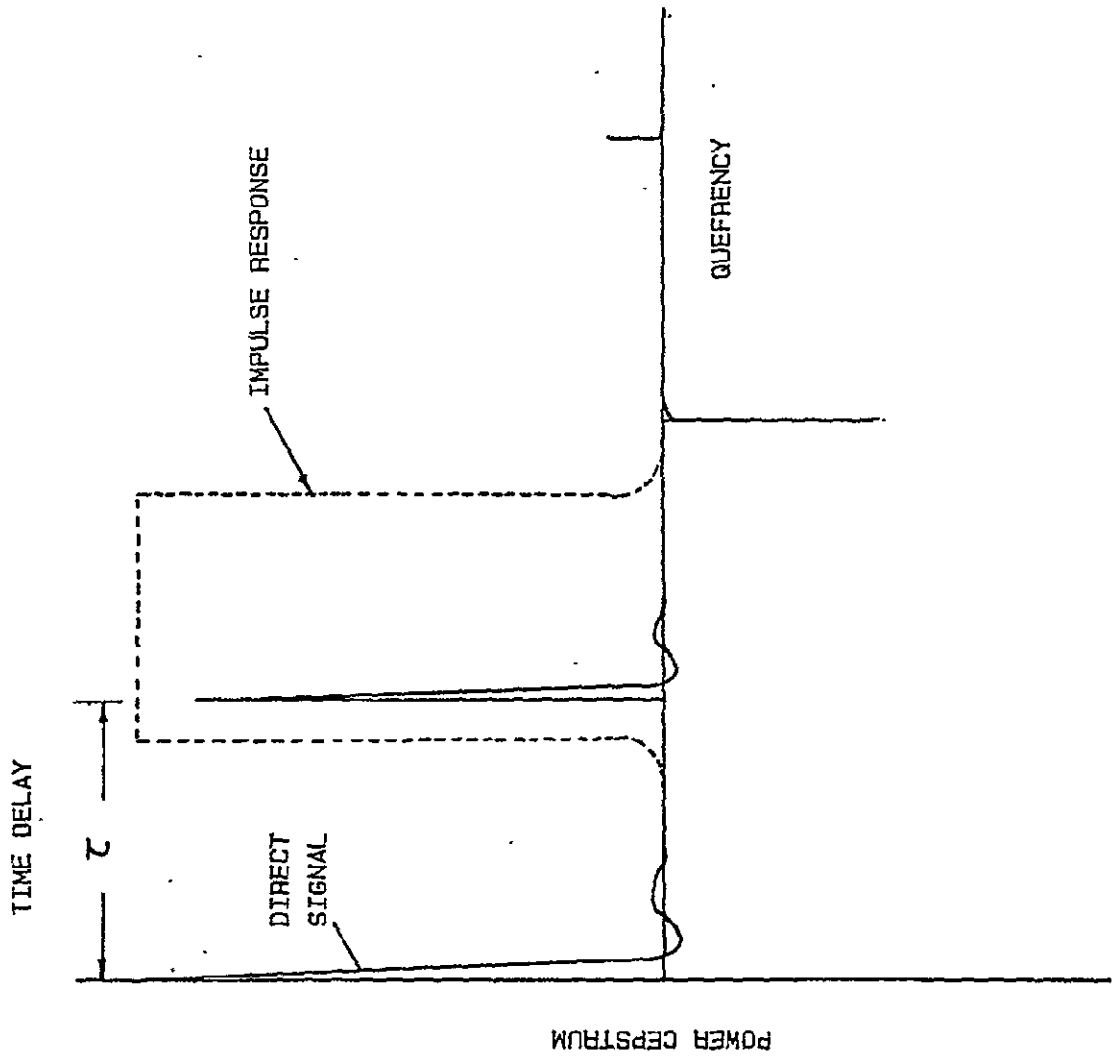

Figure 8.4: A Typical Cepstrum

direct signal and the impulse response are isolated (see References 40-42). This means that the contribution of the direction $x_{pc}(\tau)$ should become negligible before the first reflected response or before the quefrency value of τ. Reference 42 discusses in detail the enhancements that are required to obtain a "good" cepstrum that can be used for further processing. Once a good cepstrum is obtained, the impulse response is filtered out as shown in Figure 8.4 (taken from Reference 42). This impulse response is then Fourier-transformed to obtain an transfer function. Equation (8.1) is used to obtain an absorption coefficient. Even though the processing of the data using this technique appears very straightforward, several difficulties are encountered in practice. These are described in References 40-44. Some of these difficulties are discussed in the subsequent subsections.

8.5 TEST PROCEDURE

Based on the basic theory developed above, the test and analysis tasks for using this technique were identified as

1. Set up test equipment as shown in Figure 8.5.
2. Acquire data sequence y(t) at a preselected sampling rate.
3. Transfer time series to computer.
4. Repeat 2 and 3 (100-200 times).
5. Repeat 2-4 without any panel.
6. Precondition data before processing: e.g., select data length, apply time window zero pad, etc.

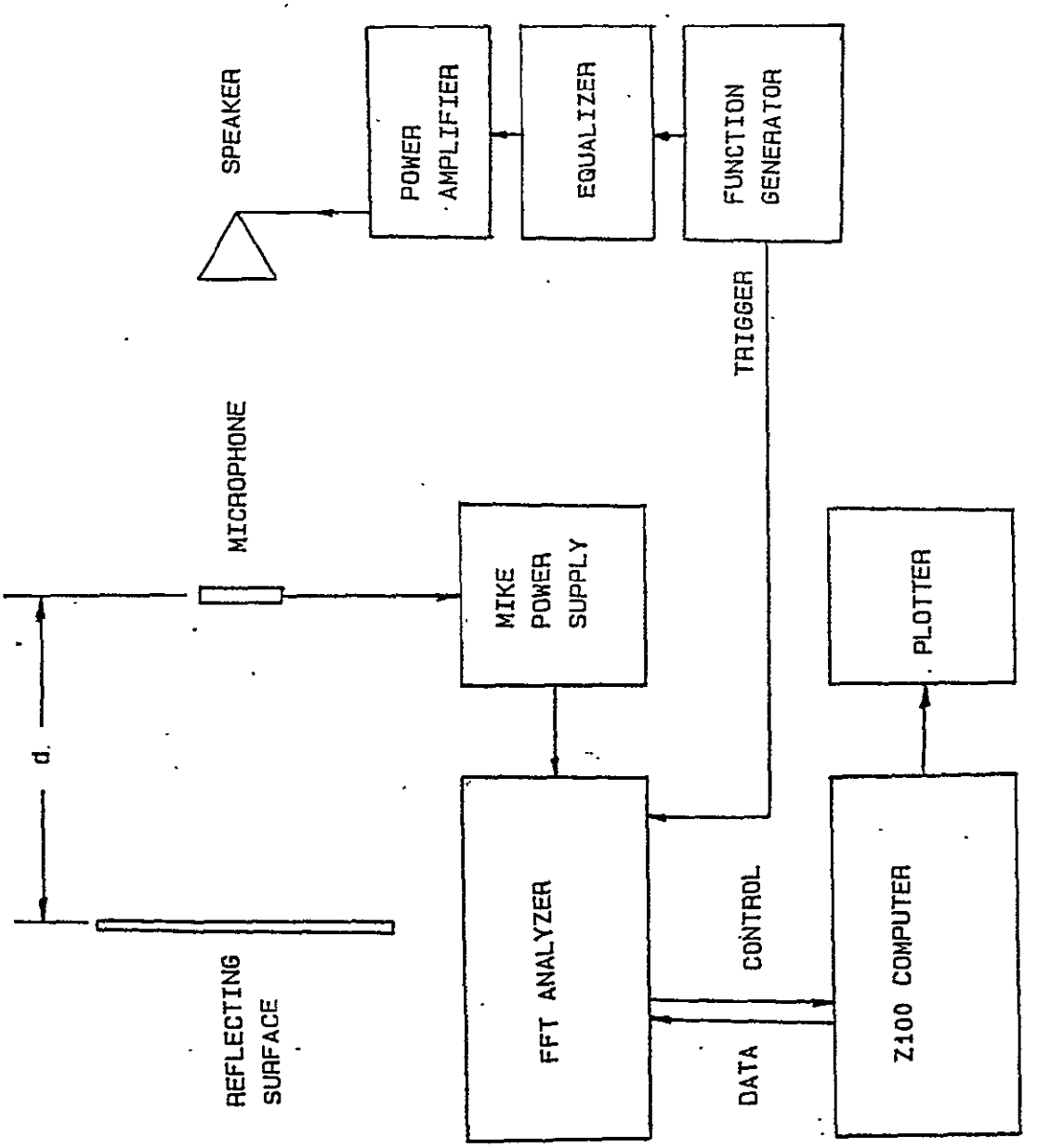

Figure 8.5: Schematic of Experimental Set-Up

7. Final ensemble averaged power spectra of both direct and composite signals.
8. Use background subtraction (see Reference 43) to remove the effect of direct signal from composite signal.
9. Find power cepstrum.
10. Filter data containing impulse response of reflecting surface (see Figure 8.4).
11. Apply window and perform FFT to obtain transfer function.
12. Calculate $\alpha(f)$ using Equation (8.8).

8.5.1 TEST SET-UP

The experimental set-up is shown in Figure 8.5. Only normal incidence was used because it avoids the need for determining exact angle of incidence. Ideally, this test should be done in free field conditions with very low ambient noise levels or in an anechoic chamber. This would avoid multiple reflections off the wall that will contaminate the test signals. Neither of these two was available at the KU-FRL. Proper time window was selected to minimize the effects of wall/floor reflections from the digitaized data.

An ideal noise source would be the one which produces a transient signal (<10 msec) and whose power spectrum is nearly flat. Properly selected pulse function would be ideal because it has the smallest correlation time. However, when this signal is sent through a speaker, the output is characterized by its impulse

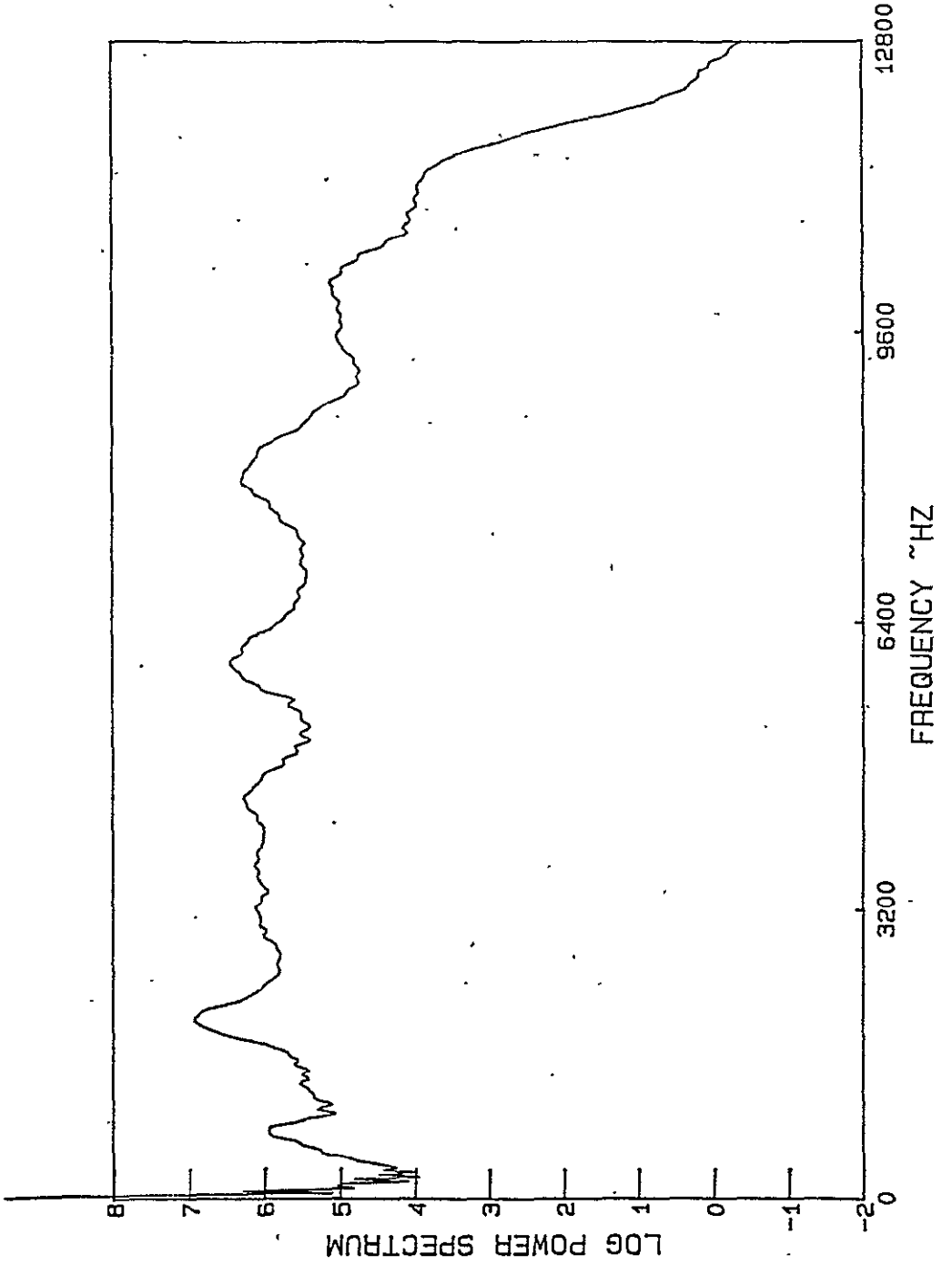

Figure 8.6: Power Spectrum of Direct Signal

response. This response became unacceptable when a large speaker was used (see discussion above). Various other noise sources such as percussion caps, etc., were tried. Even though they produced a better defined spectrum, the repeatability of tests was not good. Finally it was decided to use a four-inch Altec 405-8H speaker. This speaker had a frequency response from ~150-15000 Hz. A seven msec chirp (15 to 40000 Hz) generated by an analog sweep oscillator was used as the input. The use of an AC power amplifier sometimes produced a hum at 60 Hz, corresponding to the line frequency. This contaminated the power spectrum. A DC amplifier was selected because it minimized this problem. But the speaker and amplifier combination produced a peak at 1800 Hz in the power spectrum. The severity of this peak was reduced by the insertion of an equalizer in the input circuit. In spite of these enhancements, the power spectrum still contained a slowly varying oscillation (see Figure 8.6).

The digitizing of time signals was done using a two-channel FFT analyzer, Nicolet 660B. One channel was used for the data and the second channel for triggering. The triggering was done through a trigger on the sweep oscillator. The analyzer had an anti-aliasing filter with 48 dB/octave roll-off rate. The anti-aliasing filter was set by selecting the frequency range knob on the front panel. The data were always digitized at 2.56 times the frequency at which the anti-aliasing filter was set. For example, if a frequency range of 10 KHz was selected, the anti-aliasing filter would be set at 10

kHz and the sampling rate would be 25.6 kHz. The user had no independent control of the sampling rate. Also the number of samples for each test was constant. Each time only 1024 data could be collected. The user could not change this value. The FFT analyzer was connected to the Z-100 through RS 232C port and was communicating at 9600 Baud.

A B&K 4136, 1/4" microphone with B&K 2619 preamplifier was used to measure the signal. The upper and lower band edge of its response was well above that of the speaker. The signal was amplified through an amplifier in NAGRA SJ recorder. The tape recorder was used only as an amplifier and not as a data recorder.

8.5.2 COMPUTER PROGRAM

Computer routines were written to perform the data acquisition and analysis. The languages used were compiled Basic and Fortran. The Fortran used is a subset of Fortran 77 without complex variables. Hence all complex variables were represented by means of two real numbers. Standard FFT routines (see References 45 and 50) were used. To remain within the memory and speed of the microcomputer Z-100, the program was divided into many small routines. Figure 8.7 shows the flow chart for calculations. The listing of computer routines developed at the KU-FRL is given in Appendix D. These routines were tested with the mathematically simulated data of Reference 40, and the results of one example are shown in Figure 8.2.

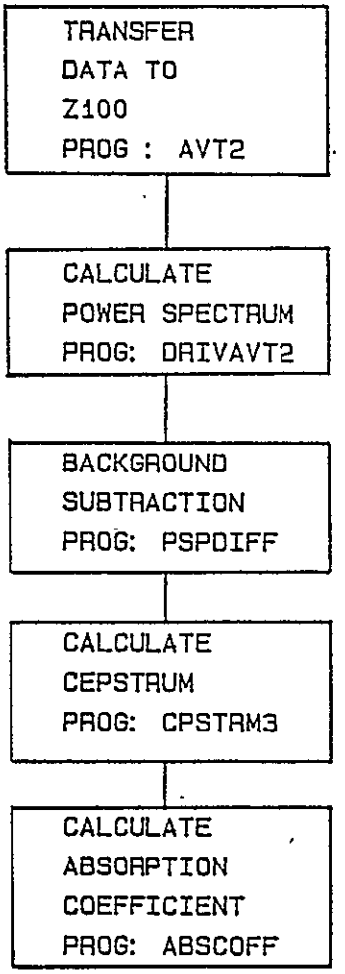

Figure 8.7: Flow Chart of Computer Program

8.6 TESTS DONE

Reference 43 describes in detail the procedures to obtain reflection coefficients of a panel in an anechoic room. The main objective of the testing program at the KU-FRL is to use this technique on a smaller sample size and in non-anechoic conditions. The test technique is slowly being evolved. At the time of this report, it has not yet been finalized. It will continue on to the next project year, 1984-85.

During the present series a vinyl sheet backed with 1/4 inch foam was used as the test sample. The sample size of the foam was four feet by five feet. It was mounted on 5/8 inch compressed particle board by means of adhesives. During the tests, the distance between the microphone and the panel was varied between 18 and 24 inches, and the distance was varied from 20 to 48 inches. Tests were done inside the KU-FRL laboratory. The line joining the centers of speaker, microphone, and the test sample was parallel to ground at five feet.

A swept size signal was generated by the analog sweep oscillator, and the triggering signal was used to trigger the data acquisition on the FFT analyzer. The anti-aliasing filter was set at 10000 Hz. This meant that 1024 samples yielded .04 secs of data. At the end of each test, the data were stored on the floppy disk. The tests were repeated 200 times with and without the absorption material.

Figure 8.8 shows the signal recorded for one such test without any panel. In this case the reflected signals off the wall can be seen after 10 msec of initial data. Also, during this series of tests, the AC/DC coupling of the FFT analyzer was set to DC. Hence at the beginning there is a DC shift. The problem of DC shift in the low-frequency region will be discussed later. Figure 8.9 shows the similar data for composite signal. In this case the AC/DC coupling switch was selected to AC coupling. As can be seen, the reflected signals overlap the incident signal. The cepstral analysis is capable of deconvolving the signals, even when they are overlapping.

For analysis first 512 points were used. The series length was extended to 1024 points by padding zeroes. A $\sin^2$ window was applied, and the power spectrum was calculated and averaged. The logarithm of power spectrum of the direct and overlapping signals is shown in Figures 8.10 and 8.11. The effect of DC shift can be seen as a peak in Figure 8.10.

As can be seen in Figures 8.10 and 8.11, the spectrum is quite irregular in the low-frequency region. This type of spectrum produces a low frequency oscillation in the cepstral domain, which will interfere with the determination of the impulse response. Hence it is nearly impossible to use only the composite signal to obtain the impulse response. To obtain good impulse response only from composite signals, the contribution due to direct signal should die down before it reaches the delay time τ. This is possible only

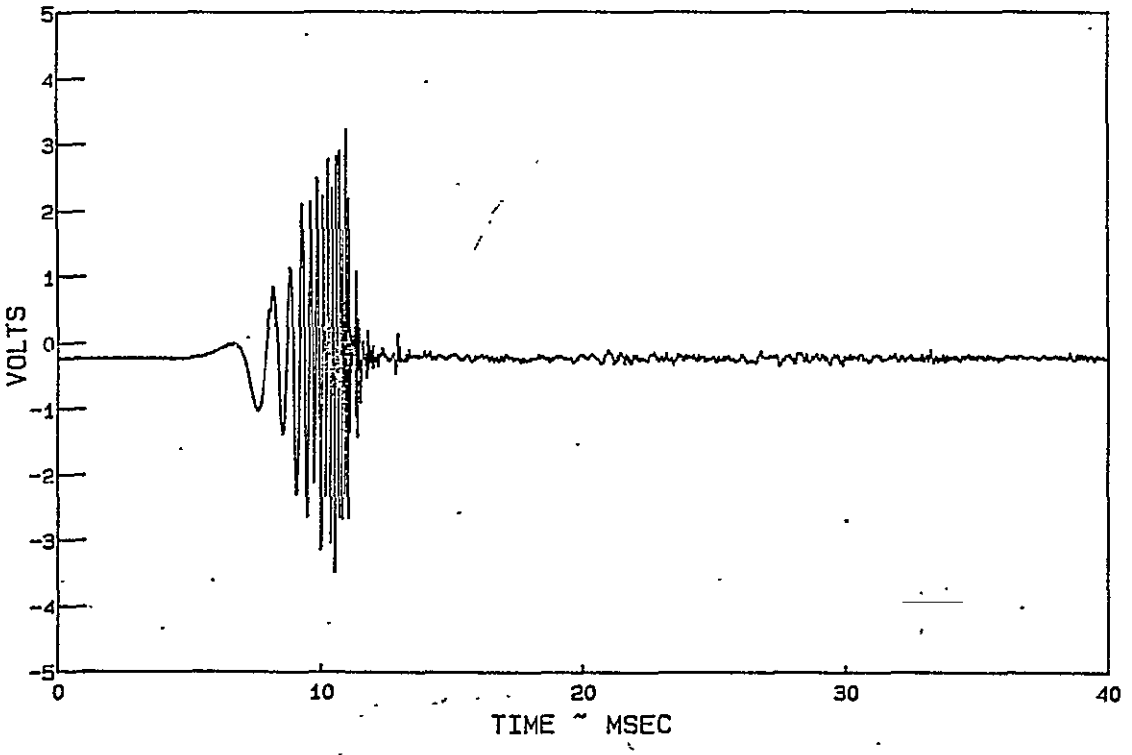

Figure 8.8: Time Series of Direct Signal

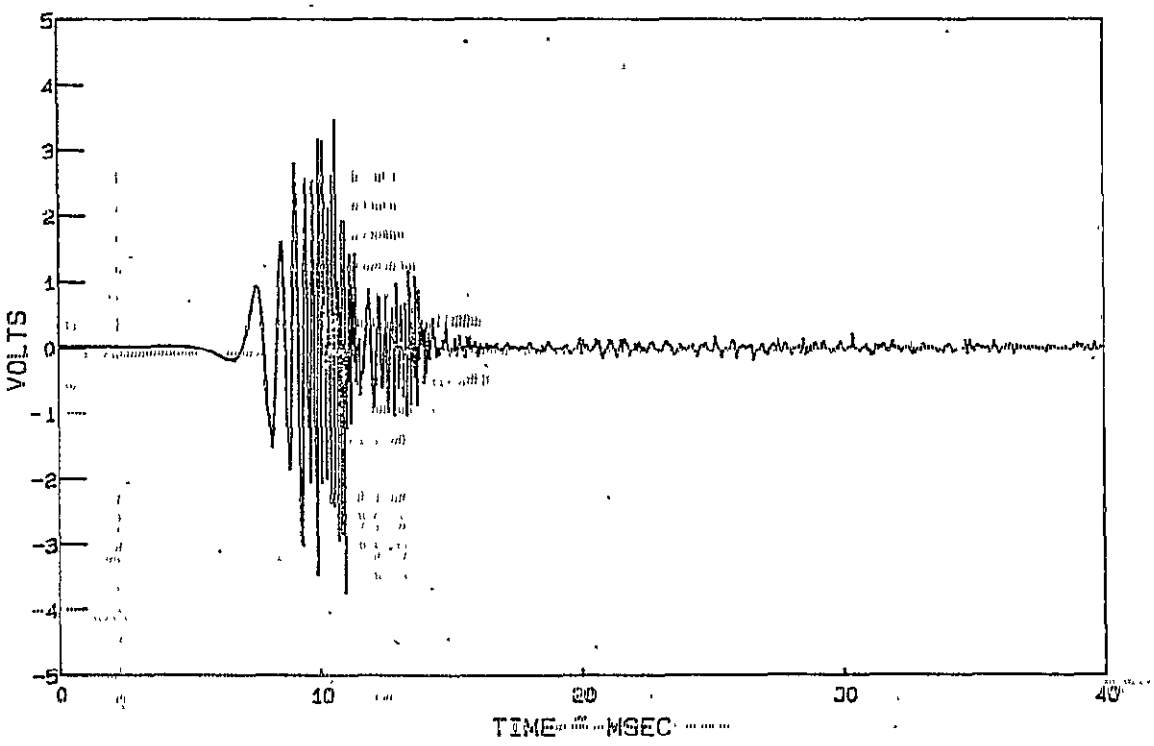

Figure 8.9: Time Series of Composite Signal

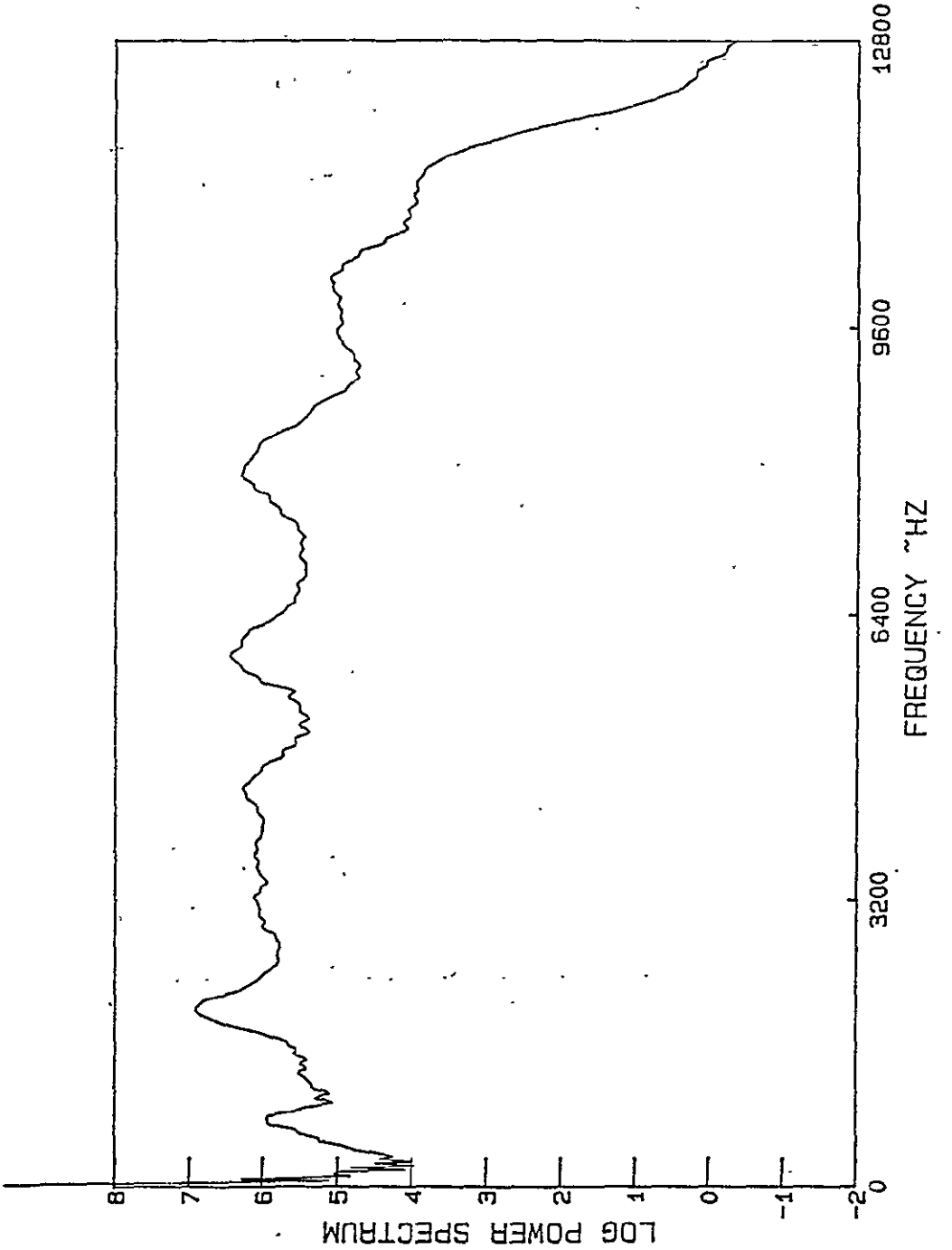

Figure 8.10: Power Spectrum of Direct Signal

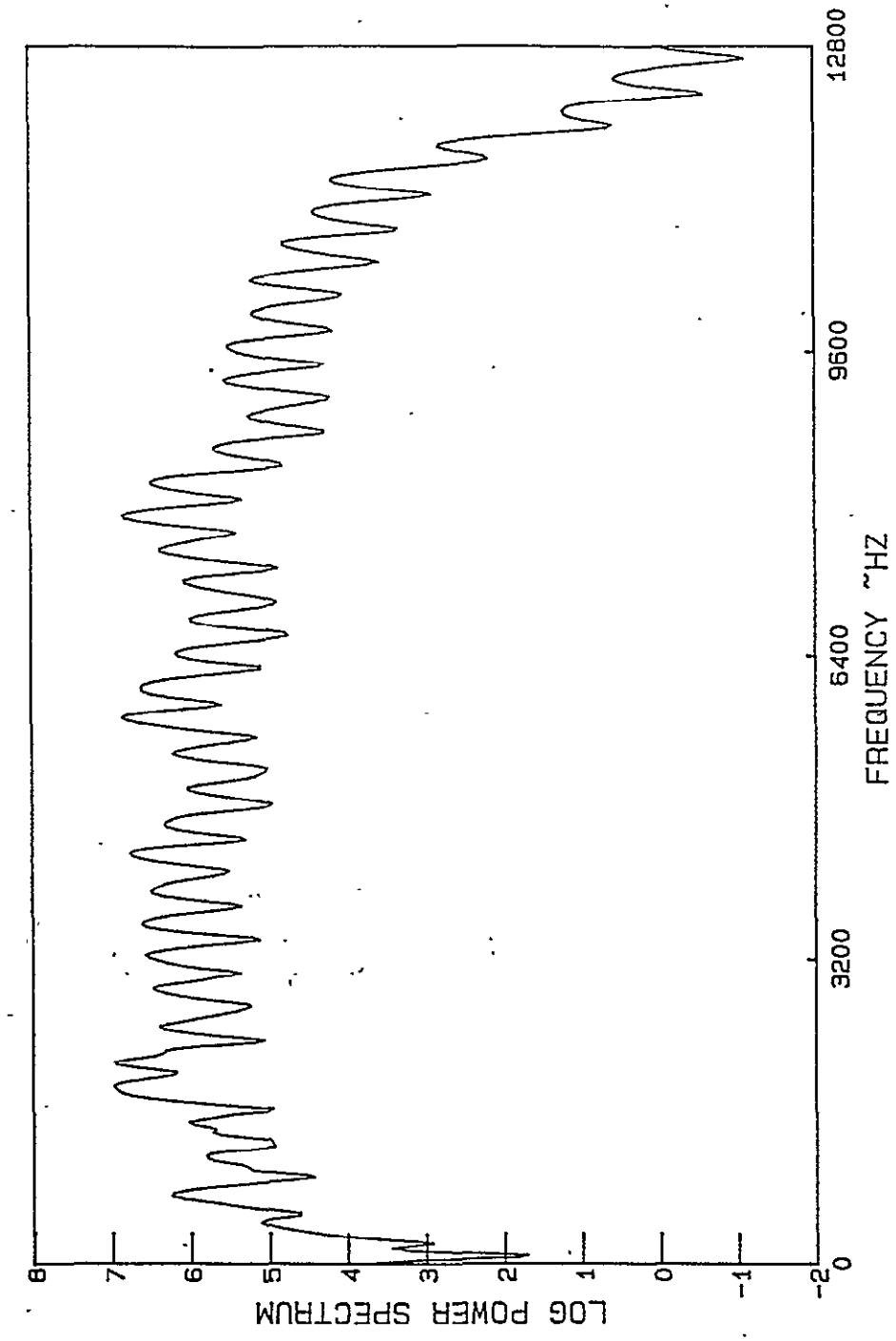

Figure 8.11: Power Spectrum of Composite Signal

if the line peaks at 60 Hz or DC shift, as in Figure 8.10 and other irregularities are removed. Because the frequency response of the speakers used is poor at such low frequencies, as in Figure 8.10, these effects cannot be fully eliminated. Some other procedure to reduce or minimize such a stringent condition is necessary. Reference 43 proposes a method called "background subtraction." In this method, the logarithm of the direct signal is subtracted from the logarithm of power spectrum of the composite signal. This difference is shown in Figure 8.12. The spectral irregularities at low frequencies can easily be seen in Figure 8.13 (with expanded X axis). In order to obtain the cepstrum, these low-frequency irregularities should be removed (Reference 43). To remove these irregularities, Reference 43 proposes spectral smoothing in this region.

When backed by a hard surface, the reflection coefficient should approach one at zero Hz. Reference 43 shows under these conditions the difference in log power spectra is given by

$$\Delta P(f) \approx \ell n(1 + 2(\frac{\ell_1}{\ell_2})\cos 2\pi f\tau + (\frac{\ell_1}{\ell_2})^2) \qquad (8.18)$$

Hence it could be assumed that at very low frequencies the rapid changes seen in Figure 8.12 are not due to reflection from material but are due to other reasons (such as noise). This part of the spectrum can be modified below a certain frequency to conform to the form shown above. This correction is shown by a dotted line in

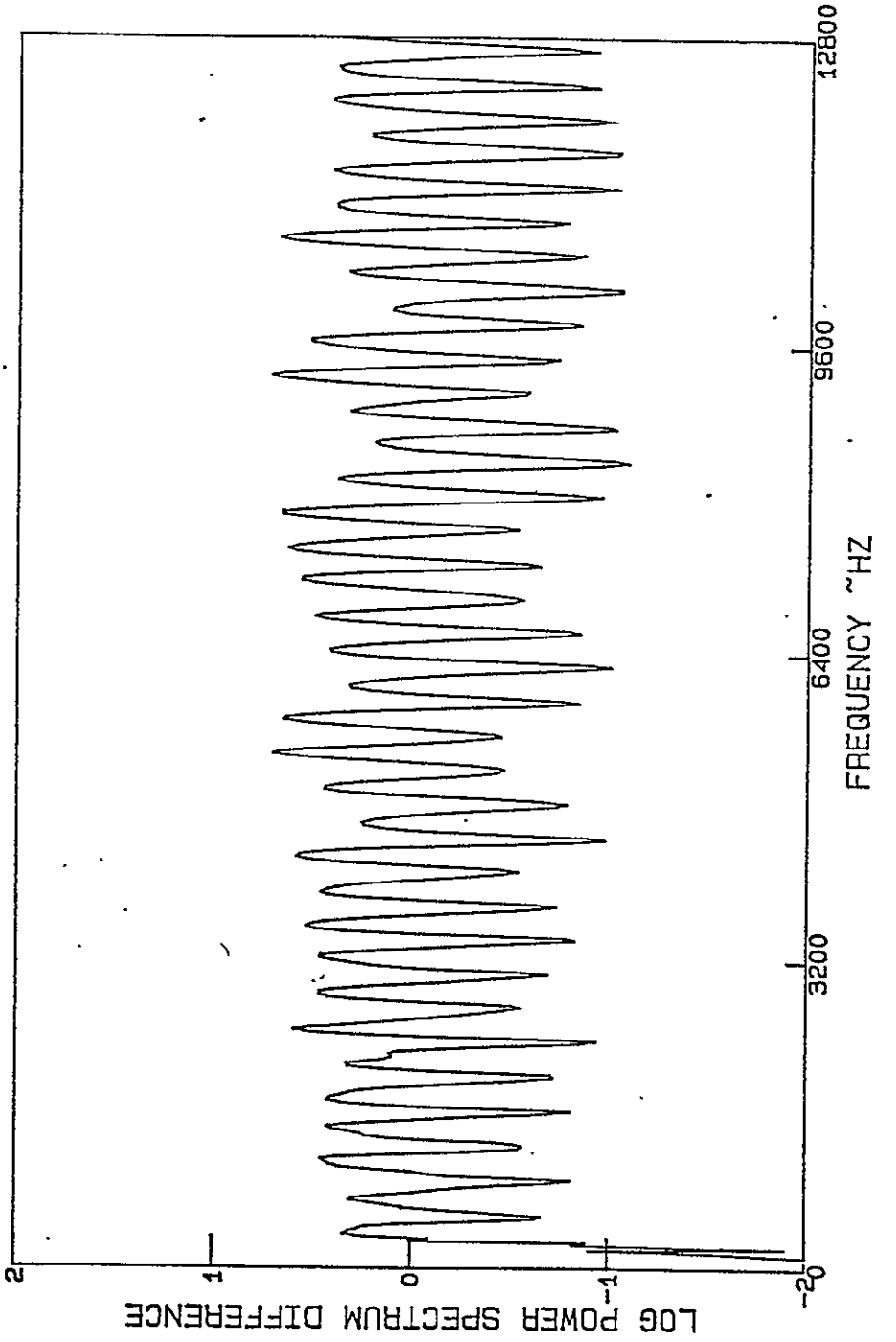

Figure 8.12: Difference between Logarithms of Composite and Direct Signal

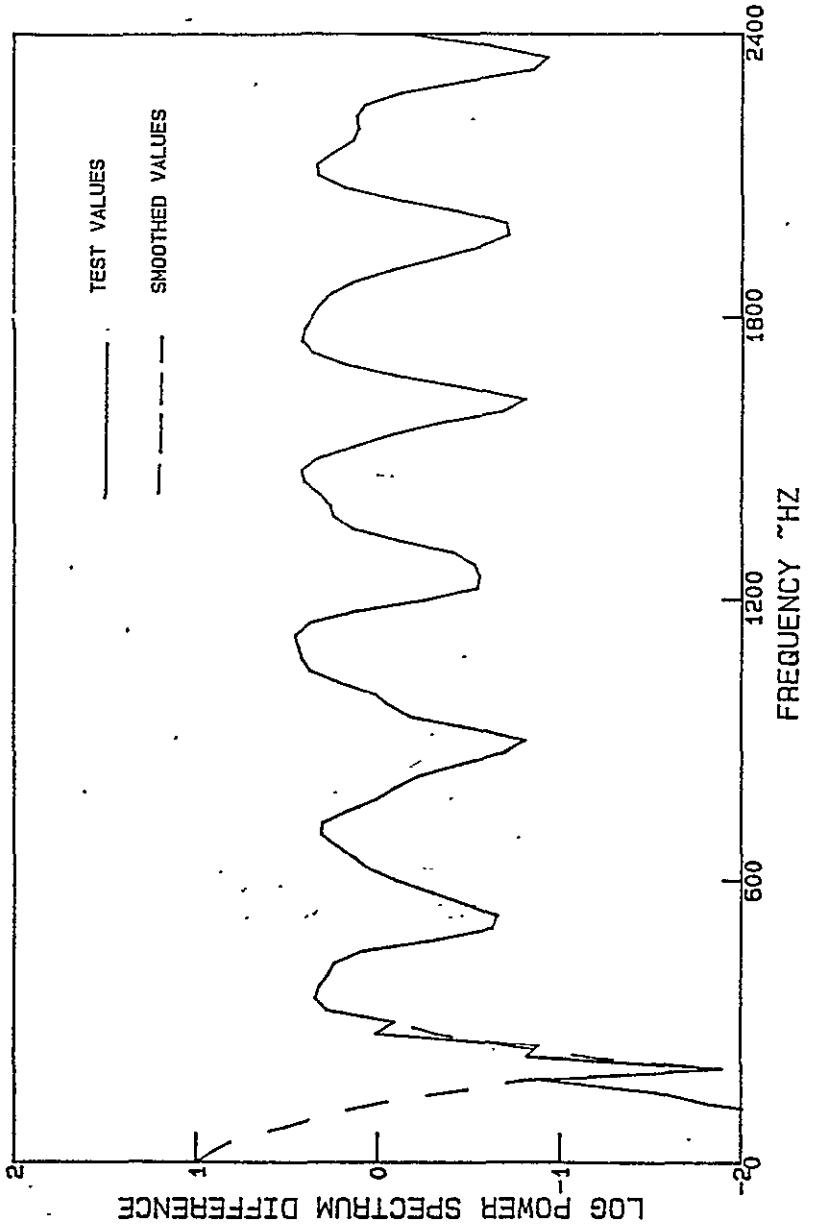

Figure 8.13: Low-Frequency Region of Difference between Logarithm of Composite and Direct Signals

Figure 8.12. However, such a modification means that absorption coefficients found will not be valid in this frequency region. In this case, this region extends up to 300 Hz.

The power cepstrum calculated from the smooth spectrum is shown in Figure 8.14. The power cepstrum shows the first peak at the correct delay time. But still certain irregularities are seen. For these reasons, the extraction of absorption coefficient still may not yield good results. Two and five tenths (2.5) msec data was extracted around this peak, the values were corrected for spherical spreading, and a $\sin^2$ window was applied to the first and last tenth of the extracted signal. The series was extended to 256 points by padding with zeroes. It was then Fourier transformed. The absorption coefficient was then calculated using Equation 8.8. The final value is shown in Figure 8.15.

8.7 DISCUSSION AND RECOMMENDATIONS

During the series of tests performed so far, the speaker has been kept at a distance of 24-48 inches from the microphone. This may violate the assumptions in the theory. When the speaker was moved far away from the microphone, the signal-to-noise ratio significantly decreased. The speaker could not handle higher power. This was traced to the fact that the sweep oscillator, even when it was not sweeping, delivered a steady state signal at frequency around its start cycle. The speaker could not handle this steady signal. However, the speaker could handle a much higher

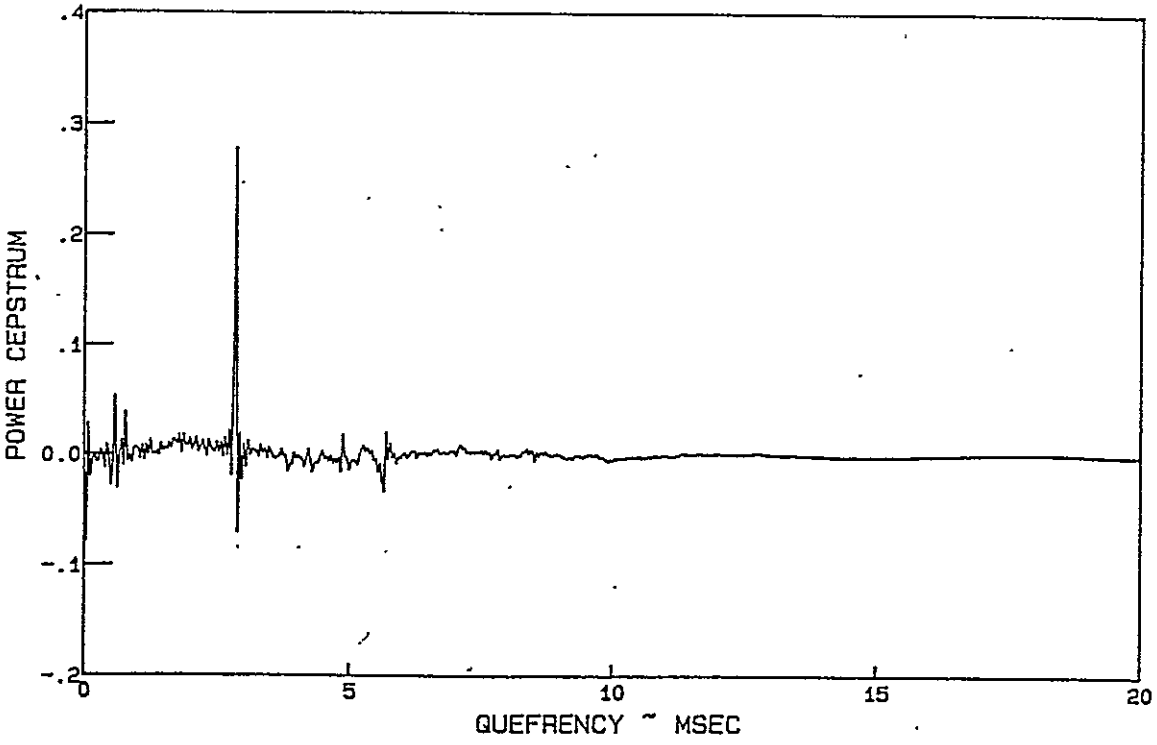

Figure 8.14: Power Cepstrum of Data

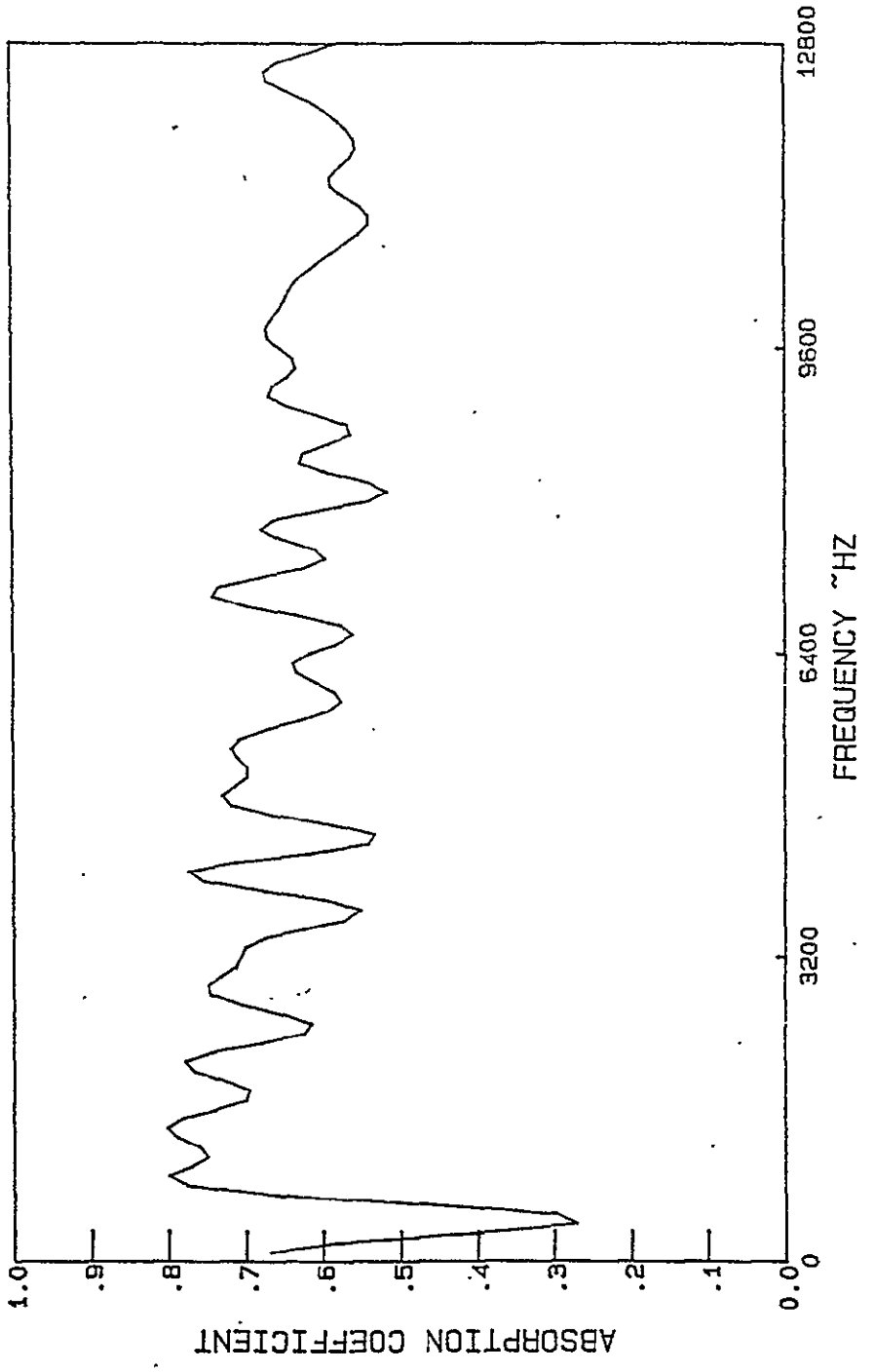

Figure 8.15: Calculated Absorption Coefficient

transient signal. Also, it is still suspected that the reflections off the floor may contaminate the signal. These, being deterministic, will not average out when ensemble averaging is done. The small sample size may also produce diffractions at the edges. The test technique has not yet progressed far enough to identify these effects. However, tests performed so far indicate that this technique can be used at general aviation aircraft companies without major cost and expertise.

Based on the experience gained during these tests, the following recommendations are made for further testing. A digitally produced signal, instead of analog signal, should be used. A 12-bit D/A card is available for the Z-100 microcomputer. This card is capable of handlig up to 70 KHz. One of the channels of this card can be used for triggering. Such triggering and digitally produced swept sine signals can produce synchronized signals. This will enable time domain averaging instead of frequency domain averaging (Reference 43). This will also reduce computation time. Use of IEEE-488 connections between the Z-100 and the Nicolet 660B will increase data transfer rate and permit checking of other parameters. Tests should also be done with speaker and microphone at least 6-8 feet above ground level. Only then can the absorption coefficients obtained be checked with published results. These tests have been proposed for the project year 1984-85.

CHAPTER 9

APPLICATION TO AIRCRAFT NOISE CONTROL DESIGN

9.1 INTRODUCTION

References 3-6 give the results of the experiments performed at the KU-FRL acoustic test facility to determine the sound transmission loss characteristics of single-wall panels. Chapter 5 of this report presents the results of double-wall panels. These panels measure only 18 inches by 18 inches. Slight changes to classical sound transmission loss model provide acceptable restuls for these panels, as can be seen from Chapter 6 (Figures 6.2-6.25). In this chapter, application of classical sound transmission theory to the design of interior noise control of an aircraft is considered. Modifications to the classical sound transmission loss theory were necessary before it could be applied to actual aircraft noise control design. The next section gives the design procedure used. Section 9.3 gives the program details and the calculations. In the last section, the theoretically predicted overall interior values are compared with the measured values. A discussion of the results concludes this chapter.

9.2 DESIGN PROCEDURE

This chapter describes attempts to design an interior noise control a business jet aircraft of Max TOW 20000 lb category. This aircraft has two aft-mounted engines. When the initial design of

the noise control treatment started, the prototype had already been built and was flying. At this stage, the interior noise levels of untreated aircraft were known. Major changes to fuselage skin/stringer/frame were not possible. Also because the aircraft was a jet aircraft, the interior noise spectrum was not very low-frequency dominant. Hence the extended calculations done in Reference 23 to find the transmission loss of untreated aircraft were not needed. Analysis of the proposed treatment had only to be confined to the effects of additional sound barrier and insulation. For these reasons, it was decided to use classical sound transmission loss theory.

For the purpose of the design of the interior noise control treatment, the interior of the aircraft was divided into four parts, as shown in Figure 9.1. The interior noise levels were measured before the application of treatment in cruise flight (35000 ft/0.8 M) at four locations along the length of the fuselage. The level at each location was representative of levels within that area. At the time of these measurements, the aircraft still had some kind of interior treatment, essentially for thermal insulation. The spectrum at each location, along with the overall values, is shown in Figure 9.2. It was noticed that even without additional treatment the contributions of the energy above 5000 Hz to the overall levels was negligible. Hence, during the design, only the frequency values to 5000 Hz were considered.

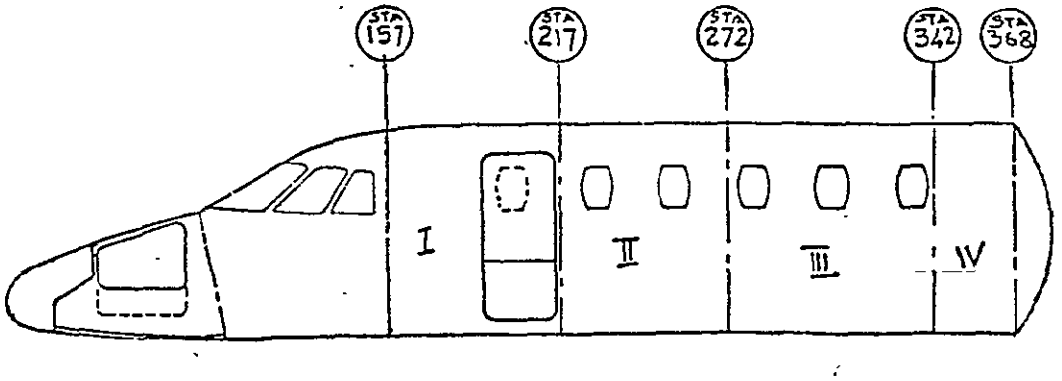

Figure 9.1: Four Areas of Treatment

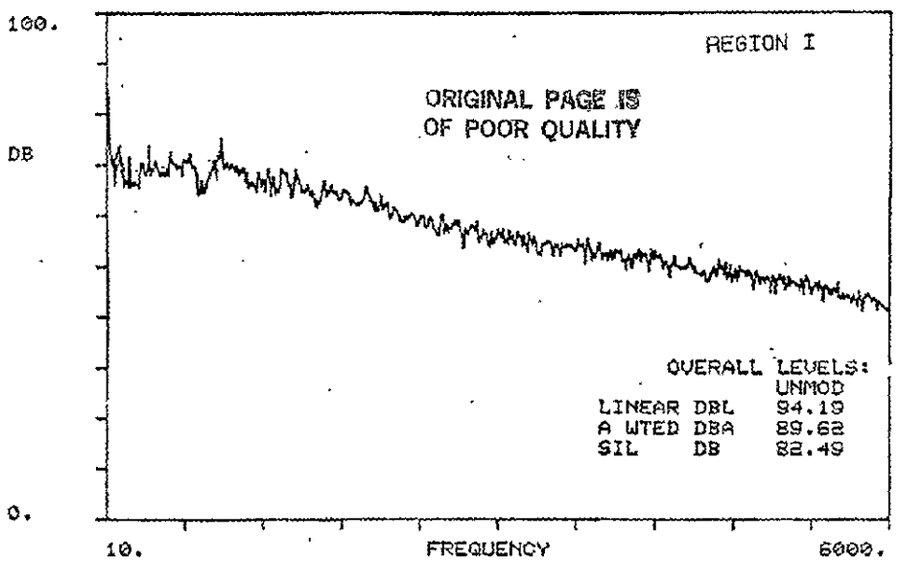

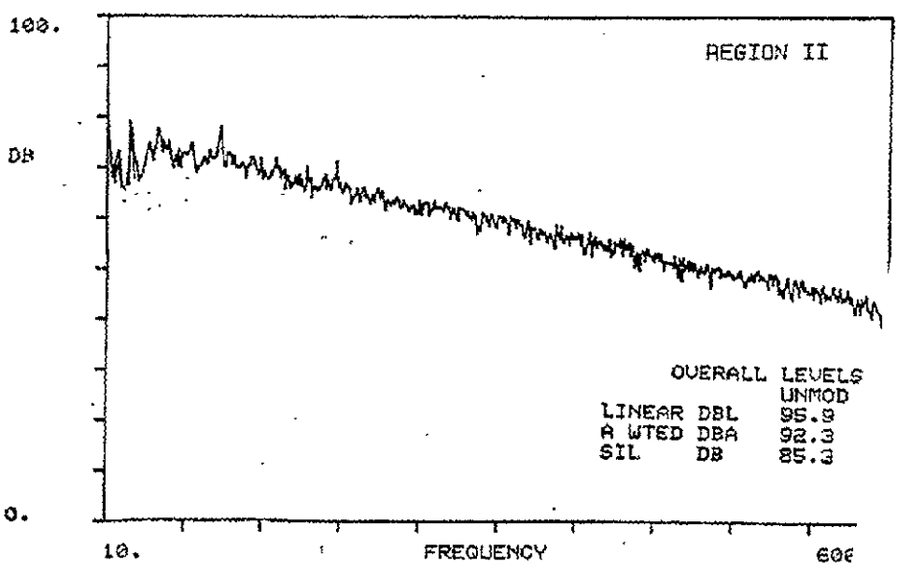

Figure 9.2: Initial Interior Noise Levels

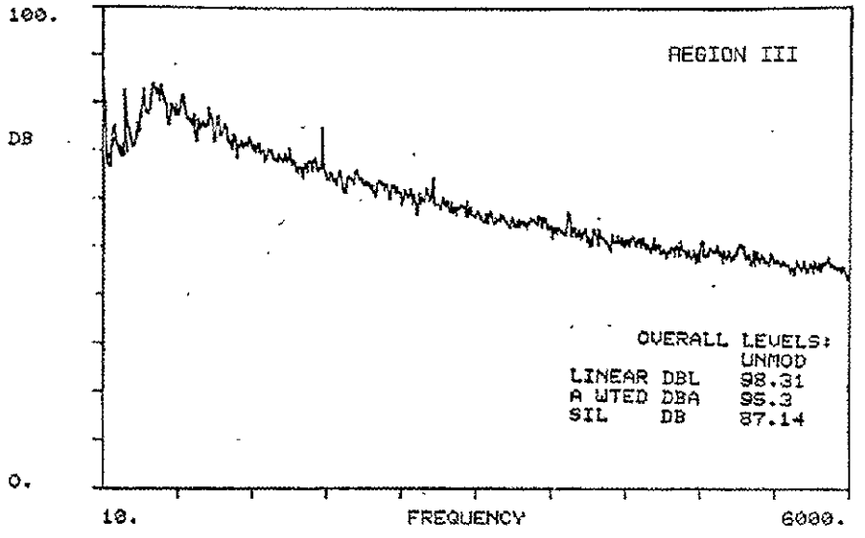

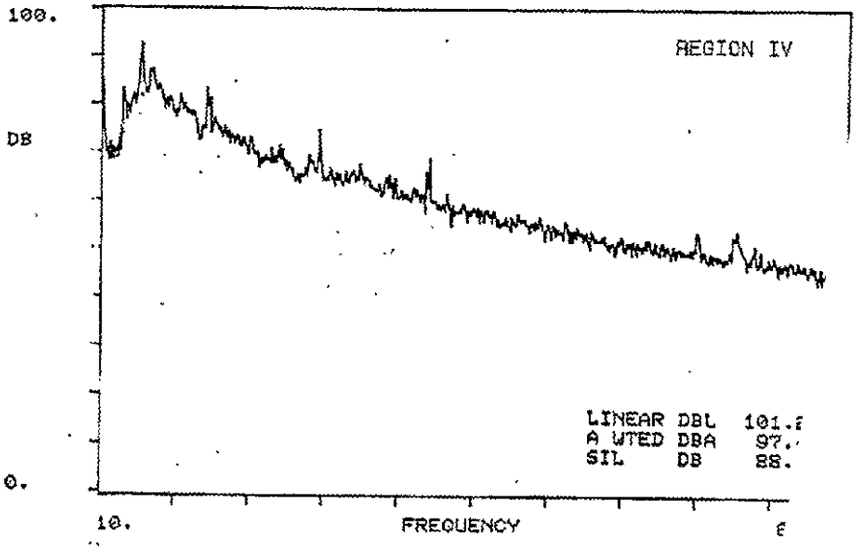

Figure 9.2: (continued)

DATA I TARY

The design of a noise control treatment involves selection of the barrier material such as leaded vinyl, proper placement of these materials along the fuselage sidewall, and selection of fiberglass insulation depth. For the sake of analysis, the source was considered to be situated outside the aircraft. In other words, in this analysis, the interior noise due to air-conditioning ducts, hydraulic motor/accumulator, etc., was assumed to be small. For the most part of the analysis, only engine noise was considered. The noise generated due to airflow over the fuselage was not considered. However, these assumptions are not restrictive in this case because during the anlaysis the measured interior levels were used. The measured levels, of course, contain the contributions from all these sources. Also the structure-borne noise from the engine into the interior through the fuselage structure was assumed to be much less compared to the noise through the airborne path. This will be the case when the engine isolators have adequate attenuation at the audio frequencies. The lack of prominant discrete tones in the measured spectrum (Figure 9.2) justifies this assumption. Under these conditions the classical sound transmission loss theory could be applied. Had any of these assumptions been violated, then the predicted interior levels with the treatment would not be achieved.

The final result of this design procedure was the prediction of the interior noise level for a given weight penalty. The following steps were involved in the design.

Calculation of theoretical transmission loss of untreated aircraft. Here the aircraft was treated as a monocoque shell, and the equations derived in Reference 51 were used to obtain the transmission loss values.

2. Calculation of additional transmission loss of the existing treatment. This is the minimal treatment used in the prototype aircraft, essentially for thermal insulation. This treatment was present when the interior noise level measurements were made. To calculate the transmission loss, the theoretical model described in Chapter 6 was used. In this case the treatment consisted essentially only of insulation.

3. Selection of additional treatment. The proposed treatments consisted of fiberglass insulation or leaded vinyls. Several densities of leaded vinyl and several thicknesses of fiberglass insulations were used. A total of 40 combinations were initially considered. Tables 9.1-9.4 list some of the treatments considered.

4. Calculation of additional transmission loss of the proposed treatment. Once again, this was done using the program in step 2 above.

5. Calculation of the difference in transmission loss (TL). This additional transmission loss is calculated by subtracting the transmission loss obtained in step 2 from transmission loss of step 4.

Table 9.1: Summary of Treatments: Region I

Location: STA #157-#217

Predicted Interior Sound Pressure Levels

Treatment		Without Absorption			With Absorption			Wt Penalty
#	Description	DBL	DBA	PSIL	DBL	DBA	PSIL	(lb)
22	3" + 20	92.9	84.7	76.7	92.6	78.5	70.1	10
23	3" + 40	92.7	83.7	75.7	92.5	77.6	69.0	17
12	3" + 60	92.6	83.5	75.2	92.4	77.3	68.6	24
24	2" + 20 + 1" + 20	92.8	82.8	71.7	92.6	77.2	65.6	17
25	2" + 20 + 1" + 40	92.6	81.5	70.6	92.4	75.9	64.8	24
13	2" + 20 + 1" + 60	92.5	80.9	69.9	92.4	75.4	64.3	31
14	2" + 40 + 1" + 20	92.5	79.2	68.0	92.4	74.2	63.0	24
26	2" + 40 + 1" + 40	92.4	78.8	67.7	92.4	73.8	62.8	31
15	2" + 40 + 1" + 60	92.3	77.9	66.8	92.3	72.8	62.1	38
27	2" + 60 + 1" + 60	92.1	75.9	64.7	92.3	71.3	60.5	45
16	2" + 80 + 1" + 80	92.1	75.3	63.4	92.3	71.1	59.3	59
17	2" +120 +1" +120	91.9	71.8	61.0	92.0	68.1	57.3	87
29	20 + 3" + 20	92.58	82.4	74.4	92.2	75.4	67	17
30	40 + 3" + 40	92.3	79.9	71.8	92.1	73.0	64.4	31
31	60 + 3" + 60	92.1	77.9	69.9	92.0	71.0	62.5	45
32	80 + 3" + 80	92.01	76.4	68.4	92.0	69.6	61.0	59
33	120 + 3" + 120	92.0	74.1	65.9	92.0	67.6	58.6	87
34	60 + 3" + 80	92.1	77.3	69.3	91.1	70.5	61.9	52
35	40 + 3" + 80	92.2	79.1	71.1	92.1	72.2	63.7	45
36	1" + 20 + 2"	93.1	84.2	73.1	92.3	77.4	65.7	10
37	1" + 20 + 2" + 20	92.8	83.0	71.8	92.2	76.2	64.6	17
38	1" + 40 + 2" + 40	92.3	78.9	67.7	92.1	72.5	61.6	31
39	1" + 60 + 2" + 60	92.3	78.2	66	92.1	72.2	60.7	45
40	1" + 80 + 2" + 80	92.1	75.0	63.5	92.0	69.4	58.8	59
41	1" +120 + 2" +120	91.9	72.0	61.1	91.93	67.0	57.2	87

Remark - Treatment Description:

1" + 120 + 2" + 120 means a four-layered treatment, with the layers in this order: one inch of fiberglass, 120 oz/yd^2 of leaded vinyl, two inches of fiberglass, followed by one more sheet of 120 oz/yd^2 of leaded vinyl. These layers were placed between the skin and the trim panel.

Table 9.2: Summary of Treatments: Region II

Location: STA #217-#272

Predicted Interior Sound Pressure Levels

Treatment		Without Absorption			With Absorption			Wt Penalty
#	Description	DBL	DBA	PSIL	DBL	DBA	PSIL	(lb)
22	3" + 20	94.5	87.6	79.4	93.4	81.6	72.9	9.5
23	3" + 40	94.1	86.6	78.4	93.2	80.6	71.8	16.0
12	3" + 60	93.9	86.3	78.0	93.2	80.3	71.4	22.5
24	2" + 20 + 1" + 20	94.5	85.0	74.5	93.5	80.6	68.1	16.0
25	2" + 20 + 1" + 40	94.0	84.7	73.5	93.2	79.3	67.1	22.5
13	1" + 20 + 1" + 60	93.8	84.1	72.8	93.1	78.8	66.5	29.0
14	2" + 40 + 1" + 20	94.0	83.4	72.2	93.3	78.6	65.5	22.5
26	2" + 40 + 1" + 40	93.8	82.9	70.8	93.2	78.1	65.2	29.0
15	2" + 40 + 1" + 60	93.5	81.8	69.9	93.1	77.0	64.5	35.5
27	2" + 60 + 1" + 60	93.2	79.5	67.5	93.0	75.0	62.6	42.0
16	2" + 80 + 1" + 80	93.1	78.6	65.8	92.9	74.4	61.4	55.0
17	2" +120 + 1" +120	92.8	75.4	63.1	92.8	71.7	59.2	81.0
29	20 + 3" + 20	93.7	85.2	77.1	92.8	78.3	70.0	16.0
30	40 + 3" + 40	93.2	82.7	74.6	92.7	75.8	67.3	29.0
31	60 + 3" + 60	92.9	80.7	72.7	92.6	73.9	65.3	42.0
32	80 + 3"+ 80	92.7	79.2	71.1	92.5	72.5	63.8	55.0
33	120 + 3" +120	92.6	76.9	68.7	92.5	70.3	61.3	81.0
34	60 + 3" + 80	92.8	80.1	72.1	92.6	73.3	64.7	48.5
35	40 + 3" + 80	93.1	81.9	73.8	92.7	75.0	66.5	42.0
36	1" + 20 + 2"	94.7	87.1	75.9	93.2	80.5	68.5	9.5
37	1" + 20 + 2" + 20	94.3	85.9	74.6	93	79.3	67.3	16.0
38	1" + 40 + 2" + 40	93.5	82.5	70.8	92.8	76.3	64.0	29.0
39	1" + 60 + 2" + 60	93.7	82.9	69.3	92.8	76.8	63.2	42.0
40	1" + 80 + 2" + 80	93.0	78.7	66.4	92.6	72.9	60.9	55.0
41	1" +120 + 2" +120	92.6	75.4	63.5	92.5	70.0	58.9	81.0

Remark - Treatment Description:

1" + 120 + 2" + 120 means a four-layered treatment, with the layers in this order: one inch of fiberglass, 120 oz/yd^2 of leaded vinyl, two inches of fiberglass, followed by one more sheet of 120 oz/yd^2 of leaded vinyl. These layers were placed between the skin and the trim panel.

Table 9.3: Summary of Treatments: Region III

Location: STA #272-#342

Predicted Interior Sound Pressure Levels

Treatment		Without Absorption			With Absorption			Wt Penalty
#	Description	DBL	DBA	PSIL	DBL	DBA	PSIL	(lb)
22	3" + 20	95.7	91	81.3	93.2	85.3	75.0	11
23	3" + 40	95	90.1	80.3	92.7	84.3	73.8	19
12	3" + 60	94.7	89.8	79.9	92.5	84.0	73.3	27
24	2" + 20 + 1" + 20	97.0	91.9	76.6	93.9	86.5	70.4	19
25	2" + 20 + 1" + 40	95.9	90.6	75.6	93.2	85.2	69.6	27
13	2" + 20 + 1" + 60	95.5	90.0	74.9	93.0	84.6	69.1	35
14	2" + 40 + 1" + 20	95.6	89.0	73.1	93.2	84.0	68.0	27
26	2" + 40 + 1" + 40	95.2	88.5	72.8	93.0	83.6	67.7	35
15	2" + 40 + 1" + 60	94.4	87.3	71.9	92.5	82.3	67.0	43
27	2" + 60 + 1" + 60	93.3	84.5	69.6	92.0	79.8	65.1	48
16	2" + 80 + 1" + 80	93.0	83.4	68.1	91.9	79.0	63.8	67
17	2" +120 + 1" +120	91.9	79.7	65.6	91.3	75.5	61.3	99
29	20 + 3" + 20	94.4	88.9	79.0	91.9	82.1	71.7	19
30	40 + 3" + 40	93.2	86.3	76.5	91.4	79.6	69.2	35
31	60 + 3" + 60	92.4	84.5	74.5	91.1	77.8	67.3	48
32	80 + 3" + 80	91.9	82.9	73.0	90.9	76.3	65.7	67
33	120 + 3" + 120	91.4	80.6	70.6	90.8	74.1	63.3	99
34	60 + 3" + 80	92.1	83.8	74.0	91.0	77.1	66.6	56
35	40 + 3" + 80	92.8	85.6	75.8	91.3	78.9	68.4	48
36	1" + 20 + 2"	97.5	93.0	77.9	93.5	86.4	70.6	11
37	1" + 20 + 2" + 20	96.6	91.8	76.7	93.0	85.2	69.5	19
38	1" + 40 + 2" + 40	94.7	88.3	72.8	92.1	82.0	66.5	35
39	1" + 60 + 2" + 60	95.3	88.9	71.2	92.4	82.7	65.6	48
40	1" + 80 + 2" + 80	93.0	84.0	68.5	91.4	78.2	63.4	67
41	1" +120 + 2" +120	91.8	80.6	65.9	90.9	74.8	61.4	99

Remark - Treatment Description:

1" + 120 + 2" + 120 means a four-layered treatment, with the layers in this order: one inch of fiberglass, 120 oz/yd^2 of leaded vinyl, two inches of fiberglass, followed by one more sheet of 120 oz/yd^2 of leaded vinyl. These layers were placed between the skin and the trim panel.

Table 9.4: Summary of Treatments: Region IV

Location: STA #342-#368

Predicted Interior Sound Pressure Levels

Treatment		Without Absorption			With Absorption			Wt Penalty
#	Description	DBL	DBA	PSIL	DBL	DBA	PSIL	(lb)
22	3" + 20	98.0	93.2	82.7	94.9	87.8	76.1	3.5
23	3" + 40	97.1	92.3	81.6	94.3	86.9	75.1	6.0
12	3" + 60	96.8	92.0	81.2	94.0	86.5	74.7	8.5
24	2" + 20 + 1" + 20	99.5	94.4	78.0	96.0	89.2	71.6	6.0
25	2" + 20 + 1" + 40	98.0	92.8	76.9	94.7	87.6	70.7	8.5
13	2" + 20 + 1" + 60	97.9	92.6	76.2	94.8	87.5	70.2	11.0
14	2" + 40 + 1" + 20	98.8	92.8	74.7	95.6	88.1	69.3	8.5
26	2" + 40 + 1" + 40	98.4	92.3	74.3	95.3	87.6	69.0	11.0
15	2" + 40 + 1" + 60	95.7	97.5	73.4	94.6	86.4	68.3	13.5
27	2" + 60 + 1" + 60	96.1	88.8	71.0	93.8	84.4	66.4	16.0
16	2" + 80 + 1" + 80	96.5	88.9	69.5	94.1	84.7	65.2	21.0
17	2" +120 + 1" +120	93.7	84.4	66.9	92.3	80.3	62.9	31.0
29	20 + 3" + 20	97.1	91.6	80.4	93.4	85.3	73.1	6.0
30	40 + 3" + 40	94.8	88.6	77.9	92.1	82.2	70.5	11.0
31	60 + 3" + 60	93.7	86.9	75.9	91.5	80.5	68.6	16.0
32	80 + 3" + 80	93.0	85.4	74.4	91.2	79.1	67	21.0
33	120 + 3" + 120	92.2	83.3	71.9	90.9	77.1	74.6	31.0
34	60 + 3" + 80	93.4	86.3	75.3	91.4	79.9	68.0	18.5
35	40 + 3" + 80	94.3	87.9	77.1	91.8	81.5	69.5	16.0
36	1" + 20 + 2"	100	95.2	79.3	95.3	88.8	72.0	3.5
37	1" + 20 + 2" + 20	98.9	94.0	78.0	94.5	87.6	70.8	6.0
38	1" + 40 + 2" + 40	97.4	91.5	74.3	93.6	85.5	67.7	11.0
39	1" + 60 + 2" + 60	98.5	92.7	72.9	94.3	86.7	67.0	16.0
40	1" + 80 + 2" + 80	95.4	88.2	70.0	92.4	82.4	64.7	21.0
41	1" +120 + 2" +120	93.5	85.0	67.3	91.5	79.3	62.7	31.0

Remark - Treatment Description:

1" + 120 + 2" + 120 means a four-layered treatment, with the layers in this order: one inch of fiberglass, 120 oz/yd^2 of leaded vinyl, two inches of fiberglass, followed by one more sheet of 120 oz/yd^2 of leaded vinyl. These layers were placed between the skin and the trim panel.

6. Correction for structure-borne path. Even though the structure-borne noise from the engines through the fuselage structure was neglected, the effect of the noise transmission through sidewall (for example, improper isolation of trim panel from skin) could not be neglected. Several studies (References 9, 23, 25, 39, and 47) have shown that in practice, the predicted transmission loss of double-wall panels is seldom achieved. In order to account for this, only 50% of theoretically calculated values (in decibels) were assumed to be effective. While this figure of 50% is based on judgement, the tests on the existing aircraft (see Appendix F) had indicated that for small differences in transmission loss values (due to treatments), this figure was not unreasonable.

7. Calculation of additional noise reduction (NR) due to increased absorption. The absorption coefficient of the interior noise would increase when the intrior was furnished. This increase is due to the increased absorption of the trim panel, seating, carpet, head liners, etc. This increase in noise reduction can be calculated from Equation 8.1.

8. Calculation of total noise reduction due to treatment. This is the sum of transmission loss obtained in step 6 and noise reduction obtained in step 7.

9. Calculation of predicted interior noise spectrum. This is obtained by subtracting the noise reduction due to treatment from measured noise levels.

10. Calculation of overall levels. From the predicted spectrum, the predicted overall levels are obtained by integration.

11. Calculation of weight penalty. From the properties of the materials used in treatment and the total area of treatment, the weight penalty for each area was calculated.

These steps are shown as a flow diagram in Figure 9.3. The actual calculation was done by three programs. The transmission loss of monocoque shell (Reference 51) was coded into a program (by Gary L. Blankenship at Cessna Aircraft Company and by Jaap Laméris at the KU-FRL) in Fortran language. This program closely follows the equations in Reference 51 and in this case was used to obtain the untreated sound transmission loss. The second program calculated the additional transmission loss across a muitilayer panel. This program was similar to the one given in Appendix B. The program (written by the author) used HP 9845B Basic language. The only difference was that the impedance of the skin panel was calculated from the values of transmission loss calculated from the first program. The impedance model with Single Degree of Freedom (SDOF) was used from Reference 27.

$$TL = 20 \log \left| 1 + \frac{Z_p}{2\rho c} \right| \qquad (9.1).$$

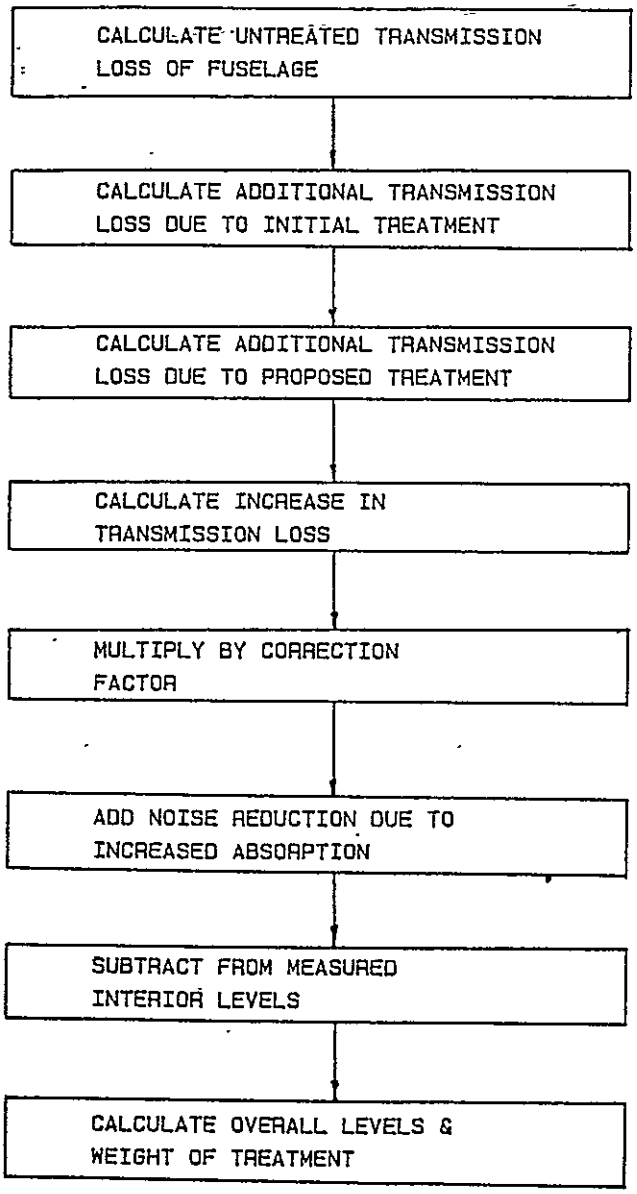

Figure 9.3: Flow Diagram of Calculation

$$\left|1 + \frac{Z_p}{2\rho c}\right|^2 = 10^{\left(\frac{TL}{10}\right)} \qquad (9.2),$$

where TL = Transmission loss

ρc = Impedance of air

Z_p = Impedance of panel having only one mode.

For a panel of only mode,

$$Z_p = 2\zeta\omega_n M + j\omega M[1 - (\frac{\omega_n}{\omega})^2] \qquad (9.3),$$

where ζ = Damping ratio

ω_n = Angular natural frequency

M = Mass of panel per unit area

ω = Angular frequency.

For small damping ratio,

$$Z_p \approx j\omega M[1 - (\frac{\omega_n}{\omega})^2] \qquad (9.4),$$

Z_p is only imaginary. The absolute value of the Z_p was found from 9.2, and it was considered to be entirely imaginary. This value of the impedance was then used for the calculations. For the trim panel, simple mass law was used. For a limp panel, the impedance (Z_p) is given by

$$Z_p = j\omega m \qquad (9.5),$$

where ω is angular frequency and M is mass per unit area. The rest of the program is the same as the program described in Chapter 6.

The average absorption value was calculated by using the equation (Reference 9),

$$\bar{\alpha} = \frac{\sum \alpha_i S_i}{S} \qquad (9.6),$$

where $\bar{\alpha}$ = average interior absorption coefficient

α_i = absorption coefficient of seat, trim, etc.

S_i = Area of treatment for seat, trim, etc.

S = Total area.

These values were then used in a program to calculate the interior spectrum and the overall values. This program was written in Time Series Language (TSL™) in PDP 11/40 at Cessna Aircraft Company and in Fortran at the KU-FRL. The driver routine in Fortran is given in Appendix F. The actual program used for the analysis was in TSL. These routines are similar to the integration routines described in Chapter 10. A listing of those routines is given in Appendix F.

9.3 CALCULATIONS

The interior noise control treatment was designed for cruise condition of 35000 ft/0.8 M. The input temperature and pressure corresponded to the standard atmospheric conditions at this altitude. The output from the monocoque shell program is given in Table 9.5. The transmission loss, due to the existing treatment at the time of initial measurement was calculated using multilayer program. The treatment consisted of fiberglass layer for thermal insulation and a thin trim material. The results are shown in Table 9.6. Next, a set of treatments was selected. These are shown in

Table 9.5: Transmission Loss, Untreated Fuselage

Frequency (Hz)	Transmission Loss (dB)
90	5.7
100	7.9
150	11.2
200	13.3
300	16.6
400	18.8
500	20.6
600	22.0
700	23.3
800	23.8
900	20.5
1000	25.5
1500	29.6
3000	35.5
4400	38.8

Table 9.6: Transmission Loss of Initial Treatment

Frequency (Hz)	Additional Transmission Loss (dB)
90	10.7
100	9.7
150	8.0
200	5.0
300	-7.7
400	8.8
500	14.5
600	17.8
700	20.1
800	21.9
900	23.6
1000	25.6
1500	32.6
3000	49.3
4400	57.8

Tables 9.1-9.4 for the four areas considered. For each treatment the multilayer program was run. The input data for this program were the untreated transmission loss values and the properties of the treatment materials. The input details for the treatments were the same as described in Chapter 6; i.e., surface density for trim panel and septum and the resistivity, porosity, density and depth for fiberglass insulation. Because porosity and resistivity of the fiberglass being used was unknown, the values of PF105 material were used. The same values were used in the noise level prediction programs described in References 23 and 24. The results of one such run are given in Table 9.7. These results were obtained for each treatment. Additional transmission loss values were calculated by subtracting the transmission value of the existing treatment and multiplying the resulting values by 0.5.

The average absorption coefficient was calculated using Equation (9.6). The absorption areas considered were divider, ceiling (or head liner), sidewall above the armrest, sidewall below the armrest, and seats. The values of absorption coefficient for these areas were found either from unpublished data at Cessna and the KU-FRL, from manufacturers' data or from experimental values published in Reference 23. The absorption areas were calculated from the drawings of aircraft. Table 9.8 gives the average calculated absorption coefficient as a function of frequency. The total area of the interior was estimated to be 320 sq ft. The details of the calculation are available in Reference 52.

Table 9.7: Typical Output Data from Multilayer Program

Frequency (Hz)	Additional Transmission Loss (dB)
90	15.0
100	12.5
150	-8.6
200	14.3
300	24.8
400	29.2
500	31.5
600	33.1
700	34.9
800	37.8
900	43.5
1000	43.8
1500	55.0
3000	74.9
4400	85.4

Table 9.8: Average Absorpiton Coefficients

Frequency (Hz)	Average Absorption Coefficient
125	.13
250	.20
500	.36
1000	.45
2000	.51
2500	.50
3000	.54
4000	.57

Both additional transmission loss and absorption values were input into the third program, to obtain the expected levels. A typical output is shown in Figure 9.4. These results are summarized in Tables 9.1-9.4. Also shown in Tables 9.1-9.4 are the expected values with a new absorption material. This material was one-inch sound foam with perforated vinyl. The vinyl was 12 mil thick. For calculation purposes this was assumed to be applied on most of the exposed areas. For each of these treatments, the weight penalty was calculated by multiplying the surface density of the treatment and multiplying the area of treatment. Then the results are plotted for four regions, as shown in Figure 9.5.

The four regions considered in this analysis were arbitrary. There were no dividers between regions 1, 2, and 3. There was a divider between regions 3 and 4 which could be closed. The levels in one of the regions would therefore determine the levels in the rest of the cabin. Hence for optimum results, the treatments should be so selected as to yield nearly the same interior levels. These treatment selections were termed "treatment strategies." For a given weight penalty one treatment strategy could be selected. One such strategy drawn for 130 lbs is given in Figure 9.6. Several such strategies, each corresponding to one given weight, were drawn up.

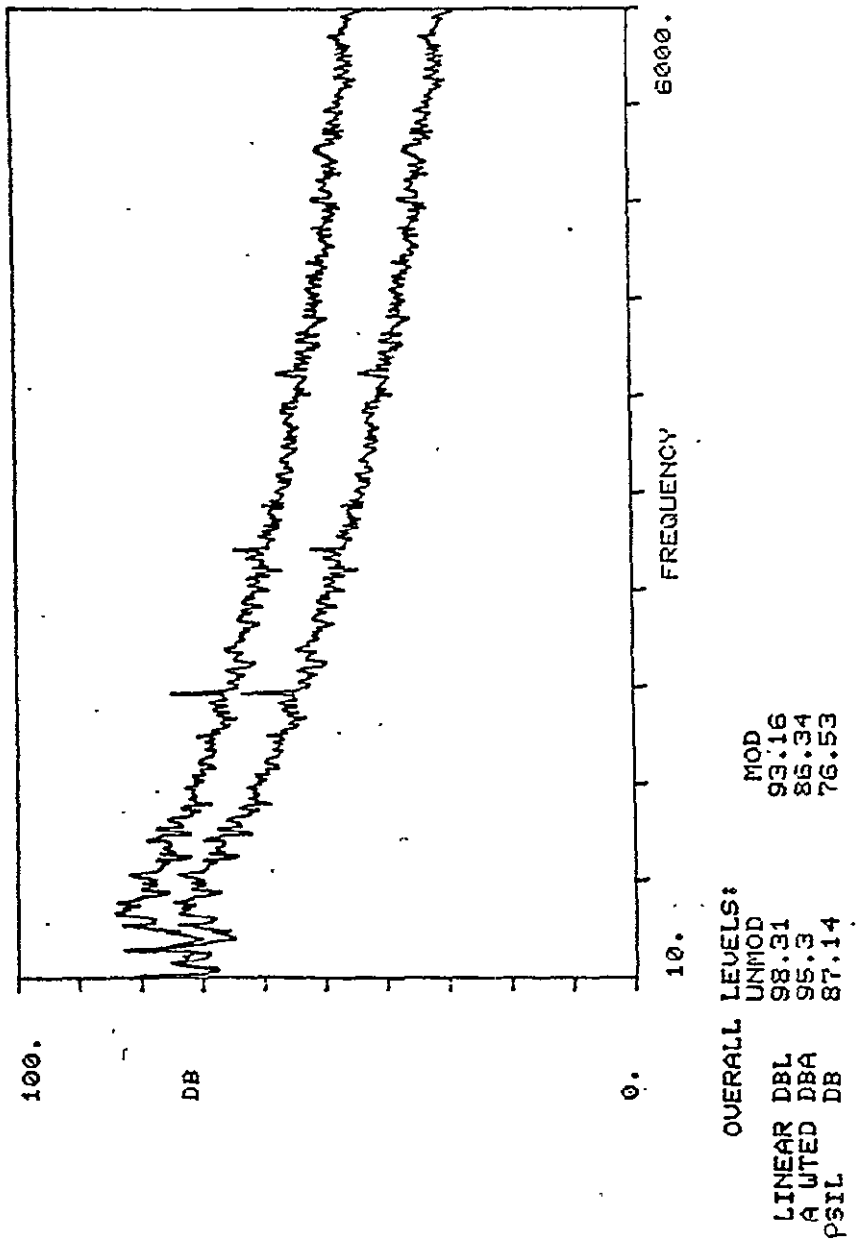

Figure 9.4: A Typical Predicted Interior Noise Spectrum

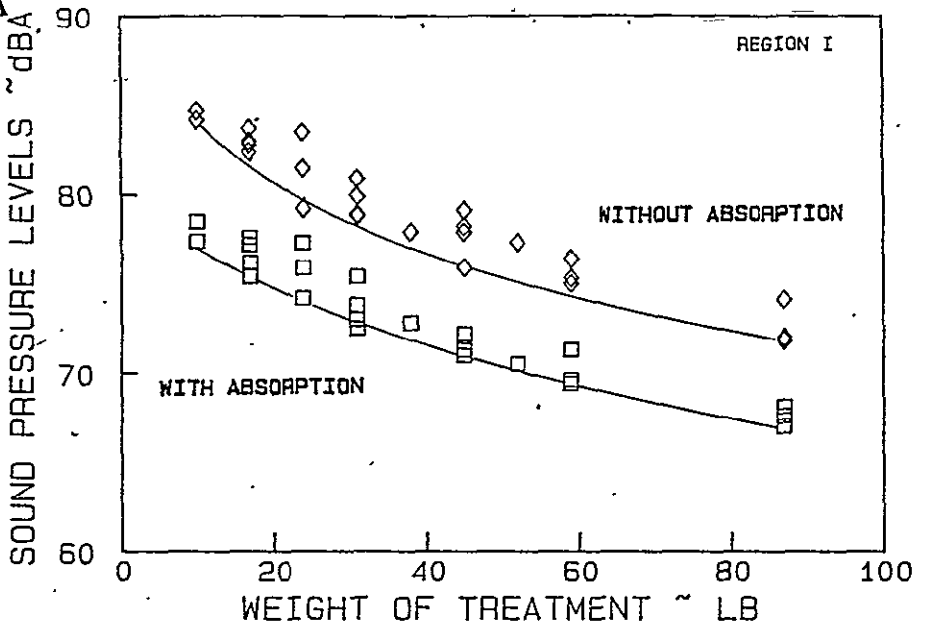

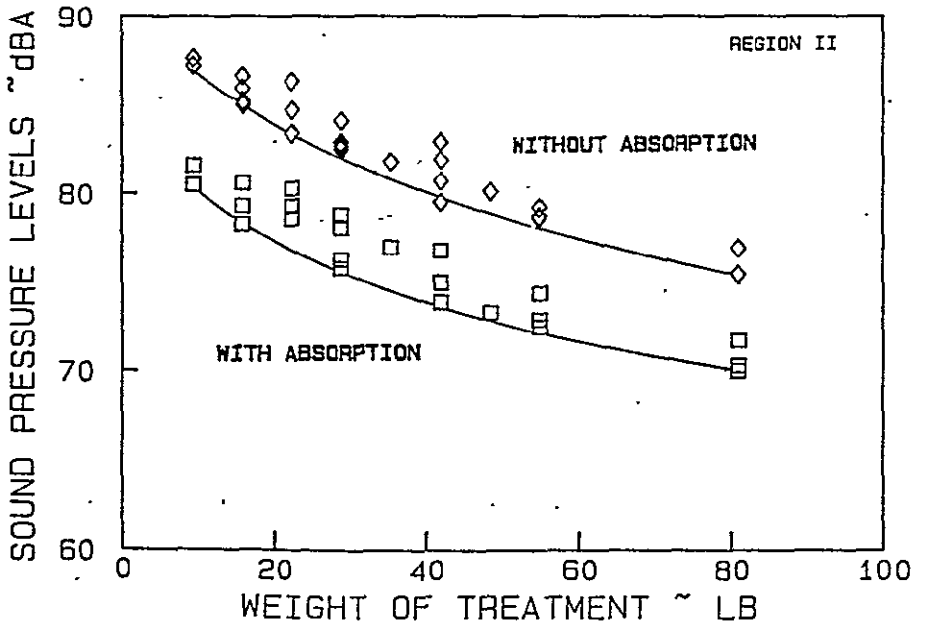

Figure 9.5: The Effect of Weight of Treatment on the Predicted Interior Level

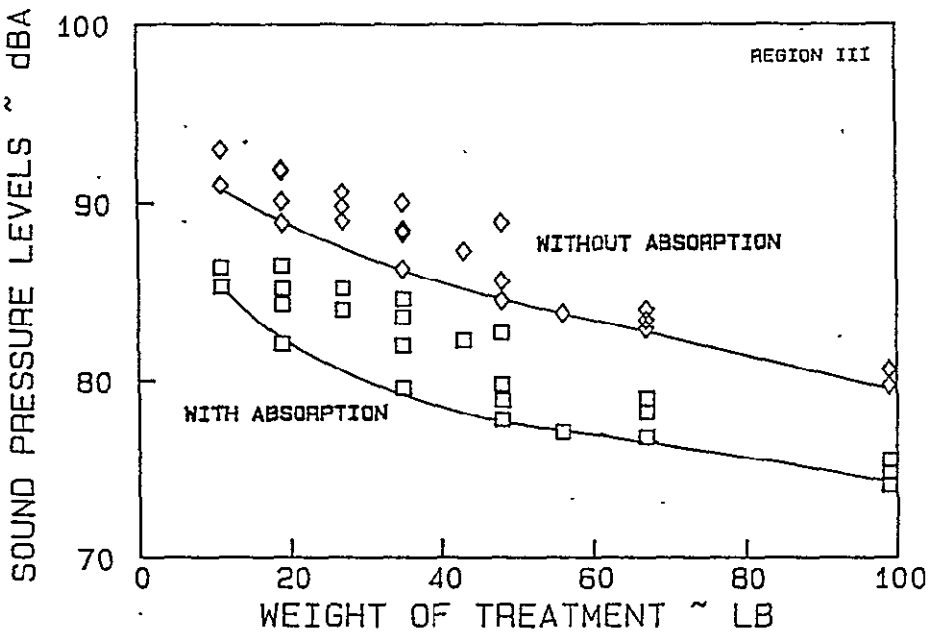

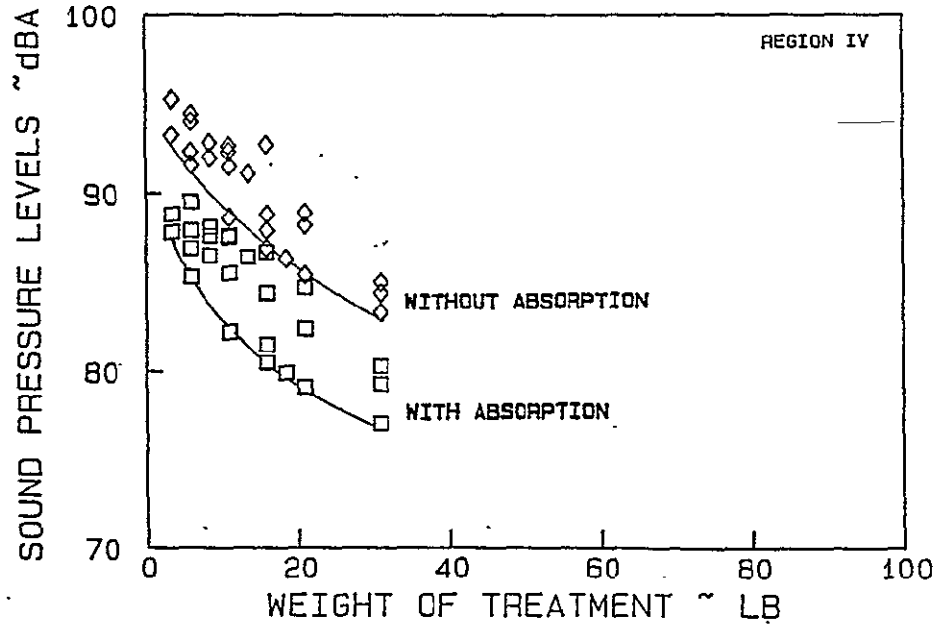

Figure 9.5: (continued)

9.4 DISCUSSION OF RESULTS AND COMPARISON WITH ACTUAL DATA

From the results shown in Tables 9.1-9.4, it was seen that equally dividing the total leaded vinyl and placing them next to the skin and trim offered at least theoretically optimum results. This was because the trim panel used was nearly as heavy as the 0.032 inch aluminum skin. Also it was seen that treatments with three inches of fiberglass material were better than treatments with two inch fiberglass material of the same weight density. Even with these treatments increased absorption tended to reduce dBA and three-octave band averages. This is significant because the two quantities indicate the energy above 500 Hz still contributes significantly to the overall interior levels.

Out of all these treatments, as an initial attempt, a treatment with 113 lb weight penalty was chosen. No special absorption material was installed. Figure 9.6 shows the selected treatment strategy. The treated aircraft was flown at 35000 ft, and the interior noise levels were measured by Cessna acoustic personnel at the same four locations. Figure 9.6 shows the levels at the four locations.

Table 9.8 compares the overall measured values with the predicted values. The predicted dBA values with the absorption material was 80 dBA throughout the cabin. As can be seen from Table 9.8, the predicted and expected values agree very well indicating

AREA	DESCRIPTION OF TREATMENT	LEVEL (DBA) a*	LEVEL (DBA) b*	WT (LB)
I	3 " FIBERGLASS & 20 OZ/SQ YD LEADED VINYL	84.7	78.5	10
II	20 OZ/SQ YD LEADED VINYL + 3" FIBERGLASS + 20 OZ/SQ YD LEADED VINYL	85.2	78.3	16
III	40 OZ/SQ YD LEADED VINYL + 3" FIBERGLASS +40 OZ/SQ YD LEADED VINYL	86.3	79.6	35
IV	80 OZ/SQ YD LEADED VINYL + 3" FIBERGLASS +80 OZ/SQ YD LEADED VINYL	85.4	79.1	21
AFT PR BULKHEAD	SAME AS REGION IV	-	-	31.5

a* WIHTOUT ABSORPTION
b* WITH ABSORPTION

WEIGHT OF ABSORPTIVE MATERIAL 16

TOTAL WEIGHT 129.5

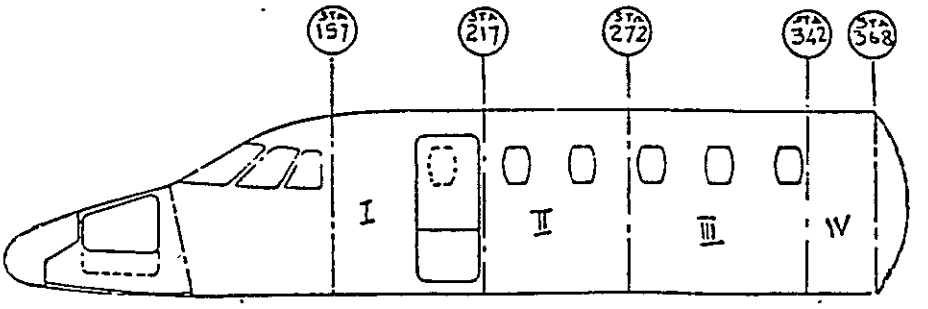

Figure 9.6: A Typical Treatment Strategy

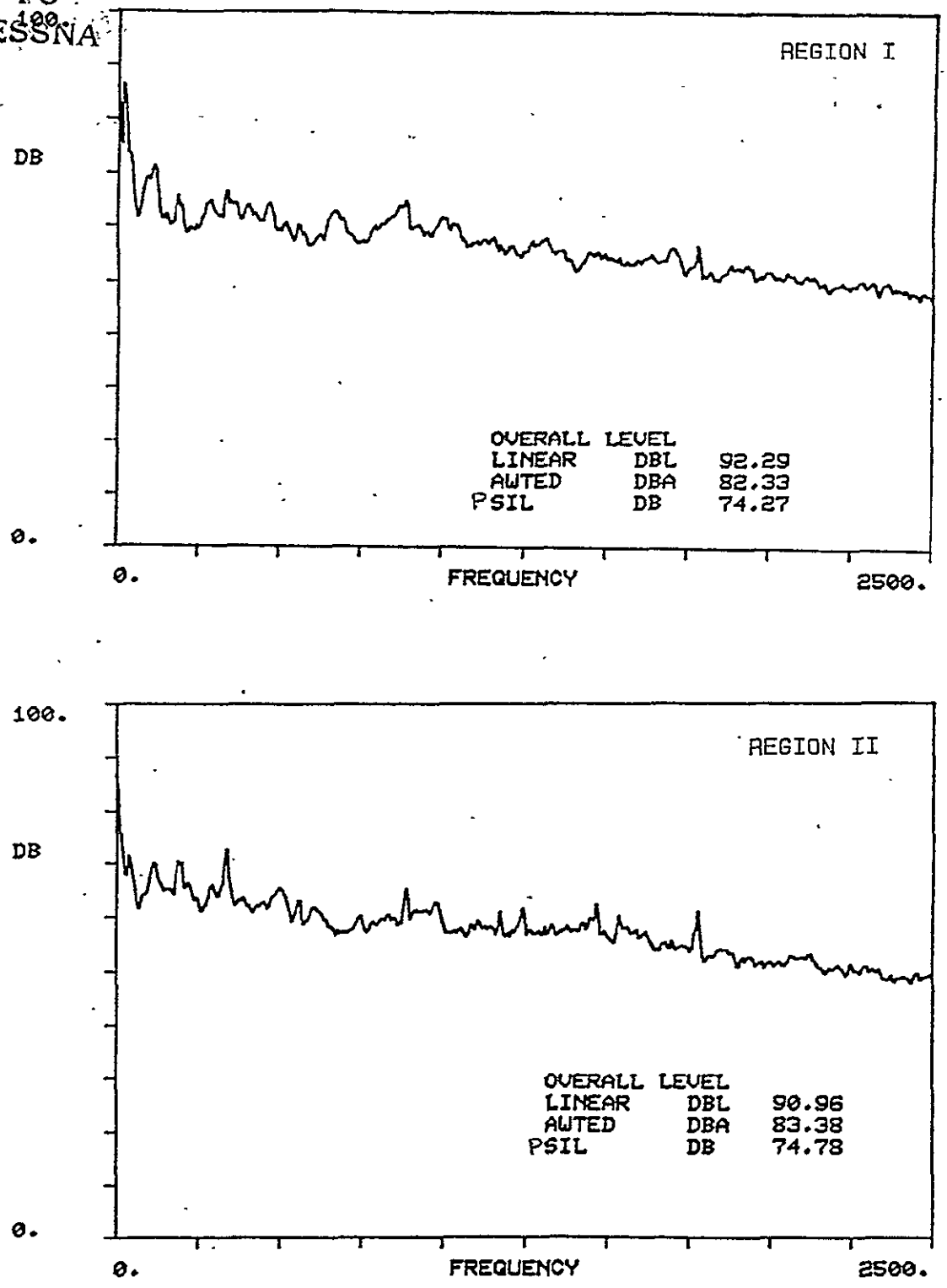

Figure 9.7: Measured Interior Noise Levels after Treatment

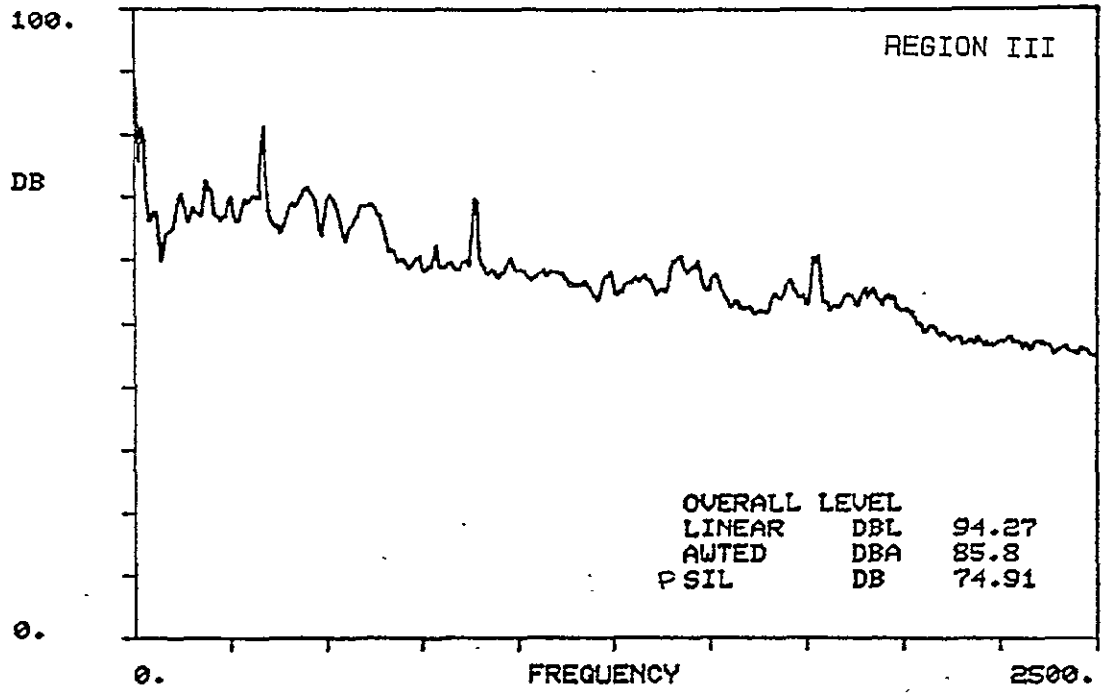

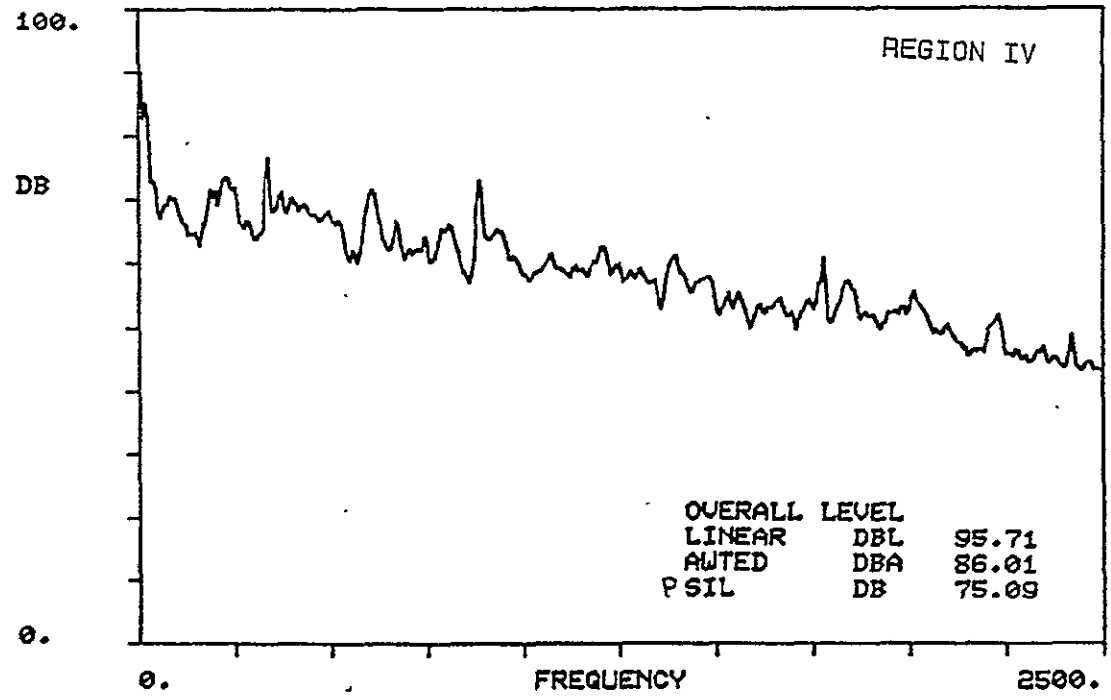

Figure 9.7: (continued)

Table 9.9: Comparison between Measured and Predicted Interior Noise Levels

Sound Pressure Levels (dBA)

Region	Predicted Values		Measured Values	
	Without Absorption	With Absorption	35000 ft	41000 ft
I	84.7	78.5	82.3	82.8
II	85.2	78.3	83.4	83.7
III	86.3	79.6	85.8	83.7
IV	85.4	79.1	86.0	85.9

Remark:

During tests, the aircraft did not have 16 lbs of absorptive material.

most of the assumptions made were reasonable. This design procedure can serve as a starting point for the control of interior noise in a new aircraft.

This agreement should be viewed with caution. It is possible that the agreement is good because the total expected reductions were only of the order of seven to ten dB. The author feels that if the initial choice of treatment weight had been large, say 200 lb, the agreement would have been poor. The reason for this is the initial assumptions. With such a heavy treatment the contribution of the sound radiated from the sidewall would have become small compared to that from other sources such as transmission through windows, internally produced sound (i.e., air-conditioning ducts, etc.). Hence these sources would determine the interior sound levels. In this treatment design no attempt had been made to account for these sources. This was confirmed by the engineers at Cessna Aircraft Company. The method suggested in this chapter offers a good initial design procedure.

CHAPTER 10

COMPUTER PROGRAM TO TROUBLESHOOT HIGH INTERIOR NOISE LEVELS

10.1 INTRODUCTION

All aircraft of the same type receive similar acoustic treatment. But it is not uncommon to find some aircraft to have higher interior noise levels than others in the same batch. In such cases, conventional noise prediction analysis may not be of any use. Such problems are normally solved by additional acoustic treatments. This additional treatment is determined by trial and error. From general aviation manufacturers it was learned that there existed no systematic way of approaching such problems.

In this chapter a computer program, developed to aid the aircraft noise control engineer in diagnosing and treating the high interior noise problem, is described. The program identifies whether the noise increase is due to discrete tones or to general increase over a band of frequencies. The program can then be used to study theoretically the effect of additional treatment on the specturm. Finally, the effect of the treatment on the overall linear, A-weighted and speech interference levels is calculated. In the subsequent sections, the details of the program, including the equations used, and typical outputs are discussed.

10.2 COMPUTER PROGRAM

The computer program was written in Time Series Language (TSL™) of Gren Rad Corporation. The reasons that dictated this choice of language are 1) it is fast and easy to operate, 2) it is an interactive language, 3) it has extensive graphics capabilities, and 4) it is specifically designed for time series application. TSL was available on PDP-11/40 system operating on RT-11 operating system with 4014 type Tektronix graphics terminal, at Cessna Aircraft Company. Also, the interior noise levels of the aircraft at Cessna Aircraft Company were analyzed on this system and the input data were available in a format compatible with TSL.

The listing of this program is given in Appendix F. It is divided into four parts:

1. Read input data and set up for further processing.
2. Problem identification:
    a. Effect of varying a discrete tone level
    b. Effect of varying the level over a band of frequency.
3. Treatment:
    a. Effect of adding mass
    b. Effect of increasing stiffness
    c. Effect of the use of double wall
    d. Effect of increasing internal absorption
    e. Effect of adding fiberglass insulation

f. Effect of adding any treatment whose additional transmission loss is known as a function of frequency.

4. Output:

a. Calculation of overall linear level

b. Calculation of overall A-weighted level .

c. Calculation of speech interference level

d. Display of interior noise spectrum with and without treatment.

This program has considerable flexibility built into it. For example, the effect of more than one treatment can be studied at a time. The program is interactive, user friendly, and menu driven. The flow chart of the program logic is given in Figure 10.1. Each treatment is covered in one subroutine in the program. These treatments are discussed below.

10.2.1 EFFECT OF A DISCRETE TONE

The effect of varying the level of one or many discrete tones by a specified amount on the overall levels can be studied using the subroutine called SPFREQ. This routine can be used for studying the effects of structure-borne noise or the effects of engine or propeller blade passage harmonics. By comparing the discrete tone levels with the average for the type of the aircraft, one can find whether the increase is due to discrete tones. The first part of this routine calls the routine PEAK, which prints the frequency

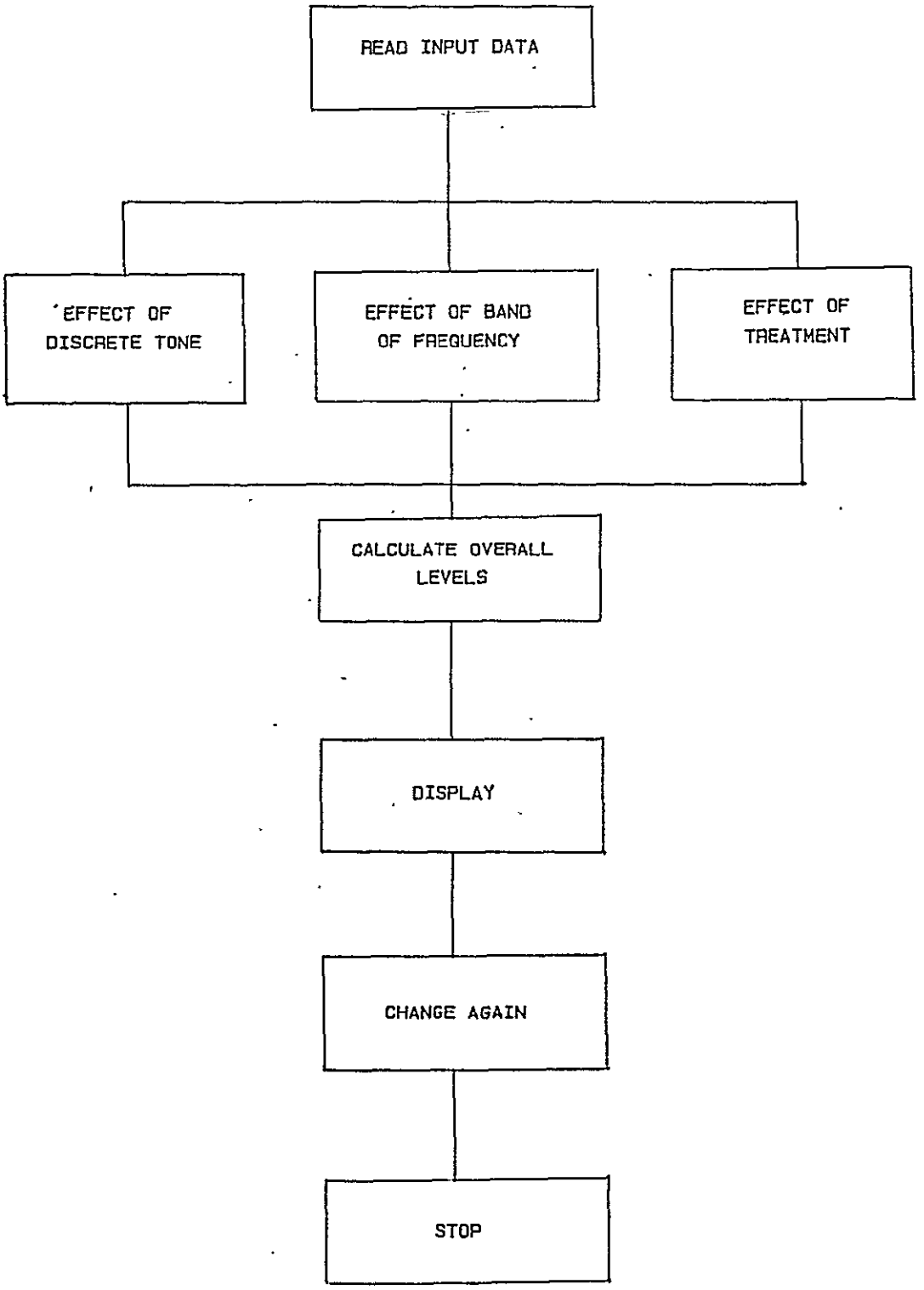

Figure 10.1: Flow Chart of the Program

values of all discrete tones and the maximum sound pressure levels at these frequencies. This permits easy identification of whether the discrete tones are high. The next part of the subroutine changes the value at a given frequency. The user can arbitrarily set the values of these discrete tones to any level (for example, levels found in other aircraft) and can calculate overall levels. If any peaks are changed, the adjacent values are also printed so that spectral leakage, if any, can be accounted for. The user has to change the value at each frequency.

10.2.2 EFFECT OF A BAND OF FREQUENCY

In some high interior noise problems, the increase in noise level is over a band of frequency: for example, increased air conditioning duct noise results in higher noise levels at 200-500 Hz. In such cases it is useful to study the contribution of a part of the interior noise spectrum on the overall noise levels. This will permit the user to concentrate only on the significant part of the spectrum during the design of the acoustic treatment. A subroutine, BNFREQ, is included. This routine changes the value of the sound pressure levels over a frequency range specified by the user. These values can either be changed by a constant value or set to a constant value. After modification, integration routines can be used to check the effect of this variation on the overall interior level.

10.2.3 EFFECT OF ADDITIONAL MASS

In normal practice, the increased transmission loss is achieved by mass loading the treatment. This is done by inserting leaded vinyl sheets (of surface density 10 oz/sq yd) between the skin and trim panel. The effect of addition of the leaded vinyl sheets can be studied using the subroutine called MASLAW. This subroutine uses classical mass law to predict the increased transmission loss at different frequencies. The following asusmptions are made in the equation (Reference 47) used in this routine:

1. Stiffness effects are neglected.
2. The entire transmission loss is assumed to follow classical-law theory.
3. The angle of incidence is normal.
4. Atmospheric conditions (speed of sound and density of air) are assumed to be the same across the panel.

From the interior noise spectrum, the effect of the transmission loss due to the existing treatment is subtracted and the effect due to combined (existing and additional) surface density is added. Under the assumptions the additional sound transmission loss at any frequency is given by (derived from Reference 47, page 297)

$$\Delta TL = 10 \log \left[\left\{1 + \left(\frac{\omega(m_1 + \Delta m)}{2\rho c}\right)^2\right\} / \left\{1 + \left(\frac{\omega m_1}{2\rho c}\right)^2\right\}\right] \quad (10.1),$$

where ΔTL = Increased transmission loss due to additional treatment (dB)

ω = Circular frequency

m = Average mass per unit area (existing; Kg/m^2)

Δm = Mass per unit area of additional treatment (Kg/m^2)

ρc = Impedance of air

ρ = Density of air (Kg/m^3)

c = Speed of sound (m/sec)

This increased transmission loss is subtracted from the measured interior noise spectrum at each frequency to obtain modified interior noise spectrum.

10.2.4 EFFECT OF ADDITIONAL STIFFNESS

The stiffness of a sidewall or window is an important parameter in the control of low-frequency noise (Reference 4). In the stiffness-controlled region the sound transmission loss can be increased by increasing the stiffness of the panel. For example, such a treatment may be recommended when it is suspected that the increased interior noise is due to the higher sound transmission through windows. In such cases window panes may be thickened, which would mean an increased stiffness as well as mass. A subroutine named STLAW is included in the program; this subroutine calculated the effect of this additional stiffness and mass on the interior noise spectrum. The following assumptions were used in deriving the equations used in subroutine STLAW:

1. Only single degree of freedom model is used.
2. Angle of incidence is normal.

3. Atmospheric conditions are the same across the panel.

The single degree of freedom model was chosen because of the limitations of TSL in handling variables and the requirement of speedy results. Also required will be a knowledge of the fundamental resonance frequency and damping ratio of the panel before and after change and other atmospheric conditions. Under the above assumptions, the increased sound transmission loss across a panel or window is given by (Reference 27, Equations 8 and 10)

$$\Delta TL = 20 \log \left| \frac{2\rho c + Zp_2}{2\rho c + Zp_1} \right| \qquad (10.2),$$

where ΔTL = Increased transmission loss due to additional stiffness

ω = Circular frequency (rad/sec)

ρ = Impedance of air

c = Density of air

Zp = Impedance of panel.

Subscript "$_1$" denotes the value before change, and subscript "$_2$" the value after change. The impedance of the panel or window is calculated using single degree of freedom model

$$Zp = 2\zeta\omega_n m + j\omega m\left(1 - \left(\frac{\omega_n}{\omega}\right)^2\right) \qquad (10.3),$$

where σ = Damping ratio

ω = Circular frequency (rad/sec)

m = Mass per unit area

ω_n = Natural frequency (rad/sec)

$j = \sqrt{-1}$.

The increased transmission loss values are then subtracted from the measured interior noise spectrum at each frequency to obtain the expected interior noise spectrum.

10.2.5 THE EFFECT OF THE USE OF DOUBLE WALL

Double-wall structures are sometimes used to obtain increased high-frequency sound transmission loss. However, at low frequencies the use of a double wall does not have any effect. The program contains an option where a double-wall structure can be used in place of a single-wall structure. For the purpose of calculation, it would be assumed that the data available is with a single-layer sidewall. Also, for simplicity it is assumed that the added wall has the same surface density as the existing skin. This can easily be changed if required. This can also be used to study the change in the interior noise levels, as the spacing between the walls is varied. The following assumptions are made in the calculations using this subroutine (DUBWAL):

1. The sidewall before treatment is a single wall layer.
2. The additional wall has the same surface density as the skin.
3. Only mass loss effects are considered.
4. It is assumed that the atmospheric conditions do not change between two sides of the wall.

Under these conditions the increased sound transmission loss of a double wall over the existing single wall can be derived from equations given in Reference 47 (page 312), as

$$\Delta TL = 10 \log\left[1 + \frac{\omega m_s \cos^2\phi}{\rho c}\left\{\cos\left(\frac{\omega d \cos\phi}{c}\right) - \frac{1}{2}\cos\phi \frac{\omega m_s}{\rho c} \sin\frac{\omega d \cos\phi}{c}\right\}^2\right] -$$

$$- 10 \log\left[1 + \left(\frac{\omega m_s \cos\phi}{2\rho c}\right)^2\right] \qquad (10.4),$$

where ΔTL = Increased transmission loss due to the double wall over the existing single wall

ω = Circular frequency

ϕ = Angle of incidence is set to normal by statement 250 of Subroutine DUBWAL. For any other incidence the cosine of the angle should be in R3.

m_s = Mass per unit area of the skin

ρc = Impedance of air

ρ = Speed of sound between walls

d = Spacing between walls.

The increased transmission loss values calculated using Equation (10.4) is then subtracted from the measured interior noise spectrum at each frequency to obtain the expected interior noise spectrum after treatment.

10.2.6 EFFECT OF INCREASED ABSORPTION

The increase in internal absorption will decrease the reflected energy of the sound waves from the sidewall, thereby decreasing the interior noise levels. The increased absorption will be useful if the cabin is made of highly reflective hard surfaces. Included is Subroutine ABS, which would calculate the additional noise reduction due to increased absorption is included. No detailed calculations are included within the program. Approximate knowledge of pretreatment absorption values is needed to use this subroutine. Three different absorption-vs-frequency tables are available. The first is based on experimental results published in Reference 23. The second and third use the absorption coefficients for noise control materials published in Reference 48. Practice shows that these values are very optimistic. Once one of these options is selected, the increased noise reduction is calculated from

$$\Delta NR = -10 \log \left| \frac{s\bar{\alpha}_u}{s\bar{\alpha}_t} \right| \qquad (10.5),$$

where ΔNR = Additional frequency at frequency f.

s = Average surface area of treatment assumed to be the same before and after treatment

$\bar{\alpha}_u$ = Average untreated absorption coefficient at frequency f

$\bar{\alpha}_t$ = Average treated absorption coefficient at frequency f.

The additional noise reduction due to increased absorption is then subtracted from the measured interior noise spectrum to obtain the expected interior noise spectrum. The absorption coefficients are

stored in ABSLO.TAB and ABSHI.TAB. These tables of absorption vs frequency can be modified to include known values of new absorption materials.

10.2.7 EFFECT OF ADDITIONAL FIBERGLASS INSULATION

The mechanism of sound transmission through fiberglass insulation is different from that through simple sound barrier material. Reference 9 discusses the mechanism of sound transmission through insulation material. Chapter 5 discusses the experimental effect of fiberglass insulation observed. The propagation of sound through the material results in two types of losses: 1) the reactive losses associated with the imaginary part of the propagation constant, and b) the resistive losses associated with the viscous losses in the material. The effects of these two losses are discussed in Chapter 6 and are taken into account in the computer program discussed in that chapter. However, as can be seen, the calculated transmission loss values are seldom realized in practice. Because of this, in the subroutine TTL2, which calculates the effect of fiberglass insulation, only the resistive losses are included. This greatly simplifies calculation because it does not account for the reactive losses. The resistive losses due to added fiberglass are calculated by (Reference 9)

$$\Delta TL = \alpha d \qquad (10.6),$$

where α = Real part of the propatation constant;

d = Thickness of the fiberglass layer.

The resistive part of the propagation constant is a complex function of

frequency, porosity, resistivity and other material properties. Reference 47 (page 270) gives the values of typical materials used in the aircraft industry. (These values are still used, as can be seen in Reference 23). At present, three options are available for users. The first option is a curve containing the values as published in Reference 47, Figure 2.22, for the pf105 type fiberglass. The other two are slightly modified versions of the first option, to have higher losses at lower frequencies and lower losses at higher frequencies. These two α-vs-frequency curves can be replaced by known α-vs-frequency curves of any other fiberglass material.

10.2.8 EFFECT OF KNOWN TREATMENT

In addition to the above treatments, a separate subroutine, TTLI, is included, where a user can input known increased transmission loss values as a function of frequency. This table can be obtained from a more sophisticated analysis which is not possible using TSL. This subroutine will prompt the user for a table of frequency vs additional transmission loss. This subroutine calculates transmission loss values at intermediate frequencies by linear interpolation. The subroutine then simply subtracts this value from the interior noise specturm at each frequency value.

10.2.9 CALCULATIONS OF OVERALL LEVELS

The linear overall levels of both modified and unmodified spectra are calculated using the energy sum method:

$$OSPL = 10 \log \sum_{i=1}^{N} (10 \frac{(SPL_i)}{10}) \qquad (10.7),$$

where OSPL = Overall sound pressure level

SPL_i = Sound pressure level of filter i

N = Number of filters.

A-weighting of sound levels is performed electronically in sound level meters to approximate the loudness level sensitivity of the human ear when listening to pure tones (References 9, 39 and 49).

Reference 39 (Table 4.1) gives in a tabular form the electrical weighting network responses at various frequencies. In this computer program, a curve was fitted through these points and this approximate equation:

$$\Delta SPL = -.8345\ f^4 + 10.07\ f^3 - 55.73\ f^2 + 160.7\ f - 184.8 \qquad (10.8).$$

This curve does not deviate from the values of Reference 49 by more than 0.05 dB. The comparison with sound level meter readings indicates this equation is invalid within 0.1 dB overall. At each frequency this response is added to the interior levels. Once again the overall levels are calculated using Equation 10.7.

The speech interference level is a simplified method of quantifying noise in terms of its interfering effect on speech communication (Reference 49). The speed interference level is calculated from the

arithmatic average of the sound pressure levels of 500, 1000, 2000 and 4000 Hz octave bands. These values should be used in conjunction with Table SIL-I in Reference 49 to indicate conversing distance over which speed is satisfactorily intelligible (corresponding to an articulation index of 0.4). When only the octave bands at 500, 1000, and 2000 Hz are used, the level obtained is called the "preferred speech interference level" (PSIL). Because normal narrow band analyzers are constant bandwidth analyzers and not proportional bandwidth analyzers, a routine was written to calculate octave band levels. Obviously, the input data should have values of at least up to the higher band edge of 4000 Hz for calculating SIL. However, the general aviation interior noise is low-frequency dominant. Hence the normal analysis is done only up to 5000 Hz. Therefore, this program uses preferred speech interference levels.

Finally, depending upon the user input, either the modified spectruum, the unmodified spectrum or both the spectra are output graphically using TSL XDISPL subroutines. The overall values are also indicated within the display area.

10.3 USE OF THE PROGRAM

This program needs less than 64 K memory. To use this program, the interior noise levels of the noisy aircraft should be measured and recorded on tape. To use this program in TSL, this recording should be analyzed using TSL and output in TSL format using BLKOUT command. This program is loaded from TSL STANDBY mode (>) by typing

```
LOAD 'MSYNTH.RN'
```

```
LOAD 'BLKIN'

LOAD 'XDISPL'
```

The program is executed by typing

```
SYNTH 'DEV:FILNAM.EXT'
```

where DEV:FILNAM.EXT is the data file containing narrow band data. Thereafter the options are presented to the user as a series of menus. A typical output is shown in Figure 10.2. A case study where this program was used, is discussed in Appendix F.2.

10.4 CONCLUSIONS

This program serves as a basis for the noise control engineer to study the effect of various treatments on the interior noise levels. This program is very general and hence can be used for any aircraft noise problem. For the same reason it cannot identify the exact cause of any particular problem but can indicate what each treatment can do.

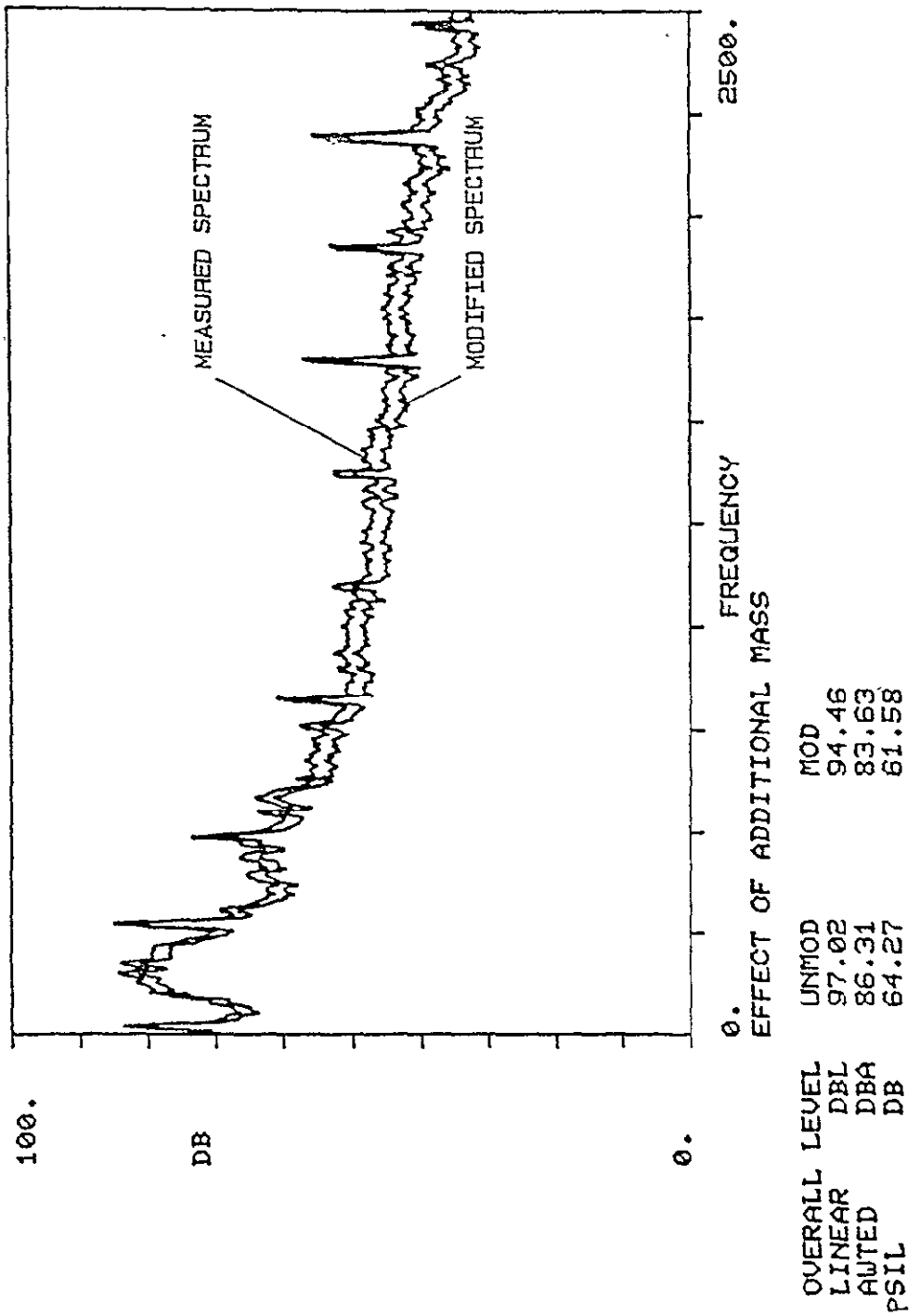

Figure 10.2: A Sample Output

CHAPTER 11

CONCLUSIONS AND RECOMMENDATIONS

The significant conclusions and recommendations resulting from this research project are summarized in the following two subsections. Additional insight into a particular area may be gained by referring to the appropriate section of the report. Overall, all of the objectives and projected technology contributions established in Section 2.1 were generally satisfied. The conclusions are presented in Section 11.1, while Section 11.2 contains the recommendations.

11.1 CONCLUSIONS

1. The broad-based approach proposed in this research--i.e., laboratory experimental investigation of sound transmission and vibration characteristics of panels, use of new data analysis techniques, and application on actual aircraft--provides a sound method to solve a complex problem such as the general aviation aircraft noise problem. The new data analysis techniques such as acoustic intensity and cepstral methods provide additional information not easily available previously to the noise control engineer.
2. The results of the experimental investigation of flat and stiffened panels with damping materials confirm that in the low-frequency region--i.e., at frequencies below the

fundamental resonance frequency--stiffness alone is the dominant parameter. In this frequency region the curvature, stiffeners, and depressurization have more effect than the type and the amount of damping material. The effect of damping material, as expected, is high only at the resonance frequency. The effect on the overall noise reduction is quite small. However, the damping tape increases noise reduction slightly while the pressurization tends to decrease the noise reduction in this region.

3. The installation effects were identified as the most important parameters on the loss factor measurements. A panel installed in the KU-FRL acoustic test facility exhibits significantly different loss factors than a free-free panel throughout the frequency region. The effect of the damping material on loss factor, was to increase it by an order of magnitude. Since loss factors are needed in the theoretical predictions, both loss factor tests and noise reduction tests should be done successively, without removing the panel, for best results.

4. Double-wall panels exhibit significantly higher noise reduction than single-wall panels in the high frequency region. However, in the low-frequency region their efficacy is low. The stiffness of skin or trim alone controls the low-frequency noise reduction. The effects of various parameters such as skin, trim panel (material and density), panel depth, and fiberglass, insulation that affect the noise reduction

characteristics of a double wall are presented. These results can serve as an aid to noise control engineers in the general aviation industry.

5. The classical sound transmission loss model for a multilayer panel is an adequate approximation to analyze the noise reduction characteristics of double-wall panels tested at this facility. This computer program helps in explaining and understanding the effects of various parameters that affect sound transmission through such panels.

6. The acoustic intensity method developed for panels at the KU-FRL acoustic test facility should serve as a valuable tool in studying the sound radiation characteristics of panels installed in the acoustic test facility. This method will be useful to study the effects of stiffeners and damping materials. This type of investigation should allow closer tailoring of treatment to obtain the highest reduction for minimum weight penalty.

7. The cepstral method promises to be an effective method to determine the absorption characteristics of trim materials. This method has not yet been fully developed. Once further tests are performed to finalize the test procedure, this method can be a valuable tool in choosing the interior trim material in the general aviation industry.

8. The application of multilayer program to actual interior noise control design confirms the trends of the noise reduction

characteristics observed at the KU-FRL acoustic test facility. It also proves that with a slight user's judgement, this model can be profitably used by the industry, as a starting point for the control of interior noise in a new aircraft.

9. The computer program developed to study the effects of treatments uses the results of classical sound transmission loss theory and results from the KU-FRL test facility. This program presents in one single program the ability to analyze the problem and study the effectiveness of noise control treatments. The engineers at Cessna Aircraft Company confirm the usefulness of such programs in noise control.

11.2 RECOMMENDATIONS

1. Starting with flat, bare aluminum panel at the beginning of this project, the complexity of the test specimen has been gradually increased to include parts of real aircraft. The noise reduction characteristics of these panels are available for use by engineers in the general aviation industry. Even with the difference in panel sizes, it is anticipated that the trends observed will still be valid.
2. The design procedure for interior noise control used in this report uses classical monocoque transmission loss program (Reference 51). However, the recommended input will be the measured (bare fuselage) transmission loss across fuselage

sections. This will increase the accuracy in prediction. Because of the cavity effect and the random errors, a number of tests need to be done to determine the transmission loss of untreated fuselages.

3. The computer program developed for the analysis of interior noise problems is recommended for use as is. Because of the approximations, at times the absolute values may not be meaningful. This program should be used to study the trends.

4. Future tests in determining noise reduction characteristics should include the effect of large panel size of the real aircraft. The size of panels will affect low-frequency noise reduction. Hence it is recommended that a systematic study similar to the one for panel type structures be undertaken with these large structures.

5. The noise reduction characteristics of trim panels indicate very wide variations in their sound transmission characteristics. The parameters include the construction details of base material, trim material, and other material properties. It is recommended that the trim panels used in the industry be studied to determine the optimum trim panel configuration from the point of view of their acoustical characteristics.

6. The tests with the cepstral techniques show great promise. It is recommended that the development of this method be

continued. The finalized test procedure should be easy and less time consuming for routine use in the industry.

7. It is recommended that the acoustic intensity technique be used to study the sound radiation pattern of stiffened panels and treatments. The results of this investigation should be useful in designing treatments with low weight penalty.

8. Finally, it is recommended that the design procedure used in this report be improved to include the analysis of very low frequency region. This will be necessary for its use in propeller-driven aircraft.

REFERENCES

1. Catherines, J. J., and Mayes, W. H., "Interior Noise Levels of Two Propeller-Driven Light Aircraft," NASA TM-X-72716, July 1975.

2. Gasaway, D. C., "Cockpit Noise Within Trainer Aircraft," SAM-TR-70-95, December 1970.

3. Peschier, T. D., "General Aviation Interior Noise Study," Doctor of Engineering Project Report, University of Kansas, August 1977.

4. Grosveld, F., "Study of Typical Parameters That Affect Sound Transmission through General Aviation Aircraft Structures," Doctor of Engineering Dissertation, University of Kansas, August 1980.

5. Navaneethan, R., "Study of Noise Reduction Characteristics of Multilayered Panels and Dual Pane Windows with Helmholtz Resonators," MS Thesis, University of Kansas, Lawrence, Kansas 66045, May 1981.

6. Laméris, J., Stevenson, S., Streeter, B., "Study of Noise Reduction Characteristics of Composite Fiber-Reinforced Panels, Interior Panel Configurations, and the Application of Tuned Damper Concept," KU-FRL-417-18, Flight Research Laboratory, University of Kansas Center for Research, Inc., Lawrence, KS, March 1982.

7. Navaneethan, R., Streeter, B., Koontz, S., "Influence of Depressurization and Damping Material on the Noise Reduction

Characteristics of Flat and Curved Stiffened Panels," KU-FRL-417-17, Flight Research Laboratory, University of Kansas Center for Reserch, Inc., October 1981.

8. Koval, L. R., "Effect of Air Flow, Panel Curvature, and Internal Pressurization on Field-Incidence Transmission Loss," Journal of Acoustic Society of America, Vol. 59, No. 6, June 1978.

9. Beranek, L. L., Noise and Vibration Control, McGraw-Hill Publications, New York, 1971.

10. Mead, Danys J., "Prediction of the Structural Damping of a Vibrating Stiffened Plate," Damping Effects in Aerospace Structures, AGARD CP 277.

11. Paz, Mario, Structural Dynamics, Van Nostrand Reinhold Company, 1980.

12. Hunt, J., "Damping Characteristics of General Aviation Aircraft Panels," MS Project Report, August 1982.

13. Blevins, R. D., Formulas for Natural Frequency and Mode Shape, Van Nostran Reinhold Company, 1979.

14. Plunkett, R., "Measurement of Damping," Section Five, Structural Damping, Ed. by Jerome E. Ruzicka, The American Society of Mechanical Engineers, Shock and Vibration Committee, 1959.

15. Heckl, M., "Measurements of Absorption Coefficients on Plates," Journal of Acoustic Society of America, Vol. 34, No. 6, June 1962.

16. Ungar, E. E., and Carbonell, J. R., "On Panel Vibration Damping Due to Structural Joints," AIAA Journal, Vol. 4, No. 8, August 1966.

17. Crandall, S. H., "The Role of Damping in Vibrtion Theory," Journal of Sound and Vibration, Vol 11, No. 1, 1970.

18. Adams, R. D., and Bacon, D. G. C., "The Dynamic Properties of Unidirectional Fibre Reinforced Composites in Fluxure and Torsion," Journal of Composite Materials, Vol. 7, January 1973.

19. Adams, et al., "Three Dynamic Properties of Unidirectional Carbon and Glass Fiber Reinforced Plastics in Torsion and Flexure," Journal of Composite Materials, Vol. 3, October 1969.

20. Henderson, T. D., "Design of an Acoustic Panel Test Facility," KU-FRL-317-3, Flight Research Laboratory, University of Kansas Center for Research, Inc., Lawrence, KS, August 1977.

21. Grosveld, F., and van Aken, J., "Investigation of the Characteristics of an Acoustic Panel Test Facility," KU-FRL-317-9, Flight Research Laboratory, University of Kansas Center for Research, Inc., Lawrence, KS, September 1978.

22. Navaneethan, R., Quayle, B., Stevenson, S., Graham, M., "Study of Noise Reduction Characteristics of Double-Wall Panels," KU-FRL-417-21, Flight Research Laboratory, University of Kansas Center for Research, Inc., Lawrence, KS, May 1983.

23. Rennison, D. C., et al., "Interior Noise Control Prediction Study for High-Speed Propeller Driven Aircraft," NASA CR 159200, NASA, September 1979.

24. Revell, J. D., Balina, F. J., and Koval, L. R., "Analytical Study of Interior Noise Control by Fuselage Design Techniques on High-Speed Propeller Driven Aircraft," NASA CR 159222, July 1978.

25. Cockburn, J. A., and Jolly, A. C., "Structural-Acoustic Response, Noise Transmission Losses and Interior Noise Levels of an Aircraft Fuselage Excited by Random Pressure Fields," AFFDL-TR-68-2, 1968.

26. Beranek, L. L., and Work, G. A., "Sound Transmission through Multiple Structures Containing Flexible Blankets," Journal of Acoustic Society of America, Vol. 21, pages 419-428, 1949.

27. Barton, C. K., "Structural Stiffening as an Interior Noise Control Technique for Light Twin Engine Aircraft," PhD Thesis, N.C. State University, Raleigh, N.C., 1979.

28. Navaneethan, R., "User's Guide to Multilayer Sound Transmission Loss Program," KU-FRL-417-20, Flight Research Laboratory, University of Kansas Center for Research, Inc., Lawrence, KS, January 1983.

29. Pierce, A. D., Acoustics: An Introduction to Its Physical Principles and Applications, McGraw-Hill Book Company, New York, 1981.

30. Chung, J. Y., "Cross-Spectral Method of Measuring Acoustical Intensity," GMR-2617, General Motors Research Laboratories, Warren, Michigan, December 1977.

31. Gade, S., "Sound Intensity (Theory)," B&K Technical Review No. 3, B&K Instruments, Inc., Massachusetts, 1982.

32. Papoulis, A., Probability, Random Variables, and Stochastic Processes, McGraw-Hill Book Company, New York, 1965.

33. Seybert, A. F., "Source Characterization Using Acoustic Intensity Measurements," Proceedings of Inter-Noise-80, Miami, Florida, Decmeber 1980.

34. Crocker, M. D., Tyrrell, R. J., and North, M. P., "The Application of Acoustic Intensity to Engine Noise Reduction, Proceedings of International Congress on Recent Development in Acoustic Intensity Measurement," Senlis, France, October 1981.

35. Bendant, J. S., and Piersol, A. G., Engineering Application of Correlation and Spectral Analysis, John Wiley and Sons, 1980.

36. Anon., "Instruction Manual for Model 660B Dual-Channel FFT Analyzer," Nicolet Scientific Corporation, N.J., 1981.

37. Navaneethan, R., and Quayle, B., "Measurement of Transmission Loss Characteristics Using Acoustic Intensity Techniques at the KU-FRL Acoustic Test Facility," KU-FRL-417-22, Flight Research Laboratory, University of Kansas Center for Research, Inc., Lawrence, KS, December 1983.

38. Walpole, R. E., and Myers, R. H., Probability and Statistics for Engineers and Scientists, Macmillan Co., New York, 1972.

39. Harris, C. M., Handbook of Noise Control, Chapter 21, McGraw-Hill Book Company, New York, 1979.

40. Hassab, J. C., and Boucher, R., "Analysis of Signal Extraction, Echo Detection and Removal by Complex Cepstrum in Presence of Distortion and Noise," Journal of Sound and Vibration, 40(3), 321-335, 1975.

41. Randall, R. B., and Hee, J., "Cepstrum Analysis," B&K Technical Review, Vol. 3, B&K Instruments Company, Marlborough, Massachusetts, 1981.

42. Bolton, J. S., and Gold, E., "The Application of Cepstral Techniques to the Measurement of Transfer Function and Acoustical Reflection Coefficients," Journal of Sound and Vibration, 93(2), 217-233, 1984.

43. Bolton, J. S., and Gold, E., "The Determinatin of Acoustical Reflections Coefficients Using Cepstral Techniques: Measurements of Polyurethene Foam," to be published.

44. Childers, D. C., Skinner, D. P., and Kemerait, R. C., "The Cepstrum: A Guide to Processing," Proceedings of the IEEE, Vol. 65, No. 10, October 1977.

45. Otnes and Enochson, Applied Time Series Analysis, John Wiley and Sons, New York, 1978.

46. Barry, T. M., "Measurement of the Absorption Spectrum Using Correlation/Spectral Density Techniques," Journal of Acoustic Society of America, Vol. 55, No. 6, June 1974.

47. Beranek, L. L., Noise Reduction, McGraw-Hill, New York, 1960.

48. Anon., "Specifications for Noise Control Materials," Anti-Phon, Inc.

49. Pearsons, K. S., and Bennet, R. L., "Hand Book of Noise Ratings," NASA CR 23767, NASA, Washington, April 1974.

50. Bloomfield, P., Fourier Analysis of Time Series: An Introduction, John Wiley and Sons, New York, 1976.

51. Navaneethan, R., Hunt, J., and Quayle, B., "Study of Damping Characteristics of General Aviation Aircraft Panels and Develoment of Computer Programs to Calculate the Effectiveness of Interior Noise Control Treatment," KU-FRL-417-19, Flight Research Laboratory, University of Kansas Center for Research, Inc., December 1982.

52. Koval, L. R., "On Sound Transmission Loss in a Thin Cylindrical shell Uncer Flight Conditions," Journal of Sound and Vibration, 48(2), 265-275, 1976.

53. Navaneethan, R., "650 Sound Treatment Analysis Data," unpublished data, Cessna Aircraft Company.

APPENDIX A

DETAIL AND CHARACTERISTICS OF THE KU-FRL ACOUSTIC TEST FACILITY

The design and construction details of the KU-FRL acoustic test facility have been described in Reference 20. Reference 21 describes the investigation carried out to determine the characteristics of the test facility. Salient features from these reports are presented below.

A.1 DESIGN AND CONSTRUCTION DETAILS

The test facility consists of two chambers: the source chamber and the receiver chamber. The test panel is mounted between these two chambers. The source chamber--consisting of a massive brick wall, a concrete collar, and a steel box--contains nine evenly spaced loudspeakers. This chamber can be considered to be a speaker box. Its purpose is to support the speakers and to prevent sound radiation to the rear and sides. It contains sound absorbing materials to minimize standing waves. These waves can induce undesirable speaker-sound radiation characteristics. A small distance, about one inch, separates the test panel from the front side of the speaker baffle. This arrangement prevents standing waves between the baffle and the test panel at frequencies in the range of interest, 20-5000 Hz. Other standing waves, parallel to the panel and the speaker baffle, could disturb the desired uniformity of excitation at the panel surface. The strength of

these waves, however, is reduced by sound absorbing material, which nearly fills all the space between the baffle and the test panel. The receiving chamber is an acoustic termination, which absorbs almost all the sound energy. To facilitate the installation of test specimens between this termination and the speaker box, the receiving chamber is mounted on wheels and rests on a steel table. Figures A.1 and A.2 show the details.

The test specimen size is 20 inches by 20 inches. One inch along the edges is used to clamp the test specimen between the two chambers. This leaves an exposed area of 18 inches by 18 inches. This is the maximum size of the test specimen that can be tested at this facility.

The loudspeakers can be driven by an amplified signal from a pure tone generator, or a frequency sweep oscillator, a random noise generator, or a tape recording of in-flight boundary layer fluctuations (Figure A.3). An equalizer is included in the sound generation system to obtain a reasonably flat input spectrum. The noise measuring system includes two 1/4" or 1/2" B&K microphones, one on each side of the test panel. The output signals of the microphones are fed to a (narrow band) real-time analyzer. The resulting spectra are transferred to an H-8 microcomputer where they are stored on floppy disks. The data are then transferred to the KU-FRL MINC computer through the phone lines, where noise reduction curves are plotted using an HP 7225B plotter.

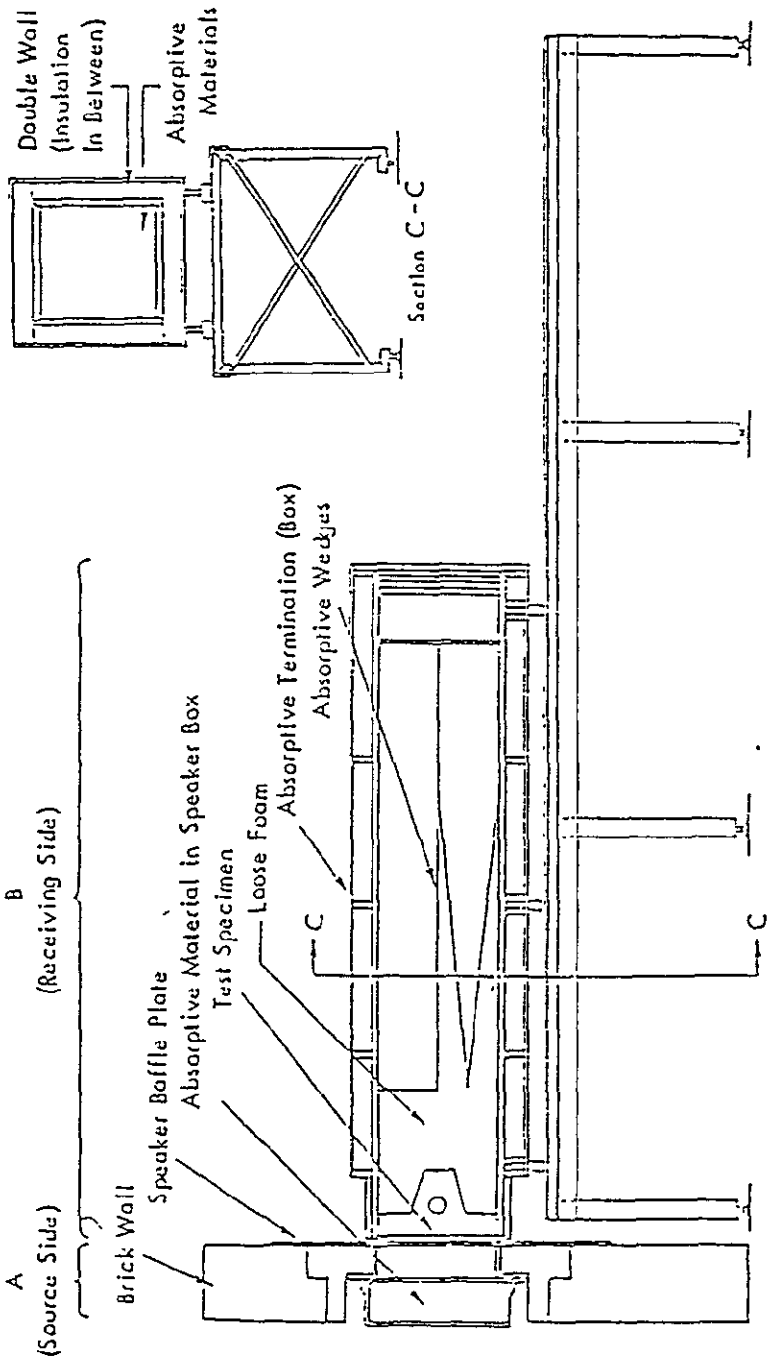

Figure A.1: KU-FRL Acoustic Test Facility

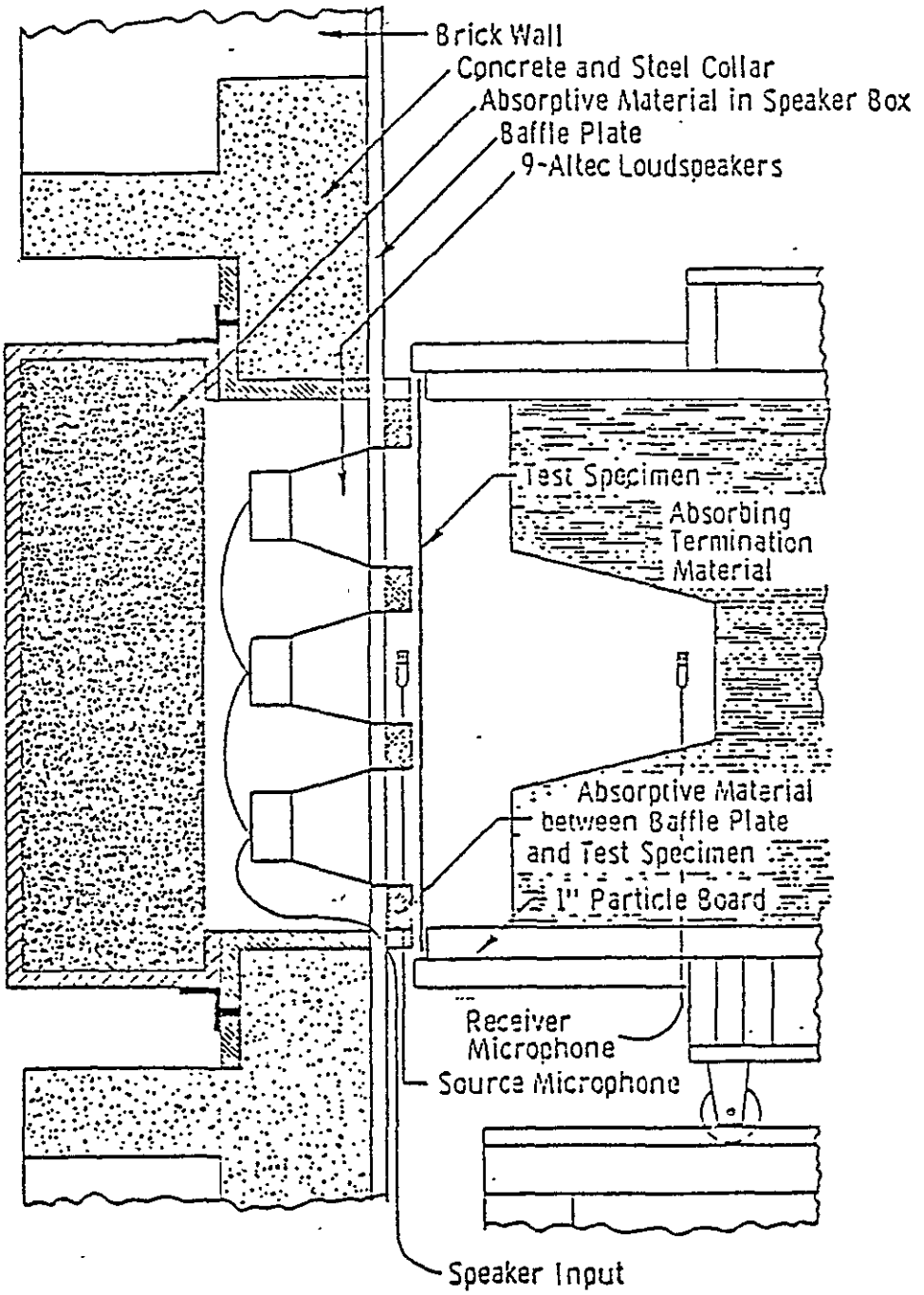

Figure A.2: KU-FRL Acoustic Test Facility, Placement of Test Specimen

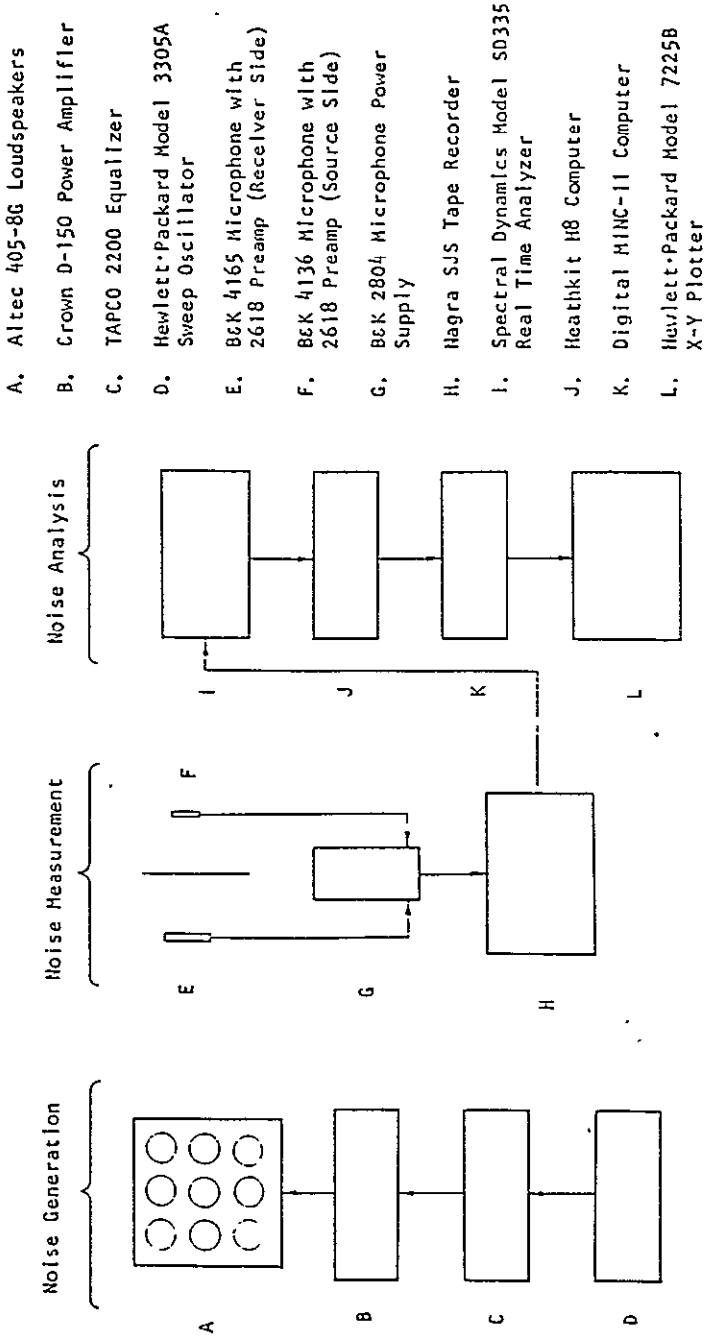

Figure A.3: General Arrangement of Electronic Equipment

The facility has a series of adaptors which are used to test the noise reduction characteristics at different angles of incidence. In addition a tension device is available which permits investigation under uniaxial or biaxial (tensile) stresses. To test the effect of pressurization on the sound transmission loss of a panel, a depressurization system has been installed. With this system the pressure in the source chamber can be reduced. At present all tests are being conducted at ambient temperature (68 to 72 degrees F).

A.2 CHARACTERISTICS OF THE TEST FACILITY

Several investigations were carried out to determine accurately the characteristics of this test facility. The results are described in References 3 and 4. Notable conclusions are given below.

1. At high frequencies using a standard panel, the slope of the noise reduction curve obtained corresponds to that predicted by mass law (i.e., 6 dB/octave). However, actual measured values exceed mass law values by 3-4 dB.
2. The plane wave approximation is justified only below a frequency of 800 Hz at short distances from the speaker baffle. However, this variation seems to have not much effect on the slope of the noise reduction curve. It is also justified over the entire frequency range tested (20 to 5000 Hz) if the distance from the source is at least 34 inches.

3. Although all the walls have been covered very carefully with high quality absorption material, standing waves have not been fully prevented.

4. In addition, the reflections from the sidewalls affect the signal measured by the receiver microphone. These reflections and the standing waves result in additional peaks and dips in the measured spectra, when narrow-band analysis is carried out.

5. The use of a sweep oscillator with a very slow sweep rate is a satisfactory substitute to measure sound transmission through aircraft structures.

6. Each of the nine speakers has its own frequency response characteistics.

7. The effect of the possible reflections off the back panel of the receiving chamber is so low that it is within the experimental scatter.

8. Removal of the back panel of the source chamber affects the results below 60 Hz.

9. The air in the closed cavity backing the test specimen acts as an additional stiffness, raising the fundamental panel resonance frequency. For a simple panel the analytical model gives an accurate account (within 5% accuracy) of this effect.

10. The edge conditions of the test panel are somewhere between simply supported and clamped, and this complicates

any comparison of measured and theoretical values in the low-frequency region. In the high-frequency region, presence of the cavity resonances and the sound absorption capability of the sound absorption materials complicate comparison of measured sound transmission with theoretical predictions. However, the results from the facility agree with the results from classical transmission loss theory when higher modes are neglected.

APPENDIX B

MULTILAYER SOUND TRANSMISSION LOSS PROGRMAM

B.1: FLOW CHART

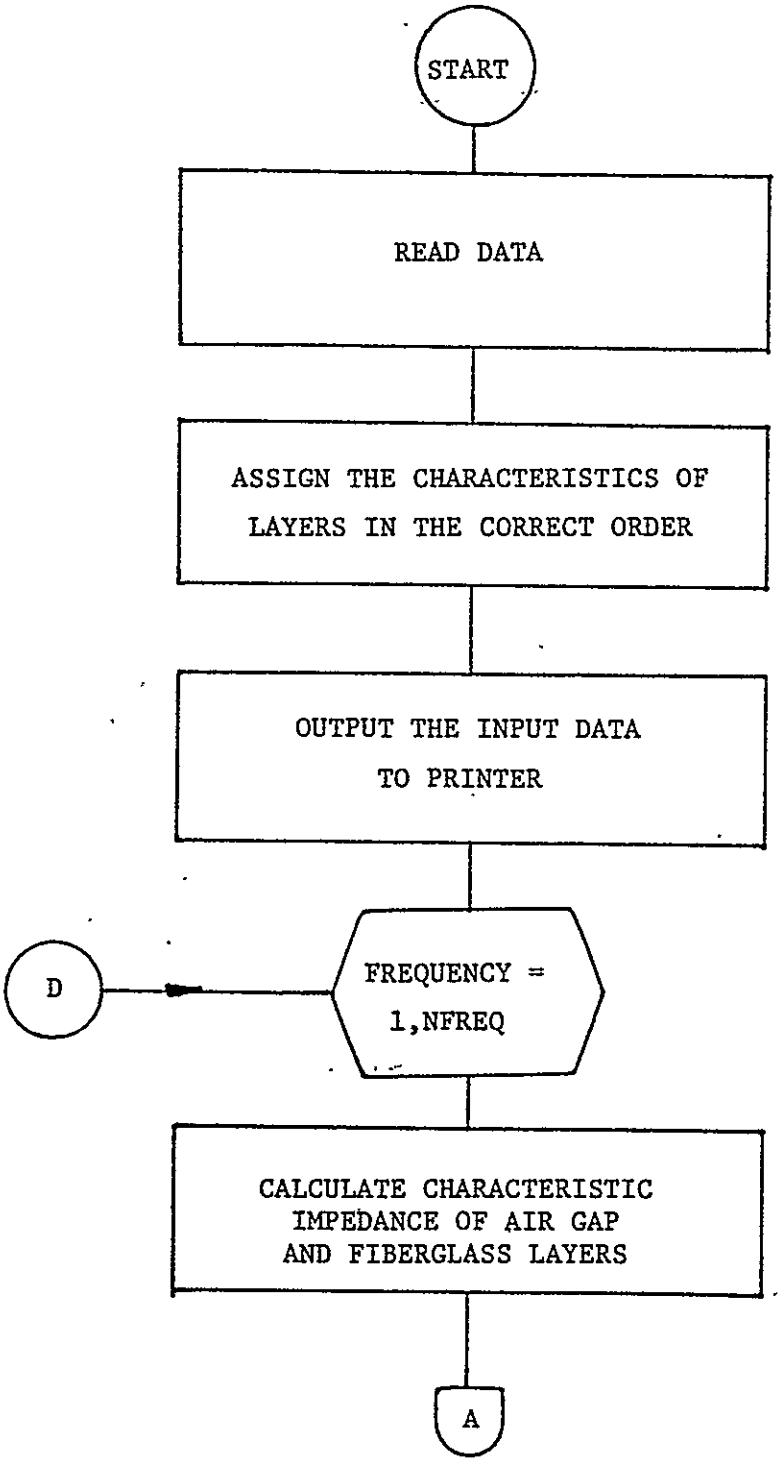

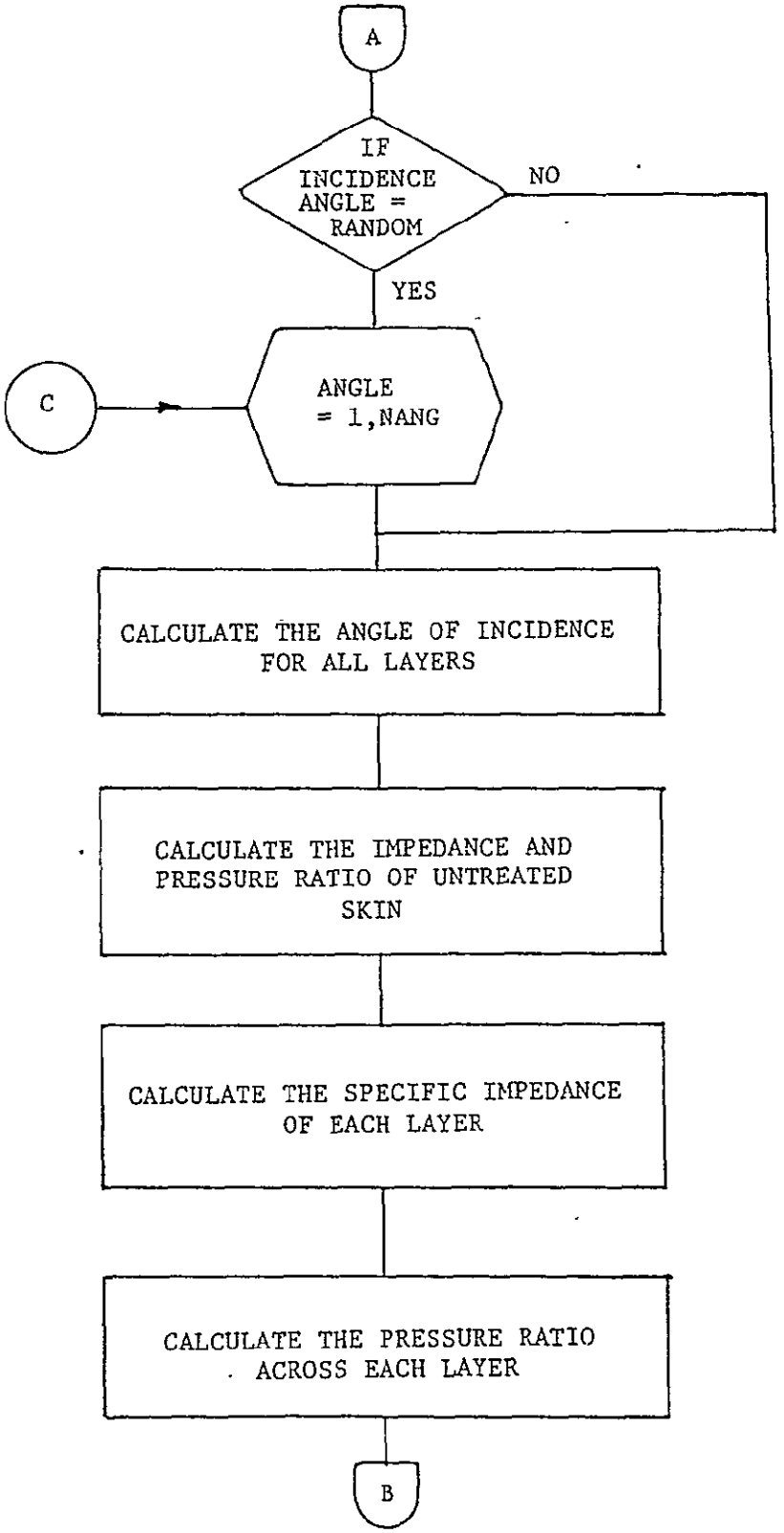

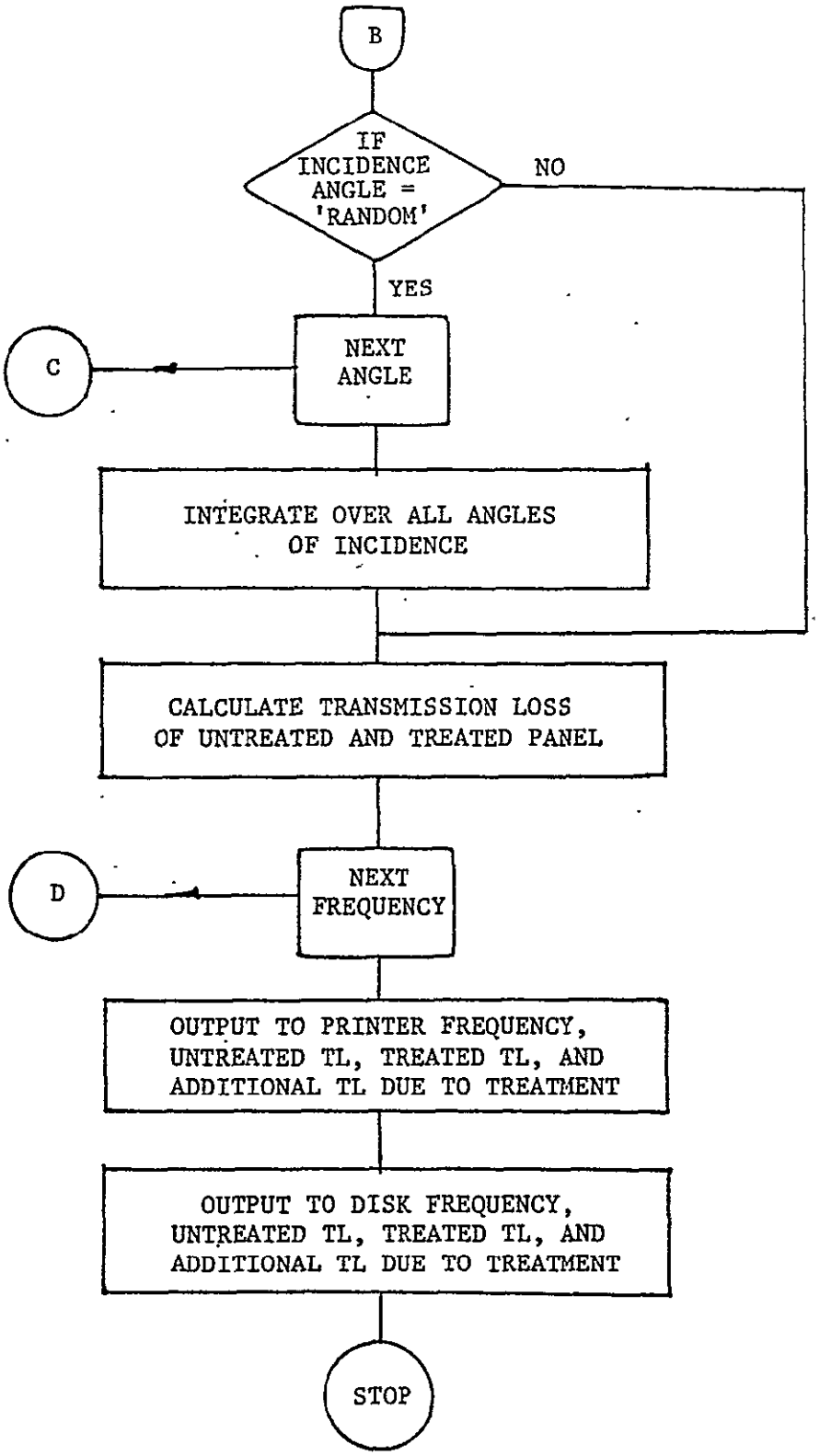
B
IF INCIDENCE ANGLE = 'RANDOM'
NO
YES
C
NEXT ANGLE
INTEGRATE OVER ALL ANGLES OF INCIDENCE
CALCULATE TRANSMISSION LOSS OF UNTREATED AND TREATED PANEL
D
NEXT FREQUENCY
OUTPUT TO PRINTER FREQUENCY, UNTREATED TL, TREATED TL, AND ADDITIONAL TL DUE TO TREATMENT
OUTPUT TO DISK FREQUENCY, UNTREATED TL, TREATED TL, AND ADDITIONAL TL DUE TO TREATMENT
STOP

B.2: LISTING OF PROGRAM

B.2.1: LISTING OF TLOSS

```
CCCCCCCCCCCCCCCCCCCCCCCCCCCCCCCCCCCCCCCCCCCCCCCCCCCCCCCCCCCCCCCCCCCCCCCCCCCCCC
C                                                                             C
C                                                                             C
C         PROGRAM TO CALCULATE THE TRANSMISSION LOSS ACROSS                   C
C                 MULTI-LAYERED AIRCRAFT SIDE-WALL                            C
C                                                                             C
C                                                                             C
CCCCCCCCCCCCCCCCCCCCCCCCCCCCCCCCCCCCCCCCCCCCCCCCCCCCCCCCCCCCCCCCCCCCCCCCCCCCCC
C
C
C#######       THIS PROGRAM CALCULATES THE TRANSMISSION LOSS OF
C#######       AIRCRAFT SIDE-WALL WITH NOISE CONTROL TREATMENTS.
C
C
C###################    VERSION     : 1              ###################
C###################    PROGRAMMER  : R.NAVANEETHAN  ###################
C###################    DATE        : 20-DEC-82      ###################
C
C
C#######
C
C         REFERENCES :
C                          1. WILBY ET AL,"INTERIOR NOISE CONTROL PREDICTION
C                             STUDY FOR A HIGH-SPEED PROPELLER DRIVEN
C                             AIRCRAFT", NASA CR 159200 SEPT 1979
C                          2. REVELL J.D. ET AL,"ANALYTICAL STUDY OF INTERIOR
C                             NOISE CONTROL BY FUSELAGE DESIGN TECHNIQUES ON
C                             HIGH-SPEED PROPELLER DRIVEN AIRCRAFT", NASA CR
C                             159222,1980.
C                          3. BERANEK L.L.,"NOISE AND VIBRATION CONTROL",
C                             MCGRAW-HILL,1971.
C
C#######
C
C         FOR FURTHER DETAILS OF THE EQUATIONS USED IN THE PROGRAM REFER
       KU-FRL REPORT KU-FRL-REP-417-19.
C
C#######
C         INPUT DATA :
C                       THE NAME OF THE DATA FILE NEEDS TO BE INPUT
C                       INTERACTIVELY.  SEE USER'S MANUAL FOR THE
C                       INPUT DATA AND FILE FORMAT
C
C        OUTPUT DATA :
C                       BOTH ON PRINTER AND DATA FILE (NAME TO BE
C                       SPECIFIED INTERACTIVELY
C
C        OTHER DETAILS:
```

```
C                     THE MAIN PROGRAM "TLOSS" IS ON THIS FILE
C                     NAMED 'MLAYER.FOR'.  THE SUBROUTINES ARE
C                     ARE AVAILABLE ON A FILE NAMED 'BLAYER.FOR'.
C                     THE FUNCTIONS NOT AVAILABLE IN THE SYSTEM
C                     LIBRARY OF MINC ARE GIVEN IN 'CLAYER.FOR'.
C                     TO EXECUTE COMPILE MLAYER,BLAYER,CLAYER AND
C                     LINK TO GET AN EXECUTABLE FILE 'MLAYER.SAV'.
C                     THIS HAS BEEN DONE. TO EXECUTE :
C                              1. PREPARE DATA FILE ACCORDING TO
C                                 USER'S MANUAL.
C                              2. TYPE 'RUN MLAYER <CR>'
C                              3. WHEN ASKED FOR,GIVE INPUT DATA
C                                 FILE AND OUTPUT DATA FILE.
C
C        FILE NAME FORMAT IN MINC :
C                     REFER RT-11 OPERATING MANUAL
C
C
      PROGRAM TLOSS
C
C#######   DIMENTION STATEMENTS
      DIMENSION L(10),THETA(10),THICK(10),SDENS(10),DENS(10),P(10)
      DIMENSION R(10),FREQ(27),ANG(23),PRESS(2),TEMP(2),THK(51)
      DIMENSION THIK(5),PT(5),RT(5),SDEN(10),DEN(5),C(10)
      DIMENSION TLT(27),TLA(27)
      REAL I01,I02,NU
      COMPLEX ZCAP(10),Z(10),B(10),X1(10),X2(10),PRATIO(10)
      COMPLEX RR,PIP(23),PIT(23),Z2UT,Z1UT,ZP,COSH,CC
      BYTE INAME(15),ONAME(15)
      COMMON/COM/TH,TH2,THETA,AMACH,PRESS,C
      COMMON/ONE1/H,RHO
      COMMON/ONE2/A1,EC1,I01,J1,A2,EC2,I02,J2,E1,G1,E2,G2
      COMMON/ONE3/ESK,NU,ETA,B1,B2,ICYL,A
      COMMON/ONE4/PAX,PCIR
      COMMON/ONE5/SKDEN,ETASK,FOSK
      COMMON/TWO/THICK
      COMMON/THREE/DENS,P,R
      COMMON/FIVE1/SDENS
      COMMON/FIVE2/ETATP,FOT,SLPFAC
      DATA INAME,ONAME/30*0/
C
C####### FREQUENCY VALUES AT WHICH TL IS CALCULATED.
C
      DATA FREQ/20.,40.,60.,80.,100.,125.,150.,175.,200.,225.,250.,300.,
     &400.,500.,600.,700.,800.,900.,1000.,1500.,2000.,2500.,3000.,
     &3500.,4000.,4500.,5000./
C
C####### ANGLES OF INCIDENCE USED IN THE RANDOM INCIDENCE INTEGRATION
```

```
C
      DATA ANG/0.,4.,8.,12.,16.,20.,24.,28.,32.,36.,40.,44.,48.,52.,
     &56.,60.,64.,68.,72.,76.,80.,84.,88./
      NFREQ=27
      NANG=23
      PI=3.141592654
C
C####### READ DATA FILE NAME
C
      TYPE*,' ENTER NAME OF THE INPUT FILE '
      ACCEPT 100,(INAME(I),I=1,14)
C
C####### READ OUTPUT FILE NAME
C
      TYPE*,' ENTER NAME OF THE OUTPUT FILE '
      ACCEPT 100,(ONAME(I),I=1,14)
 100  FORMAT(14A1)
C
C#######  OPEN INPUT DATA FILE, READ DATA AND CLOSE INPUT DATA FILE
C
      OPEN (UNIT=8,NAME=INAME,TYPE='OLD',FORM='FORMATTED')
C
C#######  READ AMBNT CONDITIONS AND INCIDENT ANGLES
C
      READ (8,105) PRESS(1),PRESS(2),TEMP(1),TEMP(2),AMACH
      READ (8,103) IA
      IF(IA.NE.1) GO TO 81
      READ (8,105) TH
      GO TO 83
81    IF(IA.NE.2) GO TO 1004
83    CONTINUE
C
C#######  READ NUMBER OF LAYERS OF TREATMENT AND TYPE OF LAYERS
C
      READ (8,103) N
      READ (8,103) NSKIN,NAIR,NFIBER,NSEPTA,NTRIM
103   FORMAT(5I5)
      IF((NSKIN+NAIR+NFIBER+NSEPTA+NTRIM).NE.N) GO TO 1000
C
C#######  READ TYPE OF IMPEDANCE MODEL FOR SKIN AND ETAILS OF SKIN
C#######  IF SKIN IS PRESENT
C
      READ (8,103) (L(I),I=1,N)
      IF(NSKIN.EQ.0) GO TO 1
      READ (8,103) ISKIN
      IF(ISKIN .NE. 1) GO TO 2
      READ (8,105) H,RHO
105   FORMAT(7F10.4)
```

```
      GO TO 1
2     CONTINUE
      IF(ISKIN.NE.2) GO TO 3
      READ (8,103)ICYL
      READ (8,105)A,H,RHO,NU,ETA,B1,B2,A1,EC1,IO1,J1,A2,EC2,IO2,J2,
      READ (8,107)ESK,E1,G1,E2,G2
107   FORMAT(5E10.2)
      GO TO 1
3     CONTINUE
      IF(ISKIN.NE.3) GO TO 19
      READ (8,105)H,R,NU,ETA,B1,B2,PAX,PCIR
      READ (8,107)ESK
      GO TO 1
19    CONTINUE
      IF(ISKIN.NE.4) GO TO 1001
      READ (8,105)SKDEN,ETASK,FOSK
1     CONTINUE
C
C#######  IF AIRGAP LAYERS ARE PRESENT READ THEIR THICKNESS
C
      IF(NAIR.EQ.0) GO TO 4
      READ (8,105) (THIK(I),I=1,NAIR)
4     CONTINUE
C
C#######  IF FIBERGLASS INSULATION LAYERS ARE PRESENT READ THEIR
C#######  CHARACTERISTICS
C
      IF(NFIBER.EQ.0) GO TO 5
      DO 611 I=1,NFIBER
      READ (8,105) DEN(I),RT(I),PT(I),THK(I)
611   CONTINUE
5     CONTINUE
C
C#######  IF SEPTA ARE PRESENT READ THEIR SURFACE DENSITIES
C
      IF(NSEPTA.EQ.0) GOTO 6
      READ(8,105)(SDEN(I),I=1,NSEPTA)
6     CONTINUE
C
C#######  IF TRIM IS PRESENT READ ITS IMPEDANCE MODEL AND
C#######  CHARACTERISTICS
C
      IF(NTRIM.EQ.0) GO TO 7
      READ(8,103) ITRIM
      IF(ITRIM.NE.1) GO TO 8
      READ(8,105) SURDEN
      GOTO 7
8     IF(ITRIM.NE.2) GO TO 1002
```

```
      READ(8,105)SURDEN,ETATP,FOT,SLPFAC
7     CONTINUE
C
C#######  END  READ STATEMENTS
C
C
C#######  CALCULATE SPEED OF SOUND AND AIR DENSITY (OUTSIDE AND INSIDE)
C
      DO 10 I=1,2
      C(I)=20.05*SQRT(273.+TEMP(I))
      RO(I)=.00348272*PRESS(I)/(TEMP(I)+273.)
10    CONTINUE
      RO(N+1)=RO(2)
      C(N+1)=C(2)
C
C#######  ASSIGN THE CHARACTERISTCS OF LAYERS IN THE CORRECT ORDER
C
      KAIR=1
      KFIBER=1
      KSEPTA=1
      KTRIM=1
      KSKIN=1
      DO 11 I=1,N
      IF(L(I).NE.1) GO TO 12
      THICK(I)=H
      KSKIN=KSKIN+1
      GO TO 11
12    IF(L(I).NE.2) GO TO 13
      THICK(I)=THIK(KAIR)
      KAIR=KAIR+1
      GO TO 11
13    IF(L(I).NE.3) GO TO 14
      DENS(I)=DEN(KFIBER)
      R(I)   =RT(KFIBER)
      P(I)   =PT(KFIBER)
      THICK(I)=THK(KFIBER)
      KFIBER=KFIBER+1
      SDENS(I)=DENS(I)*THICK(I)
      GO TO 11
14    IF(L(I).NE.4) GO TO 15
      SDENS(I)=SDEN(KSEPTA)
      KSEPTA=KSEPTA+1
      GO TO 11
15    SDENS(I)=SURDEN
      KTRIM=KTRIM+1
11    CONTINUE
      CLOSE(UNIT=8)
C
```

```
C#######  PRINT INPUT VALUES
C
      WRITE(6,200)
200   FORMAT(' ',/'                    INPUT DATA                    '//)
      WRITE(6,201)
201   FORMAT('          AMBIENT CONDITIONS  '/)
      WRITE (6,202)PRESS(1)
202   FORMAT('   OUTSIDE PRESSURE(PASCAL)  = ',F10.2)
      WRITE (6,203)TEMP(1)
203   FORMAT('   OUTSIDE TEMPERATURE(DEG C)= ',F10.2)
      WRITE (6,204)PRESS(2)
204   FORMAT('   INSIDE PRESSURE(PASCAL)   = ',F10.2)
      WRITE(6,205)TEMP(2)
205   FORMAT('   INSIDE TEMPERATURE(DEG C) = ',F10.2)
      WRITE(6,206) AMACH
206   FORMAT('   MACH NUMBER               = ',F10.2)
      IF(IA.EQ.2) GOTO 16
      WRITE(6,232)TH
232   FORMAT('   ANGLE OF INCIDENCE(DEG)   = ',F10.2)
      GO TO 17
16    WRITE(6,233)
233   FORMAT('   ANGLE OF INCIDENCE        = RANDOM')
17    CONTINUE
      DO 20 I=1,N
      IF(L(I).NE.1) GO TO 21
      WRITE(6,207)I
207   FORMAT(/'   LAYER # ',I2,' IS SKIN'/)
      WRITE (6,208) ISKIN
208   FORMAT('   IMPEDANCE MODEL FOR SKIN  = ',I1/)
      IF(ISKIN .NE. 1) GO TO 22
      WRITE (6,209) H,RHO
209   FORMAT('   THICKNESS OF SKIN(M)      = ',F8.4,/,'   DENSITY OF
     & SKIN(KG/CU M)  = ',F6.1)
      GO TO 20
22    CONTINUE
      IF(ISKIN.NE.2) GO TO 23
      WRITE(6,210)A,H,RHO,ETASK
      WRITE (6,211)
      WRITE (6,212)B1,A1,EC1,IO1,J1,E1,G1
      WRITE(6,213)
      WRITE (6,212)B2,A2,EC2,IO2,J2,E2,G2
210   FORMAT('   RADIUS OF THE PANEL(M)    = ',F8.4,/,'   THICKNESS OF
     &SKIN(M)      = ',F8.4,/,'   DENSITY OF SKIN(KG/CU M)  = ',F6.1,
     &/,'   YOUNG"S MOD OF S/M2) = ',E10.2)
211   FORMAT(/'   STRINGER (STIFFENER) CHARACTERISTICS')
213   FORMAT(/'   FRAME CHARACTERISTICS')
212   FORMAT('   SPACING(M)        = ',F8.3,/,'   X-SEC AREA(M2)    = '
     &,F8.3,/,'   ECCENTRICITY(M)   = ',F8.3,/,'   MOM OF INERTIA(M4)= '
```

```
     &,E8.2,/,'   TORSION CONST(M4) = ',E8.2,/,'   YOUNG"S MOD(N/M2) = '
     &,E8.2,/,'   SHEAR MOD(N/M2)   = ',E8.2/)
      GO TO 20
23    IF(ISKIN.NE.3)GOTO 82
      WRITE(6,215)H,RHO,B1,B2,PAX,PCIR
215   FORMAT('   THICKNESS OF SKIN(M)      = ',F8.4,/,'   DENSITY OF
     & SKIN(KG/CU M)  = ',F6.1,/'   LENGTH OF PANEL(M)         = ',F8.4,
     &/,'   WIDTH OF PANEL(M)          = ',F8.4,/,'   SKIN LOAD/UNIT
     &LENGTH(N/M)= ',F10.4,/,'   CIRCUM SKIN LOAD(N/M)      = ',F10.4)
      GOTO 20
82    WRITE(6,223)SKDEN,ETASK,FOSK
223   FORMAT('   SURFACE DENSITY(KG/SQ M)  = ',F7.4,/,'   DAMPING
     &RATIO             = ',F5.3,/,'   FUND. RESONANCE FREQ(HZ)  = '
     &,F4.0)
      GO TO 20
21    CONTINUE
      IF(L(I).NE.2) GO TO 24
      WRITE(6,216)I
216   FORMAT(/'   LAYER # ',I2,' IS AIRGAP '/)
      WRITE(6,217) THICK(I)
217   FORMAT('   THICKNESS OF AIRGAP(M)    = ',F8.4)
      GO TO 20
24    CONTINUE
      IF(L(I).NE.3) GO TO 25
      WRITE(6,225)I
225   FORMAT(/'   LAYER # ',I2,' IS FIBERGLASS '/)
      WRITE(6,218)DENS(I),R(I),P(I),THICK(I)
218   FORMAT('   DENSITY(KG/CU M)          = ',F6.1,/,'   RESISTIVITY
     &(MKS RAYLS)    = ',F7.0,/,'   POROSITY                  = ',
     &F3.1,/,'   THICKNESS(M)              = ',F8.4
      GO TO 20
25    CONTINUE
      IF(L(I).NE.4) GO TO 26
      WRITE(6,226) I
226   FORMAT(/'   LAYER # ',I2,' IS SEPTUM '/)
      WRITE(6,219)SDENS(I)
219   FORMAT('   SURFACE DENSITY(KG/SQ M)  = ',F7.4)
      GO TO 20
26    CONTINUE
      IF(L(I).NE.5) GO TO 20
      WRITE(6,227)I
227   FORMAT(/'   LAYER # ',I2,' IS TRIM'/)
      WRITE(6,220) ITRIM
220   FORMAT('   IMPEDANCE MODEL FOR TRIM  = ',I1/)
      IF(ITRIM.NE.1) GO TO 28
      WRITE(6,221) SDENS(I)
221   FORMAT('   SURFACE DENSKG/SQ M)  = ',F7.4)
      GOTO 20
```

```
28    CONTINUE
      WRITE(6,222)SDENS(I),ETATP,FOT,SLPFAC
222   FORMAT('   SURFACE DENSITY(KG/SQ M)  = ',F7.4,/,'   DAMPING
     &RATIO                 = ',F5.3,/,'   FUND. RESONANCE FREQ(HZ)  = '
     &,F4.0,/,'   SLOPE FACTOR                = ',F5.3)
20    CONTINUE
      WRITE (6,250)(INAME(KK),KK=1,14)
250   FORMAT(//10X,' INPUT FILE NAME    = ',14A1,)
      WRITE(6,251)(ONAME(KK),KK=1,14)
251   FORMAT(10X,' OUTPUT FILE NAME   = ',14A1,/)
C
C#######  START OF FREUENCY LOOP
C
      IF(IA.EQ.1)TH=TH*PI/180.
      DO 30 I=1,NFREQ
      W=2.*PI*FREQ(I)
      ZCAP(N+1)=CMPLX(RO(N+1)*C(N+1),0.)
C
C#######  CALCULATE CHARACTEISTIC IMPEDANCE FOR AIRGAPS AND POROUS
C#######  FIBERGLASS INSULATIONS
C
      DO 40 KI=1,N
      KK=KI
      IF(L(KI).NE.3) GOTO 41
      CALL PCBKT(KK,W,RO(N+1),ZCAP(KI),B(KI))
      C(KI)=W/(AIMAG(B(KI)))
      GO TO 40
41    CONTINUE
      IF(L(KI).NE.2)GO TO 40
      RO(KI)=RO(N+1)
      C(KI)=C(N+1)
      ZCAP(KI)=CMPLX((RO(I)*C(KI)),0.)
40    CONTINUE
C
C#######  FOR SPECIFIC ANGLE OF INCIDENCE SET COUNTER J=1
C
      J=1
      IF(IA.EQ.1) GOTO 31
C
C#######  LOOP FOR RANDOM ANGLES OF INCIDENCE
C
      DO 32 J=1,NANG
      TH=ANG(J)
      TH=TH*PI/180.
31    CONTINUE
      THETA(1)=TH
      ITEMP=1
      L(N+1)=2
```

```
C
C#######  CALCULATE THE ANGLE OF TRANSMISSION FOR AIRGAPS AND FIBERGLASS
C
      DO 45 KI=1,N+1
      THETA(KI)=THETA(ITEMP)
      IF((L(KI).NE.2).AND.(L(KI).NE.3))GO TO 45
      TE=C(KI)*SINA(ITEMP))/C(ITEMP)
      IF(TE.GT.1.) GO TO 1003
      CALL ASIN(TE,THETA(KI))
      ITEMP=KI
45    CONTINUE
C
C#######  CALCULATE THE IMPEDANCE AND PRESSURE RATIO OF UNTREATED SKIN,
C#######  IF PRESENT.
C
      IF(NSKIN.EQ.0) GO TO 33
      TR1=(C(2)/C(1)*COS(TH)/(1.+AMACH*COS(TH)))**2
      IF(TR1.GT.1.) GO TO 1003
      CALL ASIN(SQRT(1.-TR1),TH2)
      Z2UT = CMPLX(RO(N+1)*C(N+1)/COS(TH2),0.)
      IF(ISKIN .EQ.1) CALL DPA1(W,Z2UT,Z1UT,ZP)
      IF(ISKIN.EQ.2) CALL DPA2(W,Z2UT,Z1UT,ZP)
      IF(ISKIN.EQ.3) CALL DPA3(W,Z2UT,Z1UT,ZP)
      IF(ISKIN.EQ.4) CALL DPA4(W,Z2UT,Z1UT,ZP)
      PIP(J) = CMPLX(1.,0)
      CC=CMPLX(RO(1)*C(1)/(COS(TH)*(1.+AMACH*SIN(TH))),0.)
      PIP(J) = PIP(J)+Z1UT/Z2UT+CC/Z2UT
      GO TO 34
C
C#######  IF SKIN NOT PRESENT SET PRESSURE RATIO TO (1.,0.)
C
33    PIP(J)=CMPLX(1.,0.)
34    CONTINUE
C
C#######  CALCULATE SPECIFIC IMPEDANCE OF EACH LAYER FROM ITS
C#######  CHARACTERISTIC AND TERMINATING IMPEDANCE.  START FROM
C#######  INTERIOR.
C
      Z(N+1)=ZCAP(N+1)
      Z(N+1)=Z(N+1)/COS(THETA(N+1))
      DO 46 KI = N,1,-1
      KK=KI
      IF(L(KI).NE.5) GO TO 47
      IF(ITRIM.EQ.1) CALL TRIM1(KK,W,Z(KK+1),Z(KK),ZCAP(KK))
      IF(ITRIM.EQ.2) CALL TRIM2(KK,W,Z(KK+1),Z(KK),ZCAP(KK))
      GO TO 46
47    CONTINUE
      IF(L(KI).NE.4) GO TO 48
```

```
      CALL TRIM1(KK,W,Z(KK+1),Z(KK),ZCAP(KK))
      GO TO 46
48    CONTINUE
      IF(L(KI).NE.3) GO TO 49
      ZCAP(KI)=ZCAP(KI)/COS(THETA(KI))
      CALL GAP(KK,ZCAP(KK),B(KK),Z(KK+1),W,Z(KK),X1K),X2(KK))
      GO TO 46
49    CONTINUE
      IF(L(KI).NE.2) GO TO 50
      ZCAP(KI)=ZCAP(KI)/COS(THETA(KI))
      B(KI)=CMPLX(0.,(W/C(KI)))
      CALL GAP(KK,ZCAP(KK),B(KK),Z(KK+1),W,Z(KK),X1(KK),X2(KK))
      GO TO 46
50    CONTINUE
      IF(L(KI).NE.1) GO TO 46
      IF(ISKIN.EQ.1) CALL DPA1(W,Z(KK+1),Z(KK),ZCAP(KK))
      IF(ISKIN.EQ.2) CALL DPA2(W,Z(KK+1),Z(KK),ZCAP(KK))
      IF(ISKIN.EQ.3) CALL DPA3(W,Z(KK+1),Z(KK),ZCAP(KK))
      IF(ISKIN.EQ.4) CALL DPA4(W,Z(KK+1),Z(KK),ZCAP(KK))
      CONTINUE
C
C#######  CALCULATE PRESSURE RATIOS OF INDIVIDUAL LAYERS FROM THEIR
C#######  SPECIFIC AND THEIR TERMINATING IMPEDANCES
C
      DO 55 KI=1,N
      IF(L(KI).NE.1) GOTO 56
      PRATIO(KI)=CMPLX(1.,0.)
      CC=CMPLX(RO(1)*C(1)/(COS(TH)*(1.+AMACH*SIN(TH))),0.)
      PRATIO(KI)=PRATIO(KI)+Z(KI)/Z(KI+1)+CC/Z(KI+1)
      GO TO 55
56    CONTINUE
      IF((L(KI).NE.2).AND.(L(KI).NE.3)) GO TO 57
      PRATIO(KI)=COSH(X2(KI))/COSH(X1(KI))
      GO TO 55
57    CONTINUE
      CC=CMPLX(COS(THTA(KI)),0.)
      CC=ZCAP(KI)*CC/Z(KI+1)
      PRATIO(KI)=CMPLX(1.,0.)+CC
55    CONTINUE
C
C#######  CALCULATE THE PRESSURE RATIO ACROSS ALL LAYERS
C
      PIT(J)=(1.,0.)
      DO 60 KI=1,N
      PIT(J)=PIT(J)*PRATIO(KI)
60    CONTINUE
C
C####### EXIT ANGLE LOOP IF SPECIFIC ANGLE OF INCIDENCE
```

```
C
      IF(IA.NE.2) GO TO 61
32    CONTINUE
C
C#######  FOR RANDOM INCIDENCE INTEGRATE OVER THE ENTIRE ANGLE RANGE
C
      DO 62 KI=1,NANG
      TH=ANG(KI)*PI/180.
      Y1(KI)=CABS(PIP(KI))**2*SIN()
      Y2(KI)=CABS(PIT(KI))**2*SIN(2.*TH)
62    CONTINUE
      STEP=(88./(NANG-1))*PI/180.
      CALL SIMP(STEP,Y1,P1A,NANG)
      CALL SIMP(STEP,Y2,P2A,NANG)
C
C#######  FOR RANDOM INCIDENCE CALCULATE THE UNTREATED AND TREATED
C#######  TRANSMISSION LOSS.
C
      TLT(I)=10.*ALOG10(P2A)
      TLA(I)=10.*ALOG10(P1A)
      GO TO 30
C
C#######  FOR SPECIFIC INCIDENCE CALCULATE UNTREATED AND TREATED
C#######  TRANSMISSION LOSS
C
61    CONTINUE
      TLT(I)=10.*ALOG10(CABS(PIT(1))**2)
      TLA(I)=10.*ALOG10(CABS(PIP(1))**2)
30    CONTINUE
C
C#######  END OF FREQUENCY LOOP
C
C#######  ON THE PRINTER GO TO NEXT PAGE (FORM FEED). THIS IS DUE
C#######  INHERENT RESTRICTION OF LA 120 (DECWRITER III)
C
      CLOSE(UNIT=6)
      OPEN(UNIT=6)
C
C#######  PRINT THE FREQUENCY,UNTREATED TL,TREATED TL AND ADD. TL DUE
C#######  TO TREATMENT
C
      WRITE(6,500)
500   FORMAT(////,17X,' SOUND TRASMISSION LOSS OF TREATED PANEL'//)
      WRITE(6,501)
501   FORMAT(/T13,'FREQUENCY',T28,'UNTREATE TL',T43,' TREATED TL ',T58,
     &'ADDITIONAL TL')
      WRITE(6,502)
502   FORMAT(T16,'HERTZ',T33,'DB',T48,'DB',T63,'DB'/)
```

```
      DO 70 I=1,NFREQ
      WRITE(6,503) FREQ(I),TLA(I),TLT(I),(TLT(I)-TLA(I))
70    CONTINUE
503   FORMAT(13X,F5.0,7X,3(3X,F8.2,4X))
C
C#######  OPEN AND WRITE IN OUTPUT DATA FILE
C
      OPEN(UNIT=9,NAME=ONAME,TYPE='NEW')
      DO 71 I=1,NFREQ
71    WRITE(9,505)FREQ(I),TLA(I)
505   FORMAT(T10,F5.0,F8.2)
      DO 72 I=1,NFREQ
72    WRITE(9,505)FREQ(I),TLT(I)
      DO 73 I=1,NFREQ
73    WRITE(9,505)FREQ(I),(TLT(I)-TLA(I))
      CLOSE(UNIT=9,DISPOSE='SAVE')
      GO TO 1100
C
C#######  ERROR MESSAGES
C
1000  CONTINUE
      TYPE*,'TOTAL NUMBER OF LAYERS DO NOT MATCH WITH INDIVIDUAL LAYERS
     & SPECIFIED!'
      GO TO 1100
1001  CONTINUE
      TYPE*,' SKIN IMPEDANCE MODEL',ISKIN,' IS NOT AVAILABLE!'
      GO TO 1100
1002  CONTINUE
      TYPE*,' TRIM IMPEDANCE MODEL',ITRIM,' IS NOT AVAILABLE!'
      GO TO 1100
1003  CONTINUE
      TYPE*,' THE INCIDENCE AN IS GREATER THAN CRITICAL ANGLE FOR
     & TRANSMISSION!'
      GO TO 1100
1004  CONTINUE
      TYPE*,' ERROR IN THE SPECIFICATION OF INCIDENCE ANGLE !'
      TYPE*,' ALLOWED OPTIONS : 1 = DISCRETE AND 2 = RANDOM'
1100  CONTINUE
C
C#######  END OF PROGRAM
C
      STOP
      END
```

B.2.2: LISTING OF BLAYER

```
CCCCCCCCCCCCCCCCCCCCCCCCCCCCCCCCCCCCCCCCCCCCCCCCCCCCCCCCCCCCCCCCCCCCCCCCCCCCCCC
C                                                                              C
C                                                                              C
C                  SUB-PROGRAM FOR SOUND TRANSMISSION                          C
C                    THROUGH FOR MULTI-LAYERED PANEL                           C
C                                                                              C
C                                                                              C
CCCCCCCCCCCCCCCCCCCCCCCCCCCCCCCCCCCCCCCCCCCCCCCCCCCCCCCCCCCCCCCCCCCCCCCCCCCCCCC
C
C
C#######          THIS SUB-PROGRAM CONTAINS THE SUBROUTINES FOR THE
C#######          TRANSMISSION LOSS OF AN AIRCRAFT SIDE-WALL WITH NOISE
C#######          CONTROL TREATMENTS
C
C##################  VERSION    : 1               ####################
C##################  PROGRAMMER : R.NAVANEETHAN   ####################
C##################  DATE       : 27-DEC-82       ####################
C
C#######
C
C         FOR REFERENCES REFER TO LISTING OF THE MAIN PROGRAM
C                          "MLAYER.FOR"
C
C##############################################################################
C
C
C     SUBROUTINE FOR THE DETERMINATION OF THE IMPEDANCE OF SKIN PANEL
C                  IMPEDANCE MODEL # 1
C                                    MASS LAW
C
      SUBROUTINE DPA1(W1,Z2,Z1,ZP)
      COMMON /COM/ TH,TH2,THETA,AMACH,PRESS,C
      COMMON /ONE1/ H,RHO
      COMPLEX Z1,Z2,ZP
      REAL M,THETA(10),PRESS(2),C(10)
C
C########  CALCULATE IMPEDANCE OF THE PANEL
C
      M = RHO*H
      PI = 3.141592654
      ZP = CMPLX(0.,W1*M)
C
C########  CALCULATE THE IMPEDANCE OF THE LAYER
C
      Z1=ZP+Z2
  11  RETURN
      END
C
```

```
C
C
C     SUBROUTINE FOR THE DETERMINATION OF THE IMPEDANCE OF THE SKIN PANEL
C           IMPEDANCE MODEL # 2
C                                   MIKULAS EQUATION
C
      SUBROUTINE DPA2(W1,Z2,Z1,ZP)
      COMMON /COM/ TH,TH2,THETA,AMACH,PRESS,C
      COMMON /ONE1/ H,RHO
      COMMON /ONE2/ A1,EC1,IO1,J1,A2,EC2,IO2,J2,E1,G1,E2,G2,ICYL,A
      COMMON /ONE3/ ESK,NU,ETA,B1,B2
      COMPLEX ZP,Z2,Z1
      REAL M,IO1,IO2,THETA(10),PRESS(2),NU,C(10)
      M = H*RHO
      D = (ESK*H**3)/(12.*(1.-NU**2))
      PI = 3.141592654
C
C#######  RESONANCE FREQUENCY STIFFENED PANEL. NEGLECTS MEMBRANE
C#######  STIFFNESS OF THE CYLINDER.(MIKULAS EQUATION)
C#######  M=1 N=.5 REFER NASA CR 159200
C
C
C#######  CALCULATE BENDING AND TORSION PARAMETERS
C
      RBP=E2*(A2*EC2**2+IO2)/(D*B2)
      SBP=E1*(A1*EC1**2+IO1)/(D*B1)
      RTP=G2*J2/(D*B2)
      STP=G1*J1/(D*B1)
C
C#######  SET DEL AND M FOR FLAT PANELS
C
      IF(ICYL.EQ.2) GO TO 201
      DEL=1.
      AM=1.0
      DELP=0.
      GOTO 202
C
C#######  SET DEL AND M FOR CURVED PANELS
C
201   CONTINUE
      AN=.5
      AM=1.
      DEL=AN*B1/AM*PI*A
      DELP=(PRESS(2)-PRESS(1))*A/2.*(AM*B1/PI)**2/D*(1.+2.*DEL**2)
202   CONTINUE
C
C#######  CALCULATE THE RESONANCE FREQUENCY
C
```

```
      W02=AM**4*((1.+DEL**2)**2+(SBP+DEL**2*(RTP+STP)+DEL**4*RBP))+DELP
      W0T=(PI/B1)**2*SQRT(D/M)*SQRT(W02)
C
C#######  CALCULATE IMPEDANCE OF THE PANEL
C
      ZPR1 = ((W0T**2)/W1)*M*ETA
      ZPR2=((W1**3)ETA*((SIN(TH))**4))/((C(1)**4)*
     .      ((1.+AMACH*SIN(TH))**4))
      ZPC1 = (W1*M)-(((W0T**2)*M)/W1)
      ZPC2 = -((W0T**3)*D*((SIN(TH))**4))/((C(1)**4)*
     &((1.+AMACH*SIN(TH))**4))
      ZP = CMPLX(ZPR1+ZPR2,ZPC1+ZPC2)
C
C#######  CALCULATE THE IMPEDANCE OF THE LAYER
C
      Z1=ZP+Z2
 11   RETURN
      END
C
C
C     SUBROUTINE FOR THE DETERMINATION OF THE IMPEDANCE OF THE SKIN PANEL
C           IMPEDANCE MODEL # 3
C                                  PRESSURIZED PANEL
C
      SUBROUTINE DPA3(W1,Z2,Z1,ZP)
      COMMON /COM/ TH,TH2,THETA,AMACH,PRESS,C
      COMMON /ONE1/ H,RHO
      COMMON /ONE3/ ESK,NU,ETA,B1,B2
      COMMON /ONE4/ PAX,PCIR
      COMPLEX ZP,Z2,Z1
      REAL M,NU,THETA(10),PRESS(2),C(10)
      M = H*RHO
      D = (ESK*H**3)/(12.*(1.-NU**2))
      PI = 3.141592654
C
C#######  CALCULATE THE RESONANCE FREQUENCY
C
      W01 = (PAX/(B2**2))+(PCIR/(B1**2))+(D*PI**2)*(((1./B2**2)
     &+(1./B1**2))**2)
      W0T = (PI/SQRT(M))*SQRT(W01)
C
C#######  CALCULATE THE IEDANCE OF THE PANEL
C
      ZPR1 = ((W0T**2)/W1)*M*ETA
      ZPR2=W1**3*D*ETA*(SIN(TH)/(C(1)*(1.+AMACH*SIN(TH))))**4
      ZPC1 = (W1*M)-(((W0T**2)*M)/W1)
      ZPC2 =-((W0T**3)*D*((SIN(TH))**4))/((C(1)**4)*
     &((1.+AMACH*SIN(TH))**4))
```

```
      ZP = CMPLX(ZPR1+ZPR2,ZPC1+ZPC2)
C
C#######  CALCULATE THE IMPEDANCE OF THE LAYER
C
      Z1=ZP+Z2
11    RETURN
      END
C
C
C
C
C     SUBROUTINE FOR THE DETERMINATION OF THE IMPEDANCE OF THE SKIN PANEL
C           IMPEDANCE MODEL # 4
C

C
      SUBROUTINE DPA4(W1,Z2,Z1,ZP)
      COMMON /COM/ TH,TH2,THETA,AMACH,PRESS,C
      COMMON /ONE5/ SKDEN,ETASK,FOSK
      COMPLEX ZP,Z2,Z1
      REAL M,THETA(10),PRESS(2),C(10)
      M = SKDEN
      PI = 3.141592654
C
C#######  RESONANCE FREQUENCY IS GIVEN
C
      WOT=2.*PI*FOSK
C
C#######  CALCULATE THE IMPEDANCE OF THE PANEL
C
      ZPR1 = 2.*M*ETASK*WOT
      ZPC1 = (W1*M)*(1.-(WOT/W1)**2)
      ZP = CMPLX(ZPR1,ZPC1)
C
C#######  CALCULATE THE IMPEDANCE OF THE LAYER
C
      Z1=ZP+Z2
11    RETURN
      END
C
C
C
C
C       SUBROUTINE FOR THE  DETERMINATION OF THE IMPEDANCE OF TRIM
C              TRIM IMPEDANCE MODEL # 1
C                                    MASS LAW
C
C
```

```
      SUBROUTINE TRIM1(KK,W1,Z2,Z1,ZP)
      COMMON /FIVE1/ SDENS
      COMPLEX ZP,Z2,Z1
      REAL M,SDENS(10)
C
C#######  CALCULATE THE IMPEDANCE OF THE PANEL
C
      ZP = CMPLX(0.,W1*SDENS(KK))
C
C#######  CALCULATE THE IMPEDANCE OF THE LAYER
C
      Z1 = ZP + Z2
      RETURN
      END
C
C
C
C         SUBROUTINE FOR THE DETERMINATION OF THE IMPEDANCE OF TRIM
C           IMPEDANCE MODEL # 2
C                              EXPERIMENTAL VALUES
C
C
C
      SUBROUTINE TRIM2(KK,W1,Z2,Z1,ZP)
      COMMON /FIVE1/ SDENS
      COMMON /FIVE2/ ETATP,FOT,SLPFAC
      COMPLEX ZP,Z1,Z2
      REAL M,SDENS(10)
      PI = 3.141592654
      M=SDENS(KK)
      WOT=2.*PI*FOT
C
C########  CHANGE SLOPE IF FREQ >500.
C
      ASLP=SLPFAC
      IZR=0
      IF(W1.GT.3141.59)IZR=1
      ZPC1 = (W1**(1.-(WOT/W1)**2)
      IF(IZR.EQ.0) GO TO 13
      AK=10.**(ASLP*6/20.)
      Z500=(3141.59*M)*(1.-(WOT/3141.59)**2)
      AN=ALOG10(W1/3141.59)/ALOG10(2.)
C
C#######  CALCULATE IMPEDANCE OF THE PANEL FROM MASS-LAWW IMPEDANCE
C#######  AT 500HZ AND THE MEASURED SLOPE
C
      ZPC1 = Z500*AK**AN
```

```
13    CONTINUE
      ZP = CMPLX(2.*ETATP*WOT*M,ZPC1)
C
C#######  CALCUALTE THE IMPEDANCE OF THE LAYER
C
      Z1 = ZP+Z2
  11  RETURN
      END
C
C
C
C
C        SUBROUTINE FOR THE DETERMINATION E IMPEDANCE OF
C                   AIRGAP AND INSULATION
C
C
C
      SUBROUTINE GAP(KK,ZCP,BP,Z2,W1,Z1,X11,X22)
      COMPLEX BP,Z2,Z1,ZCP,X11,X22,ACOTH,COTH
      COMMON/COM/TH,TH2,THETA,AMACH,PRESS,C
      COMMON/TWO/THICK
      REAL THETA(10),PRESS(2),C(10),THICK(10)
      PI=3.1415962
C
C#######  CALCUALTE THE XSI1 (FUNCTION OF TERMINATING IMPEDANCE)
C
      X11 =ACOTH(Z2/ZCP)
C
C#######  CALCULATE THE XSI2 (FUNCTION OF THE IMPEDANCE OF THE LAYER)
C
      X22 = CMPLX(THICK(KK)*COS(THETK)),0.)
      X22 =X22*BP+X11
C
C#######  CALCULATE THE IMPEDANCE OF THE LAYER
C
      Z1 = ZCP*COTH(X22)
      RETURN
      END
C
C
C
C       SUBROUTINE FOR THE INTEGRATION
C                        SIMPSON'S RULE
C
C
      SUBROUTINE SIMP(INC,Y,Z,NDIM)
      REAL INC
      DIMENSION Y(NDIM)
```

```
      N1=NDIM-1
      N2=NDIM-2
      SUM1=0.
      SUM2=0.
C
      DO 5 J=2,N1,2
      SUM1=SUM1+4*Y(J)
    5 CONTINUE
C
      DO 10 J=3,N2,2
      SUM2=SUM2+2*Y(J)
   10 CONTINUE
C
      SUM = Y(1) + Y(NDIM)
      Z = (SUM + SUM1 + SUM2)*INC/3.
C
      RETURN
      END
C
C
C
C       SUBROUTINE TO CALCULATE THE CHARACTERISTIC IMPEDANCE AND
C       PROPAGATION CONSTANT OF POROUS FUBERGLASS MATERIAL
C                 (SEE REFERENCE # 3 IN MLAYER.FOR)
C
      SUBROUTINE PCBKT(KK,W1,RHO2,ZCP,BP)
      COMMON/THREE/DENS,P,R
      REAL K
      COMPLEX BP,ZCP,RHOP,JW
      REAL DENS(10),P(10),R(10)
      DENS1=DENS(KK)
      P1=P(KK)
      R1=R(KK)
      PI=3.1415962
C     .
C#######  CALCULATE THE COMPRESSIBILTY FACTOR FOR PF105 FIBERGLASS
C
      ECX1=ALOG10(W1/(2.*PI*R1))
      IF (ECX1 .LT. -3.) GO TO 1
      IF (ECX1 .GT. 1.)  GO TO 2
      K=1.E5*(((-1.821E-2*ECX1-6.099E-2)*ECX1+8.667E-2)*ECX1+1.3444)
      GO TO 3
    1 K=1.05E5
      GO TO 3
    2 K=1.3E5
C
C#######  CALCULATE STRUCTURES FACTOR AND FACTORS F1 AND F2
C
```

```
    3 SF=10.**(-3.010*ALOG10(P1))
      F1=1.+(1.2*R1/(DENS1*W1))**2
      F2=1.+(P1+DENS1/(SF*RHO2))*(1.2*R1/(DENS1*W1))**2
C
C####### CALCULAE THE COMPLEX (EFFECTIVE) DENSITY
C
      RHOP=CMPLX(RHO2*SF*F2/F1,-1.2*R1/(F1*W1))
C
C#######  CALCULATE PROPAGATION CONSTANT
C
      BP=CMPLX(P1/K,0.)
      BP=CSQRT(BP*RHOP)
      JW=CMPLX(0.,W1)
      BP=BP*JW
C
C#######  CALCULATE THE CHARACTERISTIC IMPEDANCE
C
      ZCP=CMPLX(0.,-K/(W1*P1))
      ZCP=ZCP*BP
      RETURN
      END
```

B.2.3: LISTING OF CLAYER

```
CCCCCCCCCCCCCCCCCCCCCCCCCCCCCCCCCCCCCCCCCCCCCCCCCCCCCCCCCCCCCCCCCCCCCCCCCCCCCCC
C
C
C      ********************************************************
C      *                                                      *
C      *  FUNCTIONS/SUBROUTINES NOT PRESENT IN MINC LIBRARY   *
C      *                                                      *
C      ********************************************************
C
C      PROGRAMMER : JAAP LAMeRIS      VERSION 1   5-31-'82
C                   R. NAVANEETHAN    VERSION 2  12-28-'82
C            VERSION 2 MODIFIED FOR MLAYER.FOR PROGRAM
C                      THIS SUB-PROGRAM IS CALLED CLAYER.FOR
C
CCCCCCCCCCCCCCCCCCCCCCCCCCCCCCCCCCCCCCCCCCCCCCCCCCCCCCCCCCCCCCCCCCCCCCCCCCCCCCC
C
C
C     SUBROUTINE TO CALCULATE THE ARCSINE OF A GIVEN VALUE (-1<X<1)
C
      SUBROUTINE ASIN(X,Y)
      PI=3.141592654
      IF(X.LT.0) GO TO 30
      A=0.
      C=PI/2.
      D=A
      E=C
   10 B=(D+E)/2.
      IF(ABS(X-SIN(B)).LE.1.0E-7) GO TO 45
      IF(X.GT.SIN(B)) GO TO 20
      E=B
      GO TO 10
   20 D=B
      GO TO 10
   30 A=-PI/2.
      C=0
      D=A
      E=C
      GO TO 10
C
   45 Y=B
      GO TO 50
C
   50 RETURN
      END
C
C
C     SUBROUTINE TO CALCULATE THE ARCOS OF GIVEN VALUE (-1<X<1)
C
```

```
      SUBROUTINE ACOS(X,Y)
C
      PI=3.141592654
      CALL ASIN(X,Y)
C
      ACOS=PI/2.-Y
      GO TO 20
   20 RETURN
      END
C
C
C     FUNCTION TO RETURN HYPERBOLIC COTANGENT OF GIVEN COMPLEX
C     NUMBER (X)
C
C
      FUNCTION COTH(X)
      COMPLEX X,COTH
      COTH = (CEXP(X)+CEXP(-X))/(CEXP(X)-CEXP(-X))
      RETURN
      END
C
C
C    FUNCTION TO RETURN THE INVERSE HYPERBOLIC COTANGENT A GIVEN
C    COMPLEX NUMBER (X).
C                    CALCULATES ONLY THE PRIMARY ARGUMENT
C
C
      FUNCTION ACOTH(X)
      COMPLEX X,ACOTH
      ACOTH = .5*CLOG((X+1.)/(X-1.))
      RETURN
      END
C
C
C     FUNCTION TO RETURN THE HYPERBOLIC COSINE OF A GIVEN COMPLEX
C     NUMBER (X)
C
      FUNCTION COSH(X)
      COMPLEX X,COSH
      COSH = .5*(CEXP(X)+CEXP(-X))
      RETURN
      END
```

APPENDIX C

ACOUSTIC INTENSITY COMPUTER ROUTINES

C.1: FLOW CHART OF TEST ROUTINES

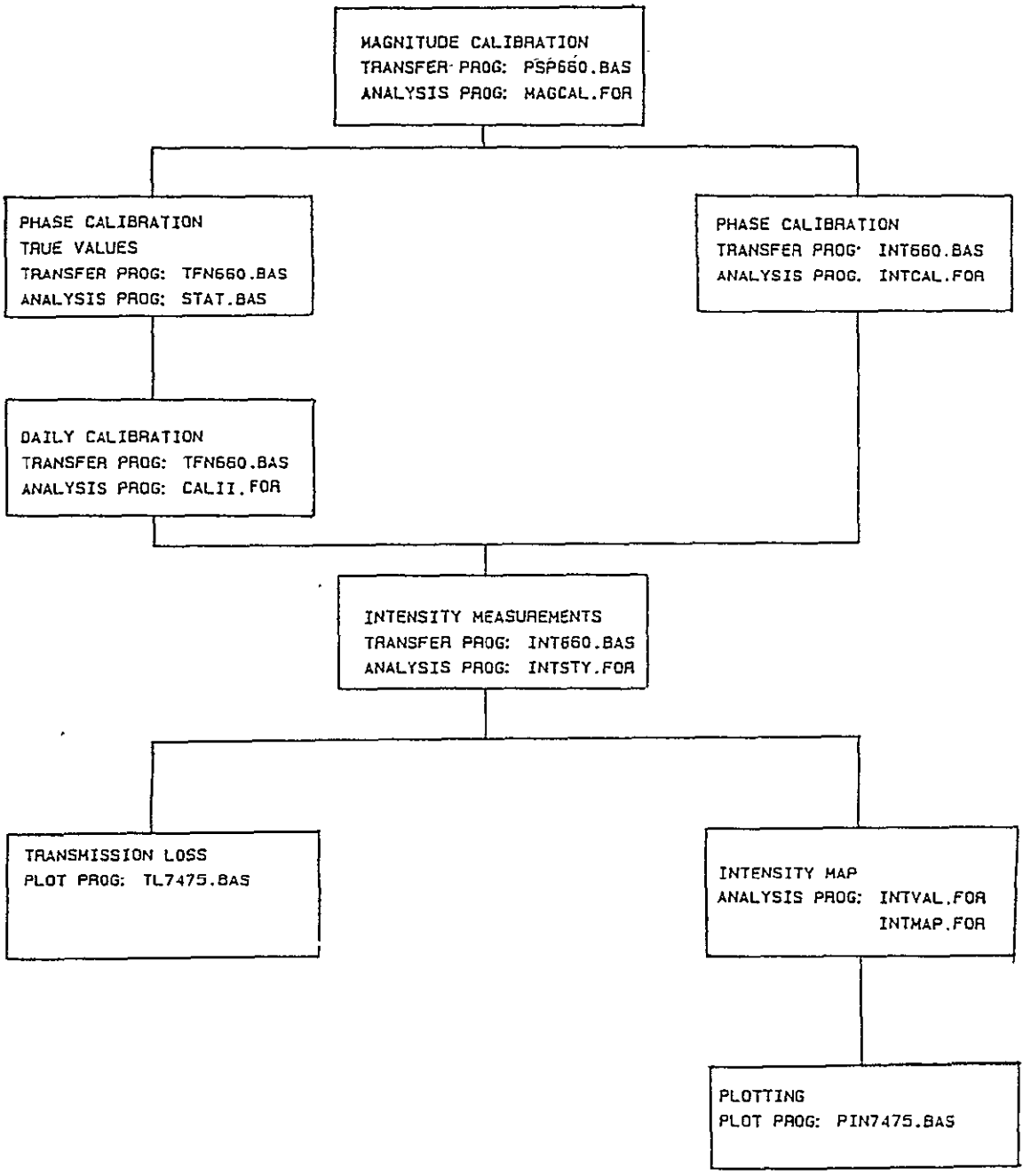

C.2: LISTING OF COMPUTER ROUTINES

C.2.1 LISTING OF PSP660.BAS

```
1 ' ##########################################################################
2 ' #                                                                        #
3 ' #    TRANSFER PROGRAM FOR POWERSPECTRUM OF CHANNEL A AND B               #
4 ' #                                                                        #
5 ' ##########################################################################
6 ' #
7 ' #                        VERSION : 4
8 ' #                     PROGRAMMER : R.NAVANEETHAN
9 ' #                           DATE : 1-23-84
10 ' #
11 ' #
100 SCREEN 0,0
110 DEFINT I-N
120 CLS:CLOSE
130 LOCATE 25,1
140 C$="ZZZ0A35SY251SY261SY272SWAJ6F1E0=8"
150 C1$="ZZZ0A35SY251SY261SY272SWAJ6F2E0=9"
160 PRINT STRING$(60," ")
170 SYN$=CHR$(22)
180 LOCATE 1,1
190 SPEED$="9600"
200 COMFIL$="COM1:"+SPEED$+",N,8,2"
210 OPEN COMFIL$ AS #1
220 OPEN "SCRN:" FOR OUTPUT AS #2
230 JC=1
240 LOCATE 25,1:PRINT "660B POWER SPECTRUM TRANSFER PROGRAM";
250 LOCATE 1,1:PRINT STRING$(60," "):LOCATE 1,1
260 IF JC=1 THEN LINE INPUT "FILE NAME FOR CHL A?
< E TO EXIT > :";DSKFIL$
270 IF JC=2 THEN LINE INPUT "FILE NAME FOR CHL B?
< E TO EXIT > :";DSKFIL$
280 IF JC=2 THEN C$=C1$
290 IF DSKFIL$="E" THEN 650
300 LOCATE 1,1:PRINT STRING$(60," "):LOCATE 1,1
310 OPEN "R",#3,DSKFIL$,72
320 FIELD #3, 72 AS R1$
330 FOR IC%=1 TO 33
340 D$=MID$(C$,IC%,1)
350 GOSUB 440
360 FOR IK%=1 TO 75
370 NEXT IK%
380 NEXT IC%
390 REM CONTINUE
400 LOCATE 1,1
410 GOSUB 470
420 CLOSE #3:JC=JC+1:CLS
430 IF JC=2 THEN GOTO 260 ELSE GOTO 650
440 PRINT #1,D$;
```

```
450 IF LOC(1)=0 THEN 450
460 A$=INPUT$(1,#1):IF ASC(A$)=6 THEN RETURN ELSE PRINT #2,
"ERROR SENDING DATA":STOP
470 J=0
480 FOR IC%=1 TO 22
490 PRINT #1,SYN$;
500 J=J+1
510 PRINT J
520 IF LOC(1)<72 THEN 520
530 H1$ = INPUT$(72,#1)
540 IF J>17 THEN GOTO 560
550 GOSUB 600
560 NEXT IC%
570 PRINT LOC(1):IF LOC(1)<>1 THEN 570
580 A$=INPUT$(1,#1)
590 RETURN
600 REM CONVERT TO REAL
610 R$=H1$
620 LSET R1$=R$
630 PUT #3
640 RETURN
650 CLOSE:END
```

C.2.2 LISTING OF MAGCAL.FOR

```
CCCCCCCCCCCCCCCCCCCCCCCCCCCCCCCCCCCCCCCCCCCCCCCCCCCCCCCCCCCCCCCCCCCCCC
C                                                                     C
C                  MAGNITUDE CALIBRATION PROGRAM                      C
C                                                                     C
CCCCCCCCCCCCCCCCCCCCCCCCCCCCCCCCCCCCCCCCCCCCCCCCCCCCCCCCCCCCCCCCCCCCCC
C
C
C
C
C#######      PROGRAMMER : R.NAVANEETHAN       ################
C#######           DATE : JAN 18, 84           ################
C#######         VERSION : 2.                  ################
C
C#######  THE MAGNITUDE CAL PROGRAM USES THE INPUT VALUES FROM
C#######  TRANSFER PROGRAM A:CALA.DAT AND A:CALB.DAT.
C
C#######  REFER TO KU-FRL REPORT KU-FRL-417-22 FOR DETAILS ON
C#######  ON THIS PROGRAM
C
C
C234567
      IMPLICIT REAL(0-Z)
      IMPLICIT REAL(B-F)
      DIMENSION CHA(402),CHB(402)
      CHARACTER*16 FSTRG,CSTRG
      CHARACTER *15 FNAME
      INTEGER*1 IJ(72)
      CHARACTER *1 HA,HB,ACHAR
      DATA HA/"A"/
      DATA HB/"B"/
      J=1
      IF(IORAND(72,72,5,0,"A:CALA.DAT")) GO TO 1000
      IF(IORAND(72,72,6,0,"A:CALB.DAT")) GO TO 1100
      DO 7 IUNIT=5,6
      KL=0
      DO 10 I=1,17
      READ(IUNIT/I)(IJ(K),K=1,72)
      DO 11 J=1,72,3
      KL=KL+1
      J1=IJ(J)
      J2=IJ(J+1)
      J3=IJ(J+2)
      IF(J3.LT.0)J3=256+J3
      JM=1
      IF(J2.LT.0) JM=-1
      JP=IABS(J2)
      CALL SUB1(JP,CSTRG)
      FSTRG=CSTRG
```

```
      CALL SUB1(J3,CSTRG)
      CALL INSERT(CSTRG,FSTRG,1)
      V=0.
      DO 20 KI=1,15
      K=16-KI
      V1=0
      CALL PUTCHR(ACHAR,1,KHAR(FSTRG,K))
      IF(ACHAR.EQ."1") V1=1
      V=V+V1/2**KI
20    CONTINUE
      IF(JM.EQ.-1)V=-V
      IF(IUNIT.EQ.5) CHA(KL)=V*2.**J1
      IF(IUNIT.EQ.6) CHB(KL)=V*2.**J1
11    CONTINUE
10    CONTINUE
7     CONTINUE
      IF (IOCLOS(5)) STOP
      IF (IOCLOS(6)) STOP
      YMCHA = CHA(1)
      YMCHB = CHB(1)
      DO 2 I=5,400
      IF (YMCHA.GE.CHA(I)) GOTO 3
      YMCHA=CHA(I)
      IAMAX=I
3     CONTINUE
      IF (YMCHB.GE.CHB(I)) GOTO 2
      YMCHB=CHB(I)
      IBMAX=I
2     CONTINUE
      YA=0.
      DO 4 I=IAMAX-3,IAMAX+3
4     YA=YA+CHA(I)
      YB=0.
      DO 5 I=IBMAX-3,IBMAX+3
5     YB=YB+CHB(I)
      PCAL=10.**(124./20.)*.00002
      AKCHA=PCAL/SQRT(YA)
      AKCHB=PCAL/SQRT(YB)
      WRITE(1,200)
200   FORMAT(' ','CHANNEL A DETAILS')
      WRITE(1,201)
201   FORMAT(' ','ENTER MAX AMPLITUDE SETTING : '$)
      READ(1,300) AMPCHA
300   FORMAT(F0.0)
      WRITE(1,202)
202   FORMAT(' ','ENTER # OF AVERAGES : '$)
      READ(1,301) NAVGA
301   FORMAT(I0)
      WRITE(1,203)
```

```
203   FORMAT(' ','CHANNEL B DETAILS')
      WRITE(1,201)
      READ(1,300) AMPCHB
      WRITE(1,202)
      READ(1,301) NAVGB
      IF (IOWRIT (8,2,0,"CALDAT.DAT")) STOP
      WRITE (8,205) AKCHA,AKCHB
205   FORMAT(' ',2E15.5)
      WRITE(8,205) AMPCHA,AMPCHB
      WRITE(8,206) NAVGA,NAVGB
206   FORMAT(' ',2I5)
      IF (IOCLOS(8)) STOP
      GOTO 6
1000  WRITE(1,500) HA
500   FORMAT(' ','ERROR OPENING DATA FILE OF CHANNEL ',A1)
      GO TO 6
1100  WRITE(1,500) HB
6     CONTINUE
      STOP
      END
      SUBROUTINE SUB1(JP,CSTRG)
      CHARACTER*16 BSTRG,B(8),CSTRG,SUBSTG
      INTEGER*2 JO(3)
      DATA B/"000","001","010","011","100","101","110","111"/
      BSTRG=""
      CSTRG=""
      JO(1) =MOD(JP,8)
      JP1  = JP/8
      JO(2) =MOD(JP1,8)
      JO(3) = JP1/8
      DO 31 JI=1,3
      JP=JO(JI)+1
31    CALL INSERT(B(JP),BSTRG,1)
      DO 32 JI=1,8
      JK= 10-JI
      CALL ADDSTG(CSTRG,SUBSTG(BSTRG,JK,JK))
32    CONTINUE
      RETURN
      END
```

C.2.3 LISTING OF TFN660.BAS

```
10 SCREEN 0,0
20 DEFINT I-N
30 CLS:CLOSE
40 LOCATE 25,1
50 C$="ZZZ0A35SY251SY261SY272SWAJ3E0E4ZZZ=8"
60 PRINT STRING$(60," ")
70 SYN$=CHR$(22)
80 LOCATE 1,1
90 SPEED$="9600"
100 COMFIL$="COM1:"+SPEED$+",N,8,2"
110 OPEN COMFIL$ AS #1
120 OPEN "SCRN:" FOR OUTPUT AS #2
130 LOCATE 25,1:PRINT "660B TRANSFER PROGRAM";
140 LOCATE 1,1:PRINT STRING$(60," "):LOCATE 1,1
150 LINE INPUT "INPUT FILE? <TYPE E TO EXIT > :";DSKFIL$
160 IF DSKFIL$="E" THEN 620
170 LOCATE 1,1:PRINT STRING$(60," "):LOCATE 1,1
180 OPEN "R",#3,DSKFIL$,72
190 FIELD #3, 72 AS R1$
200 FOR IC%=1 TO 36
210 D$=MID$(C$,IC%,1)
220 GOSUB 360
230 FOR IK%=1 TO 75
240 NEXT IK%
250 NEXT IC%
260 REM CONTINUE
270 LOCATE 1,1
280 GOSUB 390
290 D$="Z":GOSUB 360
300 D$="Z":GOSUB 360
310 D$="=":GOSUB 360
320 D$="9":GOSUB 360
330 GOSUB 390
340 CLOSE #3:CLS
350 GOTO 130
360 PRINT #1,D$;
370 IF LOC(1)=0 THEN 370
380 A$=INPUT$(1,#1):IF ASC(A$)=6 THEN RETURN ELSE PRINT #2,"ERROR SENDING
DATA":STOP
390 J=0
410 FOR IC%=1 TO 22
415 PRINT #1,SYN$;
417 J=J+1
418 PRINT J
420 IF LOC(1)<72 THEN 420
430 H1$ = INPUT$(72,#1)
470 IF J>17 THEN GOTO 490
480 GOSUB 530
490 NEXT IC%
```

```
500 PRINT LOC(1):IF LOC(1)<>1 THEN 500
510 A$=INPUT$(1,#1)
520 RETURN
530 REM CONVERT TO REAL
538 R$=H1$
539 LSET R1$=R$
600 PUT #3
610 RETURN
620 CLOSE:END
```

C.2.4 LISTING OF STAT.BAS

```
1 ' ############################################################
2 ' #                                                          #
3 ' #        PROGRAM TO DETERMINE CONFIDENCE INTERVAL          #
4 ' #                                                          #
5 ' ############################################################
6 ' #
7 ' #                        VERSION : 1
8 ' #                     PROGRAMMER : BRIAN QUAYLE
9 ' #                           DATE : 30 - OCT-84
10 ' #
11 '#
100 CLS
110 OPTION BASE 1
120 DIM X(513),X2(513),AVMAG(513),VAR(513),TAV(31),CI(513)
130 FOR I=1 TO 31
140 READ TAV(I)
150 NEXT I
160 DATA 12.71,4.303,3.182,2.776,2.571,2.447,2.365,2.306
170 DATA 2.262,2.228,2.201,2.179,2.160,2.145,2.131,2.12,2.11,2.101
180 DATA 2.093,2.086,2.08,2.074,2.069,2.064,2.06,2.056,2.052,2.048
190 DATA 2.045,2.042,2.02
200 N=0
210 INPUT "ENTER NAME OF INPUT FILE CATALOG ";A$
220 OPEN "I",#1,A$
230 INPUT "ENTER OUTPUT FILE NAME ";B$
240 INPUT "ENTER SPECTRAL LINE SPACING ";LS
250 IF EOF(1) THEN  GOTO 480
260 N=N+1
270 INPUT#1, N$
280 PRINT N$
290 OPEN "I",#2, N$
300 INPUT#1, M$
310 PRINT M$
320 OPEN "I",#3, M$
330 I=0
340 IF EOF(2) THEN GOTO 450
350 I=I+1
360 INPUT#2,A
370 INPUT#3,B
380 DEG=ATN(B/A)*(180/3.14159)
390 IF(A<0)AND(B>0) THEN DEG=DEG+180
400 IF(A<0)AND(B<0) THEN DEG=DEG-180
410 X(I)=X(I)+DEG
420 X2(I)=X2(I)+DEG^2
430 PRINT I*LS-LS;DEG;X(I);X2(I)
440 GOTO 340
450 CLOSE #3
460 CLOSE #2
```

```
470 GOTO 250
480 CLOSE #1
490 OPEN "O",#1,B$
500 K=N
510 IF N>31 THEN K=31
520 FOR J=1 TO I
530 VAR(J)=(N*X2(J)-X(J)^2)/(N*(N-1))
540 X(J)=X(J)/N
550 CI(J)=TAV(K)*(VAR(J)/N)^2
560 PRINT J*LS-LS;X(J);VAR(J);CI(J)
570 PRINT#1,USING"#####.### ";J*LS-LS,X(J),CI(J)
580 NEXT
590 CLOSE #1
600 FOR I=1 TO 3
610 BEEP
620 FOR J=1 TO 200
630 NEXT
640 NEXT
650 END
```

C.2.5 LISTING OF CALII.FOR

```
CCCCCCCCCCCCCCCCCCCCCCCCCCCCCCCCCCCCCCCCCCCCCCCCCCCCCCCCCCCCCCCCCCCCCCCCC
C                                                                       C
C         PHASE CALIBRATION PROGRAM FOR INTENSITY                       C
C               TRANSFER FUNCTION METHOD                                C
C                     TYPE I                                            C
C                                                                       C
C                                                                       C
C             VERSION : 1                                               C
C          PROGRAMMER : R.NAVANEETHAN                                   C
C               DATE : 20-MAY-83                                        C
C                                                                       C
CCCCCCCCCCCCCCCCCCCCCCCCCCCCCCCCCCCCCCCCCCCCCCCCCCCCCCCCCCCCCCCCCCCCCCCCC
C
C
C######  FOR MORE DETAILS ON THIS METHOD REFER KU-FRL REPORT
C######  KU-FRL-417-22
C
C
C######  DIMENSION STATEMENTS
C
      COMPLEX CALA (512)
      COMPLEX CMPLX
      CHARACTER *15 NAMET,NAME1,NAME2,NAME3,NAME4,NAMEC
      CHARACTER *1 AR
      REAL X(512),Y(512)
      REAL ABIB(4)
      DATA ABIB/4*0./
      DATA NAME1/"B:TFNCAL.DLO"/
      DATA NAME2/"B:TFNCAL.DHI"/
      DATA NAME3/"B:CALII.DLO"/
      DATA NAME4/"B:CALII.DHI"/
      RAD=180./3.1415962
      WRITE(1,600)
600   FORMAT(' ENTER FREQUENCY RANGE : '$)
      READ(1,601) SFREQ
601   FORMAT(F0.0)
      IFLAG=1
      NAMET=NAME1
      NAMEC=NAME3
      IF (SFREQ.GT.1000.) IFLAG=2
      IF (IFLAG.NE.2) GOTO 112
      NAMET=NAME2
      NAMEC=NAME4
112   CONTINUE
C
C########## CHANGE N DEPENDING UPON THE ANALYZER
C
      N=402
```

```
C
C##########  OPEN DATA FILE CONTAINING TRANSFER FUNCTION DATA
C
      IF(IOREAD(8,2,0,NAMET)) STOP
      J=1
      DO 1 I=1,67
      READ(8,100) (X(J1), J1=J,J+5)
      J=J+6
1     CONTINUE
      J=1
      DO 11 I=1,67
      READ(8,100) (Y(J1), J1=J,J+5)
      J=J+6
11    CONTINUE
C
C#######  CHANGE FORMAT STATEMENT DEPENDING UPON THE ANALYZER
C
100   FORMAT(6E0.0)
      IF(IOCLOS(8)) STOP
      NAMET="A:STATLO.DAT"
      IF (IFLAG.EQ.2) NAMET="A:STATHI.DAT"
      IF(IOREAD(6,2,0,NAMET)) STOP
      READ(6,114) FREQ
 114  FORMAT(F0.0)
      IF(FREQ.NE.SFREQ) GOTO 999
      BW=SFREQ*2.56/1024.
      DO 3 I=1,N
      READ(6,110) AMEAN,ALVL
110   FORMAT(F9.3,1X,F9.3)
      IF(ALVL.LT..1) ALVL=.1
      THETA1=ATAN2(Y(I),X(I))*RAD
      IF((IFLAG.EQ.2).AND.(I.GT.280)) GOTO 4
      IF(I.EQ.1) THETA1=0.0
      SIGMA=ALVL*SQRT(30.)
      ZSTAT=(AMEAN-THETA1)/(SIGMA*SQRT(1./30.+1./5.))
987   FORMAT(' ',F15.2,2F15.3)
      IF(ABS(ZSTAT).LE.1.96) GO TO 4
      WRITE(1,990)
990   FORMAT('         FREQUENCY       CAL VALUE
     &ZSTAT         ')
      FRQ=FLOAT(I-1)*BW
      WRITE(1,987) FRQ,THETA1,ZSTAT
989   WRITE(1,113)
113   FORMAT('  VALUES NOT WITHIN LIMITS! ACCEPT OR REJECT
     &<A/R> : '$)
      READ(1,988) AR
988   FORMAT(A0)
      IF((AR.NE."A").AND.(AR.NE."R")) GOTO 989
```

```
      IF(AR.EQ."R") GO TO 998
4     CONTINUE
      THETA1=-THETA1/RAD
      CALA(I)=CMPLX(COS(THETA1),SIN(THETA1))
3     CONTINUE
C
C########## OPEN PHASE CAL DATA FILE
C
      IF(IOWRIT(10,2,0,NAMEC)) STOP
      ABIB(1)=SFREQ
      ABIB(2)=2.
      WRITE(10,102)(ABIB(J),J=1,4)
102   FORMAT(' ',4F15.5)
      DO 2 I=1,N
      WRITE(10,101) CALA(I)
101   FORMAT(' ',2E15.5)
2     CONTINUE
      IF(IOCLOS(10)) STOP
      GOTO 9999
999   WRITE(1,700)
700   FORMAT(' FREQUENCY MIS-MATCH')
      GO TO 9999
998   CONTINUE
9999  CONTINUE
      STOP
      END
```

C.2.6 LISTING OF INT660.BAS

```
1 ' ##############################################################################
2 ' #                                                                            #
3 ' #             TRANSFER PROGRAM FOR CROSS SPECTRUM                            #
4 ' #                                                                            #
5 ' ##############################################################################
6 ' #
7 ' #                        VERSION : 4
8 ' #                     PROGRAMMER : R.NAVANEETHAN
9 ' #                           DATE : 1-20-84
10 ' #
11 ' #
100 SCREEN 0,0
110 DEFINT I-N
120 CLS:CLOSE
130 LOCATE 25,1
140 C$="ZZZ0A35SY251SY261SY272SWAJ2E0ZZZ=8"
150 PRINT STRING$(60," ")
160 SYN$=CHR$(22)
170 LOCATE 1,1
180 SPEED$="9600"
190 COMFIL$="COM1:"+SPEED$+",N,8,2"
200 OPEN "SCRN:" FOR OUTPUT AS #2
210 LOCATE 25,1:PRINT "660B TRANSFER PROGRAM";
220 LOCATE 1,1:PRINT STRING$(60," "):LOCATE 1,1
230 LINE INPUT "INPUT FILE? <TYPE E TO EXIT > :";DSKFIL$
240 IF DSKFIL$="E" THEN 640
250 OPEN COMFIL$ AS #1
260 LOCATE 1,1:PRINT STRING$(60," "):LOCATE 1,1
270 OPEN "R",#3,DSKFIL$,72
280 FIELD #3, 72 AS R1$
290 FOR IC%=1 TO 34
300 D$=MID$(C$,IC%,1)
310 GOSUB 430
320 NEXT IC%
330 REM CONTINUE
340 LOCATE 1,1
350 GOSUB 470
360 D$="Z":GOSUB 430
370 D$="Z":GOSUB 430
380 D$="=":GOSUB 430
390 D$="9":GOSUB 430
400 GOSUB 470
410 CLOSE #3:CLOSE #1:CLS
420 GOTO 210
430 PRINT #1,D$;
440 FOR IK%=1 TO 200:NEXT IK%
450 IF LOC(1)<>1 THEN 450
460 A$=INPUT$(1,#1):IF ASC(A$)=6 THEN RETURN ELSE PRINT #2,
```

```
"ERROR SENDING DATA":STOP
470 J=0
480 FOR IC%=1 TO 22
490 PRINT #1,SYN$;
500 J=J+1
510 IF LOC(1)<72 THEN 510
520 H1$ = INPUT$(72,#1)
530 IF J>17 THEN GOTO 550
540 GOSUB 590
550 NEXT IC%
560 IF LOC(1)<>1 THEN 560
570 A$=INPUT$(1,#1)
580 RETURN
590 REM CONVERT TO REAL
600 R$=H1$
610 LSET R1$=R$
620 PUT #3
630 RETURN
640 CLOSE:END
```

C.2.7 LISTING OF INTCAL.FOR

```
CCCCCCCCCCCCCCCCCCCCCCCCCCCCCCCCCCCCCCCCCCCCCCCCCCCCCCCCCCCCCCCCCCCCCCC
C                                                                      C
C                PHASE CALIBRATION PROGRAM FOR INTENSITY               C
C                                                                      C
C                                                                      C
C             VERSION : 1                                              C
C           PROGRAMMER : R.NAVANEETHAN                                 C
C                DATE : 02-SEP-83                                      C
C                                                                      C
CCCCCCCCCCCCCCCCCCCCCCCCCCCCCCCCCCCCCCCCCCCCCCCCCCCCCCCCCCCCCCCCCCCCCCC
C
C
C
C########  THIS PROGRAM CALCULATES THE PHASE CALIBRATION USING
C########  THE METHOD DESCRIBED IN "THE APPLICATION OF ACOUSTIC
C########  INTENSITY FOR ENGINE NOISE REDUCTION" BY M.D.CROCKER
C########  ET AL, PRESENTED AT THE INTERNATIONAL CONFERENCE ON
C########  RECENT ADVANCES IN ACOUSTIC INTENSITY METHODS,
C########  SENLIS, FRANCE, OCT 1981
C
C
C########  THE FIRST LINE OUTPUT IN ANY DATA FILE CONTAINS FOUR
C########  VARIABLES INCLUDING FREQUENCY RANGE OF ANALYSIS,
C########  DISTANCE BETWEEN MICROPHONES, AREA SWEPT BY THE
C########  MICOPHONE ETC.
C
C
C
C
C##########  DIMENSION STATEMENTS
C
C
C#########  DEPENDING UPON THE FFT ANALYSER CHARACTERISTICS THE
C#########  DIMENSION VALUES NEED TO BE CHANGED.
C
C
C
      COMPLEX CALA(408),CALB(408),C1
C
C##### THE FOLLOWING STATEMENT IS PECULIAR TO SUPERSOFT FORTRAN
C
      COMPLEX CMPLX
C
C#####
C
      REAL X(408),Y(408)
      REAL ABIB(4),BBIB(4)
      CHARACTER *12 NAME1,NAME2,NAME3
```

```
      CHARACTER*2 STR1
      CHARACTER*16 FSTRG,CSTRG
      CHARACTER*1 ACHAR
      INTEGER *1 IJ(72)
      DATA NAME1/"B:XSNORM.DLO"/
      DATA NAME2/"B:XSSWCH.DLO"/
      DATA NAME3/"B:INTCAL.DLO"/
      DATA STR1/"HI"/
      DATA ABIB/4*0./
      DATA BBIB/4*0./
C
C#########  READ DATA FROM X-SPEC DATA FROM THE FFT ANALYZER
C#########  STORED IN THE DISC
C#########  THIS FORMAT FOR OPENING THE DISK FILE IS PECULIAR
C#########  TO SUPER SOFT COMPILER
C
      WRITE(1,700)
700   FORMAT(' ENTER FREQUENCY RANGE OF ANALYSIS : '$)
      READ(1,800) SFREQ
800   FORMAT(F0.0)
      IFLAG=1
      IF(SFREQ.LT.1001.) GO TO 87
      IFLAG=2
      CALL PUTCHR(NAME1,11,KHAR(STR1,1))
      CALL PUTCHR(NAME1,12,KHAR(STR1,2))
      CALL PUTCHR(NAME2,11,KHAR(STR1,1))
      CALL PUTCHR(NAME2,12,KHAR(STR1,2))
      CALL PUTCHR(NAME3,11,KHAR(STR1,1))
      CALL PUTCHR(NAME3,12,KHAR(STR1,2))
87    CONTINUE
      IF(IORAND(72,72,5,0,NAME1)) STOP
      KL=0
      DO 10 I=1,34
      READ(5/I)(IJ(K),K=1,72)
C
C########  CONVERT 3 BYTES FROM NICOLET 660B TO 4 BYTE REAL
C########  VALUES OF SUPERSOFT FORTRAN
C
      DO 11 J=1,72,3
      KL=KL+1
      KJL=KL-408
      J1=IJ(J)
      J2=IJ(J+1)
      J3=IJ(J+2)
      IF(J3.LT.0)J3=256+J3
      JM=1
      IF(J2.LT.0) JM=-1
      JP=IABS(J2)
```

```
      CALL SUB1(JP,CSTRG)
      FSTRG=CSTRG
      CALL SUB1(J3,CSTRG)
      CALL INSERT(CSTRG,FSTRG,1)
      V=0.
      DO 20 KI=1,15
      K=16-KI
      V1=0
      CALL PUTCHR(ACHAR,1,KHAR(FSTRG,K))
      IF(ACHAR.EQ."1") V1=1
      V=V+V1/2**KI
20    CONTINUE
      IF(JM.EQ.-1)V=-V
      IF(KL.LE.408) X(KL)=V*2.**J1
      IF(KL.GT.408) Y(KJL)=V*2.**J1
11    CONTINUE
10    CONTINUE
      IF(IOCLOS(5)) STOP
      N=408
      DO 12 I=1,408
      Y(I)= -Y(I)
      CALA(I) = CMPLX(X(I),Y(I))
12    CONTINUE
C
C###### READ NEXT FILE
C
      IF(IDRAND(72,72,5,0,NAME2)) STOP
      KL=0
      DO 3110 I=1,34
      READ(5/I)(IJ(K),K=1,72)
      DO 3111 J=1,72,3
      KL=KL+1
      KJL=KL-408
      J1=IJ(J)
      J2=IJ(J+1)
      J3=IJ(J+2)
      IF(J3.LT.0)J3=256+J3
      JM=1
      IF(J2.LT.0) JM=-1
      JP=IABS(J2)
      CALL SUB1(JP,CSTRG)
      FSTRG=CSTRG
      CALL SUB1(J3,CSTRG)
      CALL INSERT(CSTRG,FSTRG,1)
      V=0.
      DO 3120 KI=1,15
      K=16-KI
      V1=0
```

```
      CALL PUTCHR(ACHAR,1,KHAR(FSTRG,K))
      IF(ACHAR.EQ."1") V1=1
      V=V+V1/2**KI
3120  CONTINUE
      IF(JM.EQ.-1)V=-V
      IF(KL.LE.408) X(KL)=V*2.**J1
      IF(KL.GT.408) Y(KJL)=V*2.**J1
3111  CONTINUE
3110  CONTINUE
      IF(IOCLOS(5)) STOP
      DO 3 I=1,N
3     CALB(I)=CMPLX(X(I),Y(I))
C
C######  END OF DATA READ
C
      IF(IOWRIT(10,2,0,NAME3)) STOP
      ABIB(1)=SFREQ
      BBIB(1)=SFREQ
      ABIB(2)=2.
      BBIB(2)=2.
      WRITE(10,102)(ABIB(J),J=1,4)
102   FORMAT(' ',4E15.5)
C
C###### FOR MORE DETAILS ON THE METHOD SEE REF ABOVE
C
      DO 21 I=1,N
C
C##########  SEE REPORT KU-FRL-417-22 FOR DETAILS
C
      C1 = CALA(I)/CALB(I)
      THETA = ATAN2(AIMAG(C1)/REAL(C1))/2.
      CALA(I)=CMPLX(COS(THETA),SIN(THETA))
C
C########  WRITE TO DISK NEW PHASE CAL VALUES
C
      WRITE(10,101) CALA(I)
101   FORMAT(' ',2E15.5)
21    CONTINUE
      IF(IOCLOS(10)) STOP
      STOP
      END
C
C###### FIND BIT PATTERN FOR GIVEN INTEGER
C
      SUBROUTINE SUB1(JP,CSTRG)
      CHARACTER*16 BSTRG,B(8),CSTRG,SUBSTG
      INTEGER*2 JO(3)
      DATA B/"000","001","010","011","100","101","110","111"/
```

```
      BSTRG=""
      CSTRG=""
      JO(1) =MOD(JP,8)
      JP1  = JP/8
      JO(2) =MOD(JP1,8)
      JO(3) = JP1/8
      DO 31 JI=1,3
      JP=JO(JI)+1
31    CALL INSERT(B(JP),BSTRG,1)
      DO 32 JI=1,8
      JK= 10-JI
      CALL ADDSTG(CSTRG,SUBSTG(BSTRG,JK,JK))
32    CONTINUE
      RETURN
      END
```

C.2.8 LISTING OF INTSTY.FOR

```
CCCCCCCCCCCCCCCCCCCCCCCCCCCCCCCCCCCCCCCCCCCCCCCCCCCCCCCCCCCCCCCCCCCCCCC
C                                                                     C
C                                                                     C
C                                                                     C
C        PROGRAM TO CALCULATE THE INTENSITY SPECTRUM                  C
C                                                                     C
C                                                                     C
C                                                                     C
CCCCCCCCCCCCCCCCCCCCCCCCCCCCCCCCCCCCCCCCCCCCCCCCCCCCCCCCCCCCCCCCCCCCCCC
C
C
C##########           VERSION   : 1.1              ###############
C##########        PROGRAMMER   : R.NAVANEETHAN    ###############
C##########              DATE   : 19-JAN-84        ###############
C
C
C########## A WORD ABOUT THE WAY THIS PROGRAM IS WRITTEN !!!!!!
C##########
C########## EACH SPECTRAL DATA ARRAY IS ASSOCIATED WITH AN
C########## ADDITIONAL ARRAY WHICH DEFINES THE RELEVANT PARA
C########## METERS ASSOCIATED WITH THE ARRAY.  FOR INTENSITY
C########## SPECTRUM THESE ARE SAMPLING FREQUENCY (ANALYSIS
C########## FREQUENCY RANGE), MIC SPACING AND AREA ASSOCITAED
C########## WITH THE MEASUREMENTS.  ADDITIONALLY, ONE MORE SPEC
C########## CAN ALSO BE INCLUDED.  THESE FOUR VALUES ARE STORED
C########## IN THE BEGINNING OF EACH INTENSITY SPECTRUM DATA
C########## ON THE DISK. THE UNIT OF INTENSITY VALUES STORED
C########## IS WATT/M^2.
C
C
C######  INPUT DATA REQUIRED:
C######      1. DATA FILE CONTAINING XPSFILE NAME, FREQUENCY
C######         RANGE, INPUT MAX AMPLITUDE CHANNEL A, INPUT
C######         MAX AMPLITUDE CHANNEL B, NUMBER OF AVERAGES
C######         MICROPHONE SPACING AND AREA ASSOCIATED WITH
C######         EACH MICROPHONE.  THIS FILE SHOULD BE NAMED
C######         XPSCAT.DAT. AND SHOULD BE AVAILABLE ON THE
C######         DISK A: REFER TO TEST PROCEDURE IN KU-FRL
C######         REPORT KU-FRL-417-22.
C######      2. MAGNITUDE CAL DATA WITH FILE NAME CALDAT.DAT
C######         THIS FILE IS AUTOMATICALLY CREATED WHEN
C######         MAGNITUDE CALIBRATION IS PERFORMED
C######      3. PHASE CALIBRATION DATA UNDER FILE NAME
C######         CALII.DLO (OR CALII.DHI).  IF METHOD II
C######         CALIBRATION IS USED, RENAME FILE INTCAL.DLO
C######         (OR INTCAL.DHI) TO CALII.DLO (OR CALII.DHI)
C
C
```

```
C######  DIMENSION STATEMENTS
C
      COMPLEX AXPS(408),CAL(408)
      COMPLEX CMPLX
      REAL BBIB(4),BINT(408),X(408),Y(408),SPL(408),AREA(100)
      REAL SFREQ(100),AIN(100),BIN(100),AVG(100),SPAC(100)
      CHARACTER*1 ANS,ACHAR
      CHARACTER*15 INAME(100),NAME
      CHARACTER *3 IN
      CHARACTER *5 OUT
      CHARACTER*16 FSTRG,CSTRG
      INTEGER*1 IJ(72)
      DATA OUT/"ASP00"/
      DATA IN/"AIN"/
      DATA NAME/"B:XSS00L.000"/
      DATA SPL/408*0.0/
C
C###### READ MAG CAL FACTORS
C
      IF(IOREAD(6,2,0,"A:CALDAT.DAT"))  GOTO 421
      GO TO 422
421   CONTINUE
      WRITE(1,423)
423    FORMAT(' ERROR OPENING FILE A:CALDAT.DAT')
      STOP
422   CONTINUE
      READ(6,700) ACAL,BCAL
      READ(6,700) ARAN,BRAN
      READ(6,701) NAVGA,NAVGB
700   FORMAT(2E15.5)
701   FORMAT(2I5)
      IF (IOCLOS(6)) STOP
C
C###### READ XPS FILENAME AND TEST DETAILS
C
      IF (IOREAD(6,2,0,"A:XPSCAT.DAT")) GOTO 671
      GO TO 672
671   WRITE(1,673)
673   FORMAT(' ERROR OPENING FILE A:XPSCAT.DAT')
      STOP
672   CONTINUE
      J=1
322   CONTINUE
      READ(6,323,ENDFILE=324)INAME(J),SFREQ(J),AIN(J),BIN(J),
     &AVG(J),SPAC(J),AREA(J)
      J=J+1
      GO TO 322
323   FORMAT(A12,1X,6F0.0)
```

```
324   JFILE=J-1
      CONTINUE
      IF (IOCLOS(6)) STOP
C
C####### READ PHASE CAL VALUES
C
      NAME="A:CALII.DLO"
      IF (SFREQ(1).GT.1001) NAME="A:CALII.DHI"
      IF(IOREAD(9,2,0,NAME)) GOTO 961
      GOTO 962
 961  WRITE(1,963)
963   FORMAT(' ERROR OPENING A:CALII.DLO OR A:CALII.DHI FILE')
      STOP
962   CONTINUE
      READ(9,103) A1,A2,A3,A4
103   FORMAT(4F15.5)
      DO 120 I=1,408
      READ(9,121) CAL(I)
121   FORMAT(2E15.5)
120   CONTINUE
      IF (IOCLOS(9)) STOP
C
C####### CHANGE DISK FOR OUTPUT FILES
C
      WRITE(1,800)
800   FORMAT(' REMOVE PROGRAM DISK IN DRIVE A:; INSERT
     &OUTPUT DISK AND HIT RETURN'$)
      PAUSE
      CONTINUE
C
C######  CHANGE N DEPENDING ON THE ANALYZER SPEC
C
      N=408
C
C#######  MAIN LOOP FOR FILES
C
      DO 900 IC=1,JFILE
      IF (IFIX(SFREQ(IC)+.05).NE.IFIX(A1+.05)) GO TO 1000
752   CONTINUE
      IF(IORAND(72,72,9,0,INAME(IC))) GO TO 750
      GO TO 751
750   CONTINUE
      WRITE(1,780)
780   FORMAT(' CHANGE INPUT FILE DISK IN DRIVE B: AND HIT
     &RETURN'$)
      PAUSE
      GO TO 752
751   CONTINUE
```

```
      WRITE(1,798) INAME(IC)
798   FORMAT(' ',A0)
      KL=0
      DO 10 I=1,34
      READ(9/I)(IJ(K),K=1,72)
C
C####### CONVERT FROM 3 BYTES FROM NICOLET 660B TO 4 BYTE
C####### REAL VALUES OF SUPERSOFT FORTRAN
C
      DO 11 J=1,72,3
      KL=KL+1
      KJL= KL-408
      J1=IJ(J)
      J2=IJ(J+1)
      J3=IJ(J+2)
      IF(J3.LT.0)J3=256+J3
      JM=1
      IF(J2.LT.0) JM=-1
      JP=IABS(J2)
      CALL SUB1(JP,CSTRG)
      FSTRG=CSTRG
      CALL SUB1(J3,CSTRG)
      CALL INSERT(CSTRG,FSTRG,1)
      V=0.
      DO 20 KI=1,15
      K=16-KI
      V1=0
      CALL PUTCHR(ACHAR,1,KHAR(FSTRG,K))
      IF(ACHAR.EQ."1") V1=1
      V=V+V1/2**KI
20    CONTINUE
      IF(JM.EQ.-1)V=-V
      IF(KL.LE.408) X(KL)=V*2.**J1
      IF(KL.GT.408) Y(KJL)=V*2.**J1
11    CONTINUE
10    CONTINUE
      IF(IOCLOS(9)) STOP
      BBIB(1)=SFREQ(IC)
      BBIB(2)=2.
      BBIB(3)=SPAC(IC)*.0254
      BBIB(4)=AREA(IC)*.0254*.0254
C
C######   DATA FOR OUTPUT FILE SPEC
C
      NAME=INAME(IC)
      CALL PUTCHR(NAME,1,KHAR(IN,1))
      CALL PUTCHR(NAME,3,KHAR(IN,2))
      CALL PUTCHR(NAME,4,KHAR(IN,3))
```

```
C
C######  CORRECT FOR MAG AND PHASE CAL
C
      TEMP=ACAL*BCAL*(AIN(IC)*BIN(IC))/(ARAN*BRAN)/(AVG(IC)
     &/FLOAT(NAVGA))
      DO 111 I=1,N
      X(I)=X(I)*TEMP
      Y(I)=Y(I)*TEMP
      AXPS(I)=CMPLX(X(I),Y(I))
111   CONTINUE
      DO 4 I=1,N
      AXPS(I)=AXPS(I)*CAL(I)
4     CONTINUE
C
C###### OPEN & WRITE OUTPUT FILE
C
      IF(IOWRIT(10,2,0,NAME)) GO TO 755
      GOTO 756
755   WRITE(1,757)
757   FORMAT(' ERROR IN OPENING OUT PUT FILE'$)
      STOP
756   CONTINUE
      WRITE(10) (BBIB(I),I=1,4)
C123   FORMAT(1X,4E15.5)
C
C
C######  CALCULATE INTENSITY
C
C
      DO 5 I=1,N
      BINT(I)=AIMAG(AXPS(I))
C
C######  STD SEA LEVEL VALUE FOR DENSITY OF AIR WAS ASSUMED.
C######  FOR BETTER ACCURACY, DENSITY SHOULD BE CALCULATED
C
      RHO=1.225
      BINT(I)=BINT(I)/(1.225*BBIB(3))
C
C######  THE FOLLOWING STATEMENT DEPENDS ON THE ANALYZER
C
      OMEGA=2.*3.1415962*FLOAT(I-1)*BBIB(1)*2.56/1024.
      BINT(I)=BINT(I)/OMEGA
      WRITE(10) BINT(I)
C104   FORMAT(' ',E15.5)
5     CONTINUE
      IF(IOCLOS(10)) STOP
      DO 6 I=1,N
      SPL(I)=SPL(I)+BINT(I)*BBIB(4)
```

```
6     CONTINUE
 900  CONTINUE
      NAME=INAME(1)
      CALL PUTCHR(NAME,1,KHAR(OUT,1))
     .CALL PUTCHR(NAME,3,KHAR(OUT,2))
      CALL PUTCHR(NAME,4,KHAR(OUT,3))
      CALL PUTCHR(NAME,6,KHAR(OUT,4))
      CALL PUTCHR(NAME,7,KHAR(OUT,5))
      WRITE(1,790)
790   FORMAT(' REMOVE OUTPUT DISK IN DRIVE A: AND INSERT SPL
     &DISK'$)
      PAUSE
      CONTINUE
      IF (IOWRIT(9,2,0,NAME)) STOP
      DO 791 I=1,N
      FR=FLOAT(I-1)*SFREQ(1)*2.56/1024.
      WRITE(9,792) FR,SPL(I)
791   CONTINUE
792   FORMAT(' ',2E15.5)
      IF (IOCLOS(9)) STOP
      GO TO 999
1000  CONTINUE
      WRITE(1,764)
764   FORMAT(' ERROR IN THE ANALYSIS RANGE SPEC')
999   CONTINUE
      STOP
      END
C
C###### FIND BIT PATTERN CORRESPONDING TO AN INTEGER
C
      SUBROUTINE SUB1(JP,CSTRG)
      CHARACTER*16 BSTRG,B(8),CSTRG,SUBSTG
      INTEGER*2 JO(3)
      DATA B/"000","001","010","011","100","101","110","111"/
      BSTRG=""
      CSTRG=""
      JO(1) =MOD(JP,8)
      JP1  = JP/8
      JO(2) =MOD(JP1,8)
      JO(3) = JP1/8
      DO 31 JI=1,3
      JP=JO(JI)+1
31    CALL INSERT(B(JP),BSTRG,1)
      DO 32 JI=1,8
      JK= 10-JI
      CALL ADDSTG(CSTRG,SUBSTG(BSTRG,JK,JK))
32    CONTINUE
      RETURN
```

C.2.9 LISTING OF TL7475.BAS

```
1 '#######################################################
2 '#                                                     #
3 '#         TRANSMISSION LOSS PLOT PROGRAM              #
4 '#                                                     #
5 '#######################################################
6 '#
7 '#                PROGRAMMER : R.NAVANEETHAN
8 '#                   VERSION : 2
9 '#                      DATE : 3-9-84
10 '#
11 '#
100 DIM TL(817),FR(817),P(6)
110 DEFINT I
120  RRAD=57.29578
130 DEF FNALOG(X)=LOG(X)/LOG(10)
140  E$=CHR$(3)
150 REM PROGRAM TRANSMISSION LOSS PLOT
160 XLBL$="FREQUENCY ~ HZ "
170 YLBL$="TRANSMISSION LOSS ~ DB"
180 INPUT"TURN ON PLOTTER, AND HIT RETURN WHEN READY", A$
190 OPEN "COM1:9600,E,7,1" AS #1
200 'CLEAR PLOTTER
210 PRINT #1,"DF;OE;"
220 FOR IK=1 TO 100:NEXT IK
230 IF LOC(1)=0 THEN 230
240 FOR IK=1 TO 100:NEXT IK
250 A$= INPUT$(LOC(1),#1)
260 IF VAL(A$)=0 THEN GOTO 290
270 PRINT ; "PRINTER ERROR ";VAL(A$);" OCCURED!"
280 STOP
290 'CONTINUE
300 PRINT #1,"IP 1543,1488,9559,7520;"
310 X1=FNALOG(20):Y1=0:X2=FNALOG(5000):Y2=60:GOSUB 2190
320 'SET CHARACTER SIZES'
330 H=1.5:AR=1.5:AOR=0!:SL=0!:GOSUB 2000
340 INPUT "ENTER PEN NUMBER (1 THRU 8) = ",I1
350 PRINT #1,("SP"+STR$(I1)+";")
360 'END OF PEN SELECTION
370 INPUT "DO YOU WANT TO DRAW AXIS <Y/N> = " ,Y$
380 IF (Y$<>"Y" AND Y$<>"N") THEN GOTO 370
390 IF Y$="N" THEN GOTO 890
400 'DRAW AXIS'
410 XCORD=FNALOG(20):YCORD=0!:II=-2!:GOSUB 1660
420 XCORD=FNALOG(5000):YCORD=0!:II=2!:GOSUB 1660
430 XCORD=FNALOG(5000):YCORD=60:II=2!:GOSUB 1660
440 XCORD=FNALOG(20):YCORD=60:II=2!:GOSUB 1660
450 XCORD=FNALOG(20):YCORD=0!:II=-1!:GOSUB 1660
460 ' X-AXIS
```

```
470 J=1
480 FOR I=2 TO 10
490 XCORD=FNALOG(10*I*J):YCORD=0!:II=0!:GOSUB 1660
500 XINC=0!:YINC=0:II=-2:GOSUB 1810
510 IF I<>10 THEN XINC=0!:YINC=.9:II=-1:GOSUB 1810
520 IF I=10 THEN XINC=0!:YINC=1.8:II=-1:GOSUB 1810
530 IF I<>10 THEN CW=-.4:CH=-1.6:GOSUB 1960
540 IF I=10 THEN CW=(-1!*FNALOG(J*100)/2):CH=-2.8:GOSUB 1960
550 L1$=RIGHT$(STR$(I),1)
560 IF(I=10 AND J=1) THEN L1$="100"
570 IF(I=10 AND J=10) THEN L1$="1000"
580 LBL$=L1$:GOSUB 2540
590 IF (J=100 AND I=5) GOTO 630
600 NEXT I
610 J=J*10
620 GOTO 480
630 'CONTINUE
640 XCORD=FNALOG(300):YCORD=0!:I=1:GOSUB 1660
650 XINC=0!:YINC=-4!:II=1:GOSUB 1810
660 CW=-7:CH=-1:GOSUB 1960
670 H=2:AR=1.5:AOR=0!:SL=0:GOSUB 2000
680 A$="LB"+XLBL$+E$
690 PRINT #1,A$
700 ' START Y AXIS
710 XCORD=FNALOG(20):YCORD=0!:II=1:GOSUB 1660
720 H=1.5:AR=1.5:AOR=0!:SL=0:GOSUB 2000
730 FOR I=0 TO 60 STEP 10
740 XCORD=FNALOG(20):YCORD=I:II=1!:GOSUB 1660
750 XINC=FNALOG(1.07):YINC=0:II=2:GOSUB 1810
760 PRINT #1,"PU;"
770 CW=-4!:CH=-.3:GOSUB 1960
780 A$="LB"+RIGHT$(STR$(I),2)+E$
790 PRINT #1,A$
800 XCORD=FNALOG(20):YCORD=I:II=1:GOSUB 1660
810 NEXT I
820 XCORD=FNALOG(20):YCORD=30:II=1:GOSUB 1660
830 XINC=-FNALOG(1.25):YINC=0:II=1:GOSUB 1810
840 H=2!:AR=1.5:AOR=90!:SL=0!:GOSUB 2000
850 CW=-10!:CH=0!:GOSUB 1960
860 A$="LB"+YLBL$+E$
870 PRINT #1,A$
880 'END OF YAXIS
890 'PLOT DATA
900 PRINT "LOW FREQUENCY DATA"
910 IKMAX=1:IFLG=1
920 GOSUB 1310
930 KIMAX=KIMAX
940 IFLG=2
```

```
950 PRINT "HIGH FREQUENCY DATA"
960 GOSUB 1310
970 IKMAX=IKMAX-1
980 'CONTINUE
990 FOR I=1 TO IKMAX
1000 X=FR(I)
1010 Y=TL(I)
1020 IF I=1 THEN XCORD=FNALOG(X):YCORD=Y:II=3:GOSUB 1660
1030 IF I<>1 THEN XCORD=FNALOG(X):YCORD=Y:II=2:GOSUB 1660
1040 NEXT I
1050 PRINT #1, "PU;"
1060 INPUT "WANT LEAST SQUARE LINE <Y/N> = ",Y$
1070 IF Y$<>"Y" THEN GOTO 1270
1080 INPUT "MIN FREQUENCY FOR LEAST SQUARE LINE? = ",AMF
1090 SUMX=0!:SUMY=0!:SUMX2=0!:SUMXY=0!
1100 N1=0
1110 FOR I=1 TO IKMAX
1120 IF FR(I)<AMF THEN GOTO 1170
1130 T1=FNALOG(FR(I))
1140 N1=N1+1
1150 SUMX=SUMX+T1:SUMY=SUMY+TL(I)
1160 SUMX2=SUMX2+T1^2:SUMXY=SUMXY+T1*TL(I)
1170 NEXT I
1180 SLOP=(SUMXY-SUMX*SUMY/N1)/(SUMX2-SUMX^2/N1)
1190 YINT = (SUMY-SLOP*SUMX)/N1
1200 X=FNALOG(AMF):Y=SLOP*X+YINT
1210 INPUT "ENTER PEN NUMBER (1 THRU 8) = ",I1
1220 PRINT #1,("SP"+STR$(I1)+";")
1230 XCORD=X:YCORD=Y:II=3:GOSUB 1660
1240 X=FNALOG(5000):Y=SLOP*X+YINT
1250 XCORD=X:YCORD=Y:II=2:GOSUB 1660
1260 PRINT #1,"SP;"
1270 'CONTINUE
1280 INPUT "WANT TO PLOT MORE CURVES <Y/N> = ",Y$
1290 IF Y$="Y" GOTO 300
1300 END
1310 'ROUTINE TO READ DATA
1320 LINE INPUT;"FILE NAME OF DATA WITHOUT PANEL = ",FILE1$
1330 PRINT
1340 OPEN "I",#2,FILE1$
1350 LINE INPUT;"FILE NAME OF DATA WITH PANEL = ",FILE2$
1360 PRINT
1370 OPEN "I",#3,FILE2$
1380 K=IKMAX
1390 K1=17:K2=401
1400 IF IFLG=2 THEN K1=41
1410 FOR I=1 TO 402
1420 INPUT #2, X1,Y1
```

```
1430 INPUT #3, X2,Y2
1440 IF((I<K1) OR (I>K2)) THEN 1510
1450 IF (Y1<0) THEN Y1=1E-12
1460 IF (Y2<0) THEN Y2=1E-12
1470 TL(K)= 10*FNALOG(Y1)-10*FNALOG(Y2)
1480 IF(IFLG=1) THEN FR(K)=(I-1)*1.25
1490 IF(IFLG=2) THEN FR(K)=(I-1)*12.5
1500 K=K+1
1510 NEXT I
1520 IKMAX=K
1530 CLOSE #2:CLOSE#3
1540 RETURN
1550 ' SUBROUTINE FIND INTEGER FROM OUTPUT STRING
1560 B$="":J=1
1570 FOR I=1 TO NLOC-1
1580 C$=MID$(A$,I,1)
1590 IF C$="," THEN GOTO 1620
1600 B$=B$+C$
1610 GOTO 1630
1620 P(J)=VAL(B$):J=J+1:B$=""
1630 NEXT I
1640 P(J)=VAL(B$)
1650 RETURN
1660 'SUBROUTINE PLOT
1670 IE=INT(II/2)*2
1680 IF(II>0 AND IE=II) THEN PRINT #1,"PD;"
1690 IF(II>0 AND IE<>II) THEN PRINT #1,"PU;"
1700 XSCL=XCORD*XRATIO+XKNST
1710 YSCL=YCORD*YRATIO+YKNST
1720 IF ABS(XSCL>32767) THEN PRINT "X TOO LARGE":RETURN
1730 IF ABS(YSCL>32767) THEN PRINT "Y TOO LARGE":RETURN
1740 IXSCL=FIX(XSCL):IYSCL=FIX(YSCL)
1750 A$="PA"+STR$(IXSCL)+","+STR$(IYSCL)
1760 PRINT #1,A$
1770 IF(II>0) THEN RETURN
1780 IF(II=IE) THEN PRINT #1,"PD;"
1790 IF(II<>IE) THEN PRINT #1,"PU;"
1800 RETURN
1810 'SUBROUTINE INCREMENTAL PLOT
1820 IE=INT(II/2)*2
1830 IF(II>0 AND IE=II) THEN PRINT #1,"PD;"
1840 IF(II>0 AND IE<>II) THEN PRINT #1,"PU;"
1850 XSCL=XINC*XRATIO
1860 YSCL=YINC *YRATIO
1870 IF ABS(XSCL>32767) THEN PRINT "X TOO LARGE":RETURN
1880 IF ABS(YSCL>32767) THEN PRINT "Y TOO LARGE":RETURN
1890 IXSCL=FIX(XSCL):IYSCL=FIX(YSCL)
1900 A$="PR"+STR$(IXSCL)+","+STR$(IYSCL)
```

```
1910 PRINT #1,A$
1920 IF(II>0) THEN RETURN
1930 IF(II=IE) THEN PRINT #1,"PD;"
1940 IF(II<>IE) THEN PRINT #1,"PU;"
1950 RETURN
1960 'SUBROUTINE CHARCATER MOVE
1970 A$="CP"+STR$(CW)+","+STR$(CH)+";"
1980 PRINT #1,A$
1990 RETURN
2000 'SET CHARACTER SIZES'
2010 RRAD=57.29578
2020 AORR=AOR/RRAD
2030 SLR=SL/RRAD
2040 PR=XNUM/YNUM
2050 W=INT(1000!*(H/AR)/PR)/1000!
2060 IF (W>127.999) THEN W=127.999
2070 IF (H>127.999) THEN H=127.999
2080 A$="SR"+STR$(W)+","+STR$(H)+";"
2090 PRINT #1,A$
2100 RISE=INT(1000!*100!*SIN(AORR))/1000!
2110 RUNN =INT(1000!*100!*COS(AORR))/1000!
2120 A$="DI"+STR$(RUNN)+","+STR$(RISE)+";"
2130 PRINT #1,A$
2140 SLR=INT(1000*SIN(SLR)/COS(SLR))/1000
2150 A$="SL"+STR$(SLR)+";"
2160 PRINT #1,A$
2170 'END OF CHAR SIZE
2180 RETURN
2190 'SET SCALE WITH ARGUMENTS X1,X2,Y1,Y2
2200 NLOC=0:A$=""
2210 PRINT #1,"OP;"
2220 IF LOC(1) =0 THEN 2220
2230 ACHR$=INPUT$(1,#1)
2240 A$=A$+ACHR$:NLOC=NLOC+1
2250 IF ASC(ACHR$)=13 THEN GOTO 2260 ELSE 2220
2260 'CONTINUE
2270 GOSUB 1550
2280 P1X= P(1):P1Y=P(2):P2X=P(3):P2Y=P(4)
2290 XNUM=P2X-P1X
2300 YNUM=P2Y-P1Y
2310 XP1=X1:XP2=X2:YP1=Y1:YP2=Y2
2320 XRATIO=XNUM/(XP2-XP1)
2330 YRATIO=YNUM/(YP2-YP1)
2340 XKNST=P1X-XP1*XRATIO
2350 YKNST=P1Y-YP1*YRATIO
2360 PRINT #1,"IW;"
2370 RETURN
2380 'END SCALE
```

```
2390 'ROUTINE LABEL PLOT WITH ARGUMENTS LBL$
2400 PRINT "ENTER LABEL (LESS THAN 80 CHARCATERS) "
2410 PRINT "PRINT ZZZ IF DONE"
2420 INPUT L$
2430 ILEN=LEN(L$)
2440 IF L$="ZZZ" THEN GOTO 2520
2450 PRINT "MOVE PEN TO DESIRED POSITION AND ";
2460 INPUT "HIT RETURN WHEN SATISFIED  ",Y$
2470 PRINT
2480 H=1.5:AR=1.5:AOR=0:SL=0:GOSUB 2000
2490 LBL$=L$:GOSUB 2540
2500 CW = -1*ILEN:CH=-1.2: GOSUB 1960
2510 GOTO 2400
2520 'CONTINUE
2530 RETURN
2540 'ROUTINE TO LABEL PLOTS WITH ARGUMENT LBL$
2550 E$=CHR$(3)
2560 A$="LB"+LBL$+E$+";"
2570 PRINT #1,A$
2580 RETURN
```

C.2.10 LISTING OF INTVAL.FOR

```
CCCCCCCCCCCCCCCCCCCCCCCCCCCCCCCCCCCCCCCCCCCCCCCCCCCCCCCCCCCCCCCCCCCCCCC
C                                                                     C
C                                                                     C
C       PROGRAM TO TO COLLECT INTENSITY VALUES AT                     C
C       A SPECIFIED FREQUENCY FROM THE INTENSITY                      C
C                      DATA FILES                                     C
C                                                                     C
C                                                                     C
CCCCCCCCCCCCCCCCCCCCCCCCCCCCCCCCCCCCCCCCCCCCCCCCCCCCCCCCCCCCCCCCCCCCCCC
C
C
C#######          PROGRAMMER : R.NAVANEETHAN
C#######             VERSION : 2
C#######                DATE : 1-MAR-84
C
C
C#######       INPUT DATA FILE: A CATALOG FILE WHICH CONTAINS
C#######                        NAMES OF ALL INTENSITY DATA
C#######                        FILES
C
      DIMENSION AINT(402)
      CHARACTER*12 NAME,NAME1
      CHARACTER*1 CHRA,CHRB
      WRITE(1,100)
2     CONTINUE
100   FORMAT(' ENTER FREQUENCY VALUE OF INTEREST')
      READ(1,101) FREQ
101   FORMAT(F0.0)
1     CONTINUE
      ICOUNT = FREQ/1.25+1
      IF (FREQ.GT.500.05) ICOUNT =FREQ/12.5+1
      IF(FREQ.LE.500.) CHRB = "L"
      IF(FREQ.GT.500.05) CHRB = "H"
      WRITE(1,103)
103   FORMAT(' ENTER CATALOG FILE NAME CONTAINING INTENSITY
     &DATA FILE NAMES')
      READ(1,104) NAME
104   FORMAT(A0)
      WRITE(1,105)
105   FORMAT(' INSERT FIRST DATA DISK IN DRIVE B:')
      PAUSE
 3    CONTINUE
      JC=0
      IF (IOREAD(6,2,0,NAME)) STOP
 4    CONTINUE
      READ(6,106,ENDFILE=5) NAME1
106   FORMAT(A0)
      WRITE(1,130) NAME1
```

```
130   FORMAT(' ',A12)
      CALL PUTCHR(CHRA,1,KHAR(NAME1,8))
      JC=JC+1
      IF(CHRA.NE.CHRB) GO TO 999
10    CONTINUE
      IF(IOREAD(7,2,0,NAME1)) GO TO 8
      GO TO 9
 8    CONTINUE
      WRITE(1,107)
107   FORMAT(' INSERT 2ND DATA DISK DRIVE IN DRIVE B:'$)
      PAUSE
      GO TO 10
9     CONTINUE
      READ(7) B1,B2,B3,B4
C
C#####  READ FROM FILE CONTAINING UNFORMATTED DATA
C
C120   FORMAT(4E15.5)
C
      DO 11 I=1,ICOUNT
      READ(7) BINT
C108   FORMAT(E15.5)
11    CONTINUE
      IF (BINT.LE.0.) BINT=1.E-12
      AINT(JC)=10.*(ALOG10(BINT/1.E-12))
      IF (IOCLOS(7)) STOP
      GO TO 4
5     CONTINUE
      IF (IOCLOS(6)) STOP
      JK=JC
      WRITE(1,109)
109   FORMAT(' ENTER NAME FOR OUTPUT FILE')
      READ(1,110) NAME
110   FORMAT(A0)
      IF (IOWRIT(10,2,0,NAME)) STOP
      DO 12 I=1,JK
      WRITE(10,111) AINT(I)
111   FORMAT(' ',F15.5)
12    CONTINUE
      IF (IOCLOS(10)) STOP
      GO TO 1000
999   WRITE(1,200)
200   FORMAT(' SOMETHING IS WRONG IN FILE NAMES!!!')
1000  CONTINUE
      STOP
      END
```

C.2.11 LISTING OF INTMAP.FOR

```
CCCCCCCCCCCCCCCCCCCCCCCCCCCCCCCCCCCCCCCCCCCCCCCCCCCCCCCCCCCCCCCCCCCCCCC
C                                                                      C
C                                                                      C
C         INTENSITY MAP INTERPOLATION PROGRAM                          C
C                                                                      C
C                                                                      C
CCCCCCCCCCCCCCCCCCCCCCCCCCCCCCCCCCCCCCCCCCCCCCCCCCCCCCCCCCCCCCCCCCCCCCC
C
C
C########                VERSION : 2
C########              PROGRAMMER : R. NAVANEETHAN
C########              DATE       : 22-FEB-84
C
C
C########  THIS PROGRAM GIVEN 81 POINTS OF INTENSITY VALUES AT
C########  81 LOCATIONS INTERPOLATES DATA AND OUPUTS DATA FILE
C########  WHICH CAN DIRECTLY PLOT INTENSITY MAP.  PLOT PROGRAM
C########  IS CALLED P7475IN. IT WILL PLOT INTENSITY MAP ON
C########  HP 7475 DIGITAL PLOTTER
C
C
C
C########  INPUT DATA : DATA FILE CONTAINING 81 INTENSITY DATA
C
C
C########  DIMENSION STATEMENTS
C
      DIMENSION A(9,9),AX(9),AY(9)
      DIMENSION B1(810),B2(810),IB3(810),IC(810)
      CHARACTER*15 INAME,ONAME
      DATA INAME/""/
      DATA ONAME/""/
      WRITE(1,700)
700   FORMAT(' ENTER INPUT FILE NAME = '$)
      READ(1,122) INAME
122   FORMAT(A0)
      WRITE(1,701)
701   FORMAT(' ENTER OUTPUT FILE NAME = '$)
      READ(1,122) ONAME
123   CONTINUE
      WRITE(1,702)
702   FORMAT(' ENTER CONTOUR INTERVAL IN dB (10. OR 5. OR 2.
     &OR 1. = '$)
      READ(1,703) CONINT
703   FORMAT(F0.0)
      IF(.NOT.((CONINT.EQ.10.).OR.(CONINT.EQ.5.).OR.
     &(CONINT.EQ.2).OR.(CONINT.EQ.1))) GO TO 123
      IF(CONINT.EQ.10.) ICON=1
```

```
      IF(CONINT.EQ.5.)  ICON = 2
      IF(CONINT.EQ.2.)  ICON = 3
      IF(CONINT.EQ.1) ICON=4
C
C######  THE FOLLOWING LOOPS ASSIGN THE INTENSITY VALUES
C######  TO AN ARRAY WHICH REPRESENTS THE TEST GRID.
C
      IF(IOREAD(8,2,0,INAME)) STOP
      DO 10 J=1,9
      DO 10 I=1,9
      READ (8,300) A(I,J)
  300 FORMAT (F0.0)
   10 CONTINUE
C
C######  THE FOLLOWING LOOPS TRANSLATE GRID LOCATIONS INTO
C######  LOCATIONS DEFINED BY THE DISTANCE FROM THE MPD EDGE.
C
      DO 11 I=1,9
      AX(I) = 1 + 2.*FLOAT(I-1)
      AY(I) = 1 + 2.*FLOAT(I-1)
   11 CONTINUE
      IF(IOCLOS(8)) STOP
C
C######  FOLLOWING LOOPS DO THE INTERPOLATION BETWEEN POINTS IN
C######  A HORIZONTAL DIRECTION.  THE LOCATION OF EACH DIVISION
C######  OF CONINT DECIBELS BETWEEN THE POINTS WILL BE FOUND
C######  FOR MAPPING PURPOSES.
C
      IF(IOWRIT(10,2,0,"INT1.TMP")) STOP
C     OPEN(UNIT=10,NAME='INT1.TMP',TYPE='NEW')
      DO 20 J=1,9
      DO 20 I=1,8
      Y2 = A((I+1),J)
      Y1 = A(I,J)
      X2 = AX(I+1)
      X1 = AX(I)
      IF(Y2.EQ.Y1) GO TO 20
C
C###### ENSURE THAT Y2 IS ALWAYS GREATER THAN Y1.
C
      IF (Y2.GE.Y1) GO TO 23
      X1TEMP = X1
      Y1TEMP = Y1
      Y1=Y2
      Y2=Y1TEMP
      X1=X2
      X2=X1TEMP
   23 CONTINUE
```

```
      SLOPE = (X2 - X1)/(Y2 - Y1)
      CALL INVAL(Y1,Y2,ZCAL,ICON)
   21 CONTINUE
      IF (ZCAL.GT.Y2) GO TO 22
      XLOC = (SLOPE*(ZCAL - Y1)) + X1
      WRITE (10,100) XLOC,AY(J),INT(ZCAL)
      ZCAL = ZCAL + CONINT
      GO TO 21
   22 CONTINUE
   20 CONTINUE
C
C###### THE FOLLOWING LOOPS DO THE INTERPOLATION BETWEEN POINTS
C###### IN VERTICAL DIRECTION.  THE LOCATION OF EACH DIVISION
C###### OF CONINT DECIBELS BETWEEN POINTS WILL BE FOUND FOR
C###### MAPPING PURPOSES.
C
      DO 30 I=1,9
      DO 30 J=1,8
      Y2 = A(I,(J+1))
      Y1 = A(I,J)
      X2 = AY(J+1)
      X1 = AY(J)
      IF(Y2.EQ.Y1) GO TO 30
C
C######  ENSURE THAT Y2 IS ALWAYS GREATER THAN Y1.
C
      IF (Y2.GE.Y1) GO TO 33
      X1TEMP = X1
      Y1TEMP = Y1
      Y1 = Y2
      Y2 = Y1TEMP
      X1 = X2
      X2 = X1TEMP
   33 CONTINUE
      SLOPE = (X2 - X1)/(Y2 - Y1)
      CALL INVAL(Y1,Y2,ZCAL,ICON)
   31 CONTINUE
      IF (ZCAL.GT.Y2) GO TO 32
      YLOC = (SLOPE*(ZCAL - Y1)) + X1
      WRITE (10,100) AX(I),YLOC,INT(ZCAL)
      ZCAL = ZCAL + CONINT
      GO TO 31
   32 CONTINUE
   30 CONTINUE
      IF(IOCLOS(10)) STOP
  100 FORMAT (1X,F6.2,1X,F6.2,1X,I3)
C
C######  SORTING DATA INTO SEQUENTIAL DIVISIONS OF CONINT DBS
```

```
C
      IF (IOREAD(9,2,0,"INT1.TMP")) STOP
C     OPEN(UNIT=9,NAME='INT1.TMP',TYPE='OLD')
      I = 1
   40 CONTINUE
      READ(9,200,ENDFILE=45) B1(I),B2(I),IB3(I)
  200 FORMAT (F6.2,1X,F6.2,1X,I3)
      I = I + 1
      GO TO 40
   41 CONTINUE
   45 NS = I - 1
      IF(IOCLOS(9)) STOP
      CALL SORT (NS,IB3,IC)
      IF(IOWRIT(11,2,0,ONAME)) STOP
C     OPEN(UNIT=11,NAME=ONAME,TYPE='NEW')
      DO 42 J=1,NS
      J2 = IC(J)
      WRITE(11,100) B1(J2),B2(J2),IB3(J2)
   42 CONTINUE
      IF(IOCLOS(11)) STOP
      STOP
      END
C
C######  A MODIFIED BUBBLE SORT WRITTEN BY R.NAVANEETHAN
C
      SUBROUTINE SORT(NS,IA,IC)
      DIMENSION IA(810),KSORT(810),IC(810)
      DO 1 IS=1,NS
      IC(IS) = IS
      KSORT(IS) = IA(IS)
    1 CONTINUE
      DO 3 IS=1,NS-1
      DO 2 JS=1,NS-IS
      IF(KSORT(JS).LE.KSORT(JS+1)) GO TO 2
      IT = KSORT(JS)
      ITC = IC(JS)
      KSORT(JS) = KSORT(JS+1)
      IC(JS) = IC(JS+1)
      KSORT(JS+1) = IT
      IC(JS+1) = ITC
    2 CONTINUE
    3 CONTINUE
      RETURN
      END
C
C###### FIND INTITIAL VALUE TO START MAPPING
C
      SUBROUTINE INVAL(Y1,Y2,ZCAL,ICONT)
```

```
      IF(ICONT.NE.1) GO TO 1
      ZCAL=FLOAT(INT(Y1/10.)*10)+10.
      GO TO 4
1     CONTINUE
      IF(ICONT.NE.2) GO TO 2
      DEC=(Y1-FLOAT(INT(Y1/10.0)*10))/10.
      IF (DEC.LT.0.5) ZCAL= FLOAT(INT(Y1/10.))*10.+5.
      IF (DEC.GE.0.5) ZCAL = FLOAT(INT((Y1 + 10.)/10.)*10.)
      GO TO 4
2     CONTINUE
      IF(ICONT.NE.3) GO TO 5
      IDEC=MOD(INT(Y1),2)
      IF(IDEC.EQ.1) ZCAL=FLOAT(INT(Y1))+1.
      IF(IDEC.EQ.0) ZCAL=FLOAT(INT(Y1))+2.
      GO TO 4
5     CONTINUE
      ZCAL=INT(Y1)+1.
4     CONTINUE
      RETURN
      END
```

C.2.12 LISTING OF PIN7475.BAS

```
1 '#####################################################
2 '#                                                   #
3 '#         INTENSITY MAP PLOTTING                    #
4 '#                                                   #
5 '#####################################################
6 '#
7 '#         PROGRAMMER : R.NAVANEETHAN
8 '#            VERSION : 1
9 '#               DATE : 3-1-84
10 '#
11 '#
100 DEFINT I
110   RAD=57.29578
120  E$=CHR$(3)
130 REM PROGRAM INTENSITY MAP PLOT
140 XLBL$="MICROPHONE HORIZONTAL LOCATION (INCHES)"
150 YLBL$="MICROPHONE VERTICAL LOCATION (INCHES)"
160 INPUT"TURN ON PLOTTER, AND HIT RETURN WHEN READY", A$
170 OPEN "COM1:9600,E,7,1" AS #1
180 'CLEAR PLOTTER
190 PRINT #1,"DF;OE;"
200 FOR IK=1 TO 100:NEXT IK
210 IF LOC(1)=0 THEN 210
220 FOR IK=1 TO 100:NEXT IK
230 A$= INPUT$(LOC(1),#1)
240 IF VAL(A$)=0 THEN GOTO 270
250 PRINT ; "PRINTER ERROR ";VAL(A$);" OCCURED!"
260 STOP
270 'CONTINUE
280 PRINT #1,"IP 2000,2000,7000,7000;"
290 X1=0!:Y1=0!:X2=18!:Y2=18!:GOSUB 1640
300 'SET CHARACTER SIZES'
310 H=2!:AR=1.5:AOR=0!:SL=0!:GOSUB 1460
320 'SET PEN VELOCITY AND PEN #1
330 PRINT "ENTER PEN VELOCITY ";
335 INPUT "0=NORMAL OTHERWISE BETWEEN 0-38 = ",I1
340 IF I1=0 THEN PRINT #1,"VS;":GOTO 360
350 PRINT #1,("VS"+RIGHT$(STR$(I1),1)+";")
360 'CONTINUE
370 INPUT "ENTER PEN NUMBER (1 THRU 8) = ",I1
380 PRINT #1,("SP"+STR$(I1)+";")
390 'END OF PEN SELECTION
400 INPUT "DO YOU WANT TO DRAW AXIS <Y/N> = " ,Y$
410 IF (Y$<>"Y" AND Y$<>"N") THEN GOTO 400
420 IF Y$="N" THEN GOTO 810
430 'DRAW AXIS'
440 XCORD=0:YCORD=0!:I=-2!:GOSUB 1120
450 XCORD=18:YCORD=0!:I=2!:GOSUB 1120
```

```
460 XCORD=18:YCORD=18!:I=2!:GOSUB 1120
470 XCORD=0:YCORD=18!:I=2!:GOSUB 1120
480 XCORD=0:YCORD=0!:I=-1!:GOSUB 1120
490 ' X-AXIS
500 FOR IJ=0 TO 18 STEP 2
510 XCORD=IJ:YCORD=0!:I=0!:GOSUB 1120
520 XINC=0!:YINC=0:I=-2:GOSUB 1270
530 XINC=0!:YINC=.3:I=-1:GOSUB 1270
540 CW=-.9:CH=-1.3:GOSUB 1420
550 A$="LB"+RIGHT$(STR$(IJ),2)+E$
560 PRINT #1,A$
570 NEXT IJ
580 XCORD=9!:YCORD=0!:I=1:GOSUB 1120
590 XINC=0!:YINC=-1.2:I=1:GOSUB 1270
600 CW=-18!:CH=-1!:GOSUB 1420
610 A$="LB"+XLBL$+E$
620 PRINT #1,A$
630 ' START Y AXIS
640 XCORD=0!:YCORD=0!:I=1:GOSUB 1120
650 FOR IJ=2 TO 18 STEP 2
660 XCORD=0:YCORD=IJ:I=0!:GOSUB 1120
670 XINC=0!:YINC=0:I=-2:GOSUB 1270
680 XINC=.3:YINC=0:I=-1:GOSUB 1270
690 CW=-3.3:CH=-.3:GOSUB 1420
700 A$="LB"+RIGHT$(STR$(IJ),2)+E$
710 PRINT #1,A$
720 NEXT IJ
730 XCORD=0!:YCORD=9!:I=1:GOSUB 1120
740 XINC=-1.2:YINC=0:I=1:GOSUB 1270
750 H=2!:AR=1.5:AOR=90!:SL=0!:GOSUB 1460
760 CW=-18!:CH=0!:GOSUB 1420
770 A$="LB"+YLBL$+E$
780 PRINT #1,A$
790 H=2!:AR=1.5:AOR=0!:SL=0!:GOSUB 1460
800 'END OF YAXIS
810 'PLOT DATA
820 INPUT "ENTER NAME OF DATA FILE = ", NFILE$
830 OPEN "I", #2,NFILE$
840 ISYM=0:IINT=-999
850 X1=0!:Y1=18:X2=18!:Y2=0!:GOSUB 1640
860 IF  EOF(2) GOTO 940
870 INPUT #2, XPOS,YPOS,INTSTY
880 IF IINT=-999 THEN IVFRST=INTSTY
890 IF IINT<>INTSTY THEN ISYM=ISYM+1:INPUT"HIT RETURN",CR$
900 IINT=INTSTY
910 XCORD=XPOS:YCORD=YPOS:I=1:GOSUB 1120
920 PRINT #1,"PU;":GOSUB 1810
930 GOTO 860
```

```
940 IVLAST=INTSTY
950 CLOSE #2
960 INPUT "WANT TO LABEL <Y/N> = ",Y$
970 IF Y$="Y" THEN GOSUB 1950
980 INPUT "WANT TO PLOT ANOTHER MAP <Y/N> = ",Y$
990 IF Y$="Y" THEN GOTO 280
1000 END
1010 ' SUBROUTINE FIND INTEGER FROM OUTPUT STRING
1020 B$="":J=1
1030 FOR I=1 TO NLOC-1
1040 C$=MID$(A$,I,1)
1050 IF C$="," THEN GOTO 1080
1060 B$=B$+C$
1070 GOTO 1090
1080 P(J)=VAL(B$):J=J+1:B$=""
1090 NEXT I
1100 P(J)=VAL(B$)
1110 RETURN
1120 'SUBROUTINE PLOT
1130 IE=INT(I/2)*2
1140 IF(I>0 AND IE=I) THEN PRINT #1,"PD;"
1150 IF(I>0 AND IE<>I) THEN PRINT #1,"PU;"
1160 XSCL=XCORD*XRATIO+XKNST
1170 YSCL=YCORD*YRATIO+YKNST
1180 IF ABS(XSCL>32767) THEN PRINT "X TOO LARGE":RETURN
1190 IF ABS(YSCL>32767) THEN PRINT "Y TOO LARGE":RETURN
1200 IXSCL=FIX(XSCL):IYSCL=FIX(YSCL)
1210 A$="PA"+STR$(IXSCL)+","+STR$(IYSCL)
1220 PRINT #1,A$
1230 IF(I>0) THEN RETURN
1240 IF(I=IE) THEN PRINT #1,"PD;"
1250 IF(I<>IE) THEN PRINT #1,"PU;"
1260 RETURN
1270 'SUBROUTINE INCREMENTAL PLOT
1280 IE=INT(I/2)*2
1290 IF(I>0 AND IE=I) THEN PRINT #1,"PD;"
1300 IF(I>0 AND IE<>I) THEN PRINT #1,"PU;"
1310 XSCL=XINC*XRATIO
1320 YSCL=YINC *YRATIO
1330 IF ABS(XSCL>32767) THEN PRINT "X TOO LARGE":RETURN
1340 IF ABS(YSCL>32767) THEN PRINT "Y TOO LARGE":RETURN
1350 IXSCL=FIX(XSCL):IYSCL=FIX(YSCL)
1360 A$="PR"+STR$(IXSCL)+","+STR$(IYSCL)
1370 PRINT #1,A$
1380 IF(I>0) THEN RETURN
1390 IF(I=IE) THEN PRINT #1,"PD;"
1400 IF(I<>IE) THEN PRINT #1,"PU;"
1410 RETURN
```

```
1420 'SUBROUTINE CHARCATER MOVE
1430 A$="CP"+STR$(CW)+","+STR$(CH)+";"
1440 PRINT #1,A$
1450 RETURN
1460 'SET CHARACTER SIZES'
1470 AORR=AOR/RAD
1480 SLR=SL/RAD
1490 PR=XNUM/YNUM
1500 W=INT(1000*(H/AR)/PR)/1000
1510 IF (W>127.999) THEN W=127.999
1520 IF (H>127.999) THEN H=127.999
1530 A$="SR"+STR$(W)+","+STR$(H)+";"
1540 PRINT #1,A$
1550 RISE=INT(1000*100*SIN(AORR))/1000
1560 RUNN =INT(1000*100*COS(AORR))/1000
1570 A$="DI"+STR$(RUNN)+","+STR$(RISE)+";"
1580 PRINT #1,A$
1590 SLR=INT(1000*SIN(SLR)/COS(SLR))/1000
1600 A$="SL"+STR$(SLR)+";"
1610 PRINT #1,A$
1620 'END OF CHAR SIZE
1630 RETURN
1640 'SET SCALE WITH ARGUMENTS X1,X2,Y1,Y2
1650 PRINT #1,"OP;"
1660 IF LOC(1) =0 THEN 1660
1670 FOR IK=1 TO 200:NEXT IK
1680 NLOC=LOC(1)
1690 A$=INPUT$(LOC(1),#1)
1700 GOSUB 1010
1710 P1X= P(1):P1Y=P(2):P2X=P(3):P2Y=P(4)
1720 XNUM=P2X-P1X
1730 YNUM=P2Y-P1Y
1740 XP1=X1:XP2=X2:YP1=Y1:YP2=Y2
1750 XRATIO=XNUM/(XP2-XP1)
1760 YRATIO=YNUM/(YP2-YP1)
1770 XKNST=P1X-XP1*XRATIO
1780 YKNST=P1Y-YP1*YRATIO
1790 PRINT #1,"IW;"
1800 'END SCALE
1810 ' ROUTINE SYMBOL WITH ARGUMENT ISYM
1820 H=2.5:AR=1.5:AOR=0!:SL=0!:GOSUB 1460
1830 PRINT #1,"SI.175,.35;"
1840 IF ISYM=1 THEN A$="UC-99,-3,-3,99,6,0,0,6,
-6,0,0,-6,-99,3,3;"
1850 IF ISYM=2 THEN A$="UC-99,0,4,99,-3,-6,6,0,
-3,6,-99,0,-4;"
1860 IF ISYM=3 THEN A$="UC-99,-3,2,99,6,0,-3,
-6,-3,6,-99,3,-2;"
```

```
1870 IF ISYM=4 THEN A$="UC-99,-1,3,99,-2,-2,0,
-2,2,-2,2,0,2,2,0,2,-2,2,-2,0,-99,1,-3;"
1880 IF ISYM=5 THEN A$="UC-99,3,0,99,-3,4,-3,
-4,3,-4,3,4,-99,-3,0;"
1890 IF ISYM=6 THEN A$="UC-99,2,2,99,-6,0,6,
-6,0,6,-99,-2,-2;"
1900 IF (ISYM <1 AND ISYM > 6) THEN GOTO 1920
1910 PRINT #1,A$
1920 'CONTINUE
1930 H=1.5:AR=1.5:AOR=0!:SL=0!:GOSUB 1460
1940 RETURN
1950 'ROUTINE LABEL PLOT WITH  IVFRST,IVLAST,ISYM
1960 ISYMM =ISYM
1970 PRINT "ENTER LABEL (LESS THAN 80 CHARCATERS) "
1980 PRINT "PRINT ZZZ IF DONE"
1990 INPUT L$
2000 ILEN=LEN(L$)
2010 IF L$="ZZZ" THEN GOTO 2090
2020 PRINT "MOVE PEN TO DESIRED POSITION AND";
2030 INPUT "HIT RETURN WHEN SATISFIED  ",Y$
2040 PRINT
2050 H=1.5:AR=1.5:AOR=0:SL=0:GOSUB 1460
2060 LBL$=L$:GOSUB 2240
2070 CW = -1*ILEN:CH=-1.2: GOSUB 1420
2080 GOTO 1970
2090 INCRMT=(IVLAST-IVFRST)/(ISYMM-1)
2100 INUM=IVFRST-INCRMT
2110 CW=3!:CH=-2.2:GOSUB 1420
2120 FOR IK=1 TO ISYMM
2130 IV=IK
2140 INUM=INUM+INCRMT
2150 IVAR=INUM
2160 L$=RIGHT$(STR$(INUM),3)
2170 ISYM=IV:GOSUB 1810
2180 CW=1!:CH=-.4:GOSUB 1420
2190 LBL$= "= "+L$+" DB": GOSUB 2240
2200 CW=-10.4:CH=-1.2:GOSUB 1420
2210 NEXT IK
2220 H=2!:AR=1.5:AOR=0:SL=0:GOSUB 1460
2230 RETURN
2240 'ROUTINE TO LABEL PLOTS WITH ARGUMENT LBL$
2250 E$=CHR$(3)
2260 A$="LB"+LBL$+E$+";"
2270 PRINT #1,A$
2280 RETURN
```

APPENDIX D

ABSORPTION COEFFICIENT MEASUREMENT ROUTINES

D.1 FLOW CHART OF TEST ROUTINES

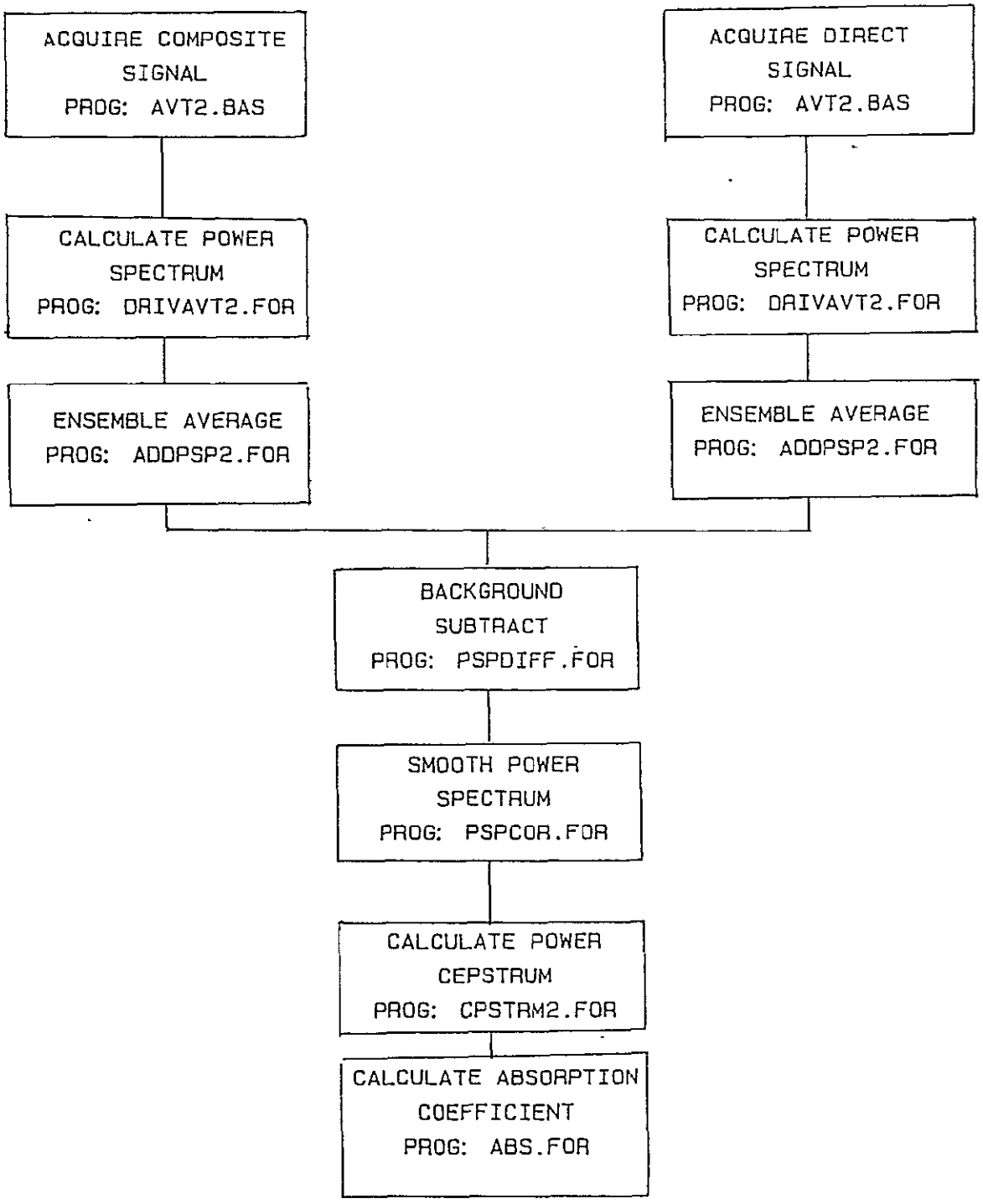

D.2 LISTING OF COMPUTER ROUTINES

D.2.1 LISTING OF AVT2.BAS

```
1 'PROGRAM AVT2
2 'THIS PROGRAM TRANSFERS AVERAGE TIME SIGNAL OF CHANNEL B
3 'THIS PROGRAM IS USED IN ABSORPTION COEFFICIENT PROGRAM
10 SCREEN 0,0
20 DEFINT I-N
30 DIM V(1030)
40 CLS:CLOSE
50 LOCATE 25,1
60 C$="ZZZ0A31SY250SY261SY296SWAJ1F2E0Z=8"
70 PRINT STRING$(60," ")
80 SYN$=CHR$(22)
90 LOCATE 1,1
100 SPEED$="9600"
110 COMFIL$="COM1:"+SPEED$+",N,8,2"
120 OPEN "SCRN:" FOR OUTPUT AS #2
130 LOCATE 25,1:PRINT "AVG TIME TRANSFER PROGRAM";
140 LOCATE 1,1:PRINT STRING$(60," "):LOCATE 1,1
150 LINE INPUT "INPUT FILE? <TYPE E TO EXIT > :";DSKFIL$
160 IF DSKFIL$="E" THEN 650
170 OPEN COMFIL$ AS #1
180 LOCATE 1,1:PRINT STRING$(60," "):LOCATE 1,1
190 OPEN "O",#3,DSKFIL$
200 J=0
210 FOR IC%=1 TO 34
220 D$=MID$(C$,IC%,1)
230 GOSUB 390
240 NEXT IC%
250 REM CONTINUE
260 LOCATE 1,1
270 GOSUB 440
280 D$="Z":GOSUB 390
290 D$="Z":GOSUB 390
300 D$="=":GOSUB 390
310 D$="9":GOSUB 390
320 GOSUB 440
330 CLOSE #1
340 FOR I= 1 TO 1024 STEP 4
350 PRINT #3,USING"###.##^^^^ ";V(I),V(I+1);V(I+2);V(I+3)
360 NEXT I
370 CLOSE #3:CLS
380 GOTO 130
390 PRINT #1,D$;
400 FOR IK%=1 TO 200:NEXT IK%
410 IF LOC(1)<>1 THEN 410
420 A$=INPUT$(1,#1)
430 IF ASC(A$)=6 THEN RETURN ELSE PRINT #2,"ERROR SENDING DATA":STOP
440 REM CONTINUE
450 FOR IC%=1 TO 65
```

```
460 PRINT #1,SYN$;
470 IF LOC(1)<96 THEN 470
480 H1$ = INPUT$(96,#1)
490 R$=H1$
500 GOSUB 550
510 NEXT IC%
520 IF LOC(1)<>1 THEN PRINT LOC(1):GOTO 520
530 A$=INPUT$(1,#1)
540 RETURN
550 K1=1:K2=8
560 IF IC%=65 THEN K2=1
570 FOR IM=K1 TO K2
580 J=J+1
590 IM2=12*(IM-1)
600 F$=MID$(R$,IM2+4,6)
610 E$=MID$(R$,IM2+10,6)
620 V(J)=VAL(F$+"E"+E$)
630 NEXT IM
640 RETURN
650 CLOSE:END
```

D.2.2 LISTING OF DRIVAVT2.FOR

```
CCCCCCCCCCCCCCCCCCCCCCCCCCCCCCCCCCCCCCCCCCCCCCCCCCCCCCCCCCCCCCCCCCCCCCCCCCC
C                                                                           C
C                                                                           C
C                  DRIVER ROUTINE FOR CEPSTRUM                              C
C                                                                           C
C                                                                           C
CCCCCCCCCCCCCCCCCCCCCCCCCCCCCCCCCCCCCCCCCCCCCCCCCCCCCCCCCCCCCCCCCCCCCCCCCCC
C
C
C
C##########  PROGRAMMER : R. NAVANEETHAN           ##################
C##########     VERSION : 3                       ##################
C##########        DATE : 29-MAR-84               ##################
C
C
      PROGRAM DRIV3
      DIMENSION XR(1024),XI(1024),TR(1025)
      CHARACTER*15 ANAME,BNAME
      DATA PI/3.14154926/
      DATA TR/1025*0./
C
C######  SET PROGRAM PARAMETERS AND READ CATALOG FILE NAME
C
      N=1024
      N3=N/2+1
      N2=2*1024
      WRITE (*,300)
300   FORMAT(' ENTER SCALE VALUE = '$)
      READ(*,*) SCL
      WRITE (*,301)
301   FORMAT (' ENTER # OF POINTS IN TIME HISTORY TO BE USED '$)
      READ (*,*) NN
      F=5.*PI/NN
      K2=NN+1
      IK=8*NN/10
      JK2=9*NN/10
      JK1=NN/10
      WRITE (*,302)
302   FORMAT(' ENTER CAT FILE NAME = '$)
      READ (*,*) BNAME
      OPEN (6,FILE=BNAME,STATUS='OLD')
1     CONTINUE
      READ(6,100,END=51) ANAME
100   FORMAT(A15)
      WRITE(*,303) ANAME
303   FORMAT(' ',A15)
C
C###### READ DATA FROM DATA FILES
```

```
C
      OPEN (9,FILE=ANAME,STATUS='OLD')
      DO 2 J=1,N,4
      READ(9,102) XI(J),XI(J+1),XI(J+2),XI(J+3)
102   FORMAT(E10.2,3(1X,E10.2))
2     CONTINUE
      CLOSE(9)
C
C###### APPLY SIN 2 WINDOW TO THE DATA SEQUENCE OF NN POINTS
C
      DO 3 I=1,NN
      XR(I)=XI(I)*SCL
      IF((I-1).LE.JK1) XR(I)=XR(I)*(SIN(F*(I-1)))**2
      IF((I-1).GE.JK2) XR(I)=XR(I)*(SIN(F*(I-1-IK)))**2
3     CONTINUE
      DO 5 I=K2,N
5     XR(I)=0.
      DO 7 I=1,N
7     XI(I)=0.
C
C###### CALCULATE FFT
C
      INV=0
      CALL FT01A(XR,XI,N,INV)
      IF(INV.EQ.-1) GOTO 1000
C
C###### FIND POWER SPECTRUM. SPEC YET TO CORRECTED FOR ANALYSIS WIDTH
C
      DO 8  I=1,N3
8     TR(I)= TR(I)+(XR(I)**2+XI(I)**2)
      GO TO 1
51    CONTINUE
C
C###### WRITE AVERAGED POWER-SPECTRUM TO DISK
C
      OPEN (10,FILE='A:POWLSP.DAT',STATUS='NEW')
      DO 9 I=1,N3
9     WRITE(10,304) TR(I)
304   FORMAT(1X,E11.5)
      CLOSE(10)
      GO TO 1010
1000  WRITE(*,501)
501   FORMAT(' ERROR IN FFT ROUTINE')
1010  CONTINUE
      STOP
      END
```

D.2.3 LISTING OF ADDPSP2.FOR

```
CCCCCCCCCCCCCCCCCCCCCCCCCCCCCCCCCCCCCCCCCCCCCCCCCCCCCCCCCCCCCCCCCCCCCCCCCCCCCC
C                                                                             C
C                    ADD POWER SPECTRUM FROM FILES                            C
C                                                                             C
CCCCCCCCCCCCCCCCCCCCCCCCCCCCCCCCCCCCCCCCCCCCCCCCCCCCCCCCCCCCCCCCCCCCCCCCCCCCCC
C
C
C##############    PROGRAMMER : R.NAVANEETHAN     ########################
C##############         DATE : 24-APR-84          ########################
C##############       VERSION : 2                 ########################
C
C
      PROGRAM ADDPSP
      REAL X(513)
      CHARACTER *15 CATFIL,FILNAM
      WRITE (*,200)
200   FORMAT('ENTER CATALOG FILENAME FOR ENERGY SUM OF PSP = '$)
      READ (*,*) CATFIL
      J=0
      OPEN (12,FILE=CATFIL,STATUS='OLD')
23    READ(12,201,END=202) FILNAM
201   FORMAT(A15)
      J=J+1
      K=J+1
      OPEN (K,FILE=FILNAM,STATUS='OLD')
      GO TO 23
202   CONTINUE
      DO 1 I=1,513
      XSUM=0.
      DO 3 JJ=1,J
      K=JJ+1
      READ (K,101) XV
      XSUM=XSUM+XV
3     CONTINUE
      X(I)=XSUM/(25.*J)
1     CONTINUE
      DO 4  JJ= 1,J
      K=JJ+1
      CLOSE(K)
4     CONTINUE
      OPEN (15,FILE='B:NNAVGPSP.DAT',STATUS='NEW')
      DO 2 I=1,513
2     WRITE(15,101) X(I)
101   FORMAT(1X,E11.5)
      CLOSE(15)
      STOP
      END
```

D.2.4 LISTING OF PSPDIFF.FOR

```
CCCCCCCCCCCCCCCCCCCCCCCCCCCCCCCCCCCCCCCCCCCCCCCCCCCCCCCCCCCCCCCCCCCCCCCCCCC
C                                                                           C
C                                                                           C
C                  PSP DIFF CALCULATION                                     C
C                                                                           C
C                                                                           C
CCCCCCCCCCCCCCCCCCCCCCCCCCCCCCCCCCCCCCCCCCCCCCCCCCCCCCCCCCCCCCCCCCCCCCCCCCC
C
C
C
C##########  PROGRAMMER : R. NAVANEETHAN          ###################
C##########     VERSION : 2                       ###################
C##########        DATE : 2-MAY-84                ###################
C
C
C234567
      PROGRAM PSPDIF
      DIMENSION TR(513)
      DOUBLE PRECISION E1,E2
      CHARACTER*15 ANAME,BNAME
      DATA PI/3.14154926/
C
C######  READ INPUT AVERAGED POWER SPECTRUM FROM A FILE
C
      WRITE (*,100)
100   FORMAT(' ENTER FILE NAME CONTAINING COMPOSITE SIGNAL = '$)
      READ (*,*) ANAME
      WRITE (*,501)
501   FORMAT (' ENTER ENSEMBLE SUM = '$)
      READ (*,*) ES1
      WRITE (*,101)
101   FORMAT(' ENTER FILE NAME CONTAINING DIRECT SIGNAL = '$)
      READ (*,*) BNAME
      WRITE (*,501)
      READ (*,*) ES2
      N=512
      N2=2*N
      NK=N+1
      OPEN (9,FILE=ANAME,STATUS='OLD')
      OPEN (8,FILE=BNAME,STATUS='OLD')
      DO 1 I=1,NK
      READ(8,201) X
      READ(9,201) Y
      E1=X/ES2
      E2=Y/ES1
1     TR(I)=DLOG(E2)-DLOG(E1)
201   FORMAT(1X,E11.5)
      CLOSE(9)
```

```
      CLOSE(8)
      OPEN(10,FILE='B:PSPDIF.DAT',STATUS='NEW')
      DO 5 I=1,NK
      WRITE(10,201)TR(I)
5     CONTINUE
      CLOSE(10)
      STOP
      END
```

D.2.5 LISTING OF PSPCOR.FOR

```
CCCCCCCCCCCCCCCCCCCCCCCCCCCCCCCCCCCCCCCCCCCCCCCCCCCCCCCCCCCCCCCCCCCCCCCCCCCCCCC
C                                                                              C
C               SMOOTH THE BACKGOROUND SUBTRACTED SPECTRUM                     C
C                                                                              C
CCCCCCCCCCCCCCCCCCCCCCCCCCCCCCCCCCCCCCCCCCCCCCCCCCCCCCCCCCCCCCCCCCCCCCCCCCCCCCC
C
C
C##############       PROGRAMMER : R.NAVANEETHAN    ####################
C##############            DATE : 23-APR-84         ####################
C##############          VERSION : 2                ####################
C
C
      PROGRAM PSPCOR
      DIMENSION X(513)
      CHARACTER *15 ANAME,BNAME
      N=512
      NK=N+1
      WRITE (*,100)
100   FORMAT (' ENTER INPUT DATA FILE = '$)
      READ (*,102) ANAME
102.  FORMAT(A15)
      WRITE (*,101)
101   FORMAT (' ENTER OUTPUT DATA FILE = '$)
      READ (*,102) BNAME
      WRITE (*,103)
103   FORMAT(' CHANGE VALUES UPTO NUMBER = '$)
      READ(*,*) I1
      OPEN (9,FILE=ANAME,STATUS='OLD')
      DO 1 I=1,NK
      READ(9,201) X(I)
201   FORMAT(1X,E11.5)
1     CONTINUE
      DO 2 I= 1,I1
      WRITE(*,104)
104   FORMAT(' ENTER NEW VALUE = '$)
      READ(*,*) AV
      X(I)=AV
2     CONTINUE
      CLOSE (9)
      OPEN (8,FILE=BNAME,STATUS='NEW')
      DO 3 I=1,NK
      WRITE(8,201) X(I)
3     CONTINUE
      CLOSE (8)
      STOP
      END
```

D.2.6 LISTING OF CPSTRM2.FOR

```
CCCCCCCCCCCCCCCCCCCCCCCCCCCCCCCCCCCCCCCCCCCCCCCCCCCCCCCCCCCCCCCCCCCCCCCCCCCCCCC
C                                                                              C
C                                                                              C
C                    CEPSTRUM CALCULATION                                      C
C                                                                              C
C                                                                              C
CCCCCCCCCCCCCCCCCCCCCCCCCCCCCCCCCCCCCCCCCCCCCCCCCCCCCCCCCCCCCCCCCCCCCCCCCCCCCCC
C
C
C
C##########  PROGRAMMER : R. NAVANEETHAN            ###################
C##########     VERSION : 6                         ###################
C##########        DATE : 2-MAY-84                  ###################
C
C
C234567
      PROGRAM CPSTRM
      DIMENSION XR(1024),XI(1024),TR(513)
      DOUBLE PRECISION E1,E2
      CHARACTER*15 ANAME,BNAME
      DATA PI/3.14154926/
C
C###### READ INPUT AVERAGED POWER SPECTRUM FROM A FILE
C
      WRITE (*,100)
100   FORMAT(' ENTER FILE NAME CONTAINING COMPOSITE SIGNAL = '$)
      READ (*,*) ANAME
      WRITE (*,501)
501   FORMAT (' ENTER ENSEMBLE SUM = '$)
      READ (*,*) ES1
      N=512
      N2=1024
      NK=N+1
      OPEN (9,FILE=ANAME,STATUS='OLD')
      DO 1 I=1,NK
      READ(9,201) Y
      TR(I)=Y
201   FORMAT(1X,E11.5)
      CLOSE(9)
      XR(1)=TR(1)
      XI(1)=0.
      DO 2 I=2,N
      XR(I)=TR(I)
      K=N2+2-I
      XR(K)=TR(I)
      XI(I)=0.
2     XI(K)=0.
      XR(NK)=TR(NK)
```

```
      XI(NK)=0.
      INV=1
      CALL FT01A(XR,XI,N2,INV)
      IF(INV.EQ.-1) GOTO 1000
      OPEN(10,FILE='B:POWCPS.DAT',STATUS='NEW')
      DO 5 I=1,NK
      WRITE(10,201)XR(I)
5     CONTINUE
      CLOSE(10)
      GO TO 1010
1000  WRITE(*,106)
106   FORMAT(' ERROR IN FFT ROUTINE')
1010  CONTINUE
      STOP
      END
```

D.2.7 LISTING OF ABSCOFF.FOR

```
CCCCCCCCCCCCCCCCCCCCCCCCCCCCCCCCCCCCCCCCCCCCCCCCCCCCCCCCCCCCCCCCCCCCCCCCCC
C                                                                       C
C                                                                       C
C       ROUTINE FOR CALCULATION OF ABS COEFF FROM CEPSTRUM              C
C                                                                       C
C                                                                       C
CCCCCCCCCCCCCCCCCCCCCCCCCCCCCCCCCCCCCCCCCCCCCCCCCCCCCCCCCCCCCCCCCCCCCCCCCC
C
C
C
C##########  PROGRAMMER : R. NAVANEETHAN          ###################
C##########     VERSION : 1                       ###################
C##########        DATE : 2-MAY-84                ###################
C
C
      PROGRAM ABSORP
      DIMENSION XR(256),XI(256),TR(129)
      DOUBLE PRECISION E
      CHARACTER*15 ANAME,BNAME,CNAME
      DATA PI/3.14154926/
      DATA TR/129*0./
C
C######  SET PROGRAM PARAMETERS AND READ CEPSTRM FILE NAME
C
      N=128
      N2=2*N
      NK=N+1
      WRITE (*,300)
300   FORMAT(' ENTER RATIO L1/L2 = '$)
      READ(*,*) SCL
301   FORMAT(' ENTER # OF POINTS FOR ANALYSIS = '$)
      WRITE (*,301)
      READ (*,*) NN
501   FORMAT(' ENTER START POINT = '$)
      WRITE(*,501)
      READ (*,*) NST
      F=5.*PI/NN
      IK=8*NN/10
      JK2=9*NN/10
      JK1=NN/10
      WRITE (*,302)
302   FORMAT(' ENTER CEPSTRUM FILE NAME = '$)
      READ (*,*) BNAME
      OPEN (6,FILE=BNAME,STATUS='OLD')
C
C###### READ DATA FROM DATA FILE
C
      OPEN (9,FILE=BNAME,STATUS='OLD')
```

```
      DO 502 J=1,NST-1
502   READ (9,201) V
      DO 2 J=1,NN
      READ(9,201) V
      XI(J)=V
2     CONTINUE
      CLOSE(9)
C
C###### APPLY SIN 2 WINDOW TO THE DATA SEQUENCE OF NN POINTS
C
      DO 3 I=1,NN
      XR(I)=XI(I)*SCL
      IF((I-1).LE.JK1) XR(I)=XR(I)*(SIN(F*(I-1)))**2
      IF((I-1).GE.JK2) XR(I)=XR(I)*(SIN(F*(I-1-IK)))**2
3     CONTINUE
C
C###### EXTEND SERIES TO 256  POINTS
C
      DO 5 I=NN+1,N2
5     XR(I)=0.
      DO 7 I=1,N2
7     XI(I)=0.
C
C###### CALCULATE FFT
      OPEN(11,FILE='B:HTAU.DAT',STATUS='NEW')
      DO 165 I=1,N2
      WRITE(11,201)XR(I)
165   CONTINUE
      CLOSE (11)
C
      INV=0
      CALL FT01A(XR,XI,N2,INV)
      IF(INV.EQ.-1) GOTO 1000
C
C###### FIND POWER SPECTRUM AND ABSORPTION COEFFICIENT
C
      DO 8  I=1,N+1
8     TR(I)= 1.-(XR(I)**2+XI(I)**2)
      OPEN(10,FILE='B:ABS.DAT',STATUS='NEW')
      DO 65 I=1,NK
      WRITE(10,201)TR(I)
201   FORMAT(1X,E11.5)
65    CONTINUE
      CLOSE(10)
      GO TO 51
1000  WRITE(*,106)
106   FORMAT(' ERROR IN FFT ROUTINE')
51    CONTINUE
```

```
STOP
END
```

APPENDIX E

COMPUTER ROUTINES USED IN PREDICTION OF INTERIOR NOISE LEVEL

E.1 LISTING OF DRIVER.FOR.

```
CCCCCCCCCCCCCCCCCCCCCCCCCCCCCCCCCCCCCCCCCCCCCCCCCCCCCCCCCCCCCCCCCCCCCCCCCCCCCCC
C                                                                              C
C                                                                              C
C                    SOUND TREATMENT CALCULATION PROGRAM                       C
C                                                                              C
C                                                                              C
CCCCCCCCCCCCCCCCCCCCCCCCCCCCCCCCCCCCCCCCCCCCCCCCCCCCCCCCCCCCCCCCCCCCCCCCCCCCCCC
C
C
C
C############           PROGRAMMER : R.NAVANEETHAN      ####################
C############             VERSION : 1                  ##################
C############                DATE : FEB 15, 1984       ####################
C
C
C#######
C         INPUT DATA :
C                      THE NAME OF THE DATA FILE NEEDS TO BE INPUT
C                      INTERACTIVELY.  SEE USER'S MANUAL FOR THE
C                      INPUT DATA AND FILE FORMAT
C
C        OUTPUT DATA :
C                      BOTH ON PRINTER AND DATA FILE (NAME TO BE
C                      SPECIFIED INTERACTIVELY
C
C        OTHER DETAILS:
C                       THE M PROGRAM DRIVER IS ON THIS FILE
C                       NAMED 'DRIV.FOR'.  THE SUBROUTINES ARE
C                       ARE AVAILABLE ON A FILE NAMED 'T2LYER.FOR'.
C                       THE FUNCTIONS NOT AVAILABLE IN THE SYSTEM
C                       LIBRARY OF MINC ARE GIVEN IN 'CLAYER.FOR'.
C                       TO EXECUTE COMPILE DRIV,T2LYER,CLAYER AND
C                       LINK TO GET AN EXECUTABLE FILE 'DRIV.SAV'.
C                       THIS HAS BEEN DONE ALREADY FOR THIS VERSION.
C                     IF FORTRAN SOURCE FILES ARE MODIFIED THEN
C                       REPEAT THE ABOVE PROCEDURE.
C
C        TO RUN THE PROGRAM:
C                                1. PREPARE DATA FILE ACCORDING TO
C                                   USER'S MANUAL.
C                                2. TYPE 'RUN DRIV <CR>'
C                                3. WHEN ASKED FOR,GIVE INPUT DATA
C                                   FILE AND OUTPUT DATA FILE.
C
C        FILE NAME FORMAT IN MINC :
C                      REFER RT11 OPERATING MANUAL
C
C
```

```
C
C234567
      PROGRAM SPL
C
C########  THIS PROGRAM CONTROLS THE SOUND TREATMENT REQUIRED FOR AN
C########  AIRCRAFT
C
      REAL DELTL(5,23),SPLWO(5,23),SPLW(5,23),SCAREA(5),SECWT(5)
      REAL SPL(5),FREQ(23),TLT(23),PR(2),TP(2),AWT(23),SPLA(5)
      BYTE INAME(15),ONAME(15),OUTFIL(5,15)
      COMMON /MAIN/ PR,TP,AMACH
      DATA INAME,ONAME/30*' '/
      DATA OUTFIL/75*' '/
      DATA FREQ/31.5,40.,50.,63.,80.,100.,125.,160.,200.,250.,315.,
     &400.,500.,630.,0.,1000.,1250.,1600.,2000.,2500.,3150.,4000.,
     &5000./
      DATA AWT/-39.4,-34.6,-30.2,-26.2,-22.5,-19.1,-16.1,-13.4,-10.9,
     &-8.6,-6.6,-4.8,-3.2,-1.9,-.8,0.,.6,1.,1.2,1.3,1.2,1.,.5/
      NFREQ=23
C
C########  READ INTERNAL SOUND PRESSURE LEVEL WITHOUT ANY TREATMENT
C
      TYPE *,' ENTER NAME OF THE INPUT FILE '
      ACCEPT 100,(INAME(I),I=1,14)
C
C########  READ OUTPUT FILE NAME
C
      TYPE*,' ENTER NAME OF THE OUTPUT FILE '
      ACCEPT 100,(ONAME(I),I=1,14)
100   FORMAT(14A1)
C
C########  OPEN AND READ INPUT DATA FILE
C
      OPEN (UNIT=8,NAME=INAME,TYPE='OLD')
      READ (8,101) ISECT
      READ (8,105) PR(1),PR(2),TP(1),TP(2),AMACH
101   FORMAT(I10)
      DO 1 I=1,ISECT
      READ (8,102) SCAREA(I)
      READ (8,105) (SPLWO(I,J),J=1,23)
105   FORMAT(7F10.5)
102   FORMAT (F10.4)
      WRITE(6,120) ISECT
120   FORMAT('       SECTION   = ',I3)
      CALL TLOSS(TLT,SECWT(I))
      DO 2 J=1,23
2     DELTL(I,J)=TLT(I)
C
```

```
C###### FORM-FEED TO THE PRINTER
C
      CLOSE(UNIT=6)
      OPEN(UNIT=6)
  1   CONTINUE
C
C######  CLOSE DATA FILE
C
      CLOSE(UNIT=8)
C
C#######  CALCULATE INTERIOR SPL WITH TREATMENT AND TREATMENT WEIGHT
C
      TOTWT=0.
      DO 5 I=1,ISECT
      SPL(I)=0.
      SPLA(I)=0.
      DO 4 J=1,NFREQ
      SPLW(I,J)= SPLWO(I,J)-DELTL(I,J)
      SPL(I)=SPL(I)+ 10.**(SPLW(I,J)/10.)
      SPLA(I)=SPLA(I)+ 10.**((SPLW(I,J)-AWT(J))/10.)
4     CONTINUE
      SPL(I)=10.*ALOG10(SPL(I))
      SECWT(I)=SECWT(I)*SCAREA(I)
      TOTWT=TOTWT+I)
5     CONTINUE
      OPEN(UNIT=9, NAME=ONAME,TYPE='NEW')
      WRITE(9,200)
      WRITE(6,200)
200   FORMAT('    NOISE CONTROL TREATMENT DESIGN RESULTS')
      WRITE(9,201) TOTWT
      WRITE(6,201) TOTWT
201   FORMAT(5X,'  TOTAL TREATMENT WEIGHT = ',F10.5,' KGS')
      WRITE(9,202)
202   FORMAT(5X,'  SECTION      PREDICTED SPL         WEIGHT OF
     & TREATMENT(KGS) ')
      WRITE(9,205)
205   FORMAT('                   DBL       DBA')
      DO 6 I =1, ISECT
      WRITE(9,203) I,SPL(I),SPLAECWT(I)
      WRITE(6,203) I,SPL(I),SPLA(I),SECWT(I)
203   FORMAT(10X,I1,10X,F6.1,10X,F6.1,12X,F6.2)
6     CONTINUE
      STOP
      END
```

APPENDIX F

COMPUTER PROGRAM USED TO STUDY HIGH INTERIOR NOISE PROBLEM

F.1 FLOW CHART

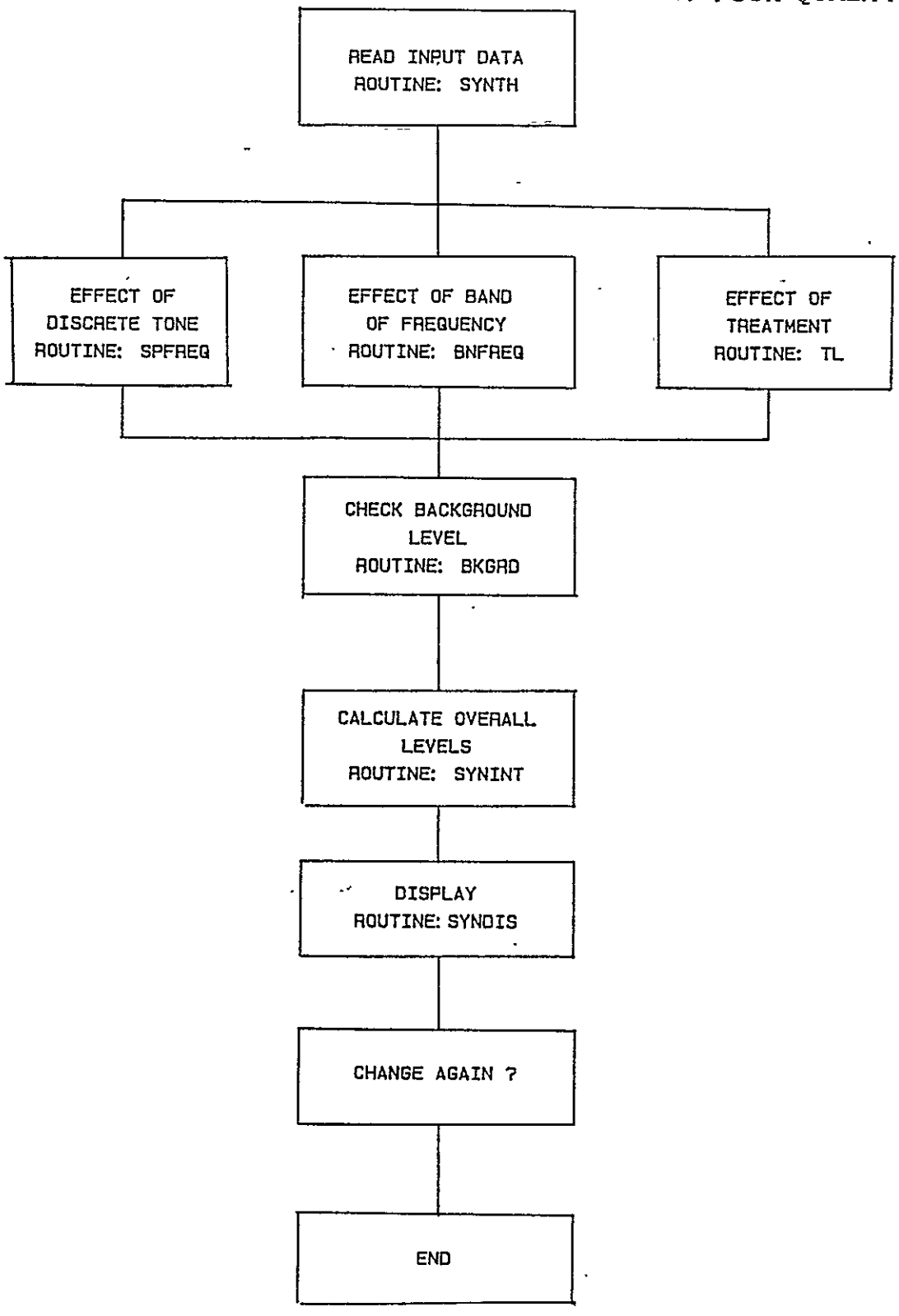

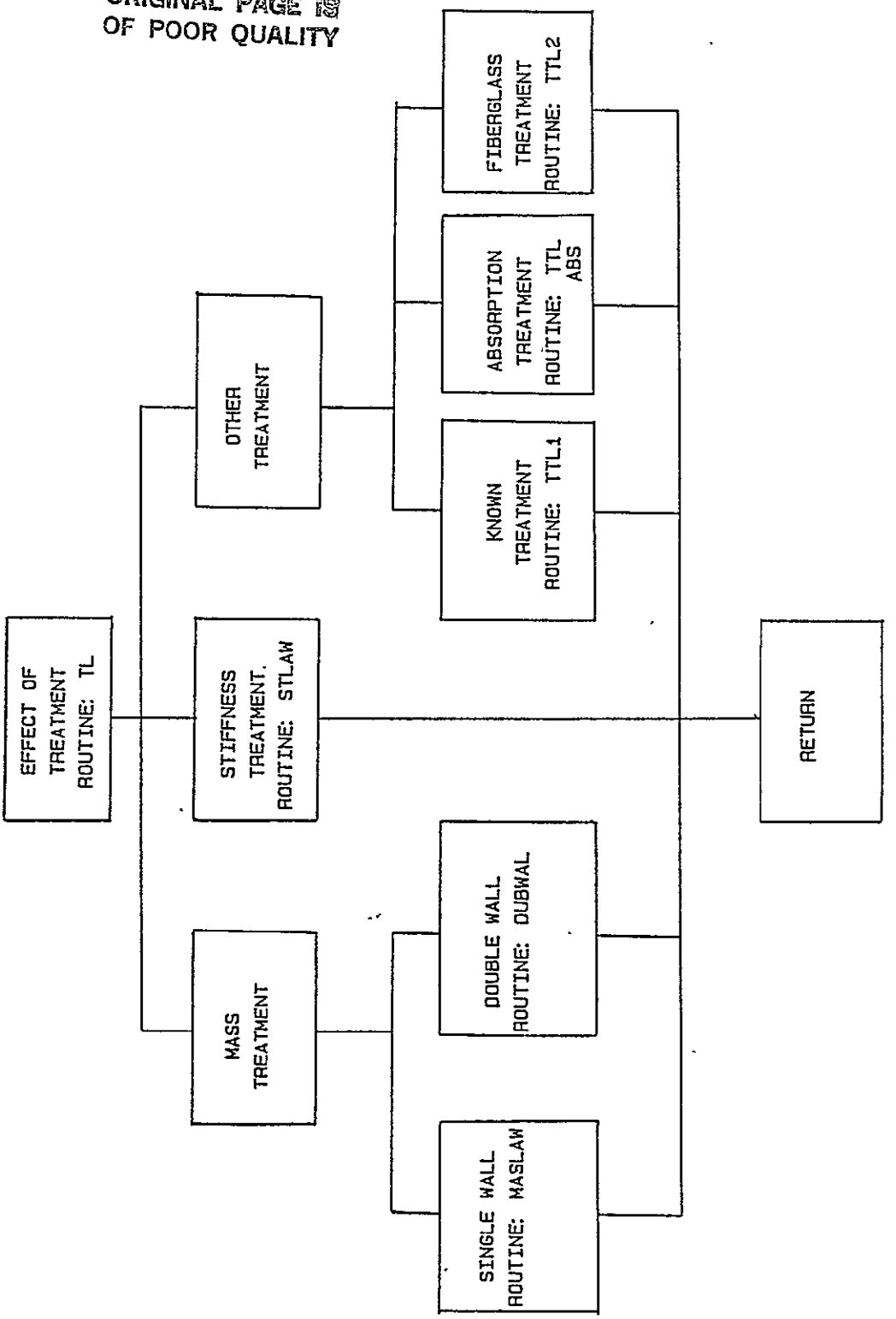

F.2 LISTING OF THE PROGRAM

```
CLEAR
CREATE SYNTH
XREF BLKIN
XREF SPFREQ
XREF BNFREQ
XREF TL
XREF BKGRD
XREF SYNINT
XREF KEYIN
XREF SYNDIS
100 BLKCLR
110 BLKIN B0,P0
120 MOVE B0,B1
130 PRINT 'OPTIONS AVAILABLE:'
140 PRINT '0= NO CHANGE'
150 PRINT '1= CHANGE THE SPL AT A SPECIFIED FREQ'
160 PRINT '2= CHANGE THE SPL OVER A FREQUENCY RANGE'
170 PRINT '3= ADD A SOUND TREATMENT'
180 INPUT I0
190 IF I0,1,290,200,220
200 SPFREQ B1
210 GOTO 290
220 IF I0,2,250,230,250
230 BNFREQ B1
240 GOTO 290
250 IF I0,3,280,260,280
260 TL B1
270 GOTO 290
280 GOTO 130
290 REMARK CONTNUE
295 BKGRD B1
300 PRINT 'CONTINUE MODIFYING'
310 HINPUT I3,'Y','N'
320 GOTO I3,300,130,330
330 BLKDEF B14,6,0
335 ZERO B14
340 SYNINT
350 PRINT 'ENTER TITLE FOR DISPLAY (40 CHR MAX)'
360 BLKDEF B15,20,1
370 KEYIN 0,39
380 SYNDIS
390 PRINT 'CONTINUE ?'
400 HINPUT I5,'Y','N'
410 GOTO I5,390,420,500
420 END
430 PRINT 'OPTIONS AVAILABLE'
440 PRINT '0= WITH ORIGINAL SPECTRUM'
450 PRINT '1= WITH MODIFIED SPECTRUM'
460 INPUT I5
470 GOTO I5,490,480
480 GOTO 130
490 GOTO 120
500 END
510 RETURN
CREATE SPFREQ
XREF PEAK
XREF BPRINT
100 STACK 100,101,103,104,114,115
110 STACK 200,201,202,203
111 PRINT 'WANT THE PEAK FREQ AND THE VALUES ?'
112 HINPUT I0,'Y','N'
113 GOTO I0,111,114,120
114 PEAK P0
120 PRINT 'ENTER VALUE OF FREQ TO BE CHANGED?'
```

```
13Ø INPUT R2
14Ø BIBSET PØ,5,IØ
15Ø BIBSET PØ,6,RØ
16Ø QUOT R1,RØ,IØ
17Ø PROD R1,R1,.5
18Ø STACK 2Ø2,2Ø1,5,1,151
19Ø DIF I14,I1,3
2ØØ SUM I15,I1,3
21Ø BPRINT PØ,I14,I15,R1
22Ø PRINT 'WANT TO CHANGE ?'
23Ø HINPUT I2,'Y','N'
24Ø GOTO I2,22Ø,25Ø,29Ø
25Ø PRINT 'ENTER CHANGED VALUE?'
26Ø PRINT 'ONLY 4 TH VALUE WILL BE CHANGED'
27Ø INPUT R3
28Ø LET PØ,I1,R3
29Ø PRINT 'CONTINUE SP FREQ CHANGE?'
3ØØ HINPUT I2,'Y','N'
31Ø GOTO I2,29Ø,12Ø,32Ø
32Ø STACK 253,252,251,25Ø
33Ø STACK 165,164,154,153,151,15Ø
34Ø RETURN
CREATE BNFREQ
XREF BPRINT
1ØØ STACK 1ØØ,1Ø1,1Ø2,1Ø3,1Ø4,114,115
11Ø STACK 2ØØ,2Ø1,2Ø2,2Ø3,2Ø4
12Ø PRINT 'ENTER LIMITS OF FREQ. RANGE'
13Ø PRINT 'MIN'
14Ø INPUT R2
15Ø PRINT 'MAX'
16Ø INPUT R3
17Ø BIBSET PØ,5,IØ
18Ø BIBSET PØ,6,RØ
19Ø QUOT R1,RØ,IØ
2ØØ PROD R1,R1,.5
21Ø STACK 2Ø2,2Ø1,5,1,164
22Ø STACK 2Ø3,2Ø1,5,1,165
23Ø PRINT 'UNCHANGED VALUES'
24Ø BPRINT PØ,I14,I15,R1
245 PRINT 'OPTIONS AVAILABLE:'
25Ø PRINT '1= CHANGE BY CONSTANT DELTA DB'
26Ø PRINT '2= CHANGE TO A CONSTANT VALUE'
27Ø INPUT IØ
28Ø GOTO IØ,25Ø,29Ø,35Ø
29Ø PRINT 'ENTER DELTA DB. REDUCTION'
3ØØ INPUT R4
31Ø FOR I1,I14,I15
32Ø DIF PØ,I1,PØ,I1,R4
33Ø NEXT I1
34Ø GOTO 4ØØ
35Ø PRINT 'ENTER NEW VALUE'
36Ø INPUT R4
37Ø FOR I1,I14,I15
38Ø LET PØ,I1,R4
39Ø NEXT I1
4ØØ PRINT 'CHANGED VALUES:'
41Ø BPRINT PØ,I14,I15,R1
42Ø PRINT 'CONTINUE ?'
43Ø HINPUT I4,'Y','N'
44Ø GOTO I4,42Ø,12Ø,45Ø
45Ø STACK 254,253,252,251,25Ø
46Ø STACK 165,164,154,153,152,151,15Ø
47Ø RETURN
CREATE TL
```

```
XREF MASLAW
XREF DUBWAL
XREF STLAW
XREF TTL
XREF TTL2
XREF TTL1
100 STACK 100
110 PRINT 'OPTIONS AVAILABLE'
120 PRINT '0= MASS LAW'
130 PRINT '1= STIFFNESS TREATMENT'
140 PRINT '2= OTHER TREATMENTS'
150 INPUT I0
160 GOTO I0,170,190,210
170 PRINT 'OPTIONS:'
172 PRINT '0= SINGLE WALL'
173 PRINT '1= DOUBLE WALL'
174 INPUT I0
175 GOTO I0,176,178
176 MASLAW P0
177 GOTO 290
178 DUBWAL P0
179 GOTO 290
180 GOTO 290
190 STLAW P0
200 GOTO 290
210 PRINT 'OPTIONS AVAILABLE'
211 PRINT '0= SOUND TREATMENT WITH KNOWN DELTA TL VS FREQ'
220 PRINT '1= ADDITIONAL ABSORPTION'
230 PRINT '2= ADDITIONAL FIBERGLASS BLANKET'
240 INPUT I0
250 GOTO I0,283,260,280
260 TTL P0
270 GOTO 290
280 TTL2 P0
281 GOTO 290
283 TTL1 P0
290 STACK 150
300 RETURN
CREATE MASLAW.
100 STACK 100,101
110 STACK 200,201,202,203,204,205,206,207,208
120 PRINT 'ENTER EXISTING AVERAGE MASS PER UNIT AREA(LB/SQFT)'
130 PRINT 'INCLUDE SKIN,TRIM,LEADED VINYL'
140 INPUT R0
150 PRINT 'ENTER MASS PER UNIT AREA OF ADDITIONAL TREATMENT'
160 INPUT R1
170 PRINT 'ENTER OUTSIDE TEMP (DEG F) AND PRESSURE (PSI)'
180 INPUT R2,R3
190 STACK 202,459.7,2,16,14.96,4,254
200 STACK 202,32.,3,.5555,4,273.,2,255
210 STACK 203,205,5,24.,4,255
220 STACK 3.14,205,5,204,5,255
230 PROD R0,R0,4.882
240 PROD R1,R1,4.882
250 SUM R1,R0,R1
260 BIBSET P0,5,I0
270 BIBSET P0,6,R6
280 QUOT R7,R6,I0
290 PROD R7,R7,.5
292 SUM I0,I0,-1
300 FOR I2,0,I0
301 LET I1,I2
302 STACK 101,0,207,4,258
320 STACK 205,208,4,201,4,253,203,203,4,1.,2,20,10.,4,253
```

```
33Ø STACK 2Ø5,2Ø8,4,2ØØ,4,252,2Ø2,2Ø2,4,1.,2,2Ø,1Ø.,4,252
34Ø SUM PØ,I1,PØ,I1,R2
35Ø DIF PØ,I1,PØ,I1,R3
36Ø NEXT I2
37Ø STACK 258,257,256,255,254,253,252,251,25Ø
38Ø STACK 151,15Ø
39Ø RETURN
CREATE BKGRD
1ØØ STACK 1ØØ,1Ø1,1Ø2,2ØØ,2Ø1,2Ø2,2Ø3,2Ø4
2ØØ BIBSET PØ,6,RØ
3ØØ BIBSET PØ,5,IØ
4ØØ STACK 2ØØ,1ØØ,Ø,5,2.,5,25Ø
5ØØ SUM IØ,IØ,-1
6ØØ FOR I1,Ø,IØ
61Ø STACK 1Ø1,Ø,2ØØ,4,251
63Ø STACK 45.,3Ø.,599Ø.,5,1Ø.,2Ø1,3,4,2,252
632 REMARK CORRECTION FOR ANALYSIS BANDWIDTH
635 STACK 2Ø2,1Ø.,12.5,2ØØ,5,2Ø,4,3,252
64Ø LET R3,PØ,I1
65Ø IF R3,R2,66Ø,7ØØ,7ØØ
66Ø LET PØ,I1,R2
7ØØ NEXT I1
71Ø STACK 254,253,252,251,25Ø,152,151,15Ø
72Ø RETURN
CREATE STLAW
1ØØ STACK 1ØØ,1Ø1
11Ø STACK 2ØØ,2Ø1,2Ø2,2Ø3,2Ø4,2Ø5,2Ø6,2Ø7,2Ø8,2Ø9,21Ø,211,212,213,214,215
12Ø PRINT 'ENTER AVERAGE MASS PER UNIT AREA OF SKIN(LB/SQ FT)'
13Ø INPUT RØ
131 PROD RØ,RØ,4.882
14Ø PRINT 'ENTER AVERAGE MASS PER UNIT AREA OF FRAMES(LB/SQ FT)'
15Ø INPUT R1
151 PROD R1,R1,4.882
16Ø PRINT 'ENTER AVERAGE STIFFNESS OF FRAMES(LB.IN)'
17Ø INPUT R2
171 PROD R2,R2,.113
18Ø PRINT 'ENTER ADITIONAL MASS PER UNIT AREA OF STIFFNES TREATMENT'
19Ø INPUT R3
191 PROD R3,R3,4.882
2ØØ PRINT 'ENTER ADDITIONAL STIFFNESS DUE TO TREATMENT'
21Ø INPUT R4
211 PROD R4,R4,.113
22Ø PRINT 'ENTER TEMP (DEG F) AND PRESSURE (PSI)'
23Ø INPUT R13,R14
24Ø STACK 213,459.7,2,16,14.96,4,265
25Ø STACK 213,32.,3,.5555,4,273.,2,262
26Ø STACK 214,212,5,24.,4,262
27Ø STACK 2.,212,4,215,4,265
28Ø STACK 2ØØ,2Ø1,2,255,2Ø2,2Ø5,5,16,255
29Ø STACK 2ØØ,2Ø1,2,2Ø3,2,256,2Ø2,2Ø4,2,2Ø6,5.,16,256
31Ø MOVE PØ,B3
32Ø BIBSET PØ,5,IØ
33Ø BIBSET PØ,6,R7
34Ø QUOT R8,R7,IØ
35Ø PROD R8,R8,.5
355 SUM IØ,IØ,-1
36Ø FOR I1,Ø,IØ
37Ø STACK 1Ø1,Ø,2Ø8,4,6.28,4,259
38Ø IF R9,R5,39Ø,39Ø,41Ø
39Ø SUM R1Ø,RØ,R1
4ØØ GOTO 42Ø
41Ø LET R1Ø,RØ
42Ø STACK 2Ø5,.Ø4,4,21Ø,4,215,2,261,211,211,4,261
43Ø LET B3,I1,R11
```

```
440 STACK 205,209,5,261,211,211,4,1.,3,11,210,4,209,4,261
450 STACK 211,211,4,261
460 SUM B3,I1,B3,I1,R11
461 LET R11,B3,I1
462 STACK 211,215,5,215,5,261
463 LET B3,I1,R11
464 NEXT I1
465 LOG B3
466 MLCONR 10.,B3
467 ADD B3,P0
468 FOR I1,0,I0
469 STACK 101,0,208,4,6.28,4,259
470 IF R9,R6,480,480,500
480 STACK 200,201,2,203,2,260
490 GOTO 510
500 STACK 200,203,2,260
510 STACK 206,.04,4,210,4,215,2,261,211,211,4,261
520 LET B3,I1,R11
530 STACK 206,209,5,261,211,211,4,1.,3,11,210,4,209,4,261
540 STACK 211,211,4,261
550 SUM B3,I1,B3,I1,R11
560 NEXT I1
565 STACK 215,215,4,265,1.,215,5,265
580 MLCONR R15,B3
600 LOG B3
620 MLCONR 10.,B3
640 SUB B3,P0
650 STACK 265,264,263,262,261,260,259,258,257,256,255,254,253,252,251,250
660 STACK 151,150
670 RETURN
CREATE TTL1
82 PRINT 'THIS SUBROUTINE USES STRAIGHT LINE INTERPOLATION BETWEEN'
83 PRINT 'FREQ. STARTING FREQ IS ZERO. ENTER WHEN ASKED FREQ AND '
84 PRINT 'THE CORRESPONDING DELTA TL'
90 STACK 100,101,201,202,203,204,205,206,207
100 BIBSET P0,6,R1
110 BIBSET P0,5,I0
120 STACK 201,100,0,5,2.,5,251
130 MOVE P0,B3
140 ZERO B3
145 LET R2,0.
146 LET R4,0.
150 GOSUB 1000
155 SUM I0,I0,-1
160 FOR I1,0,I0
170 STACK 101,0,201,4,256
180 IF R6,R3,200,200,190
190 LET R2,R3
191 LET R4,R5
192 GOSUB 1000
200 STACK 205,204,3,203,202,3,5,206,202,3,4,204,2,257
210 IF R6,100,220,230,230
220 LET R7,0.
230 IF R7,40.,250,250,240
240 LET R7,40.
250 LET B3,I1,R7
260 NEXT I1
270 SUB B3,P0
275 STACK 257,256,255,254,253,252,251,151,150
280 RETURN
1000 PRINT 'ENTER FREQ VALUE'
1010 INPUT R3
1020 PRINT 'ENTER ADD. TL DUE TO TREATMENT AT THIS FREQ
1030 INPUT R5
```

```
'104Ø RETURN
CREATE SYNMES
9Ø END
1ØØ PRINT 'TO RUN LOAD BLKIN AND XDISPL.'
11Ø PRINT 'THEN EXECUTE SYNTH TIC DEV:FILNAM.EXT TIC.'
12Ø PRINT 'FOR HELP, LOAD TIC HELP.MEW TIC AND EXECUTE'
13Ø PRINT 'HELPNT TIC OVRWRT.HLP TIC '
14Ø RETURN
CREATE TTL
XREF BLKIN
XREF ABS
1ØØ STACK 1ØØ,1Ø1
12Ø STACK 2Ø1,2Ø2,2Ø3,2Ø4,2Ø5,2Ø6
14Ø STACK 1Ø2,1Ø3
16Ø PRINT 'OPTIONS AVAILABLE:'
18Ø PRINT 'Ø= EXPERIMENTAL ABS IN CURRENT FUSELAGE DESIGN'
2ØØ PRINT '1= OPTIMISED ABS IN LO FREQ REGION'
22Ø PRINT '2= OPTIMISED ABS IN HI FREQ REGION'
24Ø INPUT I3
26Ø BIBSET PØ,5,I1
28Ø BIBSET PØ,6,R1
3ØØ STACK 2Ø1,1Ø1,Ø,5,2.,5,252
32Ø STACK 1ØØ.,2Ø2,5,1,152
34Ø DIF I1,I1,1
36Ø GOTO I3,38Ø,56Ø,68Ø
38Ø PRINT 'ENTER UNTREATED ABSORB COEFF ?'
4ØØ INPUT R3
42Ø PRINT 'ENTER MAX TREATED ABSORB:COEFF?'
44Ø INPUT R4
46Ø MOVE PØ,B3
48Ø ZERO B3
5ØØ FOR IØ,I2,I1
52Ø STACK 1ØØ,Ø,2Ø2,4,255
54Ø STACK 2Ø5,2Ø,2.,3,2Ø4,2Ø3,3,4,2Ø3,2,256
56Ø IF R5,15ØØ.,6ØØ,6ØØ,58Ø
58Ø LET R6,R4
6ØØ STACK 2Ø3,2Ø6,5,2Ø,1Ø.,4,11,256
62Ø LET B3,IØ,R6
64Ø NEXT IØ
65Ø SUB B3,PØ
655 GOTO 72Ø
66Ø BLKIN B11,'ABSLO.TAB'
665 ABS PØ
67Ø GOTO 72Ø
68Ø BLKIN B11,'ABSHI.TAB'
685 ABS PØ
72Ø STACK 153,152
74Ø STACK 256,255,254,253,252,251,151,15Ø
76Ø RETURN
CREATE TTL2
1ØØ STACK 1ØØ,1Ø1,1Ø2,2Ø1,2Ø2,2Ø3,2Ø4,2Ø5
12Ø REMARK THIS SUBROUTINE CALCULATES THE RESISTIVE LOSS DUE TO
14Ø REMARK POROUS BLANKET
16Ø PRINT 'RESISTIVE LOSS DUE TO FIBERGLASS BLANKET'
165 PRINT 'OPTIONS AVAILABLE:'
17Ø PRINT 'Ø= BLANKET TYPE A (PF1Ø5)'
172 PRINT '1= BLANKET TYPE B (PF1Ø5 WITH HIGHER LO FREQ TL)'
174 PRINT '2= BLANKET TYPE C (TYPE B WITH LOWER HI FREQ TL)'
178 INPUT I2
22Ø PRINT 'ENTER BLANKET THICKNESS IN INCH'
24Ø INPUT R5
26Ø BIBSET PØ,5,I1
28Ø BIBSET PØ,6,R1
3ØØ STACK 2Ø1,1Ø1,Ø,5,2.,5,252
```

```
32Ø DIF I1,I1,1
34Ø MOVE PØ,B3
36Ø ZERO B3
38Ø FOR IØ,1,I1
4ØØ STACK 1ØØ,Ø,2Ø2,4,253
4Ø5 STACK 2Ø3,2Ø,253
41Ø GOTO I2,42Ø,5Ø2,512
42Ø IF R3,2.,44Ø,44Ø,48Ø
44Ø STACK .Ø5,2Ø3,2Ø,4,254
46Ø GOTO 52Ø
48Ø REMARK CONTINUE
5ØØ STACK -1.234,2Ø3,4,16.53,2,2Ø3,4,53.76,3,2Ø3,4,51.37,2,254
5Ø1 GOTO 52Ø
5Ø2 IF R3,2.,5Ø3,5Ø3,5Ø5
5Ø3 STACK .6,2Ø3,4,254
5Ø4 GOTO 52Ø
5Ø5 STACK 2.5Ø3,2Ø3,4,-14.56,2,2Ø3,4,29.66,2,2Ø3,4,-19.87,2,254
5Ø6 GOTO 52Ø
512 IF R3,2.,513,513,515
513 STACK .6,2Ø3,4,254
514 GOTO 52Ø
515 STACK -1.268,2Ø3,4,14.37,2,2Ø3,4,-43.25,2,2Ø3,4,4Ø.44,2,254
52Ø STACK 2Ø4,2Ø5,4,254
54Ø LET B3,IØ,R4
56Ø NEXT IØ
58Ø SUB B3,PØ
6ØØ STACK 255,254,253,252,251,152,151,15Ø
62Ø RETURN
CREATE DUBWAL
1ØØ STACK 1ØØ,1Ø1
11Ø STACK 2ØØ,2Ø1,2Ø2,2Ø3,2Ø4,2Ø5,2Ø6,2Ø7,212,213,214,215
12Ø PRINT 'ENTER MASS PER AREA (LB/SQ FT)'
13Ø INPUT RØ
135 PROD RØ,RØ,4.882
14Ø PRINT 'ENTER SPACING IN INCH'
15Ø INPUT R1
155 PROD R1,R1,.Ø254
16Ø PRINT ' ENTER TEMP(DEG F) AND PRESS (PSI)'
17Ø INPUT R13,R14
18Ø STACK 213,459.7,2,16,14.96,4,265
19Ø STACK 213.,32.,3,.5555,4,273.,2,262
2ØØ STACK 214,212,5,24.,4,215,4,262
21Ø MOVE PØ,B3
22Ø BIBSET PØ,5,IØ
23Ø BIBSET PØ,6,R2
24Ø STACK 2Ø2.1ØØ,Ø,5,.5,4,252
25Ø LET R3,1.
26Ø SUM IØ,IØ,-1
3ØØ FOR I1,Ø,IØ
31Ø STACK 1Ø1,Ø,2Ø2,4,6.28,4,254
315 STACK 2Ø4,2ØØ,4,212,5,257
32Ø STACK 2Ø7,2Ø3,4,.5,4,255,2Ø5,2Ø5,4,255
33Ø STACK 1.,2Ø5,2,2Ø,1Ø.,4,255
34Ø SUM PØ,I1,PØ,I1,R5
38Ø STACK 2Ø4,2Ø1,4,2Ø3,4,215,5,256
39Ø STACK 2Ø6,14,2Ø7,.5,4,2Ø3,4,2Ø6,15,4,3,255
4ØØ STACK 2Ø5,2Ø5,4,2Ø7,4,2Ø3,2Ø3,4,4,1.,2,255
41Ø STACK 2Ø5,2Ø,1Ø.,4,255
42Ø DIF PØ,I1,PØ,I1,R5
43Ø NEXT I1
44Ø STACK 265,264,263,262,257,256,255,254,253,252,251,25Ø
45Ø STACK 151,15Ø
46Ø RETURN
CREATE BPRINT
```

```
100 STACK 108
110 STACK 213,214,215
120 LET R15,P3
130 PRINT '  FREQ            SPL'
131 FORMAT 1,7,2
132 FORMAT 2,7,2
140 FOR I8,P1,P2
150 STACK 108,0,215,4,264
160 LET R13,P0,I8
170 PRINT R14,'       ',R13
180 NEXT I8
181 FORMAT
190 STACK 255,264,263
200 STACK 158
210 RETURN
CREATE INTEG
5 STACK 102,101
10 STACK 100,200,201
20 LET R1,0.
22 LET I1,P1
23 LET I2,P2
30 FOR I0,I1,I2
40 LET R0,P0,I0
50 STACK 200,.1,4,22,250
60 SUM R1,R1,R0
70 NEXT I0
90 STACK 201,20,10.,4,251
100 LET P3,R1
110 STACK 251,250,150
112 STACK 151,152
120 RETURN
CREATE SYNDIS
XREF DISPLY
XREF LAB1
100 STACK 100,200,201,202
110 PRINT 'ENTER DISPLAY OPTIONS:'
120 PRINT '0= ORIGINAL SPECTRUM'
130 PRINT '1= MODIFIED SPECTRUM'
140 PRINT '2= BOTH SPECTRA'
150 INPUT I0
160 PRINT 'ENTER MAX VALUE VERTICAL SCALE'
170 INPUT R2
180 PRINT 'FREQ RANGE'
182 PRINT 'MIN'
183 INPUT R0
184 PRINT 'MAX'
186 INPUT R1
200 GOTO I0,210,230,250
210 DISPLY B0,'M','EX',R0,R1,'YLAB','DB','SC',R2,'GLAB','UNMOD SPECTRA','SUB',LAB1
220 GOTO 270
230 DISPLY B1,'M','EX',R0,R1,'YLAB','DB','SC',R2,'GLAB','MOD SPECTRUM','SUB',LAB1,
240 GOTO 270
250 DISPLY B0,'M','EX',R0,R1,'YLAB','DB','SC',R2,'GLAB',' ','SUB',LAB1,'G','R'
260 DISPLY B1,'M','EX',R0,R1,'SC',R2,'NG','G'
270 ERASE
275 PRINT 'CONTINUE DISPLAY'
280 HINPUT I0,'Y','N'
290 GOTO I0,270,110,300
300 HOLOUT 'KB',27
310 HOLOUT 'KB',12
320 STACK 252,251,250,150
330 RETURN
CREATE SYNINT
XREF INTEG
```

```
XREF AWT
XREF SIL
100 STACK 200,203,204,101,102,103
110 PRINT 'ENTER LIMITS OF INTEGRATION'
120 PRINT 'MIN'
130 INPUT R3
140 PRINT 'MAX'
150 INPUT R4
160 BIBSET B0,5,I1
170 BIBSET B0,6,R0
180 STACK 200,101,0,5,.5,4,251
190 STACK 203,201,5,1,152,204,201,5,1,153
200 INTEG B0,I2,I3,R3
210 LET B14,0,R3
220 INTEG B1,I2,I3,R3
230 LET B14,2,R3
240 MOVE B0,B3
250 AWT B3
260 INTEG B3,I2,I3,R3
270 LET B14,1,R3
280 MOVE B1,B3
290 AWT B3
300 INTEG B3,I2,I3,R3
310 LET B14,3,R3
320 STACK 200,.5,4,250
330 IF R0,5650.,380,340,340
340 SIL B0,R3
350 LET B14,4,R3
360 SIL B1,R3
370 LET B14,5,R3
380 STACK 153,152,151,254,253,250
390 RETURN
CREATE AWT
100 STACK 100,101,102,200,201,202
110 BIBSET P0,5,I1
120 BIBSET P0,6,R0
130 QUOT R1,R0,I1
140 PROD R1,R1,.5
150 LET P0,0,0.
155 SUM I1,I1,-1
160 FOR I0,1,I1
170 STACK 100,0,201,4,20,250
180 STACK 200,200,4,200,4,200,4,-.8345,4
190 STACK 200,200,4,200,4,10.07,4
200 STACK 200,200,4,-55.73,4
210 STACK 200,160.7,4,-184.8,2,2,2,2
220 STACK 250
250 LET R2,P0,I0
260 STACK 202,200,2,252
270 LET P0,I0,R2
280 NEXT I0
290 STACK 252,251,250,152,151,150
300 RETURN
CREATE KEYIN
100 SUM I0,P0,-1
110 SUM I0,I0,1
120 HOLIN 'KB',I1
130 IF I1,13,140,250,140
140 IF I1,127,210,150,210
150 SUM I0,I0,-1
160 IF I0,P0,170,190,190
170 LET I0,P0
180 GOTO 120
190 HOLOUT 'KB',92
```

```
200 GOTO 120
210 IF I0,P1,220,220,290
220 HOLOUT 'KB',I1
230 TRANS 1,B15,I0,I1
240 GOTO 110
250 IF I0,P1,260,260,290
260 FOR I1,I0,P1
270 TRANS 1,B15,I1,32
280 NEXT I1
290 PRINT
310 RETURN
CREATE BLKPRT
100 FOR I0,0,39
110 TRANS 0,B15,I0,I1
120 HOLOUT 'KB',I1
130 NEXT I0
140 PRINT
150 RETURN
CREATE LAB1
XREF BLKPRT
100 STACK 200,201,202,203,204,205,206
110 BEAMP 200,145
120 BLKPRT
130 BEAMP 0,105
140 FORMAT 1,6,2
145 FORMAT 2,6,2
150 LET R0,B14,0
160 LET R1,B14,1
170 LET R2,B14,2
180 LET R3,B14,3
182 LET R4,B14,4
184 LET R5,B14,5
200 PRINT 'OVERALL LEVEL   UNMOD        MOD'
210 PRINT 'LINEAR    DBL  ',R0,'       ',R2
220 PRINT 'AWTED     DBA  ',R1,'       ',R3
230 BIBSET B0,6,R6
240 STACK 206,.5,4,256
250 IF R6,5650.,270,260,260
260 PRINT 'SIL       DB   ',R4,'.      ',R5
270 STACK 256,255,254,253,252,251,250
280 FORMAT
290 RETURN
CREATE SIL
100 STACK 100,101,102,104,200,201,204,205
110 BIBSET B0,5,I0
120 BIBSET B0,6,R2
130 STACK 100,0,202,5,2.,4,252
140 LET R0,0.
150 LET R1,0.
160 LET I1,355
170 LET I2,705
180 STACK 102,0,202,4,1,152
190 STACK 101,0,202,4,1,151
200 FOR I0,1,4
210 FOR I4,I1,I2
220 LET R5,P0,I4
230 STACK 205,10.,5,22,255
240 SUM R0,R0,R5
250 NEXT I4
260 STACK 200,20,10.,4,250
270 STACK 201,200,2,251,102,151,102,0,2.,4,1,152
280 LET R0,0.
290 NEXT I0
300 STACK 201,4.,5,251
```

```
31Ø LET P1,R1
32Ø STACK 255,254,251,25Ø,154,152,151,15Ø
33Ø RETURN
CREATE ABS
1Ø REMARK THIS SUB CALCULATES ADD. TL  DUE TO ABSORPTION.
2Ø STACK 1ØØ,1Ø1,1Ø2,1Ø3,2ØØ,2Ø1,2Ø2,2Ø3,2Ø4,2Ø5,2Ø6,2Ø7
4Ø LET I2,Ø
5Ø BIBSET PØ,6,R1
6Ø BIBSET PØ,5,IØ
7Ø STACK 2Ø1,1ØØ,Ø,5,2.,5,251
8Ø MOVE PØ,B3
9Ø ZERO B3
1ØØ LET R2,Ø.
11Ø LET R4,Ø.
12Ø GOSUB 1ØØØ
13Ø SUM IØ,IØ,-1
14Ø FOR I1,1,IØ
15Ø STACK 1Ø1,Ø,2Ø1,4,256
155 STACK 2Ø6,2Ø,256
16Ø IF R6,R3,2ØØ,2ØØ,162
162 IF R3,3.6Ø2,165,2ØØ,2ØØ
165 LET R2,R3
17Ø LET R4,R5
18Ø GOSUB 1ØØØ
2ØØ STACK 2Ø5,2Ø4,3,2Ø3,2Ø2,3,5,2Ø6,2Ø2,3,4,2Ø4,2,257
2Ø5 STACK .1,2Ø7,5,2Ø,1Ø.,4,11,257
2Ø6 IF R7,1Ø.,21Ø,21Ø,2Ø7
2Ø7 LET R7,1Ø.
21Ø LET B3,I1,R7
22Ø NEXT I1
23Ø SUB B3,PØ
24Ø STACK 257,256,255,254,253,252,251,25Ø,153,152,151,15Ø
25Ø RETURN
1ØØØ SUM I3,I2,1
1Ø1Ø LET R3,B11,I2
1Ø2Ø STACK 2Ø3,2Ø,253
1Ø3Ø LET R5,B11,I3
1Ø4Ø SUM I2,I2,2
1Ø5Ø RETURN
CREATE PEAK
1Ø STACK 1ØØ,1Ø1,1Ø2,2ØØ,2Ø1,2Ø2
15 STACK 1Ø3,2Ø3
2Ø BIBSET PØ,5,I1
3Ø BIBSET PØ,6,RØ
4Ø STACK 2ØØ,1Ø1,Ø,5,2.,5,25Ø
5Ø ERASE
6Ø PRINT '    FREQ       PEAK VALUE'
7Ø FORMAT 1,1Ø,2
8Ø FORMAT 2,1Ø,2
9Ø DIF I1,I1,1Ø.
95 LET IØ,3
1ØØ MOVE PØ,B3
11Ø DIFF B3
12Ø SUM IØ,IØ,1
13Ø IF IØ,I1,14Ø,25Ø,25Ø
14Ø IF B3,IØ,12Ø,12Ø,15Ø
15Ø SUM IØ,IØ,1
16Ø IF B3,IØ,17Ø,15Ø,15Ø
17Ø DIF IØ,IØ,1
171 DIF I2,IØ,1
172 DIF R2,PØ,1Ø,PØ,I2
173 SUM I3,IØ,1
174 DIF R3,PØ,I3,PØ,IØ
175 STACK 2Ø3,1Ø,253
```

```
18Ø IF R2,3.,182,19Ø,19Ø
182 IF R3,3.,12Ø,19Ø,19Ø
19Ø STACK 1ØØ,Ø,2ØØ,4,251
2ØØ LET R2,PØ,IØ
21Ø PRINT R1,R2
22Ø SUM IØ,IØ,1
23Ø IF IØ,I1,12Ø,24Ø,24Ø
24Ø REMARK CONTINUE
25Ø FORMAT
255 STACK 253,153
26Ø STACK 252,251,25Ø,152,151,15Ø
27Ø RETURN
CREATE SAVSYN
XREF SYNTH
XREF SPFREQ
XREF BNFREQ
XREF TL
XREF MASLAW
XREF BKGRD
XREF STLAW
XREF TTL1
XREF SYNMES
XREF TTL
XREF TTL2
XREF DUBWAL
XREF BPRINT
XREF INTEG
XREF SYNDIS
XREF SYNINT
XREF AWT
XREF KEYIN
XREF BLKPRT
XREF LAB1
XREF SIL
XREF ABS
XREF PEAK
1Ø OSPEC 'MSYNTH.RN'
2Ø PRINT 'CLEAR'
3Ø SAVE SYNTH,'NE'
4Ø SAVE SPFREQ,'NE'
5Ø SAVE BNFREQ,'NE'
6Ø SAVE TL,'NE'
7Ø SAVE MASLAW,'NE'
75 SAVE BKGRD,'NE'
8Ø SAVE STLAW,'NE'
9Ø SAVE TTL1,'NE'
1ØØ SAVE SYNMES,'NE'
11Ø SAVE TTL,'NE'
12Ø SAVE TTL2,'NE'
122 SAVE DUBWAL,'NE'
13Ø SAVE BPRINT,'NE'
132 SAVE INTEG,'NE'
134 SAVE SYNDIS,'NE'
136 SAVE SYNINT,'NE'
14Ø SAVE AWT,'NE'
15Ø SAVE KEYIN,'NE'
16Ø SAVE BLKPRT,'NE'
17Ø SAVE LAB1,'NE'
172 SAVE SIL,'NE'
18Ø SAVE ABS,'NE'
2ØØ SAVE PEAK,'NE'
21Ø SAVE SAVSYN,'NE'
22Ø PRINT 'SYNMES'
23Ø PRINT 'END'
24Ø END
25Ø RETURN
SYNMES
END
```

F.3 A SAMPLE APPLICATION

In this appendix the application of this program during a noise control program of a noisy, production, business-jet aircraft by the engineers at Cessna Aircraft Company is described. Figure F.1 shows the interior spectrum in the aft seat area of this aircraft. The overall linear and A-weighted levels were high. The preferred Speech Interference Levels (PSIL) were acceptable. The aircraft interior spectrum was then analyzed using this program. From the low figure of PSIL it is obvious that the higher levels were due to the high low-frequency content. As can be seen in Figure F.1, the discrete tone at 270 Hz dominates the spectrum. This tone corresponds to engine N_1 tone. The use of PEAK subroutine in the program showed this value to be 97.2 dB. The levels of the neighboring band (265 and 275) were found to be 91.6 and 94.7 dB. This high value at these locations could be attributed to spectral leakage. Comparison with the normal aircraft interior spectrum showed that the peak should range from 85 to 88 dB. The effect of reducing this tone to normal levels is shown in Figure F.2. In this case the tone at 270 Hz was reduced from 97.2 to 90 dB. The values at 265 and 275 Hz were also changed correspondingly. This reduction alone decreased the overall linear and A-weighted levels from 101 dBL and 92.9 dBA to 96.6 and 88 dBA. A reduction of this peak to 84 would have reduced the levels to 95.2 dBL and 86.2 dBA. Hence, before any application of additional treatment, the engine installation interference was checked. A slight engine interference

was found. The interference was cleared by the installation of the engine and its accessories. The aircraft interior levels were measured, and Figure F.3 shows the measured spectrum. Because the interior levels were still high compared to normal aircraft (86.3 dBA instead of normal 83-85 dBA), additional treatments were contemplated. An addition of 40 oz/sq yd leaded vinyl decreased these levels to acceptable values, as shown in Figure F.4. The placement of this additional vinyl sheet was finalized based on the results from the program discussed in Chapter 6. The results from the program indicated that the maximum gain in the noise reduction would be achieved in this aircraft if this material is placed next to the trim panel. With this mass treatment and additional treatments (not known to the author) the aircraft was flown and the results are shown in Figure F.5. The aircraft was delivered with the levels of 90.7 dBL, 81.1 dBA and 63.6 dB PSIL.

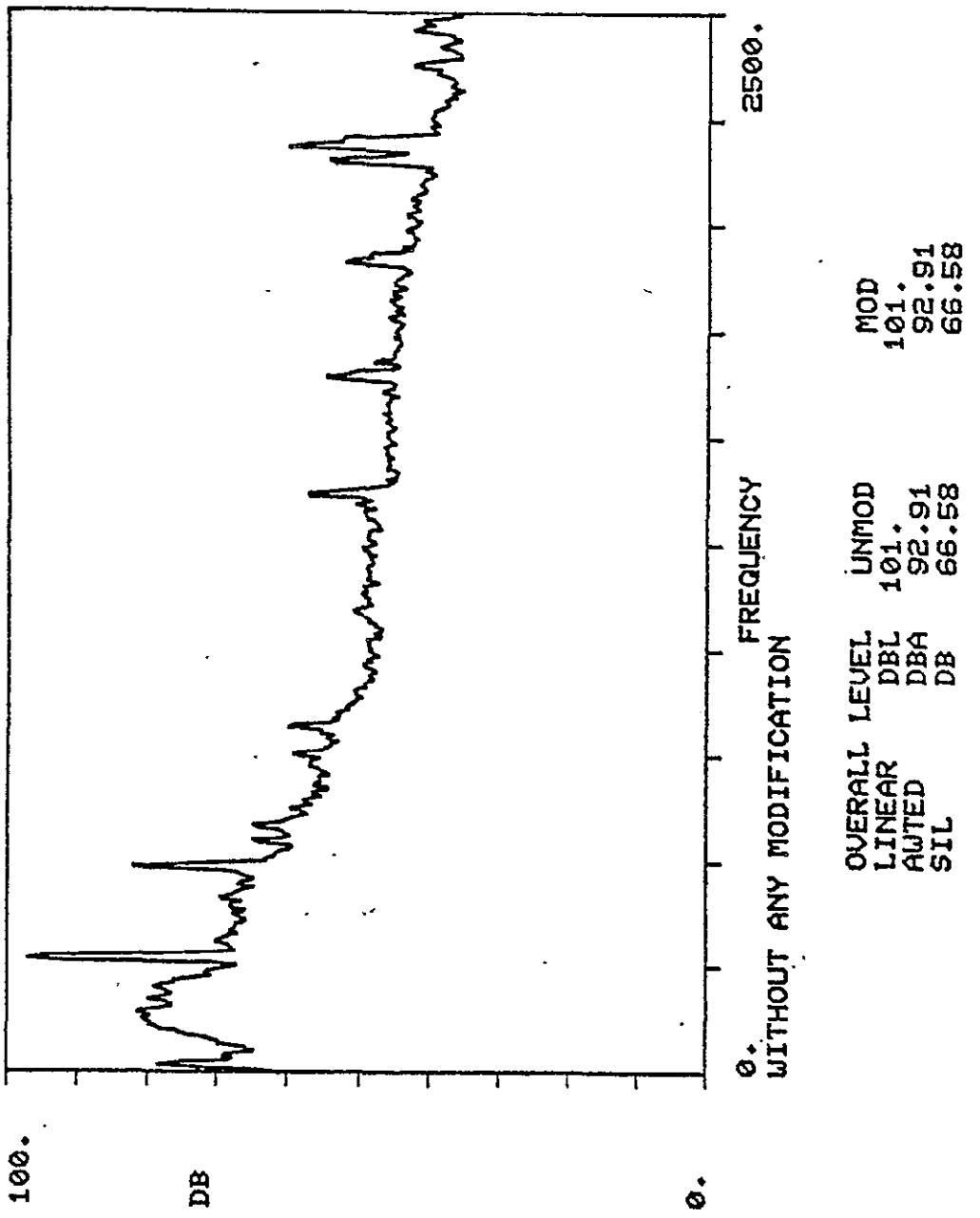

Figure F.1: Measured Interior Noise Spectrum of Noisy Aircraft

C-6

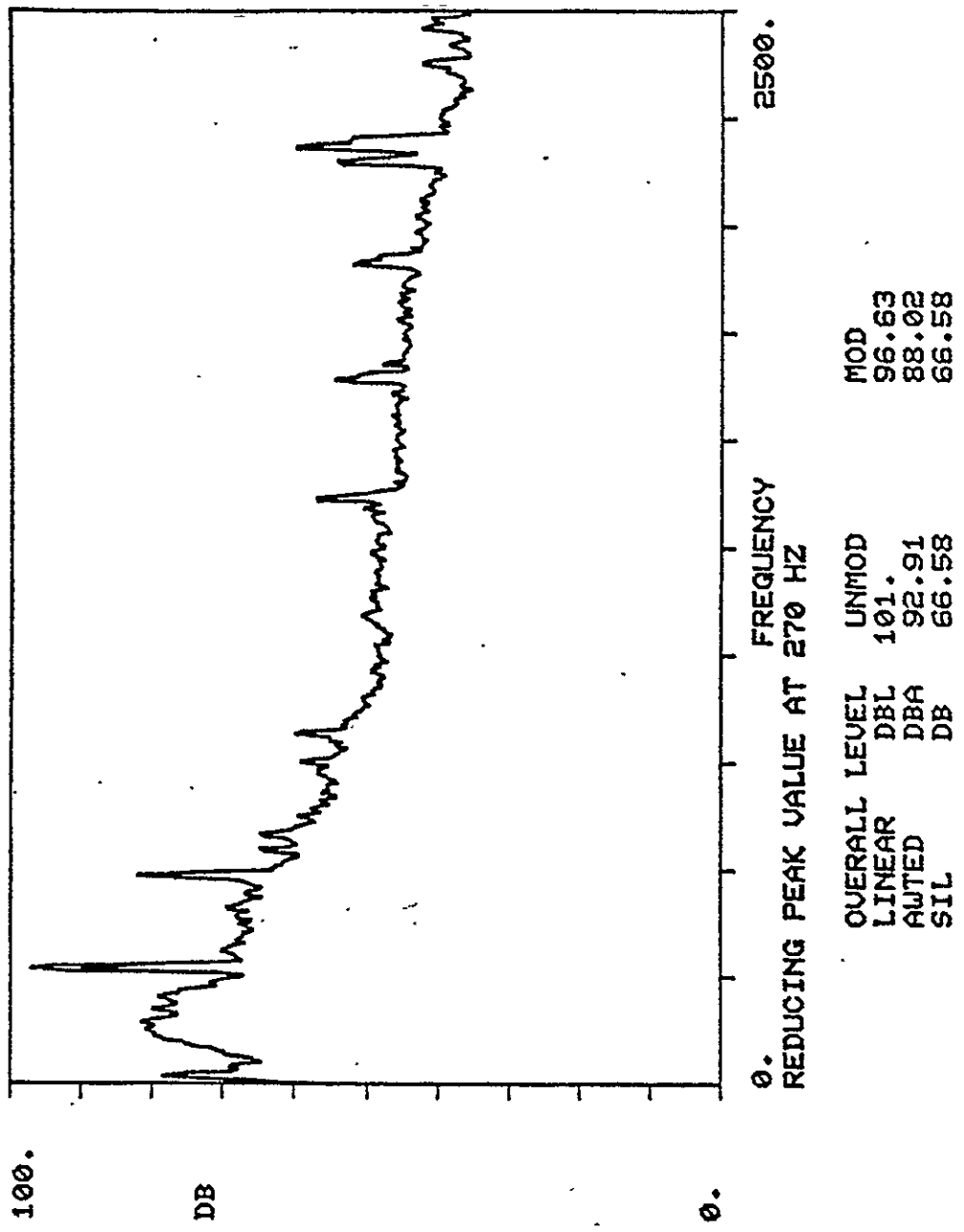

Figure F.2: Effect of Reducing the Tone at 270 Hz

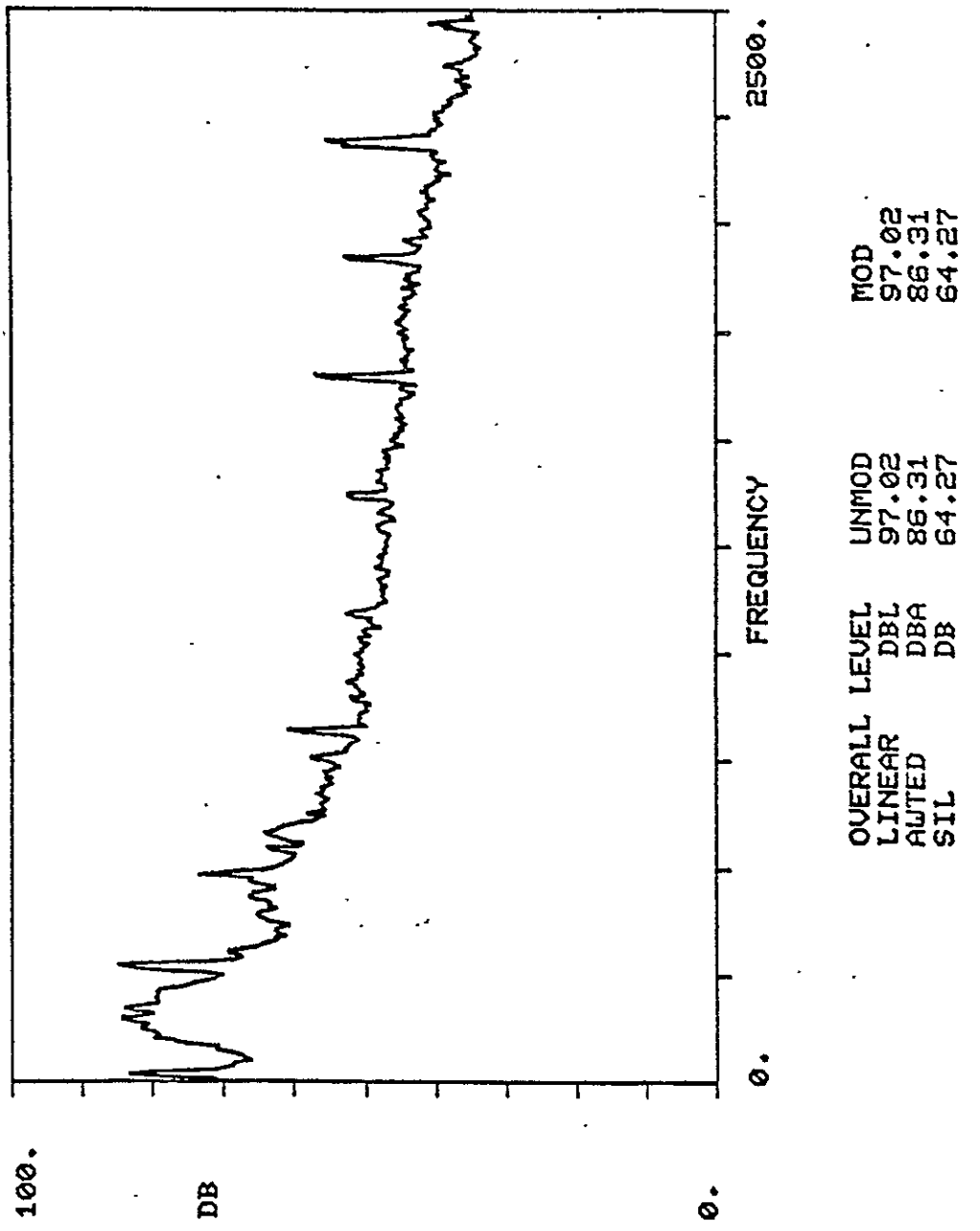

Figure F.3: Measured Interior Spectrum after Tone Reduction

DATA PROPRIETARY
TO
CESSNA

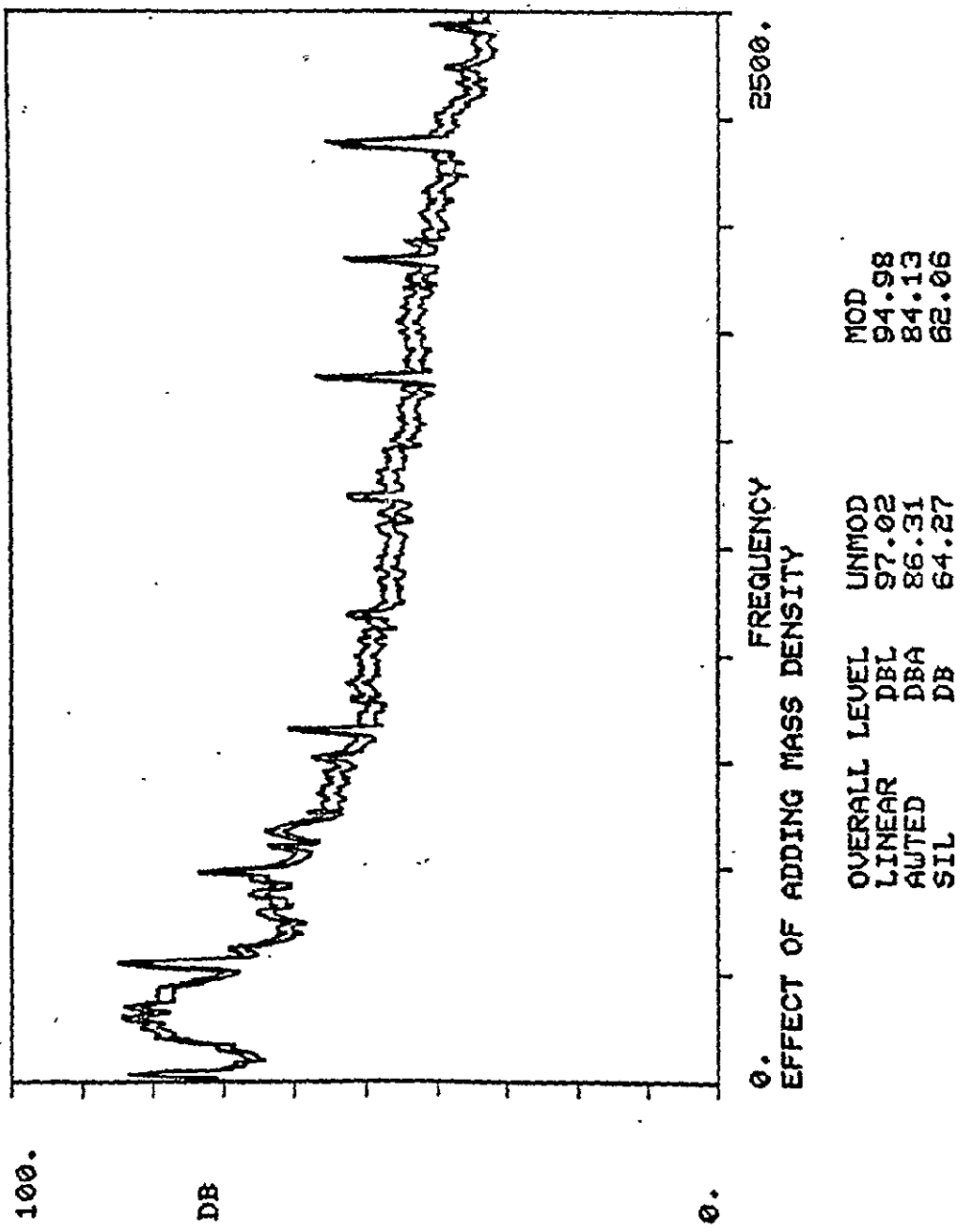

Figure F.4: Effect of Additional Mass Treatment

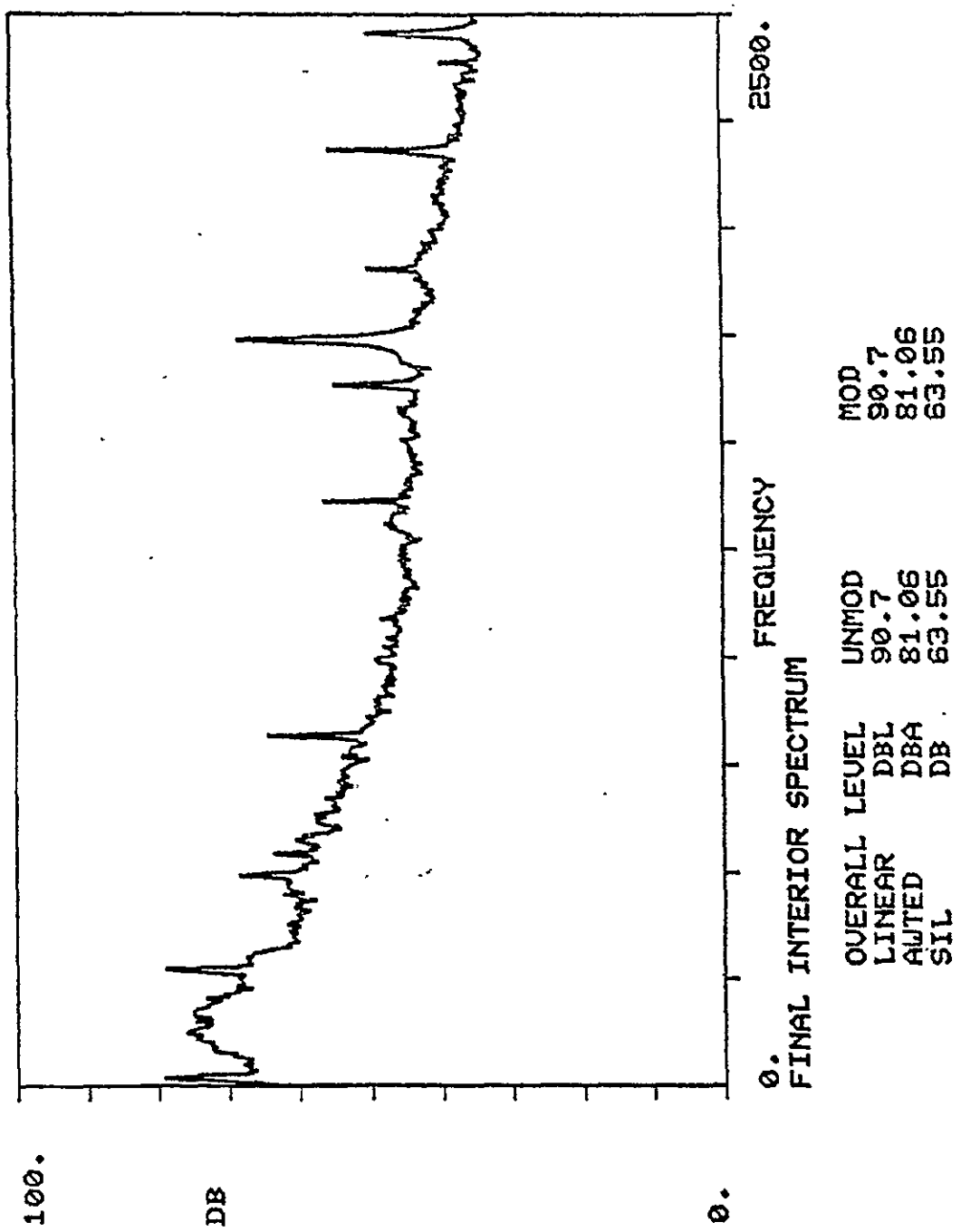

Figure F.5: Final Measured Interior Noise Spectrum